

July 20, 2023

Ms. Jennifer Meyer
Remediation and Redevelopment Program
Wisconsin Department of Natural Resources
1027 West St. Paul Avenue
Milwaukee, WI 53233

Project # 40441B

**Subject: Remedial Action Options Report
Community Within the Corridor – East Block
2748 N. 32nd Street, Milwaukee, WI 53210
BRRTS #: 02-41-263675, FID #: 241025400**

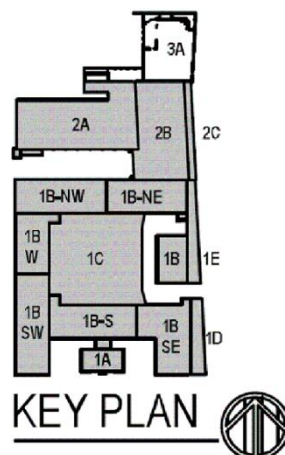
Dear Ms. Meyer:

On behalf of the Community Within the Corridor Limited Partnership (CWC), K. Singh & Associates, Inc. (KSingh) is pleased to respond to WDNR's letter dated June 7, 2023 for the Community Within the Corridor – East Block project with a Remedial Action Options Report addressing additional remedial action at the project. Please find a review fee of \$1,050 with this submittal.

Project Background

The Community Within the Corridor Limited Partnership is redeveloping the property, a former Briggs and Stratton Factory, into a mix of affordable housing, commercial spaces, and other amenities. The property has been rezoned to Industrial Mix to facilitate development of the project. No demolition of the buildings was performed. The building interiors are renovated and reconfigured. A ramp was constructed to utilize the basement as a parking garage. Paved areas were restored with asphalt.

The East Block complex is a series of buildings and additions that have been identified by the key plan included below.



A Commissioning Plan was submitted to WDNR on December 28, 2022 and updated on February 14, 2023.

Commissioning was carried out in accordance with the February 14, 2023 plan.

The results of Commissioning documented vapor intrusion of TCE into the building. The WDNR was provided test results and the City of Milwaukee issued an evacuation order on March 25, 2023. In addition, the WDNR issued an emergency order on March 31, 2023 requesting additional information.

Timeline of DNR Submittals & Responses

Please see below for a timeline of submittals following the Emergency Order:

- April 7, 2023 – An Interim Remedial Action Documentation Report (RADR) was submitted to WDNR.
- April 19, 2023 – An Emergency Corrective Action Plan (ECAP) was submitted to WDNR.
- May 8, 2023 – The WDNR responded to the Emergency Corrective Action Plan.
- May 2023 – Corrective Action activities outlined in ECAP fully commenced.
- May 26, 2023 – A response to WDNR's Technical Assistance Review of ECAP was submitted.
- June 7, 2023 – WDNR issued response to Interim and Remedial Action Status based on the Interim RADR and Status Reports from March 23, 2023 through June 5, 2023 with comments on the following areas of concern:
 - Soil Excavation
 - Soil Vapor Extraction
 - TCE in Indoor Air

Remedial Activities/Progress Update on CWC Corrective Action

The following actions have been completed or are underway with progress reported in weekly status reports.

- Sid's Sealing has performed caulk sealing work on floors, walls, sump lids, and columns throughout the complex and there was apparent improvement associated with the work. An additional sealing firm was consulted regarding Retro-Coat sealing in order to address the wooden columns, floors, and walls specifically in Units 1045 and 1050, however they could not guarantee any results on walls and columns.
- KSingh has performed portable Gas Chromatograph (GC) testing throughout the complex in association with Hartman Environmental Geoscience. Significant data has been developed and shared with the WDNR in weekly status reports.
- The gutters and downspouts near the south blowers have been redirected to divert stormwater away from the blowers and pipes from the sub-slab depressurization system.
- Constructed 14 access points for the purposes of installing inspection ports or connections to vapor mitigation system fans. Eleven of the access points have been sealed with two layers of 15-mil vapor barrier and concrete. The remaining three access points are covered with plastic and will be permanently sealed with vapor barrier and concrete soon. Please refer to Figure 1 for the location of access points.
- VS-Water Blasting, LLC televised the VMS System except for in Building 3A using the access points. No water or blockages were determined to be in the sub-slab depressurization system.
- Four sumps/drains have been added to the complex for draining water from the sub-slab depressurization system. In addition, drain tile has been installed from the sub-slab depressurization system trench to sumps associated with elevators in building 2A and building 1B-NE. Please refer to Figure 1 for locations of the sumps and drains.
- Approximately 40 tons of soil is estimated to have been generated from excavation of the sumps, drain tile trenches, and access points.

- Three additional blowers were added to the system based on data collection and analysis:
 - Blower #5, an Obar Fan GBR 123, was connected to the sub-slab depressurization system at the north side of the Fitness Room.
 - Blower #6, an Obar Fan HA 89, was connected to the sub-slab depressurization system in the hallway west of Unit 1037 in order to address depressurization concerns, based on data collected, in Units 1039, 1040, 1041, 1042, and 1043.
 - Blower #7, an Obar Fan HA 89, was connected to the sub-slab depressurization system in Unit 1035 in order to address depressurization concerns, based on data collected, in Building 1B-South.
 - With the addition of Blowers 5, 6, and 7, the capacity of air flow has increased from 1,342 cfm on May 31, 2023 to 2,294 cfm on June 22, 2023. Please refer to the locations of the blowers in Figure 1 and flow data based on anemometer readings in Table 1.
- Fliteway Technologies replaced rental Blowers 3 and 4 with permanent blowers. The 7.5HP rental blower was upgraded to a 10HP blower, so that Blowers 3 and 4 are both 10 HP Blowers.
- Details from Obar Fan and Fliteway are included in Attachment A.
- Upon the successful startup of Blower #5, continuous monitoring commenced in Units 1045 and 1050. Ventilation fans were turned off and doors to all units were closed to allow for the evaluation of the vapor mitigation system under the most challenging conditions.
- Modifications were made to Blower #8, its piping, and its vapor extraction points including an addition of a valve to direct more vacuum to the Northern Mechanical Room.

Analysis of Results

The following results were observed upon completion of the described corrective actions.

- Additional depressurization was observed immediately upon the startup of Blowers 5, 6, and 7. Depressurization was established under all residential units greater than -0.004 inches of water. During the week ending July 15, 2023, Blower #7 shut off and will be replaced and Blower #2 was temporarily shut down and was repaired. The shutdown of the blowers led to loss of depressurization in Units 1025, 1026, 1035, 1036, 1037, 1039, and 1058 and in vapor pins BB 1, BB 2, BB 4, and BB 5 to less than -0.004 inches H₂O. Vacuum is not exhibited in Stairwell 4, N. Mechanical Room, SW Garage 2, SW Garage 6, and SW Garage 19.

Restoration of vacuum is anticipated with the restoration of blowers and replacement of Blower #7 with a GBR 89. An additional blower is proposed for the SW Garage area. Connection of Stairwell 4 to the area influenced by Blower #5 is proposed to establish sufficient sustained vacuum in the stairwell. Excavation of the Northern Mechanical Room is proposed to improve vacuum draw conditions under the Northern Mechanical Room. Please refer to Table 5 and Figure 6 for a summary of depressurization measurements and the location of vapor pins for the week ending July 15, 2023.

- TCE detections in indoor air have reduced from a maximum TCE concentration of 350 ug/m³ on March 30, 2023 in Unit 1045 to less than 2.1 ug/m³ in all units except the Northern Mechanical Room as of July 14, 2023. Please refer to Table 6 for a summary of discrete TCE measurements utilizing the portable GC and Figure 7 showing where indoor air exceedances are occurring.

- Sub-slab vapor concentrations of TCE have greatly reduced and nearly all vapor pin results are less than 70 ug/m³. Please refer to Table 7 for a summary of sub-slab vapor measurements and Figure 7 showing the estimated extent of sub-slab vapors with TCE concentrations greater than 70 ug/m³.
- Emissions have shown a significant increase in concentrations of TCE being removed from approximately 30 ug/m³ prior to the startup of Blower #5 to more than 400 ug/m³ from Blower #5 after startup, greater than 1 order of magnitude improvement. Please refer to Table 1 for a summary of blower emissions concentrations of TCE and a summary of estimated flow rates based on anemometer readings.
- Resulting from the increased flow from the sub-slab depressurization system and increased concentrations of TCE in the emission, the soil vapor extraction Removal Rate has improved from approximately 0.9 pounds of TCE a year to approximately 5 to 7 pounds of TCE per year. Please refer to Table 1 for estimates of emissions. Emissions at 5 to 7 pounds per year of TCE are evidence that soil vapor extraction is occurring.

Identification and Evaluation of Remedial Action Options

The following remedial action options were identified as likely to be feasible for the facility based on the criteria of NR 722.07 and compliance with the environmental laws and standards under NR 722.09 (2).

1. Use of Biochar to sequester TCE Vapors
2. Selective Source Removal – Excavation and Disposal of Contaminated Soils to Degree and Extent Practical
3. Addition of Depressurization Fans / Improvement of Conditions for Depressurization

Chemical injection was considered technically infeasible due to the underlying clay soils. Relying on just the existing blowers was considered infeasible due to exceedances of VALs and VRSLs which did not demonstrate short-term effectiveness and the uncertain restoration time frame. Bio-degradation technologies were not considered feasible due to the technical infeasibility due to clay soils, and the uncertain restoration time frame. Complete excavation of the contaminated soils was considered infeasible due to the technical feasibility of excavation below a building which acts as a structural impediment. Biochar will be used with the thickness of Biochar still to be determined.

Based on the evaluation of the options including technical feasibility and expected short-term effectiveness, a combination of selective source removal, use of Biochar, and improvement of sub-slab conditions was considered the best remedial option for the remediating the indoor air pathway in accordance with NR 722.09.

Additional Corrective Action

The results to date have shown significant improvement in Indoor Air Quality, Sub-Slab Vapor Quality, emissions rates that demonstrate the achievement of SVE removal rates, and the achievement of depressurization under the entire building except for the Northern Mechanical Room, Stairwell 4, and parts of the garage. Subslab vapor risk screening levels for TCE were exceeded in the laundry room (room 1048), Unit 1045, Unit 1050, Unit 1044, in the southern portion of the gym at vapor pin BB 1 and 2, and the vapor pin in the SW Garage 2. The proposed plan includes additional source removal to bring Sub-Slab Vapor Quality in compliance with VRSLs and to improve vacuum performance in areas of inadequate depressurization.

The following actions are proposed:

1. Perform additional source removal to 4 feet below the top of slab in areas where there are indoor air

VAL exceedances, VRSL exceedances, and/or significant concentrations of TCE remaining in subsurface soils based on the Interim Remedial Action Documentation Report findings and GC testing data. Existing gravel will be separated and reused. Residual TCE concentrations in soil are shown on Figure 8. Excavation is limited to 4 feet to not jeopardize the structural integrity of the building foundation and 2 feet in the stairwell and gym areas. The locations of proposed excavations are shown on Figures 2, 3, and 4. Please refer to Table 2 for the areas of excavation and estimated quantities of material that are proposed to be removed. Table 3 estimates the TCE to be removed by the additional source removal to be approximately 3 pounds.

2. Collect at least two confirmatory samples from the bottom of each unit/area excavated and test for VOCs.
3. Perform smoke testing to determine if there is a loss of vacuum from leakage in the garage run of the sub-slab depressurization system. Determine if the sumps are contributing to loss of vacuum. Modify as necessary, add additional fans to the sub-slab depressurization system, and/or perform additional source removal. Additional source removal, including in the Northern Mechanical Room, will also result in an additional sub-slab gravel layer which is anticipated to expand the zone of depressurization.
4. Replace Blower #6 with an Obar GBR 123 Fan for increased depressurization and vapor removal below building 1B-SW. An Obar GBR 89 will be used to replace the malfunctioning Blower #7.
5. Following excavation and collection of confirmatory samples, a thin layer of Biochar will be placed, a geotextile will be placed atop the Biochar, the excavation will be backfilled with gravel to required grades. A typical cross-section of excavation and restoration is shown on Figure 5. Biochar is a carbon-rich product obtained when biomass, such as wood, manure, or leaves, undergoes pyrolysis, a thermochemical process that occurs under high temperatures and in the absence of oxygen. It is similar to charcoal but is designed specifically for soil application. The structure of biochar is often characterized by a high degree of porosity, a high carbon content, and a high surface area. Please refer to Attachment B for further information on BioChar.

Biochar can interact with TCE via adsorption, a process by which TCE molecules adhere to the surface of biochar. This interaction can occur in several ways:

- **Physical adsorption:** The porous structure and high surface area of biochar allow TCE molecules to be physically trapped within its structure. This process is primarily driven by van der Waals forces.
- **Chemical adsorption:** The surface of biochar often contains various functional groups that can form chemical bonds with TCE molecules, resulting in a stronger, chemically bonded form of adsorption. This process is more specific and stronger than physical adsorption.
- **π - π electron donor-acceptor (EDA) interactions:** The aromatic carbon structure of biochar may form π - π EDA interactions with the aromatic ring in TCE, further enhancing its adsorption capacity.

Given its adsorptive properties, biochar is considered a promising, environmentally sustainable option for remediation of TCE-contaminated environments, especially in soil and groundwater remediation. By adjusting the production parameters of biochar (like pyrolysis temperature and feedstock), the adsorptive properties of biochar can be tuned to enhance its effectiveness in TCE adsorption.

It's important to note that the presence of other substances in the environment could potentially compete with TCE for adsorption sites on the biochar, which may affect its performance. Therefore, the effectiveness of biochar in TCE adsorption could depend on the specific conditions of the environment where it is applied.

Please refer to Table 4 for calculations of how much Biochar is required. Based on the historical information of soil contamination coupled with the predicted adsorption capacity of the biochar, a total of approximately 2.3 tons of biochar would be required to prevent a breakthrough. The application of biochar coupled with the VMS will ensure an efficient TCE removal mechanism.

6. Atop the gravel fill, a vapor barrier at least 20-mils thick, and concrete will be placed.
7. Additional sub-slab depressurization fans will be placed to provide additional resiliency to Units 1044, 1045, 1048, 1049, and 1050 and the garage area of 1B-NW to improve sub-slab depressurization and provide resiliency to the system based on post-construction depressurization and TCE measurements.
8. Apply Biochar to wooden columns to provide additional protection against vapor intrusion using the wooden columns as preferential pathways. The biochar-alginate gel can be used in the floors and wooden columns to provide a dual purpose of sealing the cracks, as well as to act as a medium of remediation by absorbing TCE. Creating a biochar-alginate mixture generally involves creating a suspension of biochar in a solution of alginate, then using a gelling process to solidify the mixture. In order to create an effective sealing and remediation mechanism, the affected areas would need about 600 kgs of biochar to be mixed with 60 kgs of potassium alginate and solidified with about 200 kgs of calcium chloride in an aqueous media.
9. An Operations and Maintenance (O&M) Plan will be submitted following restoration of concrete throughout the complex. The O&M Plan will provide a plan for additional depressurization fans and power backup, as needed.

Sustainable Remedial Action Evaluation

The use of Biochar will allow for the beneficial reuse of organic wastes in a sustainable manner that will also limit the long-term electrical needs of the vapor mitigation system by sequestering TCE. Biochar will also reduce the generation of air pollutants. There will be no impacts to water use or impacts to water resources by the proposed plan. There will be no impacts to future land use or ecosystems from the proposed remedial action.

The Obar Fans utilized at the site have adjustable speeds and may be adjusted over time as conditions improve to limit electricity use.

Schedule / Timeline

The following is the proposed schedule for additional remedial action.

1. August 1 to September 15, 2023 Source Removal Starting in Northern Mechanical Room work to Include: Concrete Cutting, Soil Excavation and Disposal, Placement of Biochar and Geotextile, Backfilling with Permeable Stone/Gravels, Installation of Vapor Extraction Piping (where required), Vapor Barrier, and Replacement of

- | | |
|---------------------------------------|---|
| | Concrete Flooring per Table 2 and Figures 2, 3, and 4. |
| | Spread Biochar and Enclose Columns in Units 1043, 1044, 1045, 1048, 1049, 1050 and 1052. |
| | Potential Installations of Additional Fans for Units 1044, 1045, and 1050, and for Units 1048 and 1049. |
| 2. August 17, 2023 | Submit Commissioning Plan to WDNR |
| 3. September 16 to September 29, 2023 | Obtain Full Operation of Mitigation System and Post-Remedial Action Indoor Air and Sub-Slab Vapor Testing |
| 4. October 2, 2023 | 1 st Round of Commissioning |
| 5. October 27, 2023 | Submit Remedial Action Documentation Report and O&M Plan |

Closing

We request WDNR’s review and approval of the proposed Remedial Action Plan. Please note that Robert Fedorchak with Patriot Engineering and Environmental, Inc., an NRPP-Certified Radon Mitigation Specialist, has provided plan input and feedback. Please find included in Attachment C certification of the plan. The remedial actions are proposed to begin in August 2023 and we would appreciate an accelerated review in order to implement any WDNR requests before work is completed. We appreciate WDNR’s assistance with this project. Please contact us if you have any questions.

Sincerely,

K. SINGH & ASSOCIATES, INC.



Robert T. Reineke, PE
Senior Engineer



Sameer Neve, Ph.D., ENV SP
Staff Engineer



Pratap N. Singh, Ph.D., PE
Principal Engineer

cc: Shane LaFave / Roers Companies
Que El-Amin / Scott Crawford, Inc.
Robert Fedorchak, PE / Patriot Engineering and Environmental, Inc.

Tables/Figures

- | | |
|----------|--|
| Table 1. | GC TCE Measurements of Blower Effluent and Estimated Removal Rates |
| Table 2. | Estimated Additional Excavation Volumes |
| Table 3. | Estimated Additional TCE Removal |

- Table 4. Biochar Application
Table 5. Summary of Differential Pressure Measurements at Vapor Pins
Table 6. GC TCE Measurements of Indoor Air
Table 7. GC TCE Measurements of Sub-Slab Vapors
- Figure 1. Locations of Access Points, Additional Sumps and Drains, Blowers for Vapor Mitigation System, and Vapor Pins
Figure 2. Proposed Areas of Additional Excavations (1B-SW and 1C)
Figure 3. Proposed Areas of Additional Excavations (1B-W and 1B-NW)
Figure 4. Proposed Area of Additional Excavation (North Mechanical Room)
Figure 5. Cross-Section of Excavation and Restoration
Figure 6. Locations of Vapor Pins and Differential Pressure Measurements for the week of 7/15/23
Figure 7. Locations of Indoor Air TCE Concentrations and VAL Exceedances and Sub-Slab Vapor TCE Concentrations and VRSL Exceedances
Figure 8. Locations of Confirmatory Samples and Residual TCE Concentrations

Attachments

- Attachment A Obar Fan and Fliteway Blower Information
Attachment B Biochar Technical Information
Attachment C Professional Engineer Certifications

TABLES / FIGURES

Table 1
GC TCE Measurements of Blower Effluent and Estimated Removal Rates

Blower ID	Blower 1 (South 7.5 HP)				Blower 2 (South 10 HP)				Blowers 3 and 4 (Northern Blowers)				Blower 5 (Obar Fan GBR 123)				Temp Radonaway GP501C at Access Point 4				Blower 6 (Obar Fan HA 89) Replacement for GP501C				Blower 7 (Obar Fan HA 89)				Blower 8 (RP 265)				Total of All Blowers				
Date	Effluent TCE Concentration	Flow Rate	TCE Removal Rate	TCE Removal Rate	Effluent TCE Concentration	Flow Rate	TCE Removal Rate	TCE Removal Rate	Effluent TCE Concentration	Flow Rate	TCE Removal Rate	TCE Removal Rate	Effluent TCE Concentration	Flow Rate	TCE Removal Rate	TCE Removal Rate	Effluent TCE Concentration	Flow Rate	TCE Removal Rate	TCE Removal Rate	Effluent TCE Concentration	Flow Rate	TCE Removal Rate	TCE Removal Rate	Effluent TCE Concentration	Flow Rate	TCE Removal Rate	TCE Removal Rate	Effluent TCE Concentration	Flow Rate	TCE Removal Rate	TCE Removal Rate	Flow Rate	TCE Removal Rate	TCE Removal Rate		
	(ug/m3)	(cfm)	(lbs/day)	(lbs/year)	(ug/m3)	(cfm)	(lbs/day)	(lbs/year)	(ug/m3)	(cfm)	(lbs/day)	(lbs/year)	(ug/m3)	(cfm)	(lbs/day)	(lbs/year)	(ug/m3)	(cfm)	(lbs/day)	(lbs/year)	(ug/m3)	(cfm)	(lbs/day)	(lbs/year)	(ug/m3)	(cfm)	(lbs/day)	(lbs/year)	(ug/m3)	(cfm)	(lbs/day)	(lbs/year)	(cfm)	(lbs/day)	(lbs/year)		
5/31/2023	19.6	315	0.0006	0.2	33.5	335	0.0010	0.4	12.5	692	0.0008	0.3	0	0	0.0000	0.0	19.5	68	0.0001	0.0	0	0	0.0000	0.0	0	0	0.0000	0.0	0	0.0000	0.000	0	0.0000	0.000	1342	0.002	0.9
6/9/2023	19.6	315	0.0006	0.2	33.5	335	0.0010	0.4	12.5	692	0.0008	0.3	461	373	0.015	5.6	0	0	0.0001	0.0	0	0	0.0000	0.000	0	0	0.0000	0.000	0	0.0000	0.000	0	0.0000	0.000	1783	0.018	6.5
6/22/2023	16.3	328	0.0005	0.2	19.8	313	0.0006	0.2	14.9	568	0.0008	0.3	405	388	0.014	5.2	28.8	314	0.001	0.3	7	380	0.0002	0.087	180	3	0.00005	0.018	2294	0.017	6.2						
6/28/2023	17.6	363	0.0006	0.2	18.7	378	0.0006	0.2	0	0	0.0000	0.0	400.4	344	0.012	4.5	28.8*	309	0.001	0.3	7*	360	0.0002	0.083	180*	3*	0.00005	0.018	1757	0.015	5.4						
7/3/2023	20.1	372	0.0007	0.2	18.3	364	0.0006	0.2	14.9*	568*	0.0008	0.3	388.7	336	0.012	4.3	23.8	316	0.001	0.2	2.93	357	0.0001	0.034	180*	3*	0.00005	0.018	2493	0.015	5.3						

*Estimated data due to unavailability of sample

Table 2
Estimated Additional Excavation Volumes

Unit	Location	Area (square feet)	Depth (feet)	Volume (cubic yards)	Weight (tons)	Reason
Hall	Hall Outside 1044 and 1045	186	2.5	17.22	30.225	Subslab Vapor Exceedance
1044	Main	100	2.5	9.26	16.25	Subslab Vapor Exceedance
1045	Main	99	2.5	9.17	16.0875	Subslab Vapor Exceedance and Residual Soil Contamination
1045	Bedroom	100	2.5	9.26	16.25	Subslab Vapor Exceedance and Residual Soil Contamination
1050	Main	50	2.5	4.63	8.125	Subslab Vapor Exceedance and Residual Soil Contamination
Hall	Hall to 1050	126	2.5	11.67	20.475	Subslab Vapor Exceedance and Residual Soil Contamination
Hall	Corridor Outside 1048/1049	192	2.5	17.78	31.2	Residual Soil Contamination
1048	Laundry	150	2.5	13.89	24.375	Subslab Vapor Exceedance and Residual Soil Contamination
1056	Mechanical Electrical Room	92	2.5	8.52	14.95	Residual Soil Contamination
1049	Storage Room	384	2.5	35.56	62.4	Residual Soil Contamination
Hall	Hall to 1051	109.72	2.5	10.16	17.83	Residual Soil Contamination
1B-NW	Garage Near SW Garage Vapor Pin (Parking Space 2, Parking Space 6, and Parking Space 19)	400	3.5	51.85	91.00	Subslab Vapor Exceedance and Lack of Vacuum
N. Mech. Room	N. Mech. Room	100	3.5	12.96	22.75	Indoor Air Exceedance and Lack of Vacuum

Table 2
Estimated Additional Excavation Volumes

Unit	Location	Area (square feet)	Depth (feet)	Volume (cubic yards)	Weight (tons)	Reason
1B-C	SW Portion of Gym (Vapor Pin BB1)	200	1.5	11.11	19.50	Subslab Vapor Exceedance, Lack of Vacuum
1B-C	S Portion of Gym (Vapor Pin BB2)	200	1.5	11.11	19.50	Subslab Vapor Exceedance, Lack of Vacuum
NW Gym Stairwell	NW Gym Stairwell	12	1.5	0.67	1.17	Subslab Vapor Exceedance and Lack of Vacuum
Total		2,500.72	---	234.81	412.09	---

Table 3
Estimated Additional TCE Removal

Unit	Location	Area (square feet)	Depth (feet)	Volume (cubic yards)	Weight (tons)	Representative Maximum Residual TCE Concentration*	Estimated TCE to be Removed (pounds)
Hall	Hall Outside 1044 and 1045	186	2.5	17.22	30.225	3.7	0.223665
1044	Main	100	2.5	9.26	16.25	3.7	0.12025
1045	Main	99	2.5	9.17	16.0875	3.7	0.1190475
1045	Bedroom	100	2.5	9.26	16.25	3.7	0.12025
1050	Main	50	2.5	4.63	8.125	3.7	0.060125
Hall	Hall to 1050	126	2.5	11.67	20.475	3.7	0.151515
Hall	Corridor Outside 1048/1049	192	2.5	17.78	31.2	3.7	0.23088
1048	Laundry	150	2.5	13.89	24.375	3.7	0.180375
1056	Mechanical Electrical Room	92	2.5	8.52	14.95	3.7	0.11063
1049	Storage Room	384	2.5	35.56	62.4	3.7	0.46176
Hall	Hall to 1051	109.72	2.5	10.16	17.83	3.7	0.1319383
1B-NW	Garage Near SW Garage Vapor Pin (Parking Space 2)	400	3.5	51.85	91.00	3.7	0.6734
N. Mech. Room	N. Mech. Room	100	3.5	12.96	22.75	3.7	0.16835
1B-C	SW Portion of Gym (Vapor Pin BB1)	200	1.5	11.11	19.50	3.7	0.1443
1B-C	S Portion of Gym (Vapor Pin BB2)	200	1.5	11.11	19.50	3.7	0.1443
NW Gym Stairwell	NW Gym Stairwell	12	1.5	0.67	1.17	2.7	0.006318
Total		2,500.72	---	234.81	412.09	---	3

*Concentration based on Median Concentration of Remedial Action Confirmatory Samples for Hot Spots and SIR concentration for Northern Mechanical Room.

Table 4
Biochar Application

	Units	Value
Biochar source		Wood Char
Biochar C%	%	67.22
Biochar bulk density	kg/m ³	633.00
Biochar Surface Area	m ² /g	0.92
Soil Area	ft ²	2500.72
Depth of Excavation	ft	2.50
Total Soil Volume	ft ³	6251.80
Soil Density	lbs/ft ³	130.00
Soil Mass	lbs	812734.00
	kg	368649.64
TCE Concentration in Exhaust	ug/m ³	400.00
Soil Pore Volume	m ³	52.52
TCE in soil	mg/kg	3.70
Total TCE mass	g	1364.00
	lbs	3.01
Biochar adsorption capacity	mg/g	32.00
Amount of biochar needed	g	42625.11
	kg	42.63
Safety Factor		10.00
Amount blended with soil	kg	426.25
Amount used to form a barrier	kg	1050.52
Amount used for sealing	kg	600.00
Total Biochar needed	kg	2076.77
	lbs	4578.49
	ton	2.29

Table 7
GC TCE Measurements of Sub-Slab Vapors

Green cells indicate the VRSL levels below the DNR limit of 70 ug/m3							
Location		Week of 6/3	Week of 6/17	Week of 6/24	Week of 7/1	Week of 7/8	Week of 7/15
1055	Women's Locker Room		46.5	17.3	13.5	25.8	9.89
1054	Fitness Room	596	0.8	4.8	0.483	2.6	2.23
1053	Men's Locker Room		102.3	71.31	55.7	76.2	26.5
Oppo. 1054			58.9	55.6	46.9	48.2	53.3
Stairwell 4			252.5	6.3	27.4	22.1	14.2
1052	Mechanical Room		63.9	38.1	14.9	5.96	4.97
1051			47.3	32.4	22.7	25.8	12.6
1049	Storage Room	426	2.6	3.38	1.76	2	2.25
1048	Laundry Room	322	679	572	561	637	556
1050		1443	303.4	377	265	283	275
Out 1050		971	113.1	10.1	64.1	46.3	72.8
1045		750	271.6	206	253	238	222
Out 1044		456	380.5	364	419	205	376
1043			178.5	185	7.92	14.3	10.7
1042		11.8	15.93	10.4	2.67	1.22	6.43
1041			108.7	13.2	4.48	4.24	18.8
1040		1.6	11.7	16.1	3.22	1.13	3.83
1040 - out				21.3	3.1	10.3	5
1039		23.5	62.2	4.3	15.2	23.8	16.5
1037			240.4	4.3	11.04	50.1	43.7
1036			17.2	5.5	2.85	10.2	6.13
1035			0.8	7	0.534	1.4	1.61
1035 - out			87	55.4	73.2	98.9	95.1
1058 E	Electric Room		433.8	1.5	87	307	181
1058 W	Electric Room		73.3	6.99	0.1	5.3	3.19
1026			16.7	6.6	7.39	20.8	14.8
1025			2.2	2.1	1.01	10.5	2.15
1014			23.9	2.2	21.2	124	44.7
1011	Conference Room		17.5	1.6	1.5	5.24	0.6
SE Lobby	Near Exit	328	0.46	0.5	0.1	0.37	0.1
BB 1	SW of the Gym			73	25.1	553	571
BB 2	South part of the Gym		30.8	1.5	286	65	43
BB 3	SE part of the Gym		2.2	1.6	0.733	1.05	7.5
BB 4	N of the Gym		2.6	1.9	0.569	0.77	3.37
BB 5	Center of the Gym		58.9	1.9	27.5	87	86.5
SW Garage (2)			227.4	63.7	300	307	317
SW Garage (26)						24.3	22.3
SW Garage (6)						43.9	2.7
SW Garage (19)						7.49	2.61
SE Garage (11)						49.5	17.8
SE Garage (14)			10.3	1.6	1.24	2.02	1.99
NW Garage (80)			141.5	4.7	12.7	27.2	21.2
NE Garage (36)			24.8	2.8	9.87	13	6.07
N Mech Room			60.2	147	27.07	18.7	0.98

East Building Level 1

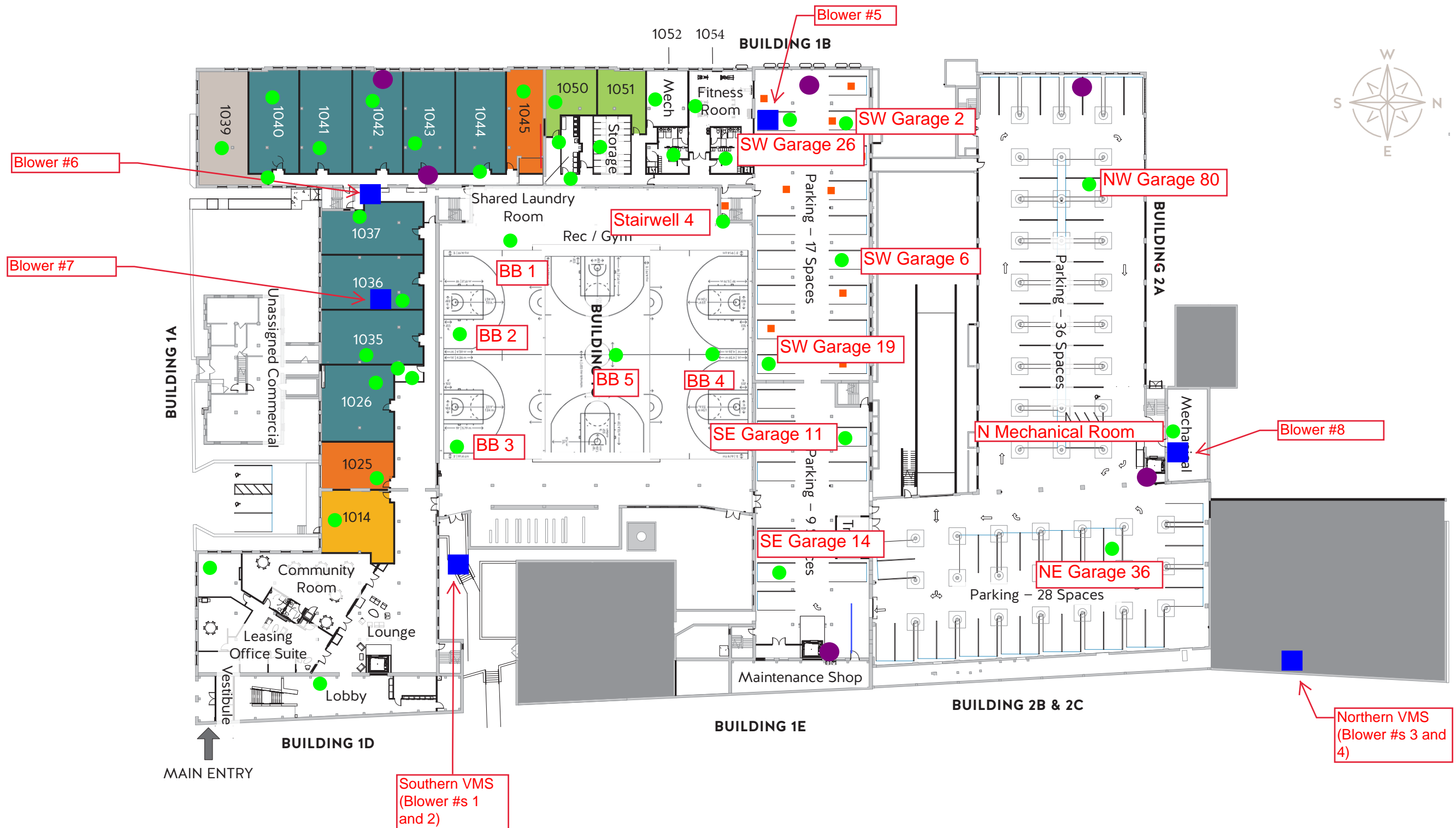


Figure 1. Locations of Access Points, Additional Sumps and Drains, Blowers for Vapor Mitigation System, and Vapor Pins

GENERAL FURTHER PLAN NOTES TO CONTRACTOR

- THIS DRAWING IS FURTHER SUPPORTED BY INFORMATION CONTAINED IN THE SPECIFICATION MANUAL. DO NOT SCALE DRAWINGS. CONTRACTOR TO VERIFY ALL CONDITIONS AND DIMENSIONS AT THE JOB SITE PRIOR TO COMMENCING CONSTRUCTION.
- FINISH FLOOR ELEVATIONS ARE TO THE TOP OF THE FINISHED FLOOR MATERIAL UNLESS OTHERWISE NOTED.
- CONTRACTORS SHALL CONTINUALLY PROVIDE AND INSTALL ALL STEPPERS, BRACING, BACKING PLATES, WALL BLOCKING AND SUPPORTING BRACKETS REQUIRED FOR THE INSTALLATION OF CASEWORK, TOILET ACCESSORIES, PARTITIONS, MILLWORK, AND ALL WORK MOUNTED OR SUSPENDED BY ALL TRADES.
- SEE SHEET A400 FOR PARTITION TYPES AND DETAILS.
- DIMENSIONS AT EXTERIOR WALLS ARE TO STRUCTURAL WALL ONLY AND DO NOT INCLUDE FINISHES. DIMENSIONS AT EXTERIOR WALLS ARE TO STRUCTURAL WALL ONLY AND DO NOT INCLUDE FINISHES.

GENERAL INFORMATION NOTES TO CONTRACTOR

- THESE DRAWINGS ARE DIAGRAMMATIC AND SHOW THE INTENT OF THE PROJECT, BUT DO NOT NECESSARILY INDICATE ALL MATERIALS OR METHODS OF CONSTRUCTION. ALL CONTRACTORS ARE RESPONSIBLE TO REVIEW THE DOCUMENTS THOROUGHLY, AND FOR PROVIDING ALL MATERIALS AND MEANS OF CONSTRUCTION NECESSARY FOR THE COMPLETION OF THE WORK IN ACCORDANCE WITH THE INTENT OF THE DRAWINGS.
- ALL WORK OF ALL TRADES SHALL BE COMPLETED IN ACCORDANCE WITH ALL LOCAL GOVERNING CODES AND ORDINANCES.
- EACH CONTRACTOR SHALL COORDINATE THEIR WORK WITH THE OWNER, THE OWNER'S OTHER CONTRACTORS, AND ALL OTHERS AT THE SITE.
- EACH CONTRACTOR IS TO OBTAIN AND PAY FOR PERMITS, LICENSES, FEES, ETC. AS REQUIRED FOR THE COMPLETION OF THEIR PORTION OF WORK.
- EACH CONTRACTOR SHALL VERIFY ALL CONDITIONS AND DIMENSIONS AT THE SITE TO SATISFY THEIR EXECUTION OF THE WORK. ANY DISCREPANCIES SHALL BE REPORTED TO THE ARCHITECT. NEITHER THE OWNER NOR THE ARCHITECT ASSUMES RESPONSIBILITY FOR CONDITIONS OR DIMENSIONS SHOWN AS EXISTING.
- IF ANY CONTRACTOR OBSERVES THAT ANY OF THE CONTRACT DOCUMENTS ARE AT VARIANCE WITH APPLICABLE LAWS, STATUTES, BUILDING CODES, OR ORDINANCES, THEY SHALL PROMPTLY NOTIFY THE ARCHITECT.
- ALL HOLES FOR PLUMBING, ELECTRICAL, HVAC, FIRE PROTECTION CONDUIT, PIPING, OR DUCTWORK ARE TO BE REPAIRED BY THE ASSOCIATED TRADE.
- ALL TRADES SHALL TAKE CARE TO MAKE HOLES ONLY AS LARGE AS NECESSARY. ALL HOLES SHALL BE NEATLY CUT, DO NOT PUNCH OR POUND HOLES IN WALLS OR ROOF DECK.
- ANY HOLES OR PENETRATIONS THROUGH FIRE RATED CONSTRUCTION SHALL BE APPROPRIATELY FIRE STOPPED, DAMPENED, OR SEALED AS REQUIRED BY CODE.
- EACH CONTRACTOR SHALL INCLUDE NECESSARY DEMOLITION AND REMOVAL OF ALL MATERIAL AS REQUIRED TO PERFORM THEIR WORK.
- REMOVAL OF ALL HAZARDOUS CONTAINING MATERIALS IS THE SOLE RESPONSIBILITY OF THE OWNER. SHOULD ANY MATERIALS BE ENCOUNTERED DURING ANY OF THE CONSTRUCTION PHASES CONTAINING, OR SUSPECTED TO BE HAZARDOUS, CONTRACTOR SHALL STOP WORK IMMEDIATELY AND NOTIFY OWNER AND ARCHITECT.
- DO NOT SCALE DRAWINGS.
- EACH CONTRACTOR SHALL PATCH LEVEL, AND PREPARE ALL WALLS AND FLOORS AS SCHEDULED AND REQUIRED TO RECEIVE NEW FINISHES.

NEW WORK PLAN LEGEND

- EXISTING TO REMAIN
- MASONRY PARTITION, SEE PARTITION TYPES FOR DETAILS
- METAL STUD PARTITION, SEE PARTITION TYPES FOR DETAILS TYPE A3 -> U.L.O.
- METAL STUD PARTITION, SEE PARTITION TYPES FOR DETAILS TYPE A2 -> U.L.O.
- NEW WORK KEY NOTE (GENERAL TO ROOM)
- Excavation to 4 Feet
- Excavation to 2 Feet
- Perforated 4-Inch Diameter Pipe
- Estimated Tunnel Extents

NEW WORK PLAN KEY NOTES - 1/8" PLANS

SEE PROJECT GENERAL CONDITIONS, GENERAL INFORMATION ON SHEET A001 AND SELECTIVE DEMOLITION, CUTTING AND PATCHING SPECIFICATIONS THAT ARE USED IN ASSOCIATION WITH THESE NOTES.

NEW WORK PLAN KEY NOTES APPLY TO ALL NEW WORK DRAWINGS AND MAY NOT BE USED ON EVERY SHEET.

- SEE UNIT 1035 ENLARGED PLAN. UNIT MAY BE MIRRORRED.
- SEE UNIT 1035 ENLARGED PLAN.
- SEE UNIT 1035 ENLARGED PLAN. UNIT MAY BE MIRRORRED.
- SEE UNIT 1037 ENLARGED PLAN.
- SEE UNIT 1035 ENLARGED PLAN.
- SEE UNIT 1040 ENLARGED PLAN.
- SEE UNIT 1041 ENLARGED PLAN.
- SEE UNIT 1042 ENLARGED PLAN.
- EXISTING HISTORIC SLIDING FIRE DOOR ASSEMBLY TO REMAIN. SECURE SLIDING DOOR IN A PARTIALLY CLOSED POSITION WITH METAL Z BRACKETS. SEE SALVAGED DOOR SCHEDULE FOR MORE INFO.
- SEE UNIT 1043 ENLARGED PLAN.
- SEE UNIT 1043 ENLARGED PLAN. UNIT IS MIRRORRED.
- SEE UNIT 2014 ENLARGED PLAN.
- SEE UNIT 2015 ENLARGED PLAN.
- SEE UNIT 2016 ENLARGED PLAN.
- SEE UNIT 2017 ENLARGED PLAN.
- SEE UNIT 2023 ENLARGED PLAN.
- SEE UNIT 2003 ENLARGED PLAN.
- SEE UNIT 2003 ENLARGED PLAN. UNIT MAY BE MIRRORRED.
- SEE UNIT 2003 ENLARGED PLAN. UNIT TYPE IS A STUDIO ON LEVEL 03.
- SEE UNIT 2017 ENLARGED PLAN.
- SEE UNIT 2017 ENLARGED PLAN.
- SEE UNIT 2019 ENLARGED PLAN.
- SEE UNIT 2002 ENLARGED PLAN. FOR UNIT 2002. SEE UNIT 2002 ENLARGED PLAN.
- SEE UNIT 2002 ENLARGED PLAN.
- SEE UNIT 2002 ENLARGED PLAN.
- SEE UNIT 2004 ENLARGED PLAN. UNIT MAY BE MIRRORRED.

NEW WORK PLAN KEY NOTES - 1/8" PLANS

SEE PROJECT GENERAL CONDITIONS, GENERAL INFORMATION ON SHEET A001 AND SELECTIVE DEMOLITION, CUTTING AND PATCHING SPECIFICATIONS THAT ARE USED IN ASSOCIATION WITH THESE NOTES.

NEW WORK PLAN KEY NOTES APPLY TO ALL NEW WORK DRAWINGS AND MAY NOT BE USED ON EVERY SHEET.

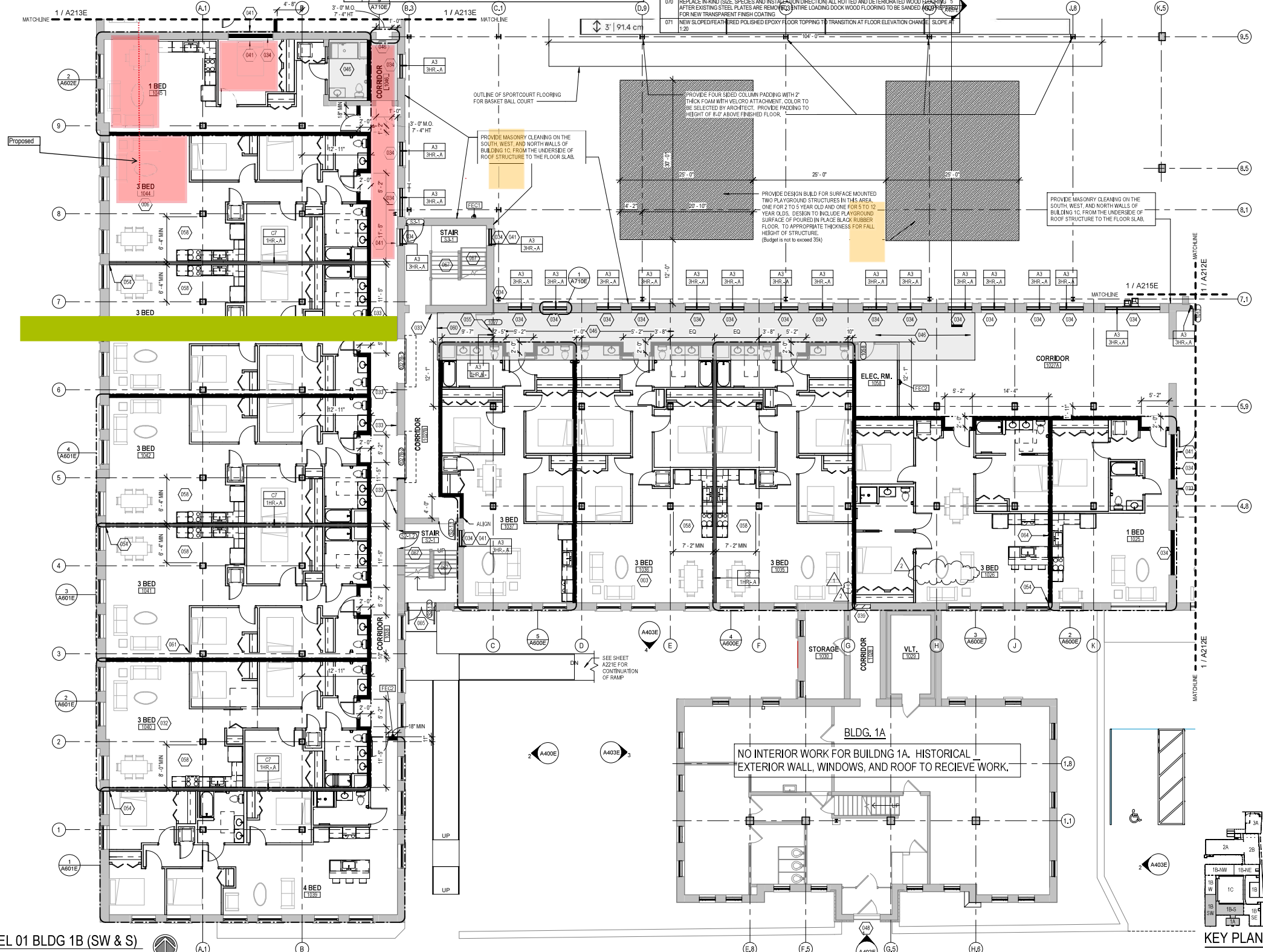
- SEE UNIT 2008 ENLARGED PLAN. UNIT MAY BE MIRRORRED.
- SEE UNIT 2111 ENLARGED PLAN. FOR UNIT 2110. SEE UNIT 2110.
- SEE UNIT 2111 ENLARGED PLAN.
- UNIT TO INCLUDE AUDIO AND VISUAL ALARM DEVICES FOR THE HEARING AND VISUALLY IMPAIRED. COORDINATE LOCATION WITH ELECTRICAL DRAWINGS.
- EXISTING HISTORIC SLIDING FIRE DOOR ASSEMBLY TO REMAIN IN PLACE. SECURE SLIDING DOOR IN A FULLY OPEN POSITION WITH METAL Z BRACKETS. SEE SALVAGED DOOR SCHEDULE FOR MORE INFO.
- NEW GYPSUM BOARD INFILL WALL ASSEMBLY AT EXISTING OPENING. SEE 3A710E.
- EXISTING HISTORIC WINDOW ASSEMBLY TO REMAIN. PREPARE EXISTING WINDOW FOR NEW PAINT FINISH. REPLACE DAMAGED OR MISSING GLAZING TO MATCH EXISTING.
- NEW CMU INFILL WALL ASSEMBLY AT EXISTING OPENING. SEE 3A710E.
- NEW METAL PANEL INFILL WALL ASSEMBLY AT EXISTING OPENING. SEE 3A610E.
- NEW BRICK AND CMU INFILL AT EXISTING WALL OPENING.
- NEW BRICK MASONRY INFILL WALL ASSEMBLY AT EXISTING OPENING. SEE 3A710E.
- EXISTING CONCRETE FLOOR WITH NEW WATERPROOF TRAFFIC COATING.
- EXISTING HISTORIC SLIDING FIRE DOOR ASSEMBLY TO REMAIN. SECURE SLIDING DOOR IN A CLOSED POSITION WITH METAL Z BRACKETS. SEE SALVAGED DOOR SCHEDULE FOR MORE INFO.
- NEW BRICK MASONRY AND GYPSUM BOARD INFILL WALL ASSEMBLY AT EXISTING OPENING. SEE 3A710E.
- NEW CMU AND GYPSUM BOARD INFILL WALL ASSEMBLY AT EXISTING OPENING. SEE 3A710E.
- NEW WOOD FLOOR INFILL. NEW WOOD FRAMING TO MATCH EXISTING. NEW WOOD SUBFLOORING TO MATCH DIMENSIONS OF EXISTING AND TO RUN IN THE SAME DIRECTION AS EXISTING. REINSTALL EXISTING SALVAGED FINISH FLOORING, RUN IN THE SAME DIRECTION AS EXISTING. SEE STRUCTURAL FOR DETAILING.
- NEW CONCRETE ON METAL DECK INFILL WITH GRAY APPLIED FIRE RESISTIVE MATERIAL AT NEW STEEL BEAMS AND ANGLES TO MATCH FLOOR ASSEMBLY FIRE RATING. SEE OVERVIEW FLOOR PLAN FOR REQUIRED FLOOR ASSEMBLY FIRE RATINGS. SEE STRUCTURAL FOR DETAIL.
- NEW CONCRETE FLOOR INFILL. SEE STRUCTURAL.
- NEW FINISHED METAL MECHANICAL LOCKER IN EXISTING MASONRY OPENING.
- ENTIRE EXISTING HISTORIC WOOD DOOR ASSEMBLY INCLUDING ALL EXTERIOR AND INTERIOR WOOD TRIM COMPONENTS TO REMAIN. ALL WOOD COMPONENTS TO BE Sanded, REPLACED IN KIND AND PREPARED FOR NEW FINISHES THAT MATCH EXISTING FINISHES. ANY MISSING WOOD COMPONENTS (DOOR ASSEMBLY, INTERIOR EXTERIOR TRIM COMPONENTS) TO BE REPLACED WITH SIMILAR WOOD SPECIES AND TO MATCH EXISTING PROFILES THAT REMAIN. ALL EXISTING DOOR HARDWARE TO BE REMOVED, Sanded AND PREPARED FOR NEW FINISH AND REINSTALLATION.

NEW WORK PLAN KEY NOTES - 1/8" PLANS(2)

SEE PROJECT GENERAL CONDITIONS, GENERAL INFORMATION ON SHEET A001 AND SELECTIVE DEMOLITION, CUTTING AND PATCHING SPECIFICATIONS THAT ARE USED IN ASSOCIATION WITH THESE NOTES.

NEW WORK PLAN KEY NOTES APPLY TO ALL NEW WORK DRAWINGS AND MAY NOT BE USED ON EVERY SHEET.

- EXISTING HISTORIC WINDOW ASSEMBLY TO REMAIN. CLEANSCRAPE/PREPARE EXISTING WINDOW FRAMES TO RECEIVE NEW PAINT. EXISTING GLAZING TO BE REMOVED.
- REPLACE ALL BROKEN/CRAACKED AND MISSING GLASS LITES AT HISTORIC LIGHT MONITOR.
- NEW GYPSUM BOARD INFILL WALL ASSEMBLY AT EXISTING OPENING TO BE 3 HOUR FIRE RATED. SEE 10A710E SM.
- LOCATION WITH ELECTRICAL DRAWINGS. PREPARE EXISTING WINDOW FOR NEW PAINT FINISH. EXISTING GLAZING TO REMAIN. NEW GLAZING NOT REQUIRED.
- EXISTING HISTORIC DOOR ASSEMBLY TO REMAIN. PREPARE EXISTING DOOR ASSEMBLY FOR NEW PAINT FINISH.
- EXISTING HISTORIC WALL WITH EDGE OF HISTORIC MASONRY OPENING.
- ALIGN CENTER OF WALL WITH CENTERLINE OF HISTORIC COLUMN.
- AT LEVEL 02, ALIGN EDGE OF DEMISING WALL WITH EDGE OF HISTORIC CONCRETE DROP SLAB. AT LEVEL 03, ALIGN EDGE OF DEMISING WALL WITH EDGE OF HISTORIC CONCRETE DROP SLAB AS IT OCCURS ON THE LEVEL BELOW.
- ALIGN CENTERLINE OF WALL WITH CENTERLINE OF WINDOW MULLION.
- CRITICAL KITCHEN CLEARANCES AT HISTORIC COLUMN. VERIFY BEFORE FRAMING DEMISING WALLS AND REPORT TO ARCHITECT IF THERE ARE ANY ISSUES.
- EXISTING HISTORIC DOOR ASSEMBLY TO REMAIN. PERMANENTLY SECURE BOTH DOORS IN CLOSED POSITION. PREPARE EXISTING DOOR ASSEMBLY FOR NEW PAINT FINISH.
- EXISTING HISTORIC OPENING AT REMOVED WINDOW. SEE DEMOLITION PLANS FOR ADDITIONAL INFORMATION.
- NEW CMU WALL TO CLOSE OFF FILLED IN UNDERGROUND TUNNEL. SEE STRUCTURAL.
- EXTEND WALL TO DEMISING WALL. TYP. SHIFT ANY PLUMBING FIXTURES OR CLOSETS AGAINST DEMISING WALL.
- EXISTING TRANSOM WINDOW ASSEMBLY TO REMAIN. PREPARE SURFACES FOR NEW PAINT. EXISTING DOOR FRAME TO REMAIN. PREPARE SURFACES FOR NEW PAINT.
- NEW CONCRETE AREA WELL WALLS. SEE STRUCTURAL.
- BUILD WALL TYPE PER UNIT DEMISING WALL WITH RESILIENT CHANNEL ON THIS SIDE.
- NEW BRICK MASONRY WALL. REBUILD WITH SALVAGED AND NEW BRICK TO MATCH EXISTING. REBUILD WALL TO MATCH FEATURES OF EXISTING. REMOVED BRICK MASONRY WALL INCLUDING, BUT NOT LIMITED TO WIDTH/DEPTH OF REMOVED WALL. HEIGHT OF REMOVED WALL AND ALL ABOVE EXISTING WINDOW OPENINGS.
- NEW BRICK MASONRY WALL. REBUILD WITH SALVAGED AND NEW BRICK TO MATCH EXISTING. REBUILD WALL TO MATCH FEATURES OF EXISTING. REMOVED BRICK MASONRY WALL INCLUDING, BUT NOT LIMITED TO WIDTH/DEPTH OF REMOVED WALL. HEIGHT OF REMOVED WALL AND ALL ABOVE EXISTING WINDOW OPENINGS.
- EXISTING HANDRAILS TO REMAIN. REFASTEN EXISTING HANDRAILS TO EXISTING WALLS IF LOOSE OR FAILING. PREPARE EXISTING HANDRAILS FOR NEW PT.
- NEW 4" PAINTED FLOOR STRIPING LEADING TO EXIT START.
- NEW 1/2" DIA. 2" TALL METAL BALL BEARING WITH TOP RAIL. PAINT PT.
- REPLACE IN KIND (SIZE, SPECIES AND INSTALLATION DIRECTION) ALL ROTTED AND DETERIORATED WOOD FLOORING. AFTER EXISTING STEEL PLATES ARE REMOVED, ENTIRE LOADING DOCK WOOD FLOORING TO BE Sanded (60 PSI) AND REFINISHED WITH NEW FINISH COATING.
- NEW SLOPED/FATHER POLISHED EPOXY FLOOR TOPPING TO TRANSITION AT FLOOR ELEVATION CHANGE. SLOPE 1:20.



NEW WORK PLAN - BASEMENT, BLDG 1A & LEVEL 01 BLDG 1B (SW & S)

Scale: 1/8" = 1'-0"



T 414.220.9640
751 N Jefferson St.
Suite 200
Milwaukee, WI 53202

CONSULTANTS

COMMUNITY WITHIN THE CORRIDOR - EAST BLOCK

3100 W. Center Street
Milwaukee, WI 53210

SHEET TITLE
Figure 2. Proposed Areas of Additional Excavations (1B-SW and 1C)

REVISIONS

1	10/09/20	Addendum #1
2	10/13/20	Addendum #2

SCALE	VARES
PROJECT NUMBER	200102
SET TYPE	CONSTRUCTION DOCUMENTS
DATE ISSUED	09/25/20
SHEET NUMBER	A211E

© COPYRIGHT 2020, CONTINUUM ARCHITECTS + PLANNERS, S.C.

GENERAL FLOOR PLAN NOTES TO CONTRACTOR

- THIS DRAWING IS FURTHER SUPPORTED BY INFORMATION CONTAINED IN THE SPECIFICATION MANUAL.
- DO NOT SCALE DRAWINGS. CONTRACTOR TO VERIFY ALL CONDITIONS AND DIMENSIONS AT THE JOB SITE PRIOR TO COMMENCING CONSTRUCTION.
- FINISH FLOOR ELEVATIONS ARE TO THE TOP OF THE FINISHED FLOOR MATERIAL, UNLESS OTHERWISE NOTED.
- CONTRACTORS SHALL JOINTLY PROVIDE AND INSTALL ALL STEENERS, BRACING, BACKING PLATES, WALL BLOCKING AND SUPPORTING BRACKETS REQUIRED FOR THE INSTALLATION OF CASEWORK, TOILET ACCESSORIES, PARTITIONS, MILL WORK, AND ALL WORK MOUNTED OR SUSPENDED BY ALL TRACES.
- SEE SHEET A401 FOR PARTITION TYPES AND DETAILS.
- DIMENSIONS AT EXTERIOR WALLS ARE TO STRUCTURAL WALL ONLY AND DO NOT INCLUDE FINISHES. DIMENSIONS AT EXTERIOR WALLS ARE TO STRUCTURAL WALL ONLY AND DO NOT INCLUDE FINISHES.

GENERAL INFORMATION NOTES TO CONTRACTOR

- THESE DRAWINGS ARE DIAGNOSTIC AND SHOW THE INTENT OF THE PROJECT, BUT DO NOT NECESSARILY INDICATE ALL MATERIALS OR METHODS OF CONSTRUCTION. ALL CONTRACTORS ARE RESPONSIBLE TO REVIEW THE DOCUMENTS THOROUGHLY, AND FOR PROVIDING ALL MATERIALS AND MEANS OF CONSTRUCTION NECESSARY FOR THE COMPLETION OF THE WORK IN ACCORDANCE WITH THE INTENT OF THE DRAWINGS.
- ALL WORK OF ALL TRADES SHALL BE COMPLETED IN ACCORDANCE WITH ALL LOCAL GOVERNING CODES AND ORDINANCES.
- EACH CONTRACTOR SHALL COORDINATE THEIR WORK WITH THE OWNER, THE OWNER'S OTHER CONTRACTORS, AND ALL OTHERS AT THE SITE.
- EACH CONTRACTOR IS TO OBTAIN AND PAY FOR PERMITS, LICENSES, FEES, ETC. AS REQUIRED FOR THE COMPLETION OF THEIR PORTION OF WORK.
- EACH CONTRACTOR SHALL VERIFY ALL CONDITIONS AND DIMENSIONS AT THE SITE TO SATISFY THEIR EXPECTATION OF THE WORK. ANY DISCREPANCIES SHALL BE REPORTED TO THE ARCHITECT. NEITHER THE OWNER NOR THE ARCHITECT ASSUMES RESPONSIBILITY FOR CONDITIONS OR DIMENSIONS SHOWN AS EXISTING.
- IF ANY CONTRACTOR OBSERVES THAT ANY OF THE CONTRACT DOCUMENTS ARE AT VARIANCE WITH APPLICABLE LAWS, STATUTES, BUILDING CODES, OR ORDINANCES, THEY SHALL PROMPTLY NOTIFY THE ARCHITECT.
- ALL HOLES FOR PLUMBING, ELECTRICAL, HVAC, FIRE PROTECTION CONDUIT, PIPING, OR DUCTWORK ARE TO BE REPAIRED BY THE ASSOCIATED TRADE.
- ALL TRADES SHALL TAKE CARE TO MAKE HOLES ONLY AS LARGE AS NECESSARY. ALL HOLES SHALL BE NEATLY CUT. DO NOT PUNCH OR POUND HOLES IN WALLS OR ROOF DECK.
- ANY HOLES OR PENETRATIONS THROUGH FIRE RATED CONSTRUCTION SHALL BE APPROPRIATELY FIRE STOPPED, DAMPENED, OR SEALED AS REQUIRED BY CODE.
- EACH CONTRACTOR SHALL INCLUDE NECESSARY DEMOLITION AND REMOVAL OF ALL MATERIAL AS REQUIRED TO PERFORM THEIR WORK.
- REMOVAL OF ALL HAZARDOUS CONTAINING MATERIALS IS THE SOLE RESPONSIBILITY OF THE OWNER. SHOULD ANY MATERIALS BE ENCOUNTERED DURING ANY OF THE CONSTRUCTION PHASES CONTAINING, OR SUSPECTED TO BE HAZARDOUS, CONTRACTOR SHALL STOP WORK IMMEDIATELY AND NOTIFY OWNER AND ARCHITECT.
- DO NOT SCALE DRAWINGS.
- EACH CONTRACTOR SHALL PATCH, LEVEL, AND PREPARE ALL WALLS AND FLOORS AS SCHEDULED AND REQUIRED TO RECEIVE NEW FINISHES.

NEW WORK PLAN LEGEND

- EXISTING, TO REMAIN
- MASONRY PARTITION, SEE PARTITION TYPES FOR DETAILS
- METAL STUD PARTITION, SEE PARTITION TYPES FOR DETAILS TYPE
- METAL STUD PARTITION, SEE PARTITION TYPES FOR DETAILS TYPE
- NEW WORK KEY NOTE (GENERAL TO ROOM)

A3 U.N.O.
 A6 THR.-A U.N.O.

Excavation to 4 Feet
 Excavation to 2 Feet
 Proposed Perforated 4-inch Diameter Pipe

NEW WORK PLAN KEY NOTES - 1B PLANS

SEE PROJECT GENERAL CONDITIONS. GENERAL INFORMATION ON SHEET A001 AND SELECTIVE DEMOLITION, CUTTING AND PATCHING SPECIFICATIONS THAT ARE USED IN ASSOCIATION WITH THESE NOTES.

NEW WORK PLAN KEY NOTES APPLY TO ALL NEW WORK DRAWINGS AND MAY NOT BE USED ON EVERY SHEET.

- SEE UNIT 1025 ENLARGED PLAN.
- SEE UNIT 1026 ENLARGED PLAN.
- SEE UNIT 1036 ENLARGED PLAN. UNIT MAY BE MIRRORRED.
- SEE UNIT 1037 ENLARGED PLAN.
- SEE UNIT 1038 ENLARGED PLAN.
- SEE UNIT 1040 ENLARGED PLAN.
- SEE UNIT 1041 ENLARGED PLAN.
- SEE UNIT 1042 ENLARGED PLAN.
- EXISTING HISTORIC SLIDING FIRE DOOR ASSEMBLY TO REMAIN. SECURE SLIDING DOOR IN A PARTIALLY CLOSED POSITION WITH METAL SPRINGETS. SEE PLAN FOR POSITION. SEE SALVAGED DOOR SCHEDULE FOR MORE INFO.
- SEE UNIT 1045 ENLARGED PLAN.
- SEE UNIT 1050 ENLARGED PLAN. UNIT IS MIRRORRED.
- SEE UNIT 2014 ENLARGED PLAN.
- SEE UNIT 2015 ENLARGED PLAN.
- SEE UNIT 2016 ENLARGED PLAN.
- SEE UNIT 2017 ENLARGED PLAN.
- SEE UNIT 2023 ENLARGED PLAN.
- SEE UNIT 2061 ENLARGED PLAN.
- SEE UNIT 2063 ENLARGED PLAN.
- SEE UNIT 2067 ENLARGED PLAN. UNIT MAY BE MIRRORRED.
- SEE UNIT 2068 ENLARGED PLAN. UNIT MAY BE MIRRORRED.
- SEE UNIT 2070 ENLARGED PLAN. UNIT TYPE IS A STUDIO ON LEVEL 03.
- SEE UNIT 2071 ENLARGED PLAN.
- SEE UNIT 2077 ENLARGED PLAN.
- SEE UNIT 2079 ENLARGED PLAN.
- SEE UNIT 2082 ENLARGED PLAN. FOR UNIT 3082. SEE UNIT 2082 ENLARGED PLAN.
- SEE UNIT 2092 ENLARGED PLAN.
- SEE UNIT 2093 ENLARGED PLAN.
- SEE UNIT 2094 ENLARGED PLAN. UNIT MAY BE MIRRORRED.

NEW WORK PLAN KEY NOTES - 1B PLANS

SEE PROJECT GENERAL CONDITIONS. GENERAL INFORMATION ON SHEET A001 AND SELECTIVE DEMOLITION, CUTTING AND PATCHING SPECIFICATIONS THAT ARE USED IN ASSOCIATION WITH THESE NOTES.

NEW WORK PLAN KEY NOTES APPLY TO ALL NEW WORK DRAWINGS AND MAY NOT BE USED ON EVERY SHEET.

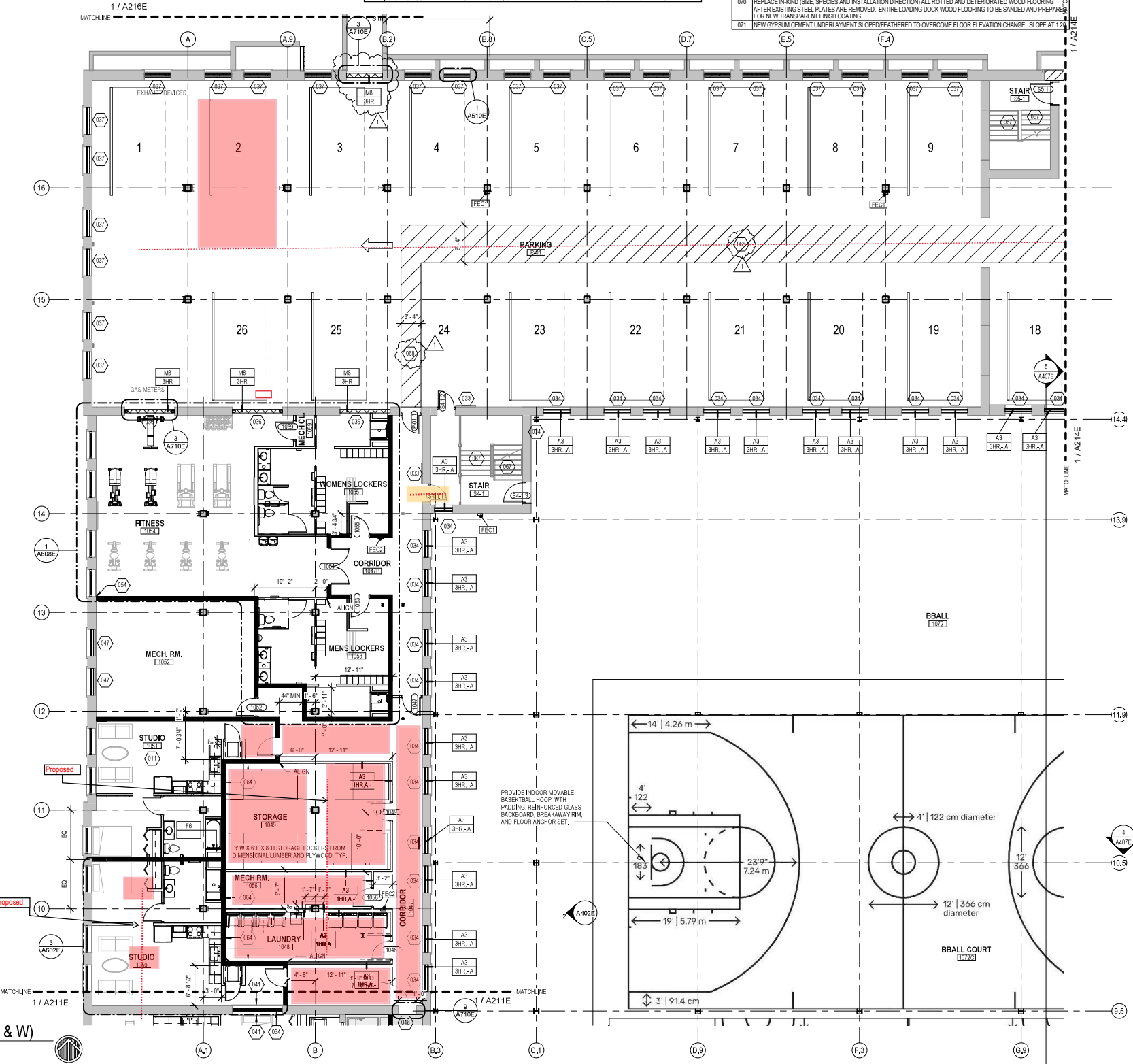
- SEE UNIT 2085 ENLARGED PLAN. UNIT MAY BE MIRRORRED.
- SEE UNIT 2111 ENLARGED PLAN. FOR UNIT 3110. SEE UNIT 2110.
- SEE UNIT 2117 ENLARGED PLAN.
- UNIT TO INCLUDE AUDIO AND VISUAL ALARM DEVICES FOR THE HEARING AND VISUALLY IMPAIRED. COORDINATE LOCATION WITH ELECTRICAL DRAWINGS.
- EXISTING HISTORIC SLIDING FIRE DOOR ASSEMBLY TO REMAIN IN PLACE. SECURE SLIDING DOOR IN A FULLY OPEN POSITION WITH METAL SPRINGETS. SEE SALVAGED DOOR SCHEDULE FOR MORE INFO.
- NEW GYPSUM BOARD INFILL WALL ASSEMBLY AT EXISTING OPENING. SEE 3A710E.
- EXISTING HISTORIC WINDOW ASSEMBLY TO REMAIN. PREPARE EXISTING WINDOW FOR NEW PAINT FINISH. REPLACE DAMAGED OR MISSING GLAZING TO MATCH EXISTING.
- NEW CMU INFILL WALL ASSEMBLY AT EXISTING OPENING. SEE 3A710E.
- NEW METAL PANEL INFILL WALL ASSEMBLY AT EXISTING OPENING. SEE 11A510E.
- NEW BRICK AND CMU INFILL AT EXISTING WALL OPENING.
- NEW BRICK MASONRY INFILL WALL ASSEMBLY AT EXISTING OPENING. SEE 3A710E.
- EXISTING CONCRETE FLOOR WITH NEW WATERPROOF TRAFFIC COATING.
- EXISTING HISTORIC SLIDING FIRE DOOR ASSEMBLY TO REMAIN. SECURE SLIDING DOOR IN A CLOSED POSITION WITH METAL SPRINGETS. SEE SALVAGED DOOR SCHEDULE FOR MORE INFO.
- NEW BRICK MASONRY AND GYPSUM BOARD INFILL WALL ASSEMBLY AT EXISTING OPENING. SEE 5A710E.
- NEW CMU AND GYPSUM BOARD INFILL WALL ASSEMBLY AT EXISTING OPENING. SEE 6A710E.
- NEW WOOD FLOOR INFILL. NEW WOOD FRAMING TO MATCH EXISTING. NEW WOOD SUBFLOORING TO MATCH DIMENSIONS OF EXISTING AND TO RUN IN THE SAME DIRECTIONS AS EXISTING. REINSTALL EXISTING SALVAGED FINISH FLOORING, RUN IN THE SAME DIRECTION AS EXISTING. SEE STRUCTURAL FOR DETAILING.
- NEW CONCRETE ON METAL DECK INFILL WITH SPRAY-APPLIED FIRE RESISTIVE MATERIAL AT NEW STEEL BEAMS AND ANGLES TO MAINTAIN FLOOR ASSEMBLY FIRE RATING. SEE OVERVIEW FLOOR PLANS FOR REQUIRED FLOOR ASSEMBLY FIRE RATINGS. SEE STRUCTURAL FOR DETAIL.
- NEW CONCRETE FLOOR INFILL. SEE STRUCTURAL.
- NEW PRECAST/CAST-IN-PLACE METAL MECHANICAL COVER IN EXISTING MASONRY OPENING.
- ENTIRE EXISTING HISTORIC WOOD DOOR ASSEMBLY INCLUDING ALL EXTERIOR AND INTERIOR WOOD TRIM COMPONENTS TO REMAIN. ALL WOOD COMPONENTS TO BE SANDED, REPLACED IN KIND AND PREPARED FOR NEW FINISHES THAT MATCH EXISTING FINISHES. ANY MISSING WOOD COMPONENTS (DOOR ASSEMBLY, INTERIOR/EXTERIOR TRIM COMPONENTS) TO BE REPLACED WITH SIMILAR WOOD SPECIES AND TO MATCH EXISTING PROFILES THAT REMAIN. ALL EXISTING DOOR HARDWARE TO BE REMOVED, SANDED AND PREPARED FOR NEW FINISH AND REINSTALLATION.

NEW WORK PLAN KEY NOTES - 1B PLANS(2)

SEE PROJECT GENERAL CONDITIONS. GENERAL INFORMATION ON SHEET A001 AND SELECTIVE DEMOLITION, CUTTING AND PATCHING SPECIFICATIONS THAT ARE USED IN ASSOCIATION WITH THESE NOTES.

NEW WORK PLAN KEY NOTES APPLY TO ALL NEW WORK DRAWINGS AND MAY NOT BE USED ON EVERY SHEET.

- EXISTING HISTORIC WINDOW ASSEMBLY TO REMAIN. CLEANSRAPE/PREPARE EXISTING WINDOW FRAMES TO RECEIVE NEW PAINT. EXISTING GLAZING TO BE REMOVED.
- REPLACE ALL BROKEN/CRAKLED AND MISSING GLASS LITES AT HISTORIC LIGHT MONITOR.
- NEW GYPSUM BOARD INFILL WALL ASSEMBLY AT EXISTING OPENING TO BE 3 HOUR FIRE RATED. SEE 10A170E SIM.
- EXISTING HISTORIC WINDOW ASSEMBLY TO REMAIN. PREPARE EXISTING WINDOW FOR NEW PAINT FINISH. EXISTING GLAZING TO REMAIN. NEW GLAZING NOT REQUIRED.
- EXISTING HISTORIC DOOR ASSEMBLY TO REMAIN. PREPARE EXISTING DOOR ASSEMBLY FOR NEW PAINT FINISH.
- ALIGN DEMISING WALL WITH EDGE OF HISTORIC MASONRY OPENING.
- EXISTING HISTORIC WINDOW ASSEMBLY TO REMAIN. PREPARE EXISTING WINDOW FOR NEW PAINT FINISH.
- ALIGN CENTERLINE OF WALL WITH CENTERLINE OF HISTORIC COLUMN.
- ALIGN LEVEL 02. ALIGN EDGE OF DEMISING WALL WITH EDGE OF HISTORIC CONCRETE DROP SLAB. AT LEVEL 03. ALIGN EDGE OF DEMISING WALL WITH EDGE OF HISTORIC CONCRETE DROP SLAB AS IT OCCURS ON THE LEVEL BELOW.
- NEW METAL PANEL INFILL WALL ASSEMBLY AT EXISTING WALL OPENING.
- CRITICAL KITCHEN CLEARANCES AT HISTORIC COLUMNS. VERIFY BEFORE FRAMING DEMISING WALLS AND REPORT TO ARCHITECT IF THERE ARE ANY ISSUES.
- EXISTING HISTORIC DOOR ASSEMBLY TO REMAIN. PERMANENTLY SECURE BOTH DOORS IN CLOSED POSITION. PREPARE EXISTING DOOR ASSEMBLY FOR NEW PAINT FINISH.
- EXISTING HISTORIC OPENING AT REMOVED WINDOW. SEE DEMOLITION PLANS FOR ADDITIONAL INFORMATION.
- NEW CMU WALL TO CLOSE OFF FILLED-IN UNDERGROUND TUNNEL. SEE STRUCTURAL.
- EXTEND WALL TO DEMISING WALL. TYP. SHIFT ANY PLUMBING FIXTURES OR CLOSETS AGAINST DEMISING WALL.
- EXISTING TRANSOM WINDOW ABOVE TO REMAIN. PREPARE SURFACES FOR NEW PAINT. EXISTING DOOR FRAME TO REMAIN. PREPARE SURFACES FOR NEW PAINT.
- NEW CONCRETE AREA WELL WALLS. SEE STRUCTURAL.
- BUILD WALL TYPE PU UNIT DEMISING WALL WITH RESILIENT CHANNEL ON THIS SIDE.
- NEW CONCRETE STAIR WITH POST WALLS. SEE STRUCTURAL.
- NEW BRICK MASONRY WALL REBUILT WITH SALVAGED AND NEW BRICK TO MATCH EXISTING. REBUILT WALL TO MATCH FEATURES OF EXISTING. REMOVED BRICK MASONRY WALL INCLUDING, BUT NOT LIMITED TO WIDTH/DEPTH OF REMOVED WALL. HEIGHT OF REMOVED WALL, AND ALL ARCHES ABOVE EXISTING WINDOW OPENINGS.
- EXISTING HANDRAILS TO REMAIN. REFASTEN EXISTING HANDRAILS TO EXISTING WALLS IF LOOSE OR FAILING. PREPARE EXISTING HANDRAILS FOR NEW PT.
- NEW 4" PAINTED FLOOR STRIPING LEADING TO EXIT STAIR.
- NEW 1/2" DIA. 3" TALL METAL SKYLIGHT WITH ONE TOP RAIL. PAINT PT.
- REPLACE IN-KIND (SIZE, SPECIES AND INSTALLATION DIRECTION) ALL ROTTED AND DETERIORATED WOOD FLOORING AFTER EXISTING STEEL PLATES ARE REMOVED. ENTIRE LOADING DOCK WOOD FLOORING TO BE SANDED AND PREPARED FOR NEW TRANSPARENT FINISH COATING.
- NEW GYPSUM CEMENT UNDERLAYMENT SLOPED/FEATHERED TO OVERCOME FLOOR ELEVATION CHANGE. SLOPE AT 12%.



NEW WORK PLAN - LEVEL 01, BLDG 1B (NW & W)
 Scale: 1/8" = 1'-0"

T 414.220.9640
 751 N Jefferson St.
 Suite 200
 Milwaukee, WI 53202

CONSULTANTS

COMMUNITY WITHIN THE CORRIDOR - EAST BLOCK
 3100 W. Center Street
 Milwaukee, WI 53210
 SHEET TITLE: **Figure 3. Proposed Areas of Additional Excavations (1B-W and 1B-NW)**

REVISIONS	
1	10/09/20 Addendum #1

SCALE	VARES
PROJECT NUMBER	200102
SET TYPE	CONSTRUCTION DOCUMENTS
DATE ISSUED	09/25/20
SHEET NUMBER	A213E

© COPYRIGHT 2020, CONTINUUM ARCHITECTS + PLANNERS S.C.

NEW WORK PLAN KEY NOTES - 1/8" PLANS

SEE PROJECT GENERAL CONDITIONS, GENERAL INFORMATION ON SHEET A01 AND SELECTIVE DEMOLITION, CUTTING AND PATCHING SPECIFICATIONS THAT ARE USED IN ASSOCIATION WITH THESE NOTES.

NEW WORK PLAN KEY NOTES APPLY TO ALL NEW WORK DRAWINGS AND MAY NOT BE USED ON EVERY SHEET.

001	SEE UNIT 1025 ENLARGED PLAN.
002	SEE UNIT 1026 ENLARGED PLAN.
003	SEE UNIT 1028 ENLARGED PLAN. UNIT MAY BE MIRRORRED.
004	SEE UNIT 1037 ENLARGED PLAN.
005	SEE UNIT 1039 ENLARGED PLAN.
006	SEE UNIT 1040 ENLARGED PLAN.
007	SEE UNIT 1041 ENLARGED PLAN.
008	SEE UNIT 1042 ENLARGED PLAN.
009	EXISTING HISTORIC SLIDING FIRE DOOR ASSEMBLY TO REMAIN. SECURE SLIDING DOOR IN A PARTIALLY CLOSED POSITION WITH METAL Z-BRACKETS. SEE PLAN FOR POSITION. SEE SALVAGED DOOR SCHEDULE FOR MORE INFO.
010	SEE UNIT 1045 ENLARGED PLAN.
011	SEE UNIT 1050 ENLARGED PLAN. UNIT IS MIRRORRED.
012	SEE UNIT 2014 ENLARGED PLAN.
013	SEE UNIT 2015 ENLARGED PLAN.
014	SEE UNIT 2016 ENLARGED PLAN.
015	SEE UNIT 2017 ENLARGED PLAN.
016	SEE UNIT 2020 ENLARGED PLAN.
017	SEE UNIT 2021 ENLARGED PLAN.
018	SEE UNIT 2023 ENLARGED PLAN.
019	SEE UNIT 2025 ENLARGED PLAN. UNIT MAY BE MIRRORRED.
020	SEE UNIT 2028 ENLARGED PLAN. UNIT MAY BE MIRRORRED.
021	SEE UNIT 2070 ENLARGED PLAN. UNIT TYPE IS A STUDIO ON LEVEL 03.
022	SEE UNIT 2071 ENLARGED PLAN.
023	SEE UNIT 2077 ENLARGED PLAN.
024	SEE UNIT 2079 ENLARGED PLAN.
025	SEE UNIT 2082 ENLARGED PLAN. FOR UNIT 3082. SEE UNIT 2082 ENLARGED PLAN.
026	SEE UNIT 2082 ENLARGED PLAN.
027	SEE UNIT 2084 ENLARGED PLAN.
028	SEE UNIT 2084 ENLARGED PLAN. UNIT MAY BE MIRRORRED.

NEW WORK PLAN KEY NOTES - 1/8" PLANS

SEE PROJECT GENERAL CONDITIONS, GENERAL INFORMATION ON SHEET A01 AND SELECTIVE DEMOLITION, CUTTING AND PATCHING SPECIFICATIONS THAT ARE USED IN ASSOCIATION WITH THESE NOTES.

NEW WORK PLAN KEY NOTES APPLY TO ALL NEW WORK DRAWINGS AND MAY NOT BE USED ON EVERY SHEET.

029	SEE UNIT 2085 ENLARGED PLAN. UNIT MAY BE MIRRORRED.
030	SEE UNIT 2111 ENLARGED PLAN. FOR UNIT 3110. SEE UNIT 2110.
031	SEE UNIT 2111 ENLARGED PLAN.
032	UNIT TO INCLUDE AUDIO AND VISUAL ALARM DEVICES FOR THE HEARING AND VISUALLY IMPAIRED. COORDINATE LOCATION WITH ELECTRICAL DRAWINGS.
033	EXISTING HISTORIC SLIDING FIRE DOOR ASSEMBLY TO REMAIN IN PLACE. SECURE SLIDING DOOR IN A FULLY OPEN POSITION WITH METAL Z-BRACKETS. SEE SALVAGED DOOR SCHEDULE FOR MORE INFO.
034	NEW GYPSUM BOARD INFILL WALL ASSEMBLY AT EXISTING OPENING. SEE 1A170E.
035	EXISTING HISTORIC WINDOW ASSEMBLY TO REMAIN. PREPARE EXISTING WINDOW FOR NEW PAINT FINISH. REPLACE DAMAGED OR MISSING GLAZING TO MATCH EXISTING.
036	NEW CMU INFILL WALL ASSEMBLY AT EXISTING OPENING. SEE 3A170E.
037	NEW METAL PANEL INFILL WALL ASSEMBLY AT EXISTING OPENING. SEE 1A510E.
038	NEW BRICK AND CMU INFILL AT EXISTING WALL OPENING.
039	NEW BRICK MASONRY INFILL WALL ASSEMBLY AT EXISTING OPENING. SEE 3A170E.
040	EXISTING CONCRETE FLOOR WITH NEW WATERPROOFING/TRAFFIC COATING.
041	EXISTING HISTORIC SLIDING FIRE DOOR ASSEMBLY TO REMAIN. SECURE SLIDING DOOR IN A CLOSED POSITION WITH METAL Z-BRACKETS. SEE SALVAGED DOOR SCHEDULE FOR MORE INFO.
042	NEW BRICK MASONRY AND GYPSUM BOARD INFILL WALL ASSEMBLY AT EXISTING OPENING. SEE 3A170E.
043	NEW CMU AND GYPSUM BOARD INFILL WALL ASSEMBLY AT EXISTING OPENING. SEE 3A170E.
044	NEW WOOD FLOOR INFILL. NEW WOOD FRAMING TO MATCH EXISTING. NEW WOOD SUBFLOORING TO MATCH DIMENSIONS OF EXISTING AND TO RUN IN THE SAME DIRECTION AS EXISTING. REINSTALL EXISTING SALVAGED FINISH FLOORING. RUN IN THE SAME DIRECTION AS EXISTING. SEE STRUCTURAL FOR DETAILING.
045	NEW CONCRETE ON METAL DECK INFILL WITH GRAY APPLIED FIRE RESISTIVE MATERIAL AT NEW STEEL BEAMS AND ANGLES TO MATCH FLOOR ASSEMBLY FIRE RATING. SEE OVERVIEW/FLOOR PLANS FOR REQUIRED FLOOR ASSEMBLY FIRE RATINGS. SEE STRUCTURAL FOR DETAIL.
046	NEW CONCRETE FLOOR INFILL. SEE STRUCTURAL.
047	NEW FINISHED METAL MECHANICAL LOCKER IN EXISTING MASONRY OPENING.
048	ENTIRE EXISTING HISTORIC WOOD DOOR ASSEMBLY INCLUDING ALL EXTERIOR AND INTERIOR WOOD TRIM COMPONENTS TO REMAIN. ALL WOOD COMPONENTS TO BE SANDED, REPLACED IN KIND AND PREPARED FOR NEW FINISHES THAT MATCH EXISTING FINISHES. ANY MISSING WOOD COMPONENTS (DOOR ASSEMBLY, INTERIOR/EXTERIOR TRIM COMPONENTS) TO BE REPLACED WITH SIMILAR WOOD SPECIES AND TO MATCH EXISTING PROFILES THAT REMAIN. ALL EXISTING DOOR HARDWARE TO BE REMOVED, SANDED AND PREPARED FOR NEW FINISH AND REINSTALLATION.

NEW WORK PLAN KEY NOTES - 1/8" PLANS(2)

SEE PROJECT GENERAL CONDITIONS, GENERAL INFORMATION ON SHEET A01 AND SELECTIVE DEMOLITION, CUTTING AND PATCHING SPECIFICATIONS THAT ARE USED IN ASSOCIATION WITH THESE NOTES.

NEW WORK PLAN KEY NOTES APPLY TO ALL NEW WORK DRAWINGS AND MAY NOT BE USED ON EVERY SHEET.

049	EXISTING HISTORIC WINDOW ASSEMBLY TO REMAIN. CLEAN/SCRAPE/PREPARE EXISTING WINDOW FRAMES TO RECEIVE NEW PAINT. EXISTING GLAZING TO BE REMOVED.
050	REPLACE ALL BROKEN/CRAKED AND MISSING GLASS LITES AT HISTORIC LIGHT MONITOR.
051	NEW GYPSUM BOARD INFILL WALL ASSEMBLY AT EXISTING OPENING TO BE 3 HOUR FIRE RATED. SEE 10A710E SIM.
052	EXISTING HISTORIC WINDOW ASSEMBLY TO REMAIN. PREPARE EXISTING WINDOW FOR NEW PAINT FINISH. EXISTING GLAZING TO REMAIN. NEW GLAZING NOT REQUIRED.
053	EXISTING HISTORIC DOOR ASSEMBLY TO REMAIN. PREPARE EXISTING DOOR ASSEMBLY FOR NEW PAINT FINISH.
054	ALIGN DEMISING WALL WITH EDGE OF HISTORIC MASONRY OPENING.
055	ALIGN CENTER OF WALL WITH CENTERLINE OF HISTORIC COLUMN.
056	AT LEVEL 02: ALIGN EDGE OF DEMISING WALL WITH EDGE OF HISTORIC CONCRETE DROP SLAB. AT LEVEL 03: ALIGN EDGE OF DEMISING WALL WITH EDGE OF HISTORIC CONCRETE DROP SLAB AS IT OCCURS ON THE LEVEL BELOW.
057	ALIGN CENTERLINE OF WALL WITH CENTERLINE OF WINDOW MULLION.
058	CRITICAL KITCHEN CLEARANCES AT HISTORIC COLUMN. VERIFY BEFORE FRAMING DEMISING WALLS AND REPORT TO ARCHITECT IF THERE ARE ANY ISSUES.
059	EXISTING HISTORIC DOOR ASSEMBLY TO REMAIN. PERMANENTLY SECURE BOTH DOORS IN CLOSED POSITION. PREPARE EXISTING DOOR ASSEMBLY FOR NEW PAINT FINISH.
060	EXISTING HISTORIC OPENING AT REMOVED WINDOW. SEE DEMOLITION PLANS FOR ADDITIONAL INFORMATION.
061	NEW CMU WALL TO CLOSE OFF FILLED IN UNDERGROUND TUNNEL. SEE STRUCTURAL.
062	EXTEND WALL TO DEMISING WALL. TYP. SHIFT ANY PLUMBING FIXTURES OR CLOSETS AGAINST DEMISING WALL.
063	EXISTING TRANSOM WINDOW ABOVE TO REMAIN. PREPARE SURFACES FOR NEW PAINT. EXISTING DOOR FRAME TO REMAIN. PREPARE SURFACES FOR NEW PAINT.
064	NEW CONCRETE AREA WELL WALLS. SEE STRUCTURAL.
065	BUILD WALL TYPE PER UNIT DEMISING WALL WITH RESISTIVE CHANNEL ON THIS SIDE.
066	NEW CONCRETE STOP WITH FROST WALLS. SEE STRUCTURAL.
067	NEW BRICK MASONRY WALL REBUILT WITH SALVAGED AND NEW BRICK TO MATCH EXISTING. REBUILT WALL TO MATCH FEATURES OF EXISTING. REMOVED BRICK MASONRY WALL INCLUDING, BUT NOT LIMITED TO WIDTH/DEPTH OF REMOVED WALL HEIGHT OR REMOVED WALL AND ALL ARCHES ABOVE EXISTING WINDOW OPENINGS.
068	EXISTING HANDRAILS TO REMAIN. REFASTEN EXISTING HANDRAILS TO EXISTING WALLS IF LOOSE OR FAILING. PREPARE EXISTING HANDRAILS FOR NEW PT.
069	NEW 4" PAINTED FLOOR STRIPING LEADING TO EXIT STAR.
070	REPLACE IN KIND (SIZE, SPECIES AND INSTALLATION DIRECTION) ALL ROTTED AND DETERIORATED WOOD FLOORING AFTER EXISTING STEEL PLATES ARE REMOVED. ENTIRE LOADING DOCK WOOD FLOORING TO BE SANDED AND PREPARED FOR NEW TRANSPARENT FINISH COATING.
071	NEW SLOPED/FATHERED POLISHED EPOXY FLOOR TOPPING TO TRANSITION AT FLOOR ELEVATION CHANGE. SLOPE AT 1:20.

GENERAL FLOOR PLAN NOTES TO CONTRACTOR

- THIS DRAWING IS FURTHER SUPPORTED BY INFORMATION CONTAINED IN THE SPECIFICATION MANUAL.
- DO NOT SCALE DRAWINGS. CONTRACTOR TO VERIFY ALL CONDITIONS AND DIMENSIONS AT THE JOB SITE PRIOR TO COMMENCING CONSTRUCTION.
- FINISH FLOOR ELEVATIONS ARE TO THE TOP OF THE FINISHED FLOOR MATERIAL UNLESS OTHERWISE NOTED.
- CONTRACTORS SHALL JOINTLY PROVIDE AND INSTALL ALL STIFFENERS, BRACING, BACKING PLATES, WALL BLOCKING AND SUPPORTING BRACKETS REQUIRED FOR THE INSTALLATION OF CASEWORK, TOILET ACCESSORIES, PARTITIONS, MILLWORK, AND ALL WORK MOUNTED OR SUSPENDED BY ALL TRADES.
- SEE SHEET A002 FOR PARTITION TYPES AND DETAILS.
- DIMENSIONS AT EXTERIOR WALLS ARE TO STRUCTURAL WALL ONLY AND DO NOT INCLUDE FINISHES. DIMENSIONS AT EXTERIOR WALLS ARE TO STRUCTURAL WALL ONLY AND DO NOT INCLUDE FINISHES.

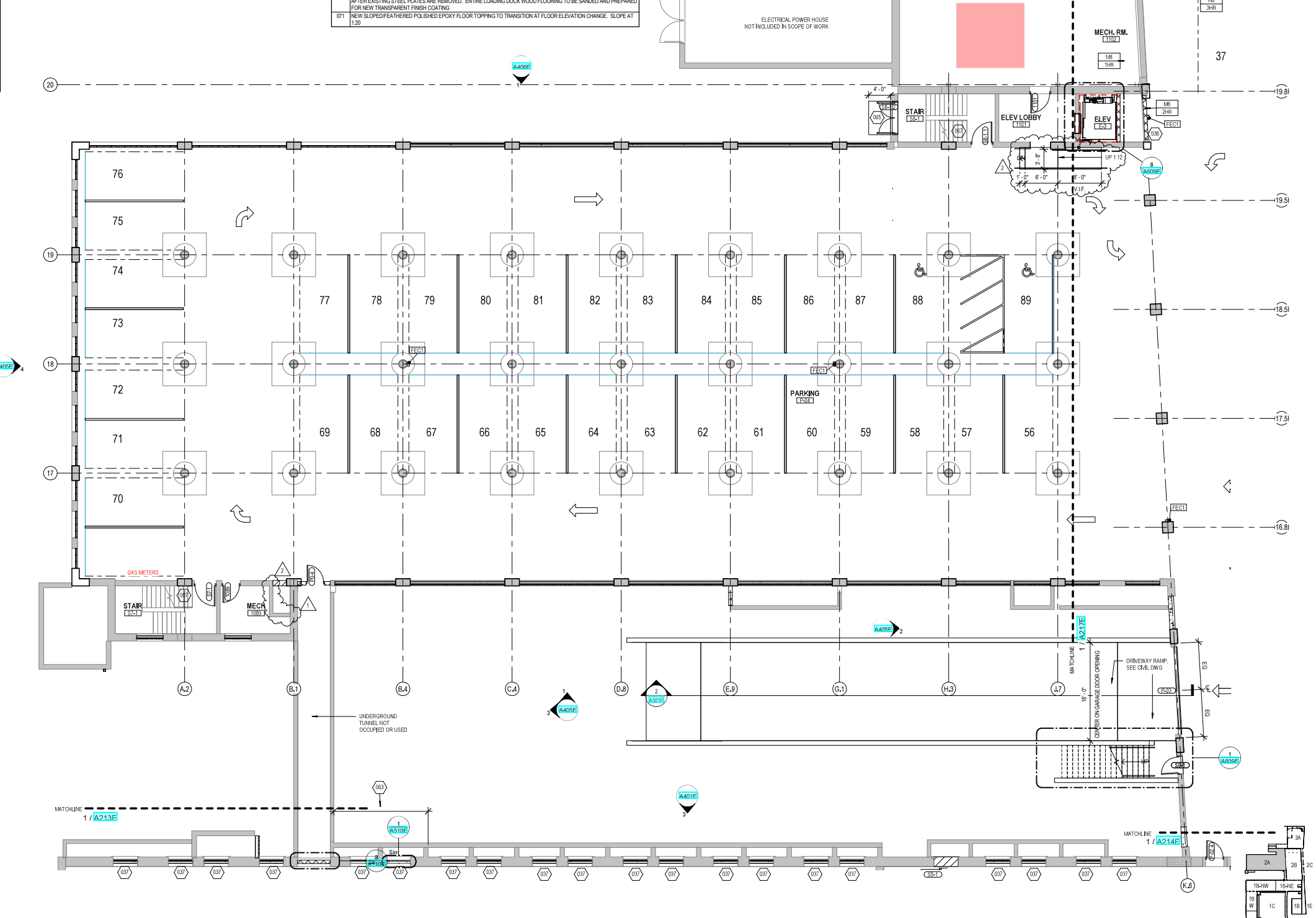
GENERAL INFORMATION NOTES TO CONTRACTOR

- THESE DRAWINGS ARE DIAGRAMMATIC AND SHOW THE INTENT OF THE PROJECT, BUT DO NOT NECESSARILY INDICATE ALL MATERIALS OR METHODS OF CONSTRUCTION. ALL CONTRACTORS ARE RESPONSIBLE TO REVIEW THE DOCUMENTS THOROUGHLY, AND FOR PROVIDING ALL MATERIALS AND MEANS OF CONSTRUCTION NECESSARY FOR THE COMPLETION OF THE WORK IN ACCORDANCE WITH THE INTENT OF THE DRAWINGS.
- ALL WORK OF ALL TRADES SHALL BE COMPLETED IN ACCORDANCE WITH ALL LOCAL GOVERNING CODES AND ORDINANCES.
- EACH CONTRACTOR SHALL COORDINATE THEIR WORK WITH THE OWNER, THE OWNER'S OTHER CONTRACTORS, AND ALL OTHERS AT THE SITE.
- EACH CONTRACTOR IS TO OBTAIN AND PAY FOR PERMITS, LICENSES, FEES, ETC. AS REQUIRED FOR THE COMPLETION OF THEIR PORTION OF WORK.
- EACH CONTRACTOR SHALL VERIFY ALL CONDITIONS AND DIMENSIONS AT THE SITE TO SATISFY THEIR EXECUTION OF THE WORK. ANY DISCREPANCIES SHALL BE REPORTED TO THE ARCHITECT. NEITHER THE OWNER NOR THE ARCHITECT ASSUMES RESPONSIBILITY FOR CONDITIONS OR DIMENSIONS SHOWN AS EXISTING.
- IF ANY CONTRACTOR OBSERVES THAT ANY OF THE CONTRACT DOCUMENTS ARE AT VARIANCE WITH APPLICABLE LAWS, STATUTES, BUILDING CODES, OR ORDINANCES, THEY SHALL PROMPTLY NOTIFY THE ARCHITECT.
- ALL HOLES FOR PLUMBING, ELECTRICAL, HVAC, FIRE PROTECTION CONDUIT, PIPING, OR DUCTWORK ARE TO BE REPAIRED BY THE ASSOCIATED TRADE.
- ALL TRADES SHALL TAKE CARE TO MAKE HOLES ONLY AS LARGE AS NECESSARY. ALL HOLES SHALL BE NEATLY CUT. DO NOT PUNCH OR POUND HOLES IN WALLS OR ROOF DECK.
- ANY HOLES OR PENETRATIONS THROUGH FIRE RATED CONSTRUCTION SHALL BE APPROPRIATELY FIRE STOPPED, DAMPENED, OR SEALED AS REQUIRED BY CODE.
- EACH CONTRACTOR SHALL INCLUDE NECESSARY DEMOLITION AND REMOVAL OF ALL MATERIAL AS REQUIRED TO PERFORM THEIR WORK.
- REMOVAL OF ALL HAZARDOUS CONTAINING MATERIALS IS THE SOLE RESPONSIBILITY OF THE OWNER. SHOULD ANY MATERIALS BE ENCOUNTERED DURING ANY OF THE CONSTRUCTION PHASES CONTAINING, OR SUSPECTED TO BE HAZARDOUS, CONTRACTOR SHALL STOP WORK IMMEDIATELY AND NOTIFY OWNER AND ARCHITECT.
- DO NOT SCALE DRAWINGS.
- EACH CONTRACTOR SHALL PATCH, LEVEL, AND PREPARE ALL WALLS AND FLOORS AS SCHEDULED AND REQUIRED TO RECEIVE NEW FINISHES.

NEW WORK PLAN LEGEND

	EXISTING, TO REMAIN
	MASONRY PARTITION. SEE PARTITION TYPES FOR DETAILS
	METAL STUD PARTITION. SEE PARTITION TYPES FOR DETAILS TYPE
	METAL STUD PARTITION. SEE PARTITION TYPES FOR DETAILS TYPE U.N.O.
	METAL STUD PARTITION. SEE PARTITION TYPES FOR DETAILS TYPE U.N.O.
	NEW WORK KEY NOTE (GENERAL TO ROOM)

Excavation to 4 Feet



1 NEW WORK PLAN - LEVEL 01, BLDG 2A
Scale: 1/8" = 1'-0"

414.220.9640
751 N Jefferson St.
Suite 200
Milwaukee, WI 53202

CONSULTANTS

COMMUNITY WITHIN THE CORRIDOR - EAST BLOCK

3100 W. Center Street
Milwaukee, WI 53210

SHEET TITLE
Figure 4. Proposed Area of Additional Excavation (Northern Mechanical Room)

REVISIONS

1	10/09/20	Addendum #1
2	10/13/20	Addendum #2

SCALE	VARES
PROJECT NUMBER	200102
SET TYPE	CONSTRUCTION DOCUMENTS
DATE ISSUED	09/25/20
SHEET NUMBER	A216E

© COPYRIGHT 2020, CONTINUUM ARCHITECTS + PLANNERS S.C.

CONSULTANT

CONSULTANT

CONSULTANT

PROJECT TITLE: COMMUNITY WITHIN THE CORRIDOR
2748 N 32ND STREET
MILWAUKEE, WI 53210
PROJECT NUMBER: 40441

CLIENT:
COMMUNITY WITHIN THE CORRIDOR LIMITED
PARTNERSHIP

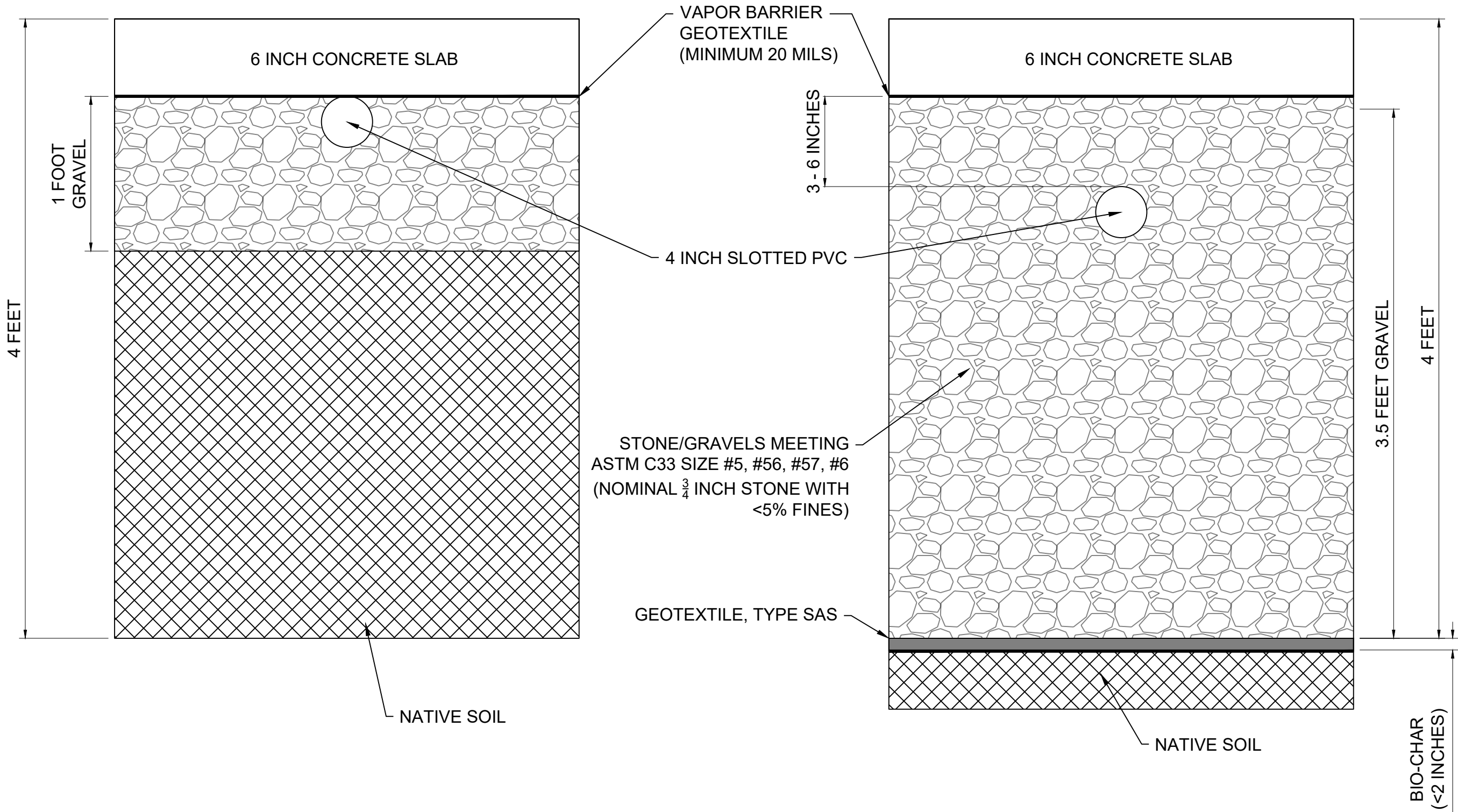
REVISIONS	DATE	DESCRIPTION
DRAWN BY	DATE	
	4/7/2023	
CHECKED BY	DATE	
	4/7/2023	
SHEET TITLE		

CROSS SECTIONS OF
EXCAVATION AND RESTORATION

FIGURE 5

EXCAVATION CROSS SECTION

RESTORATION CROSS SECTION



East Building Level 1

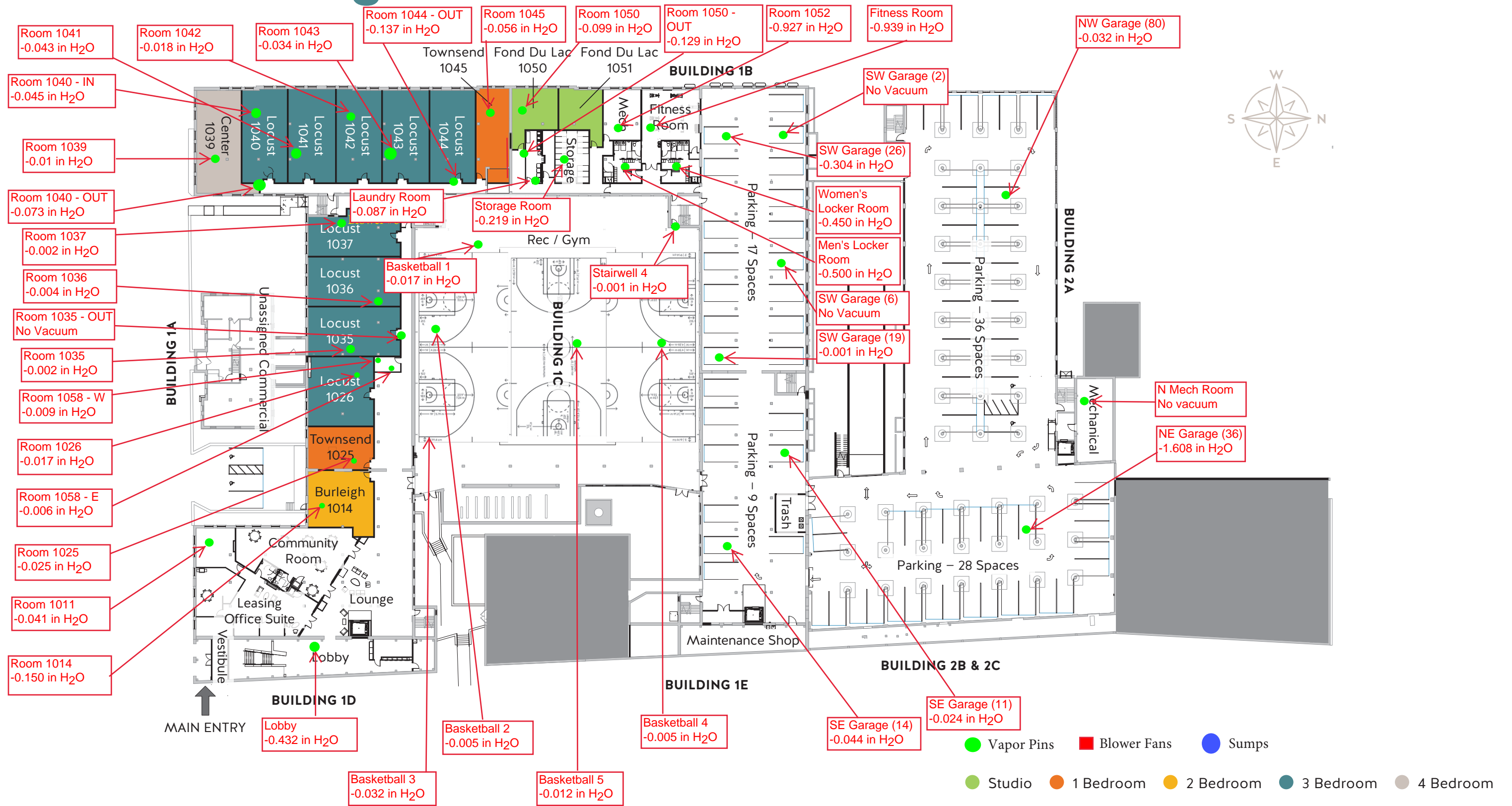
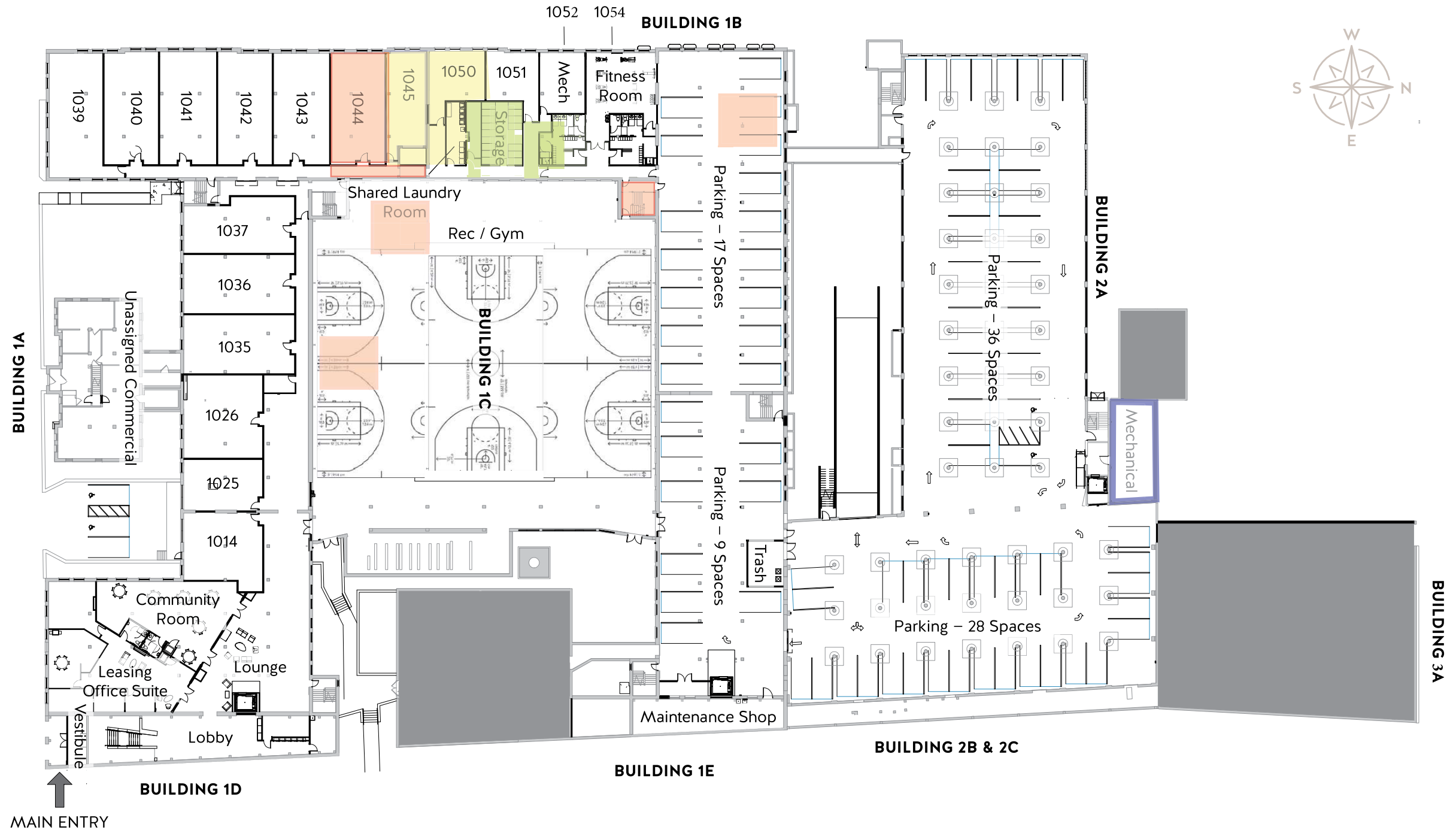


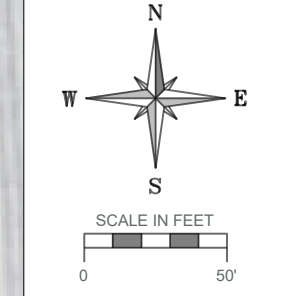
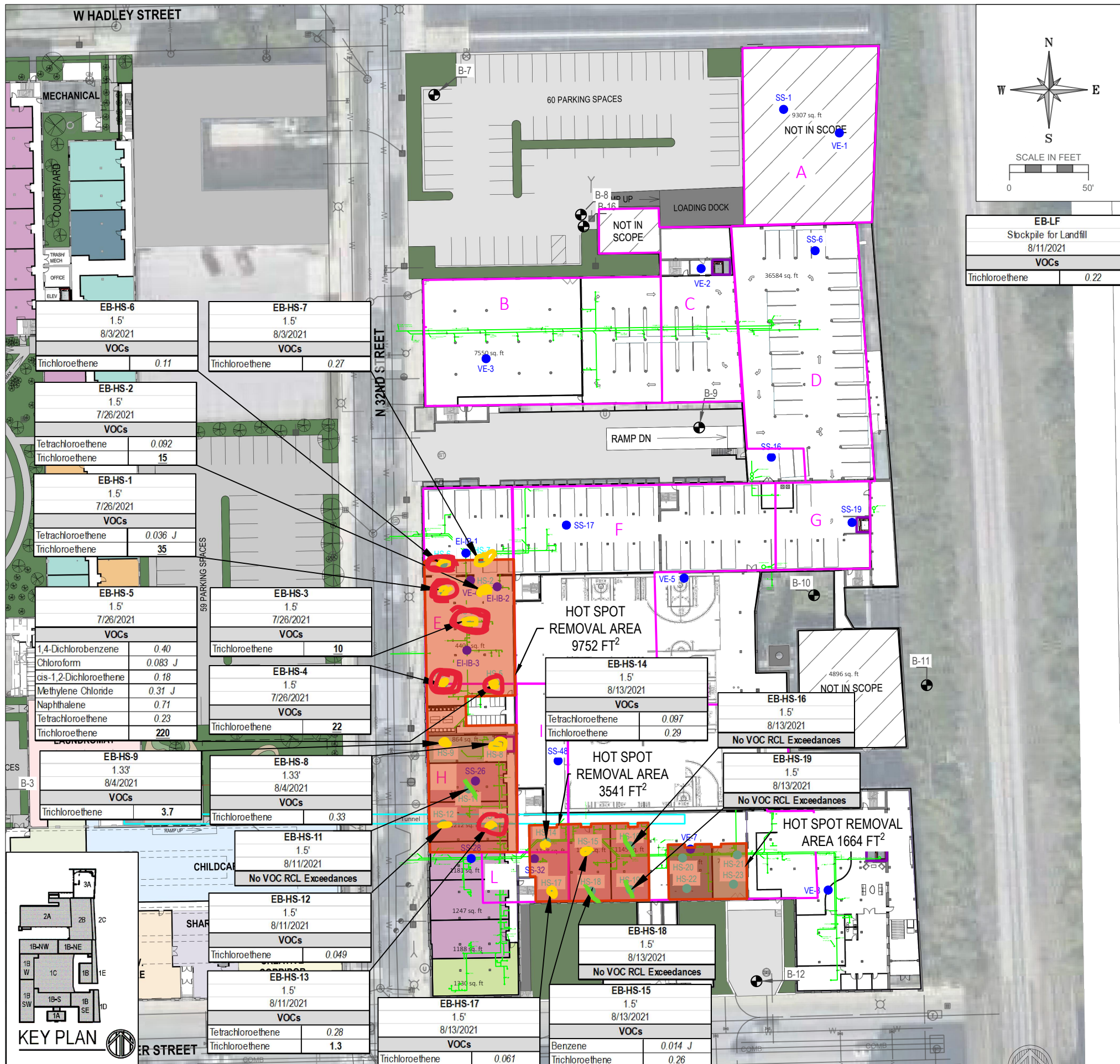
Figure 6. Locations of Vapor Pins and Average Differential Pressure Measurements for the week of 7/15/23

East Building Level 1



- VRSL Hotspot Areas based on sub-slab TCE Levels higher than VRSL (70 ug/m³)
- Areas with Indoor air TCE levels higher than VAL (2.1 ug/m³)
- Areas with Residual Soil Contamination
- VRSL Hotspot Areas based on sub-slab TCE Levels higher than VRSL (70 ug/m³) and Residual Soil Contamination

Figure 7. Locations of VAL and VRSL Exceedances and Residual Soil Contamination



EB-LF	
Stockpile for Landfill	
8/11/2021	
VOCs	
Trichloroethene	0.22

LEGEND

- Soil Sampling Locations
- Previous Soil Boring Locations
- Known Elevator Shaft
- 1 - Bedroom Apartment
- 2 - Bedroom Apartment
- 3 - Bedroom Apartment
- 4 - Bedroom Apartment
- Studio Apartment
- Underground Plumbing
- Underground Tunnel
- TCE Zones for Mass Calculations
- TCE Hot Spot Removal Area

NOTE:
 ● COMBINATION OF EXISTING AND PROPOSED PLUMBING

Analyte	NR 720 RCLs for GW Protection (1)	NR 720 RCLs - Non-Industrial Use for Direct Contact Protection (1)	NR 720 RCLs - Industrial Use for Direct Contact Protection (1)
Volatile Organic Compounds (VOCs)			
1,4-Dichlorobenzene	0.144	3.74	16.4
Benzene	0.0051	1.6	7.07
Chloroform	0.0033	0.454	1.98
cis-1,2-Dichloroethene	0.0412	156	2,340
Methylene Chloride	0.0026	61.8	1,150
Naphthalene	0.658182	5.52	24.10
Tetrachloroethene	0.0045	33	145
Trichloroethene	0.0036	1.3	8.41

- NOTES:
- (1) FROM WDNR RCLs WORKSHEET DATED DECEMBER 2018
 - REPORTED UNITS IN MG/KG
 - ONLY EXCEEDANCES SHOWN
 - ITALICS = VALUE EXCEEDS GROUNDWATER PROTECTION OR DIRECT CONTACT RCLs
 - BOLD = VALUE EXCEEDS NON-INDUSTRIAL DIRECT CONTACT RCLs
 - BOLD UNDERLINED** = VALUE EXCEEDS INDUSTRIAL DIRECT CONTACT RCLs
 - "J" = ANALYTE DETECTED BETWEEN 'LIMIT OF DETECTION' AND 'LIMIT OF QUANTITATION'
 - SAMPLING LOCATIONS ARE APPROXIMATE

CONSULTANT
 CONSULTANT
 CONSULTANT

PROJECT TITLE: COMMUNITY WITHIN THE CORRIDOR
 2748 N 32ND STREET
 MILWAUKEE, WI 53210
 PROJECT NUMBER: 40441

CLIENT:
 COMMUNITY WITHIN THE CORRIDOR LIMITED
 PARTNERSHIP

REVISIONS	DATE	DESCRIPTION

DRAWN BY: AMZ DATE: 09/09/2021
 CHECKED BY: RTR DATE: 09/09/2021

FIGURE 8

ATTACHMENT A
Obar Fan and Fliteway Blower Information

THE OBAR GBR89 COMPACT RADIAL BLOWER



Based on 25 years of experience and 2 years of research and development, the patent pending GBR series of compact radial blowers provide the perfect combination of performance and design.

PERFORMANCE

- GBR89 HA 14" WC at 100CFM max flow 500 CFM.
- Built in speed control to customize performance.
- Condensate bypass built in.
- 12 month warranty 40,000 hr sealed bearings.



GBR89 WITH ROOF MOUNT

DESIGN

- Our modular design means the blower and manifold assembly can be removed and replaced as a unit. This makes repairs cost effective and easy and allows contractors to upgrade systems simply by swapping assemblies.
- The GBR series is based on a bypass blower designed to handle combustible materials.
- The housing is not required to be air tight so you can add gauges and alarms without compromising the system.
- Built in condensate bypass.
- Built in speed control.
- Quick disconnect electrical harness.
- All UL listed components including UL listed enclosure for outside use.
- Wall fastening lugs included.
- GBR series roof and wall mounts available to quickly configure the blowers for your installation while providing a custom built look.
- Compact design 18"x 16"x 10" weighing only 26 lbs.
- 4" schedule 40 inlet and 6" schedule 40 exhaust.

Enclosure Specifications

Rating:

Ingress Protection (EN 60529): 66/67

Electrical insulation: Totally insulated

Halogen free (DIN/VDE 0472, Part 815): yes

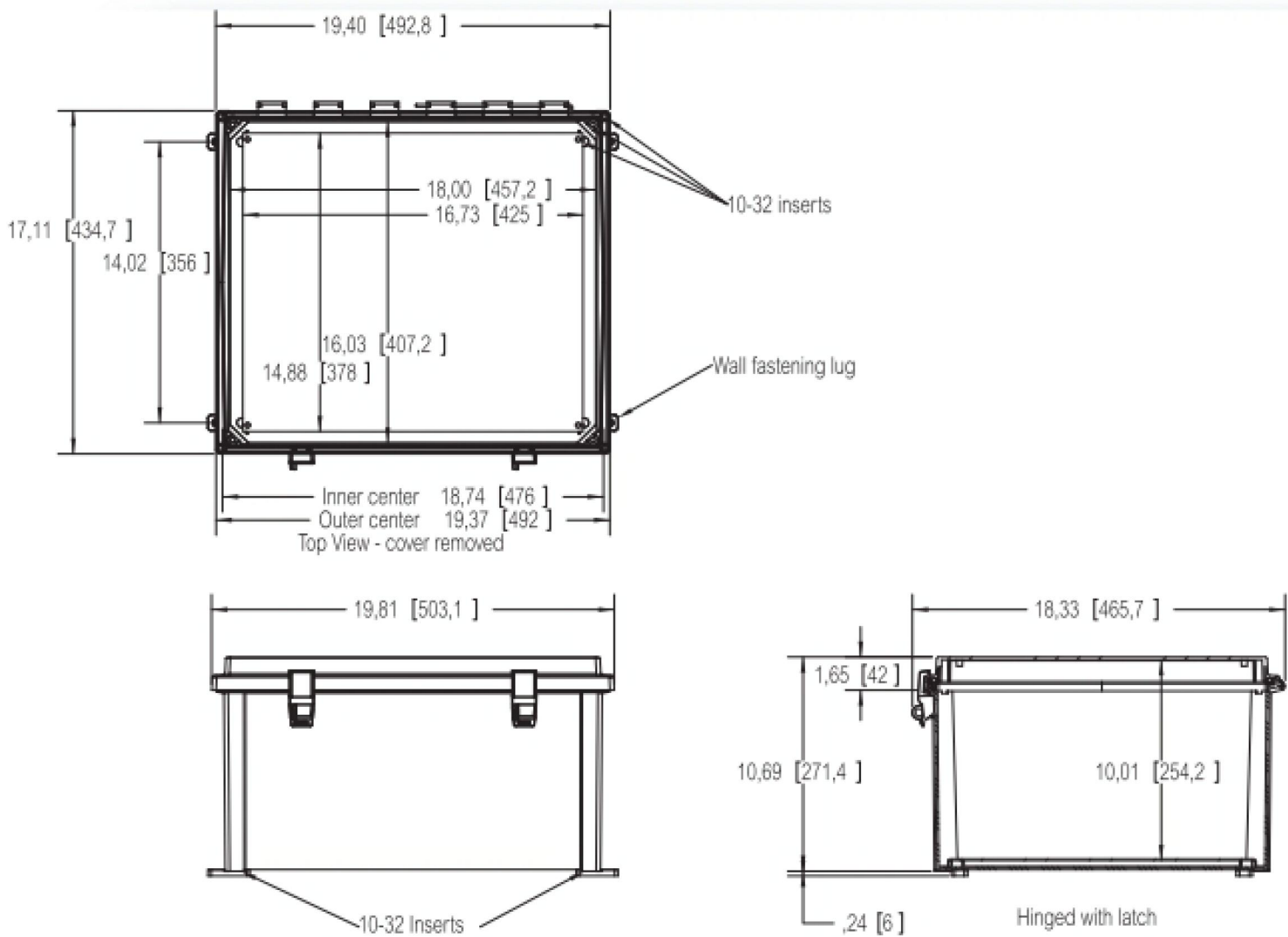
UV resistance: UL 508

Flammability Rating (UL 746 C 5): complies with UL 508

Glow Wire Test (IEC 695-2-1) °C: 960

NEMA Class: UL Type 4, 4X, 6, 6P, 12 and 13

Certificates: Underwriters Laboratories

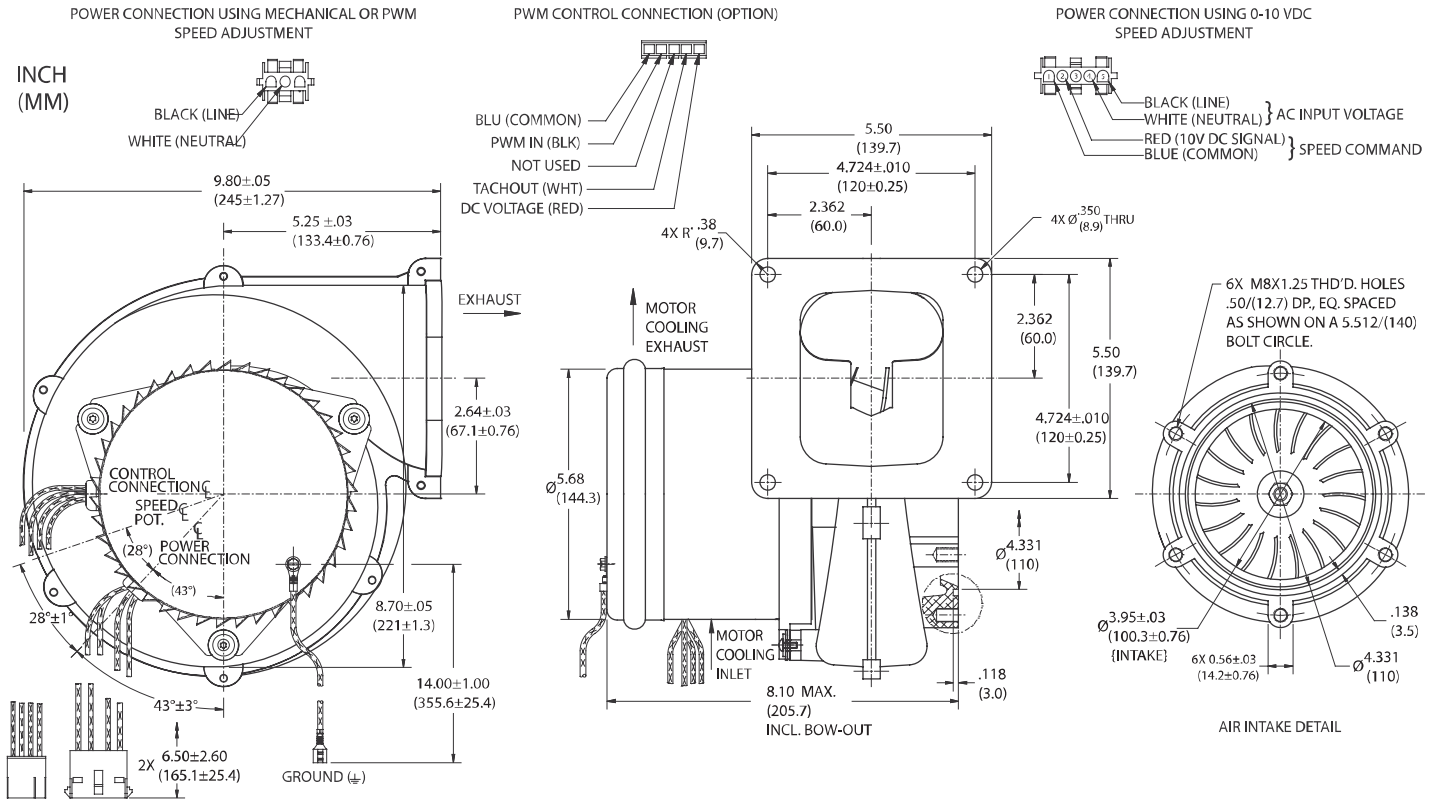


High Voltage Brushless DC Blowers

Nautilair (TM) 8.9" (226mm) Variable Speed Blower

240 Volt AC Input, Single Phase, High Output

Nautilair



		Part/ Model Number		
Specification	Units	150240	150241	150242
Speed Control	-	Mechanical	0-10 VDC	PWM

Notes:

- **Input Voltage Range:** 216 - 264 Volts AC RMS, 50/60 Hz, single phase.
 - **Input Current:** 10 amps AC RMS
 - **Operating Temperature (Ambient Air and Working Air):** 0°C to 50°C
 - **Storage Temperature:** -40°C to 85°C
 - **Dielectric Testing:** 1800 Volts AC RMS 60 Hz applied for one second between input pins and ground, 3mA leakage maximum.
 - **Speed Control Methods:** PWM (Pulse Width Modulation). Speed control input signal of 15 - 45 VDC @ 500 Hz - 10 kHz, and tachometer output (2 Pulses / Revolution).
Optional tachometer output (3 Pulses / Revolution).
 - **0 to 10 VDC** with a speed control input current of 5 mA to 20 mA at 10 VDC Input with multi-turn potentiometer set to minimum resistance (fully clockwise).
Mechanical: A potentiometer is available for speed control of the blower. The potentiometer can be preset for a specific speed. Access for speed adjustment located in motor housing. 4-20mA speed control available.
 - **Approximate Weight:** 9.3 Lbs. / 4.2 Kg.
 - **Option Card available for Customization**
 - **Regulatory Agency Certification:** Underwriters Laboratories Inc. UL507 Recognized under File E94403 and CSA C22.2#133 under File LR43448
 - **Design Features:** Designed to provide variable airflow for low NOx & CO emission in high efficiency gas fired combustion systems. Built with non-sparking materials. Blower housing assembly constructed of die cast aluminum. Impeller constructed from hardened aluminum. Rubber isolation mounts built into blower construction to dampen vibration within the motor. Two piece blower housing assembly sealed with O-ring gasket for combustion applications. Customer is responsible to check for any leakage once the blower is installed into the final application.
 - **Miscellaneous:** Blower inlet, discharge, and all motor cooling inlet and discharge vents must not be obstructed. Motor ventilation air to be free of oils and other foreign particles, (i.e. breathing quality air). Blower is to be mounted so ventilation air cannot be re-circulated.
- POWER CONNECTION (3 CAVITY):** Blower connector, AMP Universal MATE-N-LOK, part no. 1-480701-0.
- POWER CONNECTION (5 CAVITY):** Blower connector, AMP Universal MATE-N-LOK, part no. 350810-1.
- SPEED CONNECTION (5 CAVITY):** Blower connector, Molex Mini-Fit Jr., part no. 39-01-4057.
- Mating harnesses available upon request.

This document is for informational purposes only and should not be considered as a binding description of the products or their performance in all applications. The performance data on this page depicts typical performance under controlled laboratory conditions. AMETEK is not responsible for blowers driven beyond factory specified speed, temperature, pressure, flow or without proper alignment. Actual performance will vary depending on the operating environment and application. AMETEK products are not designed for and should not be used in medical life support applications. AMETEK reserves the right to revise its products without notification. The above characteristics represent standard products. For product designed to meet specific applications, contact AMETEK Technical & Industrial Products Sales department.

AMETEK TECHNICAL & INDUSTRIAL PRODUCTS

627 Lake Street, Kent OH 44240

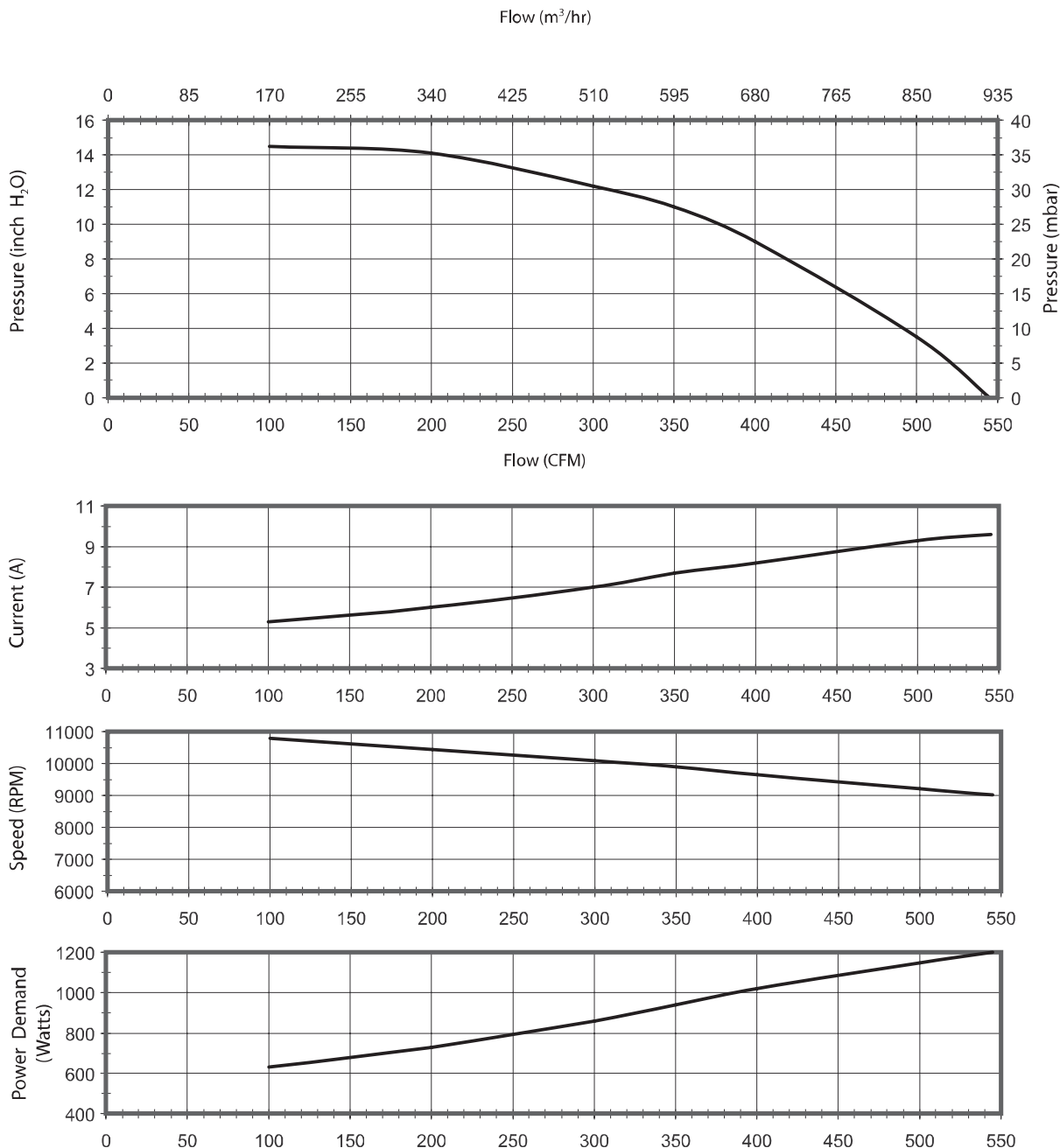
USA: +1 215-256-6601 - Europe: +44 (0) 845 366 9664 - Asia: +86 21 5763 1258

www.ametektip.com

B 47

AMETEK
PRECISION MOTION CONTROL

Typical Performance



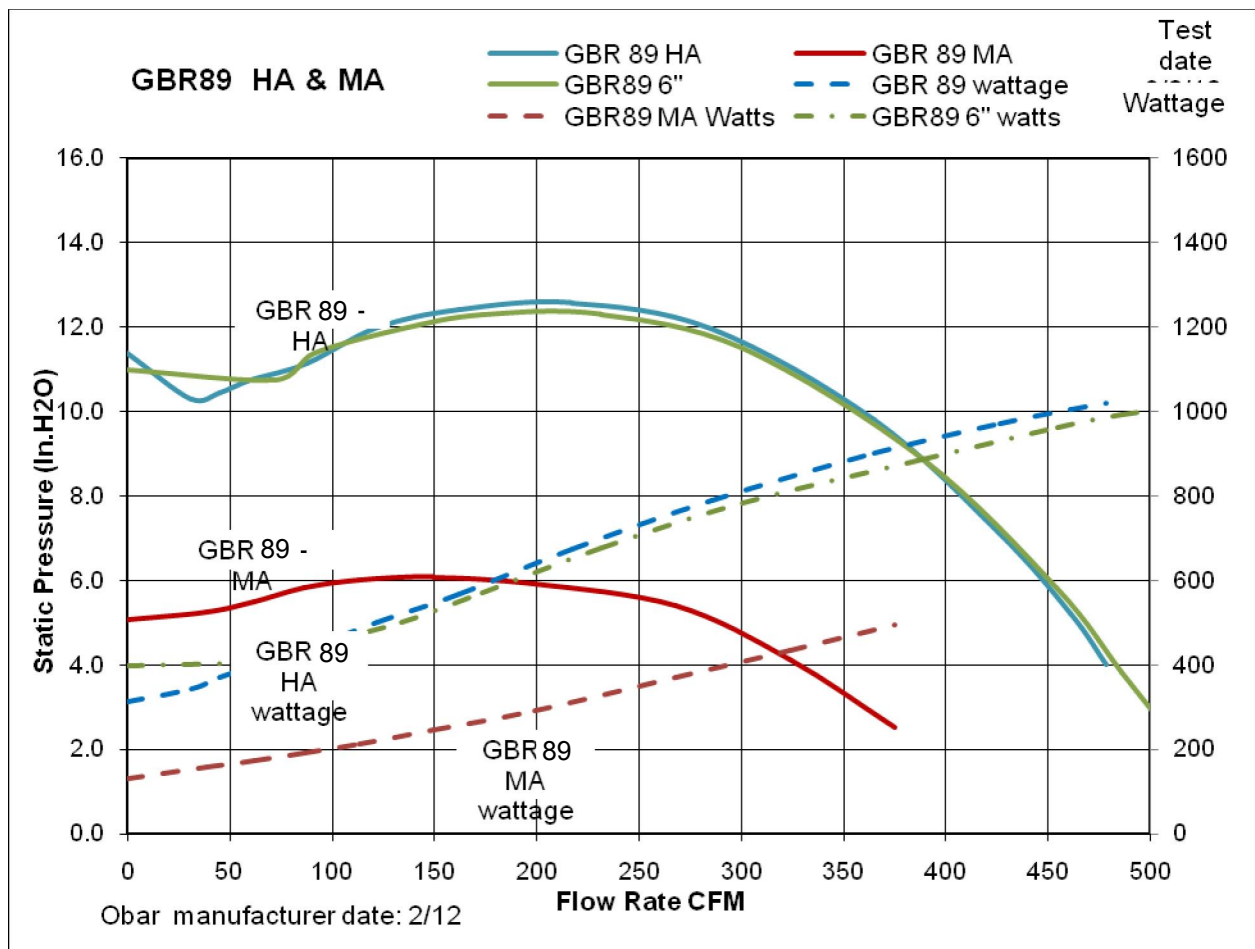
Data presented represents blower performance at STANDARD AIR DENSITY, .075 lb/ft³ (29.92" Hg, Sea Level, 68° F)
 Vacuum performance available upon request.

This document is for informational purposes only and should not be considered as a binding description of the products or their performance in all applications. The performance data on this page depicts typical performance under controlled laboratory conditions. AMETEK is not responsible for blowers driven beyond factory specified speed, temperature, pressure, flow or without proper alignment. Actual performance will vary depending on the operating environment and application. AMETEK products are not designed for and should not be used in medical life support applications. AMETEK reserves the right to revise its products without notification. The above characteristics represent standard products. For product designed to meet specific applications, contact AMETEK Technical & Industrial Products Sales department.

GBR89 HA tested at full voltage with 8 feet of 4" inlet (Blue Lines) and 6" Inlet (Green lines)

Maximum airflow with no exhaust piping and 8' of 6" piping is 529 CFM

GBR89 MA tested with speed control set to half the wattage consumption (Red Line)

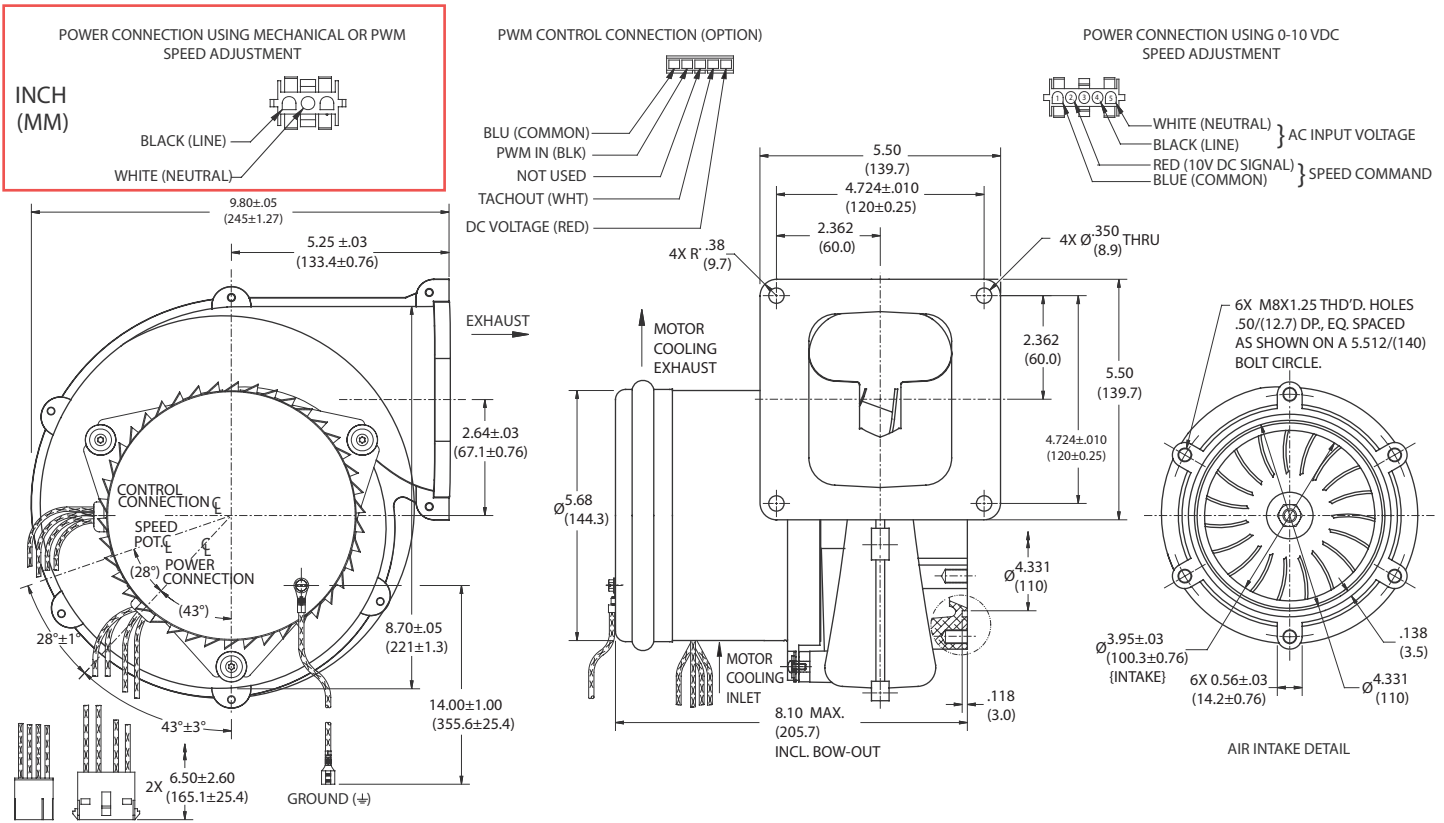


High Voltage Brushless DC Blowers

Nautilair (TM) 8.9" (226mm) Variable Speed Blower

120 Volt AC Input, Single Phase, High Output

Nautilair



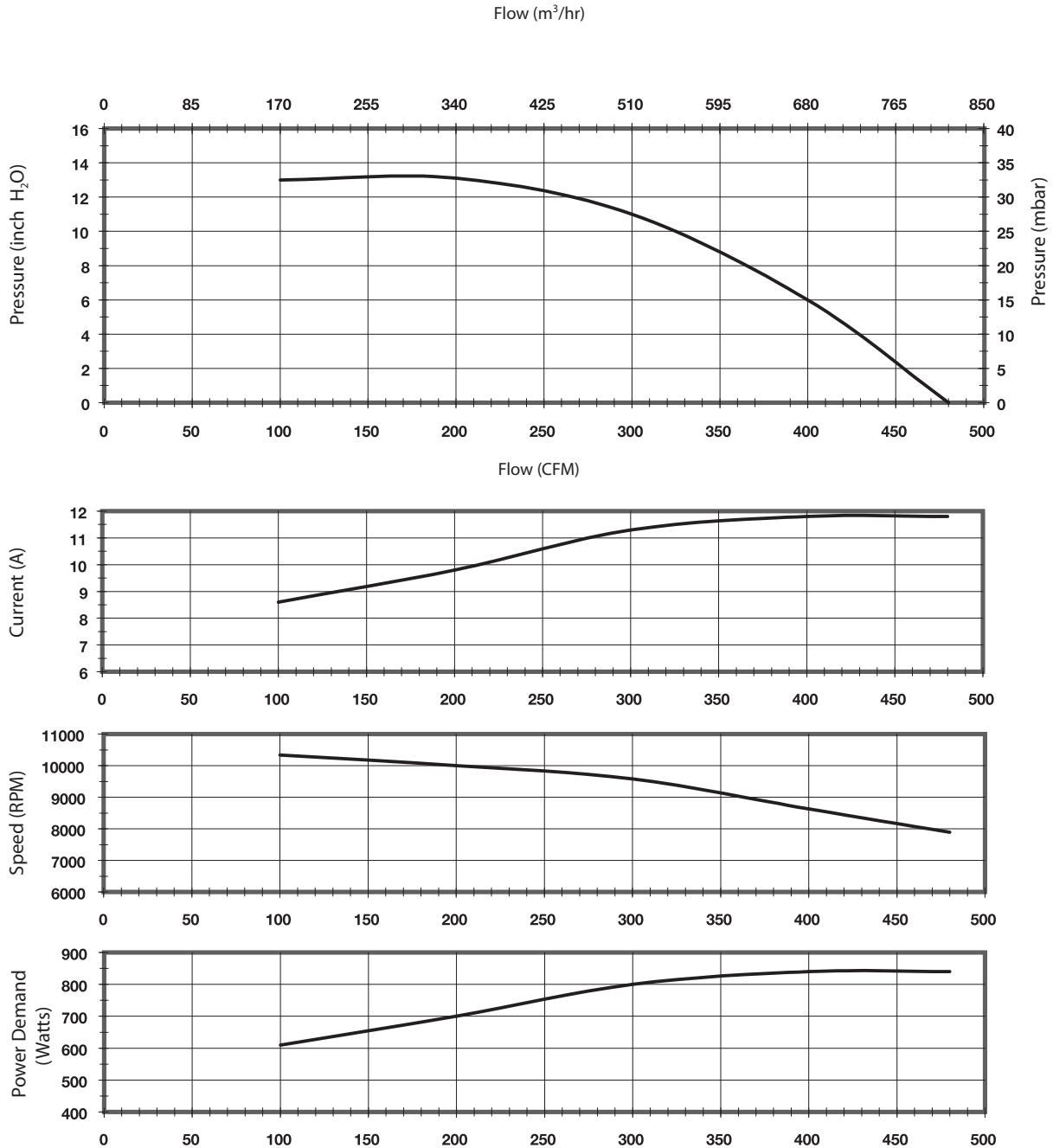
Specification	Units	150230	150231	150232
Speed Control	-	Mechanical	0-10 VDC	PWM

Notes:

- Input Voltage Range:** 108 - 132 Volts AC RMS, 50/60 Hz, single phase.
 - Input Current:** 12 amps AC RMS
 - Operating Temperature (Ambient Air and Working Air):** 0°C to 50°C
 - Storage Temperature:** -40°C to 85°C
 - Dielectric Testing:** 1500 Volts AC RMS 60 Hz applied for one second between input pins and ground, 3mA leakage maximum.
 - Speed Control Methods:** PWM (Pulse Width Modulation). Speed control input signal of 15 - 45 VDC @ 500 Hz - 10 kHz, and tachometer output (2 Pulses / Revolution). Optional tachometer output (3 Pulses / Revolution).
0 to 10 VDC speed control.
Mechanical: A potentiometer is available for speed control of the blower. The potentiometer can be preset for a specific speed. Access for speed adjustment located in motor housing.
4-20mA speed control available.
 - Approximate Weight:** 9.3 Lbs. / 4.2 Kg
 - Option Card available for Customization**
 - Regulatory Agency Certification:** Underwriters Laboratories Inc. UL507 Recognized under File E94403 and CSA C22.2#133 under File LR43448
 - Design Features:** Designed to provide variable airflow for low NOx & CO emission in high efficiency gas fired combustion systems. Built with non-sparking materials. Blower housing assembly constructed of die cast aluminum. Impeller constructed from hardened aluminum. Rubber isolation mounts built into blower construction to dampen vibration within the motor. Two piece blower housing assembly sealed with O-ring gasket for combustion applications. Customer is responsible to check for any leakage once the blower is installed into the final application.
 - Miscellaneous:** Blower inlet, discharge, and all motor cooling inlet and discharge vents must not be obstructed. Motor ventilation air to be free of oils and other foreign particles. (i.e. breathing quality air). Blower is to be mounted so ventilation air cannot be re-circulated.
 - POWER CONNECTION (3 CAVITY):** Blower connector, AMP Universal MATE-N-LOK, part no. 1-480701-0.
 - POWER CONNECTION (5 CAVITY):** Blower connector, AMP Universal MATE-N-LOK, part no. 350810-1.
 - SPEED CONNECTION (5 CAVITY):** Blower connector, Molex Mini-Fit Jr., part no. 39-01-4057.
- Mating harnesses available upon request.

This document is for informational purposes only and should not be considered as a binding description of the products or their performance in all applications. The performance data on this page depicts typical performance under controlled laboratory conditions. AMETEK is not responsible for blowers driven beyond factory specified speed, temperature, pressure, flow or without proper alignment. Actual performance will vary depending on the operating environment and application. AMETEK products are not designed for and should not be used in medical life support applications. AMETEK reserves the right to revise its products without notification. The above characteristics represent standard products. For product designed to meet specific applications, contact AMETEK Technical & Industrial Products Sales department.

Typical Performance

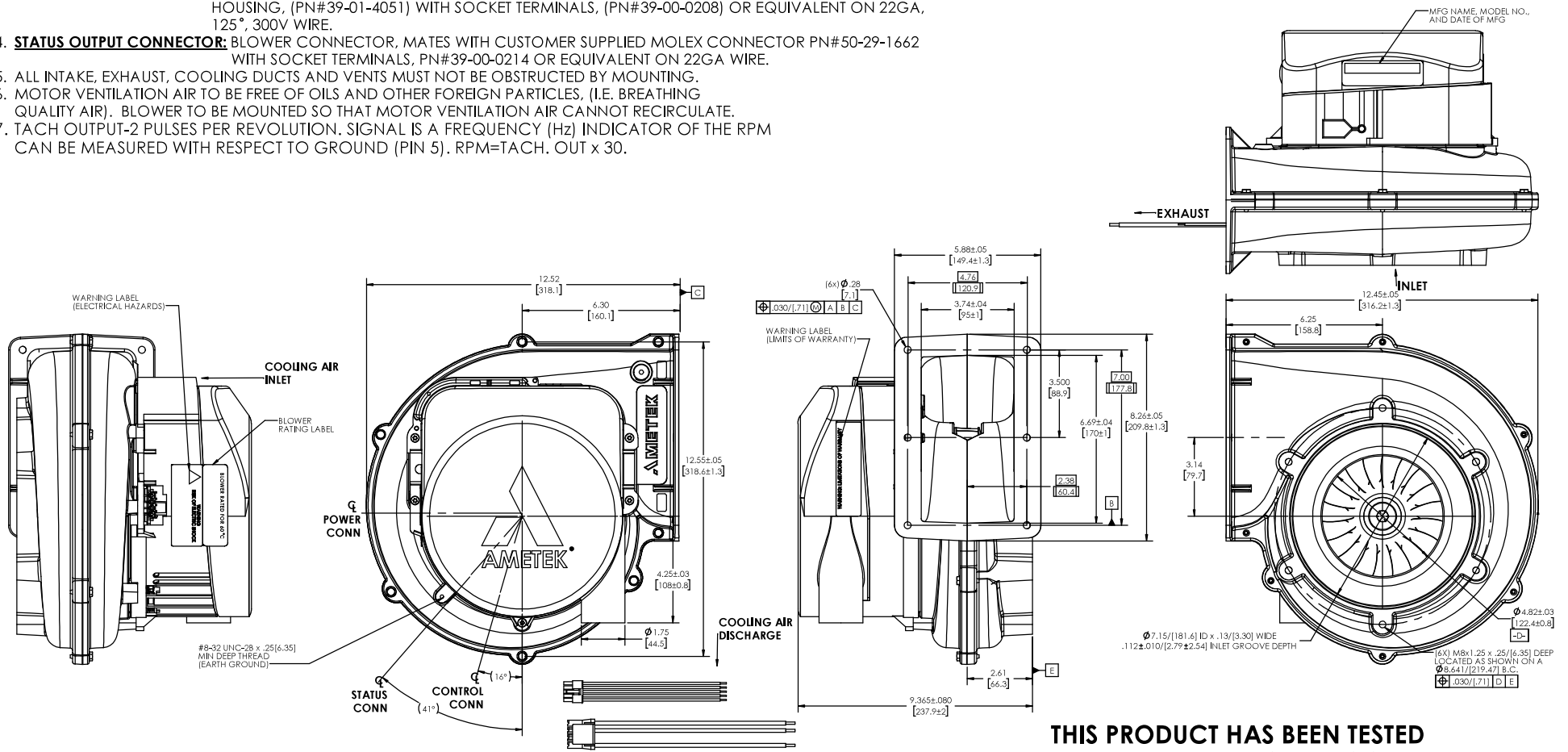


Data presented represents blower performance at STANDARD AIR DENSITY, .075 lb/ft³ (29.92" Hg, Sea Level, 68° F)
 Vacuum performance available upon request.

This document is for informational purposes only and should not be considered as a binding description of the products or their performance in all applications. The performance data on this page depicts typical performance under controlled laboratory conditions. AMETEK is not responsible for blowers driven beyond factory specified speed, temperature, pressure, flow or without proper alignment. Actual performance will vary depending on the operating environment and application. AMETEK products are not designed for and should not be used in medical life support applications. AMETEK reserves the right to revise its products without notification. The above characteristics represent standard products. For product designed to meet specific applications, contact AMETEK Technical & Industrial Products Sales department.

NOTES:

1. ROHS AND REACH COMPLIANCE. REFERENCE AMETEK ENVIRONMENTAL SPECIFICATION ES0010 FOR DETAILS.
2. **POWER CONNECTION:** BLOWER CONNECTOR, MATES WITH CUSTOMER SUPPLIED MOLEX CONNECTOR PN#172672-2004 WITH SOCKET TERMINALS, PN#171825 OR EQUIVALENT ON 12GA WIRE.
3. **CONTROL CONNECTION:** BLOWER CONNECTOR, MATES WITH CUSTOMER SUPPLIED MOLEX SERIES 5557 CONNECTOR HOUSING, (PN#39-01-4051) WITH SOCKET TERMINALS, (PN#39-00-0208) OR EQUIVALENT ON 22GA, 125°, 300V WIRE.
4. **STATUS OUTPUT CONNECTOR:** BLOWER CONNECTOR, MATES WITH CUSTOMER SUPPLIED MOLEX CONNECTOR PN#50-29-1662 WITH SOCKET TERMINALS, PN#39-00-0214 OR EQUIVALENT ON 22GA WIRE.
5. ALL INTAKE, EXHAUST, COOLING DUCTS AND VENTS MUST NOT BE OBSTRUCTED BY MOUNTING.
6. MOTOR VENTILATION AIR TO BE FREE OF OILS AND OTHER FOREIGN PARTICLES, (I.E. BREATHING QUALITY AIR). BLOWER TO BE MOUNTED SO THAT MOTOR VENTILATION AIR CANNOT RECIRCULATE.
7. TACH OUTPUT-2 PULSES PER REVOLUTION. SIGNAL IS A FREQUENCY (Hz) INDICATOR OF THE RPM CAN BE MEASURED WITH RESPECT TO GROUND (PIN 5). RPM=TACH. OUT x 30.



POWER CONNECTION

PIN #	CONTROL	DESCRIPTION	COLOR
1	-	GROUND	GREEN
2	-	-	-
3	INPUT	A/C INPUT	WHITE
4	INPUT	A/C INPUT	BLACK

CONTROL CONNECTION

PIN #	CONTROL	DESCRIPTION	COLOR
1	INPUT	15V-40V (OPTIONAL)	RED
2	OUTPUT	TACH-OUTPUT	WHITE
3	OUTPUT	5V OUTPUT	YELLOW
4	INPUT	ANALOG INPUT	GREEN
5	INPUT	COMMON	BLACK

STATUS OUTPUT CONNECTION

PIN #	CONTROL	DESCRIPTION	COLOR
2	OUTPUT	ISOLATED +15VDC	BLUE
3	OUTPUT	OPEN COLLECTOR TRANSISTOR	BLACK

THIS PRODUCT HAS BEEN TESTED AND VALIDATED TO BE ACCEPTABLE IN OUR APPLICATION.

APPROVED BY: _____

PRINT NAME: _____

TITLE: _____

DATE: _____

COMPANY: _____

NAUTILAIR

Model: 150644-02P

MECHANICAL

DIAMETER: 12.3" (312mm)
DISCHARGE TYPE: Tangential
DISCHARGE: Large Rectangular Flange
APPROXIMATE WEIGHT: 28lbs/12.7kg

PERFORMANCE

FLOW CLASSIFICATION: High Energy
STAGES: 1 Stage

TEMPERATURE

OPERATING TEMP: 0°C to 60°C
STORAGE TEMP: -40°C to 85°C

ELECTRICAL

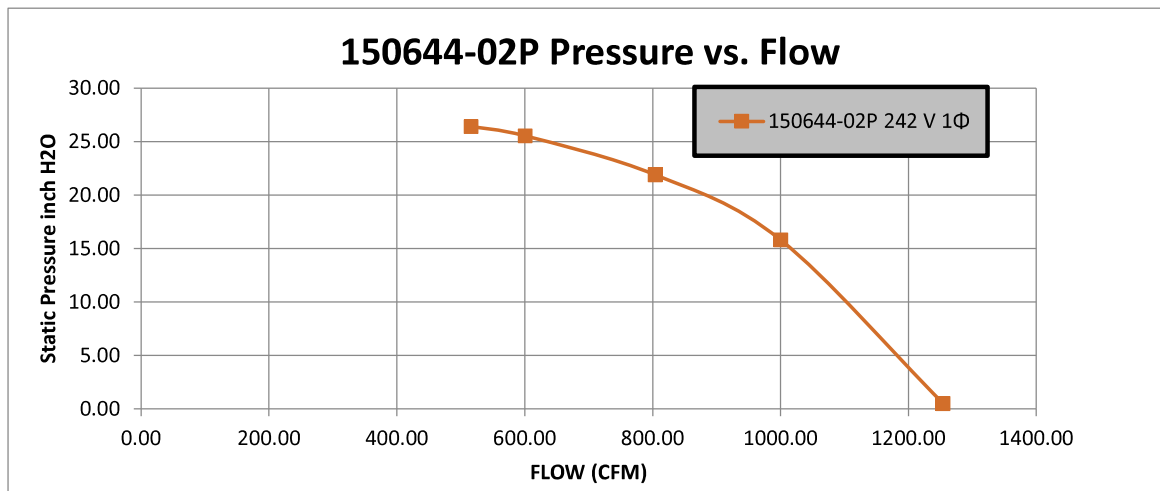
OPERATING INPUT VOLTAGE: RANGE: 180-264 VAC
OPERATING INPUT VOLTAGE: 240V 1Ø

OPTIONAL FEATURES

SPEED CONTROL: Remote Pot., Open Loop, 4-Pin Power, 5-Pin Control, 3-Pin Status

REGULATORY CERTIFICATIONS

COMPLIANCE: RoHS and Reach
UL FILE NUMBER: E94403
AGENCY FULL LOAD AMPS: 30A
REFERENCE: E-54147

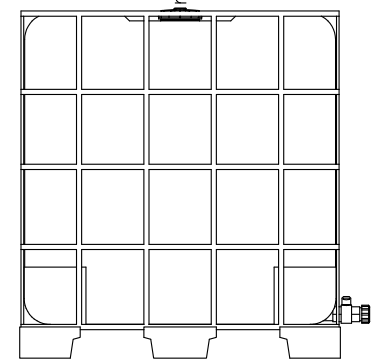
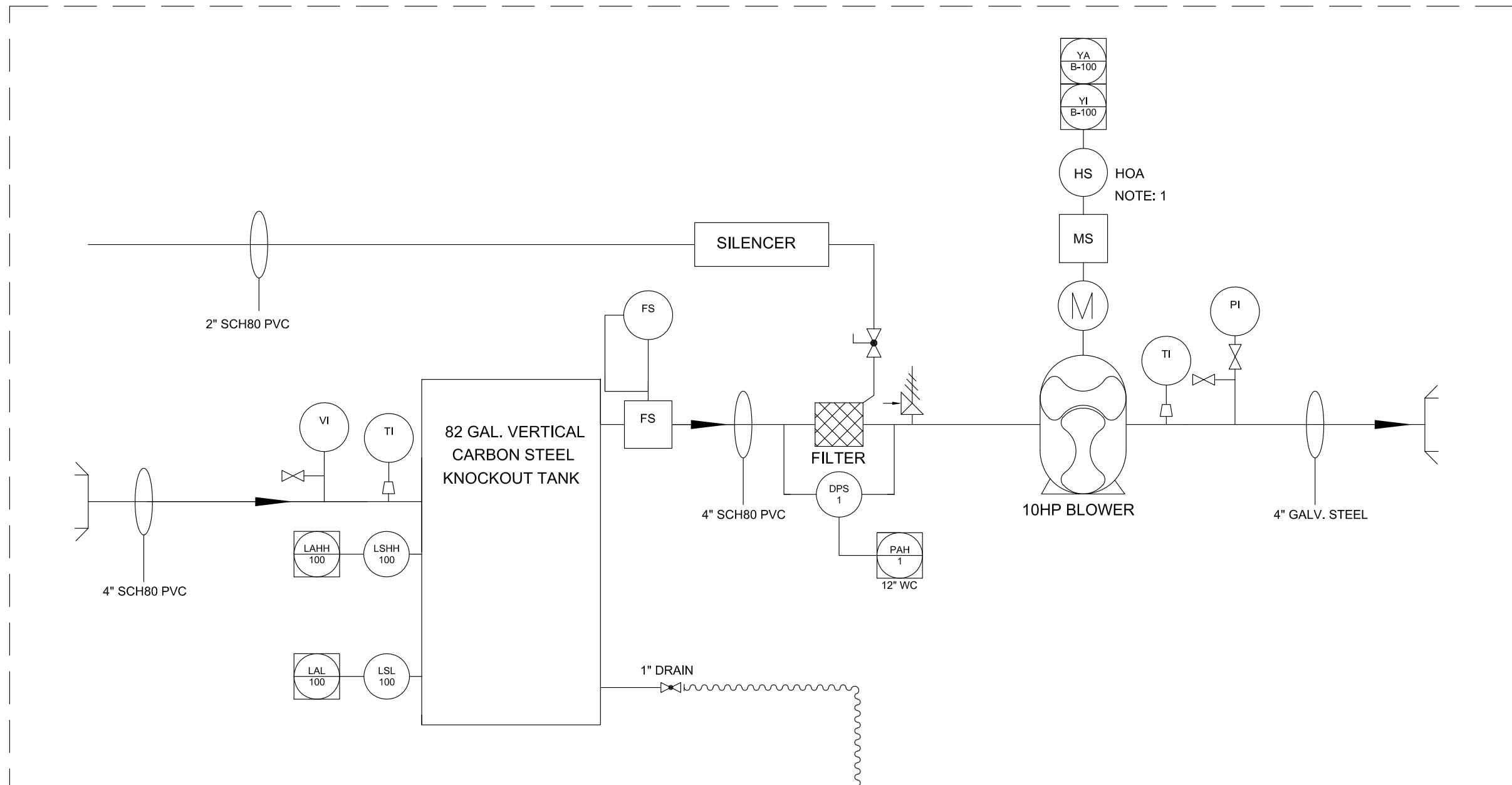


Flow Rate <i>cfm</i>	Static Pressure <i>inch H2O</i>	Total Pressure <i>inch H2O</i>	Current <i>A</i>	Power Demand <i>W</i>	Voltage <i>V</i>	Flow Temp. <i>°C</i>	Rotational Speed <i>rpm</i>	Static Efficiency <i>%</i>	Total Efficiency <i>%</i>
1254.13	0.50	1.31	22.94	3668.54	241.71	26.45	7620	2.05	5.32
999.97	15.82	16.33	24.99	4002.16	241.73	27.99	8700	47.31	48.83
804.13	21.90	22.23	22.93	3651.93	241.61	28.78	9150	57.80	58.67
600.63	25.54	25.73	20.40	3214.99	242.38	29.50	9510	57.31	57.72
515.85	26.41	26.54	19.19	2994.57	243.03	29.99	9690	54.69	54.97

WARNING PERFORMANCE DATA IS FOR REFERENCE ONLY

DESIGN APPLICATION: Designed to provide variable airflow for low NOx and CO emission in high efficiency gas fired combustion systems. Built with non-sparking materials. Blower housing assembly constructed of die cast aluminum. Impeller constructed from hardened aluminum. Rubber isolation mounts built into blower construction to dampen vibration within the motor. Two-piece blower housing assembly sealed, and factory leak checked. Customer is responsible to check for any leakage once the blower is installed into the final application.

MISCELLANEOUS: Motor cooling inlet and discharge vents must not be obstructed. Motor ventilation air to be free of oils and other foreign particles. Blower is to be mounted so ventilation air cannot be re-circulated.



© FITWAY TECHNOLOGIES, INC.

REV.	ISSUED DATE	DESCRIPTION	BY	CK'D
0	08/02/2022	DRAFT	GPR	JK

SEAL

Prepared for:
RENTAL SYSTEM

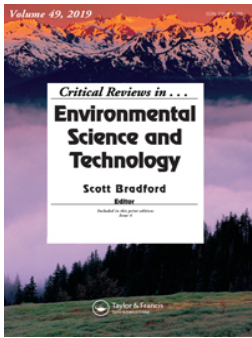
Prepared by:
Fitway Technologies, Inc.
2129 E Birchwood Ave.
Cudahy, WI 53110
Tel: (414) 483-5600 Fax: (414) 483-1957
www.fitway.com

**TYPICAL OF 10-HP SSDS
P&ID**

SHEET TITLE

APPROVED BY JK	CHECKED BY MPS
DESIGNED BY BDC	DRAWN BY BDC
PROJECT NUMBER RV	DRAWING NUMBER
SHEET 1 OF 1	

ATTACHMENT B
Biochar Technical Information



Critical Reviews in Environmental Science and Technology

ISSN: 1064-3389 (Print) 1547-6537 (Online) Journal homepage: <https://www.tandfonline.com/loi/best20>

Alginate-based composites for environmental applications: a critical review

Bing Wang, Yongshan Wan, Yuling Zheng, Xinqing Lee, Taoze Liu, Zebin Yu, Jun Huang, Yong Sik Ok, Jianjun Chen & Bin Gao

To cite this article: Bing Wang, Yongshan Wan, Yuling Zheng, Xinqing Lee, Taoze Liu, Zebin Yu, Jun Huang, Yong Sik Ok, Jianjun Chen & Bin Gao (2019) Alginate-based composites for environmental applications: a critical review, *Critical Reviews in Environmental Science and Technology*, 49:4, 318-356, DOI: [10.1080/10643389.2018.1547621](https://doi.org/10.1080/10643389.2018.1547621)

To link to this article: <https://doi.org/10.1080/10643389.2018.1547621>



Published online: 20 Dec 2018.



Submit your article to this journal [↗](#)



Article views: 1167





View related articles [↗](#)



Citing articles: 28 View citing articles [↗](#)



Alginate-based composites for environmental applications: a critical review

Bing Wang^{a,b} , Yongshan Wan^c, Yuling Zheng^b, Xinqing Lee^a, Taoze Liu^a, Zebin Yu^d, Jun Huang^{e,f}, Yong Sik Ok^g, Jianjun Chen^h, and Bin Gao^b 

^aState Key Laboratory of Environmental Geochemistry, Institute of Geochemistry Chinese Academy of Sciences, Guiyang, China; ^bDepartment of Agricultural and Biological Engineering, University of Florida, Gainesville, Florida, USA; ^cNational Health and Environmental Effects Research Laboratory, US EPA, Gulf Breeze, Florida, USA; ^dSchool of Resources, Environment and Materials, Guangxi University, Nanning, China; ^eHualan Design & Consulting Group Co. Ltd, Nanning, China; ^fCollege of Civil Engineering and Architecture Guangxi University, Nanning, China; ^gKorea Biochar Research Center & Division of Environmental Science and Ecological Engineering, Korea University, Seoul, Republic of Korea; ^hMid-Florida Research & Education Center, University of Florida, Apopka, Florida, USA

ABSTRACT



Alginate-based composites have been extensively studied for applications in energy and environmental sectors due to their biocompatible, nontoxic, and cost-effective properties. This review is designed to provide an overview of the synthesis and application of alginate-based composites. In addition to an overview of current understanding of alginate biopolymer, gelation process, and cross-linking mechanisms, this work focuses on adsorption mechanisms and performance of different alginate-based composites for the removal of various pollutants including dyes, heavy metals, and antibiotics in water and wastewater. While encapsulation in alginate gel beads confers protective benefits to engineered nanoparticles, carbonaceous materials, cells and microbes, alginate-based composites typically exhibit enhanced adsorption performance. The physical and chemical properties of alginate-based composites determine the effectiveness under different application conditions. A series of alginate-based composites and their physicochemical and sorptive properties have been summarized. This critical review not only summarizes recent advances in alginate-based composites but also presents a perspective of future work for their environmental applications.

KEYWORDS

Alginate; hydrogel; nanocomposites; dyes; heavy metals; antibiotics

1. Introduction

Achieving environmental goals while supporting robust economic growth demands innovative technologies for water and wastewater treatment (Gupta and Ali, 2012; Lim & Aris, 2014; Michael et al., 2013; Yagub, Sen, Afroze, & Ang, 2014). Adsorption technology has been considered as one

CONTACT Bin Gao  bg55@ufl.edu  Agricultural & Biological Engineering, University of Florida, PO Box 110570, Gainesville, FL, USA.

Color versions of one or more of the figures in the article can be found online at www.tandfonline.com/best.

© 2018 Taylor & Francis Group, LLC

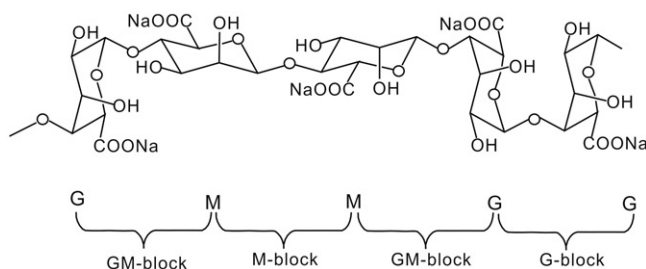


Figure 1. The molecular structure of sodium alginate (SA).

of the most effective and environmentally sound methods for remediating contaminants that are difficult to degrade in the environment (Ali, 2012; Ali and Gupta, 2006; Fu & Wang, 2011; Lim & Aris, 2014; Wan et al., 2018). Recently, various biomaterials have been developed for improving adsorption capacities, increasing environmental compatibility and operation efficiency as alternatives for conventional activated carbon (Burakov et al., 2018; Gupta, Carrott, Ribeiro Carrott, & Suhas, 2009). As a low cost and highly efficient absorbent, alginate-based composites have been extensively studied for the removal of heavy metals, industrial dyes, pesticides, antibiotics, and other pollutants in water and wastewater (Fomina & Gadd, 2014; Wan Ngah, Teong, & Hanafiah, 2011; Wang, Gao, & Wan, 2018b; Wang, Gao, Zimmerman, & Lee, 2018; Wang, Gao, Zimmerman, Zheng, & Lyu, 2018; Yagub et al., 2014).

Alginate is an anionic polysaccharide found in the outer cell wall of brown algae, such as kelps. The major component of alginate is alginic acid while sodium alginate (SA) is Na-salt of alginic acid, which is a polymer with abundant free hydroxyl and carboxyl groups distributed along the backbone chain of the polymer (Figure 1). The linear, anionic polysaccharide consists of two kinds of 1,4-linked hexuronic acid residues, namely β -D-mannuronopyranosyl (M) and α -L-guluronopyranosyl (G) residues, arranged in blocks of repeating M residues (MM blocks), blocks of repeating G residues (GG blocks), and blocks of mixed M and G residues (MG-blocks) (Yang, Xie, & He, 2011). Sodium alginate itself is nontoxic, stable in the environment with strong gelation, film-forming, and complexing abilities. The sodium alginate gel is soft and soluble in alkaline solution. It can go through an irreversible chemical process with polyvalent cations (except magnesium) to form a crosslinking bond, and finally the formation of a thermo-irreversible gel. For example, when Ca^{2+} is added to the SA solution, Ca^{2+} displaces part of H^+ and Na^+ to form a calcium alginate (CA) gel. Due to its nontoxicity, biocompatibility, and the ability to form crosslinks with cations, alginate has been utilized for encapsulation of chemical and biological compounds with a wide range of application in agriculture, food technologies, pharmaceutical cosmetics, chemical

engineering, environmental engineering, paper and textile industry, and many other areas.

Environmental applications of alginate hinge partly on the fact that the rich surface functional groups (e.g., carboxyl and hydroxyl) in alginate could capture metallic or cationic ions via ion exchange between the cross-linking cations and target pollutants such as heavy metals or dyes. However, alginate gel has disadvantages such as high rigidity and fragility with poor elasticity and mechanical properties (Thakur, Pandey, & Arotiba, 2016). Organic and inorganic alginate-based composites have been synthesized to enhance mechanical and thermal stability, and swelling properties of pure alginate gels (Thakur et al., 2016). These composites possess unique physicochemical properties and excellent biocompatibility. Over the past decade, alginate-based composites combining alginate gels and other polymers, natural and engineered nanoparticles, and microorganisms are extensively studied for the removal of pollutants from aqueous solution (Ali, Al-Othman, & Sanagi, 2015; Ali, Al-Othman, & Al-Warthan, 2016a; Ali, Al-Othman, & Al-Warthan, 2016b; Wang, Gao, & Wan, 2018a; Wang et al., 2018b; Wang, Gao, Zimmerman, & Lee, 2018; Zhao, Qin, & Feng, 2016). However, these studies are scattered, aiming to report the adsorption performance of specific composites. No comprehensive literature reviews on alginate-based composites as adsorbents for environmental applications are currently available.

The objective of this paper is to provide a systematic synthesis of the existing literature over the past two decades regarding environmental applications of alginate-based composites with respect to their adsorption capacities and experimental conditions. Most of these studies focus on the removal of dyes and heavy metals, as well as dozens of studies on antibiotics and other pollutants. This review starts with an examination of the synthesis of alginate-based composites and their special functionalities resulting from various materials encapsulated in alginate. Subsequently, the adsorption mechanisms and performance of different alginate-based composites for the removal of dyes, heavy metals, and antibiotics from aqueous solutions are reviewed. Future perspectives on application of alginate-based composites for environmental remediation is presented.

2. Synthesis of alginate-based composites as adsorbents

Properties and potential applications of alginate-based composites depend largely on their synthesis, i.e. physical and chemical crosslinking methods (Ching, Bansal, & Bhandari, 2017; Idris, Ismail, Hassan, Misran, & Ngomsik, 2012). Four common methods including ionic crosslinking, emulsification, electrostatic complexation, and self-assembly have been used

for synthesis of alginate-based composites (Akhtar, Hanif, & Ranjha, 2016; Mane, Ponrathnam, & Chavan, 2015; Paques, Van Der Linden, Van Rijn, & Sagis, 2014). Physically crosslinked hydrogels are synthesized by ionic interaction, crystallization, stereocomplex formation, hydrophobized polysaccharides, protein interaction and hydrogen bond. In contrast, chemically crosslinked hydrogels are synthesized by chain growth polymerization, addition and condensation polymerization and gamma and electron beam polymerization (Maitra & Shukla, 2014). These synthesis methods have their own advantages and disadvantages. The synthesis of physically crosslinked sodium alginate hydrogel is simple, and the conditions are gentle, but the gel strength is poor. The structural regularity of chemically crosslinked sodium alginate hydrogel is better, and the preparation conditions are more complicated, requiring complete removal of the unreacted cross-linking agents for post-treatment.

Sodium alginate contains a large number of functional groups, such as active hydroxyl group and carboxyl group along with its backbone chain and can be chemically modified by chemical crosslinking, esterification and etherification. The fundamental process involving gel formation is the interaction between sodium alginate and divalent cations (such as calcium ions) or cationic polymers. Sodium alginate has a -COO- group in the molecule. When a divalent cation is added to the sodium alginate solution, sodium alginate undergoes a cross-linking reaction, Na^+ from the guluronic acid (G) blocks is exchanged with these divalent cations to form a water-insoluble gel with a characteristic “egg-box” structure. Different cations show different affinity for alginate, the ability of sodium alginate to bind to multivalent cations follows the sequence of $\text{Pb}^{2+} > \text{Cu}^{2+} > \text{Cd}^{2+} > \text{Ba}^{2+} > \text{Sr}^{2+} > \text{Ca}^{2+} > \text{Co}^{2+} > \text{Ni}^{2+} > \text{Zn}^{2+} > \text{Mn}^{2+}$ (Russo, Malinconico, & Santagata, 2007). In this ionic cross-linking process of sol-gel reaction, the solution concentration, pH value, and metal ion intensity all affect the stability, mechanical strength, shape and structure of the gel beads (Chan, Jin, & Heng, 2002).

In order to improve the performance and stability of alginate for environmental applications, various materials have been incorporated into alginate hydrogel (microspheres) (De-Bashan, Moreno, Hernandez, & Bashan, 2002; Hong et al., 2017; Rezaei, Haghshenasfard, & Moheb, 2017; Wang, Gao, Zimmerman, Zheng, et al., 2018; Zhuang et al., 2016). Synthesis of these composites typically starts with mixing the material with sodium alginate solution before the gelation of calcium alginate (Figure 2). A comprehensive review of the literature indicates that the materials encapsulated in alginate for environmental applications include activated carbon (AC), biochar, carbon nanotube (CNT), graphene oxide (GO), nanoparticle, magnetic materials and microorganism (Figure 2). Selection of the materials to

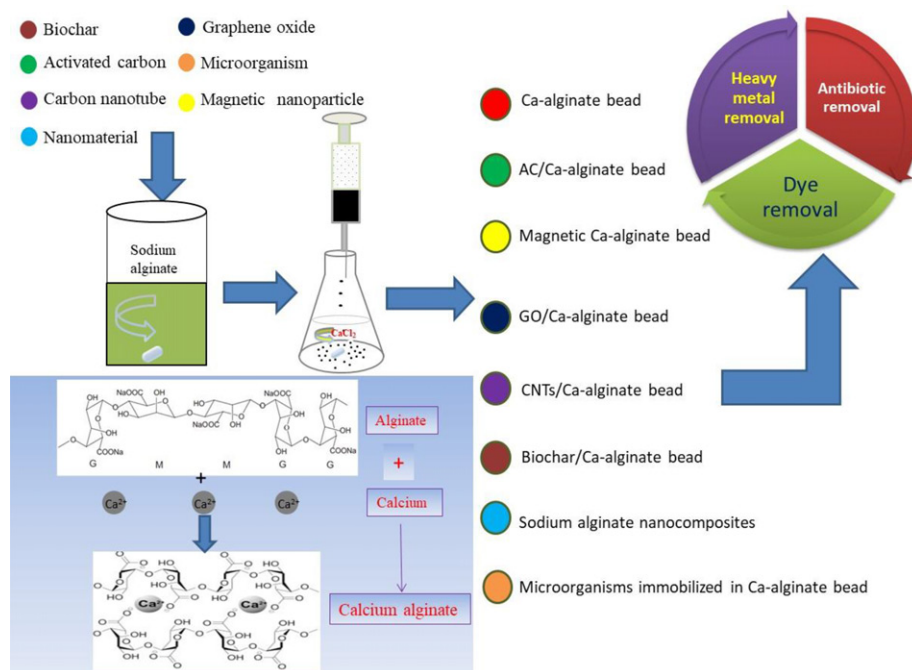


Figure 2. Fabrication of different alginate-based composites.

be encapsulated depends on the functionality of the material and the intended application so that synergetic benefits can be attained by the composite. While alginate-based composites typically exhibit enhanced physical/mechanical properties for bioengineering applications [24-25], a few other benefits achieved through fabrication are worth mentioning here.

First, alginate beads may serve as a stable matrix for other types of adsorbents that are too fine in particle size and too difficult to separate from aqueous solution. These adsorbents are typically carbon-based, such as AC, biochar, CNTs, and GO (Mohammadi, Khani, Gupta, Amereh, & Agarwal, 2011; Gupta, Nayak, Agarwal, & Tyagi, 2014; Robati et al., 2016). AC has been widely used for wastewater treatment (Maneerung et al., 2016). However, AC is mostly used as a fine powder, and the difficulty in separation and regeneration from the effluent may result in significant loss of the adsorbent. Biochar has been recently used as a cost-effective alternative of AC in water/wastewater treatment (Ahmad et al., 2014; Fang, Zhan, Ok, & Gao, 2018; Inyang et al., 2016; Mohan, Sarswat, Ok, & Pittman, 2014; Wang, Gao, & Fang, 2017). Biochar can be ball milled to increase its surface areas (Lyu et al., 2017; Lyu, Gao, He, Zimmerman, Ding, Huang, et al., 2018; Lyu, Gao, He, Zimmerman, Ding, Tang, et al., 2018). Like AC powders, ball milled biochar is difficult to separate from water due to its small particle size (Wang et al., 2018b; Wang, Gao, Zimmerman, Zheng, et al., 2018). CNTs and GO both have been intensively studied for removal

of organic and inorganic pollutants because of their unique structural features and large specific areas (Chen, Gao, & Li, 2015; Gupta, Kumar, Nayak, Saleh, & Barakat, 2013). The facts that GO disperses extremely well in water and CNTs are very small and form aggregates make it difficult to separate them from aqueous solution (Ding, Hu, Morales, & Gao, 2014; Inyang, Gao, Zimmerman, Zhang, & Chen, 2014; Tian et al., 2012; Wang, Yang, & Hsieh, 2010). Encapsulation of these carbonaceous materials into alginate hydrogels or beads offer ease of separation and regeneration for water/wastewater treatment (Wang et al., 2018a, 2018b; Wang, Gao, Zimmerman, & Lee, 2018; Wang, Gao, Zimmerman, Zheng, et al., 2018).

Second, fabricating magnetic materials and nanoparticles into alginate brings in nano-effects and magnetic technology into the composites while attaining excellent absorption performance and reducing the potential environmental risk of nanoparticles. Nanotechnology and magnetic technology have been increasingly used in water and wastewater treatment (Qu, Alvarez, & Li, 2013; Theron, Walker, & Cloete, 2008). Alginate/nanomaterial composites are blends of alginate and nanomaterials with enhanced adsorption capacity (Figure 3). Furthermore, a magnetic adsorbent (called magsorbent) can be developed by encapsulating magnetic functionalized nanoparticles in alginate beads along with different cross-linking agents (Lee et al., 2000; Russo et al., 2007). For example, incorporating maghemite with the alginate in bead form is very useful in isolation or recovery process (Idris et al., 2012). Magnetic technology has the advantage of simple operation and easy separation.

Third, alginate can serve a carrier of microorganisms to optimize the microbial processes for environmental and agricultural applications (Cohen, 2001; Covarrubias, De-Bashan, Moreno, & Bashan, 2012; Martins, Martins, Fiúza, & Santaella, 2013). Compared with the conventional suspension system, alginate microorganism composites offer a multitude of advantages, such as high biomass, high metabolic activity and strong resistance to toxic chemicals (An, Zhou, Li, Fu, & Sheng, 2008; Cai, Chen, Ren, Cai, & Zhang, 2011; Junter & Jouenne, 2004; Liu, Guo, Liao, & Wang, 2012). Moreover, immobilized microorganisms can be used several times without significant loss of activity (Rhee, Lee, & Lee, 1996). Therefore, alginate immobilized microorganism technology has received substantial attention for wastewater treatment (An et al., 2008).

3. Alginate-based composites as adsorbents for environmental applications

Alginate-based composites are fabricated as adsorbents for both inorganic and organic contaminants. The adsorption mechanisms typically involve ion exchange and electrostatic interactions (Figure 4). Special functionalities

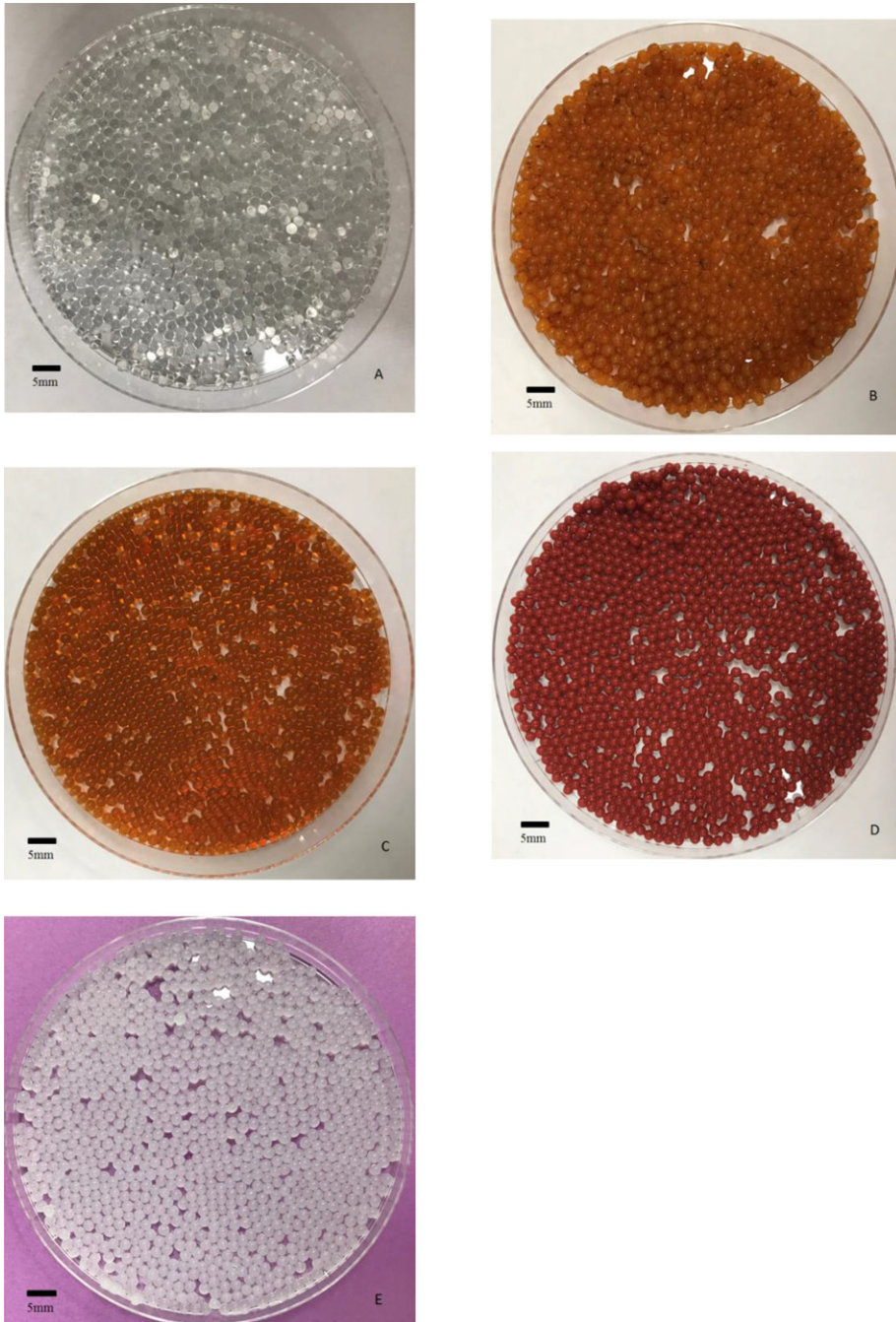


Figure 3. Photographs of different nanomaterial-alginate hybrid beads. Ca-alginate beads (A); Zero-valent iron nanoparticle-alginate composite beads (B); Silver nanoparticle-alginate composite beads (C); Fe₂O₃ nanoparticle-alginate composite beads (D); MgO nanoparticle-alginate composite beads (E).

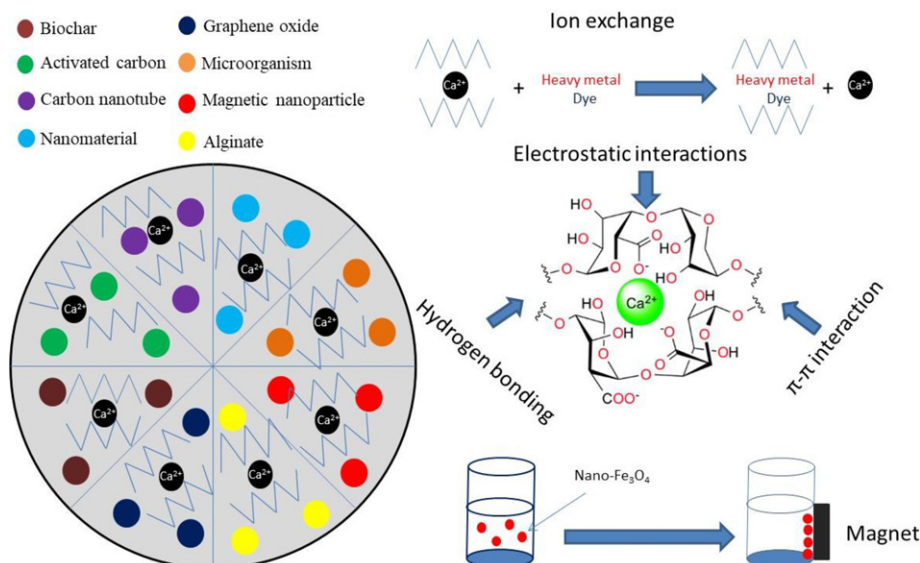


Figure 4. Adsorption mechanisms of different alginate-based composites on organic and inorganic contaminants in water.

of encapsulated materials may bring in other benefits depending on the needs and applications. This section is intended to discuss the performance and mechanisms of various types of composites for the removal of dyes, heavy metals, and antibiotics.

3.1. Dyes

Dyes are intensely colored complex organic compounds which have been heavily used in the textile industry. Release of processed dye wastes into the aquatic environment may result in harmful impacts on human health and the environment. The most obvious impact is the reduction of light penetration, thereby affecting the primary productivity of aquatic ecosystems. Some dyes and their derivatives are toxic to aquatic plants, fish, and shell fish. The removal of dye from wastewater is largely based on the adsorption technique whereby the dissolved dye is adsorbed by the sorbent (Fang, Gao, Mosa, & Zhan, 2017; Fang, Gao, Zimmerman, Ro, & Chen, 2016; Gupta & Suhas, 2009; Robinson, McMullan, Marchant, & Nigam, 2001; Zhang & Gao, 2013). Alginate itself is an excellent sorbent for dye removal. The potential use of pure calcium alginate beads for removal of black dyes was studied in a dynamic batch mode by Aravindhan et al. (Aravindhan, Fathima, Rao, & Nair, 2007). The adsorption isotherm suggested a Langmuir adsorption capacity of 57.70 mg g^{-1} . The performance of alginate-based composites for dye removal is summarized in Table 1 for a subset of studies. Each type of the composites is highlighted below.

Table 1. Alginate-based composites for the removal of synthetic dyes from aqueous solution.

Adsorbent	Adsorbate	Adsorption capacity (mg g ⁻¹)	pH	Temperature (°C)	Ref
GO/CA fibers	Methylene blue	181.81	5.4	25	(Li et al., 2013)
Calcium alginate beads	Basic black dye	57.70	4.0	30	(Aravindhan et al., 2007)
Graphene/alginate nanocomposite	Methylene blue	2300	8.0	25	(Zhuang, Yu, Chen, & Ma, 2016)
Alginate-halloysite nanotube	Methylene blue	250	—	35	(Liu, Wan, et al., 2012)
CA/MWCNTs	Methylene blue	606.1	—	25	(Sui et al., 2012)
CA/MWCNTs	Methyl orange	12.5	—	25	(Sui et al., 2012)
CA/AC beads	Methylene blue	892	—	20	(Hassan, Abdel-Mohsen, & Fouda, 2014)
CA/AC beads	Methylene blue	730	—	40	(Hassan, Abdel-Mohsen, & Fouda, 2014)
AC–bentonite–alginate beads	Methylene blue	756.97	—	30	(Benhouria et al., 2015)
AC–bentonite–alginate beads	Methylene blue	982.47	—	40	(Benhouria et al., 2015)
AC–bentonite–alginate beads	Methylene blue	994.06	—	50	(Benhouria et al., 2015)
Sodium alginate- Fe ₃ O ₄	Malachite green	47.84	7.0	25	(Mohammadi et al., 2014)
AC/CA beads	Rhodamine 6G	—	—	—	(Annadurai et al., 2002)
Alginate/polyaspartate beads	Methylene blue	700	—	25	(Jeon, Lei, & Kim, 2008)
Alginate/polyaspartate beads	Malachite green	350	—	25	(Jeon et al., 2008)
Magnetic alginate beads	Methylene blue	22.06	6.7	—	(Rocher et al., 2008)
Magnetic alginate beads	Methyl orange	0.65	6.7	—	(Rocher et al., 2008)
Magnetic alginate beads cross-linked with epichlorohydrin	Methylene blue	261.73	—	—	(Rocher et al., 2010)
Magnetic alginate beads cross-linked with epichlorohydrin	Methyl orange	6.55	—	—	(Rocher et al., 2010)
CABI nano-goethite	Congo red	181.1	3.0	25	(Munagapati & Kim, 2017)
SA/n-TiO ₂	Direct Red 80	163.9	2.0	25	(Mahmoodi, Hayati, Arami, & Bahrami, 2011)
SA/n-TiO ₂	Acid Green 25	151.5	2.0	25	(Mahmoodi et al., 2011)
Activated organo-bentonite/SA	Methylene blue	414	—	23	(Belhouchat, Zaghouane-Boudiaf, & Viseras, 2017)
Activated organo-bentonite/SA	Methylene orange	116	—	23	(Belhouchat et al., 2017)
Methylcellulose/CA beads	Methylene blue	336.7	—	20	(Li et al., 2016)
Silver nanocomposite hydrogel	Methylene blue	213.7	—	Room T	(Devi, Kumar, & Kumar, 2016)
Montmorillonite/CA composite	Basic red 46 (BR46)	35	—	—	(Hassani et al., 2015)
SA/poly(N-vinyl-2-pyrrolidone) beads	Reactive red-120 (RR)	116.82	—	25	(Inal & Erduran, 2015)
Magnetic ferrite nanoparticle–alginate composite	Basic Blue 9 (BB9)	106	—	25	(Mahmoodi, 2013)
Magnetic ferrite nanoparticle–alginate composite	Basic Blue 41 (BB41)	25	—	25	(Mahmoodi, 2013)
Magnetic ferrite nanoparticle–alginate composite	Basic Red 18 (BR18)	56	—	25	(Mahmoodi, 2013)
SA/poly(N-vinyl-2-pyrrolidone) beads	Cibacron brilliant red 3B-A	73.3	—	25	(Inal & Erduran, 2015)
SA/poly(N-vinyl-2-pyrrolidone) beads	Remazol brilliant blue R	55.28	—	25	(Inal & Erduran, 2015)
Alginate–montmorillonite composite beads	Methylene blue	181.8	—	40	(Uyar, Kaygusuz, & Erim, 2016)

3.1.1. Activated carbon/alginate beads

Recent studies have shown that AC immobilized into calcium alginate removed a significant amount of dyes from wastewater (Hassan, Abdel-Mohsen, & Fouda, 2014). Benhouria et al. prepared bentonite-alginate beads, activated carbon-alginate beads, and activated carbon-bentonite-alginate beads via a simple fabrication method to remove methylene blue

(MB). The results showed that maximum monolayer adsorption capacity of activated carbon-bentonite-alginate beads was 756.97 mg g^{-1} at 30°C with high resilience on adsorption efficiency after six regeneration cycles (Benhouria, Islam, Zaghouane-Boudiaf, Boutahala, & Hameed, 2015). Annadurai et al. studied batch adsorption equilibrium of Rhodamine 6G using activated carbon incorporated into calcium alginate beads and obtained high percentages of adsorption of Rhodamine 6G (Annadurai, Juang, & Lee, 2002).

Although the activated carbon and alginate composite processes excellent adsorption properties for dyes, the cost and reuse of activated carbon is still of concern. In order to make the activated carbon-alginate beads a magnetically separable adsorbent, the magnetic beads were prepared with a high magnetic sensitivity under an external magnetic field [31]. This provides an easy and efficient way to separate the beads from aqueous solution.

3.1.2. Graphene oxide/alginate composites

The GO and alginate biopolymer composites offer great potential for dye removal from wastewaters. For example, Yin et al. successfully fabricated graphene oxide (GO)/sodium alginate (SA)/polyacrylamide (PAM) (GO/SA/PAM) composite hydrogels for adsorption of cationic dyes (R6G, MB, MG, and BG) and anionic dyes (CA, MO, BR and RB) (Fan, Shi, Lian, Li, & Yin, 2013). In addition, Fan et al. fabricated a novel graphene oxide (GO)/sodium alginate (SA)/polyacrylamide (PAM) ternary nanocomposite hydrogel through free-radical polymerization of acrylamide (AAM) and SA in the presence of GO in an aqueous system followed with ionically cross-linking of calcium ions. The GO/SA/PAM ternary nanocomposite hydrogel exhibited excellent adsorption properties for water-soluble dyes. After introducing GO, the dye adsorption capacities of the hydrogel were significantly improved (Fan et al., 2013). Li et al. prepared the calcium alginate-GO composites and found that the maximum MB adsorption capacity obtained from Langmuir isotherm equation was 181.81 mg g^{-1} . The adsorption reaction was exothermic and spontaneous in nature, occurring on the homogenous surface of GO/CA by monolayer adsorption (Li et al., 2013).

3.1.3. Carbon nanotubes (CNTs)/Ca-alginate beads

Carbon nanotubes (CNTs) have been intensively studied as a potential material to be used in a variety of applications based on their specific physical and chemical properties (Wang, Gao, Zimmerman, & Lee, 2018, Gupta, Kumar, Nayak, Saleh, & Barakat 2013; Gupta & Saleh 2013). Sui et al. investigated the adsorption of methylene blue (MB) and methyl orange

(MO) ionic dyes onto calcium alginate/multi-walled carbon nanotubes (CA/MWCNT) composite fibers with varying MWCNTs content and pH values. The results showed that an introduction of MWCNTs increased the adsorption capacity of MO by 3 times, and enhanced the adsorption rate for MB compared to that of native CA (Sui et al., 2012). Li et al. prepared the CA/MWCNTs composite fiber to remove MO anionic dyes and the results illustrated that the introduction of MWCNTs obviously increased the adsorption capacity of MO, reaching about 14.13 mg g^{-1} (Li et al., 2012). Although the adsorption capacity increased using CNTs, the tedious centrifugation separation process might be a limiting factor and thus introducing magnetic properties into multi-wall carbon nanotube system will help with the separation process (Gong et al., 2009).

3.1.4. Other alginate nanocomposites

In addition to GO and CNTs, alginate has been blended with other natural and engineered nanoparticles to form nanocomposites to enhance the adsorption capacity (Tesh & Scott, 2014; Wang et al., 2018a, 2018b; Wang, Gao, Zimmerman, Zheng, et al., 2018). Mohammadi et al. prepared superparamagnetic sodium alginate-coated Fe_3O_4 nanoparticles for removal of malachite green (MG) from aqueous solutions. The maximum adsorption capacity obtained from Langmuir isotherm equation was 47.84 mg g^{-1} (Mohammadi, Daemi, & Barikani, 2014). Liu et al. prepared a new kind of porous beads by immobilizing halloysite nanotubes with alginate and found that the maximum MB adsorption capacity of about 250 mg g^{-1} . After 10 successive adsorption-desorption cycles, the removal efficiency of MB could be kept above 90% (Liu, Wan, et al., 2012). The alginate gel beads populated by halloysite nanotubes improved their ability to capture the dye so that they can have important implications for the enhancement of controlled adsorption. Compared to the unloaded gel beads, the hybrid gel beads are very effective and efficient for removing positively charged dye from the aqueous phase with enhanced properties (Cavallaro, Gianguzza, Lazzara, Milioto, & Piazzese, 2013).

Some novel synthesized composites showed great promise in removal of dyes. Nano-sized montmorillonite (MMT)/calcium alginate (CA) composite synthesized by Hassani et al. removed basic red 46 (BR46) in aqueous solution with the maximum adsorption capacity of about 35 mg g^{-1} (Hassani, Soltani, Karaca, & Khataee, 2015). Wang, Wang, and Wang (2013) prepared a series of NaAlg-g-p(AA-co-St)/organo-I/S nanocomposite absorbents to remove methylene blue (MB) and found that the nanocomposite can rapidly adsorb MB with an adsorption capacity of $1843.46 \text{ mg g}^{-1}$. TiO_2 immobilized in a Ca-alginate bead retained its photoactivity during all of the experiments and the TiO_2 -gel beads presented good stability in

water for maintaining its shape after several uses (Albarelli, Santos, Murphy, & Oelgemöller, 2009). Impregnated calcium alginate beads with nano-goethite (CABI nano-goethite) removed Congo red (CR) from an aqueous solution, the maximum monolayer adsorption capacity was 181.1 mg g^{-1} at pH 3.0 and the adsorption process was endothermic and favored at high temperature (Munagapati & Kim, 2017).

3.1.5. Magnetic Ca-alginate beads

A series of studies have reported that alginate beads containing magnetic nanoparticles and activated carbon (AC-MAB) can selectively remove two dyes with different charges: positively charged MB and negatively charged methyl orange (MO). The adsorption capacity of beads was found to be higher than non encapsulated AC for MB and of the same order of magnitude for MO. The AC-MAB system selectively and strongly adsorbs MB due to the presence of carboxylate functions of both alginate and magnetic nanoparticles through ionic exchange with calcium ions (Rocher, Siaugue, Cabuil, & Bee, 2008).

Rocher et al. prepared another magnetic alginate beads by an extrusion technique and crosslinked with epichlorohydrin which contains both magnetic nanoparticles and activated carbon (Rocher, Bee, Siaugue, & Cabuil, 2010). With the addition of magnetic properties, the beads can be easily recovered or manipulated by an external magnetic field. Two mechanisms can be explained the adsorption process: (1) a hydrophobic adsorption onto encapsulated activated carbon which depends neither on the electrical charge of the dye, nor of the solution pH; (2) an ionic exchange between the positively charged dye and calcium ions and sodium ions, the counter ions of the carboxylate functions of both alginate and citrate-coated magnetic nanoparticles (Rocher et al., 2010).

Rosales et al. studied the decolorization of dyes under electro-Fenton process using Fe alginate gel beads and found that around 98-100% of dye decolorization was obtained for both dyes by an electro-Fenton process in successive batches (Rosales, Iglesias, Pazos, & Sanromán, 2012). Mahmoodi synthesized magnetic ferrite nanoparticle-alginate composite used to remove dyes from the binary system. The maximum dye adsorption capacity of MFN-alginate was 106 mg g^{-1} , 25 mg g^{-1} , and 56 mg g^{-1} for BB9, BB41, and BR18, respectively (Mahmoodi, 2013).

3.1.6. Microalgae immobilized in Ca-alginate beads

Immobilization of microbial cells in alginate beads has received increasing interest for dye removal. Chen et al. developed an efficient sol-gel method for fabricating alginate-silicate organic-inorganic gel beads for immobilization

of *P. luteola* cells and demonstrated the usefulness of such immobilized cells system in azo dye decolorization. The results indicated that the alginate-silicate matrix showed improvement over other synthetic or natural polymer gel matrices for immobilizing *P. luteola* in decolorization of Reactive Red 22 (Chen & Lin, 2007). Enayatzamir et al. studied the ability of white-rot fungus *Phanerochaete chrysosporium* immobilized on Ca-alginate beads to decolorize different recalcitrant azo dyes. The results showed that the MnP secreted by the fungus played the main role while adsorption was found to be negligible except for the dye BB in this decoloration process (Enayatzamir, Alikhani, Yakhchali, Tabandeh, & Rodríguez-Couto, 2010). Daâssi et al. found that the immobilization of *P. laccase* into Ca-alginate beads improved its thermal and storage stabilities and the immobilized *P. laccase* exhibited efficient textile dye decolorization in several successive batches (Daâssi, Rodríguez-Couto, Nasri, & Mechichi, 2014).

3.2. Heavy metals

Heavy metals in wastewater of industry and mining enterprises are of great environmental concerns due to their low toxicity thresholds and cumulative biological effects (Inyang et al., 2012; Xue et al., 2012; Zhou et al., 2013). It is extremely expensive to remove heavy metals from wastewater and reduce their toxicity in the environment. Several low-cost adsorbents and biopolymers, such as alginate and chitosan extracted from microalgae, shrimp, crab, and fungi are known to bind metal ions and could be used for heavy metal removal from wastewater (Babel & Kurniawan, 2003; Zhou et al., 2014; Zhou, Gao, Zimmerman, & Cao, 2014; Zhou et al., 2013). Alginate is rich in carboxyl, hydroxyl and other active functional groups, which can react with heavy metals through ion exchange or complex reaction. Therefore, it can be used as adsorption material to remove heavy metals. The performance of alginate-based composites for heavy metal removal is summarized in Table 2. Each type of the composites is highlighted below.

3.2.1. Ca-alginate beads

Alginate with a high M/G ratio, extracted from *Laminaria digitata*, was evaluated for Cu(II), Cd(II) and Pb(II) sorption in acidic solutions, in the form of calcium cross-linked beads. The high M/G ratio of alginate extracted from this algal species is most likely the determining factor for the increased adsorption capacity of the investigated metals, and the manuronic acid in particular is responsible for the ion exchange mechanism. The presence of carboxyl groups in the alginate structure enhances the adsorption of many metal ions compared with other adsorbents. There are

Table 2. Alginate-based composites for the removal of heavy metals from aqueous solution.

Adsorbent	Adsorbate	Adsorption capacity (mg g ⁻¹)	pH	Temperature (°C)	Ref.
Biochar-alginate beads	Cd(II)	9.73	6.0	—	(Roh et al., 2015)
Graphite nano carbon beads	Co(II)	11.63	5.0	Ambient T	(Jung et al., 2015)
Graphite nano carbon beads	Ni(II)	11.48	5.0	Ambient T	(Jung et al., 2015)
Chitosan coated calcium alginate	Ni(II)	222.2	5.0	Room T	(Vijaya, Popuri, Boddu, & Krishnaiah, 2008)
Alginate–chitosan hybrid gel beads	Cu(II)	8.38	3.5	25	(Gotoh, Matsushima, & Kikuchi, 2004b)
Alginate–chitosan hybrid gel beads	Cd(II)	6.63	3.5	25	(Gotoh et al., 2004b)
Alginate–chitosan hybrid gel beads	Co(II)	3.18	3.5	25	(Gotoh et al., 2004b)
Iron oxide loaded alginate beads	As(V)	0.0226	7.0	—	(Zouboulis & Katsoyiannis, 2002)
Waste metal (hydr)oxide in CA beads	As(III)	126.5	8.0	20	(Escudero, Fiol, Villaescusa, & Bollinger, 2009)
Waste metal (hydr)oxide in CA beads	As(V)	41.6	8.0	20	(Escudero et al., 2009)
CA/GO beads	Cu(II)	60.2	—	—	(Algothmi, Bandaru, Yu, Shapter, & Ellis, 2013)
Biochar-alginate capsule	Pb(II)	263.158	5.0	27	(Do & Lee, 2013)
CA beads from Laminaria digitata	Cu(II)	88.95	4.5	25	(Papageorgiou et al., 2006)
CA beads from Laminaria digitata	Cd(II)	130.77	4.5	25	(Papageorgiou et al., 2006)
CA beads from Laminaria digitata	Pb(II)	374.67	4.5	25	(Papageorgiou et al., 2006)
Orange peel cellulose immobilized CA beads	Cu(II)	166.7	—	28	(Lai, Thirumavalavan, & Lee, 2010)
Orange peel cellulose immobilized CA beads	Pb(II)	128.2	—	28	(Lai et al., 2010)
Orange peel cellulose immobilized CA beads	Zn(II)	156.25	—	28	(Lai et al., 2010)
Banana peel cellulose immobilized CA beads	Cu(II)	163.93	—	28	(Lai et al., 2010)
Banana peel cellulose immobilized CA beads	Pb(II)	121.95	—	28	(Lai et al., 2010)
Banana peel cellulose immobilized CA beads	Zn(II)	183.85	—	28	(Lai et al., 2010)
Ca-alginate beads	Cu(II),	84.39	4.5	25	(Papageorgiou, Katsaros, Kouvelos, & Kanellopoulos, 2009)
Ca-alginate beads	Cd(II)	141.97	4.5	25	(Papageorgiou et al., 2009)
Ca-alginate beads	Pb(II)	360.11	4.5	25	(Papageorgiou et al., 2009)
Sodium alginate	Cu(II)	167.1	4.5	—	(Wang, Lu, & Li, 2016)
Sodium alginate	Cd(II)	179.0	4.5	—	(Wang, Lu, et al., 2016)
Sodium alginate	Pb(II)	435.3	4.5	—	(Wang, Lu, et al., 2016)
Polyvinyl alcohol (PVA)- SA beads	Cu(II)	0.69	—	—	(Cai et al., 2016)
Halloysite/alginate nanocomposite beads	Pb(II)	325	5.0	25	(Chiew et al., 2016)
Polyvinyl alcohol (PVA)- SA beads	Cd(II)	0.52	—	—	(Cai et al., 2016)
Polyvinyl alcohol (PVA)- SA beads	Pb(II)	0.60	—	—	(Cai et al., 2016)
Ca-Fe beads	As(V)	352	—	—	(Min & Hering, 1998)
SA-hydroxyapatite-CNT beads	Co(II)	347.8	6.8	21	(Karkeh-Abadi, Saber-Samandari, & Saber-Samandari, 2016)
Fe ₀ -Fe ₃ O ₄ nanocomposites embedded polyvinyl alcohol (PVA)/sodium alginate	Cr(VI)		5.0	30	(Lv et al., 2013)
Magnetic alginate beads	Pb(II)	100	4.7	Room T	(Bée et al., 2011)
Magnetic alginate beads	Pb(II)	50	7.0	30	(Idris et al., 2012)
Alginate-montmorillonite/polyaniline nanocomposite	Cr(VI)	29.89	—	—	(Olad & Farshi Azhar, 2014)

(continued)

Table 2. Continued.

Adsorbent	Adsorbate	Adsorption capacity (mg g ⁻¹)	pH	Temperature (°C)	Ref.
Bio-polymeric beads	Cr(VI)	0.833	6.0	—	(Bajpai, Shrivastava, & Bajpai, 2004)
Fe ₃ O ₄ @Alg-Ce magnetic beads	Cr(VI)	9.166	5.0	30	(Gopalakannan & Viswanathan, 2015)
Fe ₃ O ₄ @Alg-Ce magnetic beads	Cr(VI)	11.069	5.0	40	(Gopalakannan & Viswanathan, 2015)
Fe ₃ O ₄ @Alg-Ce magnetic beads	Cr(VI)	12.503	5.0	50	(Gopalakannan & Viswanathan, 2015)
Chitosan–alginate beads	Cu (II)	67.66	4.5	Room T	(Ngh & Fatinathan, 2008)
Microgel/SA composite	Cu(II)	46.39	—	—	(Zhao et al., 2016)
Alginate activated carbon beads	Phenol	96.0	3	25	(Kim et al., 2008)
Alginate activated carbon beads	Phenol	85.6	7	25	(Kim et al., 2008)
Alginate activated carbon beads	Phenol	69.6	10	25	(Kim et al., 2008)
Nanochitosan/SA/microcrystalline cellulose beads	Cu(II)	43.32	—	—	(Vijayalakshmi, Gomathi, Latha, Hajeeth, & Sudha, 2016)
Magnetic nanocomposite beads	Cu(II)	72.99	6.0	25	(Bakr et al., 2015)
Graphene/alginate double-network nanocomposite	Cu(II)	169.5	4.0	—	(Zhuang et al., 2016)
Graphene/alginate double-network nanocomposite	Cr(VI)	72.5	4.0	—	(Zhuang et al., 2016)
Sodium alginate/graphene oxide aerogel	Cu(II)	98.0	5.0	30	(Jiao et al., 2016)
Sodium alginate/graphene oxide aerogel	Pb(II)	267.4	5.5	30	(Jiao et al., 2016)
Nanohydroxyapatite–alginate composite	Pb(II)	270.3	5.0	Ambient T	(Googerdchian et al., 2012)
Halloysite nanotube–alginate hybrid beads	Cu(II)	74.13	—	—	(Wang et al., 2014)
Silica nanopowders/alginate composite	Pb(II)	83.33	5.0	—	(Soltani et al., 2014)
Alginate activated carbon bead	Zn(II)	135	6.8	32	(Choi et al., 2009)
Alginate activated carbon bead	Toluene	215	6.8	32	(Choi et al., 2009)
Alginate <i>Pleurotus ostreatus</i>	Pb(II)	121.21	6.5	25	(Xiangliang, Jianlong, & Daoyong, 2005)
White-rot fungus <i>Trametes versicolor</i> in CA bead	Cd(II)	120.6	6.0	25	(Arıca et al., 2001)
<i>Lentinus sajor-caju</i> immobilized Ca-alginate	Cd(II)	123.5	6.0	25	(Bayramoglu et al., 2002)
Alginate–Ayouos wood sawdust (<i>Triplochiton scleroxylon</i>)	Cd(II)	6.21	—	—	(Njimou, Măicăneanu, Indolean, Nanseu-Njiki, & Ngameni, 2016)
CA immobilized <i>Phanerochaete chrysosporium</i>	Cd(II)	85.4	6.0	25	(Kaçar et al., 2002)
CA immobilized <i>Phanerochaete chrysosporium</i>	Hg(II)	112.6	6.0	25	(Kaçar et al., 2002)
Fe ₃ O ₄ nanoparticles embedded SA	Cd(II)	97.8	6.2	—	(Jiao, Qi, Liu, Wang, & Shan, 2015)
CA immobilized <i>Phanerochaete chrysosporium</i>	Pb(II)	355	7.0	25	(Yakup Arıca et al., 2003)
CA immobilized <i>Phanerochaete chrysosporium</i>	Zn(II)	48	7.0	25	(Yakup Arıca et al., 2003)
<i>Spirulina platensis</i> TISTR 8217 immobilized in alginate	Cd(II)	70.92	7.0	26	(Rangsayatorn et al., 2004)
Ca-alginate immobilized wood-rotting fungus	Hg(II)	403.2	6.0	20	(Arıca et al., 2001)
Ca-alginate immobilized wood-rotting fungus	Zn(II)	54.0	6.0	20	(Arıca et al., 2001)
Ca-alginate immobilized wood-rotting fungus	Cd(II)	191.6	6.0	20	(Arıca et al., 2001)

(continued)

Table 2. Continued.

Adsorbent	Adsorbate	Adsorption capacity (mg g ⁻¹)	pH	Temperature (°C)	Ref.
Ca-alginate immobilized-algal beads	Hg(II)	116.8	5.0	25	(Bayramoğlu, Tuzun, Celik, Yilmaz, & Arica, 2006)
Ca-alginate immobilized-algal beads	Cd(II)	88.6	5.0	25	(Bayramoğlu et al., 2006)
Ca-alginate immobilized-algal beads	Pb(II)	384.4	5.0	25	(Bayramoğlu et al., 2006)
Bacterial consortia immobilized in alginate beads	Cr(VI)	657	3.0	30	(Samuel et al., 2013)
Alginate–goethite beads	Cr(III)	20.67	3.0	20	(Lazaridis & Charalambous, 2005)
Alginate–goethite beads	Cr(VI)	23.38	3.0	20	(Lazaridis & Charalambous, 2005)
<i>Scenedesmus quadricauda</i> immobilized Ca-alginate beads	Cu(II)	75.6	5.0	25	(Bayramoğlu & Yakup Arica, 2009)
<i>Scenedesmus quadricauda</i> immobilized Ca-alginate beads	Zn(II)	55.2	5.0	25	(Bayramoğlu & Yakup Arica, 2009)
<i>Scenedesmus quadricauda</i> immobilized Ca-alginate beads	Ni(II)	30.4	5.0	25	(Bayramoğlu & Yakup Arica, 2009)
SA-polyaniline nanofibers	Cr(VI)	73.34	4.2	30	(Karthik & Meenakshi, 2015)
SA-polyaniline nanofibers	Cr(VI)	74.46	4.2	40	(Karthik & Meenakshi, 2015)
SA-polyaniline nanofibers	Cr(VI)	75.82	4.2	50	(Karthik & Meenakshi, 2015)
Ca-alginate immobilized sericite bead	Ni(II)	10.743	7.5	—	(Jeon & Cha, 2015)
Goethite impregnated calcium alginate beads	As(V)	30.44	5.0	25	(Basu, Singhal, Pimple, & Reddy, 2015)
Phosphate-embedded calcium alginate beads	Pb(II)	263.16	4.0	25	(Wang, Yao, et al., 2016)
Phosphate-embedded calcium alginate beads	Cd(II)	82.64	5.5	25	(Wang, Yao, et al., 2016)
SA-graft-poly(methyl methacrylate) beads	Pb(II)	526	—	—	(Salisu, Sanagi, Abu Naim, Wan Ibrahim, & Abd Karim, 2016)
Alginate graft polyacrylonitrile beads	Pb(II)	454	—	—	(Salisu, Sanagi, Abu Naim, Abd Karim, et al., 2016)
SA-carboxymethyl cellulose gel beads	Pb(II)	1727	5.0	37	(Ren et al., 2016)
Quercetin loaded nanoparticles based on alginate	Pb(II)	140.37	7.0	25	(Qi, Jiang, Cui, Zhao, & Zhou, 2015)
Functional CNTs-SA	U(II)	6.01	6.0	Ambient T	(Allaboun, Fares, & Abu Al-Rub, 2016)
CNTs/CA	Cu(II)	84.88	5.0	20	(Li et al., 2010)

pronounced differences between sorption capacities of the alginate beads for different metals examined, with a general order of Pb(II) > Cu(II) > Cd(II) (Papageorgiou et al., 2006). Alginate gel beads showed a high affinity for heavy metal ions of Cu(II) and Mn(II), especially in a low concentration region. After covalently cross-linked with 1,6-diaminohexane bridges, the matrix of alginate gel beads was expected to improve the mechanical strength and resistance to chemical and microbial degradation of the beads, without the change in adsorption property. Ca-alginate beads also were applied to remove U(VI) ions from the solution and the results indicated that the interaction between uranium ions and Ca-alginate beads is endothermic in nature. Values of entropy and Gibbs free energy change

suggested that the adsorption of uranium on Ca-alginate is a spontaneous process (Gok & Aytas, 2009). That is, the covalently cross-linked alginate gel beads are expected to be a good candidate for adsorbents to remove heavy metal ions from low heavy metal concentration wastewater (Gotoh, Matsushima, & Kikuchi, 2004a).

3.2.2. Activated carbon/Ca-alginate beads

While AC has used widely to remove organic substances, AC immobilized in alginate beads has been studied for the removal of heavy metals in water and wastewater (Hassan, Abdel-Mohsen, & Elhadidy, 2014). Hassan et al. investigated three different adsorbent materials namely; KOH-activated carbon-based apricot stone (C), calcium alginate beads (G) and calcium alginate/activated carbon composite beads (GC) for the As removal. The results indicated that GC exhibited the maximum As(V) adsorption (66.7 mg g^{-1} at 30°C) (Hassan, Abdel-Mohsen, & Elhadidy, 2014). Kim et al. studied adsorption equilibrium characteristics of Cu and phenol onto powdered AC, alginate bead and alginate-activated carbon (AAC) bead. The adsorption capacity of Cu(II) onto different adsorbents was in the following order: alginate bead > AAC bead > AC; that of phenol was: AC > AAC bead > alginate bead (Kim, Jin, Park, Kim, & Cho, 2008). Choi et al. produced a novel alginate complex by impregnating synthetic zeolite and powdered activated carbon (PAC) into alginate gel bead and found that the composite could simultaneously remove zinc and toluene from aqueous solution. The maximum adsorption capacity of alginate complex for zinc and toluene obtained from Langmuir adsorption isotherm was 4.3 g kg^{-1} and 13.0 g kg^{-1} , respectively (Choi, Yang, Kim, & Lee, 2009).

3.2.3. Biochar/Ca-alginate composites

Previous studies have indicated that engineered biochar serves as a low-cost AC alternative for adsorption of heavy metals (Ding, Hu, Wan, Wang, & Gao, 2016; Lyu, Gao, He, Zimmerman, Ding, Huang, et al., 2018; Wan et al., 2016; Wan, Wu, He, Zhou, Wang, Bin, & Chen 2017; Wang, Lee, Lehmann, & Gao, 2018). Adsorption of Cd(II) by biochar-alginate bead was studied using batch systems and continuous fixed bed columns and the results indicated that biochar-alginate beads, *Ambrosia trifida* L. var. Trifida biochar-alginate beads (ATLB-AB) can be applied as an eco-friendly and potential adsorbent for the removal of Cd(II) from groundwaters (Roh et al., 2015; Wang et al., 2018b). Do and Lee also synthesized a biochar-alginate capsule to remove lead ions Pb(II) from an aqueous solution. The maximum adsorption capacity for Pb(II) was found to be $263.158 \text{ mg g}^{-1}$ at pH of 5.0 (Do & Lee, 2013).

3.2.4. Graphene oxide/Ca-alginate beads

In the last decade, GO has been studied for the removal of heavy metals, synthetic dyes, and other organic compounds (Bai et al., 2016; Chen, Gao, & Li, 2014; Chen et al., 2015; Zhang, Gao, Cao, & Yang, 2013). However, regeneration and separation of GO from aqueous media are difficult because it disperses so well in water. To solve this problem, several attempts were made to couple magnetic nanoparticles with fabrication of GO composites (Chandra et al., 2010; Liu, Gao, Fang, Wang, & Cao, 2016; Shen et al., 2010; Zhang, Gao, Li, Zhang, & Hardin, 2013; Zhang, Gao, Yao, Xue, & Inyang, 2012). Vu et al. fabricated magnetite GO encapsulated in calcium alginate beads (mGO/beads) to absorb Cr(VI) and As(V) from wastewater (Vu et al., 2017). They found that the mGO/bead maintained its activity in wastewater and exhibited greater adsorption efficiency for both Cr(VI) and As(V) than activated carbon and carbon nanotube. Lv et al. introduced graphene oxide (GO) into alginate gel before mixing with zero-valent iron nanoparticles (Fe_0 NPs) to create Fe_0 NPs embedded graphene oxide alginate beads (Fe@GOA beads), which were further reduced to Fe_0 NPs embedded reduced graphene oxide-alginate beads (Fe@GA beads) (Lv et al., 2017). The Fe@GA beads were examined for Cr(VI) removal. The result showed that 1% of alginate and 1.5-2.0% of Fe_0 by weight performed the best with a maximum adsorption capacity of about 34 mg g^{-1} .

3.2.5. Carbon nanotubes (CNTs)/Ca-alginate beads

CNTs-alginate beads show synergistic effects on removal of heavy metals (Wang, Gao, Zimmerman, & Lee, 2018). Studies have shown that the introduction of carbon nanotubes into alginate can improve the physicochemical properties of alginate-based composites, thereby enhancing its ability to adsorb heavy metals (Wang, Gao, Zimmerman, & Lee, 2018). Li et al. mixed CNTs and SA and added to the CaCl_2 solution to prepare CNTs-CA composites. The results show that the specific surface area and pore size of CA gel is $28 \text{ m}^2 \text{ g}^{-1}$ and $0.06 \text{ cm}^3 \text{ g}^{-1}$, respectively. When combined with CNTs, the high specific surface area and pore size of CNTs can form microchannels in the composites. The specific surface area and pore size of CNTs-CA composites were $76 \text{ m}^2 \text{ g}^{-1}$ and $0.37 \text{ cm}^3 \text{ g}^{-1}$, respectively. Under the same conditions, the adsorption capacity of Cu (II) on CA gel was better than that of CNTs. When the equilibrium concentration was 5 mg L^{-1} , the adsorption capacity was 52.1 mg g^{-1} for CA gel and increased to 67.9 mg g^{-1} for CNTs-CA (Li et al., 2010). Under the same conditions, the adsorption performance of CNTs-CA composites to Cu(II) was significantly higher than that of CNTs.

3.2.6. Other alginate nanocomposites

Alginate nanocomposites have excellent functional properties, biocompatibility and special nano-effects for heavy metal remediation. Googerdchian et al. prepared the natural hydroxyapatite nanoparticles by mechanical activation method, and then compounded the particles with sodium alginate to prepare the granular and film SA/nano-hydroxyapatite composites for adsorption of Pb(II). The SA/nanohydroxyapatite composite membrane exhibited strong Pb(II) adsorption ability (Googerdchian, Moheb, & Emadi, 2012). Soltani et al. entrapped silica nanopowders within calcium alginate and reported that an optimal initial pH of 5.0 was good for Pb(II) adsorption with the maximum adsorption capacity of 83.33 mg g^{-1} (Soltani, Khorramabadi, Khataee, & Jorfi, 2014). The potential of Hal/alginate nanocomposite beads for the removal of Pb(II) in aqueous solutions was investigated, and the Hal/alginate beads removed Pb(II) through ion exchange with Ca(II) followed by coordination with carboxylate groups of alginate, in addition to physisorption on Hal nanotubes (Chiew et al., 2016). Wang, Zhang, Wang, Zhang, and Liu (2014) examined the adsorption behavior of Cu(II) onto the halloysite nanotube-alginate hybrid bead by a continuous fixed bed column adsorption experiment and demonstrated that the adsorption capacity reached 74.13 mg g^{-1} . Lazaridis et al. developed a composite alginate-goethite sorbent material for the removal of trivalent and hexavalent chromium ions from binary aqueous solutions. The sorption capacities for Cr(VI) and Cr(III) increased from 20.5 to 29.5 mg g^{-1} and 20.7 to 25.3 mg g^{-1} , respectively, when temperature increased from 20 to 60°C (Lazaridis & Charalambous, 2005).

3.2.7. Magnetic alginate beads

Several reports documented that magnetic materials fabricated in alginate had excellent performance for the removal of Co(II), Pb(II), Ni(II), Cu(II), Cr(VI), Au(III) (Bakr, Moustafa, Khalil, Yehia, & Motawea, 2015; Bée, Talbot, Abramson, & Dupuis, 2011; Gopalakannan & Viswanathan, 2015). Bée et al. developed a magsorbent by encapsulation of magnetic functionalized nanoparticles in calcium-alginate beads and reported that it was easily collected from aqueous media by using an external magnetic field. The authors concluded that magnetic alginate beads could be efficiently used to remove heavy metals in a water treatment process (Bée et al., 2011). Synthesis of magnetic alginate hybrid beads was also tested for efficient removal of chromium (VI) (Gopalakannan & Viswanathan, 2015). The removal of nickel ions from aqueous solution using magnetic alginate microcapsules was studied and the result indicated that the sorption capacity of nickel increases with increasing pH (Ngomsik, Bee, Siaugue, Cabuil, & Cote, 2006). Metal uptake capacity at low pH is attributed to an

ionic exchange between protons and nickel ions. At higher pH, the adsorption of Ni is pH-dependent and corresponds to a competition between nickel and calcium ions. A new calcium-alginate magnetic sorbent was prepared by an electrostatic extrusion technique with a maximum adsorption capacities of arsenic and copper ions of 6.75 and 60.24 mg g⁻¹, respectively, much higher than those of commercial adsorbents (Lim & Chen, 2007). The introduction of magnetic properties into calcium-alginate beads system combines the high adsorption capacity of calcium-alginate beads and the separation convenience of magnetic materials, offering a viable technique for future applications.

3.2.8. Microorganisms immobilized in Ca-alginate beads

Alginate can be used as an immobilizing carrier to maintain the biological activity of microorganisms and enzymes for the removal of heavy metal ions. A large number of studies have shown that microbial immobilization is effective for treatment of wastewaters with low concentrations of heavy metals to meet discharge standards. Natural polymers, such as cellulose derivatives, alginate, chitosan, and chitin have been used as the matrix for immobilization of microbial cells. These polymers are also known to bind metal ions (Zargar, Asghari, & Dashti, 2015). Arica et al. used calcium alginate to immobilize white rot fungi to adsorb different metal ions in wastewater. The maximum experimental biosorption capacities for entrapped live and dead fungal mycelia of *T. versicolor* were 102.3 mg g⁻¹ and 120.6 mg g⁻¹, respectively (Arica, Kaçar, & Genç, 2001). Then Arica et al. immobilized the basidio spores of *Phanerochaete chrysosporium* in alginate gel beads to remove Pb(II) and Zn(II) ions from artificial wastewater. The results indicated that the maximum biosorption capacity of alginate beads and both immobilized live and heat inactivated fungus were 230, 282 and 355 mg for Pb(II) and 30, 37 and 48 mg for Zn(II) per gram of dry biosorbents, respectively (Yakup Arica, Arpa, Ergene, Bayramoğlu, & Genç, 2003). Arica et al. also immobilized *Funalia trogii* biomass in Ca-alginate gel beads to adsorb Hg(II), Cd(II) and Zn(II) ions. The results indicated that the metal biosorption capacities of the heat-inactivated immobilized *F. trogii* for Hg(II), Cd(II) and Zn(II) were 403.2, 191.6, and 54.0 mg g⁻¹, respectively, while Hg(II), Cd(II) and Zn(II) biosorption capacities of the immobilized live form were 333.0, 164.8 and 42.1 mg g⁻¹, respectively (Arica et al., 2001).

Bayramoglu et al. entrapped a white rot fungus species (*Lentinus sajor-caju*) biomass into alginate gel via a liquid curing method in the presence of Ca(II) to remove Cd(II) in a batch system. The maximum experimental biosorption capacities for entrapped live and dead fungal mycelia of *L. sajor-caju* were found to be 104.8 and 123.5 mg g⁻¹, respectively. The

Table 3. Alginate-based composites for the removal of antibiotics from aqueous solution.

Adsorbent	Adsorbate	Adsorption capacity (mg g ⁻¹)	pH	Temperature (°C)	Ref.
EPCs@CMCS gel beads	Tetracycline	136.9	6.0	25	(He et al., 2016)
CMCS gel beads	Tetracycline	9.47	6.0	25	(He et al., 2016)
SA/graphene oxide beads	Ciprofloxacin	86.12	—	25	(Fei et al., 2016)
GO/CA fibers	Ciprofloxacin	39.06	5.9	Room T	(Wu et al., 2013)
GO/CA fibers	Tetracycline	131.6	6.0	25	(Zhu et al., 2018)
Alginate/graphene double network hydrogel	Tetracycline	290.70	8.0	25	(Zhuang et al., 2017)
Alginate/graphene double network hydrogel	Ciprofloxacin	344.83	8.0	25	(Zhuang et al., 2017)

kinetics of cadmium biosorption were fast, with approximately 85% of biosorption taking place within 30 min (Bayramoglu, Denizli, Bektas, & Yakup Arica, 2002). Kacar et al. immobilized basidiospores of *Phanerochaete chrysosporium* into Ca-alginate beads via entrapment, and the beads incubated for vegetation at 30 °C for 5 days. The alginate beads and both entrapped live and heat inactivated fungal mycelia of *P. chrysosporium* were used for the removal of Hg(II) and Cd(II) ions from aqueous solution in the concentrations range of 30-500 mg L⁻¹. The adsorption capacities of the immobilized live and heat inactivated fungal biomass reached 66.1 and 112.6 mg g⁻¹ for mercury and 50.0 and 85.4 mg g⁻¹ for cadmium, respectively (Kaçar et al., 2002).

A large body of evidence shows that algae can effectively absorb and enrich heavy metals in sewage (Prakasham, Merrie, Sheela, Saswathi, & Ramakrishna, 1999; Rangsayatorn, Pokethitiyook, Upatham, & Lanza, 2004). The enrichment factor can reach several thousand times with an enrichment capacity up to 10% of its dry weight. Immobilization can increase the resistance of algal cells to heavy metal toxicity. Some scholars studied the removal rate of the immobilization system and compared heavy metal adsorption with dead and live algae. Prakasham et al. indicated that immobilized microbial on sodium alginate effectively removed hexavalent chromium at pH =2. The adsorbed metal ions can be desorbed by dilute sulfuric acid (Prakasham et al., 1999). Rangsayatorn et al. studied biosorption of cadmium by immobilized *Spirulina platensis* on alginate gel and silica gel and found that the maximum biosorption capacities for alginate immobilized cells and silica immobilized cells were 70.92 and 36.63 mg g⁻¹ biomass, respectively (Rangsayatorn et al., 2004).

3.3. Antibiotics

As an emerging pollutant, antibiotics pose a great threat to human health and the environment in spite of their low concentrations in the aquatic environment (Kümmerer, 2009). Traditional wastewater treatment

processes do not normally work well with most antibiotics. Therefore, alginate-based composites have been investigated as a new adsorbent to remediate antibiotic pollution (Table 3).

3.3.1. Magnetic alginate beads

There are a few reports about removal of antibiotics in water using magnetic alginate beads. Kim et al. found that nZVI-immobilized alginate beads removed trichloroethylene (TCE) from aqueous solution by >99.8% (Kim et al.). Konwar et al. prepared magnetic alginate-Fe₃O₄ hydrogel fibers using a simple laboratory micropipette and found that the magnetic alginate-Fe₃O₄ hydrogel fibers were effective in adsorption of ciprofloxacin hydrochloride, while the blank alginate hydrogel fiber did not show any significant adsorption. Anion exchange mechanism mainly controlled the adsorption of antibiotic and the formation of hydrogen bonding between the antibiotic and magnetic alginate beads can also result in the increase of adsorption capacity (Konwar, Gogoi, & Chowdhury, 2015). Such magnetic alginate-Fe₃O₄ hydrogel fibers can serve as a simple and cost-effective probe for adsorption/separation of antibiotics, with additional advantages of being easy to fabricate and having high thermal stability and mechanical strength (Konwar et al., 2015).

3.3.2. Graphene oxide/Ca-alginate beads

Wu et al. prepared a new biocomposite fibers by a wet spinning method using graphene oxide doped calcium alginate (GO/CA) (Wu et al., 2013). The comparative study indicated that the addition of GO could significantly improve the adsorption capacities of ciprofloxacin onto GO/CA fibers. The encapsulation of GO into SA made the materials more porous, provided π - π electron donor-acceptor interactions between graphene oxide and ciprofloxacin, and introduced C=O bonds into the composite (Fei, Li, Han, & Ma, 2016). Zhu et al. prepared graphene oxide/calcium alginate (GO/CA) composite fibers via a freeze-drying method using calcium chloride as a cross-linking reagent between graphene oxide and sodium alginate. The maximum tetracycline adsorption capacity of the GO/CA composite fibers predicted by the Langmuir model reached 131.6 mg g⁻¹. The mechanism of adsorption was the hydrogen bonding and π - π interaction which serve as predominant contributions to the significantly enhanced adsorption capability (Zhu, Chen, Liu, & Li, 2018). To improve the adsorption capacity of double network hydrogel, physical and chemical modifications were made on alginate/graphene double network hydrogel. The modified hydrogel featured a more porous structure and more functional groups than that before modification. The maximum adsorption capacities of

Table 4. Alginate-based composites for the removal of other pollutants from aqueous solution.

Adsorbent	Adsorbate	Adsorption capacity (mg g ⁻¹)	pH	Temperature (°C)	Ref.
MnO ₂ -alginate beads	Sr(II)	102.0	—	25	(Hong et al., 2017)
Alginate/Fe ₃ O ₄ composite	Sr(II)	12.5	6.0	25	(Hong et al., 2016)
Calcium alginates	Yi (III)	97.087	6.0	24	(Khotimchenko et al., 2015)
Sodium alginates	Yi (III)	181.818	6.0	24	(Khotimchenko et al., 2015)
Zirconium alginate beads	Fluoride	28.05	2.0	30	(Qiusheng et al., 2015)
Hydrous ferric oxide doped alginate beads	Fluoride	8.90	7.0	Ambient T	(Sujana et al., 2013)
n-HApAlgLa Composite Beads	Fluoride	4.536	—	Room T	(Pandi & Viswanathan, 2015)
n-HApAlgLa Composite Beads	Fluoride	4.916	—	Room T	(Pandi & Viswanathan, 2015)
n-HApAlgLa Composite Beads	Fluoride	5.271	—	Room T	(Pandi & Viswanathan, 2015)
Iron oxide loaded CA beads	La(III)	123.5	5.0	25	(Wu et al., 2010)
Magnetic alginate beads	La(III)	250	4.0	25	(Elwakeel et al., 2017)
nZnO-entrapped alginate (alginate-nZnO) beads	H ₂ S	—	—	—	(Gautam, Rahman, Bezbaruah, & Borhan, 2016; Gautam et al., 2017)
nZnO-entrapped alginate (alginate-nZnO) beads	Greenhouse gases'	—	—	—	(Gautam et al., 2016; Gautam et al., 2017)
Silver nanoparticle-alginate composite beads	Disinfecting bacteria	—	—	—	(Lin et al., 2013)
Ammonium molybdophosphate-CA composite	Rb(I)	49.57	3.5–4.5	25	(Ye et al., 2009)
Ammonium molybdophosphate-CA composite	Cs(I)	91.70	3.5–4.5	25	(Ye et al., 2009)
Alginate/Iron (III) Chloride Capsules	Phosphate	—	—	20	(Siwek et al., 2016)
Electrochemically modified biochar CA beads	Phosphate	214.2	4.0	10	(Jung et al., 2017)
Electrochemically modified biochar CA beads	Phosphate	292.98	4.0	20	(Jung et al., 2017)
Electrochemically modified biochar CA beads	Phosphate	342.67	4.0	30	(Jung et al., 2017)

tetracycline and ciprofloxacin on GAD were 290.70 and 344.83 mg g⁻¹, respectively (Zhuang, Yu, Ma, & Chen, 2017).

3.4. Other environmental applications

In addition to dyes, heavy metals and antibiotics, alginate-based composites have also been used for remediation of other pollutants (Table 4). For example, MnO₂-alginate beads and alginate/Fe₃O₄ composite were used to remove Sr(II) from seawater (Hong et al., 2016; Hong et al., 2017). Removal of some rare earth elements and radionuclides from water was reported using different alginate-based composites (Elwakeel, Daher, Abd

El-Fatah, Abd El Monem, & Khalil, 2017; Khotimchenko, Kovalev, Khozhaenko, & Khotimchenko, 2015; Wu, Zhao, Zhang, Wu, & Yang, 2010; Ye et al., 2009). Besides removal of cations, alginate-based nanomaterial composites were also studied for removal of some anions in water (Pandi & Viswanathan, 2015; Qiusheng, Xiaoyan, Jin, Jing, & Xuegang, 2015; Siwek, Bartkowiak, Włodarczyk, & Sobecka, 2016; Sujana, Mishra, & Acharya, 2013). Electrochemically modified biochar calcium-alginate beads was also applied to remove phosphate under batch and continuous fixed-bed column conditions (Jung, Jeong, Choi, Ahn, & Lee, 2017). With continued research and development, alginate-based nanocomposites will be increasingly applied to various fields of environmental remediation in the future.

4. Conclusions and future perspectives

Alginate-based composites have been fabricated by encapsulating various materials, such as AC, biochar, GO, CNT, magnetic and nanomaterials, as well as microorganisms into alginate hydrogels/beads with demonstrated utility as a biosorbent for environmental application. These composites offer great potential for real world applications for the removal of dyes, heavy metals, antibiotics, and other pollutants from water and wastewater. While alginate-based composites typically exhibit enhanced physical/mechanical properties over pure alginate gels or beads, the biocompatibility of alginate coupled with new properties of the encapsulated materials often lend synergetic functionalities of the new derivatives. Among these are ease of separation and regeneration of the biosorbent for wastewater treatment, reduced environmental risk of the encapsulated materials such as nanomaterials, and optimized bioprocesses of microbial immobilization technology.

Future environmental applications of alginate-based composites, which will likely evolve considerably, require further research on the mechanisms involved in pollutant uptakes by various alginate-based composites should be emphasized. Comparative studies among the composites under controlled laboratory settings can be conducted. Another research need is to optimize existing and engineer new alginate-based composites with distinct properties and novel functionalities for targeted applications. While new techniques, such as genetic engineering will likely advance the design and creation of new composite, more effective combination of materials to improve the adsorption capacity and mechanical, chemical and thermal stability when crosslinking with alginate beads can still be explored in a systematic fashion. Although not a focus in this paper, encapsulation strategies can be directly relevant to the production of new alginate-based composites to meet different applications. Parallel to this research need is

the investigation into what chemically modifies alginate, which will benefit alginate-based composites. Because alginate contains abundant free hydroxyl and carboxyl groups distributed along the polymer chain backbone, chemical modifications of these two types of functional groups that alter the characteristics of alginate can be a future research area to fabricate new alginate-based composites for targeted environmental applications.

Most of the reported studies described in this review were conducted in a laboratory setting. Scaling up for real world applications in an uncontrolled environment requires further testing as the characteristics and mechanical/thermal stability of alginate-based composites may change. For example, the dynamic swelling of alginate-based composites in soil would be influenced by varying soil physical and chemical properties in the field. Therefore, the performance of alginate-based composites under field conditions can be explored further. Such work can also be realized in studies involving multicomponent solutions and/or complex effluents under dynamic conditions to mimic the field conditions. Potential risks associated with nanomaterials or metals encapsulated in alginate should also be evaluated when considering applications in ambient soil and water environments.

In attempts to test alginate-based composites in large-scale applications, cost and effectiveness are the important factors to be evaluated. Because microbial treatment is potentially less harmful to the environment and more cost-effective than chemical treatment or physical removal of soil or water to an off-site location, encapsulation of microorganisms in alginate beads as a carrier will be cost effective. Investigating the further effectiveness of immobilization technology, particularly in the areas of microbial survival, binding, and transport, as well as *in-situ* bioremediation of contaminated soil or groundwater will evolve alginate based technology and make it more competitive for use in remediation applications.

Acknowledgments

The authors would like to thank Dr. Elizabeth George and two anonymous reviewers for their comments and suggestions. The views expressed in this article are those of the authors and do not necessarily reflect the views or policies of the funding agencies or the U.S. Environmental Protection Agency.

Funding

This work was financially supported by the National Key Research and Development Program of China (2016YFC0502602), the Key Agriculture R & D Program of Guizhou Province (NZ [2013]3012), the International Scientific and Technological Cooperation Project of Guizhou Province (G[2012]7050), the High-Level Overseas Talent Innovation

and Entrepreneurship Project of Guizhou Province and the Opening Fund of State Key Laboratory of Environmental Geochemistry (SKLEG2018907).

ORCID

Bing Wang  <http://orcid.org/0000-0002-2773-2370>

Bin Gao  <http://orcid.org/0000-0003-3769-0191>

References

- Ahmad, M., Rajapaksha, A. U., Lim, J. E., Zhang, M., Bolan, N., Mohan, D., ... Ok, Y. S. (2014). Biochar as a sorbent for contaminant management in soil and water: A review. *Chemosphere*, 99, 19–33. doi:10.1016/j.chemosphere.2013.10.071
- Akhtar, M. F., Hanif, M., Ranjha, N. M. (2016). Methods of synthesis of hydrogels: A review. *Saudi Pharmaceutical Journal*, 24(5), 554–559.
- Albarelli, J. Q., Santos, D. T., Murphy, S., & Oelgemöller, M. (2009). Use of Ca-alginate as a novel support for TiO₂ immobilization in methylene blue decolorisation. *Water Science and Technology*, 60(4), 1081–1087.
- Algothmi, W. M., Bandaru, N. M., Yu, Y., Shapter, J. G., & Ellis, A. V. (2013). Alginate–graphene oxide hybrid gel beads: An efficient copper adsorbent material. *Journal of Colloid and Interface Science*, 397, 32–38. doi:10.1016/j.jcis.2013.01.051
- Ali, I. (2012). New generation adsorbents for water treatment. *Chemical reviews*, 112, 5073–5091.
- Ali, I., Al-Othman, Z. A., & Al-Warthan, A. (2016a). Molecular uptake of congo red dye from water on iron composite nano particles. *Journal of Molecular Liquids*, 224, 171–176.
- Ali, I., Al-Othman, Z. A., & Al-Warthan, A. (2016b). Removal of sebumeton herbicide from water on composite nanoadsorbent. *Desalination and Water Treatment*, 57, 10409–10421.
- Ali, I., Al-Othman, Z. A., & Sanagi, M. M. (2015). Green synthesis of iron nano-impregnated adsorbent for fast removal of fluoride from water. *Journal of Molecular Liquids*, 211, 457–465.
- Ali, I., & Gupta, V. (2006). Advances in water treatment by adsorption technology. *Nature protocols*, 1, 2661–2667.
- Allaboun, H., Fares, M. M., & Abu Al-Rub, F. A. (2016). Removal of uranium and associated contaminants from aqueous solutions using functional carbon nanotubes-sodium alginate conjugates. *Minerals*, 6(1), 9. doi:10.3390/min6010009
- An, T., Zhou, L., Li, G., Fu, J., & Sheng, G. (2008). Recent patents on immobilized micro-organism technology and its engineering application in wastewater treatment. *Recent Patents on Engineering*, 2(1), 28–35. doi:10.2174/187221208783478543
- Annadurai, G., Juang, R.-S., & Lee, D.-J. (2002). Factorial design analysis for adsorption of dye on activated carbon beads incorporated with calcium alginate. *Advances in Environmental Research*, 6(2), 191–198. doi:10.1016/S1093-0191(01)00050-8
- Aravindhan, R., Fathima, N. N., Rao, J. R., & Nair, B. U. (2007). Equilibrium and thermodynamic studies on the removal of basic black dye using calcium alginate beads. *Colloids and Surfaces A: Physicochemical and Engineering Aspects*, 299(1-3), 232–238. doi:10.1016/j.colsurfa.2006.11.045

- Arica, M. Y., Bayramoglu, G., Yilmaz, M., Bektaş, S., & Genç, O. (2004). Biosorption of Hg^{2+} , Cd^{2+} , and Zn^{2+} by Ca-alginate and immobilized wood-rotting fungus *Funalia trogii*. *Journal of Hazardous Materials*, 109(1-3), 191–199.
- Arica, M. Y., Kaçar, Y., & Genç, Ö. (2001). Entrapment of white-rot fungus *Trametes versicolor* in Ca-alginate beads: Preparation and biosorption kinetic analysis for cadmium removal from an aqueous solution. *Bioresource Technology*, 80(2), 121–129. doi:10.1016/S0960-8524(01)00084-0
- Babel, S., & Kurniawan, T. A. (2003). Low-cost adsorbents for heavy metals uptake from contaminated water: A review. *Journal of Hazardous Materials*, 97(1-3), 219–243.
- Bai, J., Sun, H. M., Yin, X. J., Yin, X. Q., Wang, S. S., & Creamer, A. E. (2016). Oxygen-content-controllable graphene oxide from electron-beam-irradiated graphite: Synthesis, characterization, and removal of aqueous lead [Pb(II)]. *ACS Applied Materials & Interfaces*, 8, 25289–25296. doi:10.1021/acsami.6b08059
- Bajpai, J., Shrivastava, R., & Bajpai, A. K. (2004). Dynamic and equilibrium studies on adsorption of Cr(VI) ions onto binary bio-polymeric beads of cross linked alginate and gelatin. *Colloids and Surfaces A: Physicochemical and Engineering Aspects*, 236(1-3), 81–90. doi:10.1016/j.colsurfa.2004.01.021
- Bakr, A.-S., A., Moustafa, Y. M., Khalil, M. M., Yehia, M. M., & Motawea, E. A. (2015). Magnetic nanocomposite beads: Synthesis and uptake of Cu(II) ions from aqueous solutions. *Canadian Journal of Chemistry*, 93(3), 289–296. doi:10.1139/cjc-2014-0282
- Basu, H., Singhal, R., Pimple, M., & Reddy, A. (2015). Arsenic removal from groundwater by goethite impregnated calcium alginate beads. *Water, Air, & Soil Pollution*, 226, 22.
- Bayramoglu, G., Denizli, A., Bektaş, S., & Yakup Arica, M. (2002). Entrapment of lentinus sajor-caju into Ca-alginate gel beads for removal of Cd(II) ions from aqueous solution: Preparation and biosorption kinetics analysis. *Microchemical Journal*, 72(1), 63–76. doi:10.1016/S0026-265X(01)00151-5
- Bayramoğlu, G., Tuzun, I., Celik, G., Yilmaz, M., & Arica, M. Y. (2006). Biosorption of mercury(II), cadmium(II) and lead(II) ions from aqueous system by microalgae *Chlamydomonas reinhardtii* immobilized in alginate beads. *International Journal of Mineral Processing*, 81(1), 35–43. doi:10.1016/j.minpro.2006.06.002
- Bayramoğlu, G., & Yakup Arica, M. (2009). Construction a hybrid biosorbent using *Scenedesmus quadricauda* and ca-alginate for biosorption of Cu(II), Zn(II) and Ni(II): Kinetics and equilibrium studies. *Bioresource Technology*, 100(1), 186–193. doi:10.1016/j.biortech.2008.05.050
- Bée, A., Talbot, D., Abramson, S., & Dupuis, V. (2011). Magnetic alginate beads for Pb(II) ions removal from wastewater. *Journal of Colloid and Interface Science*, 362(2), 486–492.
- Belhouchat, N., Zaghouane-Boudiaf, H., & Viseras, C. (2017). Removal of anionic and cationic dyes from aqueous solution with activated organo-bentonite/sodium alginate encapsulated beads. *Applied Clay Science*, 135, 9–15. doi:10.1016/j.clay.2016.08.031
- Benhouria, A., Islam, M. A., Zaghouane-Boudiaf, H., Boutahala, M., & Hameed, B. (2015). Calcium alginate–bentonite–activated carbon composite beads as highly effective adsorbent for methylene blue. *Chemical Engineering Journal*, 270, 621–630. doi:10.1016/j.cej.2015.02.030
- Burakov, A. E., Galunin, E. V., Burakova, I. V., Kucherova, A. E., Agarwal, S., Tkachev, A. G., & Gupta, V. K. (2018). Adsorption of heavy metals on conventional and nano-structured materials for wastewater treatment purposes: A review. *Ecotoxicology and Environmental Safety*, 148, 702–712. doi:10.1016/j.ecoenv.2017.11.034

- Cai, C.-X., Xu, J., Deng, N.-F., Dong, X.-W., Tang, H., Liang, Y., ... Li, Y.-Z. (2016). A novel approach of utilization of the fungal conidia biomass to remove heavy metals from the aqueous solution through immobilization. *Scientific Reports*, 6, 36546.
- Cai, T., Chen, L., Ren, Q., Cai, S., & Zhang, J. (2011). The biodegradation pathway of triethylamine and its biodegradation by immobilized *Arthrobacter protophormiae* cells. *Journal of Hazardous Materials*, 186(1), 59–66. doi:10.1016/j.jhazmat.2010.10.007
- Cavallaro, G., Gianguzza, A., Lazzara, G., Milioto, S., & Piazzese, D. (2013). Alginate gel beads filled with halloysite nanotubes. *Applied Clay Science*, 72, 132–137. doi:10.1016/j.clay.2012.12.001
- Chan, L. W., Jin, Y., & Heng, P. W. S. (2002). Cross-linking mechanisms of calcium and zinc in production of alginate microspheres. *International Journal of Pharmaceutics*, 242(1–2), 255–258. doi:10.1016/S0378-5173(02)00169-2
- Chandra, V., Park, J., Chun, Y., Lee, J. W., Hwang, I.-C., & Kim, K. S. (2010). Water-dispersible magnetite-reduced graphene oxide composites for arsenic removal. *ACS Nano*, 4(7), 3979–3986. doi:10.1021/nn1008897
- Chen, H., Gao, B., & Li, H. (2014). Functionalization, pH, and ionic strength influenced sorption of sulfamethoxazole on graphene. *Journal of Environmental Chemical Engineering*, 2(1), 310–315. doi:10.1016/j.jece.2013.12.021
- Chen, H., Gao, B., & Li, H. (2015). Removal of sulfamethoxazole and ciprofloxacin from aqueous solutions by graphene oxide of sulfamethoxazole and ciprofloxacin from aqueous solutions by graphene oxide. *Journal of Hazardous Materials*, 282, 201–207.
- Chen, J.-P., & Lin, Y.-S. (2007). Decolorization of azo dye by immobilized *Pseudomonas luteola* entrapped in alginate–silicate sol–gel beads. *Process Biochemistry*, 42(6), 934–942. doi:10.1016/j.procbio.2007.03.001
- Chiew, C. S. C., Yeoh, H. K., Pasbakhsh, P., Krishnaiah, K., Poh, P. E., Tey, B. T., & Chan, E. S. (2016). Halloysite/alginate nanocomposite beads: Kinetics, equilibrium and mechanism for lead adsorption. *Applied Clay Science*, 119, 301–310. doi:10.1016/j.clay.2015.10.032
- Ching, S. H., Bansal, N., & Bhandari, B. (2017). Alginate gel particles—A review of production techniques and physical properties. *Critical Reviews in Food Science and Nutrition*, 57(6), 1133–1152. doi:10.1080/10408398.2014.965773
- Choi, J.-W., Yang, K.-S., Kim, D.-J., & Lee, C. E. (2009). Adsorption of zinc and toluene by alginate complex impregnated with zeolite and activated carbon. *Current Applied Physics*, 9(3), 694–697. doi:10.1016/j.cap.2008.06.008
- Cohen, Y. (2001). Biofiltration—the treatment of fluids by microorganisms immobilized into the filter bedding material: A review. *Bioresource Technology*, 77(3), 257–274. doi:10.1016/S0960-8524(00)00074-2
- Covarrubias, S. A., De-Bashan, L. E., Moreno, M., & Bashan, Y. (2012). Alginate beads provide a beneficial physical barrier against native microorganisms in wastewater treated with immobilized bacteria and microalgae. *Applied Microbiology and Biotechnology*, 93(6), 2669–2680. doi:10.1007/s00253-011-3585-8
- Daâssi, D., Rodríguez-Couto, S., Nasri, M., & Mechichi, T. (2014). Biodegradation of textile dyes by immobilized laccase from *Corioliopsis gallica* into Ca-alginate beads. *International Biodeterioration & Biodegradation*, 90, 71–78. doi:10.1016/j.ibiod.2014.02.006
- De-Bashan, L. E., Moreno, M., Hernandez, J.-P., & Bashan, Y. (2002). Removal of ammonium and phosphorus ions from synthetic wastewater by the microalgae *Chlorella vulgaris* coimmobilized in alginate beads with the microalgae growth-promoting bacterium *Azospirillum brasilense*. *Water Research*, 36(12), 2941–2948. doi:10.1016/S0043-1354(01)00522-X

- Devi, G. K., Kumar, P. S., & Kumar, K. S. (2016). Green synthesis of novel silver nanocomposite hydrogel based on sodium alginate as an efficient biosorbent for the dye wastewater treatment: Prediction of isotherm and kinetic parameters. *Desalination and Water Treatment*, 57, 27686–27699.
- Ding, Z. H., Hu, X., Morales, V. L., & Gao, B. (2014). Filtration and transport of heavy metals in graphene oxide enabled sand columns. *Chemical Engineering Journal*, 257, 248–252. doi:10.1016/j.cej.2014.07.034
- Ding, Z. H., Hu, X., Wan, Y. S., Wang, S. S., & Gao, B. (2016). Removal of lead, copper, cadmium, zinc, and nickel from aqueous solutions by alkali-modified biochar: Batch and column tests. *Journal of Industrial and Engineering Chemistry*, 33, 239–245. doi:10.1016/j.jiec.2015.10.007
- Do, X. H., & Lee, B. K. (2013). Removal of Pb^{2+} using a biochar-alginate capsule in aqueous solution and capsule regeneration. *Journal of Environmental Management*, 131, 375–382. doi:10.1016/j.jenvman.2013.09.045
- Elwakeel, K. Z., Daher, A., Abd El-Fatah, A., Abd El Monem, H., & Khalil, M. M. (2017). Biosorption of lanthanum from aqueous solutions using magnetic alginate beads. *Journal of Dispersion Science and Technology*, 38(1), 145–151. doi:10.1080/01932691.2016.1146617
- Enayatzamir, K., Alikhani, H., Yakhchali, B., Tabandeh, F., & Rodríguez-Couto, S. (2010). Decolouration of azo dyes by *Phanerochaete chrysosporium* immobilised into alginate beads. *Environmental Science and Pollution Research*, 17(1), 145–153. doi:10.1007/s11356-009-0109-5
- Escudero, C., Fiol, N., Villaescusa, I., & Bollinger, J.-C. (2009). Arsenic removal by a waste metal (hydr)oxide entrapped into calcium alginate beads. *Journal of Hazardous Materials*, 164(2-3), 533–541. doi:10.1016/j.jhazmat.2008.08.042
- Fan, J., Shi, Z., Lian, M., Li, H., & Yin, J. (2013). Mechanically strong graphene oxide/sodium alginate/polyacrylamide nanocomposite hydrogel with improved dye adsorption capacity. *Journal of Materials Chemistry A*, 1(25), 7433–7443. doi:10.1039/c3ta10639j
- Fang, J., Gao, B., Mosa, A., & Zhan, L. (2017). Chemical activation of hickory and peanut hull hydrochars for removal of lead and methylene blue from aqueous solutions. *Chemical Speciation and Bioavailability*, 29(1), 197–204. doi:10.1080/09542299.2017.1403294
- Fang, J., Gao, B., Zimmerman, A. R., Ro, K. S., & Chen, J. J. (2016). Physically (CO_2) activated hydrochars from hickory and peanut hull: Preparation, characterization, and sorption of methylene blue, lead, copper, and cadmium. *RSC Advances*, 6(30), 24906–24911. doi:10.1039/C6RA01644H
- Fang, J., Zhan, L., Ok, Y. S., & Gao, B. (2018). Minireview of potential applications of hydrochar derived from hydrothermal carbonization of biomass. *Journal of Industrial and Engineering Chemistry*, 57, 15–21. doi:10.1016/j.jiec.2017.08.026
- Fei, Y., Li, Y., Han, S., & Ma, J. (2016). Adsorptive removal of ciprofloxacin by sodium alginate/graphene oxide composite beads from aqueous solution. *Journal of Colloid and Interface Science*, 484, 196–204. doi:10.1016/j.jcis.2016.08.068
- Fomina, M., & Gadd, G. M. (2014). Biosorption: Current perspectives on concept, definition and application. *Bioresource Technology*, 160, 3–14. doi:10.1016/j.biortech.2013.12.102
- Fu, F., & Wang, Q. (2011). Removal of heavy metal ions from wastewaters: A review. *Journal of Environmental Management*, 92(3), 407–418.
- Gautam, D. P., Rahman, S., Bezbaruah, A. N., & Borhan, M. S. (2016). Evaluation of calcium alginate entrapped nano zinc oxide to reduce gaseous emissions from liquid dairy manure. *Applied Engineering in Agriculture*, 32, 89–102.

- Gautam, D. P., Rahman, S., Fortuna, A.-M., Borhan, M. S., Saini-Eidukat, B., & Bezbaruah, A. N. (2017). Characterization of zinc oxide nanoparticle (NZNO) alginate beads in reducing gaseous emission from swine manure. *Environmental Technology*, 38(9), 1061–1074. doi:10.1080/09593330.2016.1217056
- Gok, C., & Aytas, S. (2009). Biosorption of uranium(VI) from aqueous solution using calcium alginate beads. *Journal of Hazardous Materials*, 168(1), 369–375. doi:10.1016/j.jhazmat.2009.02.063
- Gong, J.-L., Wang, B., Zeng, G.-M., Yang, C.-P., Niu, C.-G., Niu, Q.-Y., ... Liang, Y. (2009). Removal of cationic dyes from aqueous solution using magnetic multi-wall carbon nanotube nanocomposite as adsorbent. *Journal of Hazardous Materials*, 164(2-3), 1517–1522. doi:10.1016/j.jhazmat.2008.09.072
- Googerdchian, F., Moheb, A., & Emadi, R. (2012). Lead sorption properties of nanohydroxyapatite–alginate composite adsorbents. *Chemical Engineering Journal*, 200, 471–479. doi:10.1016/j.cej.2012.06.084
- Gopalakannan, V., & Viswanathan, N. (2015). Synthesis of magnetic alginate hybrid beads for efficient chromium (VI) removal. *International Journal of Biological Macromolecules*, 72, 862–867. doi:10.1016/j.ijbiomac.2014.09.024
- Gotoh, T., Matsushima, K., & Kikuchi, K.-I. (2004a). Adsorption of Cu and Mn on covalently cross-linked alginate gel beads. *Chemosphere*, 55(1), 57–64.
- Gotoh, T., Matsushima, K., & Kikuchi, K.-I. (2004b). Preparation of alginate-chitosan hybrid gel beads and adsorption of divalent metal ions. *Chemosphere*, 55(1), 135–140.
- Gupta, V. K., & Ali, I. (2012). *Environmental water: Advances in treatment, remediation and recycling*; Newnes.
- Gupta, V. K., Carrott, P. J. M., Ribeiro Carrott, M. M. L. & Suhas. (2009). Low-cost adsorbents: Growing approach to wastewater treatment: A review. *Critical Reviews in Environmental Science and Technology*, 39, 783–842.
- Gupta, V. K., Nayak, A., Agarwal, S., & Tyagi, I. (2014). Potential of activated carbon from waste rubber tire for the adsorption of phenolics: Effect of pre-treatment conditions. *Journal of Colloid and Interface Science*, 417, 420–430.
- Gupta, V. K., & Saleh, T. A. (2013). Sorption of pollutants by porous carbon, carbon nanotubes and fullerene—an overview. *Environmental Science and Pollution Research*, 20, 2828–2843.
- Gupta, V. K., Kumar, R., Nayak, A., Saleh, T. A., & Barakat, M. A. (2013). Adsorptive removal of dyes from aqueous solution onto carbon nanotubes: A review. *Advances in Colloid and Interface Science*, 193-194, 24–34. doi:10.1016/j.cis.2013.03.003
- Gupta, V. K. & Suhas. (2009). Application of low-cost adsorbents for dye removal: A review. *Journal of Environmental Management*, 90, 2313–2342.
- Hassan, A., Abdel-Mohsen, A., & Elhadidy, H. (2014). Adsorption of arsenic by activated carbon, calcium alginate and their composite beads. *International Journal of Biological Macromolecules*, 68, 125–130. doi:10.1016/j.ijbiomac.2014.04.006
- Hassan, A., Abdel-Mohsen, A., & Fouda, M. M. (2014). Comparative study of calcium alginate, activated carbon, and their composite beads on methylene blue adsorption. *Carbohydrate Polymers*, 102, 192–198. doi:10.1016/j.carbpol.2013.10.104
- Hassani, A., Soltani, R. D. C., Karaca, S., & Khataee, A. (2015). Preparation of montmorillonite–alginate nanobiocomposite for adsorption of a textile dye in aqueous phase: Isotherm, kinetic and experimental design approaches. *Journal of Industrial and Engineering Chemistry*, 21, 1197–1207. doi:10.1016/j.jiec.2014.05.034
- He, J., Dai, J., Xie, A., Tian, S., Chang, Z., Yan, Y., & Huo, P. (2016). Preparation of macroscopic spherical porous carbons@ carboxymethylcellulose sodium gel beads and

- application for removal of tetracycline. *RSC Advances*, 6(87), 84536–84546. doi:10.1039/C6RA14877H
- Hong, H.-J., Jeong, H. S., Kim, B.-G., Hong, J., Park, I.-S., Ryu, T., ... Ryu, J. (2016). Highly stable and magnetically separable alginate/Fe₃O₄ composite for the removal of strontium (Sr) from seawater. *Chemosphere*, 165, 231–238. doi:10.1016/j.chemosphere.2016.09.034
- Hong, H.-J., Kim, B.-G., Hong, J., Ryu, J., Ryu, T., Chung, K.-S., ... Park, I.-S. (2017). Enhanced Sr adsorption performance of mno₂-alginate beads in seawater and evaluation of its mechanism. *Chemical Engineering Journal*, 319, 163–169. doi:10.1016/j.cej.2017.02.132
- Idris, A., Ismail, N. S. M., Hassan, N., Misran, E., & Ngomsik, A.-F. (2012). Synthesis of magnetic alginate beads based on maghemite nanoparticles for Pb(II) removal in aqueous solution. *Journal of Industrial and Engineering Chemistry*, 18(5), 1582–1589. doi:10.1016/j.jiec.2012.02.018
- Inal, M., & Erduran, N. (2015). Removal of various anionic dyes using sodium alginate/poly(N-vinyl-2-pyrrolidone) blend hydrogel beads. *Polymer Bulletin*, 72, 1735–1752. doi:10.1007/s00289-015-1367-7
- Inyang, M., Gao, B., Yao, Y., Xue, Y., Zimmerman, A. R., Pullammanappallil, P., & Cao, X. (2012). Removal of heavy metals from aqueous solution by biochars derived from anaerobically digested biomass. *Bioresource Technology*, 110, 50–56. doi:10.1016/j.biortech.2012.01.072
- Inyang, M., Gao, B., Zimmerman, A., Zhang, M., & Chen, H. (2014). Synthesis, characterization, and dye sorption ability of carbon nanotube–biochar nanocomposites. *Chemical Engineering Journal*, 236, 39–46. doi:10.1016/j.cej.2013.09.074
- Inyang, M. I., Gao, B., Yao, Y., Xue, Y., Zimmerman, A., Mosa, A., ... Cao, X. (2016). A review of biochar as a low-cost adsorbent for aqueous heavy metal removal. *Critical Reviews in Environmental Science and Technology*, 46(4), 406–433. doi:10.1080/10643389.2015.1096880
- Jeon, C., & Cha, J.-H. (2015). Removal of nickel ions from industrial wastewater using immobilized sericite beads. *Journal of Industrial and Engineering Chemistry*, 24, 107–112. doi:10.1016/j.jiec.2014.09.016
- Jeon, Y. S., Lei, J., & Kim, J.-H. (2008). Dye adsorption characteristics of alginate/polyaspartate hydrogels. *Journal of Industrial and Engineering Chemistry*, 14(6), 726–731. doi:10.1016/j.jiec.2008.07.007
- Jiao, C., Xiong, J., Tao, J., Xu, S., Zhang, D., Lin, H., & Chen, Y. (2016). Sodium alginate/graphene oxide aerogel with enhanced strength–toughness and its heavy metal adsorption study. *International Journal of Biological Macromolecules*, 83, 133–141. doi:10.1016/j.ijbiomac.2015.11.061
- Jiao, L., Qi, P., Liu, Y., Wang, B., & Shan, L. (2015). Fe₃O₄ nanoparticles embedded sodium alginate/PVP/calcium gel composite for removal of Cd²⁺. *Journal of Nanomaterials*, 16, 257. doi:10.1155/2015/940985
- Jung, K.-W., Jeong, T.-U., Choi, J.-W., Ahn, K.-H., & Lee, S.-H. (2017). Adsorption of phosphate from aqueous solution using electrochemically modified biochar calcium-alginate beads: Batch and fixed-bed column performance. *Bioresource Technology*, 244, 23–32. doi:10.1016/j.biortech.2017.07.133
- Jung, W., Jeon, B.-H., Cho, D.-W., Roh, H.-S., Cho, Y., Kim, S.-J., & Lee, D. S. (2015). Sorptive removal of heavy metals with nano-sized carbon immobilized alginate beads. *Journal of Industrial and Engineering Chemistry*, 26, 364–369. doi:10.1016/j.jiec.2014.12.010

- Junter, G.-A., Jouenne, T. (2004). Immobilized viable microbial cells: From the process to the proteome em leader or the cart before the horse. *Biotechnology Advances*, 22(8), 633–658.
- Kaçar, Y., Arpa, Ç., Tan, S., Denizli, A., Genç, Ö., & Arıca, M. Y. (2002). Biosorption of Hg(II) and Cd(II) from aqueous solutions: Comparison of biosorptive capacity of alginate and immobilized live and heat inactivated *Phanerochaete chrysosporium*. *Process Biochemistry*, 37(6), 601–610. doi:10.1016/S0032-9592(01)00248-5
- Karkeh-Abadi, F., Saber-Samandari, S., & Saber-Samandari, S. (2016). The impact of functionalized CNT in the network of sodium alginate-based nanocomposite beads on the removal of Co(II) ions from aqueous solutions. *Journal of Hazardous Materials*, 312, 224–233. doi:10.1016/j.jhazmat.2016.03.074
- Karthik, R., & Meenakshi, S. (2015). Removal of Cr(VI) ions by adsorption onto sodium alginate-polyaniline nanofibers. *International Journal of Biological Macromolecules*, 72, 711–717. doi:10.1016/j.ijbiomac.2014.09.023
- Khotimchenko, M., Kovalev, V., Khozhaenko, E., & Khotimchenko, R. (2015). Removal of yttrium (iii) ions from water solutions by alginate compounds. *International Journal of Environmental Science and Technology*, 12(10), 3107–3116. doi:10.1007/s13762-014-0737-2
- Kim, H., Hong, H.-J., Jung, J., Kim, S.-H., & Yang, J.-W. (2010). Degradation of trichloroethylene (TCE) by nanoscale zero-valent iron (NZVI) immobilized in alginate bead. *Journal of Hazardous Materials*, 176(1-3), 1038–1043.
- Kim, T. Y., Jin, H. J., Park, S. S., Kim, S. J., & Cho, S. Y. (2008). Adsorption equilibrium of copper ion and phenol by powdered activated carbon, alginate bead and alginate-activated carbon bead. *Journal of Industrial and Engineering Chemistry*, 14(6), 714–719. doi:10.1016/j.jiec.2008.07.004
- Konwar, A., Gogoi, A., & Chowdhury, D. (2015). Magnetic alginate-Fe₃O₄ hydrogel fiber capable of ciprofloxacin hydrochloride adsorption/separation in aqueous solution. *RSC Advances*, 5(99), 81573–81582. doi:10.1039/C5RA16404D
- Kümmerer, K. (2009). Antibiotics in the aquatic environment: A review. Part I. *Chemosphere*, 75(4), 417–434. doi:10.1016/j.chemosphere.2008.11.086
- Lai, Y.-L., Thirumavalavan, M., & Lee, J.-F. (2010). Effective adsorption of heavy metal ions (Cu²⁺, Pb²⁺, Zn²⁺) from aqueous solution by immobilization of adsorbents on Ca-alginate beads. *Toxicological and Environ Chemistry*, 92(4), 697–705. doi:10.1080/02772240903057382
- Lazaridis, N. K., & Charalambous, C. (2005). Sorptive removal of trivalent and hexavalent chromium from binary aqueous solutions by composite alginate–goethite beads. *Water Research*, 39(18), 4385–4396. doi:10.1016/j.watres.2005.09.013
- Lee, K. Y., Rowley, J. A., Eiselt, P., Moy, E. M., Bouhadir, K. H., & Mooney, D. J. (2000). Controlling mechanical and swelling properties of alginate hydrogels independently by cross-linker type and cross-linking density. *Macromolecules*, 33(11), 4291–4294. doi:10.1021/ma9921347
- Li, Y., Du, Q., Liu, T., Sun, J., Wang, Y., Wu, S., ... Xia, L. (2013). Methylene blue adsorption on graphene oxide/calcium alginate composites. *Carbohydrate Polymers*, 95(1), 501–507. doi:10.1016/j.carbpol.2013.01.094
- Li, Y., Liu, F., Xia, B., Du, Q., Zhang, P., Wang, D., ... Xia, Y. (2010). Removal of copper from aqueous solution by carbon nanotube/calcium alginate composites. *Journal of Hazardous Materials*, 177(1–3), 876–880. doi:10.1016/j.jhazmat.2009.12.114
- Li, Y., Sui, K., Liu, R., Zhao, X., Zhang, Y., Liang, H., & Xia, Y. (2012). Removal of methyl orange from aqueous solution by calcium alginate/multi-walled carbon nanotubes composite fibers. *Energy Procedia*, 16, 863–868. doi:10.1016/j.egypro.2012.01.138

- Li, Z. M., Yao, Y., Wei, G. T., Jiang, W. Y., Wang, Y. Z., & Zhang, L. Y. (2016). Adsorption and heat-energy-aid desorption of cationic dye on a new thermo-sensitive adsorbent: Methyl cellulose/calcium alginate beads. *Polymer Engineering & Science*, 56(12), 1382–1389. doi:10.1002/pen.24373
- Lim, A. P., & Aris, A. Z. (2014). A review on economically adsorbents on heavy metals removal in water and wastewater. *Reviews in Environmental Science and Bio/Technology*, 13(2), 163–181. doi:10.1007/s11157-013-9330-2
- Lim, S. F., & Chen, J. P. (2007). Synthesis of an innovative calcium-alginate magnetic sorbent for removal of multiple contaminants. *Applied Surface Science*, 253(13), 5772–5775. doi:10.1016/j.apsusc.2006.12.049
- Lin, S., Huang, R., Cheng, Y., Liu, J., Lau, B. L. T., & Wiesner, M. R. (2013). Silver nanoparticle-alginate composite beads for point-of-use drinking water disinfection. *Water Research*, 47(12), 3959–3965. doi:10.1016/j.watres.2012.09.005
- Liu, H., Guo, L., Liao, S., & Wang, G. (2012). Reutilization of immobilized fungus *Rhizopus* sp. Lg04 to reduce toxic chromate. *Journal of Applied Microbiology*, 112(4), 651–659. doi:10.1111/j.1365-2672.2012.05257.x
- Liu, L., Wan, Y., Xie, Y., Zhai, R., Zhang, B., & Liu, J. (2012). The removal of dye from aqueous solution using alginate-halloysite nanotube beads. *Chemical Engineering Journal*, 187, 210–216. doi:10.1016/j.cej.2012.01.136
- Liu, T. Z., Gao, B., Fang, J. N., Wang, B., & Cao, X. D. (2016). Biochar-supported carbon nanotube and graphene oxide nanocomposites for Pb(II) and Cd(II) removal. *RSC Advances*, 6(29), 24314–24319. doi:10.1039/C6RA01895E
- Lv, X., Jiang, G., Xue, X., Wu, D., Sheng, T., Sun, C., & Xu, X. (2013). Fe₀-Fe₃O₄ nanocomposites embedded polyvinyl alcohol/sodium alginate beads for chromium(VI) removal. *Journal of Hazardous Materials*, 262, 748–758. doi:10.1016/j.jhazmat.2013.09.036
- Lv, X., Zhang, Y., Fu, W., Cao, J., Zhang, J., Ma, H., & Jiang, G. (2017). Zero-valent iron nanoparticles embedded into reduced graphene oxide-alginate beads for efficient chromium (VI) removal. *Journal of Colloid and Interface Science*, 506, 633–643. doi:10.1016/j.jcis.2017.07.024
- Lyu, H., Gao, B., He, F., Zimmerman, A. R., Ding, C., Huang, H., & Tang, J. (2018). Effects of ball milling on the physicochemical and sorptive properties of biochar: Experimental observations and governing mechanisms. *Environmental Pollution*, 233, 54–63.
- Lyu, H. H., Gao, B., He, F., Ding, C., Tang, J. C., & Crittenden, J. C. (2017). Ball-milled carbon nanomaterials for energy and environmental applications. *ACS Sustainable Chemistry & Engineering*, 5, 9568–9585. doi:10.1021/acssuschemeng.7b02170
- Lyu, H., Gao, B., He, F., Zimmerman, A. R., Ding, C., Tang, J., & Crittenden, J. C. (2018). Experimental and modeling investigations of ball-milled biochar for the removal of aqueous methylene blue. *Chemical Engineering Journal*, 335, 110–119. doi:10.1016/j.cej.2017.10.130
- Mahmoodi, N. M. (2013). Magnetic ferrite nanoparticle-alginate composite: Synthesis, characterization and binary system dye removal. *Journal of the Taiwan Institute of Chemical Engineers*, 44(2), 322–330. doi:10.1016/j.jtice.2012.11.014
- Mahmoodi, N. M., Hayati, B., Arami, M., & Bahrami, H. (2011). Preparation, characterization and dye adsorption properties of biocompatible composite (alginate/titania nanoparticle). *Desalination*, 275(1-3), 93–101. doi:10.1016/j.desal.2011.02.034
- Maitra, J., & Shukla, V. K. (2014). Cross-linking in hydrogels: A review. *American Journal of Polymer Science*, 4, 25–31.

- Mane, S., Ponrathnam, S., & Chavan, N. (2015). Effect of chemical cross-linking on properties of polymer microbeads: A review. *Can. Chem. Trans*, 3, 473–485.
- Maneerung, T., Liew, J., Dai, Y., Kawi, S., Chong, C., & Wang, C.-H. (2016). Activated carbon derived from carbon residue from biomass gasification and its application for dye adsorption: Kinetics, isotherms and thermodynamic studies. *Bioresource Technology*, 200, 350–359. doi:10.1016/j.biortech.2015.10.047
- Martins, S. C. S., Martins, C. M., Fiúza, L. M. C. G., & Santaella, S. T. (2013). Immobilization of microbial cells: A promising tool for treatment of toxic pollutants in industrial wastewater. *African Journal of Biotechnology*, 12(28), 4412–4418.
- Michael, I., Rizzo, L., Mc Ardell, C. S., Manaia, C. M., Merlin, C., Schwartz, T., ... Fatta-Kassinos, D. (2013). Urban wastewater treatment plants as hotspots for the release of antibiotics in the environment: A review. *Water Research*, 47(3), 957–995. doi:10.1016/j.watres.2012.11.027
- Min, J. H., & Hering, J. G. (1998). Arsenate sorption by Fe(III)-doped alginate gels. *Water Research*, 32(5), 1544–1552. doi:10.1016/S0043-1354(97)00349-7
- Mohammadi, A., Daemi, H., & Barikani, M. (2014). Fast removal of malachite green dye using novel superparamagnetic sodium alginate-coated Fe₃O₄ nanoparticles. *International Journal of Biological Macromolecules*, 69, 447–455. doi:10.1016/j.ijbiomac.2014.05.042
- Mohammadi, N., Khani, H., Gupta, V. K., Amereh, E., & Agarwal, S. (2011). Adsorption process of methyl orange dye onto mesoporous carbon material—kinetic and thermodynamic studies. *Journal of Colloid and Interface Science*, 362, 457–462.
- Mohan, D., Sarawat, A., Ok, Y. S., & Pittman, C. U. (2014). Organic and inorganic contaminants removal from water with biochar, a renewable, low cost and sustainable adsorbent: A critical review. *Bioresource Technology*, 160, 191–202. doi:10.1016/j.biortech.2014.01.120
- Munagapati, V. S., & Kim, D. S. (2017). Equilibrium isotherms, kinetics, and thermodynamics studies for congo red adsorption using calcium alginate beads impregnated with nano-goethite. *Ecotoxicology and Environmental Safety*, 141, 226–234. doi:10.1016/j.ecoenv.2017.03.036
- Ngah, W. S. W., & Fatinathan, S. (2008). Adsorption of Cu(II) ions in aqueous solution using chitosan beads, chitosan–GLA beads and chitosan–alginate beads. *Chemical Engineering Journal*, 143(1–3), 62–72. doi:10.1016/j.cej.2007.12.006
- Ngomsik, A.-F., Bee, A., Siaugue, J.-M., Cabuil, V., & Cote, G. (2006). Nickel adsorption by magnetic alginate microcapsules containing an extractant. *Water Research*, 40(9), 1848–1856. doi:10.1016/j.watres.2006.02.036
- Njimou, J. R., Măicăneanu, A., Indolean, C., Nansu-Njiki, C. P., & Ngameni, E. (2016). Removal of Cd(II) from synthetic wastewater by alginate-ayous wood sawdust (*Triplochiton scleroxylon*) composite material. *Environmental Technology*, 37(11), 1369–1381. doi:10.1080/09593330.2015.1116609
- Olad, A., & Farshi Azhar, F. (2014). A study on the adsorption of chromium (VI) from aqueous solutions on the alginate-montmorillonite/polyaniline nanocomposite. *Desalination and Water Treatment*, 52(13–15), 2548–2559. doi:10.1080/19443994.2013.794711
- Pandi, K., & Viswanathan, N. (2015). Synthesis of alginate beads filled with nanohydroxyapatite: An efficient approach for fluoride sorption. *Journal of Applied Polymer Science*, 132(19), 41937.
- Papageorgiou, S. K., Katsaros, F., Kouvelos, E., & Kanellopoulos, N. (2009). Prediction of binary adsorption isotherms of Cu²⁺, Cd²⁺ and Pb²⁺ on calcium alginate beads from

- single adsorption data. *Journal of Hazardous Materials*, 162(2-3), 1347–1354. doi: [10.1016/j.jhazmat.2008.06.022](https://doi.org/10.1016/j.jhazmat.2008.06.022)
- Papageorgiou, S. K., Katsaros, F. K., Kouvelos, E. P., Nolan, J. W., Le Deit, H., & Kanellopoulos, N. K. (2006). Heavy metal sorption by calcium alginate beads from *Laminaria digitata*. *Journal of Hazardous Materials*, 137(3), 1765–1772. doi:[10.1016/j.jhazmat.2006.05.017](https://doi.org/10.1016/j.jhazmat.2006.05.017)
- Paques, J. P., Van Der Linden, E., Van Rijn, C. J. M., & Sagis, L. M. C. (2014). Preparation methods of alginate nanoparticles. *Advances in Colloid and Interface Science*, 209, 163–171. doi:[10.1016/j.cis.2014.03.009](https://doi.org/10.1016/j.cis.2014.03.009)
- Prakasham, R. S., Merrie, J. S., Sheela, R., Saswathi, N., & Ramakrishna, S. V. (1999). Biosorption of chromium vi by free and immobilized *Rhizopus arrhizus*. *Environmental Pollution*, 104(3), 421–427. doi:[10.1016/S0269-7491\(98\)00174-2](https://doi.org/10.1016/S0269-7491(98)00174-2)
- Qi, Y., Jiang, M., Cui, Y.-L., Zhao, L., & Zhou, X. (2015). Synthesis of quercetin loaded nanoparticles based on alginate for Pb(II) adsorption in aqueous solution. *Nanoscale Research Letters*, 10, 408.
- Qiusheng, Z., Xiaoyan, L., Jin, Q., Jing, W., & Xuegang, L. (2015). Porous zirconium alginate beads adsorbent for fluoride adsorption from aqueous solutions. *RSC Advances*, 5(3), 2100–2112. doi:[10.1039/C4RA12036A](https://doi.org/10.1039/C4RA12036A)
- Qu, X., Alvarez, P. J., & Li, Q. (2013). Applications of nanotechnology in water and wastewater treatment. *Water Research*, 47(12), 3931–3946.
- Rangsayatorn, N., Pokethitiyook, P., Upatham, E. S., & Lanza, G. R. (2004). Cadmium biosorption by cells of *Spirulina platensis* TISTR 8217 immobilized in alginate and silica gel. *Environment International*, 30(1), 57–63. doi:[10.1016/S0160-4120\(03\)00146-6](https://doi.org/10.1016/S0160-4120(03)00146-6)
- Ren, H., Gao, Z., Wu, D., Jiang, J., Sun, Y., & Luo, C. (2016). Efficient Pb(II) removal using sodium alginate–carboxymethyl cellulose gel beads: Preparation, characterization, and adsorption mechanism. *Carbohydrate Polymers*, 137, 402–409. doi:[10.1016/j.carbpol.2015.11.002](https://doi.org/10.1016/j.carbpol.2015.11.002)
- Rezaei, H., Haghshenasfard, M., & Moheb, A. (2017). Optimization of dye adsorption using Fe_3O_4 nanoparticles encapsulated with alginate beads by Taguchi method. *Adsorption Science & Technology*, 35, 55–71. doi:[10.1177/02636174166667508](https://doi.org/10.1177/02636174166667508)
- Rhee, S.-K., Lee, G., & Lee, S.-T. (1996). Influence of a supplementary carbon source on biodegradation of pyridine by freely suspended and immobilized *Pimelobacter* sp. *Applied Microbiology and Biotechnology*, 44, 816–822. doi:[10.1007/BF00178624](https://doi.org/10.1007/BF00178624)
- Robati, D., Mirza, B., Rajabi, M., Moradi, O., Tyagi, I., Agarwal, S., et al. (2016). Removal of hazardous dyes-br 12 and methyl orange using graphene oxide as an adsorbent from aqueous phase. *Chemical Engineering Journal*, 284, 687–697.
- Robinson, T., McMullan, G., Marchant, R., & Nigam, P. (2001). Remediation of dyes in textile effluent: A critical review on current treatment technologies with a proposed alternative. *Bioresource Technology*, 77(3), 247–255. doi:[10.1016/S0960-8524\(00\)00080-8](https://doi.org/10.1016/S0960-8524(00)00080-8)
- Rocher, V., Bee, A., Siaugue, J.-M., & Cabuil, V. (2010). Dye removal from aqueous solution by magnetic alginate beads crosslinked with epichlorohydrin. *Journal of Hazardous Materials*, 178(1-3), 434–439. doi:[10.1016/j.jhazmat.2010.01.100](https://doi.org/10.1016/j.jhazmat.2010.01.100)
- Rocher, V., Siaugue, J.-M., Cabuil, V., & Bee, A. (2008). Removal of organic dyes by magnetic alginate beads. *Water Research*, 42(4-5), 1290–1298.
- Roh, H., Yu, M.-R., Yakkala, K., Koduru, J. R., Yang, J.-K., & Chang, Y.-Y. (2015). Removal studies of Cd (II) and explosive compounds using buffalo weed biochar-alginate beads. *Journal of Industrial and Engineering Chemistry*, 26, 226–233. doi:[10.1016/j.jiec.2014.11.034](https://doi.org/10.1016/j.jiec.2014.11.034)

- Rosales, E., Iglesias, O., Pazos, M., & Sanromán, M. A. (2012). Decolourisation of dyes under electro-fenton process using Fe alginate gel beads. *Journal of Hazardous Materials*, 213, 369–377. doi:10.1016/j.jhazmat.2012.02.005
- Russo, R., Malinconico, M., & Santagata, G. (2007). Effect of cross-linking with calcium ions on the physical properties of alginate films. *Biomacromolecules*, 8(10), 3193–3197.
- Salisu, A., Sanagi, M. M., Abu Naim, A., Wan Ibrahim, W. A., & Abd Karim, K. J. (2016). Removal of lead ions from aqueous solutions using sodium alginate-graft-poly (methyl methacrylate) beads. *Desalination and Water Treatment*, 57(33), 15353–15361. doi:10.1080/19443994.2015.1071685
- Salisu, A., Sanagi, M. M., Abu Naim, A., Abd Karim, K. J., Wan Ibrahim, W. A., & Abdulganiyu, U. (2016). Alginate graft polyacrylonitrile beads for the removal of lead from aqueous solutions. *Polymer Bulletin*, 73(2), 519–537. doi:10.1007/s00289-015-1504-3
- Samuel, J., Pulimi, M., Paul, M. L., Maurya, A., Chandrasekaran, N., & Mukherjee, A. (2013). Batch and continuous flow studies of adsorptive removal of Cr(VI) by adapted bacterial consortia immobilized in alginate beads. *Bioresource Technology*, 128, 423–430. doi:10.1016/j.biortech.2012.10.116
- Shen, J., Hu, Y., Shi, M., Li, N., Ma, H., & Ye, M. (2010). One step synthesis of graphene oxide – magnetic nanoparticle composite. *The Journal of Physical Chemistry C*, 114(3), 1498–1503. doi:10.1021/jp909756r
- Siwek, H., Bartkowiak, A., Włodarczyk, M., & Sobecka, K. (2016). Removal of phosphate from aqueous solution using alginate/iron (III) chloride capsules: A laboratory study. *Water, Air, & Soil Pollution*, 227, 427.
- Soltani, R. D. C., Khorramabadi, G. S., Khataee, A. R., & Jorfi, S. (2014). Silica nanopowders/alginate composite for adsorption of lead (II) ions in aqueous solutions. *Journal of the Taiwan Institute of Chemical Engineers*, 45(3), 973–980. doi:10.1016/j.jtice.2013.09.014
- Sui, K., Li, Y., Liu, R., Zhang, Y., Zhao, X., Liang, H., & Xia, Y. (2012). Biocomposite fiber of calcium alginate/multi-walled carbon nanotubes with enhanced adsorption properties for ionic dyes. *Carbohydrate Polymers*, 90(1), 399–406. doi:10.1016/j.carbpol.2012.05.057
- Sujana, M. G., Mishra, A., & Acharya, B. C. (2013). Hydrous ferric oxide doped alginate beads for fluoride removal: Adsorption kinetics and equilibrium studies. *Applied Surface Science*, 270, 767–776. doi:10.1016/j.apsusc.2013.01.157
- Tesh, S. J., & Scott, T. B. (2014). Nano-composites for water remediation: A review. *Advanced Materials (Deerfield Beach, Fla.)*, 26(35), 6056–6068.
- Thakur, S., Pandey, S., & Arotiba, O. A. (2016). Development of a sodium alginate-based organic/inorganic superabsorbent composite hydrogel for adsorption of methylene blue. *Carbohydrate Polymers*, 153, 34–46. doi:10.1016/j.carbpol.2016.06.104
- Theron, J., Walker, J., & Cloete, T. (2008). Nanotechnology and water treatment: Applications and emerging opportunities. *Critical Reviews in Microbiology*, 34(1), 43–69. doi:10.1080/10408410701710442
- Tian, Y., Gao, B., Morales, V. L., Wu, L., Wang, Y., Muñoz-Carpena, R., ... Yang, L. (2012). Methods of using carbon nanotubes as filter media to remove aqueous heavy metals. *Chemical Engineering Journal*, 210, 557–563. doi:10.1016/j.cej.2012.09.015
- Uyar, G., Kaygusuz, H., & Erim, F. B. (2016). Methylene blue removal by alginate–clay quasi-cryogel beads. *Reactive and Functional Polymers*, 106, 1–7. doi:10.1016/j.reactfunctpolym.2016.07.001
- Vijaya, Y., Popuri, S. R., Boddu, V. M., & Krishnaiah, A. (2008). Modified chitosan and calcium alginate biopolymer sorbents for removal of nickel (II) through adsorption. *Carbohydrate Polymers*, 72(2), 261–271. doi:10.1016/j.carbpol.2007.08.010

- Vijayalakshmi, K., Gomathi, T., Latha, S., Hajeeth, T., & Sudha, P. (2016). Removal of copper (II) from aqueous solution using nanochitosan/sodium alginate/microcrystalline cellulose beads. *International Journal of Biological Macromolecules*, 82, 440–452. doi: [10.1016/j.ijbiomac.2015.09.070](https://doi.org/10.1016/j.ijbiomac.2015.09.070)
- Vu, H. C., Dwivedi, A. D., Le, T. T., Seo, S.-H., Kim, E.-J., & Chang, Y.-S. (2017). Magnetite graphene oxide encapsulated in alginate beads for enhanced adsorption of Cr(VI) and As(V) from aqueous solutions: Role of crosslinking metal cations in pH control. *Chemical Engineering Journal*, 307, 220–229. doi: [10.1016/j.cej.2016.08.058](https://doi.org/10.1016/j.cej.2016.08.058)
- Wan Ngah, W. S., Teong, L. C., & Hanafiah, M. A. K. M. (2011). Adsorption of dyes and heavy metal ions by chitosan composites: A review. *Carbohydrate Polymers*, 83(4), 1446–1456. doi: [10.1016/j.carbpol.2010.11.004](https://doi.org/10.1016/j.carbpol.2010.11.004)
- Wan, S., Wu, J., Zhou, S., Wang, R., Gao, B., & He, F. (2018). Enhanced lead and cadmium removal using biochar-supported hydrated manganese oxide (HMO) nanoparticles: Behavior and mechanism. *Science of the Total Environment*, 616, 1298–1306. doi: [10.1016/j.scitotenv.2017.10.188](https://doi.org/10.1016/j.scitotenv.2017.10.188)
- Wan, S. L., He, F., Wu, J. Y., Wan, W. B., Gu, Y. W., & Gao, B. (2016). Rapid and highly selective removal of lead from water using graphene oxide-hydrated manganese oxide nanocomposites. *Journal of Hazardous Materials*, 314, 32–40. doi: [10.1016/j.jhazmat.2016.04.014](https://doi.org/10.1016/j.jhazmat.2016.04.014)
- Wan, S., Wu, J., He, F., Zhou, S., Wang, R., Gao, B., & Chen, J. (2017). Phosphate removal by lead-exhausted bioadsorbents simultaneously achieving lead stabilization. *Chemosphere*, 168, 748–755. doi: [10.1016/j.chemosphere.2016.10.142](https://doi.org/10.1016/j.chemosphere.2016.10.142)
- Wang, B., Gao, B., & Fang, J. (2017). Recent advances in engineered biochar productions and applications. *Critical Reviews in Environmental Science and Technology*, 47(22), 2158–2207. doi: [10.1080/10643389.2017.1418580](https://doi.org/10.1080/10643389.2017.1418580)
- Wang, B., Gao, B., & Wan, Y. (2018a). Comparative study of calcium alginate, ball-milled biochar, and their composites on methylene blue adsorption from aqueous solution. *Environmental Science and Pollution Research*. doi: [10.1007/s11356-018-1497-1](https://doi.org/10.1007/s11356-018-1497-1)
- Wang, B., Gao, B., & Wan, Y. S. (2018b). Entrapment of ball-milled biochar in calcium alginate beads for the removal of aqueous Cd(II). *Journal of Industrial and Engineering Chemistry*, 61, 161–168. doi: [10.1016/j.jiec.2017.12.013](https://doi.org/10.1016/j.jiec.2017.12.013)
- Wang, B., Gao, B., Zimmerman, A., & Lee, X. (2018). Impregnation of multiwall carbon nanotubes in alginate beads dramatically enhances their adsorptive ability to aqueous methylene blue. *Chemical Engineering Research and Design*, 133, 235–242. doi: [10.1016/j.cherd.2018.03.026](https://doi.org/10.1016/j.cherd.2018.03.026)
- Wang, B., Gao, B., Zimmerman, A. R., Zheng, Y., & Lyu, H. (2018). Novel biochar-impregnated calcium alginate beads with improved water holding and nutrient retention properties. *Journal of Environmental Management*, 209, 105–111. doi: [10.1016/j.jenvman.2017.12.041](https://doi.org/10.1016/j.jenvman.2017.12.041)
- Wang, F., Lu, X., & Li, X.-Y. (2016). Selective removals of heavy metals (Pb²⁺, Cu²⁺, and Cd²⁺) from wastewater by gelation with alginate for effective metal recovery. *Journal of Hazardous Materials*, 308, 75–83. doi: [10.1016/j.jhazmat.2016.01.021](https://doi.org/10.1016/j.jhazmat.2016.01.021)
- Wang, J.-P., Yang, H.-C., & Hsieh, C.-T. (2010). Adsorption of phenol and basic dye on carbon nanotubes/carbon fabric composites from aqueous solution. *Separation Science and Technology*, 46(2), 340–348. doi: [10.1080/01496395.2010.508066](https://doi.org/10.1080/01496395.2010.508066)
- Wang, Q., Wang, B., Lee, X., Lehmann, J., & Gao, B. (2018). Sorption and desorption of Pb(II) to biochar as affected by oxidation and pH. *Science of the Total Environment*, 634, 188–194.

- Wang, Y.-Y., Yao, W.-B., Wang, Q.-W., Yang, Z.-H., Liang, L.-F., & Chai, L.-Y. (2016). Synthesis of phosphate-embedded calcium alginate beads for Pb(II) and Cd(II) sorption and immobilization in aqueous solutions. *Transactions of Nonferrous Metals Society of China*, 26(8), 2230–2237. doi:10.1016/S1003-6326(16)64340-6
- Wang, Y., Wang, W., & Wang, A. (2013). Efficient adsorption of methylene blue on an alginate-based nanocomposite hydrogel enhanced by organo-illite/smectite clay. *Chemical Engineering Journal*, 228, 132–139. doi:10.1016/j.cej.2013.04.090
- Wang, Y., Zhang, X., Wang, Q., Zhang, B., & Liu, J. (2014). Continuous fixed bed adsorption of Cu (II) by halloysite nanotube-alginate hybrid beads: An experimental and modelling study. *Water Science and Technology*, 70(2), 192–199. doi:10.2166/wst.2014.148
- Wu, D., Zhao, J., Zhang, L., Wu, Q., & Yang, Y. (2010). Lanthanum adsorption using iron oxide loaded calcium alginate beads. *Hydrometallurgy*, 101(1-2), 76–83. doi:10.1016/j.hydromet.2009.12.002
- Wu, S., Zhao, X., Li, Y., Zhao, C., Du, Q., Sun, J., ... Xia, L. (2013). Adsorption of ciprofloxacin onto biocomposite fibers of graphene oxide/calcium alginate. *Chemical Engineering Journal*, 230, 389–395. doi:10.1016/j.cej.2013.06.072
- Xiangliang, P., Jianlong, W., & Daoyong, Z. (2005). Biosorption of Pb(II) by *Pleurotus ostreatus* immobilized in calcium alginate gel. *Process Biochemistry*, 40(8), 2799–2803. doi:10.1016/j.procbio.2004.12.007
- Xue, Y., Gao, B., Yao, Y., Inyang, M., Zhang, M., & Zimmerman, A. R. (2012). Hydrogen peroxide modification enhances the ability of biochar (hydrochar) produced from hydrothermal carbonization of peanut hull to remove aqueous heavy metals: Batch and column tests. *Chemical Engineering Journal*, 200, 673–680. doi:10.1016/j.cej.2012.06.116
- Yagub, M. T., Sen, T. K., Afroze, S., & Ang, H. M. (2014). Dye and its removal from aqueous solution by adsorption: A review. *Advances in Colloid and Interface Science*, 209, 172–184.
- Yakup Arica, M., Arpa, Ç., Ergene, A., Bayramoğlu, G., & Genç, Ö. (2003). Ca-alginate as a support for Pb(II) and Zn(II) biosorption with immobilized *Phanerochaete chrysosporium*. *Carbohydrate Polymers*, 52(2), 167–174. doi:10.1016/S0144-8617(02)00307-7
- Yang, J.-S., Xie, Y.-J., & He, W. (2011). Research progress on chemical modification of alginate: A review. *Carbohydrate Polymers*, 84(1), 33–39. doi:10.1016/j.carbpol.2010.11.048
- Ye, X., Wu, Z., Li, W., Liu, H., Li, Q., Qing, B., ... Ge, F. (2009). Rubidium and cesium ion adsorption by an ammonium molybdophosphate-calcium alginate composite adsorbent. *Colloids and Surfaces A: Physicochemical and Engineering Aspects*, 342(1-3), 76–83. doi:10.1016/j.colsurfa.2009.04.011
- Zargar, V., Asghari, M., & Dashti, A. (2015). A review on chitin and chitosan polymers: Structure, chemistry, solubility, derivatives, and applications. *ChemBioEng Reviews*, 2, 204–226. doi:10.1002/cben.201400025
- Zhang, M., & Gao, B. (2013). Removal of arsenic, methylene blue, and phosphate by biochar/aloooh nanocomposite. *Chemical Engineering Journal*, 226, 286–292. doi:10.1016/j.cej.2013.04.077
- Zhang, M., Gao, B., Cao, X. D., & Yang, L. Y. (2013). Synthesis of a multifunctional graphene-carbon nanotube aerogel and its strong adsorption of lead from aqueous solution. *RSC Advances*, 3(43), 21099–21105. doi:10.1039/c3ra44340j
- Zhang, M., Gao, B., Li, Y., Zhang, X. W., & Hardin, I. R. (2013). Graphene-coated pyrogenic carbon as an anode material for lithium battery. *Chemical Engineering Journal*, 229, 399–403. doi:10.1016/j.cej.2013.06.025

- Zhang, M., Gao, B., Yao, Y., Xue, Y. W., & Inyang, M. (2012). Synthesis, characterization, and environmental implications of graphene-coated biochar. *Science of the Total Environment*, 435, 567–572. doi:10.1016/j.scitotenv.2012.07.038
- Zhao, F., Qin, X., & Feng, S. (2016). Preparation of microgel/sodium alginate composite granular hydrogels and their Cu²⁺ adsorption properties. *RSC Advances*, 6(102), 100511–100518. doi:10.1039/C6RA21546G
- Zhou, Y., Gao, B., Zimmerman, A. R., Chen, H., Zhang, M., & Cao, X. D. (2014). Biochar-supported zerovalent iron for removal of various contaminants from aqueous solutions. *Bioresource Technology*, 152, 538–542. doi:10.1016/j.biortech.2013.11.021
- Zhou, Y. M., Gao, B., Zimmerman, A. R., & Cao, X. D. (2014). Biochar-supported zerovalent iron reclaims silver from aqueous solution to form antimicrobial nanocomposite. *Chemosphere*, 117, 801–805. doi:10.1016/j.chemosphere.2014.10.057
- Zhou, Y. M., Gao, B., Zimmerman, A. R., Fang, J., Sun, Y. N., & Cao, X. D. (2013). Sorption of heavy metals on chitosan-modified biochars and its biological effects. *Chemical Engineering Journal*, 231, 512–518. doi:10.1016/j.ccej.2013.07.036
- Zhu, H., Chen, T., Liu, J., & Li, D. (2018). Adsorption of tetracycline antibiotics from an aqueous solution onto graphene oxide/calcium alginate composite fibers. *RSC Advances*, 8(5), 2616–2621. doi:10.1039/C7RA11964J
- Zhuang, Y., Yu, F., Chen, H., Zheng, J., Ma, J., & Chen, J. (2016). Alginate/graphene double-network nanocomposite hydrogel beads with low-swelling, enhanced mechanical properties, and enhanced adsorption capacity. *Journal of Materials Chemistry A*, 4(28), 10885–10892.
- Zhuang, Y., Yu, F., Chen, J., & Ma, J. (2016). Batch and column adsorption of methylene blue by graphene/alginate nanocomposite: Comparison of single-network and double-network hydrogels. *Journal of Environmental Chemical Engineering*, 4(1), 147–156. doi:10.1016/j.jece.2015.11.014
- Zhuang, Y., Yu, F., Ma, J., & Chen, J. (2017). Enhanced adsorption removal of antibiotics from aqueous solutions by modified alginate/graphene double network porous hydrogel. *Journal of Colloid and Interface Science*, 507, 250–259. doi:10.1016/j.jcis.2017.07.033
- Zouboulis, A. I., & Katsoyiannis, I. A. (2002). Arsenic removal using iron oxide loaded alginate beads. *Industrial & Engineering Chemistry Research*, 41, 6149–6155. doi:10.1021/ie0203835



Removal of trichloroethylene by biochar supported nanoscale zero-valent iron in aqueous solution



Haoran Dong^{*}, Cong Zhang, Kunjie Hou, Yujun Cheng, Junmin Deng, Zhao Jiang, Lin Tang, Guangming Zeng

College of Environmental Science and Engineering, Hunan University, Changsha, Hunan 410082, China

Key Laboratory of Environmental Biology and Pollution Control (Hunan University), Ministry of Education, Changsha, Hunan 410082, China

ARTICLE INFO

Article history:

Received 15 June 2017

Received in revised form 12 July 2017

Accepted 13 July 2017

Available online 14 July 2017

Keywords:

Nanoscale zero-valent iron

Biochar

Trichloroethylene

Adsorption

Degradation

ABSTRACT

Nanoscale zero-valent iron (NZVI) has been widely used for the degradation of trichloroethylene (TCE) in contaminated water, however, it is suffering from being easy to aggregate and having low adsorption capacity for TCE. In order to overcome the shortcomings of NZVI, modified NZVI particles with biochar (NZVI/BC) were applied in this study for removal and degradation of TCE, given the high stability and adsorption capacity of BC. The effects of pyrolysis temperature of BC, mass ratio of NZVI/BC and solution pH on the removal and degradation efficiency of TCE were studied. The different pyrolysis temperatures of BC resulted in the differences on the surface areas, aromaticity and noncarbonized fractions, which determined the sorption capacity of TCE. Compared with pure NZVI, the NZVI/BC at different mass ratios could increase the removal efficiency of TCE to 99%, which was attributed to the higher adsorption capacity of BC for TCE. Besides, the yield of final products (ethane, ethylene and acetylene) differed at different mass ratios of NZVI/BC. Generally, the main product was ethylene in all reactions and the yield of acetylene and ethane were relatively low. Solution pH had little effect on the total removal of TCE but significantly influenced the yield of final products. The yield of ethylene decreased with the increasing pH. The results indicate that solution pH could not affect the sorption of TCE but influenced the degradation rate of TCE by NZVI/BC.

© 2017 Elsevier B.V. All rights reserved.

1. Introduction

In recent years, increasing numbers of chlorinated hydrocarbons have been released into soil and groundwater, owing to their common use in industrial production [1,2]. The chlorinated hydrocarbons often have the following characters: non-aqueous phase liquid, higher density than water, and low solubility in water [3], thus they may serve as contamination sources of groundwater and soil [4–6], and pose threats to the health and safety of the environment [7].

Trichloroethylene (TCE), as a representative of chlorinated hydrocarbons, has attracted wide attention since it was firstly detected in the environment in late 1970s [8]. For the remediation of contaminated soil or groundwater with TCE, biotic and abiotic methods have been employed [1,9]. While biotic methods utilize microorganisms to dechlorinate TCE completely or into less chlorinated by-products under aerobic or anaerobic conditions [10,11], abiotic methods generally include physical adsorption [12] and

chemical oxidation [13] or reduction [14] of TCE. Among these methods, nanoscale zero-valent iron (NZVI) has been widely used in TCE dechlorination in groundwater because of its simplicity, low cost and environmental friendliness [15–18]. However, there are still many challenges regarding the removal of TCE with NZVI, one of which is the agglomeration of NZVI particles [19–21]. Due to the high surface energy and magnetic interaction, NZVI particles can easily attach to each other and form large-sized aggregates, resulting in declined reactivity [19–21]. In order to hinder the aggregation of NZVI, researchers have employed different materials as the support for NZVI to provide better distribution, which include bentonite [22], mesoporous silica [23], activated carbon [24] and biochar [25]. Among these materials, biochar has been regarded as one of the best adsorbents because of its high adsorption capacity [26] and low cost [27]. Biochar has been used as an adsorbent to remove organic pollutants such as TCE [28]. However, biochar does not decompose TCE into other harmless products. Therefore, modifying NZVI particles with biochar could compensate the deficiencies of them in removing TCE.

In recent years, there are many studies about removing TCE by biochars or NZVI, but far fewer about combining biochars and NZVI [18,29]. Therefore, this study investigated the feasibility and

^{*} Corresponding author at: College of Environmental Science and Engineering, Hunan University, Changsha, Hunan 410082, China.

E-mail address: dongh@hnu.edu.cn (H. Dong).

mechanisms of degradation of TCE by NZVI supported by biochar. The specific objectives of this study were (1) to investigate the effects of pyrolysis temperature, the ratio of NZVI to biochar and the solution pH on the removal of TCE, (2) to examine the differences in quantity and species of reaction products under different conditions, and (3) to probe into the reaction mechanisms of removing TCE by the biochar supported NZVI (NZVI/BC).

2. Materials and methods

2.1. Reagents

The cornstalk was purchased from a local agricultural field at Lianyungang City, Jiangsu Province, China. NaBH_4 (98%), $\text{FeCl}_3 \cdot 6\text{H}_2\text{O}$ (Analytical Reagent) and methanol (Analytical Reagent) were purchased from Sinopharm Chemical Reagent Co., Ltd. TCE (Analytical Reagent) was purchased from Huihong reagent co., Ltd, Hunan province, China. Hexane (HPLC) was purchased from Tianjin chemical reagent research institute co., LTD, China, and was used as extractant for TCE detection. Gaseous alkene standards (3.11% ethane, 12.3% ethylene and 8.1% acetylene) were obtained from Huategas Co., Ltd, Guangdong province, China.

2.2. Preparation of biochar, NZVI, and biochar-modified NZVI

The cornstalk was used as raw feedstocks to produce biochar. The feedstocks were dried in an air-forced oven at 60 °C for a day and ground to less than 150 μm (100 mesh sieve). The grounded feedstocks were placed in a quartz porcelain boat and pyrolyzed in a tube furnace at 7 °C min^{-1} under a limited oxygen condition (via purging nitrogen). The different peak temperatures, i.e. 500, 600 and 700 °C, were adapted to carbonize each feedstock, where they were held for 2 h followed by being cooled to room temperature inside the furnace [30]. Then the biochar was washed with 1 M HCl (1/20, v/v) for demineralization of cations such as K^+ , Na^+ , Ca^{2+} and Mg^{2+} , and was purified by using ultrapure water until the solution pH achieved stability before being dried at 60 °C in an air-forced oven [30]. The developed biochars (BC) at different pyrolysis temperatures (i.e., 500, 600 and 700 °C) were saved in air-tight containers, and referred to as BC500, BC600 and BC700, respectively.

NZVI particles were synthesized via the method as described in previous studies [15,31]. In the synthesis of NZVI/BC composites with different mass ratios of NZVI/BC at 1:1, 1:3 and 1:5 (referred to as NZVI/BC_(1:1), NZVI/BC_(1:3), NZVI/BC_(1:5)), ferric chloride solution ($\text{FeCl}_3 \cdot 6\text{H}_2\text{O}$, 0.05 M) was mixed with BC of different amounts (0.28 g, 0.84 g and 1.4 g, respectively) for one night. All solvents were purged with N_2 for more than 60 min prior to use and the whole synthesis process was under N_2 atmosphere. The FeCl_3 -BC solution was added in a 3-mouth container with mechanical stirring at least an hour. An equal volume of 0.2 M potassium borohydride (KBH_4) was dropwisely added into the 3-mouth container. Another 30 min was needed for the generation of Fe^0 and uniformly attached to the surface of the biochar. Afterwards, the composite was separated with refrigerated centrifuge, and washed with ethanol. The NZVI/BC slurry was finally dried in a vacuum drying oven at 60 °C for 8 h. The synthesized NZVI/BC powders were stored in vacuum bag and used in batch experiments within 2 days.

2.3. Characterizations

The surface morphologies of BC and NZVI/BC were examined by using a field emission scanning electron microscope (FE-SEM) (JSM-6700F, JEOL, Japan) equipped with an energy dispersive spec-

troscopy (Oxford Inca EDS). X-ray diffractometer (XRD, Philips Electronic Instruments) was used to determine oxidation state of Fe on the surface of BC. The specific surface areas of BC were analyzed by an ASAP 2020 N_2 -Brunauer-Emmett-Teller (BET) -surface area analyzer (Micromeritics, USA). The spectral properties of BC pyrolyzed at different temperatures were measured by Fourier transform infrared spectroscopy (FTIR), and spectra was obtained in a wavelength range of 450–4000 cm^{-1} .

2.4. Adsorption and dechlorination experiments

Batch experiment was conducted in 40-mL glass vials under anoxic conditions. The ultra-pure water was purged with Helium (He) for 30 min (dissolved oxygen <0.2 mg/L). 100 mg pure NZVI or NZVI/BC were added into the vials, followed by adding 20 mL anaerobic ultrapure water. Then 50 μL of 12 g/L TCE solution (diluted from the analytical reagent TCE with acetone) was added, which made the initial TCE concentration come to 30 mg/L. The vials were capped and transferred to a horizontal shaker at 250 rpm at room temperature.

Liquid sample was taken from the glass vials, and extracted through 0.45 μm needle filter to remove the solid impurities. Then, the remaining TCE in the aqueous phase was extracted with n-hexane. The mixture was analyzed by the means of common GC method for TCE (Rtx-5MS chromatographic column 30 mm \times 0.25 mm \times 0.25 μm , MS detection). Gas sample was taken from the headspace over the reaction solution and analyzed using the same method as described above for the determination of ethane, ethylene and acetylene.

3. Results and discussion

3.1. Characterization of biochar and NZVI/BC

3.1.1. SEM-EDS

The morphologies of NZVI and NZVI/BC were observed by using FE-SEM as shown in Fig. 1. SEM images show that biochar had abundant porous structure and NZVI particles were distributed on the porous structure as well as the surface of biochar. To verify the successful synthesis of NZVI/BC, the EDS mapping and XRD spectrum of the synthesized composites were presented in Fig. 2. The elemental mapping as illustrated in Fig. 2(B and C) showed the uniform distribution of C and Fe. XRD analysis (Fig. 2D) further demonstrated that the Fe existed in the form of Fe^0 . The results reveal that NZVI particles were successfully synthesized and uniformly dispersed on the surface of biochar.

3.1.2. BET

The BET surface area, pore volume and pore size of the derived biochars at 500 °C(BC500), 600 °C(BC600) and 700 °C(BC700) and NZVI/BC were presented in Table 1. The BET surface area of biochar increased with the increase of the pyrolysis temperatures. As shown in Table 1, compared with BC500 and BC600 (28.5 $\text{m}^2 \text{g}^{-1}$ and 31.2 $\text{m}^2 \text{g}^{-1}$ for BC500 and BC600, respectively), BC700 had a larger BET surface area (64.8 $\text{m}^2 \text{g}^{-1}$). The previous research has shown that the pyrolysis temperature in the biochar production process is closely related to the biochar structure [32]. During the thermal decomposition of biomass, coal tar would be produced, which forms pores on the surface of the biochar and increases the related specific surface area. At a higher pyrolyzed temperature, more pores are easily produced because of volatilization of the biomass components [32]. Therefore, the pore volume of the biochar is also closely related to the BET surface area [33]. As shown in Table 1, the data of pore volume displayed an upward trend with the increasing pyrolyzed temperature (0.023, 0.0241 and

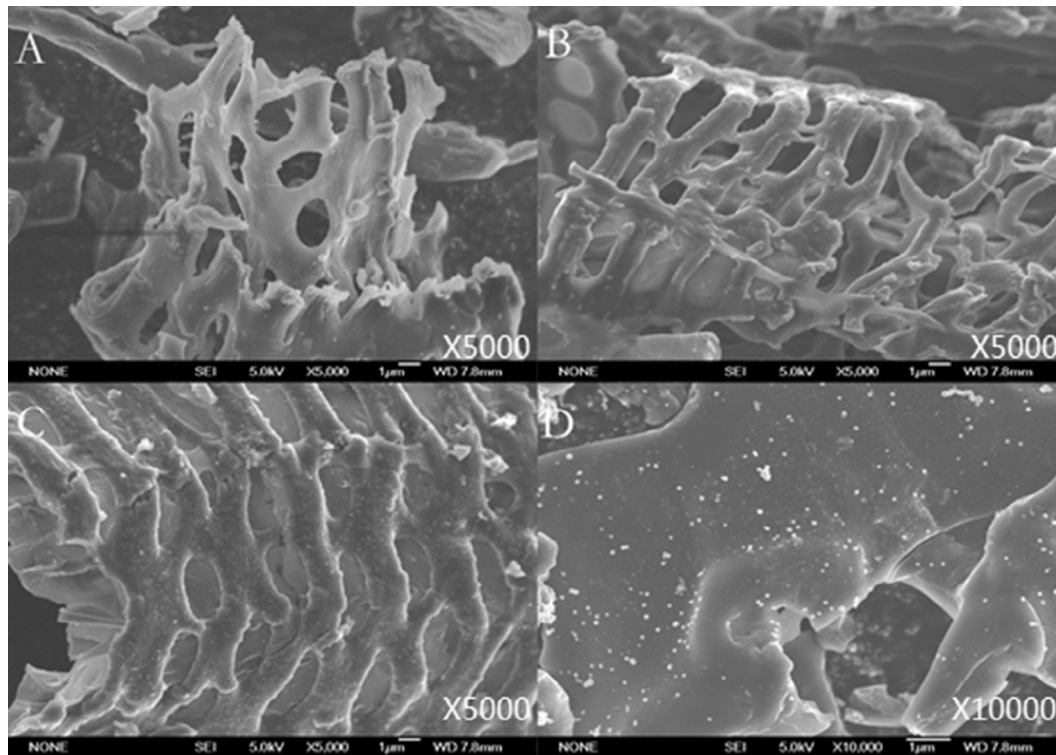


Fig. 1. SEM images of biochar at different pyrolysis temperatures: (A) 500 °C; (B) 600 °C; (C) 700 °C and (D) the synthesized NZVI/BC (biochar pyrolyzed at 600 °C).

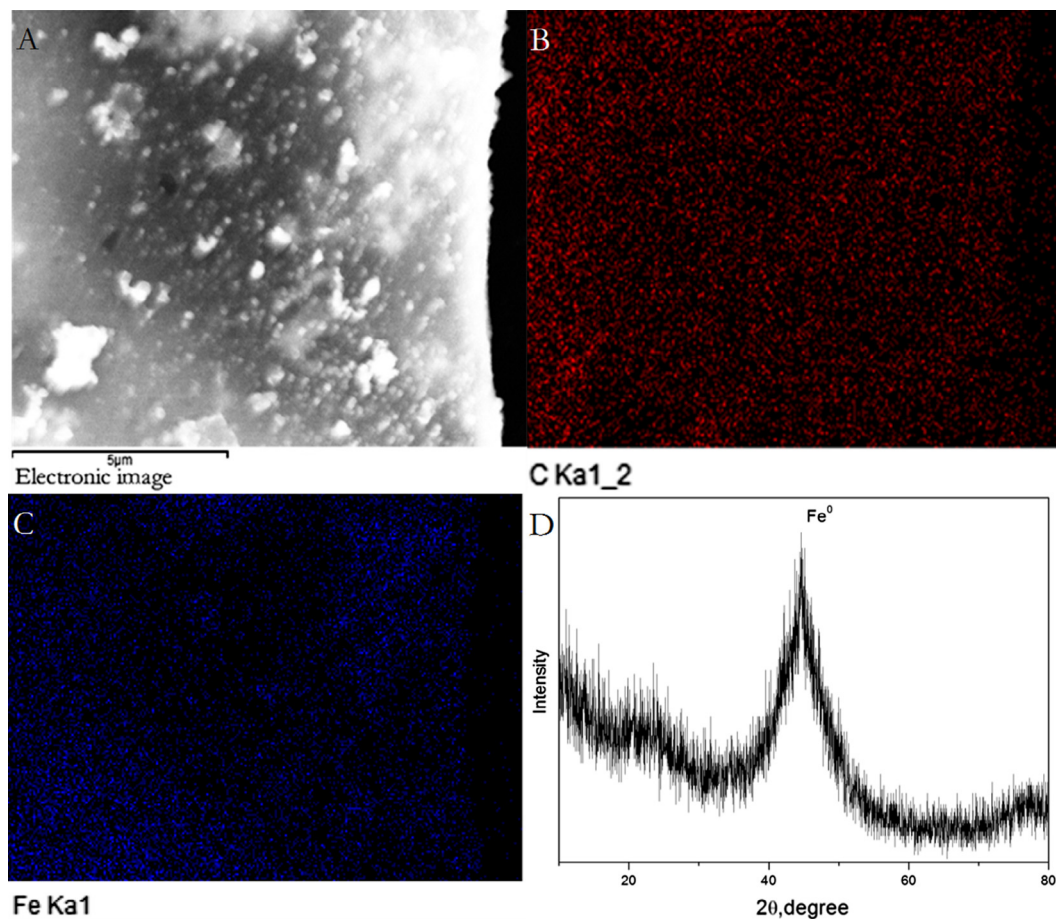


Fig. 2. (A) SEM image of NZVI/BC composite (biochar pyrolyzed at 600 °C). (B) and (C) Elemental spot mapping of C (B) and Fe (C) measured by SEM-EDS in the area shown in (A). (D) XRD analysis of NZVI/BC.

Table 1

BET surface area, pore volume and pore size of the derived biochars at 500 °C (BC500), 600 °C (BC600) and 700 °C (BC700) and NZVI/BC (biochar pyrolyzed at 600 °C and mass ratio of NZVI and BC at 1:3).

	BET surface area (m ² g ⁻¹)	Pore volume (cm ³ g ⁻¹)	Pore size (nm)
BC500	28.5	0.0230	3.24
BC600	31.2	0.0241	3.08
BC700	64.8	0.185	11.4
NZVI/BC	7.95	0.0236	11.9

0.185 cm³ g⁻¹ for BC500, BC600 and BC700, respectively). The average pore sizes of BC500, BC600 and BC700 were 3.24 nm, 3.08 nm and 11.4 nm, respectively. The results reveal that the surface areas of biochars were all dominated by mesopores (the pore sizes ranging from 2.0 to 50.0 nm were defined as mesopores) [34]. In order to reflect the differences between NZVI/BC and biochar more explicitly, the BET surface area, pore volume and pore size of NZVI/BC are also presented in Table 1. Compared with the pure biochar, NZVI/BC had a much smaller BET surface area, which might be ascribed to the blocking effect of the loaded NZVI on the inner surface of the biochar.

3.1.3. FTIR analysis

FTIR spectra of biochars pyrolyzed at different temperatures are presented in Fig. 3. Different spectra reflect the changes of the surface functional groups of biochar produced at different temperatures. The main adsorption bands in biochars at 3424, 2926, 1600, and 1105 cm⁻¹ were assigned to —OH stretching, —CH₂ stretching, aromatic C=O and C=C stretching, and C—O functional groups, respectively. And the peaks at 871 and 770 cm⁻¹ in biochar were assigned to aromatic C—H, indicating the presence of adjacent aromatic hydrogen [12]. The subordinate band at 2348 cm⁻¹ represented CO₂ asymmetric stretching vibrations which might be due to the fact that biochar absorbed CO₂ in the air environment during the FTIR analysis. The peak of —OH bond at 3424 cm⁻¹ from the intermolecular hydrogen bonding of alcohols and phenols decreased slightly with the increase of the temperature. The peak at 2926 cm⁻¹, representing the presence of long linear aliphatic

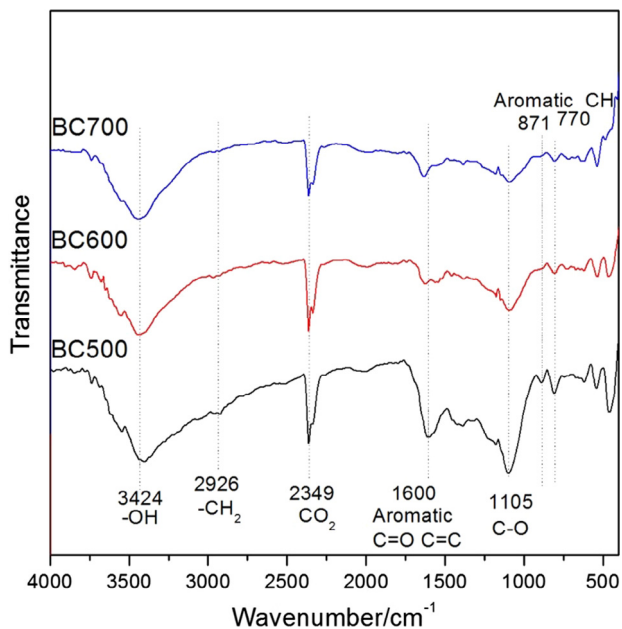


Fig. 3. FTIR analysis of biochar pyrolyzed at different temperatures.

chain —CH₂ groups, decreased with the increase of the temperature, and disappeared in BC700. Adsorption at 1105 cm⁻¹ suggested the presence of C—O function groups in biochar, which declined with increasing temperatures. The peaks of the aromatic C=O and C=C at 1600 cm⁻¹ decreased significantly at 700 °C as compared with 500 °C. These results indicate a decrease in the polar functional groups with the increase of pyrolysis temperature of biochar. The O and H functional groups decreased with increasing the temperature, resulting in the drops in surface acidity and polarity, but the increase in aromaticity of biochar.

Generally, the results of the FTIR analysis indicate that the pyrolysis temperature considerably influenced the surface properties of biochar. The findings are in consistent with the studies of Ahmad et al. [12] who reported the decrease in acidity and increase in aromaticity in biochar developed from soybean stover at 300 and 700 °C. Therefore, it was speculated that the changing surface properties of biochar derived from different pyrolysis temperatures might affect the adsorption behavior of TCE, thus affecting the TCE degradation by the NZVI/BC composites.

3.2. Removal of TCE

3.2.1. Effect of pyrolysis temperatures of BC on the removal of TCE by NZVI/BC

The effect of different pyrolysis temperatures of biochar on the removal of TCE by the NZVI/BC composites is illustrated in Fig. 4. The removal efficiencies of 97.19%, 97.94% and 87.10% were achieved by NZVI/BC500, NZVI/BC600 and NZVI/BC700, respectively, within 4-h reaction time. All the three NZVI/BC composites showed a better TCE removal than the pure NZVI (63.97%, within 4 h). On the one hand, the NZVI/BC composites could serve more sorption sites than the pure NZVI for the uptake of TCE because of the large specific surface area of biochar; on the other hand, the NZVI particles, distributed on the surface or in the porous structure of BC, could provide more active sites than the pure NZVI for the reaction with TCE due to less potential of agglomeration for NZVI once deposited onto BC [23–25]. In regard to the differences among the three NZVI/BC composites, as demonstrated in Fig. 4A, NZVI/BC600 displayed the best performance within 4 h, while all the three types of NZVI/BC achieved a nearly complete TCE removal when the reaction time was prolonged up to 60 h. As discussed in the previous section, the different pyrolysis temperatures resulted in the different specific surface areas and aromaticity of biochar [12], which should contribute to the different TCE removal efficiencies of NZVI/BC. In order to explore the effect of biochar on the TCE removal, the TCE removal by pure biochar generated at different pyrolysis temperatures is also illustrated in Fig. 4B. The removal efficiencies of TCE reached to 90.75%, 93.29% and 75.51% for BC500, BC600 and BC700, respectively, within 4 h, which were only slightly lower than that of the NZVI/BC composites but showed a similar trend. This reveals that the biochar played a major role in the removal of TCE. As demonstrated in the characterization of biochars, BC700 had higher aromaticity, lower polarity and larger surface area than BC500 and BC600, but it exhibited the slowest removal of TCE. This is contrary to the findings of Ahmad et al. [12], who reported that biochars produced from soybean stover at higher temperature (700 °C) had a high adsorption capacity of TCE due to their high aromaticity, low polarity and large surface area. The differences might result from the use of different feedstocks (cornstalk was used in this study) for the production of biochars, therefore, the results cannot be compared directly. Moreover, it was presumed that the removal of TCE might not only be associated with the above mentioned properties (i.e., aromaticity, polarity and surface area) of biochars but also be affected by the other factors. Chen et al. [35] reported that a lower pyrolysis temperature would increase the hydrophobicity of biochar because

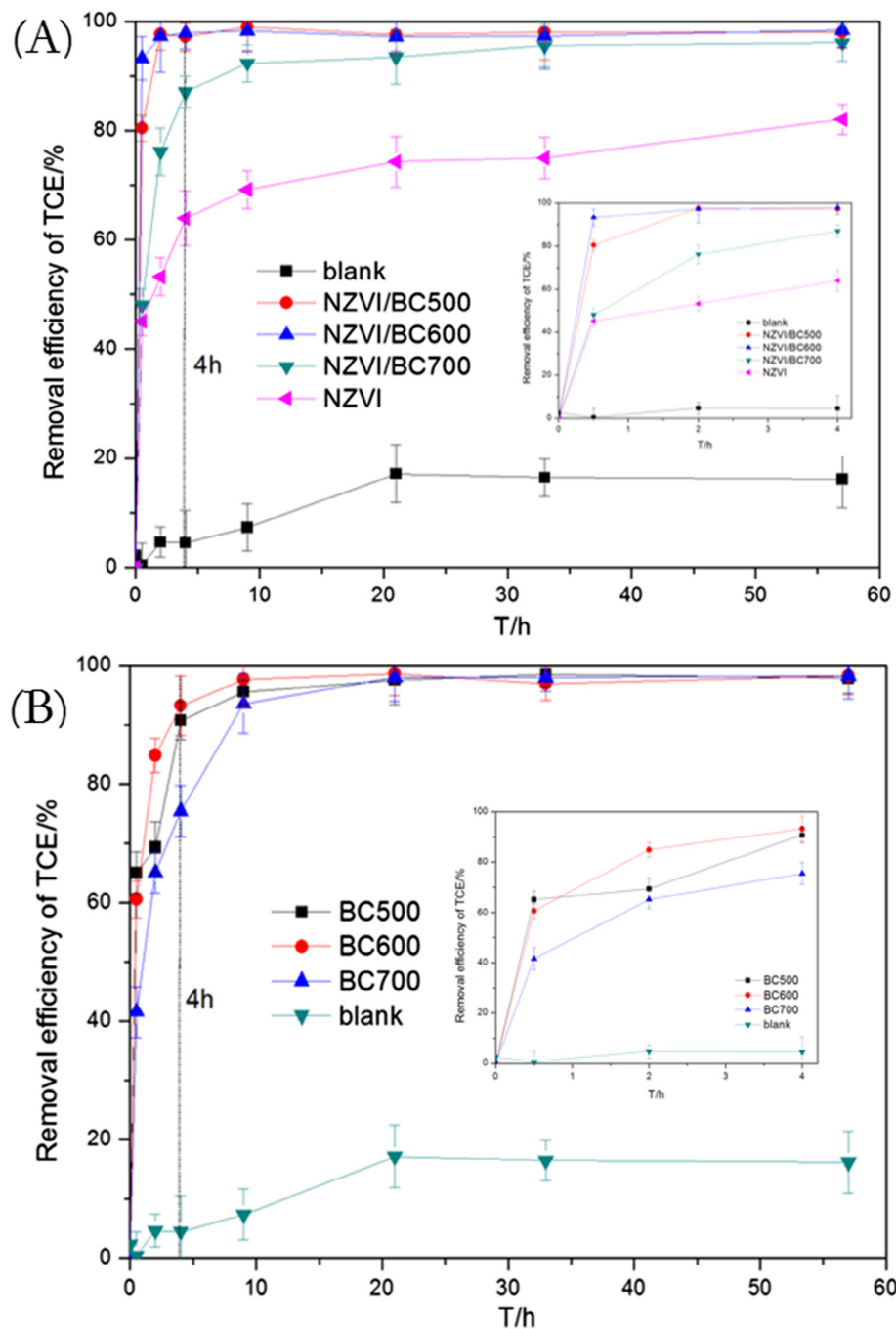


Fig. 4. Effect of pyrolysis temperature of biochar on the removal of TCE by (A) NZVI/BC and (B) BC. Inset figures show the removal of TCE in the first 4-h reaction. 'Blank' refers to the sample with only TCE. (NZVI = NZVI/BC = BC = 5 g/L; TCE = 30 mg/L; pH = 6.25).

of the biological organic residues from the biomass, which was suitable for sorption of hydrophobic organic compounds. Sorption mechanisms of biochars are partitioning-dominant at low pyrolytic temperatures, but are adsorption-dominant at higher pyrolytic temperatures [35–37]. The contributions of adsorption and partition are determined by the carbonized and noncarbonized fractions, besides their surface and bulk properties. The carbonization fractions increased with the pyrolytic temperature. The non-carbonized organic matter is expected to behave as partition phase and the carbonized organic matter as an adsorbent; adsorption is typically nonlinear, whereas partition is essentially linear [35]. As shown in Fig. 4B, generally, the sorption of TCE showed a linear trend in the first few hours, and then a nonlinear trend with

prolonged reaction time. In this sense, it was presumed that the sorption of TCE to biochars resulted from both partition with non-carbonized fractions and adsorption with carbonized fractions. Therefore, the best performance of BC600 should be ascribed to the combined contributions of noncarbonized fractions (for partition) and their surface and bulk properties (for adsorption). The BC600 was thus employed as supporting material for NZVI in the following experiments.

3.2.2. Effect of mass ratio of NZVI/BC on the removal of TCE

The effects of mass ratios of NZVI/BC (1:1, 1:3, 1:5) on the removal of TCE are illustrated in Fig. 5A. The removal efficiency of 63.97% was achieved by NZVI alone within 4-h reaction time,

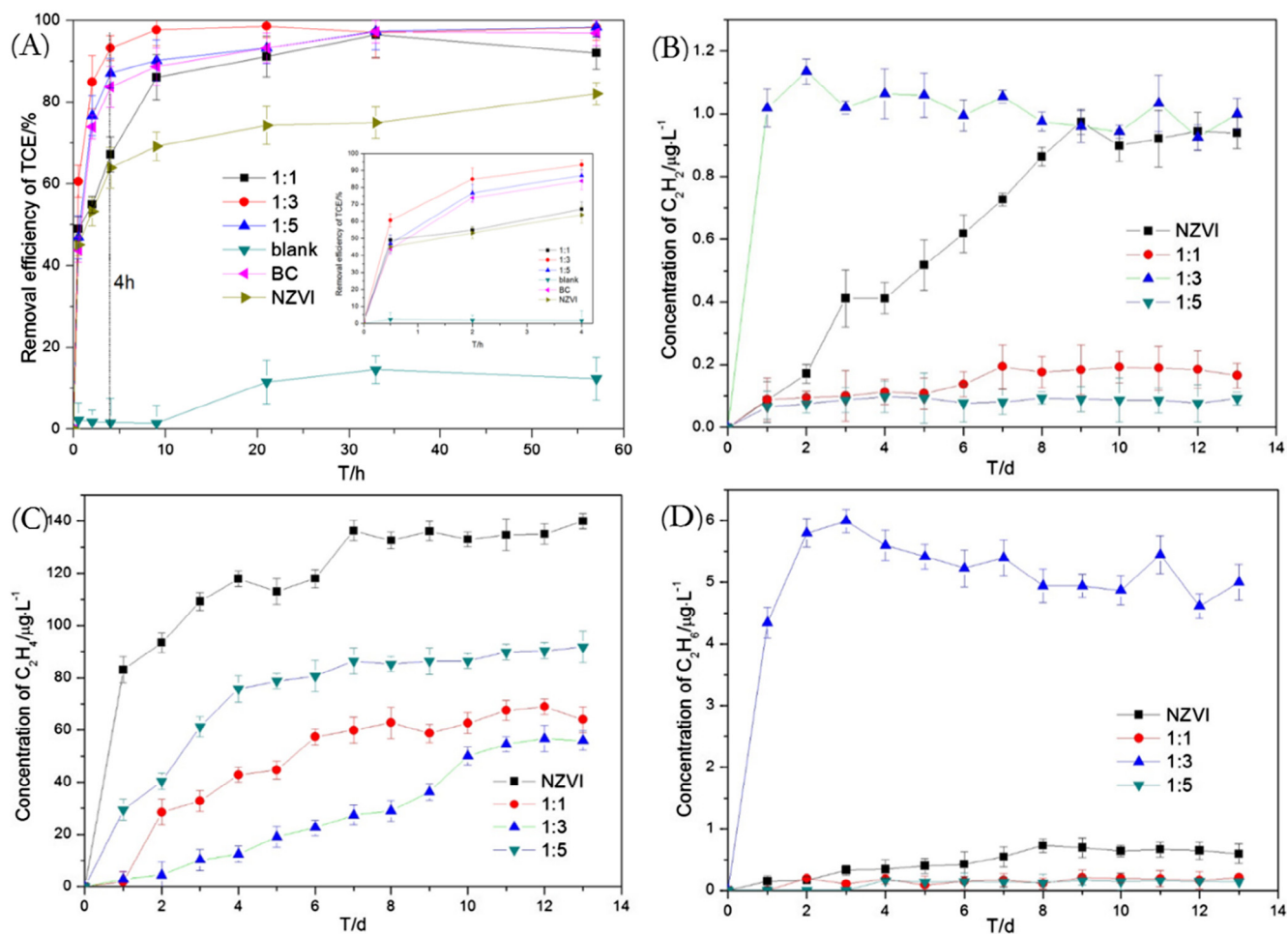


Fig. 5. Effect of mass ratio of NZVI/BC on the removal of TCE (A) and the main reaction products: (B) C_2H_2 , (C) C_2H_4 and (D) C_2H_6 . Inset figure shows the removal of TCE in the first 4-h reaction. 'Blank' refers to the sample with only TCE. (NZVI = NZVI/BC = BC = 5 g/L; TCE = 30 mg/L; pH = 6.25).

while it was able to reach 83.78% for biochar alone. The removal efficiency of TCE were 67.22%, 93.29% and 87.11% for NZVI/BC_(1:1), NZVI/BC_(1:3) and NZVI/BC_(1:5), respectively, within 4-h reaction time. However, with prolonged reaction time, the final removal efficiency of TCE for the different NZVI/BC materials could reach more than 96%, while the pure NZVI could only reach 82%. The NZVI/BC_(1:1) showed a slower TCE removal than that of NZVI/BC_(1:3) and NZVI/BC_(1:5), which might be ascribed to the larger amount of NZVI distributed on the surface of biochar occupied the sorption sites for TCE. However, the removal efficiency of TCE by NZVI/BC_(1:5) (87.11%) was slightly lower than that of NZVI/BC_(1:3) (93.28%) within 4-h reaction time. It was deduced that the excessive biochar might block the active sites on the NZVI surfaces, inhibiting the redox reaction of TCE with NZVI. Besides, the larger biochar loading provided more pore structures, which might result in the distribution of more NZVI particles onto the inner surfaces of pore structures of biochar (as displayed in Fig. 1D), having a lower probability to react with the TCE in the bulk solution [24]. As a result, the mass ratio of NZVI/BC at 1:3 achieved the best removal efficiency of TCE in this experiment.

3.2.3. Analysis of final products of TCE degradation at different mass ratios of NZVI/BC

At different mass ratios of NZVI and BC, the concentrations of the main final products of TCE degradation (i.e., ethane, ethylene and acetylene) were detected and shown in Fig. 5B–D. It was found that the concentrations of the gas products were trivial within

hours of reaction, although TCE was rapidly removed by NZVI and NZVI/BC within hours (Fig. 5A). This indicates that the rapid TCE removal in the first few hours was due to the adsorption rather than degradation. To probe the kinetics of TCE degradation, the reactions were prolonged to 13 days (Fig. 5B–D). The results showed that the NZVI/BC could instantaneously sorb >90% of TCE from aqueous solutions and then decomposed TCE into non-chlorinated products gradually. Based on the proposed dechlorination mechanisms of TCE by NZVI in previous studies [18,38,39], the dechlorination process of TCE by NZVI/BC may react as follows: ① adsorption of TCE on biochar, ② β -elimination for TCE, ③ hydrogenolysis reaction for chloroacetylene, ④ hydrogenation reaction for acetylene, and ⑤ hydrogenation reaction for ethylene. Although the dechlorination reactions certainly involve some other intermediate steps, only the dominated dechlorination processes of TCE were discussed in this paper. In addition, compared with the study by Gao et al. [18] who found the degradation products of TCE are mainly C3–C6 compounds, the primary products in this research are ethylene, ethane and acetylene which are all C2 compounds. As illustrated in Fig. 5, the concentrations of final products (ethane, ethylene and acetylene) were detected quantitatively. Due to the high reactivity of chloroacetylene and other intermediates, they could only be detected qualitatively. As demonstrated in Fig. 5B–D, the main reaction product was ethylene for all reactions. The concentrations of acetylene and ethane were relatively low, which might result from the incompleteness of the hydrogenation reaction and the relative stable chemical properties of ethylene.

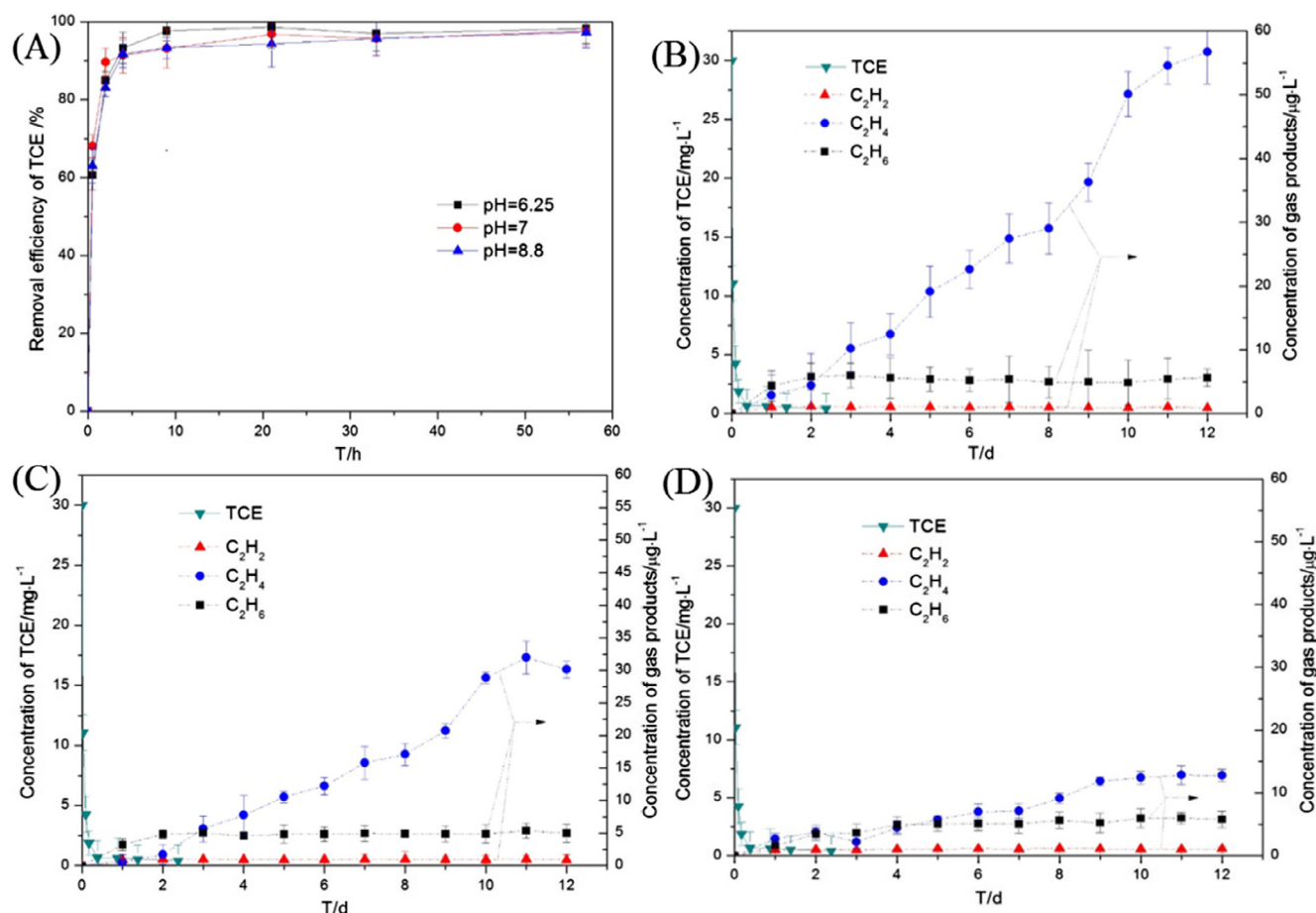


Fig. 6. Effect of pH on the removal of TCE by NZVI/BC (A); and the main reaction products at different pH: (B) pH = 6.25, (C) pH = 7, (D) pH = 8.8 (NZVI/BC = 5 g/L; TCE = 30 mg/L).

Thus, the higher concentration of ethane observed in the reaction between TCE and NZVI/BC_(1:3) reveals a more complete degradation of TCE. In Fig. 5A, it can be noticed that bare BC and NZVI/BC had a better removal efficiency of TCE than bare NZVI. Moreover, although the mass of the NZVI in the NZVI/BC system is decreasing with decreasing mass ratio of NZVI/BC, the degree of TCE degradation presents a positive relationship with the mass of biochar, of which total concentrations of final products were 89, 62, 60 µg/L with NZVI/BC_(1:5), NZVI/BC_(1:3), NZVI/BC_(1:1), respectively according to Fig. 5(B,C,D). The results indicate that the biochar can not only facilitate the adsorption of TCE, but also promote the degradation of TCE. Nevertheless, the degradation results by NZVI/BC were all much lower than bare NZVI which was 141 µg/L. On the basis of previous research [18,38,39], the above results might be due to three reasons: (i) NZVI played a dominant role in the degradation of TCE, which is the reason why the bare NZVI showed the best degradation efficiency of TCE; (ii) biochar might also play an important role (e.g., as adsorbent and electron shuttle [29]) in NZVI/BC system, which is the reason why the degradation efficiency of NZVI/BC_(1:5), NZVI/BC_(1:3), and NZVI/BC_(1:1) gradually decreased (i.e., with the decrease of biochar mass); (iii) in NZVI/BC system, a certain proportion of biochar could also hinder the contact of NZVI with TCE which was adsorbed by biochar and the decrease of the mass of NZVI in NZVI/BC system led to a decrease of TCE degradation compared with bare NZVI.

In addition, it should be noted that although the generation of intermediates were not qualified, they were detected from all the reactions between TCE and NZVI/BC. A high level of intermediate

products were detected in the first day for all the materials including NZVI/BC_(1:5), NZVI/BC_(1:3), NZVI/BC_(1:1) and bare NZVI, however, the amount of intermediate products generated by NZVI/BC_(1:5) and NZVI/BC_(1:3) began to decrease respectively from the second and the fourth day, while it still maintained a high level throughout the experiment with pure NZVI and NZVI/BC_(1:1). The results also explained why the final degradation products of NZVI/BC_(1:1) were less than NZVI/BC_(1:3) and NZVI/BC_(1:5), although it contained more NZVI. In the case of NZVI/BC_(1:1), it was presumed that a proportion of TCE was only partially degraded to intermediate products, which could not be further degraded.

3.2.4. Effect of pH on the removal of TCE by NZVI/BC

As illustrated in Fig. 6(A), TCE removal by NZVI/BC_(1:3) was studied at different pH values (6.25, 7 and 8.8). It was found that the removal efficiencies of TCE by NZVI/BC_(1:3) were 93.28%, 91.33% and 91.74% at pH 6.25, 7 and 8.8, respectively, within 4 h, which did not have a big difference. Nevertheless, the analysis of final products in Fig. 6(B–D) proved that the degradation efficiency of TCE decreased with the increasing pH values. In addition, the concentrations of main final products (acetylene, ethylene and ethane) had a diverse tendency at different pH values. According to Fig. 6, it is obvious the yield of ethylene was disparate at different pH values, whereas the yields of acetylene and ethane were similar. The concentration of ethylene could be achieved to 56 µg/L at pH 6.25, which were only 31.9 µg/L and 12.8 µg/L at pH 7 and 8.8, respectively, what is to say, the production of ethylene appeared a negative relationship with pH. Those phenomena might be accounted for (i) the sorption of TCE on biochar played a primary

role in the removal of TCE, and was less dependent on pH; (ii) the degradation of TCE was determined by NZVI, and was dependent on pH. Obviously, H^+ can promote the corrosion of iron oxide on the surface of NZVI and inhibit the passivation of NZVI [40,41], which would facilitate the reductive β -elimination and hydrogenation reaction for TCE [18,38,39,42].

4. Conclusion

Herein, we discussed the effects of the pyrolysis temperature of biochar (BC), the mass ratios of NZVI to BC and the solution pH on the removal of TCE by NZVI/BC. It was found that the pyrolysis temperature (500, 600 and 700 °C) of BC had an influence on the removal of TCE due to the fact that the physicochemical properties of BC varied at different pyrolysis temperatures, which can impact the sorption of TCE on BC. And the TCE removal efficiency reached a maximum with biochar pyrolysed at 600 °C. Besides, the mass ratio of NZVI to BC (1:5, 1:3 and 1:1) greatly influenced the removal of TCE and the generation of final products. A synergistic effect was found in NZVI/BC system, in which BC contributed to the sorption of TCE and NZVI contributed to the degradation of TCE. The results showed that TCE achieved a maximum value in degradation as well gained a high removal efficiency when the mass ratio of NZVI/BC was 1:5. However, A more thorough degradation was noticed when the mass ratio of NZVI to BC was 1:3. The solution pH has little influence on the removal efficiency of TCE but significantly influenced the yield of final products generated from TCE degradation. The results showed that the production of ethylene decreased with the increasing of pH, while ethane and acetylene were kept at relatively low concentrations.

Acknowledgments

This research was supported by the National Natural Science Foundation of China (51409100, 51521006, 51378190), the Fundamental Research Funds for the Central Universities and the Program for Changjiang Scholars and Innovative Research Team in University (IRT-13R17).

References

- [1] Z. Wei, Y. Seo, Trichloroethylene (TCE) adsorption using sustainable organic mulch, *J. Hazard. Mater.* 181 (2010) 147–153.
- [2] T. Seyama, K. Adachi, S. Yamazaki, Kinetics of photocatalytic degradation of trichloroethylene in aqueous colloidal solutions of TiO₂ and WO₃ nanoparticles, *J. Photochem. Photobiol. A Chem.* 249 (2012) 15–20.
- [3] X. Yu, T. Wu, X. Yang, J. Xu, J. Auzam, R. Semiat, Han Yf, Degradation of trichloroethylene by hydrodechlorination using formic acid as hydrogen source over supported Pd catalysts, *J. Hazard. Mater.* 305 (2015) 178–189.
- [4] K. Klasson, L. Wartelle, I. Lima, W. Marshall, D. Akin, Activated carbons from flax shive and cotton gin waste as environmental adsorbents for the chlorinated hydrocarbon trichloroethylene, *Biores. Technol.* 100 (2009) 5045–5050.
- [5] Y.J. Jo, J.Y. Lee, M.J. Yi, H.S. Kim, K.K. Lee, Soil contamination with TCE in an industrial complex: contamination levels and implication for groundwater contamination, *Geosci. J.* 14 (2010) 313–320.
- [6] H.R. Dong, Q. He, G.M. Zeng, L. Tang, L.H. Zhang, Y.K. Xie, Y.L. Zeng, F. Zhao, Degradation of trichloroethene by nanoscale zero-valent iron (nZVI) and nZVI activated persulfate in the absence and presence of EDTA, *Chem. Eng. J.* 316 (2017) 410–418.
- [7] C. Collins, F. Laturnus, A. Nepovim, Remediation of BTEX and trichloroethene, *Environ. Sci. Pollut. Res.* 9 (2002) 86–94.
- [8] F. Schaumburg, Banning trichloroethylene: Responsible reaction or overkill?, *Environ. Sci. Technol.* 24 (2005) 17–22.
- [9] X. Liang, Y. Dong, T.R. Kuder, R.P. Philp, E.C. Butler, Distinguishing abiotic and biotic transformation of tetrachloroethylene and trichloroethylene by stable carbon isotope fractionation, *Environ. Sci. Technol.* 41 (2007) 7094–7100.
- [10] K.V. Volč, J. Hoffmann, J. Růžička, M. Sergejevov, Trichloroethylene (TCE) removal in a single pulse suspension bioreactor, *J. Environ. Manage.* 74 (2005) 293–304.
- [11] H.B. Shao, E.C. Butler, The relative importance of abiotic and biotic transformation of carbon tetrachloride in anaerobic soils and sediments, *Soil Sediment Contamination Int. J.* 268 (2009) 455–469.
- [12] M. Ahmad, S.S. Lee, X. Dou, D. Mohan, J.K. Sung, J.E. Yang, Y.S. Ok, Effects of pyrolysis temperature on soybean stover- and peanut shell-derived biochar properties and TCE adsorption in water, *Bioresour. Technol.* 118 (2012) 536–544.
- [13] G. Chen, G.E. Hoag, P. Chedda, F. Nadim, B.A. Woody, G.M. Dobbs, The mechanism and applicability of in situ oxidation of trichloroethylene with Fenton's reagent, *J. Hazard. Mater.* 87 (2001) 171–186.
- [14] S.R. Rajajayavel, S. Ghoshal, Enhanced reductive dechlorination of trichloroethylene by sulfidated nanoscale zerovalent iron, *Water Res.* 78 (2015) 144–153.
- [15] H.R. Dong, K. Ahmad, G.M. Zeng, Z.W. Li, G.Q. Chen, Q. He, Y.K. Xie, Y.N. Wu, F. Zhao, Y.L. Zeng, Influence of fulvic acid on the colloidal stability and reactivity of nanoscale zero-valent iron, *Environ. Pollut.* 211 (2016) 363–369.
- [16] F. He, D. Zhao, C. Paul, Field assessment of carboxymethyl cellulose stabilized iron nanoparticles for in situ destruction of chlorinated solvents in source zones, *Water Res.* 44 (2010) 2360–2370.
- [17] D. O'Carroll, B. Sleep, K. Magdalena, B. Hardiljeet, K. Christopher, Nanoscale zero valent iron and bimetallic particles for contaminated site remediation, *Adv. Water Resour.* 51 (2013) 104–122.
- [18] J. Gao, W. Wang, A.J. Rondinone, F. He, L. Liang, Degradation of trichloroethene with a novel ball milled Fe-C nanocomposite, *J. Hazard. Mater.* 300 (2015) 443–450.
- [19] H.R. Dong, Q. He, G. Zeng, L. Tang, C. Zhang, Y. Xie, Y. Zeng, F. Zhao, Y. Wu, Chromate removal by surface-modified nanoscale zero-valent iron: Effect of different surface coatings and water chemistry, *J. Colloid Interface Sci.* 471 (2016) 7–13.
- [20] H.R. Dong, Y. Xie, G. Zeng, L. Tang, J. Liang, Q. He, F. Zhao, Y. Zeng, Y. Wu, The dual effects of carboxymethyl cellulose on the colloidal stability and toxicity of nanoscale zero-valent iron, *Chemosphere* 144 (2016) 1682–1689.
- [21] Y.K. Xie, H.R. Dong, Guangming Zeng, Lin Tang, Zhao Jiang, Cong Zhang, Junmin Deng, Lihua Zhang, Yi Zhang, The interactions between nanoscale zero-valent iron and microbes in the subsurface environment: a review, *J. Hazard. Mater.* 321 (2017) 390–407.
- [22] L.N. Shi, X. Zhang, Z.L. Chen, Removal of chromium (VI) from wastewater using bentonite-supported nanoscale zero-valent iron, *Water Res.* 45 (2) (2011) 886–892.
- [23] E. Petala, K. Dimos, A. Douvalis, T. Bakas, J. Tucek, R. Zbořil, M.A. Karakassides, Nanoscale zero-valent iron supported on mesoporous silica: characterization and reactivity for Cr(VI) removal from aqueous solution, *J. Hazard. Mater.* 261 (13) (2013) 295–306.
- [24] H. Zhu, Y. Jia, X. Wu, H. Wang, Removal of arsenic from water by supported nano zero-valent iron on activated carbon, *J. Hazard. Mater.* 172 (2–3) (2009) 1591–1596.
- [25] H.R. Dong, J.M. Deng, Y.K. Xie, C. Zhang, Z. Jiang, Y.J. Cheng, K.J. Hou, G.M. Zeng, Stabilization of nanoscale zero-valent iron (nZVI) with modified biochar for Cr (VI) removal from aqueous solution, *J. Hazard. Mater.* 332 (2017) 79–86.
- [26] X. Cao, W. Harris, Properties of dairy-manure-derived biochar pertinent to its potential use in remediation, *Biores. Technol.* 101 (2010) 5222–5228.
- [27] M. Ahmad, S.S. Lee, A.U. Rajapaksha, M. Vitthanage, M. Zhang, J.S. Cho, S.E. Lee, Y.S. Ok, Trichloroethylene adsorption by pine needle biochars produced at various pyrolysis temperatures, *Biores. Technol.* 143 (2013) 615–622.
- [28] J.E. Kilduff, T. Karanfil, Trichloroethylene adsorption by activated carbon preloaded with humic substances: effects of solution chemistry, *Water Res.* 36 (2002) 1685–1698.
- [29] H. Tang, D. Zhu, T. Li, H. Kong, W. Chen, Reductive dechlorination of activated carbon-adsorbed trichloroethylene by zero-valent iron: carbon as electron shuttle, *J. Environ. Qual.* 40 (6) (2011) 1878–1885.
- [30] L. Han, S. Xue, S. Zhao, J. Yan, L. Qian, M. Chen, Biochar supported nanoscale iron particles for the efficient removal of methyl orange dye in aqueous solutions, *PLoS one* 10 (2015) e0132067.
- [31] H.R. Dong, Feng Zhao, Qi He, Yankai Xie, Yalan Zeng, Lihua Zhang, Lin Tang, Guangming Zeng, Physicochemical transformation of carboxymethyl cellulose-coated zero-valent iron nanoparticles (nZVI) in simulated groundwater under anaerobic conditions, *Sep. Purif. Technol.* 175 (2017) 376–383.
- [32] R.A. Brown, A.K. Kercher, T.H. Nguyen, Production and characterization of synthetic wood chars for use as surrogates for natural sorbents, *Org. Geochem.* 37 (2006) 321–333.
- [33] A. Downie, A. Crosky, P. Munroe, Physical properties of biochar: Science and Technology, Publisher, Earthscan, London, 2009, pp. 13–32.
- [34] F. Rouquerol, J. Rouquerol, K. Sing, Assessment of microporosity, in: *Adsorption by Powder Sand Porous Solids*, Academic Press, London, 1999, pp. 219–236.
- [35] B.L. Chen, D.D. Zhou, L.Z. Zhu, Transitional adsorption and partition of nonpolar and polar aromatic contaminants by biochars of pine needles with different pyrolytic temperatures, *Environ. Sci. Technol.* 42 (2008) 5137–5143.
- [36] C. Lattao, X.Y. Cao, J.D. Mao, K. Schmidt-Rohr, J.J. Pignatello, Influence of molecular structure and adsorbent properties on sorption of organic compounds to a temperature series of wood chars, *Environ. Sci. Technol.* 48 (2014) 4790–4798.
- [37] S.Y. Oh, Y.D. Seo, Factors affecting sorption of nitro explosives to biochar: pyrolysis temperature, surface treatment, competition, and dissolved metals, *J. Environ. Qual.* 44 (2015) 833–840.
- [38] W.A. Arnold, A.L. Roberts, Pathways and kinetics of chlorinated ethylene and chlorinated acetylene reaction with Fe(0) particles, *Environ. Sci. Technol.* 34 (2000) 1794–1805.

- [39] Y. Liu, G.V. Lowry, Effect of particle age (Fe0 content) and solution pH on NZVI reactivity: H₂ evolution and TCE dechlorination, *Environ. Sci. Technol.* 40 (2006) 6085–6090.
- [40] H.R. Dong, F. Zhao, G.M. Zeng, L. Tang, C.Z. Fan, L.H. Zhang, Y.L. Zeng, Q. He, Y.K. Xie, Y.N. Wu, Aging study on carboxymethyl cellulose-coated zero-valent iron nanoparticles in water: Chemical transformation and structural evolution, *J. Hazard. Mater.* 312 (2016) 234–242.
- [41] Y.K. Xie, H.R. Dong, G.M. Zeng, L.H. Zhang, Y.J. Cheng, K.J. Hou, Z. Jiang, C. Zhang, J.M. Deng, The comparison of Se(IV) and Se(VI) sequestration by nanoscale zero-valent iron in aqueous solutions: The roles of solution chemistry, *J. Hazard. Mater.* 338 (2017) 306–312.
- [42] Matheson LJ And, P.G. Tratnyek, Reductive Dehalogenation of Chlorinated Methanes by Iron Metal, *Environ. Sci. Technol.* 28 (1994) 2045–2053.



Effects of pyrolysis temperature on soybean stover- and peanut shell-derived biochar properties and TCE adsorption in water

Mahtab Ahmad^a, Sang Soo Lee^a, Xiaomin Dou^b, Dinesh Mohan^c, Jwa-Kyung Sung^d, Jae E Yang^a, Yong Sik Ok^{a,*}

^a Korea Biochar Research Center, Department of Biological Environment, Kangwon National University, Chuncheon 200-701, Republic of Korea

^b Department of Environmental Science and Engineering, Beijing Forestry University, P.O. Box 60, Beijing 100083, PR China

^c School of Environmental Sciences, Jawaharlal Nehru University, New Delhi 110067, India

^d National Academy of Agricultural Science, RDA, Suwon 441-707, Republic of Korea

HIGHLIGHTS

- ▶ Pyrolysis temperature influenced crop residue-derived biochar (BC) properties.
- ▶ High pyrolysis temperature led to increased surface area and aromaticity of BC.
- ▶ TCE adsorption capacity was related to aromaticity and polarity of BC.

ARTICLE INFO

Article history:

Received 20 January 2012

Received in revised form 9 May 2012

Accepted 11 May 2012

Available online 18 May 2012

Keywords:

Crop residue

Biomass

Carbonization

Proximate analysis

Agricultural waste

ABSTRACT

Conversion of crop residues into biochars (BCs) via pyrolysis is beneficial to environment compared to their direct combustion in agricultural field. Biochars developed from soybean stover at 300 and 700 °C (S-BC300 and S-BC700, respectively) and peanut shells at 300 and 700 °C (P-BC300 and P-BC700, respectively) were used for the removal of trichloroethylene (TCE) from water. Batch adsorption experiments showed that the TCE adsorption was strongly dependent on the BCs properties. Linear relationships were obtained between sorption parameters (K_M and S_M) and molar elemental ratios as well as surface area of the BCs. The high adsorption capacity of BCs produced at 700 °C was attributed to their high aromaticity and low polarity. The efficacy of S-BC700 and P-BC700 for removing TCE from water was comparable to that of activated carbon (AC). Pyrolysis temperature influencing the BC properties was a critical factor to assess the removal efficiency of TCE from water.

© 2012 Elsevier Ltd. All rights reserved.

1. Introduction

Biochar (BC) is biomass-derived black C that has been recently recognized as a multifunctional material related to C sequestration, metal immobilization, and fertilization in soils (Awad et al., 2012; Chen et al., 2011; Uchimiya et al., 2010). Biochar is produced by thermal decomposition of biomass under a negligible or limited supply of oxygen (Novak et al., 2009). Various types of biomass including poultry litter, dairy manure, sewage sludge, and paper sludge have been used to produce BCs. The diverse natured BCs are being commonly applied to soils as conditioners; however, their use in soil and groundwater remediation is very scarce.

The proper strategies of BCs applications are needed because of the variation in BCs' characteristics. For example, the crop residues originated from agricultural byproducts are essential sources to maintain the plant nutrition cycle in soils and to sustain soil quality or crop yield (Ok et al., 2011). However, an excessive supply of crop residue also causes environmental pollution when burned directly in the field, dumped into the ocean or fertile land (Karlen et al., 2009). As a possible solution, the excessive crop residues may be transformed efficiently to bioenergy via pyrolysis. An estimated 5.7×10^5 tons of crop residue was used for biofuel production in Korea in 2009 (Kim et al., 2010). The BC being generated as a by-product during bio-oil production would offset the associated environmental problems and contribute to mitigate climate change with lower CO₂ emission (Boateng et al., 2010).

Application of BC immobilizes heavy metals and herbicides in soils (Ahmad et al., 2012a; Cao and Harris, 2010). One of the most important functions of BCs is their capability to adsorb organic pollutants from the surrounding environment (Chen et al., 2011). The

* Corresponding author. Address: Korea Biochar Research Center, Department of Biological Environment, Kangwon National University, 192-1 Hyoja 2-Dong, Chuncheon 200-701, Republic of Korea. Tel.: +82 33 250 6443; fax: +82 33 241 6640.

E-mail address: soilok@kangwon.ac.kr (Y.S. Ok).

structured C matrix with medium-to-high surface area evokes the BC to act as an adsorbent similar to activated carbon (AC) (Cao and Harris, 2010). The use of BC as an adsorbent for organic contaminants is not only economical but also readily accessible due to the wide availability of feedstock and absence of activation processes versus AC (Qiu et al., 2009). The development of porosity during carbonization may also influence the specific surface area of BC (Novak et al., 2009). However, the attempt to clarify the changes in chemical properties of BC by the preparation conditions/performance is still lacking.

Release of chlorinated hydrocarbons is a continual threat to groundwater (Yang et al., 2011). Trichloroethylene (TCE), a chlorinated hydrocarbon exists as a dense non-aqueous phase liquid. TCE is water soluble having 1.1 kg m^{-3} solubility at 25°C and is commonly used as an industrial solvent (Wei and Seo, 2010). TCE spills or improper release is not rapidly washable due to its high relative density (1460 kg m^{-3}), thereby inducing severe contamination of soil and groundwater (Jo et al., 2010). Moreover, the high resistance of TCE to biological degradation may aggravate environmental contamination (Klasson et al., 2009).

The high levels of TCE residues are frequently detected and reported in groundwater near industrial or urban areas in Korea (Lee and Lee, 2004). Baek and Lee (2010) reported that the groundwater in the industrial complex in Wonju city has been contaminated by TCE. Yu et al. (2006) indicated that the industrial complex of $300,000 \text{ m}^2$ located in Wonju city, Korea is suffering TCE contamination, indicating $\geq 1.52 \text{ mg L}^{-1}$ TCE concentration in the groundwater (vs. Korean regulation level of $\leq 0.03 \text{ mg L}^{-1}$ for residence and $\leq 0.06 \text{ mg L}^{-1}$ for industrial area). The authors revealed that a TCE plume was formed at the groundwater zone near the investigated industrial area, which reached to the bedrock aquifer. Jo et al. (2010) supported their studies and examined TCE contamination levels in soil and groundwater. They reported a maximum TCE level of 14703 mg kg^{-1} in soil and an equilibrium concentration of 19.36 mg L^{-1} in groundwater based on the distribution coefficient, which is 645 times higher than the Korean regulation level for residence. Consequently, the Korean Ministry of Environment has focused on the technology development for TCE removal in groundwater.

Various adsorbents to remediate TCE from groundwater have been reported (Erto et al., 2010; Karanfil and Dastgheib, 2004; Wei and Seo, 2010). Among them, thermally modified biomass or wood materials, namely BCs, is receiving much attention. The BCs have been considered as natural adsorbents originated from bio-source waste or residuals to remove organic contaminants from water. However, the detailed investigations are lacked to understand the mechanism or effectiveness of BCs for TCE removal. This is the first in a series of studies investigating the feasibility of BCs and factors affecting the removal of TCE from contaminated groundwater. In this study, the value-added BCs derived from soybean stover and peanut shells were tested to remediate TCE from contaminated water and were compared with commercially available AC.

2. Methods

2.1. Biomass pyrolysis for biochar production

Soybean stover and peanut shells collected from a local agricultural field in Chungju-city, Korea and household wastes, respectively, were used as raw feedstocks to produce BCs. The raw feedstocks were dried in an air-forced oven at 60°C for 3 days and ground to $<1 \text{ mm}$. The ground feedstock was placed in ceramic crucible with a lid and pyrolyzed in a muffle furnace (MF 21GS, Jeio Tech, Seoul, Korea) at 7°C min^{-1} under a limited oxygen condition.

Two different peak temperatures, i.e. 300 and 700°C , were adapted to carbonize each feedstock, where they were held for 3 h followed by cooling to room temperature inside the furnace. These subjected temperatures were selected based on the results of earlier reports (Chen et al., 2008; Chun et al., 2004). The developed BCs were stored in air-tight containers, and hereafter referred to as S-BC300, P-BC300, S-BC700, and P-BC700, where the prefix letters S and P represent soybean stover and peanut shells, respectively, and suffix numbers represent the pyrolysis temperatures.

2.2. Characterization of biochar

2.2.1. Proximate analysis

The modified thermal analysis methods by McLaughlin et al. (2009) were employed to characterize the BCs. Moisture was determined by calculating the weight loss after heating the BCs at 105°C for 24 h to a constant weight. Mobile matter (analogous to volatile matter), reflecting the non-carbonized portion in BC, was determined as the weight loss after heating in a covered crucible at 450°C for 30 min. Ash content was also measured as the residue remained after heating at 700°C in an open-top crucible. The portion of the BC that is not ash is called resident matter (analogous to fixed matter) and was calculated by the difference in moisture, ash, and mobile matter. Each sample was analyzed in duplicate.

2.2.2. Surface area and morphological analyses

Surface areas of BCs were measured from N_2 isotherms at 77 K using a gas sorption analyzer (NOVA-1200; Quantachrome Corp., Boynton Beach, FL, USA). The samples were degassed for 6 h under vacuum at 473 K prior to conducting adsorption measurements. The N_2 adsorbed per g of BC was plotted versus the relative vapor pressure (P/P_0) of N_2 ranging from 0.02 to 0.2, and the data were fitted to the Brunauer–Emmett–Teller equation (BET) to calculate surface area. Total pore volume was estimated from N_2 adsorption at $P/P_0 \sim 0.5$. The Barret–Joyner–Halender method was used to determine the pore size distribution from the N_2 desorption isotherms (Park and Komarneni, 1998).

The surface physical morphology was examined using a field emission scanning electron microscope (FE-SEM) equipped with an energy dispersive spectroscopy (SU8000, Hitachi, Tokyo, Japan). Feedstocks and BCs were placed on double-sided platinum coated tape, and images were recorded from a $50\text{-}\mu\text{m}$ area in scanning mode.

2.2.3. Spectral and elemental analyses

The spectral properties of raw feedstocks and BCs were examined by Fourier transform infrared spectroscopy (FTIR) (Bio-Rad Excalibur 3000MX spectrophotometer, Hercules, CA, USA). Spectra were obtained in a wavelength range of $600\text{--}4000 \text{ cm}^{-1}$ with 32 successive scans at a resolution of 4 cm^{-1} . The elemental composition of BCs including C, H, N, S, and O was determined by dry combustion using an elemental analyzer (EA1110, CE Instruments, Milan, Italy). These data were used to calculate molar ratios of H/C, O/C, (O + N)/C, and (O + N + S)/C.

The pH of developed BCs was estimated in a suspension of 1:5 BC/de-ionized water using a digital pH meter (Orion, Thermo Electron Corp., Waltham, MA, USA). The suspension was shaken for 1 h before measurement.

2.3. Sorption experiments

Reagent grade TCE (99% purity; Wako Pure Chemical Industries, Osaka, Japan) and hexane (95% purity; J.T. Baker Chemical Co., Phillipsburg, NJ, USA) were used. Ultra-pure water was prepared using a water purification system (Arium Pro UV/DI Water

Purification System, Sartorius Stedium Biotech, Goettingen, Germany). The TCE stock solution (100 mg L^{-1}) was prepared in ultra-pure water by mixing 24 h to ensure complete dissolution. Five different adsorbents including four lab-produced BCs and an AC (Sigma–Aldrich, St. Louis, MO, USA) were used for single-solute-adsorption experiments. Adsorption isotherms were achieved at the concentration range of $2\text{--}20 \text{ mg L}^{-1}$ TCE buffered at pH 7 with 1-mM phosphate buffer ($0.5\text{-mM Na}_2\text{HPO}_4\cdot\text{H}_2\text{O}$ and $0.5\text{-mM NaH}_2\text{PO}_4$). An adsorbent dose of 0.3 g L^{-1} was used. The adsorbent was equilibrated with TCE aqueous solutions in Teflon-lined screw capped glass vials on a horizontal shaker at 50 rpm for 48 h. All experiments were conducted at 25°C . The vials were filled to remove headspace and to minimize volatilization loss of TCE. Three replicates of each sample and blank (without sorbent) were performed (Wei and Seo, 2010).

2.4. Analytical methods

After the adsorption equilibrium time, a 5 mL aliquot from each vial was filtered through a $0.45\text{-}\mu\text{m}$ pore size syringe filter and extracted with hexane for gas chromatography (GC) analysis (HP 6890, Dallas, TX, USA). A DB-624 column (Agilent Technologies, Santa Clara, CA, USA) having a length of 30 m, an inside diameter of 0.53 mm , and a thickness of $3.0 \text{ }\mu\text{m}$ was used for volatile organic compounds. The carrier gas was N_2 and the column flow rate was 3.0 mL min^{-1} . The inlet was set to splitless mode at 250°C , and the injection volume was $3.0 \text{ }\mu\text{L}$. A flame ionization detector was used at 250°C . The initial oven temperature was 50°C , ramped to $10^\circ\text{C min}^{-1}$, and held at a 210°C final temperature for 4 min.

2.5. Adsorption models

The TCE concentration adsorbed on BCs or AC was calculated as a function of TCE concentration that remained in solution at equilibrium using the Eq. [1] (Ok et al., 2007; Wei and Seo, 2010):

$$Q_e = V/M \times [(C_o - C_e)] \quad (1)$$

where Q_e is the equilibrium TCE concentration in mg g^{-1} ; V is the volume of TCE aqueous solution in L; M is the adsorbent mass in g; C_o is the initial TCE concentration in mg L^{-1} ; and C_e is the aqueous TCE concentration at equilibrium in mg L^{-1} .

Sorption isotherms were fitted to the Freundlich (Eq. [2]) and Langmuir (Eq. [3]) equations to quantify the adsorption capacity of different BCs and AC (Jung et al., 2011).

$$\log(Q_e) = \log(K_F) + 1/n_F \log(C_e) \quad (2)$$

$$C_e/Q_e = 1/K_L S_M + C_e/S_M \quad (3)$$

where K_F is the Freundlich constant representing adsorptive capacity in $[\text{mg g}^{-1}]/[\text{mg L}^{-1}]^{1/n_F}$; n_F is the constant related to adsorption intensity; K_L is the Langmuir constant indicating binding energy in mg^{-1} ; and S_M is the maximum amount of sorption corresponding to complete surface coverage in mg g^{-1} (Wei and Seo, 2010).

The percentage TCE removed from aqueous solution by the different BCs and AC was also calculated using Eq. [4] (Ahmad et al., 2012b):

$$\% \text{TCE removed} = [(C_o - C_e)/C_o] \times 100 \quad (4)$$

2.6. Statistics

Mean values of three replicates were used to draw the isotherms and to calculate the adsorption isotherm constants. Isotherm regression curves were plotted using the linear regression. Pearson's correlation coefficient (r) and probability (P)

values were determined using the SAS ver. 9.1, (SAS Institute, Cary, NC, USA).

3. Results and discussion

3.1. Characterization of biochars

3.1.1. Proximate analysis

Moisture content, yield, ash, mobile matter, and resident matter contents of BCs derived from soybean stover and peanut shells at two different carbonization temperatures of 300 and 700°C are given in Table 1. The BC yield was reduced from 37% to 22% with increase in temperature from 300 to 700°C . This may be due to lignin and cellulose decomposition in the feedstock (Novak et al., 2009). Removing H_2O , CO_2 , CO , CH_4 , and H_2 from feedstock at $>600^\circ\text{C}$ have been known to contribute to a reduction of BC weight loss (Varhegyi et al., 1998). Resident or fixed matter in the BC is the portion corresponding to its stability in the soil, considering BC as an important source of C sequestration in soil. Resident matter is also indicative of fully carbonized organic matter (OM) in BC (Chen et al., 2008). The increase in resident matter in the BCs was 29% for soybean stover and 21% for peanut shell as temperature increases from 300 to 700°C . On the other hand, mobile matter decreases by 32% for soybean stover and 28% for peanut shell with rise in temperature from 300 to 700°C . It was mainly due to the loss of OM at high temperature. The considerable amount of resident matter in BCs reflects their ability to act as a C sink in the soil because of their slow chemical transformation and microbial decomposition, whereas the presence of mobile matter in BCs supplies organic material to soil microorganisms and improves soil quality (Lehmann et al., 2011). Ash content ranged from 1.24–17.18% in different BCs depending on feedstock types. Higher ash content of 10% and 17% in S-BC300 and S-BC700, respectively, was due to the mixed stems and blades of the soybean stover versus 1% and 10% in P-BC300 and P-BC700, respectively. Ash content increases with rise in temperature due to the concentrations of minerals and OM combustion residues (Cao and Harris, 2010).

3.1.2. Surface area and morphology

The surface area of S-BC700 ($420 \text{ m}^2 \text{ g}^{-1}$) and P-BC700 ($448 \text{ m}^2 \text{ g}^{-1}$) was extremely high compared to that of S-BC300 ($6 \text{ m}^2 \text{ g}^{-1}$) and P-BC300 ($3 \text{ m}^2 \text{ g}^{-1}$), indicating the temperatures effects on carbonization (Table 2). Spectral analyses are presented in Fig. S1 under Supplementary Data. The removal of H and O carrying functional groups of main aliphatic alkyl- CH_2 , ester C=O , aromatic $-\text{CO}$, and phenolic $-\text{OH}$ groups in BCs produced at 700°C greatly enlarges their surface areas (Chen et al., 2008). Generally, the increase in surface area at high carbonization temperature is due to the removal of volatile material resulting in increased micropore volume (Lee et al., 2010). The present findings are in agreement with this notion as shown by the pore volumes of 0.19 and $0.20 \text{ cm}^3 \text{ g}^{-1}$ for S-BC700 and P-BC700, respectively.

Solid particle morphology can be described by SEM, providing information about the structural variations in BC particles after thermal treatment. SEM images of feedstocks and BCs are shown in Fig. S2 (provided under Supplementary Data). These images were taken to compare the morphological changes in the pore structure of raw feedstocks and BCs during carbonization. The original plant cell structure was observed in the feedstocks and then reduced after carbonizing into the BCs at 700°C . A reduction in pore size, appearance of internal pores, and an increase in porosity due to the escape of volatiles during carbonization can also be observed in BCs. Additionally, the formation of channel structures in BCs may also lead to specialized pore structures.

Table 1Percentage yield, moisture, mobile matter, resident matter, and ash contents of the biochars (BCs)^a.

Sample	Yield wt.%	Moisture	Mobile matter	Resident matter	Ash
S-BC300	37.03 ± 0.48	4.50 ± 0.36	46.34 ± 2.99	38.75 ± 3.15	10.41 ± 0.52
P-BC300	36.91 ± 1.68	1.29 ± 0.12	60.47 ± 5.43	37.00 ± 5.39	1.24 ± 0.08
S-BC700	21.59 ± 0.83	0.42 ± 0.01	14.66 ± 1.68	67.74 ± 1.92	17.18 ± 0.25
P-BC700	21.89 ± 2.47	0.35 ± 0.07	32.65 ± 0.74	58.09 ± 0.59	8.91 ± 0.08

^a mean ± standard deviation in duplicate.**Table 2**

pH value (1:5 biochar/water suspension), elemental composition (moisture- and ash-free basis), molar ratio, BET surface area, and pore volume of biochars (BCs) and activated carbon (AC).

Sample	pH ^a	Elemental composition (wt %)					H/C	O/C	(O + N)/C	(O + N + S)/C	Surface area m ² g ⁻¹	Pore volume cm ³ g ⁻¹
		C	H	N	S	O						
S-BC300	7.27 ± 0.03	68.81	4.29	1.88	0.04	24.99	0.74	0.27	0.30	0.30	5.61	
P-BC300	7.76 ± 0.06	68.27	3.85	1.91	0.09	25.89	0.67	0.29	0.31	0.31	3.14	
S-BC700	11.32 ± 0.02	81.98	1.27	1.30	0.00	15.45	0.19	0.14	0.16	0.16	420.3	0.19
P-BC700	10.57 ± 0.05	83.76	1.75	1.14	0.00	13.34	0.25	0.12	0.13	0.13	448.2	0.20
AC	9.54 ± 0.06	90.85 ^b	0.90 ^b	0.00	0.00	8.24 ^b	0.12	0.07	0.07	0.07	1110	0.64

^a mean ± standard deviation in duplicate.^b values obtained from Qiu et al., 2008.

3.1.3. pH and elemental composition

The pH values and the elemental compositions of the BCs are given in Table 2. Elemental compositions were converted to moisture- and ash-free values. BCs produced at 700 °C exhibited a pH >10, which may be attributed to separation of alkali salts from the organic matrix in the feedstock (Shinogi and Kanri, 2003). The C contents of 69% and 68% in S-BC300 and P-BC300, respectively, were increased to 82% and 84% in S-BC700 and P-BC700, respectively, indicating high carbonization at high temperature. In contrast, the H, N, and O contents decreased in BCs produced at 700 °C than those produced at 300 °C. The S contents in all types of BCs were negligibly low (<0.1%). Molar ratios of elements were calculated to estimate the aromaticity (H/C) and polarity (O/C, (O + N)/C, and (O + N + S)/C) of the BCs (Uchimiya et al., 2010). Lower molar ratios were obtained in BCs produced at 700 °C. The molar H/C ratios of S-BC700 and P-BC700 were 0.19 and 0.25, respectively, showing that the BC is highly carbonized and exhibits higher aromaticity at 700 °C compared to 300 °C (Chun et al., 2004). Conversely, the relatively higher H/C ratios of S-BC300 and P-BC300 than S-BC700 and P-BC700 suggested the presence of original organic residues (Chen et al., 2008). The molar O/C ratio was also lower in S-BC700 (0.14) and P-BC700 (0.12), indicating that the surface of BCs becomes less hydrophilic at high temperature (Chun et al., 2004). In other words, the hydrophobicity of the BCs increased due to considerable removal of O content from 25% in S-BC300 to 15% in S-BC700 and from 26% in P-BC300 to 13% in P-BC700. Similar study was reported by Li et al. (2002) showing that the reduction of O at high temperature resulted in the removal of various acidic functional groups, causing the surfaces of the BCs to become more basic. The higher pH values of S-BC700 and P-BC700 compared to S-BC300 and P-BC300 also supported this finding. The ratios of (O + N)/C, as a polarity index indicator, decreased in the BCs produced at 700 °C than those produced at 300 °C. These results indicate an increased aromaticity and decreased polarity of BCs produced at 700 °C. This may be due to the formation of aromatic structures by a higher degree of carbonization of the OM and the removal of polar surface functional groups, similar to studies of Chen et al. (2008) and Uchimiya et al. (2010).

3.1.4. Spectral characteristics

FTIR spectra of BCs and their respective feedstocks are presented in Fig. S1 (Supplementary Data). Different spectra reflected

changes in the surface functional groups of BCs produced at different temperatures. Spectroscopic assignments based on Coates (2000) spectral interpretations, indicated that the band at 3337 cm⁻¹ corresponds to the stretching vibration of the -OH group of bonded water. The bands at 2922, 2854, and 1375 cm⁻¹ were assigned to -CH₂ stretching vibrations, whereas the peaks at 1734, 1616, and 1506 cm⁻¹ represented C=O stretching of the ester bond, C=C and C=O stretching in the aromatic ring, and C=C-C stretching in the aromatic ring, respectively. Aromatic C-H and C-N stretching vibrations were observed at 1242 and 1024 cm⁻¹. The peak at 871 cm⁻¹ in S-BC700 and P-BC700 was assigned to the aromatic C-H out of the plane bend, indicating the presence of adjacent aromatic hydrogen. The absorption band at 1420 cm⁻¹ in S-BC700 and P-BC700 represented the inorganic CO₃²⁻.

Specific lignin peaks at 1504–1630 cm⁻¹ decrease significantly in BCs produced at 700 °C. The broad band at 3337 cm⁻¹ indicated the strong hydrogen bonding in the feedstocks. However, the hydrogen bondings from S-BC300 and P-BC300 became weaker and it ultimately diminished in S-BC700 and P-BC700. Absorption at 2922 and 2854 cm⁻¹ suggested the presence of long linear aliphatic chain -CH₂ groups in the feedstocks, which were reduced in the S-BC300 and P-BC300, and disappeared in S-BC700 and P-BC700. These results suggested a decrease in the polar functional groups with an increase in carbonization temperature (Chen et al., 2008). The peak of the ester C=O bond at 1734 cm⁻¹ in the feedstocks disappeared in BCs, whereas the band at 1616 cm⁻¹ (aromatic C=O and C=C) remained in S-BC300 and P-BC300, and was ultimately diminished in S-BC700 and P-BC700. The maximum loss was obtained in -OH, -CH₂, and C-O functional groups in BCs produced at 700 °C, which was also apparent from their elemental composition (Table 1). Relatively low values of O, H, and H/C in S-BC700 and P-BC700 than those in S-BC300 and P-BC300 revealed the significant elimination of polar functional groups (-OH and C-O). Thermal destruction of cellulose and lignin in the feedstocks may result in the exposure of aliphatic alkyl -CH₂, hydroxyl -OH, ester C=O, and aromatic C=O functional groups in BCs (Chen et al., 2008).

Generally, the results of the BC characterization indicated that feedstocks carbonization temperature greatly influenced the BC properties. The yield, moisture, mobile matter, H, N, and O contents of BCs decreased, whereas resident matter, ash, pH, and C contents

increased with a rise in carbonization temperature from 300 to 700 °C. The O and H functional groups from the surfaces of BCs produced at 700 °C were removed, resulting in the decreases in surface acidity and polarity, and the increase in aromaticity. These findings agree with the study of Chun et al. (2004) who reported the decrease in acidity and increase in aromaticity in BC produced from wheat residue pyrolyzed at 300–700 °C. Thus, it may be speculated that the structural changes in BCs by carbonization temperature determine their adsorptive behavior towards TCE.

3.2. TCE adsorption

The adsorption isotherms for all the BCs and AC are shown in Fig. 1. Among the tested BCs, the P-BC700 has the highest Q_e (30.74 mg g⁻¹) followed by the S-BC700 (25.38 mg g⁻¹) at 9 mg L⁻¹ TCE equilibrium concentration in water, which was comparable to that of AC (34.04 mg g⁻¹) at an equilibrium concentration of 6 mg L⁻¹ TCE. However, the relatively low Q_e values of 9.85 mg g⁻¹ and 7.79 mg g⁻¹ were obtained for S-BC300 and P-BC300, respectively, at a maximum equilibrium concentration of 14 mg L⁻¹ TCE. Similarly, Klasson et al. (2009) reported 50 mg g⁻¹ loading of TCE on commercial AC (Calgon Filtrasorb 300) at an equilibrium concentration of 4 mg L⁻¹, indicating a higher TCE loading than present findings of 25 mg g⁻¹ for BCs produced at 700 °C and 30 mg g⁻¹ for AC. Wei and Seo (2010) also reported a 1.1 mg g⁻¹ Q_e value for TCE adsorption on pine mulch at a 50 mg L⁻¹ initial concentration which is lower than present findings.

Table 3 shows the Freundlich and Langmuir isotherm constants and the TCE adsorption correlation coefficients for the different BCs

Table 3

Freundlich and Langmuir isotherm constants for trichloroethylene (TCE) adsorption onto different biochars (BCs) and activated carbon (AC).

Adsorbent	Freundlich K_F (mg g ⁻¹)	$1/n_F$	R^2	Langmuir K_L (mg ⁻¹)	S_M (mg g ⁻¹)	R^2
S-BC300	3.39	0.40	0.68	0.22	12.48	0.82
P-BC300	2.35	0.46	0.66	0.13	12.12	0.51
S-BC700	12.16	0.46	0.89	0.78	31.74	0.97
P-BC700	13.65	0.36	0.77	1.23	32.02	0.98
AC	12.26	0.61	0.95	0.36	50.01	0.99

and AC. The parameter K_F in the Freundlich equation was higher for S-BC700 (12 mg g⁻¹) and P-BC700 (14 mg g⁻¹) than that of S-BC300 (3 mg g⁻¹) and P-BC300 (2 mg g⁻¹), reflecting the high adsorption capacity of BCs produced at 700 °C. The $1/n_F$ values were <1 in all cases, thereby indicating nonlinearity in the isotherms similar to other studies of Chen et al. (2008) and Uchimiya et al. (2010). The maximum adsorption capacity (S_M) as determined by the Langmuir equation was 32 mg g⁻¹ for BCs produced at 700 °C which is 2.7 times higher than that of BCs produced at 300 °C (12 mg g⁻¹), providing an evidence of a higher binding energy (K_L). The tested AC showed the greatest adsorption affinity for TCE with an S_M value of 50 mg g⁻¹. The AC has been extensively used as an adsorbent for removing TCE from water. The high efficiency of AC is related to its high surface area and microporosity as a result of thermal or chemical activation (Karanfil and Dastgheib, 2004; Klasson et al., 2009). The results showed that the Langmuir model well described the TCE adsorption on BCs and AC based on the correlation coefficients, indicating monolayer coverage of adsorbate on planar surfaces of adsorbents.

The percentage removal of TCE from water by BCs and AC is presented in Fig. 2. At the same carbonization temperature, the percentage removals of TCE were not significantly different when BCs derived from soybean stover and peanut shells were applied. At the relatively low TCE initial concentrations, P-BC700 was more effective than the other BCs and AC, which may be attributed to its high K_L value (1.23 mg⁻¹; Table 3) permitting more binding sites to attach TCE at low initial concentrations. The TCE removal efficiency of BCs or AC can be decreased with increasing initial TCE concentration due to the low availability of binding sites to attach TCE in the adsorbents (Ahmad et al., 2012b).

3.3. Interaction between BC properties and TCE adsorption

The adsorptive behavior of a sorbent for a non-ionic organic compound depends on its physical and chemical properties (Kim et al., 2012). The adsorption capacity of BCs was correlated with

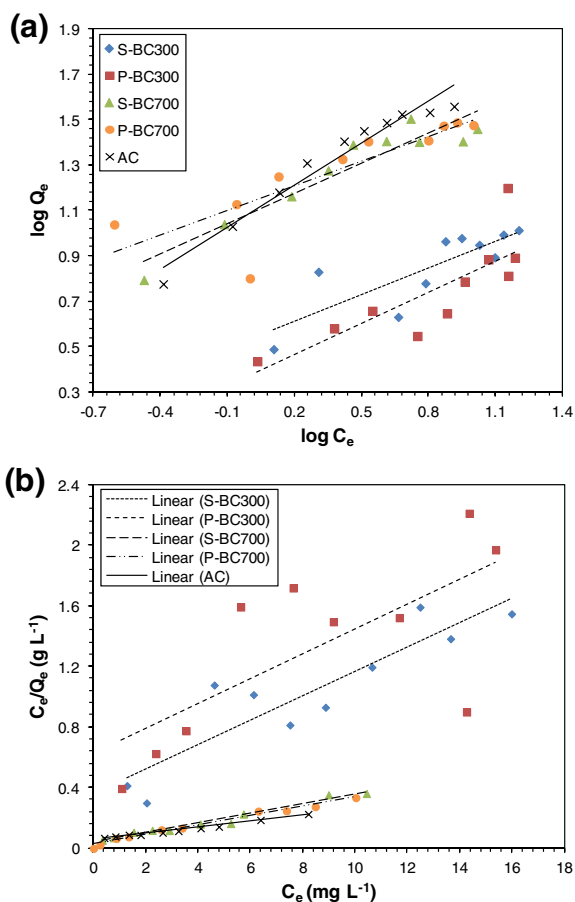


Fig. 1. Freundlich (a) and Langmuir (b) isotherms of trichloroethylene (TCE) adsorption on biochars (BCs) and activated carbon (AC).

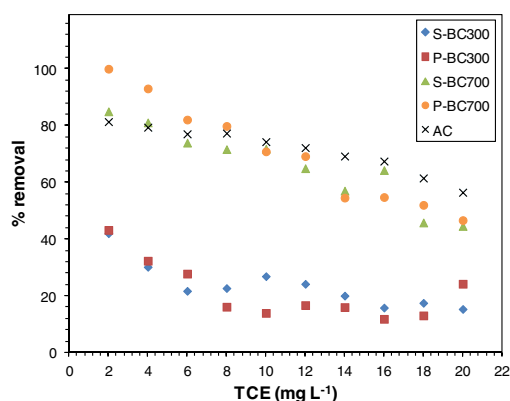


Fig. 2. Percentage removal of trichloroethylene (TCE) using biochars (BCs) and activated carbon (AC).

their properties including C and O content, molar H/C, O/C, and (O + N)/C ratios, and surface area (Fig. 3). The TCE adsorption capacities (Q_{e6}) of different BCs and AC were taken from the adsorption isotherms at a constant TCE equilibrium concentration of 6 mg L^{-1} and plotted against various sorbent properties taken from Table 2. The Q_{e6} was positively correlated with C content. The highest C content occurred with AC followed by P-BC700 and S-BC700 due to their high carbonization temperatures, and indicated the presence of more carbonized OM to serve as an adsorbent (Chen et al., 2008). In contrast, at a relatively low carbonization temperature of 300°C , the presence of non-carbonized mobile matter showed the low C contents and hindered the adsorptive properties.

The Q_{e6} was negatively correlated with the O contents of BCs and AC. As mentioned earlier, the low O content resulted in the increased hydrophobicity of S-BC700, P-BC700, and AC because of the removal of acidic functional groups favoring the adsorption

of hydrophobic TCE. The molar H/C ratio, as an indicator of aromaticity, was negatively correlated with the Q_{e6} values of BCs and AC. Adsorption of organic contaminants generally increases with aromaticity of C materials. Similar to H/C, the low molar ratios of O/C, (O + N)/C, and (O + N + S)/C promoted the TCE adsorption capacity of BCs. A decrease of polarity, as indicated by the low O/C and (O + N)/C ratios of BCs produced at 700°C and AC, greatly influenced their adsorption capacities. The polarity of the C surface is critical to determine C–H₂O interactions. Polar sites hinder the removal of hydrophobic organic contaminants such as TCE via formation of water clusters (Karanfil and Dastgheib, 2004). The O-containing functional groups adsorb water as a result of hydrogen bonding preventing the access of organic contaminant to hydrophobic sites on the C surface (Li et al., 2002). The low O contents in BCs produced at 700°C hindered the formation of water clusters and facilitated TCE adsorption. The positive correlation between the Q_{e6} values of BCs or AC and their surface area

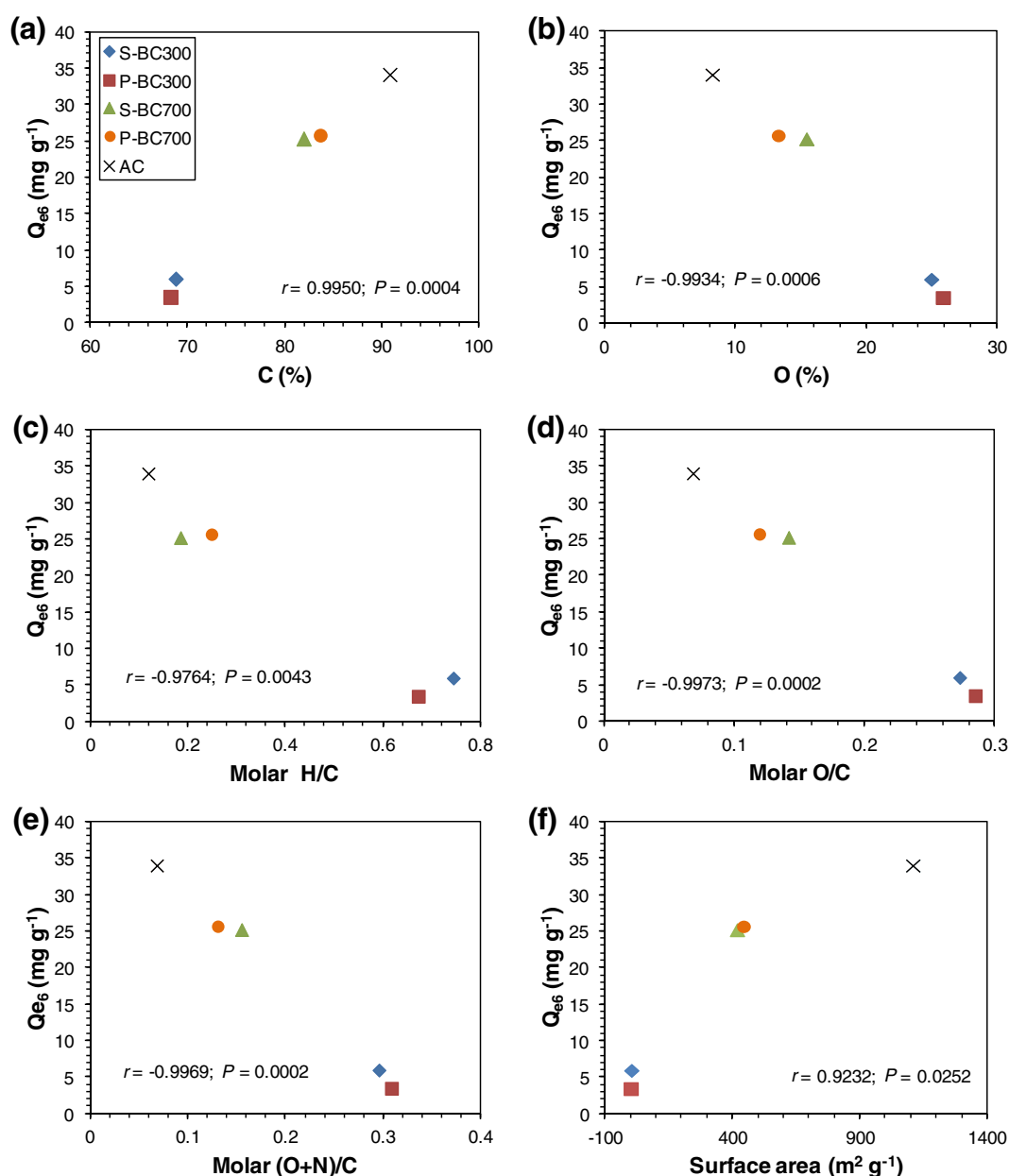


Fig. 3. Trichloroethylene (TCE) adsorption capacities of biochars (BCs) and activated carbon (AC) at 6 mg L^{-1} TCE equilibrium concentration as functions of (a) C, (b) O, (c) H/C, (d) O/C, (e) (O + N)/C, and (f) surface area.

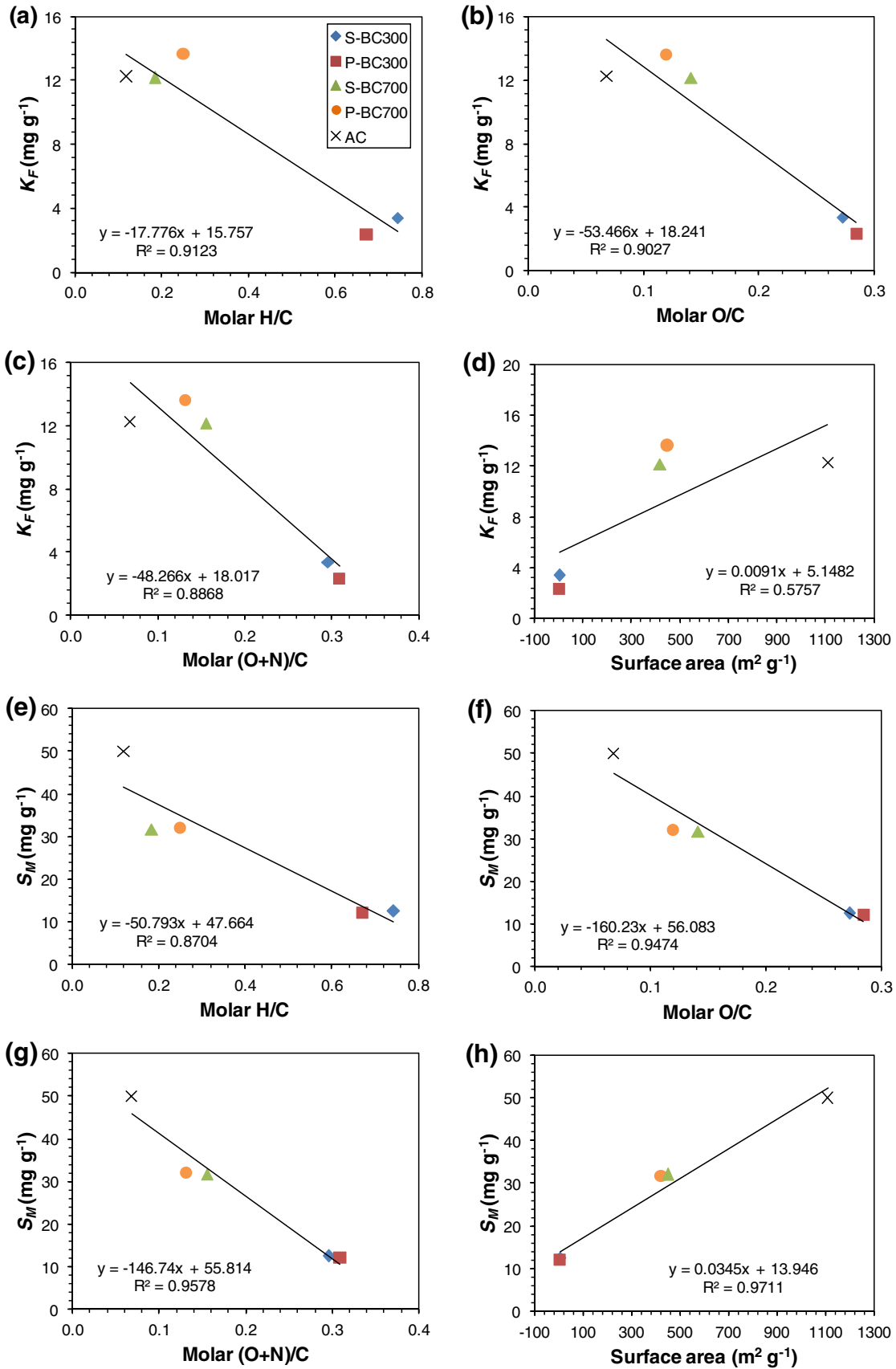


Fig. 4. Correlation among Freundlich adsorptive capacity (K_F) and Langmuir maximum adsorption capacity (S_M) versus molar ratios of H/C, O/C, (O + N)/C, and surface area of biochars (BCs) and activated carbon (AC).

indicated their interdependence. A similar dependence of adsorption capacity on surface area has been reported by Chen et al. (2008) and Erto et al. (2010). The removal of volatile matter from BCs at high temperature (700 °C) would have resulted in the development of micropores causing increased surface area leading to greater diffusion of TCE into these micropores.

To further elucidate the TCE adsorption, Freundlich adsorptive capacity (K_F) and Langmuir adsorption capacity (S_M) were plotted versus the elemental ratios and surface area of BCs and AC (Fig. 4). A linear decrease in K_F and S_M as a function of molar H/C, O/C, and (O + N)/C ratios, whereas a linear increase in K_F and S_M as a function of surface area were obtained. Specifically, the aromaticity was the best for correlation with the K_F ($R^2 = 0.91$), whereas the polarity was well fitted with the S_M ($R^2 = 0.96$). Similar linearity between sorption parameters and aromaticity was reported by Chen et al. (2008) and Uchimiya et al. (2010). The BC properties influenced by carbonization temperature further affected their adsorption characteristics. High aromaticity and decreased polarity of S-BC700 and P-BC700 promoted their adsorption capacities for removing TCE in water compared to S-BC300 and P-BC300.

3.4. TCE desorption

To evaluate the regeneration of BC, TCE was desorbed using *n*-hexane solvent. Details are given in the Supplementary Data. A maximum of 56% TCE desorption was observed from AC, while <20% of TCE desorption occurred from BCs (Fig. S3; Supplementary Data). Such behavior indicated that BCs have more strong binding affinity to TCE than AC and there is less release risk of adsorbed TCE from BCs than AC. Among BCs, P-BC700 and S-BC700 showed higher TCE desorption compared to P-BC300 and S-BC300, respectively. This suggested that adsorption of TCE onto BC may differ to that of AC. Possibly, diffusion processes may have limited the desorption of TCE from BC, and/or the presence of non-carbonized fraction may have shielded the pores of BC resulting in less desorption, specifically from BCs produced at low temperature of pyrolysis. However, the extended desorption experiments for long-time period using different solvents can help to verify such speculations and to further demonstrate the regeneration of BC. Nevertheless, the low cost of BC and the regeneration properties, it may be economical to use BC one time without regeneration.

3.5. Environmental implications

The use of BC as an alternative adsorbent to remediate organic contaminants could be advantageous. Production of BC is cheap compare to AC because of less energy requirements and no pre- or post-activation processes. The estimated break-even price of BC is US\$246 per ton, which is approximately 1/6 of AC (~US\$1500 per ton) (Klasson et al., 2009; McCarl et al., 2009). Additionally, BC is also obtained from bio-oil manufacturing as a byproduct, which can effectively be used as adsorbent to remediate contaminants. This will further bring down the cost of bio-oil production. Transformation of waste biomass by pyrolysis into BC can also provide a beneficial way to reuse the waste materials. In the present study, BCs produced at 700 °C were effective in removing TCE from water. Especially, the BCs at high temperature have potential to mitigate CO₂ as a greenhouse gas, resulting from their high stability in the soil. Other co-benefits of BC can be related to its application in soil where it can improve soil fertility by reducing the loss of soil nutrients and retaining moisture contents.

4. Conclusions

Carbonization temperature strongly influenced the physical and chemical properties of BCs produced from soybean stover and

peanut shells. Structural, elemental, and morphological properties were similar in BCs produced at the same temperatures. Removing oxygen-containing functional groups from BCs during carbonization resulted in increasing hydrophobicity and surface area and decreasing polarity. It also induced the condensation of the aromatic structure of BCs. Moreover, the characteristics of BC generated at different carbonization temperatures determine the behavior or capacity of TCE adsorption.

Acknowledgements

This study was supported by the Ministry of Environment, Republic of Korea as “The GAIA Project (No. 173-092-010)” and the National Research Foundation of Korea Grant funded by the Korean Government (Project No. 2009-0071439). Instrumental analysis was supported by the Korea Basic Science Institute, the Environmental Research Institute and the Central Laboratory of Kangwon National University, Korea.

Appendix A. Supplementary data

Supplementary data associated with this article can be found, in the online version, at <http://dx.doi.org/10.1016/j.biortech.2012.05.042>.

References

- Ahmad, M., Lee, S.S., Yang, J.E., Ro, H.M., Lee, Y.H., Ok, Y.S., 2012a. Effects of soil dilution and amendments (mussel shell, cow bone, and biochar) on Pb availability and phytotoxicity in military shooting range soil. *Ecotoxicol. Environ. Saf.* 79, 225–231.
- Ahmad, M., Usman, A.R.A., Lee, S.S., Kim, S.C., Joo, J.H., Yang, J.E., Ok, Y.S., 2012b. Eggshell and coral wastes as low cost sorbents for the removal of Pb²⁺, Cd²⁺ and Cu²⁺ from aqueous solutions. *J. Ind. Eng. Chem.* 18, 198–204.
- Awad, Y.M., Blagodatskaya, E., Ok, Y.S., Kuzyakov, Y., 2012. Effects of polyacrylamide, biopolymer and biochar on decomposition of soil organic matter and plants residues as determined by ¹⁴C and enzyme activities. *Eur. J. Soil Biol.* 48, 1–10.
- Baek, W., Lee, J.Y., 2010. Source apportionment of trichloroethylene in groundwater of the industrial complex in Wonju, Korea: a 15-year dispute and perspective. *Water Environ. J.* 25, 336–344.
- Boateng, A.A., Mullen, C.A., Goldberg, N.M., Hicks, K.B., Devine, T.E., Lima, I.M., McMurtrey, J.E., 2010. Sustainable production of bioenergy and biochar from the straw of high-biomass soybean lines via fast pyrolysis. *Environ. Prog. Sustain. Energy* 29, 175–183.
- Cao, X., Harris, W., 2010. Properties of dairy-manure-derived biochar pertinent to its potential use in remediation. *Bioresour. Technol.* 101, 5222–5228.
- Chen, B., Chen, Z., Lv, S., 2011. A novel magnetic biochar efficiently sorbs organic pollutants and phosphate. *Bioresour. Technol.* 102, 716–723.
- Chen, B., Zhou, D., Zhu, L., 2008. Transitional adsorption and partition of nonpolar and polar aromatic contaminants by biochars of pine needles with different pyrolytic temperatures. *Environ. Sci. Technol.* 42, 5137–5143.
- Chun, Y., Sheng, G., Chiou, C.T., Xing, B., 2004. Compositions and sorptive properties of crop residue-derived chars. *Environ. Sci. Technol.* 38, 4649–4655.
- Coates, J., 2000. Interpretation of Infrared Spectra, a Practical Approach. In: Meyers, R.A. (Ed.), *Encyclopedia of Analytical Chemistry*. John Wiley & Sons Ltd, Chichester, pp. 10815–10837.
- Erto, A., Andreozzi, R., Lancia, A., Musmarra, D., 2010. Factors affecting the adsorption of trichloroethylene onto activated carbons. *Appl. Surf. Sci.* 256, 5237–5242.
- Jo, Y.J., Lee, J.Y., Yi, M.J., Kim, H.S., Lee, K.K., 2010. Soil contamination with TCE in an industrial complex: contamination levels and implication for groundwater contamination. *Geosci. J.* 14, 313–320.
- Jung, K., Ok, Y.S., Chang, S.X., 2011. Sulfate adsorption properties of acid-sensitive soils in the Athabasca oil sands region in Alberta, Canada. *Chemosphere* 84, 457–463.
- Karanfil, T., Dastgheib, S.A., 2004. Trichloroethylene adsorption by fibrous and granular activated carbons: aqueous phase, gas phase, and water vapor adsorption studies. *Environ. Sci. Technol.* 38, 5834–5841.
- Karlen, D.L., Lal, R., Follett, R.F., Kimble, J.M., Hatfield, J.L., Miranowski, J.M., Cambardella, C.A., Manale, A., Anex, R.P., Rice, C.W., 2009. Crop residues: The rest of the story. *Environ. Sci. Technol.* 43, 8011–8015.
- Kim, J., Kim, M., Hyun, S., Kim, J.G., Ok, Y.S., 2012. Sorption of acidic organic solute onto kaolinitic soils from methanol-water mixtures. *J. Environ. Sci. Health, Part B* 47, 22–29.
- Kim, J.S., Park, S.C., Kim, J.W., Park, J.C., Park, S.M., Lee, J.S., 2010. Production of bioethanol from lignocelluloses: Status and perspectives in Korea. *Bioresour. Technol.* 101, 4801–4805.

- Klasson, K.T., Wartelle, L.H., Lima, I.M., Marshall, W.E., Akin, D.E., 2009. Activated carbons from flax shive and cotton gin waste as environmental adsorbents for the chlorinated hydrocarbon trichloroethylene. *Bioresour. Technol.* 100, 5045–5050.
- Lee, J.Y., Lee, K.K., 2004. A short note on investigation and remediation of contaminated groundwater and soil in Korea. *J. Eng. Geol.* 14, 123–130.
- Lehmann, J., Rillig, M.C., Thies, J., Maseillo, C.A., Hockaday, W.C., Crowley, D., 2011. Biochar effects on soil biota – A review. *Soil Biol. Biochem.* 43, 1812–1836.
- Li, L., Quinlivan, P.A., Knappe, D.R.U., 2002. Effects of activated carbon surface chemistry and pore size structure on the adsorption of organic contaminants from aqueous solution. *Carbon* 40, 2085–2100.
- McCarl, B.A., Peacocke, C., Chrisman, R., Kung, C.C., Sands, R.D., 2009. Economics of Biochar Production, Utilization and Greenhouse Gas Offsets. In: Lehmann, J., Joseph, A.S. (Eds.), *Biochar for Environmental Management: Science and Technology*. Earthscan, London, pp. 341–358.
- McLaughlin, H., Anderson, P.S., Shields, F.E., Reed, T.B., 2009. All biochars are not created equal and how to tell them apart. Presented at: North America Biochars Conference, 9–12 August, Boulder, CO., USA.
- Novak, J.M., Lima, I., Xing, B., Gaskin, J.W., Steiner, C., Das, K.C., Ahmedna, M., Rehrh, D., Watts, D.W., Busscher, W.J., Schomberg, H., 2009. Characterization of designer biochar produced at different temperatures and their effects on a loamy sand. *Ann. Environ. Sci.* 3, 195–206.
- Ok, Y.S., Usman, A.R.A., Lee, S.S., Abd El-Azeem, S.A.M., Choi, B., Hashimoto, Y., Yang, J.E., 2011. Effects of rapeseed residue on lead and cadmium availability and uptake by rice plants in heavy metal contaminated paddy soil. *Chemosphere* 85, 677–682.
- Ok, Y.S., Yang, J.E., Zhang, Y.S., Kim, S.J., Chung, D.Y., 2007. Heavy metal adsorption by a formulated zeolite–Portland cement mixture. *J. Hazard. Mater.* 147, 91–96.
- Park, M., Komarneni, S., 1998. Stepwise functionalization of mesoporous crystalline silica materials. *Microporous Mesoporous Mater.* 25, 75–80.
- Qiu, Y., Cheng, H., Xu, C., Sheng, G.D., 2008. Surface characteristics of crop-residue-derived black carbon and lead(II) adsorption. *Water Res.* 42, 567–574.
- Qiu, Y., Zheng, Z., Zhou, Z., Sheng, G.D., 2009. Effectiveness and mechanisms of dye adsorption on a straw-based biochar. *Bioresour. Technol.* 100, 5348–5351.
- Shinogi, Y., Kanri, Y., 2003. Pyrolysis of plant, animal and human waste: physical and chemical characterization of the pyrolysis products. *Bioresour. Technol.* 90, 241–247.
- Uchimiya, M., Wartelle, L.H., Lima, I.M., Klasson, K.T., 2010. Sorption of deisopropylatrazine on broiler litter biochars. *J. Agric. Food Chem.* 58, 12350–12356.
- Varhegyi, G., Szabó, P., Till, F., Zelei, B., 1998. TG, TG-MS, and FTIR characterization of high yield biomass charcoals. *Energy Fuels* 12, 969–974.
- Wei, Z., Seo, Y., 2010. Trichloroethylene (TCE) adsorption using sustainable organic mulch. *J. Hazard. Mater.* 181, 147–153.
- Yang, J.E., Skogley, E.O., Ok, Y.S., 2011. Carbonaceous resin capsule for vapor-phase monitoring of volatile monoaromatic hydrocarbons in soil. *Soil Sediment Contam.* 20, 205–220.
- Yu, S.Y., Chae, G.T., Jeon, K.H., Jeong, J.S., Park, J.G., 2006. Trichloroethylene contamination in fractured bedrock aquifer in Wonju, South Korea. *Bull. Environ. Contam. Toxicol.* 76, 341–348.



Biochar Application to Soils

**A Critical Scientific Review
of Effects on Soil Properties, Processes and Functions**

F. Verheijen, S. Jeffery, A.C. Bastos, M. van der Velde, I. Dias



EUR 24099 EN - 2010

The mission of the JRC-IES is to provide scientific-technical support to the European Union's policies for the protection and sustainable development of the European and global environment.

European Commission,
Joint Research Centre
Institute for Environment and Sustainability

Contact information

Address: Dr. Frank Verheijen, European Commission, Joint Research Centre, Land Management and Natural Hazards Unit, TP 280, via E. Fermi 2749, I-21027 Ispra (VA) Italy
E-mail: frank.verheijen@jrc.ec.europa.eu
Tel.: +39-0332-785535
Fax: +39-0332-786394

<http://ies.jrc.ec.europa.eu/>
<http://www.jrc.ec.europa.eu/>

Legal Notice

Neither the European Commission nor any person acting on behalf of the Commission is responsible for the use which might be made of this publication.

***Europe Direct is a service to help you find answers
to your questions about the European Union***

Freephone number (*):

00 800 6 7 8 9 10 11

(*) Certain mobile telephone operators do not allow access to 00 800 numbers or these calls may be billed.

A great deal of additional information on the European Union is available on the Internet.

It can be accessed through the Europa server <http://europa.eu/>

JRC 55799

EUR 24099 - EN
ISBN 978-92-79-14293-2
ISSN 1018-5593
DOI 10.2788/472

Luxembourg: Office for Official Publications of the European Communities

© European Communities, 2010

Reproduction is authorised provided the source is acknowledged

Title page artwork: Charcoal drawing by Marshall Short
Printed in Italy

Biochar Application to Soils

A Critical Scientific Review of Effects on Soil Properties, Processes and Functions

F. Verheijen¹, S. Jeffery¹, A.C. Bastos², M. van der Velde¹, I. Diafas¹

¹ Institute for Environment and Sustainability, Joint Research Centre (Ispra)

² Cranfield University (UK)

* Corresponding author: frank.verheijen@jrc.ec.europa.eu

ACKNOWLEDGEMENTS

The preparation of this report was an institutional initiative. We have received good support from Luca Montanarella, our soil colleagues in DG ENV provided helpful reviews and comments along the way, and two external experts reviewed the document in detail, thereby improving the quality of the final version.

This volume should be referenced as: Verheijen, F.G.A., Jeffery, S., Bastos, A.C., van der Velde, M., and Diafas, I. (2009). Biochar Application to Soils - A Critical Scientific Review of Effects on Soil Properties, Processes and Functions. EUR 24099 EN, Office for the Official Publications of the European Communities, Luxembourg, 149pp.

EXECUTIVE SUMMARY

Biochar application to soils is being considered as a means to sequester carbon (C) while concurrently improving soil functions. The main focus of this report is providing a critical scientific review of the current state of knowledge regarding the effects of biochar application to soils on soil properties, processes and functions. Wider issues, including atmospheric emissions and occupational health and safety associated to biochar production and handling, are put into context. The aim of this review is to provide a sound scientific basis for policy development, to identify gaps in current knowledge, and to recommend further research relating to biochar application to soils. See Table 1 for an overview of the key findings from this report. Biochar research is in its relative infancy and as such substantially more data are required before robust predictions can be made regarding the effects of biochar application to soils, across a range of soil, climatic and land management factors.

Definition

In this report, biochar is defined as: “charcoal (biomass that has been pyrolysed in a zero or low oxygen environment) for which, owing to its inherent properties, scientific consensus exists that application to soil at a specific site is expected to sustainably sequester carbon and concurrently improve soil functions (under current and future management), while avoiding short- and long-term detrimental effects to the wider environment as well as human and animal health.” Biochar as a material is defined as: “charcoal for application to soils”. It should be noted that the term 'biochar' is generally associated with other co-produced end products of pyrolysis such as 'syngas'. However, these are not usually applied to soil and as such are only discussed in brief in the report.

Biochar properties

Biochar is an organic material produced via the pyrolysis of C-based feedstocks (biomass) and is best described as a ‘soil conditioner’. Despite many different materials having been proposed as biomass feedstock for biochar (including wood, crop residues and manures), the suitability of each feedstock for such an application is dependent on a number of chemical, physical, environmental, as well as economic and logistical factors. Evidence suggests that components of the carbon in biochar are highly recalcitrant in soils, with reported residence times for wood biochar being in the range of 100s to 1,000s of years, i.e. approximately 10-1,000 times longer than residence times of most soil organic matter (SOM). Therefore, biochar addition to soil can provide a potential sink for C. It is important to note, however, that there is a paucity of data concerning biochar produced from feedstocks other than wood. Owing to the current interest in climate change mitigation, and the irreversibility of biochar application to soil, an effective evaluation of biochar stability in the environment and its effects on soil processes and functioning is paramount. The current state of knowledge concerning these factors is discussed throughout this report.

Pyrolysis conditions and feedstock characteristics largely control the physico-chemical properties (e.g. composition, particle and pore size distribution) of

the resulting biochar, which in turn, determine the suitability for a given application, as well as define its behaviour, transport and fate in the environment. Reported biochar properties are highly heterogeneous, both within individual biochar particles but mainly between biochar originating from different feedstocks and/or produced under different pyrolysis conditions. For example, biochar properties have been reported with cation exchange capacities (CECs) from negligible to approximately 40 cmolc g^{-1} , C:N ratios from 7 to 500 (or more). The pH is typically neutral to basic and as such relatively constant. While such heterogeneity leads to difficulties in identifying the underlying mechanisms behind reported effects in the scientific literature, it also provides a possible opportunity to engineer biochar with properties that are best suited to a particular site (depending on soil type, hydrology, climate, land use, soil contaminants, etc.).

Effects on soils

Biochar characteristics (e.g. chemical composition, surface chemistry, particle and pore size distribution), as well as physical and chemical stabilisation mechanisms of biochar in soils, determine the effects of biochar on soil functions. However, the relative contribution of each of these factors has been assessed poorly, particularly under the influence of different climatic and soil conditions, as well as soil management and land use. Reported biochar loss from soils may be explained to a certain degree by abiotic and biological degradation and translocation within the soil profile and into water systems. Nevertheless, such mechanisms have been quantified scarcely and remain poorly understood, partly due to the limited amount of long-term studies, and partly due to the lack of standardised methods for simulating biochar aging and long-term environmental monitoring. A sound understanding of the contribution that biochar can make as a tool to improve soil properties, processes and functioning, or at least avoiding negative effects, largely relies on knowing the extent and full implications of the biochar interactions and changes over time within the soil system.

Extrapolation of reported results must be done with caution, especially when considering the relatively small number of studies reported in the primary literature, combined with the small range of climatic, crop and soil types investigated when compared to possible instigation of biochar application to soils on a national or European scale. To try and bridge the gap between small scale, controlled experiments and large scale implementation of biochar application to a range of soil types across a range of different climates (although chiefly tropical), a statistical meta-analysis was undertaken. A full search of the scientific literature led to a compilation of studies used for a meta-analysis of the effects of biochar application to soils and plant productivity. Results showed a small overall, but statistically significant, positive effect of biochar application to soils on plant productivity in the majority of cases. The greatest positive effects were seen on acidic free-draining soils with other soil types, specifically calcarosols showing no significant effect (either positive or negative). There was also a general trend for concurrent increases in crop productivity with increases in pH up on biochar addition to soils. This suggests that one of the main mechanisms behind the reported positive effects of biochar application to soils on plant

productivity may be a liming effect. However, further research is needed to confirm this hypothesis. There is currently a lack of data concerning the effects of biochar application to soils on other soil functions. This means that although these are qualitatively and comprehensively discussed in this report, a robust meta-analysis on such effects is as of yet not possible. Table 0.1 provides an overview of the key findings - positive, negative, and unknown - regarding the (potential) effects on soil, including relevant conditions.

Preliminary, but inconclusive, evidence has also been reported concerning a possible priming effect whereby accelerated decomposition of SOM occurs upon biochar addition to soil. This has the potential to both harm crop productivity in the long term due to loss of SOM, as well as releasing more CO₂ into the atmosphere as increased quantities of SOM is respired from the soil. This is an area which requires urgent further research.

Biochar incorporation into soil is expected to enhance overall sorption capacity of soils towards anthropogenic organic contaminants (e.g. polycyclic aromatic hydrocarbons - PAHs, pesticides and herbicides), in a mechanistically different (and stronger) way than amorphous organic matter. Whereas this behaviour may greatly mitigate toxicity and transport of common pollutants in soils through reducing their bioavailability, it might also result in their localised accumulation, although the extent and implications of this have not been fully assessed experimentally. The potential of biochar to be a source of soil contamination needs to be evaluated on a case-by-case basis, not only with concern to the biochar product itself, but also to soil type and environmental conditions.

Implications

As highlighted above, before policy can be developed in detail, there is an urgent need for further experimental research with regard to long-term effects of biochar application on soil functions, as well as on the behaviour and fate in different soil types (e.g. disintegration, mobility, recalcitrance), and under different management practices. The use of representative pilot areas, in different soil ecoregions, involving biochars produced from a representative range of feedstocks is vital. Potential research methodologies are discussed in the report. Future research should also include biochars from non-lignin-based feedstocks (such as crop residues, manures, sewage and green waste) and focus on their properties and environmental behaviour and fate as influenced by soil conditions. It must be stressed that published research is almost exclusively focused on (sub)tropical regions, and that the available data often only relate to the first or second year following biochar application.

Preliminary evidence suggests that a tight control on the feedstock materials and pyrolysis conditions might substantially reduce the emission levels of atmospheric pollutants (e.g. PAHs, dioxins) and particulate matter associated to biochar production. While implications to human health remain mostly an occupational hazard, robust qualitative and quantitative assessment of such emissions from pyrolysis of traditional biomass feedstock is lacking.

Biochar potentially affects many different soil functions and ecosystem services, and interacts with most of the ‘threats to soil’ outlined by the Soil Thematic Strategy ([COM\(2006\) 231](#)). It is because of the wide range of implications from biochar application to soils, combined with the irreversibility of its application that more interdisciplinary research needs to be undertaken before policy is implemented. Policy should first be designed with the aim to invest in fundamental scientific research in biochar application to soil. Once positive effects on soil have been established robustly for certain biochars at a specific site (set of environmental conditions), a tiered approach can be imagined where these combinations of biochar and specific site conditions are considered for implementation first. A second tier would then consist of other biochars (from different feedstock and/or pyrolysis conditions) for which more research is required before site-specific application is considered.

From a climate change mitigation perspective, biochar needs to be considered in parallel with other mitigation strategies and cannot be seen as an alternative to reducing emissions of greenhouse gases. From a soil conservation perspective, biochar may be part of a wider practical package of established strategies and, if so, needs to be considered in combination with other techniques.

Table 0.1 Overview of key findings (numbers in parentheses refer to relevant sections)

	Description	Conditions
Positives	Empirical evidence of charcoal in soils exists (long term)	Biochar analogues (pyrogenic BC and charcoal) are found in substantial quantities in soils of most parts of the world (1.2-1.4)
	The principle of improving soils has been tried successfully in the past	Anthrosols can be found in many parts of the world, although normally of very small spatial extent. Contemplation of Anthrosol generation at a vast scale requires more comprehensive, detailed and careful analysis of effects on soils as well as interactions with other environmental components before implementation (1.2-1.3 and throughout)
	Plant production has been found to increase significantly after biochar addition to soils	Studies have been reported almost exclusively from tropical regions with specific environmental conditions, and generally for very limited time periods, i.e. 1-2 yr. Some cases of negative effects on crop production have also been reported (3.3).
	Liming effect	Most biochars have neutral to basic pH and many field experiments show an increase in soil pH after biochar application when the initial pH was low. On alkaline soils this may be an undesirable effect. Sustained liming effects may require regular applications (3.1.4)
	High sorption affinity for HOC may enhance the overall sorption capacity of soils towards these trace contaminants	Biochar application is likely to improve the overall sorption capacity of soils towards common anthropogenic organic compounds (e.g. PAHs, pesticides and herbicides), and therefore influence toxicity, transport and fate of such contaminants. Enhanced sorption capacity of a silt loam for diuron and other anionic and cationic herbicides has been observed following incorporation of biochar from crop residues (3.2.2)
	Microbial habitat and provision of refugia for microbes whereby they are protected from grazing	Biochar addition to soil has been shown to increase microbial biomass and microbial activity, as well as microbial efficiency as a measure of CO ₂ released per unit microbial biomass C. The degree of the response appears to be dependent on nutrient availability in soils

	Increases in mycorrhizal abundance which is linked to observed increases in plant productivity	Possibly due to: a) alteration of soil physico-chemical properties; b) indirect effects on mycorrhizae through effects on other soil microbes; c) plant–fungus signalling interference and detoxification of allelochemicals on biochar; or d) provision of refugia from fungal grazers (3.2.6)
	Increases in earthworm abundance and activity	Earthworms have been shown to prefer some soils amended with biochar than those soils alone. However, this is not true of all biochars, particularly at high application rates (3.2.6)
Negatives	The use of biochar analogues for assessing effects of modern biochars is very limited	Charcoal in Terra Preta soils is limited to Amazonia and have received many diverse additions other than charcoal. Pyrogenic BC is found in soils in many parts of the world but are of limited feedstock types and pyrolysis conditions (Chapter 1)
	Soil loss by erosion	Top-dressing biochar to soil is likely to increase erosion of the biochar particles both by wind (dust) and water. Many other effects of biochar in soil on erosion can be theorised, but remain untested at present (4.1)
	Soil compaction during application	Any application carries a risk of soil compaction when performed under inappropriate conditions. Careful planning and management could prevent this effect (4.6)
	Risk of contamination	Contaminants (e.g. PAHs, heavy metals, dioxins) that may be present in biochar may have detrimental effects on soil properties and functions. The occurrence of such compounds in biochar is likely to derive from either contaminated feedstocks or the use of processing conditions that may favour their production. Evidence suggests that a tight control over the type of feedstock used and lower pyrolysis temperatures (<500°C) may be sufficient to reduce the potential risk for soil contamination (3.2.4)
	Residue removal	Removal of crop residues for use as a feedstock for biochar production can forego incorporation of the crop residue into the soil, potentially leading to multiple negative effects on soils (3.2.5.5)
	Occupational health and fire hazards	Health (e.g. dust exposure) and fire hazards associated to the production, transport, application and storage of biochar need to be considered when determining the suitability for biochar application. In the context of occupational health, tight health and safety measures need to be put in place in order to reduce such risks. Some of these measures have already proved adequate (5.2)
	Reduction in earthworm survival rates (limited number of cases)	High biochar application rates of >67 t ha ⁻¹ (produced from poultry litter) were shown to have a negative effect on earthworm survival rates, possibly due to increases in pH or salt levels (3.2.6)
Unknown	Empirical evidence is extremely scarce for many modern biochars in soils under modern arable management	Biochar analogues do not exist for many feedstocks, or for some modern pyrolysis conditions. Biochar can be produced with a wide variety of properties and applied to soils with a wide variety of properties. Some short term (1-2 yr) evidence exists, but only for a small set of biochar, environmental and soil management factors and almost no data is available on long term effect (1.2-1.4)
	C Negativity	The carbon storage capacity of biochar is widely hypothesised, although it is still largely unquantified and depends on many factors (environmental, economic, social) in all parts of the life cycle of biochar and at the several scales of operation (1.5.2 and Chapter 5)
	Effects on N cycle	N ₂ O emissions depend on effects of biochar addition on soil hydrology (water-filled pore volume) and associated microbial processes. Mechanisms are poorly understood and thresholds largely unknown (1.5.2)
	Biochar Loading Capacity (BLC)	BLC is likely to be crop as well as soil dependent leading to potential incompatibilities between the irreversibility of biochar once applied to soil and changing crop demands (1.5.1)
	Environmental behaviour	The extent and implications of the changes that biochar undergoes in soil remain largely unknown. Although biochar physical-chemical

mobility and fate	properties and stabilization mechanisms may explain biochar long mean residence times in soil, the relative contribution of each factor for its short- and long-term loss has been sparsely assessed, particularly when influenced by soil environmental conditions. Also, biochar loss and mobility through the soil profile and into the water resources has been scarcely quantified and transport mechanisms remain poorly understood (3.2.1)
Distribution and availability of contaminants (e.g. heavy metals, PAHs) within biochar	Very little experimental evidence is available on the short- and long-term occurrence and bioavailability of such contaminants in biochar and biochar-enriched soil. Full and careful risk assessment in this context is urgently required, in order to relate the bioavailability and toxicity of the contaminant to biochar type and 'safe' application rates, biomass feedstock and pyrolysis conditions, as well as soil type and environmental conditions (3.2.4)
Effect on soil organic matter dynamics	Various relevant processes are acknowledged but the way these are influenced by combinations of soil-climate-management factors remains largely unknown (Section 3.2.5)
Pore size and connectivity	Although pore size distribution in biochar may significantly alter key soil physical properties and processes (e.g. water retention, aeration, habitat), experimental evidence on this is scarce and the underlying mechanisms can only be hypothesised at this stage (2.3 and 3.1.3)
Soil water retention/availability	Adding biochar to soil can have direct and indirect effects on soil water retention, which can be short or long lived, and which can be negative or positive depending on soil type. Positive effects are dependent on high applications of biochar. No conclusive evidence was found to allow the establishment of an unequivocal relation between soil water retention and biochar application (3.1.2)
Soil compaction	Various processes associated with soil compaction are relevant to biochar application, some reducing others increasing soil compaction. Experimental research is lacking. The main risk to soil compaction could probably be reduced by establishing a guide of good practice regarding biochar application (3.1.1 and 4.6)
Priming effect	Some inconclusive evidence of a possible priming effect exists in the literature, but the evidence is relatively inconclusive and covers only the short term and a very restricted sample of biochar and soil types (3.2.5.4)
Effects on soil megafauna	Neither the effects of direct contact with biochar containing soils on the skin and respiratory systems of soil megafauna are known, nor the effects or ingestion due to eating other soil organisms, such as earthworms, which are likely to contain biochar in their guts (3.2.6.3)
Hydrophobicity	The mechanisms of soil water repellency are understood poorly in general. How biochar might influence hydrophobicity remains largely untested (3.1.2.1)
Enhanced decomposition of biochar due to agricultural management	It is unknown how much subsequent agricultural management practices (planting, ploughing, etc.) in an agricultural soil with biochar may influence (accelerate) the disintegration of biochar in the soil, thereby potentially reducing its carbon storage potential (3.2.3)
Soil CEC	There is good potential that biochar can improve the CEC of soil. However, the effectiveness and duration of this effect after addition to soils remain understood poorly (2.5 and 3.1.4)
Soil Albedo	That biochar will lower the albedo of the soil surface is fairly well established, but if and where this will lead to a substantial soil warming effect is untested (3.1.3)

TABLE OF CONTENTS

ACKNOWLEDGEMENTS	4
EXECUTIVE SUMMARY	5
TABLE OF CONTENTS	11
LIST OF FIGURES	15
LIST OF TABLES	19
LIST OF ACRONYMS	21
LIST OF UNITS	23
LIST OF CHEMICAL ELEMENTS AND FORMULAS	25
LIST OF KEY TERMS	27
1. BACKGROUND AND INTRODUCTION	31
1.1 Biochar in the attention	33
1.2 Historical perspective on soil improvement	35
1.3 Different solutions to similar problems	37
1.4 Biochar and pyrogenic black carbon	37
1.5 Carbon sequestration potential	38
1.5.1 <i>Biochar loading capacity</i>	40
1.5.2 <i>Other greenhouse gasses</i>	41
1.6 Pyrolysis	42
1.6.1 <i>The History of Pyrolysis</i>	43
1.6.2 <i>Methods of Pyrolysis</i>	43
1.7 Feedstocks	45
1.8 Application Strategies	49
1.9 Summary	50
2. PHYSICOCHEMICAL PROPERTIES OF BIOCHAR	51
2.1 Structural and Chemical Composition	51
2.1.1 <i>Structural composition</i>	51
2.1.2 <i>Chemical composition and surface chemistry</i>	52
2.2 Particle size distribution	54
2.2.1 <i>Biochar dust</i>	56
2.3 Pore size distribution and connectivity	56
2.4 Thermodynamic stability	58
2.5 CEC and pH	58
2.6 Summary	58
3. EFFECTS ON SOIL PROPERTIES, PROCESSES AND FUNCTIONS	61
3.1 Properties	61
3.1.1 <i>Soil Structure</i>	61
3.1.1.1 <i>Soil Density</i>	61
3.1.1.2 <i>Soil pore size distribution</i>	63
3.1.2 <i>Water and Nutrient Retention</i>	64
3.1.2.1 <i>Soil water repellency</i>	66
3.1.3 <i>Soil colour, albedo and warming</i>	67
3.1.4 <i>CEC and pH</i>	68

3.2	Soil Processes	69
3.2.1	<i>Environmental behaviour, mobility and fate</i>	69
3.2.2	<i>Sorption of Hydrophobic Organic Compounds (HOCs)</i>	72
3.2.3	<i>Nutrient retention/availability/leaching</i>	76
3.2.4	<i>Contamination</i>	78
3.2.5	<i>Soil Organic Matter (SOM) Dynamics</i>	81
3.2.5.1	<i>Recalcitrance of biochar in soils</i>	81
3.2.5.2	<i>Organomineral interactions</i>	82
3.2.5.3	<i>Accessibility</i>	83
3.2.5.4	<i>Priming effect</i>	83
3.2.5.5	<i>Residue Removal</i>	85
3.2.6	<i>Soil Biology</i>	85
3.2.6.1	<i>Soil microbiota</i>	87
3.2.6.2	<i>Soil meso and macrofauna</i>	89
3.2.6.3	<i>Soil megafauna</i>	90
3.3	Production Function	91
3.3.1	<i>Meta-analysis methods</i>	91
3.3.2	<i>Meta-analysis results</i>	93
3.3.3	<i>Meta-analysis recommendations</i>	98
3.3.4	<i>Other components of crop production function</i>	98
3.4	Summary	98
4.	BIOCHAR AND 'THREATS TO SOIL'	101
4.1	Soil loss by erosion	101
4.2	Decline in soil organic matter	103
4.3	Soil contamination	103
4.4	Decline in soil biodiversity	105
4.6	Soil compaction	106
4.7	Soil salinisation	106
4.8	Summary	107
5.	WIDER ISSUES	109
5.1	Emissions and atmospheric pollution	109
5.2	Occupational health and safety	111
5.3	Monitoring biochar in soil	113
5.4	Economic Considerations	113
5.4.1	<i>Private costs and benefits</i>	113
5.4.2	<i>Social costs and benefits</i>	116
5.5	Is biochar soft geo-engineering?	117
5.6	Summary	118
6.	KEY FINDINGS	121
6.1	Summary of Key Findings	121
6.1.1	<i>Background and Introduction</i>	124
6.1.2	<i>Physicochemical properties of Biochar</i>	124
6.1.3	<i>Effects on soil properties, processes and functions</i>	125
6.1.4	<i>Biochar and soil threats</i>	127
6.1.5	<i>Wider issues</i>	127
6.2	Synthesis	128
6.2.1	<i>Irreversibility</i>	128
6.2.2	<i>Quality assessment</i>	128
6.2.3	<i>Scale and life cycle</i>	129

6.2.4 <i>Mitigation/adaptation</i>	129
6.3 Knowledge gaps	131
6.3.1 <i>Safety</i>	131
6.3.2 <i>Soil organic matter dynamics</i>	131
6.3.3 <i>Soil biology</i>	132
6.3.4 <i>Behaviour, mobility and fate</i>	132
6.3.5 <i>Agronomic effects</i>	133
References	135

LIST OF FIGURES

- Figure 1.1 Google Trends™ result of “biochar”, “*Terra Preta*” and “black earth”. The scale is based on the average worldwide traffic of “biochar” from January 2004 until June 2009 (search performed on 04/12/2009) 33
- Figure 1.2 Google Trends™ geographical distribution of the search volume index of “biochar” of the last 12 months from June 2008 to June 2009 (search performed on 16/09/2009). Data is normalised against the overall search volume by country 34
- Figure 1.3 Scientific publications registred in Thompson’s ISI Web of Science indexed for either biochar or bio-char including those articles that mention charcoal (search performed on 4/12/2009) 35
- Figure 1.4 Distribution of Anthrosols in Amazonia (left; Glaser et al., 2001) and Europe (middle and right; Toth et al., 2008; Blume and Leinweber, 2004) 35
- Figure 1.5 Comparing tropical with temperate Anthrosols. The left half shows a profile of a fertile Terra Preta (Anthrosol with charcoal) created by adding charcoal to the naturally-occurring nutrient poor Oxisol (far left; photo courtesy of Bruno Glaser). The right half (far right) is a profile picture of a fertile European Plaggen Soil (Plaggic Anthrosol; photo courtesy of Erica Micheli) created by adding peat and manure to the naturally-occurring nutrient poor sandy soils (Arenosols) of The Netherlands 36
- Figure 1.6 Terms and properties of pyrogenic BC (adopted from Preston and Schmidt, 2006) 38
- Figure 1.7 Diagram of the carbon cycle. The black numbers indicate how much carbon is stored in various reservoirs, in billions of tons (GtC = Gigatons of Carbon and figures are circa 2004). The purple numbers indicate how much carbon moves between reservoirs each year, i.e. the fluxes. The sediments, as defined in this diagram, do not include the ~70 million GtC of carbonate rock and kerogen (NASA, 2008) 39
- Figure 1.9 A graph showing the relative proportions of end products after fast pyrolysis of aspen poplar at a range of temperatures (adapted from IEA, 2007) 44
- Figure 2.1 Putative structure of charcoal (adopted from Bourke et al., 2007). A model of a microcristalline graphitic structure is shown on on the left and an aromatic structure containing oxygen and carbon free radicals on the right 51

- Figure 3.1 Typical representation of the soil water retention curve as provided by van Genuchten (1980) and the hypothesized effect of the addition of biochar to this soil 66
- Figure 3.2 The percentage change in crop productivity upon application of biochar at different rates, from a range of feedstocks along with varying fertiliserco-amendments. Points represent mean and bars represent 95% confidence intervals. Numbers next to bars denote biochar application rates ($t\ ha^{-1}$). Numbers in the two columns on the right show number of total 'replicates' upon which the statistical analysis is based (**bold**) and the number of 'experimental treatments' which have been grouped for each analysis (*italics*) 93
- Figure 3.3 Percentage change in crop productivity upon application of biochar at different rates along with varying fertiliserco-amendments grouped by change in pH caused by biochar addition to soil. Points represent mean and bars represent 95% confidence intervals. Values next to bars denote change in pH value. Numbers in the two columns on the right show number of total 'replicates' upon which the statistical analysis is based (**bold**) and the number of 'experimental treatments' which have been grouped for each analysis (*italics*) 94
- Figure 3.4 The percentage change in crop productivity o upon application of biochar at different rates along with varying fertiliserco-amendments to a range of different soils. Points shows mean and bars so 95% confidence intervals. Numbers in the two columns on the right show number of total 'replicates' upon which the statistical analysis is based (**bold**) and the number of 'experimental treatments' which have been grouped for each analysis (*italics*) 95
- Figure 3.5 The percentage change in crop productivity of either the biomass or the grain upon application of biochar at different rates along with varying fertiliserco-amendments. Points shows mean and bars so 95% confidence intervals. Numbers in the two columns on the right show number of total 'replicates' upon which the statistical analysis is based (**bold**) and the number of 'experimental treatments' which have been grouped for each analysis (*italics*) 96
- Figure 3.6 The percentage change in crop productivity upon application of biochar along with a co-amendment of organic fertiliser(o), inorganic fertiliser(I) or no fertiliser(none). Points shows mean and bars so 95% confidence intervals. Numbers in the two columns on the right show number of total 'replicates' upon which the statistical analysis is based (**bold**) and the number of 'experimental treatments' which have been grouped for each analysis (*italics*) 97
- Figure 5.1 Effect of transportation distance in biochar systems with bioenergy production using the example of late stover feedstock (high

revenue scenario) on net GHG, net energy and net revenue
(adopted from Roberts et al., 2009)

LIST OF TABLES

Table 0.1	Overview of key findings	
Table 1.1	The mean post-pyrolysis feedstock residues resulting from different temperatures and residence times (adapted from IEA, 2007)	45
Table 1.2	Summary of key components (by weight) in biochar feedstocks (adapted from Brown et al., 2009)	46
Table 1.3	Examples of the proportions of nutrients (g kg^{-1}) in feedstocks (adapted from Chan and Xu, 2009)	47
Table 2.1	Relative proportion range of the four main components of biochar (weight percentage) as commonly found for a variety of source materials and pyrolysis conditions (adapted from Brown, 2009; Antal and Gronli, 2003)	52
Table 2.2	Summary of total elemental composition (C, N, C:N, P, K, available P and mineral N) and pH ranges and means of biochars from a variety of feedstocks (wood, green wastes, crop residues, sewage sludge, litter, nut shells) and pyrolysis conditions ($350\text{-}500^\circ\text{C}$) used in various studies (adapted from Chan and Xu, 2009)	53
Table 3.1	Pore size classes in material science vs. soil science	63
Table 6.1	Overview of key findings	121

LIST OF ACRONYMS

BC	Black carbon
CEC	Cation Exchange Capacity
DOM	Dissolved Organic Matter
HOCs	Hydrophobic Organic Compounds
NOM	Natural (or Native) Organic Matter
NPs	Nanoparticles
OM	Organic Matter
PAHs	Polycyclic Aromatic Hydrocarbons
PCDD/PCDFs	Dioxins and furans
(S)OC	(Soil) Organic Carbon
SOM	Soil Organic Matter
SWR	Soil Water Repellency
VOCs	Volatile Organic Compounds

LIST OF UNITS

μm	Micrometer ($= 10^{-6} \text{ m}$)
Bar	1 bar = 100 kPa = 0.987 atm
$\text{Cmol}_c \text{ g}^{-1}$	Centimol of charge ($1 \text{ cmol kg}^{-1} = 1 \text{ meq } 100\text{g}^{-1}$) <i>per gram</i>
Gt y^{-1}	Gigatonnes <i>per year</i>
$\text{J g}^{-1} \text{ K}^{-1}$	Joule ($1\text{J} = 1 \text{ kg m}^2 \text{ sec}^{-2}$) <i>per gram per Kelvin</i>
$\text{J g}^{-1} \text{ K}^{-1}$	Joule <i>per gram per Kelvin</i>
K	Kelvin ($1 \text{ K} = ^\circ\text{C} + 273,15$)
kJ mol^{-1}	Kilojoule ($= 10^3 \text{ J}$) <i>per mole</i> ($1 \text{ mol} \approx 6.022 \times 10^{23}$ atoms or molecules of the pure substance measured)
Mg ha^{-1}	Megagram ($= 10^6 \text{ g}$) <i>per hectare</i>
nm	Nanometer ($= 10^{-9} \text{ m}$)
$^\circ\text{C sec}^{-1}$	Degrees Celsius <i>per second</i> (rate of temperature increase)
t ha^{-1}	Tonnes <i>per hectare</i>
v v^{-1}	Volume <i>per volume</i> (e.g. 1 ml <i>per</i> 100 ml)
w w^{-1}	Weight <i>per weight</i> (e.g. 1 g <i>per</i> 100 g)

LIST OF CHEMICAL ELEMENTS AND FORMULAS

Al	Aluminium
Ar	Arsenic
C	Carbon
CaCO ₃	Calcium carbonate
CaO	Calcium oxide
CH ₄	Methane
Cl	Chlorine
CO ₂	Carbon dioxide
Cr	Chromium
Cu	Copper
H	Hydrogen
H ₂	Hydrogen gas
Hg	Mercury
K	Potassium
K ₂ O	Potassium oxide
Mg	Magnesium
N	Nitrogen
N ₂ O	Nitrous oxide
Na ₂ O	Sodium oxide
NH ₄ ⁺	Ammonium (ion)
Ni	Nickel
NO ₃ ⁻	Nitrate (ion)
O	Oxygen
P	Phosphorus
Pb	Lead
S	Sulphur
Si	Silicon
SiO ₂	Silica (silicon dioxide)
Zn	Zinc

LIST OF KEY TERMS

Accelerated soil erosion	Soil erosion, as a result of anthropogenic activity, in excess of natural soil formation rates causing a deterioration or loss of one or more soil functions
Activated carbon	<i>(noun)</i> Charcoal produced to optimise its reactive surface area (e.g. by using steam during pyrolysis)
Anthrosol	<i>(count noun)</i> A soil that has been modified profoundly through human activities, such as addition of organic materials or household wastes, irrigation and cultivation (WRB, 2006)
Biochar	<p><i>i)</i> <i>(Material)</i> charcoal for application to soil</p> <p><i>ii)</i> <i>(Concept)</i> "charcoal (biomass that has been pyrolysed in a zero or low oxygen environment) for which, owing to its inherent properties, scientific consensus exists that application to soil at a specific site is expected to sustainably sequester carbon and concurrently improve soil functions (under current and future management), while avoiding short- and long-term detrimental effects to the wider environment as well as human and animal health."</p>
Black carbon	<i>(noun)</i> All C-rich residues from fire or heat (including from coal, gas or petrol)
Black Earth	<i>(mass noun)</i> Term synonymous with Chernozem used (e.g. in Australia) to describe self-mulching black clays (SSSA, 2003)
Char	<i>(mass noun)</i> 1. Synonym of 'charcoal'; 2. charred organic matter as a result of wildfire (Lehmann and Joseph, 2009)
Charcoal	<i>(verb)</i> synonym of the term 'pyrolyse'
Chernozem	<i>(mass noun)</i> charred organic matter
Coal	<i>(count noun)</i> A black soil rich in organic matter; from the Russian 'chernij' meaning 'black' and 'zemlja' meaning 'earth' or 'land' (WRB, 2006)
Combustion	<i>(mass noun)</i> Combustible black or dark brown rock consisting chiefly of carbonized plant matter, found mainly in underground seams and used as fuel (OED, 2003)
Decline in soil biodiversity	<i>(mass noun)</i> <i>chemistry</i> Rapid chemical combination of a substance with oxygen, involving the production of heat and light (OED, 2003)
Decline in soil organic matter (SOM)	<i>(soil threat)</i> Reduction of forms of life living in the soil (both in terms of quantity and variety) and of related functions, causing a deterioration or loss of one or more soil functions
Desertification	<i>(soil threat)</i> A negative imbalance between the build-up of SOM and rates of decomposition leading to an overall decline in SOM contents and/or quality, causing a deterioration or loss of one or more soil functions
Dust	<i>(soil threat)</i> land degradation in arid, semi-arid and dry sub-humid areas resulting from various factors, including climatic variations and human activities, causing a deterioration or loss of one or more soil functions
Ecosystem functions	The finest fraction of biochar, rather than the particulate matter emitted during pyrolysis. This fraction comprises distinct particle sizes within the micro- and nano-size range.
Feedstock	The capacity of natural processes and components to provide goods and services that satisfy human needs, directly or indirectly
Landslides	<i>(noun)</i> Biomass that is pyrolysed in order to produce biochar
Nanoparticle	The movement of a mass of rock, debris, artificial fill or earth down a slope, under the force of gravity
	<i>(noun)</i> Any particle with at least one dimension smaller than 100 nm (e.g. fullerenes or fullerene-like structures, crystalline forms of

Organic carbon	silica, cristobalite and tridymite) (<i>noun</i>) <i>biology</i> C that was originally part of an organism; (<i>chemistry</i>) C that is bound to at least one hydrogen (H) atom
Pyrolysis	(<i>mass noun</i>) The thermal degradation of biomass in the absence of oxygen leading to the production of condensable vapours, gases and charcoal
Soil	(<i>mass noun</i>) The unconsolidated mineral or organic matter on the surface of the earth that has been subjected to and shows effects of genetic and environmental factors of: climate (including water and temperature effects), and macro- and microorganisms, conditioned by relief, acting on parent material over a period of time (ENVASSO, 2008). (<i>count noun</i>) a spatially explicit body of soil, usually differentiated vertically into layers formed naturally over time, normally one of a specific soil class (in a specified soil classification system) surrounded by soils of other classes or other demarcations like hard rock, a water body or artificial barriers (ENVASSO, 2008)
Soil compaction	(<i>soil threat</i>) The densification and distortion of soil by which total and air-filled porosity are reduced, causing a deterioration or loss of one or more soil functions
Soil contamination	(<i>soil threat</i>) The accumulation of pollutants in soil above a certain level, causing a deterioration or loss of one or more soil functions.
Soil erosion	(<i>soil threat</i>) The wearing away of the land surface by physical forces such as rainfall, flowing water, wind, ice, temperature change, gravity or other natural or anthropogenic agents that abrade, detach and remove soil or geological material from one point on the earth's surface to be deposited elsewhere. When the term 'soil erosion' is used in the context of it representing a soil threat it refers to 'accelerated soil erosion'.
Soil functions	A subset of ecosystem functions: those ecosystem functions that are maintained by soil Usage: Most soil function systems include the following: 1) Habitat function 2) Information function 3) Production function 4) Engineering function 5) Regulation function
Soil organic matter	(<i>noun</i>) The organic fraction of the soil exclusive of undecayed plant and animal residues (SSSA, 2001)
Soil salinisation	(<i>soil threat</i>) Accumulation of water soluble salts in the soil, causing a deterioration or loss of one or more soil functions.
Soil sealing	(<i>soil threat and key issue</i>) The destruction or covering of soil by buildings, constructions and layers, or other bodies of artificial material which may be very slowly permeable to water (e.g. asphalt, concrete, etc.), causing a deterioration or loss of one or more soil functions
Soil threats	A phenomenon that causes a deterioration or loss of one or more soil functions. Usage: Eight main threats to soil identified by the EC (2002) with the addition of desertification: 1. Soil erosion 2. Decline in soil organic matter 3. Soil contamination 4. Soil sealing 5. Soil compaction 6. Decline in soil biodiversity 7. Soil salinisation 8. Landslides

Soil water
repellency

Terra Preta

9. Desertification

the reduction of the affinity of soils to water such that they resist wetting for periods ranging from a few seconds to hours, days or weeks (King, 1981)

(noun) Colloquial term for a kind of Anthrosol where charcoal (or biochar) has been applied to soil along with many other materials, including pottery shards, turtle shells, animal and fish bones, etc. Originally found in Brazil. From the Portuguese 'terra' meaning 'earth' and 'preta' meaning 'black'.

1. BACKGROUND AND INTRODUCTION

Biochar is commonly defined as charred organic matter, produced with the intent to deliberately apply to soils to sequester carbon and improve soil properties (based on: Lehmann and Joseph, 2009). The only difference between biochar and charcoal is in its utilitarian intention; charcoal is produced for other reasons (e.g. heating, barbeque, etc.) than biochar. In a physicochemical sense, biochar and charcoal are essentially the same material. It could be argued that biochar is a term that is used for other purposes than scientific, i.e. to re-brand charcoal into something more attractive-sounding to serve a commercial purpose. However, from a soil science perspective it is useful to be able to distinguish between any charcoal material and those charcoal materials where care has been taken to avoid deleterious effects on soils and to promote beneficial ones. As this report makes clear, the wide variety of soil groups and associated properties and processes will require specific charcoal properties for specific soils in order to meet the intention of biochar application. Considering the need to make this distinction, a new term is required and since biochar is the most common term currently used, it was selected for this report. The definition of the concept of biochar used in this report is:

“charcoal (biomass that has been pyrolysed in a zero or low oxygen environment) for which, owing to its inherent properties, scientific consensus exists that application to soil at a specific site is expected to sustainably sequester carbon and concurrently improve soil functions (under current and future management), while avoiding short- and long-term detrimental effects to the wider environment as well as human and animal health.” As a material, biochar is defined as: “charcoal for application to soil”.

The distinction between biochar as a concept and as a material is important. For example, a particular biochar (material) may comply with all the conditions in the concept of biochar when applied to field A, but not when applied to field B. This report investigates the evidence for when, where and how actual biochar application to soil complies with the concept, or not.

The terms ‘charcoal’ and ‘pyrogenic black carbon (BC)’ are also used in this report when appropriate according to their definitions above and in the List of Key Terms. Additionally, BC refers to C-rich residues from fire or heat (including from coal, gas or petrol).

This report aims to review the state-of-the-art regarding the interactions between biochar application to soil and its effects on soil properties, processes and functioning. A number of recent publications have addressed parts of this objective as well (Sohi et al., 2009; Lehmann and Joseph, 2009; Collison et al., 2009). This report sets itself apart by i) addressing the issue from an EU perspective, ii) inclusion of quantitative meta-analyses of selected effects, and iii) a discussion of biochar for the threats to soil as identified by the Thematic Strategy for Soil Protection ([COM\(2006\) 231](#)). In addition, this report is independent, objective and critical.

Biochar is a stable carbon (C) compound created when biomass (feedstock) is heated to temperatures between 300 and 1000°C, under low (preferably zero) oxygen concentrations. The objective of the biochar concept is to abate

the enhanced greenhouse effect by sequestering C in soils, while concurrently improving soil quality. The proposed concept through which biochar application to soils would lead to C sequestration is relatively straightforward. Carbon dioxide from the atmosphere is fixed in vegetation through photosynthesis. Biochar is subsequently created through pyrolysis of the plant material thereby potentially increasing its recalcitrance with respect to the original plant material. The estimated residence time of biochar-carbon is in the range of hundreds to thousands of years while the residence time of carbon in plant material is in the range of decades. Consequently, this would reduce the CO₂ release back to the atmosphere if the carbon is indeed persistently stored in the soil. The carbon storage potential of biochar is widely hypothesised, although it is still largely unquantified, particularly when also considering the effects on other greenhouse gasses (see Section 1.3), and the secondary effects of large-scale biochar deployment. Concomitant with carbon sequestration, biochar is intended to improve soil properties and soil functioning relevant to agronomic and environmental performance. Hypothesised mechanisms that have been suggested for potential improvement are mainly improved water and nutrient retention (as well as improved soil structure, drainage).

Considering the multi-dimensional and cross-cutting nature of biochar, an imminent need is anticipated for a robust and balanced scientific review to effectively inform policy development on the current state of knowledge with reference to biochar application to soils.

How to read this report?

Chapter 1 introduces the concept of biochar and its origins, including a comparison with European conditions/history.

Chapter 2 reviews the range of physical and chemical properties of biochars that are most relevant to soils.

Chapter 3 focuses on the interactions between biochar application to soil and soil properties, processes and functions.

Chapter 4 outlines how biochar application can be expected to influence threats to soils.

Chapter 5 discusses some key issues regarding biochar that are beyond the scope of this report.

Chapter 6 summarises the main findings of the previous chapters, synthesises between these and identifies the key findings. Suggestions for further reading are inserted where appropriate.

1.1 Biochar in the attention

The concept of biochar is increasingly in the attention in both political and academic arenas, with several countries (e.g. UK, New Zealand, U.S.A.) establishing 'biochar research centres'; as well as in the popular media where it is often portrayed as a miracle cure (or as a potential environmental disaster). The attention of the media and public given to biochar can be illustrated by contrasting a Google™ search for 'biochar' with a search for 'biofuels'. A Google search for biochar yields 185,000 hits while biofuels yields 5,210,000 hits. Another illustration is given by comparing the search volumes of 'biochar', '*Terra Preta*' and 'black earth' over the last years, testifying the recent increase in attention in and exposure of biochar (Figure 1.1, made with Google Trends™).

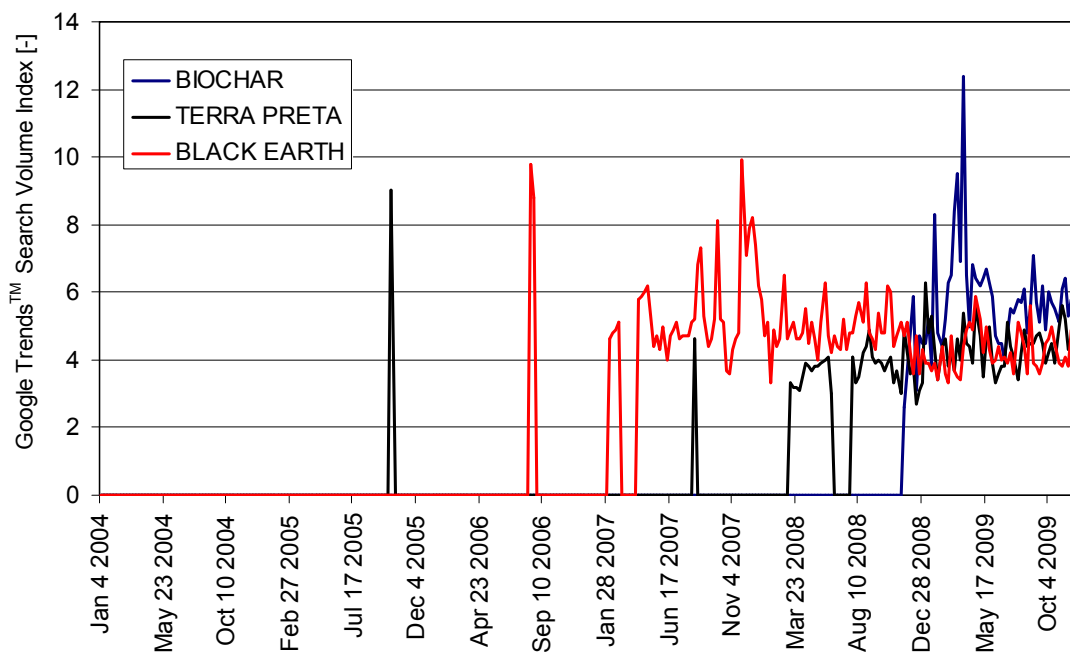


Figure 1.1 Google Trends™ result of “biochar”, “*Terra Preta*” and “black earth”. The scale is based on the average worldwide traffic of “biochar” from January 2004 until June 2009 (search performed on 04/12/2009)

The geographical interest in biochar can be explored further by using the search volume index of biochar; the total number of searches normalised by the overall search volume by country. Over the last 12 months the search volume index for biochar was highest in Australia and New Zealand (Figure 1.2). The actual attention for biochar in Australia may even be higher, since in Australia biochar is also referred to as ‘Agrichar’, one of its trade names.



Figure 1.2 Google Trends™ geographical distribution of the search volume index of “biochar” of the last 12 months from June 2008 to June 2009 (search performed on 16/09/2009). Data is normalised against the overall search volume by country

An indication for the attention devoted to biochar by the scientific community is provided by performing a search in the scientific literature search engines Thompson’s ISI Web of Science and Google Scholar™. A search in Google Scholar™ yielded 724 hits for biochar and 48,600 hits for biofuels (searches undertaken on 16/09/2009). If we consider ‘*Terra Preta*’ – a Horticultural Anthrosol found in Amazonia – in comparison to biochar, a search yielded 121,000 hits on Google and 1,490 on Google Scholar. A search in the ISI Web of Science for those articles indexed for either biochar or bio-char yielded a total of 81 articles (Figure 1.3). Three authors are independently involved in 22 articles (~25%) of these 81 articles (Lehmann (9); Derimbas (8); Davaajav (8)). Out of the 81 articles 27 articles include a reference to charcoal (Figure 1.3). This is an indication of the relative small number of scientists currently involved in biochar research, although the number of articles is rapidly increasing (Figure 1.3). Finally, the oldest paper appearing in either ISI Web of Science™ or Scopus™ dealing with ‘biochar’, ‘*Terra Preta*’ or ‘black earth’ dates from 1998, 1984 and 1953, respectively.

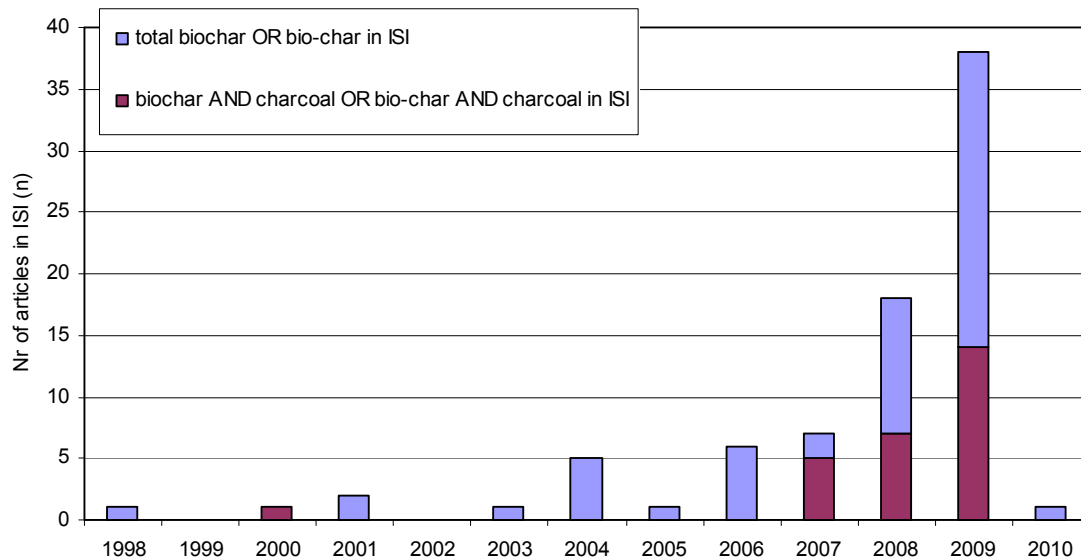


Figure 1.3 Scientific publications registered in Thompson’s ISI Web of Science indexed for either biochar or bio-char including those articles that mention charcoal (search performed on 4/12/2009)

1.2 Historical perspective on soil improvement

Man-made soils (Anthrosols) enriched with charcoal are found as small pockets (10s – 200 m in diameter) close to both current and historic human settlements throughout Amazonia (see Figure 1.4) which are estimated to cover a total area of 6,000 – 18,000 km² (Sombroek and Carvalho de Souza, 2000). A rapidly expanding body of scientific literature has reached the consensus that these soils were created by indigenous people, as far back as 10,000 yr BP (Woods et al., 2009), with varying depth (down to 1 m).

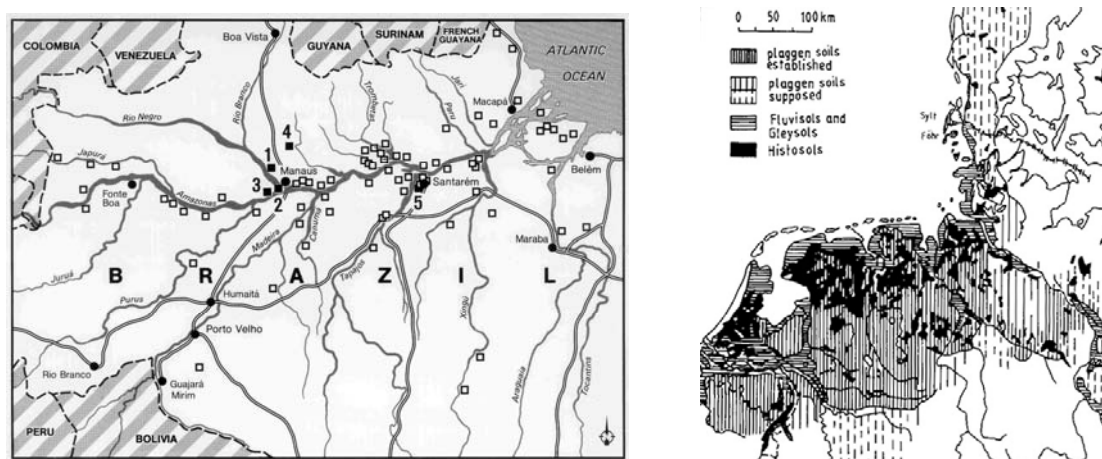


Figure 1.4 Distribution of Anthrosols in Amazonia (left; Glaser et al., 2001) and Europe (right; Blume and Leinweber, 2004)

The first Anthrosols in Europe, which are mostly enriched with organic material from peatlands and heathlands, have been dated to 3,000 yr BP on

the German island of Sylt (Blume and Leinweber, 2004). The largest expanse, from a 3,500 km² total European area of man-made soils (Plaggic Anthrosols), was created during the Middle Ages in the nutrient poor, dry sandy soils (Arenosols) of The Netherlands, northern Belgium and north-western Germany (Figure 1.4) to similar depths as their Amazonian counterparts (i.e. down to 1 m).

Such a vast single area of Anthrosols is rare, if not unique, and may be explained by the relatively high population density (and subsequent food demand) combined with environmental factors, i.e. the presence of extensive peat deposits in close proximity to the nutrient poor free-draining soil. Much more common are small scale Anthrosols, pockets of man-made soils close to settlements, as an inevitable consequence or planned soil conditioning, by a 'permanent' human settlement that continuously produces organic waste. Many Anthrosols do not appear on the EU soil distribution map because of their small size in relation to the 1:1,000,000 scale of the Soil Geographical Database of Eurasia, which is the basis of the map (Toth et al., 2008). However, numerous small scale Anthrosols have been reported across the European continent, e.g. Scotland (Meharg et al., 2006; Davidson et al., 2006), Ireland, Italy, Spain and northwest Russia (Giani et al., 2004). Based on their formation, it can be assumed that Anthrosols exist in other parts of Europe as well, but data are lacking.



Figure 1.5 Comparing tropical with temperate Anthrosols. The left half shows a profile of a fertile Terra Preta (Anthrosol with charcoal) created by adding charcoal to the naturally-occurring nutrient poor Oxisol (far left; photo courtesy of Bruno Glaser). The right half (far right) is a profile picture of a fertile European Plaggic Soil (Plaggic Anthrosol; photo courtesy of Erica Micheli) created by adding peat and manure to the naturally-occurring nutrient poor sandy soils (Arenosols) of The Netherlands

Although both European and Amazonian Anthrosols were enriched to increase their agricultural performance, there is an important distinction between the Plaggic Anthrosols of Europe and the Horticultural Anthrosols of Amazonia (Figure 1.5). Plaggic is from the Dutch 'Plag' meaning a cut out section of the organic topsoil layer, including vegetation (grass or heather) while Horticultural Anthrosol translates freely into 'kitchen soil'. These names are reflected in their composition, i.e. Plaggic Anthrosols were made by adding organic topsoil material and peat (early Middle Ages) and mixed with manure (late Middle Ages) while Horticultural Anthrosols were created by a wide variety of organic and mineral materials, ranging from animal bones to charcoal and pottery fragments. What sets the Terra Preta apart from other Horticultural

Anthrosols is the high proportion of charcoal. It is assumed that the charcoal was made deliberately for application to soil, i.e. not just charred remains from clearing and burning the forest.

1.3 Different solutions to similar problems

The challenges faced by the people of two very different environments (tropical rain forest vs. temperate climate on largely open or partially deforested land) appear similar in the sense of needing to grow crops on soils that naturally had low nutrient and water retention. One can only speculate as to what exactly the reasons were for the people living at the time to either add or not add charcoal to their soils. In addition to the available supply of organic materials, possible explanations may be related to the relative value of the different organic materials and contrasting residence times of SOM. In a simplified scenario, the colder climate in Europe means that microbial decomposition occurs much more slowly than in the tropics, leading to much longer residence times of organic matter. The recalcitrance of the peat and plaggen that were added to the soil meant that the benefits from increased water and (to a lesser degree) nutrient retention lasted long enough to make it worth the investment. In tropical soils, however, the recalcitrance of the organic matter that was added to the soil needed to be greater to get a return that was worth the investment. Charring organic matter may have been a conscious policy to achieve this. Of course, wood and charcoal were being produced in Europe at the time as well. However, other uses of these materials were likely to be more valuable, e.g. the burning of wood in fire places to heat living accommodations and the use of charcoal to achieve high enough temperatures for extracting metals from ores.

Because of the relatively small areal extent of Anthrosols, many of their locations may not be known or recognised presently. It is possible that small pockets of Anthrosols exist in Europe, created at different times in history, where greater amounts of charcoal are present than in the Plaggic Anthrosols. Potentially, identification and study of these sites (including chronosequences) could provide valuable information regarding the interactions between charcoal and environmental factors prevalent in Europe.

1.4 Biochar and pyrogenic black carbon

A potential analogue for biochar may be found in the charcoal produced by wildfires (or pyrogenic black carbon – BC – as it is often referred to) found naturally in soils across the world, and in some places even makes up a larger proportion of total organic C in the soil than in some Terra Preta soils. Preston and Schmidt (2006) showed an overview of studies on non-forested sites in different parts of the world with BC making up between 1 and 80% of total SOC. For example, BC was found to constitute 10-35% of the total SOC content for five soils from long-term agricultural research sites across the U.S.A. (Skjemstad et al., 2002). Schmidt et al. (1999) studied pyrogenic BC contents of chernozemic soils (Cambisol, Luvisol, Phaeozem, Chernozem and Greyzem) in Germany and found BC to make up 2-45% of total SOC (mean of 14%).

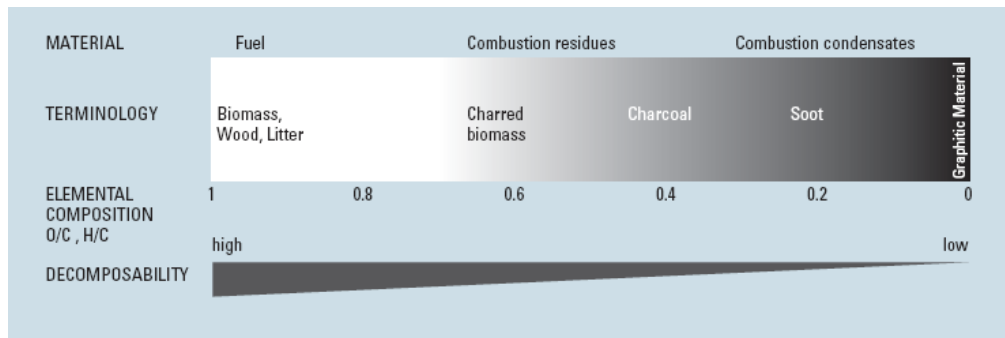


Figure 1.6 Terms and properties of pyrogenic BC (adopted from Preston and Schmidt, 2006)

However, it is important to bear in mind that, while the range of BC materials produced by wildfire overlaps with the range of biochar materials (i.e. the continuum from charred biomass to soot and graphite; Figure 1.6), the composition and properties of biochar can be very different to pyrogenic BC (see Chapter 2). The two main responsible factors are feedstock and pyrolysis conditions. In a wildfire, the feedstock is the aboveground biomass (and sometimes peat and roots) while for biochar any organic feedstock can theoretically be used from wood and straw to chicken manure (Chapter 2). In a pyrolysis oven, the pyrolysis conditions can be selected and controlled, including maximum temperature and duration but also the rate of temperature increase, and inclusion of steam, or e.g. KOH, activation and oxygen conditions.

1.5 Carbon sequestration potential

Globally, soil is estimated to hold more organic carbon (1,100 Gt; 1 Gt=1,000,000,000 tonnes) than the atmosphere (750 Gt) and the terrestrial biosphere (560 Gt) (Post et al., 1990; Sundquist, 1993). In the Kyoto Protocol on Climate Change of 1997, which was adopted in the United Nations Framework Convention on Climate Change, Article 3.4 allows organic carbon stored in arable soils to be included in calculations of net carbon emissions. It speaks of the possibility of subtracting the amounts of CO₂ removed from the atmosphere into agricultural sinks, from the assigned target reductions for individual countries. SOC sequestration in arable agriculture has been researched (Schlesinger, 1999; Smith et al., 2000a, b; Freibauer et al., 2002; West & Post, 2002; Sleutel et al., 2003; Janzen, 2004; King et al., 2004; Lal, 2004) against the background of organic carbon (OC) credit trading schemes (Brown et al., 2001; Johnson & Heinen, 2004). However, fundamental knowledge on attainable SOC contents (relative to variation in environmental factors) is still in its infancy, and it is mostly approached by modelling (Falloon et al., 1998; Pendall et al., 2004).

The principle of using biochar for carbon (C) sequestration is related to the role of soils in the C-cycle (Figure 1.7). As Figure 1.7 shows, the global flux of CO₂ from soils to the atmosphere is in the region of 60 Gt of C per year. This CO₂ is mainly the result of microbial respiration within the soil system as the microbes decompose soil organic matter (SOM). Components of biochar are proposed to be considerably more recalcitrant than SOM and as such are only decomposed very slowly, over a time frame which can be measured in

hundreds or thousands of years. This means that biochar allows carbon input into soil to be increased greatly compared to the carbon output through soil microbial respiration, and it is this that is the basis behind biochar's possible carbon negativity and hence its potential for climate change mitigation.

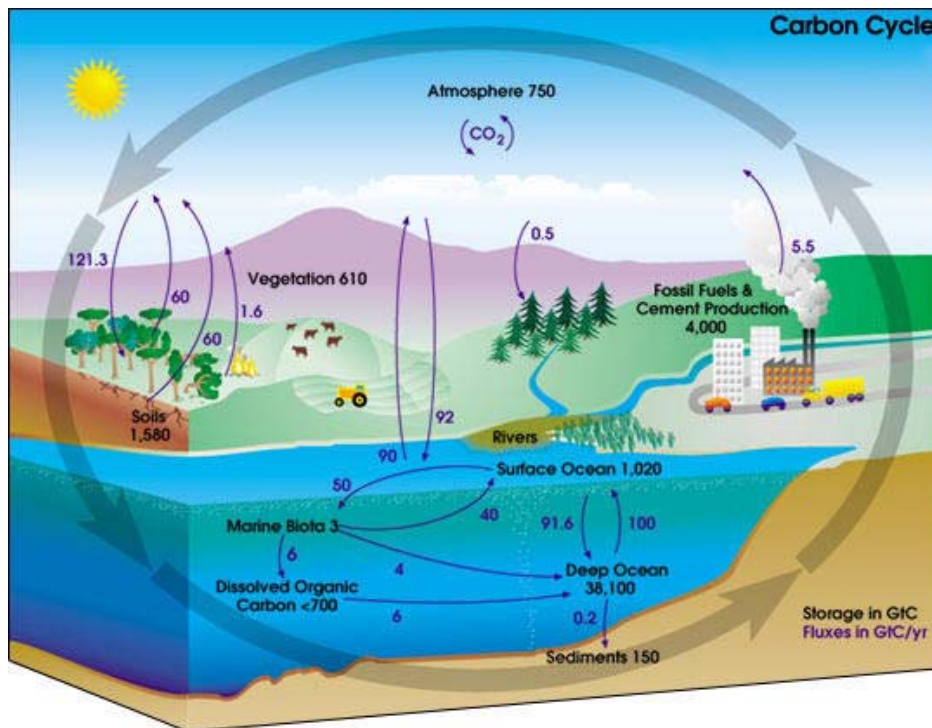


Figure 1.7 Diagram of the carbon cycle. The black numbers indicate how much carbon is stored in various reservoirs, in billions of tons (GtC = Gigatons of Carbon and figures are circa 2004). The purple numbers indicate how much carbon moves between reservoirs each year, i.e. the fluxes. The sediments, as defined in this diagram, do not include the ~70 million GtC of carbonate rock and kerogen (NASA, 2008)

Although Figure 1.7 is clearly a simplification of the C-cycle as it occurs in nature, the numbers are well established (NASA, 2008) and relatively uncontroversial. A calculation of the fluxes, while being more a 'back of the envelope' calculation, than precise mathematics, is highly demonstrative of the anthropogenic influence on atmospheric CO₂ levels. When all of the sinks are added together (that is the fluxes of CO₂ leaving the atmosphere) the total amount of C going into sinks is found to be in the region of 213.35 Gt per year. Conversely, when all of the C fluxes emitted into the atmosphere from non-anthropogenic (natural) sources are added, they total 211.6 Gt per year. This equates to a net loss of carbon from the atmosphere of 1.75 Gt C.

It is for this reason that the relatively small flux of CO₂ from anthropogenic sources (5.5 Gt C per year) is of such consequence as it turns the overall C flux from the atmosphere from a *loss* of 1.75 Gt per year, to a *net gain* of 3.75 Gt C per year. This is in relatively close agreement with the predicted rate of CO₂ increase of about 3 Gt of C per year (IPCC, 2001). It is mitigation of this net gain of CO₂ to the atmosphere that biochar's addition to soil is posited for.

Lehmann et al. (2006) estimate a potential global C-sequestration of 0.16 Gt yr⁻¹ using current forestry and agricultural wastes, such as forest residues, mill residues, field crop residues, and urban wastes for biochar production. Using

projections of renewable fuels by 2100, the same authors estimate sequestration to reach a potential range of 5.5-9.5 Gt yr⁻¹, thereby exceeding current fossil fuel emissions. However, the use of biochar for climate change mitigation is beyond the scope of this report that focuses on the effects of biochar addition to soils with regard to physical, chemical and biological effects, as well as related effects on soil and ecosystem functioning.

1.5.1 Biochar loading capacity

Terra Preta soils have been shown to contain about 50 t C ha⁻¹ in the form of BC, down to a depth of approximately 1 meter (approximately double the amount relative to pre-existing soil), and these soils are highly fertile when compared to the surrounding soils. This has led to the idea of biochar being applied to soil to sequester carbon and maintain or improve the soil production function (e.g. crop yields), as well as the regulation function and habitat function of soils. Controlled experiments have been undertaken to look at the effects of different application rates of biochar to soils.

At present, however, it is not clear whether there is a maximum amount of C, in the form of biochar, which can be safely added to soils without compromising other soil functions or the wider environment; that is, what is the 'biochar loading capacity' (BLC) of a given soil? It will be important to determine if the BLC varies between soil types and whether it is influenced by the crop type grown on the soil. In order to maximise the amount of biochar which can be stored in soils without impacting negatively on other soil functions, the biochar loading capacity of different soils exposed to different environmental and climatic conditions specific to the site will have to be quantified for different types of biochar.

The organic matter fractions of some soils in Europe have been reported to consist of approximately 14% (up to 45%) BC or charcoal (see Section 1.4), which are both analogues of biochar as previously discussed. Lehmann and Rondon (2005) reported that at loadings up to 140 t C ha⁻¹ (in a weathered tropical soil) positive yield effects still occurred. However, it should be noted that some experiments report that some crops experience a loss of the positive effects of biochar addition to soil at a much lower application rate. For example, Rondon et al. (2007) reported that the beans (*Phaseolus vulgaris* L.) showed positive yield effects on biochar application rates up to 50 t C ha⁻¹ that disappeared at an application rate of 60 t C ha⁻¹ with a negative effect on yield being reported at application rates of 150 t C ha⁻¹. This shows that the BLC is likely to be crop dependent as well as probably both soil and climate dependent. Combined with the irreversibility of biochar application to soil, this highlights the complex nature of calculating a soil's BLC as future croppings should be taken into account to ensure that future crop productivity is not compromised if the crop type for a given field is changed. Apart from effects on plant productivity, it can be imagined that other effects, on for example soil biology or transport of fine particles to ground and surface water, should be taken into account when 'calculating' or deriving the BLC for a specific site. Also, the BLC concept would need to be developed for both total (final) amount and the rate of application, i.e. the increase in the total amount over time. The rate of application would need to consist of a long term rate (i.e. t ha⁻¹ yr⁻¹ over 10 or 100 years) as well as a 'per application' rate, both

determined by evidence of direct and indirect effects on soil and the wider environment.

Another consideration regarding the biochar loading capacity of a soil is the risk of smouldering combustion. Organic soils that dry out sufficiently are capable of supporting below ground smouldering combustion that can continue for long time periods (years in some cases). It is feasible that soils which experience very high to extreme loading rates of biochar and are subject to sufficiently dry conditions could support smouldering fires. Ignition of such fires could occur both naturally, e.g. by lightning strike, or anthropogenically. What the biochar content threshold would be, how the threshold would change according to environmental conditions, and how much a risk this would be in non-arid soils remains unclear, but is certainly worthy of thought and future investigation.

1.5.2 Other greenhouse gasses

Carbon dioxide is not the only gas emitted from soil with the potential to influence the climate. Methane (CH₄) production also occurs as a part of the carbon cycle. It is produced by the soil microbiota under anaerobic conditions through a process known as methanogenesis and is approximately 21 times more potent as a greenhouse gas than CO₂ over a time horizon of 100 years.

Nitrous oxide (N₂O) is produced as a part of the nitrogen (N) cycle through process known as nitrification and denitrification which are carried out by the soil microbiota. Nitrous oxide is 310 times more potent as a greenhouse gas than CO₂ over a time horizon of 100 years (U.S. Environmental Protection Agency, 2002).

Whilst these gases are more potent greenhouse gases than CO₂, only approximately 8% of emitted greenhouse gases are CH₄ and only 5% are N₂O, with CO₂ making up approximately 83% of the total greenhouse gases emitted. Eighty percent of N₂O and 50% of CH₄ emitted are produced by soil processes in managed ecosystems (US Environmental Protection Agency, 2002). It should be noted that these figures detail total proportions of each greenhouse gas and are not weighted to account for climatic forcing.

In one study, biochar addition to soils has been shown to reduce the emission of both CH₄ and N₂O. Rondon et al. (2005) reported that a near complete suppression of methane upon biochar addition at an application rate of 2% w w⁻¹ to soil. It was hypothesised that the mechanism leading to reduced emission of CH₄ is increased soil aeration leading to a reduction in frequency and extent of anaerobic conditions under which methanogenesis occurs. Pandolfo et al. (1994) investigated CH₄ adsorption capacity of several activated carbons (from coconut feedstock) in a series of laboratory experiments. Their results showed increased CH₄ 'adsorption' with increase surface area of the activated carbon, particularly for micropores (<2µm). These charcoal materials were activated using steam or KOH, however, and it remains to be tested how different biochar materials added to soils in the field will interact with methane dynamics. The influence of biochar on SOM dynamics are discussed later in this report (Section 3.2.5).

A reduction in N₂O emissions of 50% in soybean plantations and 80% in grass stands was also reported (Rondon et al. 2005). The authors

hypothesised that the mechanism leading to this reduction in N₂O emissions was due to slower N cycling, possibly as a result of an increase in the C:N ratio. It is also possible that the N that exists within the biochar is not bioavailable when introduced to the soil as it is bound up in heterocyclic form (Camps, 2009; Personal communication). Yanai et al. (2007) measured N₂O emissions from soils after rewetting in the laboratory and found variable results, i.e. an 89% suppression of N₂O emissions at 73-78% water-filled pore space contrasting to a 51% increase at 83% water-filled pore space. These results indicate that the effect of biochar additions to soils on the N cycle depend greatly on the associated changes in soil hydrology and that thresholds of water content effects on N₂O production may be very important and would have to be studied for a variety of soil-biochar-climate conditions. Furthermore, if biochar addition to soil does slow the N-cycle, this could have possible consequences on soil fertility in the long term. This is because nitrate production in the soil may be slowed beyond the point of plant uptake, meaning that nitrogen availability, often the limiting factor for plant growth in soils, may be reduced leading to concurrent reduction in crop productivity. Yanai et al. (2007) reported that this effect did change over time, but their experiment only ran for 5 days and so extrapolation of the results to the time scales at which biochar is likely to persist in soil is not possible. Further research is therefore needed to better elucidate the effects and allow extrapolation to the necessary time scales.

1.6 Pyrolysis

Pyrolysis is the chemical decomposition of an organic substance by heating in the absence of oxygen. The word is derived from Greek word 'pyro' meaning fire and "lysis" meaning decomposition or breaking down into constituent parts. In practice it is not possible to create a completely oxygen free environment and as such a small amount of oxidation will always occur. However, the degree of oxidation of the organic matter is relatively small when compared to combustion where almost complete oxidation of organic matter occurs, and as such a substantially larger proportion of the carbon in the feedstock remains and is not given off as CO₂. However, with pyrolysis much of the C from the feedstock is still not recovered in charcoal form, but converted to either gas or oil.

Pyrolysis occurs spontaneously at high temperatures (generally above approximately 300°C for wood, with the specific temperature varying with material). It occurs in nature when vegetation is exposed to wildfires or comes into contact with lava from volcanic eruptions. At its most extreme, pyrolysis leaves only carbon as the residue and is called carbonization. The high temperatures used in pyrolysis can induce polymerisation of the molecules within the feedstocks, whereby larger molecules are also produced (including both aromatic and aliphatic compounds), as well as the thermal decomposition of some components of the feedstocks into smaller molecules. This is discussed in more detail in Section 3.2.5.1.

The process of pyrolysis transforms organic materials into three different components, being gas, liquid or solid in different proportions depending upon both the feedstock and the pyrolysis conditions used. Gases which are produced are flammable, including methane and other hydrocarbons which

can be cooled whereby they condense and form an oil/tar residue which generally contains small amounts of water. The gasses (either condenses or in gaseous form) and liquids can be upgraded and used as a fuel for combustion.

The remaining solid component after pyrolysis is charcoal, referred to as biochar when it is produced with the intention of adding it to soil to improve it (see List of Key terms). The physical and chemical properties of biochar are discussed in more detail in Chapter 2.

The process of pyrolysis has been adopted by the chemical industry for the production of a range of compounds including charcoal, activated carbon, methanol and syngas, to turn coal into coke as well as producing other chemicals from wood. It is also used for the breaking down, or 'cracking' of medium-weight hydrocarbons from oil to produce lighter hydrocarbons such as petrol.

A range of compounds in the natural environment are produced by both anthropogenic and non-anthropogenic pyrolysis. These include compounds released from the incomplete burning of petrol and diesel in internal combustion engines, through to particles produced from wood burned in forest fires, for example. These substances are generally referred to as black carbon (see List of Key terms) in the scientific literature and exist in various forms ranging from small particulate matter found in the atmosphere, through to a range of sizes found in soils and sediments where it makes up a significant part of the organic matter (Schmidt et al., 1999; Skjemstad et al., 2002; Preston et al., 2006; Hussain et al. 2008).

1.6.1 The History of Pyrolysis

While it is possible that pyrolysis was first used to make charcoal over 7,000 years ago for the smelting of copper, or even 30,000 years ago for the charcoal drawings of the Chauvet cave (Antal, 2003), the first definitive evidence of pyrolysis for charcoal production comes from over 5,500 years ago in Southern Europe and the Middle East. By 4,000 years ago, the start of the Bronze Age, pyrolysis use for the production of charcoal must have been widespread. This is because only burning charcoal allowed the necessary temperatures to be reached to smelt tin with copper and so produce bronze (Earl, 1995).

A range of compounds can be found in the natural environment that is produced by both anthropogenic and non-anthropogenic pyrolysis. These include compounds released from the incomplete burning of petrol and diesel in internal combustion engines, through to being produced from wood in forest fires for example.

1.6.2 Methods of Pyrolysis

Although the basic process of pyrolysis, that of heating a C-containing feedstock in an limited oxygen environment, is always the same, different methodologies exist, each with different outputs.

Apart from the feedstocks used, which are discussed further in Section 1.7, the main variables that are often manipulated are pyrolysis temperature, and

the residence time of the feedstock in the pyrolysis unit. Temperature itself can have a large effect on the relative proportions of end product from a feedstock (Fig. 1.9).

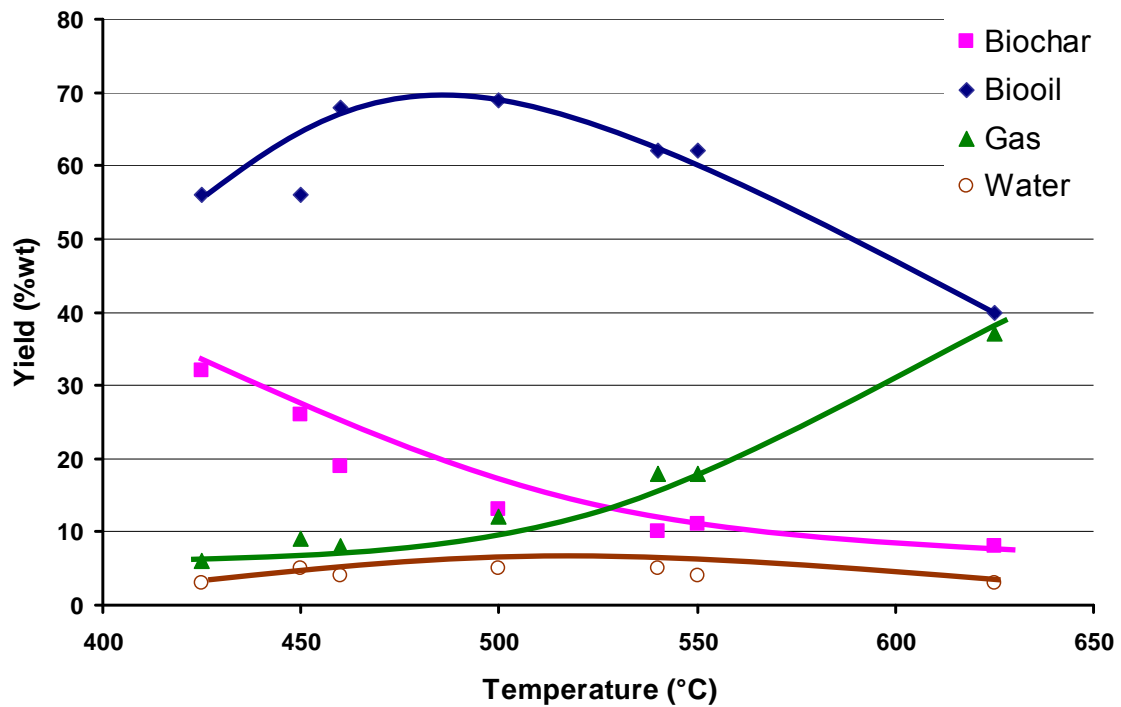


Figure 1.8 A graph showing the relative proportions of end products after fast pyrolysis of aspen poplar at a range of temperatures (adapted from IEA, 2007)

Residence times of both the solid constituents and the hot vapor produced under pyrolysis conditions can also have a large effect on the relative proportions of each end product of pyrolysis (Table 1.1). In the nomenclature, four different types of pyrolysis are generally referred to, with the difference between each being dependent on temperature and residence time of solid or vapour in the pyrolysis unit, or a combination of both. The four different types of pyrolysis are fast, intermediate and slow pyrolysis (with slow pyrolysis often referred to as “carbonisation” due to the relatively high proportion of carbonaceous material it produces: biochar) along with gasification (due to the high proportion of syngas produced).

Table 1.1 shows that different pyrolysis conditions lead to different proportions of each end product (liquid, char or gas). This means that specific pyrolysis conditions can be tailored to each desired outcome. For example, the IEA report (2007) stated that fast pyrolysis was of particular interest as liquids can be stored and transported more easily and at lower cost than solid or gaseous biomass forms. However, with regard to the use of biochar as a soil amendment and for climate change mitigation it is clear that slow pyrolysis, would be preferable, as this maximises the yield of char, the most stable of the pyrolysis end products.

Table 1.1 The mean post-pyrolysis feedstock residues resulting from different temperatures and residence times (adapted from IEA, 2007)

Mode	Conditions	Liquid	Biochar	Syngas
Fast pyrolysis	Moderate temperature, ~500°C, short hot vapour residence time of ~ 1 s	75%	12%	13%
Intermediate Pyrolysis	Moderate temperature ~500°C, moderate hot vapour residence time of 10 – 20 s	50%	20%	30%
Slow Pyrolysis (Carbonisation)	Low temperature ~400°C, very long solids residence time	30%	35%	35%
Gasification	High temperature ~800°C, long vapour residence time	5%	10%	85%

Owing to the fact that end products such as flammable gas can be recycled into the pyrolysis unit and so provide energy for subsequent pyrolysis cycles, costs, both in terms of fuel costs, and of carbon emission costs, can be minimised. Furthermore, the pyrolysis reaction itself becomes exothermic after a threshold is passed, thereby reducing the required energy input to maintain the reaction. However, it is important to note that other external costs are associated with pyrolysis, most of which will be discussed in Section 2.4. For example, fast pyrolysis requires that the feedstock is dried to less than 10% water ($w w^{-1}$). This is done so that the bio-oil is not contaminated with water. The feedstock then needs to be ground to a particle size of *ca.* 2 mm to ensure that there is sufficient surface area to ensure rapid reaction under pyrolysis conditions (IEA, 2007). The grinding of the feedstock, and in some cases also the drying require energy input and will increase costs, as well as of the carbon footprint of biochar production if the required energy is not produced by carbon neutral sources.

As well as different pyrolysis conditions, the scale at which pyrolysis is undertaken can also vary greatly. The two different scales discussed throughout this report are that of ‘Closed’ vs ‘Open’ scenarios. Closed refers to the scenario in which relatively small, possibly even mobile, pyrolysis units are used on each farm site, with crop residues and other bio-wastes being pyrolysed on site and added back to the same farm’s soils. Open refers to biowastes being accumulated and pyrolysed off-site at industrial scale pyrolysis plants, before the biochar is redistributed back to farms for application to soil. The scales at which these scenarios function are very different, and each brings its own advantages and disadvantages.

1.7 Feedstocks

Feedstock is the term conventionally used for the type of biomass that is pyrolysed and turned into biochar. In principle, any organic feedstock can be pyrolysed, although the yield of solid residue (char) respective to liquid and gas yield varies greatly (see Section 1.6.2) along with physico-chemical properties of the resulting biochar (see Chapter 2).

Feedstock is, along with pyrolysis conditions, the most important factor controlling the properties of the resulting biochar. Firstly, the chemical and

structural composition of the biomass feedstock relates to the chemical and structural composition of the resulting biochar and, therefore, is reflected in its behaviour, function and fate in soils. Secondly, the extent of the physical and chemical alterations undergone by the biomass during pyrolysis (e.g. attrition, cracking, microstructural rearrangements) are dependent on the processing conditions (mainly temperature and residence times). Table 1.2 provides a summary of some of the key components in representative biochar feedstocks.

Table 1.2 Summary of key components (by weight) in biochar feedstocks (adapted from Brown et al., 2009)

	Ash	Lignin (w w ⁻¹)	Cellulose
Wheat straw	11.2	14	38
Maize residue	2.8-6.8	15	39
Switchgrass	6	18	32
Wood (poplar, willow, oak)	0.27 - 1	26 - 30	38 - 45

Cellulose and lignin undergo thermal degradation at temperatures ranging between 240-350°C and 280-500°C, respectively (Sjöström, 1993; Demirbas, 2004). The relative proportion of each component will, therefore, determine the extent to which the biomass structure is retained during pyrolysis, at any given temperature. For example, pyrolysis of wood-based feedstocks generates coarser and more resistant biochars with carbon contents of up to 80%, as the rigid ligninolytic nature of the source material is retained in the biochar residue (Winsley, 2007). Biomass with high lignin contents (e.g. olive husks) have shown to produce some of the highest biochar yields, given the stability of lignin to thermal degradation, as demonstrated by Demirbas (2004). Therefore, for comparable temperatures and residence times, lignin loss is typically less than half of cellulose loss (Demirbas, 2004).

Whereas woody feedstock generally contains low proportions (< 1% by weight) of ash, biomass with high mineral contents such as grass, grain husks and straw residues generally produce ash-rich biochar (Demirbas 2004). These latter feedstocks may contain ash up to 24% or even 41% by weight, such as rice husk (Amonette and Joseph, 2009) and rice hulls (Antal and Grønly, 2003), respectively. The mineral content of the feedstock is largely retained in the resulting biochar, where it concentrates due to the gradual loss of C, hydrogen (H) and oxygen (O) during processing (Demirbas 2004). The mineral ash content of the feedstock can vary widely and evidence seems to suggest a relationship between that and biochar yield (Amonette and Joseph, 2009). Table 1.3 provides an example of the elemental composition of representative feedstocks.

Table 1.3 Examples of the proportions of nutrients (g kg^{-1}) in feedstocks (adapted from Chan and Xu, 2009)

	Ca	Mg	K	P
	(g kg^{-1})			
Wheat straw	7.70	4.30	2.90	0.21
Maize cob	0.18	1.70	9.40	0.45
Maize stalk	4.70	5.90	0.03	2.10
Olive kernel	97.0	20.0	-	-
Forest residue	130	19.0	-	-

In the plant, Ca occurs mainly within cell walls, where it is bound to organic acids, while Mg and P are bound to complex organic compounds within the cell (Marschner, 1995). Potassium is the most abundant cation in higher plants and is involved in plant nutrition, growth and osmoregulation (Schachtman and Schroeder, 1994). Nitrogen, Mn and Fe also occur associated to a number of organic and inorganic forms. During thermal degradation of the biomass, potassium (K), chlorine (Cl) and N vaporize at relatively low temperatures, while calcium (Ca), magnesium (Mg), phosphorus (P) and sulphur (S), due to increased stability, vaporise at temperatures that are considerably higher (Amonette and Joseph, 2009). Other relevant minerals can occur in the biomass, such as silicon (Si), which occurs in the cell walls, mostly in the form of silica (SiO_2).

Many different materials have been proposed as biomass feedstocks for biochar, including wood, grain husks, nut shells, manure and crop residues, while those with the highest carbon contents (e.g. wood, nut shells), abundance and lower associated costs are currently used for the production of activated carbon (e.g. Lua et al., 2004; Martinez et al., 2006; González et al., 2009;). Other feedstocks are potentially available for biochar production, among which biowaste (e.g. sewage sludge, municipal waste, chicken litter) and compost. Nevertheless, a risk is associated to the use of such source materials, mostly linked to the occurrence of hazardous components (e.g. organic pollutants, heavy metals). Crystalline silica has also been found to occur in some biochars. Rice husk and rice straw contain unusually high levels of silica (220 and 170 g kg^{-1}) compared to that in other major crops. High concentrations of calcium carbonate (CaCO_3) can be found in pulp and paper sludge (van Zwieten et al., 2007) and are retained in the ash fraction of some biochars.

Regarding the characteristics of some plant feedstocks, Collison et al. (2009) go further, suggesting that even within a biomass feedstock type, different composition may arise from distinct growing environmental conditions (e.g. soil type, temperature and moisture content) and those relating to the time of harvest. In corroboration, Wingate et al. (2009) have shown that the adsorbing properties of a charcoal for copper ions can be improved 3-fold by carefully selecting the growth conditions of the plant biomass (in this case, stinging nettles). Even within the same plant material, compositional heterogeneity has

also been found to occur among different parts of the same plant (e.g. maize cob and maize stalk, Table 1.3).

Lignocellulosic biomass is an obvious feedstock choice because it is one of the most abundant naturally occurring available materials (Amonette and Joseph, 2009). The spatio-temporal occurrence of biomass feedstock will influence the availability of specific biochars and its economic value (e.g. distance from source to field). For example, in an area with predominantly root crops on calcareous sandy arable soils and a dry climate, biochars that provide more water retention and are mechanically strong (e.g. woody feedstocks) are likely to be substantially more valuable than in an area of predominantly combinable crops on acidic sandy soils and a 'year round' wet climate. In the latter case, biochars with a greater CEC, liming capacity and possibly a lower mechanical strength (e.g. crop residue feedstock) may be more in demand.

In Terra Pretas potential feedstocks were limited to wood from the trees and organic matter from other vegetation. Nowadays any biomass material, including waste, is considered as a feedstock for biochar production. Considering that historical sites contain either biochar (Terra Preta) or BC (from wildfires), chronosequence studies can only give us information about the long term consequences and dynamics of those limited natural feedstocks. This implies an important methodological challenge for the study of the long term dynamics of soils with biochar produced from feedstocks other than natural vegetation. Even for trees and plants, careful consideration needs to be given to specific species that bioaccumulate certain metals, or, in the case of crop residues, that may contain relevant concentrations of herbicides, pesticides, fungicides, and in the case of animal manures that may contain antibiotics or their secondary metabolites. See Section 5.1.5 for a more detailed discussion on the (potential) occurrence of contaminants within biochar.

In addition, chronosequence studies using historic sites are often poor predictors of structural disintegration and concomitant chemical reactivity and mobility of biochars, because they are either not in arable land use, or have not been subject to the intense physical disturbance of modern arable tillage and cultivation (e.g. the power harrow).

A detailed description of all biochar feedstocks is beyond the scope of this report and feedstocks have been reviewed in other works (Collison et al., 2009; Lehmann and Joseph, 2009). The key point is that the suitability of each biomass type as a potential source for biochar, is dependent on a number of chemical, physical, environmental, as well as economic and logistical factors (Collison et al., 2009), as discussed, where appropriate, throughout this report. It is important to stress, however, that for any material to be considered as a feedstock for biochar production, and therefore also for application to soil, a rigorous procedure needs to be developed in order to assess the biochar characteristics and long term dynamics in the range of soil, other environmental conditions, and land use and management factors that are considered for its application.

1.8 Application Strategies

Biochar application strategies have been studied very little, although the way biochar is applied to soils can have a substantial impact on soil processes and functioning, including aspects of the behaviour and fate of biochar particles in soil and the wider environment (Chapter 3) as well as on 'threats to soil' (Chapter 4), occupational health and safety (5.2), and economic considerations (Section 5.4). Broadly speaking there are three main approaches: i) topsoil incorporation, ii) depth application, and iii) top-dressing.

For topsoil incorporation biochar can be applied on its own or combined with composts or manures. The degree of mixing will depend on the cultivation techniques used. In conventional tillage systems the biochar (and compost/manure/slurry) will generally be mixed more or less homogeneously throughout the topsoil (in most arable soils from 0-15/30 cm depth). Water and wind erosion will remove biochar along with other soil material, i.e. that would erode without biochar additions as well, and possibly more biochar will be eroded from the surface because of its low density. Potentially, the application of biochar combined with compost or manure would reduce this risk, but studies evidencing this are lacking. In conservation tillage systems the incorporation depth will be reduced (leading to greater biochar concentrations at equal application rates) and possibly a concentration gradient decreasing with depth. In no-till systems any incorporation would be through natural processes (see top-dressing below). Deep mouldboard ploughing effectively results in (temporary) 'depth application' (see below), with more topsoil homogenisation occurring during subsequent ploughing.

Depth application of biochar has been described mostly as 'deep-banded' application (e.g. Blackwell et al., 2007). The placement of the biochar directly into the rhizosphere is thought to be more beneficial for crop growth and less susceptible to erosion. The application can be either by pneumatic systems, which can operate at high rates, or by applying the biochar in furrows or trenches and subsequently levelling the soil surface. Deep mouldboard ploughing essentially results in temporary 'depth application', although horizontally continuous (unlike the 'deep-banded' application). Subsequent mouldboard ploughing and cultivation will then further homogenise the biochar distribution through the topsoil.

Top-dressing of biochar is the spreading of biochar (dust fraction mostly) to the soil surface and relying on natural processes for the incorporation of the biochar into the topsoil. This form of application is being considered mainly for those situations where mechanical incorporation is not possible, e.g. no-till systems, forests, and pastures. An obvious drawback is the risk of erosion by water and wind, as well as human health (inhalation) and impacts on other ecosystem components (e.g. surface water, leaf surfaces, etc.). It is also largely unknown what the rates of incorporation would be for different soil-climate-land use combinations.

The dust fraction of biochar is an issue for all application strategies during the storing, handling, and applying phases of the biochar (see Sections 2.2.1 and 5.2 for more detailed information about the properties and implications of

biochar's dust fraction). This aspect needs to be investigated thoroughly before implementation. Like any trafficking on soil, there is a risk of (sub)soil compaction during biochar application. This may be particularly the case for the relatively heavy machinery involved in 'depth application'.

Both topsoil incorporation and top-dressing can be applied with a range of frequencies, i.e. a 'one-off' application, every few years, or every year. For specific effects on soil, e.g. nutrient availability (from a feedstock like poultry manure) or liming effect, a more frequent application may be more beneficial to the soil and/or less detrimental to the environment (nitrate leaching).

1.9 Summary

As a concept biochar is defined as 'charcoal (biomass that has been pyrolysed in a zero or low oxygen environment) for which, owing to its inherent properties, scientific consensus exists that application to soil at a specific site is expected to sustainably sequester carbon and concurrently improve soil functions (under current and future management), while avoiding short- and long-term detrimental effects to the wider environment as well as human and animal health'. Inspiration is derived from the anthropogenically created Terra Preta soils (Hortic Anthrosols) in Amazonia where charred organic material plus other (organic and mineral) materials appear to have been added purposefully to soil to increase its agronomic quality. Ancient Anthrosols have been found in Europe as well, where organic matter (peat, manure, 'plaggen') was added to soil, but where charcoal additions appear to have been limited or non-existent. Furthermore, charcoal from wildfires (pyrogenic black carbon - BC) has been found in many soils around the world, including European soils where pyrogenic BC can make up a large proportion of total soil organic carbon.

Biochar can be produced from a wide range of organic feedstocks under different pyrolysis conditions and at a range of scales. Many different materials have been proposed as biomass feedstocks for biochar. The suitability of each biomass type for such an application is dependent on a number of chemical, physical, environmental, as well as economic and logistical factors. The original feedstock used, combined with the pyrolysis conditions will determine the properties, both physical and chemical, of the biochar product. It is these differences in physicochemical properties that govern the specific interactions which will occur with the endemic soil biota upon addition of biochar to soil, and hence how soil dependent ecosystem functions and services are affected. The application strategy used to apply biochar to soils is an important factor to consider when evaluating the effects of biochar on soil properties and processes. Furthermore, the biochar loading capacity of soils has not been fully quantified, or even developed conceptually.

2. PHYSICOCHEMICAL PROPERTIES OF BIOCHAR

This chapter provides an overview of the physical and chemical properties of biochar, as determined mainly by feedstock and the pyrolysis operational conditions. The combined heterogeneity of the feedstock and the wide range of chemical reactions which occur during processing, give rise to a biochar product with a unique set of structural and chemical characteristics (Antal and Gronli, 2003; Demirbas, 2004). A primary focus was given to those characteristics that are more likely to impact on soil properties and processes when biochar is incorporated into soil. The implications of such characteristics in the context of the biochar-soil mixture are discussed in Chapter 3. More detailed information on a wider range of biochar properties can be found in the relevant scientific literature (e.g. Lehmann and Joseph, 2009; and others).

2.1 Structural and Chemical Composition

2.1.1 Structural composition

Thermal degradation of cellulose between 250 and 350°C results in considerable mass loss in the form of volatiles, leaving behind a rigid amorphous C matrix. As the pyrolysis temperature increases, so thus the proportion of aromatic carbon in the biochar, due to the relative increase in the loss of volatile matter (initially water, followed by hydrocarbons, tarry vapours, H₂, CO and CO₂), and the conversion of alkyl and O-alkyl C to aryl C (Baldock and Smernik, 2002; Demirbas 2004). Around 330°C, polyaromatic graphene sheets begin to grow laterally, at the expense of the amorphous C phase, and eventually coalesce. Above 600°C, carbonization becomes the dominant process. Carbonization is marked by the removal of most remaining non-C atoms and consequent relative increase of the C content, which can be up to 90% (by weight) in biochars from woody feedstocks (Antal and Gronli, 2003; Demirbas, 2004).

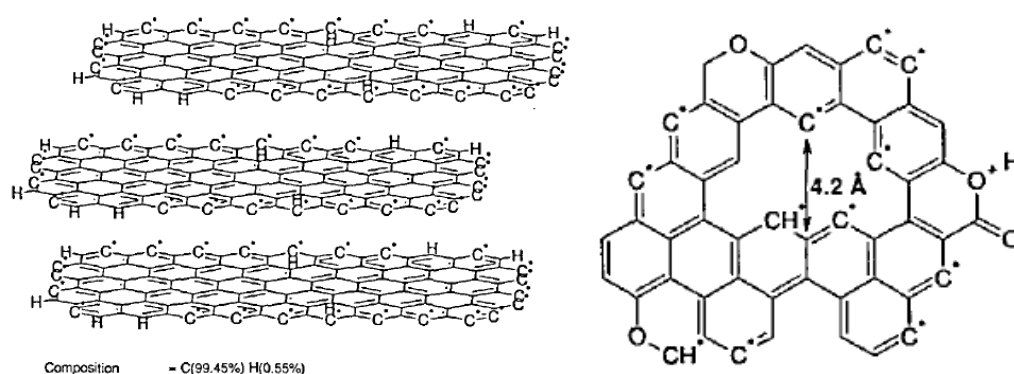


Figure 2.1 Putative structure of charcoal (adopted from Bourke et al., 2007). A model of a microcrystalline graphitic structure is shown on the left and an aromatic structure containing oxygen and carbon free radicals on the right

It is commonly accepted that each biochar particle comprises of two main structural fractions: stacked crystalline graphene sheets and randomly

ordered amorphous aromatic structures (Figure 2.1). Hydrogen, O, N, P and S are found predominantly incorporated within the aromatic rings as heteroatoms (Bourke et al., 2007). The presence of heteroatoms is thought to be a great contribution to the highly heterogeneous surface chemistry and reactivity of biochar (see the next section).

2.1.2 Chemical composition and surface chemistry

Biochar composition is highly heterogeneous, containing both stable and labile components (Sohi et al., 2009). Carbon, volatile matter, mineral matter (ash) and moisture are generally regarded as its major constituents (Antal and Gronli, 2003). Table 2.1 summarizes their relative proportion ranges in biochar as commonly found for a variety of source materials and pyrolysis conditions (Antal and Gronli, 2003; Brown, 2009).

Table 2.1 Relative proportion range of the four main components of biochar (weight percentage) as commonly found for a variety of source materials and pyrolysis conditions (adapted from Brown, 2009; Antal and Gronli, 2003)

Component	Proportion (w w⁻¹)
Fixed carbon	50-90
Volatile matter (e.g. tars)	0-40
Moisture	1-15
Ash (mineral matter)	0.5-5

The relative proportion of biochar components determines the chemical and physical behaviour and function of biochar as a whole (Brown, 2009), which in turn determines its suitability for a site specific application, as well as transport and fate in the environment (Downie, 2009). For example, coarser and more resistant biochars are generated by pyrolysis of wood-based feedstocks (Winsley, 2007). In contrast, biochars produced from crop residues (e.g. rye, maize), manures and seaweed are generally finer and less robust (lower mechanical strength). The latter are also nutrient-rich, and therefore, more readily degradable by microbial communities in the environment (Sohi et al., 2009). The ash content of biochar is dependent on the ash content of the biomass feedstock. Grass, grain husks, straw residues and manures generally produce biochar with high ash contents, in contrast to that from woody feedstocks (Demirbas 2004). For instance, manure (e.g. chicken litter) biochars can contain 45% (by weight) as ash (Amonette and Joseph, 2009). Moisture is another critical component of biochar (Antal and Gronli, 2003), as higher moisture contents increase the costs of biochar production and transportation for unit of biochar produced. Keeping the moisture content up to 10% (by weight) appears to be desirable (Collison et al., 2009). In order for this to be achieved, pre-drying the biomass feedstock may be a necessity, which can be a challenge in biochar production.

Despite the feasibility of biochar being produced from a wide range of feedstocks under different pyrolysis conditions, its high carbon content and strongly aromatic structure are constant features (Sohi et al., 2009). According to Sohi et al. (2009), these features largely account for its chemical stability. Similarly, pH shows little variability between biochars, and is typically

>7. Table 2.2 summarizes total elemental composition (C, N, C:N, P, K, available P – *Pa* - and mineral N) and pH ranges of biochars from a variety of feedstocks (wood, green wastes, crop residues, sewage sludge, litter, nut shells) and pyrolysis conditions (350-500°C) used in various studies (adapted from Brown, 2009).

Table 2.2 Summary of total elemental composition (C, N, C:N, P, K, available P and mineral N) and pH ranges and means of biochars from a variety of feedstocks (wood, green wastes, crop residues, sewage sludge, litter, nut shells) and pyrolysis conditions (350-500°C) used in various studies (adapted from Chan and Xu, 2009)

		pH	C (g kg ⁻¹)	N (g kg ⁻¹)	N (NO ₃ ⁻ +NH ₄ ⁺) (mg kg ⁻¹)	C:N	P (g kg ⁻¹)	<i>Pa</i> (g kg ⁻¹)	K (g kg ⁻¹)
Range	From	6.2	172	1.7	0.0	7	0.2	0.015	1.0
	To	9.6	905	78.2	2.0	500	73.0	11.6	58
Mean		8.1	543	22.3	-	61	23.7	-	24.3

Total carbon content in biochar was found to range between 172 to 905 g kg⁻¹, although OC often accounts for < 500 g kg⁻¹, as reviewed by Chan and Xu (2009) for a variety of source materials. Total N varied between 1.8 and 56.4 g kg⁻¹, depending on the feedstock (Chan and Xu, 2009). Despite seemingly high, biochar total N content may not be necessarily beneficial to crops, since N is mostly present in an unavailable form (mineral N contents < 2 mg k⁻¹; Chan and Xu, 2009). Nuclear magnetic resonance (NMR) spectroscopy has shown that aromatic and heterocyclic N-containing structures in biochar occur as a result of biomass heating, converting labile structures into more recalcitrant forms (Almendros et al., 2003). C:N (carbon to nitrogen) ratio in biochar has been found to vary widely between 7 and 500 Chan and Xu, (2009), with implications for nutrient retention in soils (see Sections 3.2.3). C:N ratio has been commonly used as an indicator of the capacity of organic substrates to release inorganic N when incorporated into soils.

Total P and total K in biochar were found to range broadly according to feedstock, with values between 2.7 - 480 and 1.0 - 58.0 g kg⁻¹, respectively (Chan and Xu, 2009). Interestingly, total ranges of N, P and K in biochar are wider than those reported in the literature for typical organic fertilizers. Most minerals within the ash fraction of biochar are thought to occur as discrete associations independent of the carbon matrix, with the exception of K and Ca (Amonette and Joseph, 2009). Typically, each mineral association comprises more than one type of mineral. Joseph et al. (2009) emphasize that our current understanding of the role of high-mineral ash biochars is yet limited, as we face the lack of available data on their long-term effect on soil properties.

The complex and heterogeneous chemical composition of biochars is extended to its surface chemistry, which in turn explains the way biochar interacts with a wide range of organic and inorganic compounds in the environment. Breaking and rearrangement of the chemical bounds in the biomass during processing results in the formation of numerous functional groups (e.g. hydroxyl -OH, amino-NH₂, ketone -OR, ester -(C=O)OR, nitro -

NO₂, aldehyde -(C=O)H, carboxyl -(C=O)OH) occurring predominantly on the outer surface of the graphene sheets (e.g. Harris, 1997; Harris and Tsang, 1997) and surfaces of pores (van Zwielen et al., 2009). Some of these groups act as electron donors, while others as electron acceptors, resulting on coexisting areas which properties can range from acidic to basic and from hydrophilic to hydrophobic (Amonette and Joseph 2009). Some functional groups also contain other elements, such as N and S, particularly in biochars from manures, sewage sludge and rendering wastes.

There is experimental evidence that demonstrates that the composition, distribution, relative proportion and reactivity of functional groups within biochar are dependent on a variety factors, including the source material and the pyrolysis methodology used (Antal and Gronli, 2003). Different processing conditions (temperature of 700°C or 450°C) explained differences in N contents between three biochars from poultry litter (Lima and Marshall, 2005; Chan et al., 2007). As the pyrolysis temperature rises, so does the proportion of aromatic carbon in the biochar, while N contents peak at around 300°C (Baldock and Smernik, 2002). In contrast, low processing temperatures (<500°C) favour the relative accumulation of a large proportion of available K, Cl (Yu et al., 2005), Si, Mg, P and S (Bourke et al., 2007; Schnitzer et al., 2007). Therefore, processing temperatures < 500°C favour nutrient retention in biochar (Chan and Xu, 2009) , while being equally advantageous in respect to yield (Gaskin et al., 2008). Nevertheless, it is important to stress that different permutations of those processing conditions, including temperature, may affect differently each source material.

This emphasises the need for a case-by-case assessment of the chemical and physical properties of biochar prior to its application into soil. Relating the adverse effect of a particular constituent (or its concentration) of biochar to a desirable biochar application rate (biochar loading capacity concept; Section 1.5.1) is difficult, as the exact biochar composition is often not provided in the literature. The review of relevant literature has indicated that the full knowledge on the composition of biochar as a soil amendment, and the way it is influenced by those parameters, as well as the implications for soil functioning, is still scarce. Partially, this can be explained by the fact that most characterisation work has involved charcoals with high carbon and low ash content, as required by the increasingly demanding market for activated carbon. Another factor is the wide variety of processing conditions and feedstocks available. The Black Carbon Steering Committee has developed reference charcoal materials (from chestnut wood and rice grass) under standardised pyrolysis conditions, representative of natural samples created by forest fires, for comparison of quantification methods for BCs in soils and sediments. Nevertheless, the current sparsity of biochar standards is largely reflected on the poor understanding of the link between biochar composition and its behaviour and function in soil.

2.2 Particle size distribution

Initially, particle size distribution in biochar is influenced mainly by the nature of the biomass feedstock and the pyrolysis conditions (Cetin et al., 2004).

Shrinkage and attrition of the organic material occur during processing, thereby generating a range of particle sizes of the final product. The intensity of such processes is dependent on the pyrolysis technology (Cetin et al., 2004). The implications of biochar particle size distribution on soils will be discussed further throughout Chapter 3.

Particle size distribution in biochar also has implications for determining the suitability of each biochar product for a specific application (Downie et al., 2009), as well as for the choice of the most adequate application method (see Section 1.8). In addition, health and safety issues relating to handling, storage and transport of biochar are also largely determined by its particle size distribution, as discussed in this report in regard to its dust fraction (see Sections 2.2.1 and 5.2).

The influence of the type of feedstock on particle size distribution was discussed by Sohi et al. (2009), among others. Wood-based feedstocks generate biochars that are coarser and predominantly xylemic in nature, whereas biochars from crop residues (e.g. rye, or maize) and manures offer a finer and more brittle structure (Sohi et al., 2009). Downie et al. (2009) have further provided evidence of the influence of feedstock and processing conditions on particle size distribution in biochar. Sawdust and woodchips under different pre-treatments were pyrolysed using continuous slow pyrolysis (heating rate of 5-10°C min⁻¹), after which particle size distribution in the resulting biochar was assessed through dry sieving. Generally, particle size was found to decrease as the pyrolysis heat treatment temperature increased (450°C-700°C range) for both feedstocks, due to a reduction of the biomass material resistance to attrition during processing (Downie et al., 2009).

The operating conditions during pyrolysis (e.g. heating rate, high treatment temperature -HTT, residence time, pressure, flow rate of the inert gas, reactor type and shape) and pre- (e.g. drying, chemical activation) and post- (e.g. sieving, activation) treatments can greatly affect biochar physical structure (Gonzalez et al., 1997; Antal and Grønli, 2003; Cetin et al., 2004; Lua et al., 2004; Zhang et al., 2004; Brown et al., 2006). Such observations were derived mainly from studies involving activated carbon produced from a variety of feedstocks, including maize hulls (Zhang et al., 2004), nut shells (Lua et al., 2004; González et al., 2009) and olive stones (González et al., 2009). Similarly, heating rate, residence time and pressure during processing were shown to be determinant factors for the generation of finer biochar particles, independently of the original material (Cetin et al., 2004). For instance, for higher heating rates (e.g. up to 105-500°C sec⁻¹) and shorter residence times, finer feedstock particles (50-2000 µm) are required in order to facilitate heat and mass transfer reactions, resulting in finer biochar material (Cetin et al., 2004). In contrast, slow pyrolysis (heating rates of 5-30°C min⁻¹) can use larger feedstock particles, thereby producing coarser biochars (Downie et al., 2009). Increasing the proportion of larger biochar particles can also be obtained by increasing the pressure (from atmospheric to 5, 10 and 20 bars) during processing, which was explained by both particle swelling and clustering, as a result of melting (i.e. plastic deformation) followed by fusion (Cetin et al., 2004).

2.2.1 Biochar dust

The term 'dust' is described in this report as referring to the fine and ultrafine fraction of biochar, comprising various organic and inorganic compounds of distinct particle sizes within the micro- and nano-size range (Harris and Tsang, 1997; Cornelissen et al., 2005). Harris and Tsang (1997) researched the micro- and nano-sized fraction of chars, although so far, this issue remains poorly understood. Biomass precursor (feedstock) and the pyrolysis conditions (Donaldson et al., 2005; Hays and van der Wal, 2007) are likely to be primary factors influencing the properties of biochar dust (Downie et al., 2009), including the type and size of its particles, as well as the proportion of micro- and nanoparticles, as discussed previously

Harris and Tsang (1997) used high resolution electron microscopy (HREM) for studying the smaller fraction of charcoal resulting from the pyrolysis (700°C) of sucrose and concluded that charcoal dust consists of round fullerene-like nanoparticles (Harris and Tsang, 1997). Brodowski et al. (2005) corroborates the finding of porous spherical-shaped particles (with surface texture ranging from smooth to rough) within the <2 µm fraction of charcoals in a field-plot topsoil (0-10 cm), although no reference to the word "fullerene" was found. What is important in this context is that, considering the small size of such particles and their reactivity, the proportion of dust within the biochar (which may also apply to biochars with high ash contents) has relevant practical, as well as health and safety implications (see Section 5.2).

The proportion of dust in biochar is also key in determining the suitability of a given application strategy (Blackwell et al., 2009). For example, Holownicki (2000) suggested that this fine fraction could be successfully employed in precision agriculture for spraying fungicide preparations in orchards and vineyards. When injection is appropriate, Blackwell et al. (2009) pointed out that the application of biochar dust may in fact be preferred when used in combination with liquid manure in selected crops.

On the other hand, biochar dust has been identified in the literature as a better sorbent for a wide range of trace hydrophobic contaminants (e.g. PAHs, polychlorinated biphenyls - PCBs, pesticides, polychlorinated dibenzo-p-dioxins and -furans - PCDD/PCDFs), when compared to larger biochar particles or to particulate organic matter (Hiller et al., 2007; Bucheli and Gustafsson, 2001, 2003). As such, the addition of biochar dust to soils may increase the sorption affinity of the soil for common environmental pollutants (see Section 3.2.2 for a more detailed discussion on the sorption of hydrophobic compounds to biochar), as demonstrated for dioxin sorption in a marine system (Persson et al., 2002).

2.3 Pore size distribution and connectivity

Biomass feedstock and the processing conditions are the main factors determining pore size distribution in biochar, and therefore its total surface area (Downie et al., 2009). During thermal decomposition of biomass, mass loss occurs mostly in the form of organic volatiles, leaving behind voids, which form an extensive pore network. This section focuses on pore size distribution

in biochar, while biochar density is discussed in the context of the biochar-soil mixture in Section 3.1.1.

Biochar pores are classified in this review into three categories (Downie et al., 2009), according to their internal diameters (ID): macropores (ID >50 nm), mesopores (2 nm < ID < 50 nm) and micropores (ID < 2 nm). These categories are orders of magnitude different to the standard categories for pore sizes in soil science (see Table 3.1). The elementary porosity and structure of the biomass feedstock is retained in the biochar product formed (Downie et al., 2009). The vascular structure of the original plant material, for example, is likely to contribute for the occurrence of macropores in biochar, as demonstrated for activated carbon from coal and wood precursors (Wildman and Derbyshire, 1991). In contrast, micropores are mainly formed during processing of the parent material. While macropores have been identified as a 'feeder' to smaller pores (Martinez et al., 2006), micropores effectively account for the characteristically large surface area in charcoals (Brown, 2009).

Among those operating parameters, HTT is thought to be the most significant factor for the resulting pore distribution in charcoals (Lua et al., 2004), as the physical changes undergone by the biomass feedstock during processing are often temperature-dependent (Antal and Grønli, 2003).

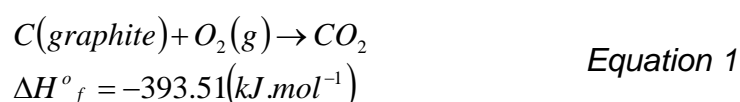
The development of microporosity in biochar, which is linked to an increase in structural and organisational order, has been showed to be favoured by higher HTT and retention times, as previously demonstrated for activated carbon (e.g. Lua et al., 2004). For example, increasing pyrolysis temperature from 250 to 500°C enhanced the development of micropores in chars derived from pistachio-nut shells, due to increased evolution of volatiles. For subsequent increases in temperature (>800°C), a reduction of the overall surface area of the char was observed and was attributed to partial melting of the char structure (Lua et al., 2004). Similarly, heating rate and pressure during processing have also been found to influence the mass transfer of volatiles produced at any given temperature range, and are therefore regarded as key contributing parameters influencing pore size distribution (Antal and Grønli, 2003). For instance, Lua et al. (2004) observed a peak in surface area of pistachio-nut shell char at low heating rates (10°C), whereas higher heating rates resulted in a decrease in surface area.

It is important to stress, however, that the relative influence of each processing parameter on the final microporosity in biochar is determined by the type of feedstock, as noted from the above studies (e.g. Cetin et al., 2004; Lua et al., 2004; Pastor-Villegas et al., 2006; González et al., 2009). In particular, the lignocellulosic composition of the parent material largely determines the rate of its thermal decomposition, and therefore, the development of porosity (González et al., 2009). In the case of charcoals from almond tree pruning, a greater volume of meso and macropores was obtained, which was accounted for by the slow decomposition rate of such precursor during the initial stages of pyrolysis (González et al., 2009). The

opposite was found for almond shell, probably due to its inherently high initial thermal decomposition rate (González et al., 2009).

2.4 Thermodynamic stability

The thermodynamic equilibrium concerning carbonised residues, such as biochar, favours the production of CO₂.



The standard enthalpy of formation is represented as ΔH°_f and the degree sign denotes the standard conditions (P = 1 bar and T = 25°C)

Equation 1 shows that the oxidation of graphite, being the most thermodynamically stable form of carbon, will occur spontaneously as shown by the negative energy value (meaning that 393.51 kJ of energy is emitted for every mole of CO₂ 'produced'). Since the oxidation of graphite to carbon dioxide will occur, albeit very slowly under normal conditions (Shneour, 1966), all other forms of carbon which are less thermodynamically stable than graphite, will also undergo oxidation to CO₂ in the presence of oxygen. The speed at which this oxidation occurs depends on a number of factors, such as the precise chemical composition, as well as the temperature and moisture regime to which the compound is exposed. Furthermore, residence time of biochar in soils will also be affected by microbial processes. The recalcitrance of biochar in soil is discussed in more depth in Sections 3.2.1 and 3.2.5.1.

2.5 CEC and pH

CEC variation in biochars ranges from negligible to around 40 cmol_c g⁻¹ and has been reported to change following incorporation into soils (Lehmann, 2007). This may occur by a process of leaching of hydrophobic compounds from the biochar (Briggs et al., 2005) or by increasing carboxylation of C via abiotic oxidation (Cheng et al. 2006; Liang et al. 2006). Glaser et al. (2001) discussed the importance of ageing to obtain the increases in CEC of black BC found in the Terra Preta soils of the Amazon.

Considering the very large heterogeneity of its properties, biochar pH values are relatively homogeneous, that is to say they are largely neutral to basic. Chan and Xu (2009) reviewed biochar pH values from a wide variety of feedstocks and found a mean of pH 8.1 in a total range of pH 6.2 – 9.6. The lower end of this range seems to be from green waste and tree bark feedstocks, with the higher end from poultry litter feedstocks.

2.6 Summary

Biochar is comprised of stable carbon compounds created when biomass is heated to temperatures between 300 to 1000°C under low (preferably zero) oxygen concentrations. The structural and chemical composition of biochar is highly heterogeneous, with the exception of pH, which is typically > 7. Some properties are pervasive throughout all biochars, including the high C content

and degree of aromaticity, partially explaining the high levels of biochar's inherent recalcitrance. Nevertheless, the exact structural and chemical composition, including surface chemistry, is dependent on a combination of the feedstock type and the pyrolysis conditions (mainly temperature) used. These same parameters are key in determining particle size and pore size (macro, meso and micropore; distribution in biochar. Biochar's physical and chemical characteristics may significantly alter key soil physical properties and processes and are, therefore, important to consider prior to its application to soil. Furthermore, these will determine the suitability of each biochar for a given application, as well as define its behaviour, transport and fate in the environment. Dissimilarities in properties between different biochar products emphasises the need for a case-by-case evaluation of each biochar product prior to its incorporation into soil at a specific site. Further research aiming to fully evaluate the extent and implications of biochar particle and pore size distribution on soil processes and functioning is essential, as well as its influence on biochar mobility and fate (see Section 3.2.1).

3. EFFECTS ON SOIL PROPERTIES, PROCESSES AND FUNCTIONS

This chapter discusses the effects of biochars with different characteristics (Chapter 2) on soil properties and processes. First, effects on the soil properties are discussed, followed by effects on soil physical, chemical and biological processes. The agricultural aspect of the production function of soil is reviewed in detail (including meta-analyses)

3.1 Properties

3.1.1 Soil Structure

The incorporation of biochar into soil can alter soil physical properties such as texture, structure, pore size distribution and density with implications for soil aeration, water holding capacity, plant growth and soil workability (Downie et al., 2009). Particularly in relation to soil water retention, Sohi et al. (2009) propose an analogy between the impact of biochar addition and the observed increase in soil water repellency as a result of fire. Rearrangement of amphiphilic molecules by heat from a fire, as proposed by Doerr et al. (2000), would not affect the soil, but could affect the biochar itself during pyrolysis. In addition, the soil hydrology may be affected by partial or total blockage of soil pores by the smallest particle size fraction of biochar, thereby decreasing water infiltration rates (see Sections 3.1.1 and 3.2.3). In that sense, further research aiming to fully evaluate the extent and implications of biochar particle size distribution on soil processes and functioning is essential, as well as its influence on biochar mobility and fate (see Section 3.2.1).

3.1.1.1 Soil Density

Biochar has a bulk density much lower than that of mineral soils and, therefore, application of biochar can reduce the overall bulk density of the soil, although increases in bulk density are also possible. If 100 t ha^{-1} of biochar with a bulk density of 0.4 g cm^{-3} is applied to the top 20 cm of a soil with a bulk density of 1.3 g cm^{-3} , and the biochar particles do not fill up existing soil pore space, then the soil surface in that field will be raised by *ca.* 2.5 cm with an overall bulk density reduction (assuming homogeneous mixing) of 0.1 g cm^{-3} to 1.2 g cm^{-3} . However, if the biochar that is applied has a low mechanical strength and disintegrates relatively quickly into small particles that fill up existing pore spaces in the soil, then the dry bulk density of the soil will increase.

In agronomy, relatively small differences in soil bulk density can be associated with agronomic benefits. Conventionally, i.e. without biochar additions, lower bulk density is associated with higher SOM content leading to nutrient release and retention (fertiliser saving) and/or lower soil compaction due to better soil management (potentially leading to improved seed germination and cost savings for tillage and cultivation). Biochar application to soil by itself may improve nutrient retention directly (see Section 3.2.2), but nutrient release is mostly very small (except for some biochars in the first years, especially in ash-rich biochars) and the application of biochar with heavy machinery may compact the subsoil, depending on the application method and timing

Soil compactibility is closely related to soil bulk density. Soane (1990) reviewed the effect of SOM, i.e. not including biochar, on compactibility and proposed several mechanisms by which SOM may influence the ability of the soil to resist compactive loads:

- 1) Binding forces between particles and within aggregates. Many of the long-chain molecules present in SOM are very effective in binding mineral particles. This is of great importance within aggregates which "...are bound by a matrix of humic material and mucilages" (Oades in Soane, 1990).
- 2) Elasticity. Organic materials show a higher degree of elasticity under compression than do mineral particles. The relaxation ratio – R – is defined as the ratio of the bulk density of the test material under specified stress to the bulk density after the stress has been removed. Relaxation effects of materials such as straw are therefore much greater than material like slurry or biochar.
- 3) Dilution effect. The bulk density of SOM is usually appreciably lower than mineral soil. It can however differ greatly, from 0.02 t m^{-3} for some types of peat to 1.4 t m^{-3} for peat moss, compared to 2.65 t m^{-3} for mineral particles (Ohu et al. in Soane, 1990).
- 4) Filament effect. Roots, fungal hyphae and other biological filaments have the capacity to bind the soil matrix.
- 5) Effect on electrical charge. Solutions/suspensions of organic compounds may increase the hydraulic conductivity of clays by changing the electrical charge on the clay particles causing them to move closer together, flocculate and shrink, resulting in cracks and increased secondary – macro - porosity (Soane, 1990). Biochar's ash fraction could cause similar effects.
- 6) Effect on friction. An organic coating on particles and organic material between particles is likely to increase the friction between particles (Beekman in: Soane, 1990). The direct effect of biochar on soil friction has not been studied.

The effect of biochar application on soil compactibility has not been tested experimentally yet. From the above mechanisms, however, direct effects of biochar are probably mostly related to bullet points 3, 5 and 6 above. The very low elasticity of biochar suggests that resilience to compaction, i.e. how quickly the soil 'bounces back', is unlikely to be increased directly by biochar. The resistance to compaction of soil with biochar could potentially be enhanced via direct or indirect effects (interaction with SOM dynamics and soil hydrology). For example, some studies have shown an increase in mycorrhizal growth after additions of biochar to soil (see Section 3.2.6) while under specific conditions plant productivity has also been shown to increase (see Section 3.3). The enhanced development of hyphae and roots will have an effect on soil compaction. However, experimental research into the mechanisms and subsequent modeling work is required before any conclusions can be drawn regarding the overall effect of biochar on soil compaction.

3.1.1.2 Soil pore size distribution

The incorporation of biochar into soil can alter soil physical properties such as texture, structure, pore size distribution and density with implications for soil aeration, water holding capacity, plant growth and soil workability. The soil pore network can be affected by biochar's inherent porosity as well as its other characteristics, in several ways. Biochar particle size and pore size distribution and connectivity, the mechanical strength of the biochar particles, and the translocation and interaction of biochar particles in the soil are all determining factors that will lead to different outcomes in different soil-climate-management combinations. As described in the above section, these factors can cause the overall porosity of the soil to increase or decrease following biochar incorporation into soils.

There is evidence that suggests that biochar application into soil may increase the overall net soil surface area (Chan et al., 2007) and consequently, may improve soil water retention (Downie et al., 2009; see Section 3.1.2) and soil aeration (particularly in fine-textured soils; Kolb, 2007). An increased soil-specific surface area may also benefit native microbial communities (Section 3.2.6) and the overall sorption capacity of soils (Section 3.2.2). In addition, soil hydrology may be affected by partial or total blockage of soil pores by the smallest particle size fraction of biochar, thereby decreasing water infiltration rates (see Sections 3.1.1, 3.1.2 and 3.2.3). Nevertheless, experimental evidence of such mechanisms is scarce and, therefore, any effects of the pore size distribution of biochar on soil properties and functions is still uncertain at this stage. Further research aiming to fully evaluate the extent and implications of biochar particle size distribution on soil processes and functioning is essential, as well as its influence on biochar mobility and fate in the environment (see Section 3.2.1).

Table 3.1 shows the classifications of pore sizes in material science and soil science. Fundamental differences, i.e. orders of magnitude difference for classes with the same names, are obstacles in communicating to any audience outside of biochar research and also hinder the communication efficiency within interdisciplinary research groups that work on biochar in soils. Therefore, it is recommended that existing classifications are modified to resolve this confusion. However, in this review we will use the existing terminology and the relevant classification will need to be retrieved from the context.

Table 3.1 Pore size classes in material science vs. soil science

	Material science	Soil science
		Pore size (μm)
Cryptospores	na	<0.1
Ultramicropores	na	0.1-5
Micropores	<0.002	5-30
Mesopores	0.002-0.05	30-75
Macropores	>0.05	>75

3.1.2 Water and Nutrient Retention

The addition of biochar to soil will alter both the soil's chemical and physical properties. The net effect on the soil physical properties will depend on the interaction of the biochar with the physicochemical characteristics of the soil, and other determinant factors such as the climatic conditions prevalent at the site, and the management of biochar application.

Adding biochar affects the regulation and production function of the agricultural soil. To what extent biochar is beneficial to agriculture, and the dominant mechanisms that determine this, is still under scientific scrutiny. Agronomic benefits of biochar are often attributed to improved water and/or nutrient retention. However, many of the scientific studies are limited to site-specific soil conditions, and performed with biochar derived from specific feedstocks. Of more concern, and as of yet underexposed, is the stability of the structural integrity of the biochar. Especially when biochar is used in today's intensive agriculture with the use of heavy machinery, opposed to the smallholder system that led to the formation of Terra Preta. Another concern relates to the potential externalities of bringing large quantities of biochar in the environment (see Chapter 5).

The mechanisms that lead to biochar-provided potential improvements in water retention are relatively straightforward. Adding biochar to soil can have direct and indirect effects on soil water retention, which can be short or long lived. Water retention of soil is determined by the distribution and connectivity of pores in the soil-medium, which is largely regulated by soil particle size (texture), combined with structural characteristics (aggregation) and SOM content.

The direct effect of biochar application is related to the large inner surface area of biochar. Biochars with a range in porous structures will result from feedstocks as variable as straw, wood and manure (see Sections 1.7, 2.1 and 2.3). Kishimoto and Sugiura (1985) estimated the inner surface area of charcoal formed between 400 and 1000°C to range from 200 to 400 m² g⁻¹. Van Zwieten et al. (2009) measured the surface area of biochar derived from papermill waste with slow pyrolysis at 115 m² g⁻¹.

The hypothesised indirect effects of biochar application on water retention of soil relate to improved aggregation or structure. Biochar can affect soil aggregation due to interactions with SOM, minerals and microorganisms. The surface charge characteristics, and their development over time, will determine the long term effect on soil aggregation. Aged biochar generally has a high CEC, increasing its potential to act as a binding agent of organic matter and minerals. Macro-aggregate stability was reported to increase with 20 to 130% with application rates of coal derived humic acids between 1.5 Mg ha⁻¹ and 200 t ha⁻¹ (Mbagwu and Piccolo, 1997). Brodowski et al (2006) found indications that BC acted as a binding agent in microaggregates in soils under forest, grassland and arable land use in Germany. In-situ enhancement of soil aggregation by biochar requires further analysis.

The mechanical stability and recalcitrance of biochar once incorporated in the soil will determine long term effects on water retention and soil structure. This is determined by feedstock type and operating conditions as well as the prevalent physical-chemical conditions that determine its weathering and the

compaction and compression of the biochar material in time. The effect of the use of heavy agricultural machinery on compaction of the soil-biochar matrix has yet to be studied in detail. Another factor contributing to the uncertainty in long-term beneficial effects of biochar application to soil is the potential clogging or cementation of soil pores with disintegrated biochar material.

Glaser et al. (2002b) reported that Anthrosols rich in charcoal with surface areas three times higher than those of surrounding soils had an increased field capacity of 18%. Tryon (1948) studied the effect of charcoal on the percentage of available moisture in soils of different textures. In sandy soil the addition of charcoal increased the available moisture by 18% after adding 45% of biochar by volume, while no changes were observed in loamy soil, and in clayey soil the available soil moisture decreased with increasing coal additions. This was attributed to hydrophobicity of the charcoal, although another factor could simply be that the biochar was replacing clay with a higher water retention capacity. Biochar's high surface area can thus lead to increased water retention, although the effect seems to depend on the initial texture of the soil. Therefore, improvements of soil water retention by charcoal additions may only be expected in coarse-textured soils or soils with large amounts of macropores. A draw-back is the large volume of biochar that needs to be added to the soil before it leads to increased water retention.

The capacity of the agricultural soil to store water regulates the time and amount water is kept available for crop transpiration. Tseng and Tseng (2006) found that activated biochar contained over 95% of micropores with a diameter <2 nm. Since the porosity of biochar largely consists of micropores, the actual amount of additional plant available water will depend on the biochar feedstock and the texture of the soil it is applied to. The agronomic water-storage benefit of biochar application will thus depend on the relative modification of the proportion of micro, meso and macro pores in the root zone. In sandy soils, the additional volume of water and soluble nutrients stored in the biochar micropores may become available as the soil dries and the matric potential increases. This may lead to increased plant water availability during dry periods.

The potential co-benefits or negative externalities of the use of biochar in irrigated agricultural systems have not been explored in detail. If the water holding capacity of the soil increases this may hypothetically reduce the irrigation frequency or irrigation volume. However, the potential susceptibility of disintegrated biochar particles to cement or clog the soil may also result in increased runoff and lower infiltration rates.

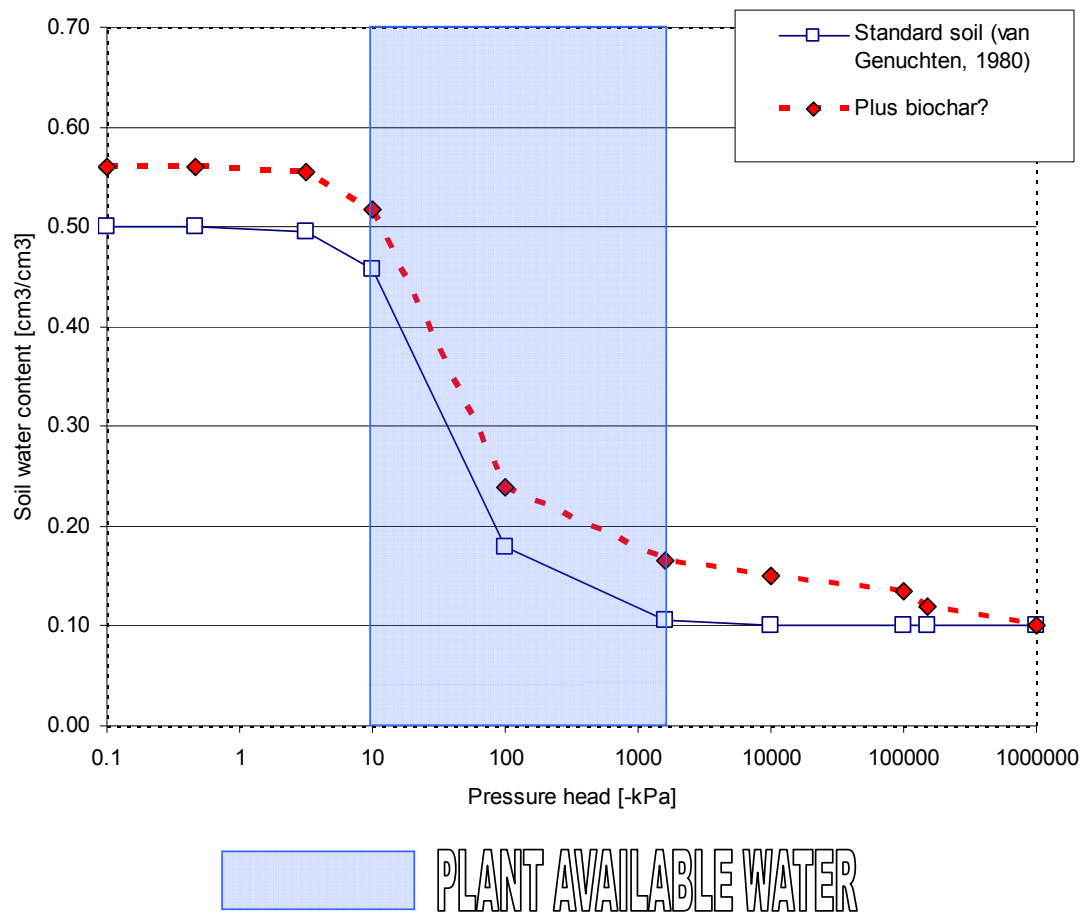


Figure 3.1 Typical representation of the soil water retention curve as provided by van Genuchten (1980) and the hypothesized effect of the addition of biochar to this soil

Figure 3.1 shows a typical representation of the soil water retention curve (van Genuchten, 1980) and the hypothesised effect of the addition of biochar to this soil. Notice that in this conceptual example most of the water that is stored additionally in the soil will not be available for plant water uptake since it occurs at tensions superior to the range wherein plant roots are able to take up water. In this hypothetical representation this is mainly due to the pore size distribution of the biochar which largely consists of very small pores and only very little pores in the range relevant for plant water uptake. Although this is a hypothetical consideration; it highlights the need for a further understanding of the direct and indirect effects of biochar addition on soil water retention, and its longevity.

3.1.2.1 Soil water repellency

Soil water repellency (SWR), or hydrophobicity, is defined functionally as “the reduction of the affinity of soils to water such that they resist wetting for periods ranging from a few seconds to hours, days or weeks” (King, 1981). SWR is a widespread phenomenon associated with decreased infiltration rates, fingered flow infiltration, and increased runoff. In the case of agricultural land, fertiliser and biocide (herbicide, pesticide) leaching to the groundwater via bypass flow (secondary porosity) can be costly to the farmer and the

environment. Most of the literature on soil water repellency focuses the effect of the heat wave from a (wild)fire on the hydrophobic properties of the SOM. Reorientation of amphiphilic molecules is one of the hypothesised mechanisms (Doerr et al., 2000) explaining the water repellent effect, although other mechanisms are also hypothesised. In relation to soil water retention, Sohi et al. (2009) propose an analogy between the impact of biochar addition and the observed increase in soil water repellency as a result of fire. Rearrangement of amphiphilic molecules by heat from a fire, as proposed by Doerr et al. (2000), would not affect the soil, but could affect the biochar itself during pyrolysis.

Field studies on water repellent properties of biochar or charcoal are absent from the scientific literature and very limited even for charcoal produced by wildfires. Briggs et al. (2005) measured WR of charcoal particles after a wildfire in a pine forest and found very large differences in WR between charcoal particles on the surface and in the mineral soil vs. those on the border of the litter layer and mineral soil. The water drop penetration time, that is the time it takes a droplet of water to infiltrate, was >2 h for the former and <10 s for the latter. The authors proposed leaching by organic acids as a mechanism explaining the reduction of water repellent properties underneath the litter layer. How biochar may influence soil water repellency, directly or indirectly, is a topic that still requires a substantial research effort before the mechanisms are understood and predictions can be made. A trade off appears to exist between the capacity to bind HOCs, like PAHs (see Section 3.2.2), and the capacity to bind water molecules.

3.1.3 Soil colour, albedo and warming

From the Anthrosol profile pictures (Figure 1.5) it is obvious that high concentrations of biochar in soil darken its colour. Briggs et al. (2005) measured changes in dry soil colour from charcoal additions and found the Munsell value to decrease from 5.5 to 4.8 at charcoal concentrations of 10 g kg⁻¹, and down to 3.6 at 50 g kg⁻¹. Oguntunde et al. (2008) compared the soil colour of charcoal sites (i.e. where charcoal used to be produced) with that of adjacent soil and found the Munsell value to decrease from 3.1 (± 0.6) to 2.5 (± 0.4). The degree of darkening is dependent on i) the colour of the soil prior to biochar additions (Munsell value 1-9), ii) the colour of the biochar (probably Munsell value 0-2), iii) the biochar concentration in the soil, iv) the degree of mixing (related to particle size of both the biochar and the soil), v) the surface roughness, and vi) the change in water retention at the soil surface that accompanies the addition of biochar (moist soil is darker in colour). Wang et al. (2005) conducted three years of continuous measurement in a semi-desert area in Tibet and showed an exponential relationship between soil moisture content (v v⁻¹) and surface albedo. The combined effects of the changes in these factors subsequently determine the albedo effect of the soil.

Land surface albedo is an important component of global and regional climate change models. However, almost exclusively, the albedo of the vegetation is used, not that of soil. Levis et al. (2004) introduced a modification to soil albedo into their community climate system model and found this change to

be the key for the model output to resemble the botanic evidence for climate-vegetation interactions in mid-Holocene North Africa. Model simulations with a darker soil colour led to an intensified monsoon which brought precipitation further north; testifying the importance of changes in soil albedo on climate feedbacks.

The principle that biochar application to soils decreases the albedo of bare soil and thereby contributes to further warming of the planet is accepted, however, if, and where, that would lead to an effect of relevant magnitude is much less certain. Bare soil is limited to the winter months on fields growing spring crops, or in orchards without ground cover (e.g. olive orchards, vineyards). In the former case, the warming effect may be relatively small because solar radiation reaching the surface is low in winter months, however, many orchards and vineyards are in more southern parts that receive a greater solar input and the bare soil conditions persist throughout the year. Post et al. (2000) investigated the influence of soil colour and moisture content on the albedo of 26 different soils ranging widely in colour and texture. They found that wet samples had their albedo reduced by a mean of 48% (ranging between 32-58%), and that Munsell colour value is linearly related to soil albedo.

The amount of solar radiation that reaches the soil surface (as affected by sun angle and slope and vegetation cover) and the specific heat of soils, largely control the rate at which soils warm up in the spring, and thus influence the emergence of seedlings. Soil colour and soil moisture content are the main factors determining the specific heat of soil. For pure water the specific heat is about $4.18 \text{ J g}^{-1} \text{ K}^{-1}$; that of dry soil is about $0.8 \text{ J g}^{-1} \text{ K}^{-1}$. Therefore, although soils high in biochar content are usually dark in colour, if the biochar increases the water retention of the soil concomitantly (see Section 3.1.2) then the associated extra energy absorption is countered by a high water content, which causes the soil to warm up much more slowly (Brady, 1990). This implies that biochar with low water retention capacity (e.g. because of water repellent properties, see Section 3.1.2.1) will cause the greatest increase in soil warming, and that this impact will be greatest where biochar is applied to light-coloured soils (high Munsell value) with spring crops (i.e. bare soil in spring) or orchards/vineyards.

3.1.4 CEC and pH

The cation exchange capacity (CEC) of soils is a measure for how well some nutrients (cations) are bound to the soil, and, therefore, available for plants uptake and 'prevented' from leaching to ground and surface waters. It is at negatively charged sites on the reactive surface area of biochar (and clay and organic matter) where cations can be electro-statically bound and exchanged. Cations compete with each other as well as with water molecules and can be excluded when the pore size at the charged site is smaller than their size. Cheng et al. (2006) assessed the effects of climatic factors on biochar oxidation in natural systems. The CEC of biochar was correlated to the mean temperature and the extent of biochar oxidation was related to its external surface area, being seven times higher on the external surfaces than in its interior (Cheng et al., 2008). It is not known at present how the CEC of

biochar will change as the biochar disintegrates by weathering and tillage operations, 'ages' and moves through the soil.

Anions are bound very poorly by soils under neutral or basic pH conditions. This is one of the reasons why crops need fertilising, as anionic nutrients (e.g. phosphates) are leached or flushed from the soil into ground/surface waters (eutrophication). Cheng et al. (2007) found biochar to exhibit an anion exchange capacity (at pH 3.5) which decreased to zero as it aged in soil (over 70 years). If biochar can play a role in anion exchange capacity of soils remains an unanswered question and a research effort is required into the mechanisms to establish under what conditions (e.g. more neutral pH) anions may be retained.

As previously discussed, biochar pH is mostly neutral to basic (see Table 2.2). The liming effect has been discussed in the literature as one of the most likely mechanisms behind increases in plant productivity after biochar applications, and the meta-analysis in this report (Section 3.3) provides supporting evidence for that mechanism. Lower pH values in soils (greater acidity) often reduce the CEC and thereby the nutrient availability. In addition, for many of the tropical soils studied, reduced aluminium toxicity by reducing the acidity is proposed as the most likely chemical mechanism behind plant productivity increases.

For the experimental studies used in the meta-analysis on plant productivity (see Section 3.3.1) the average pre-amendment soil pH was 5.3 and post-amendment 6.2, although for poultry litter biochar on acidic soils the change was as large as from pH 4.8 to 7.8. Therefore, a scientific consensus on a short term liming effect of biochar applied to soil is apparent. This implies that biochars with greater liming capacity can provide greater benefit to arable soils that require liming, by being applied more frequently at lower application rates. Thereby reducing, or potentially cutting, a conventional liming operation, and hence providing a clear cost saving.

3.2 Soil Processes

3.2.1 Environmental behaviour, mobility and fate

An effective evaluation of biochar stability in the environment is paramount, particularly when considering its feasibility as a carbon sequestration tool. A sound understanding of the contribution that biochar can make to improve soil processes and functioning relies on knowing the extent and implications of the changes biochar undergoes in soil over time. Such knowledge remains, however, sparse and most experimental evidence has been gathered for other forms of black carbon. Energy-dispersive X-ray spectrometry looks promising as a tool for providing evidence of such changes in soil (Glaser et al., 2000; Brodowski et al., 2005a).

Current evaluations of the age of black carbon particles from both wildfires and anthropogenic activity indicate great stability of (at least) a significant component of biochar, ranging from several millennia to hundreds of years (e.g. Skjemstad et al., 2001; Lehmann et al., 2009). Such stability has been employed as a tool for evaluating, dating and modelling of ancient cropping

and management practices (Scott et al., 2000; Ferrio et al., 2006). Yet, establishing the mean residence time of biochars in natural systems remains a challenge, partly due to their inherent heterogeneity, and partly due to different interactions with both the biotic (e.g. microbial communities, flora) and abiotic (e.g. clays, humic substances) components of soil (Brodowski et al., 2005a, 2006).

Analysis of biochar-enriched agricultural soil using X-ray spectrometry and scanning electron microscopy showed that biochar particles in soil occur either as discrete particles or as particles embedded and bound to minerals (mainly clay and silt; Brodowski et al., 2005). This corroborates earlier studies reporting that most biochar in Amazonian Terra Preta was found in the light ($<0.2 \text{ g cm}^{-3}$) fraction of soil (Gu et al., 1995), which Hammes and Schmidt (2009) refer to as “intrinsically refractory”, while a minor amount occurred adsorbed to the surface of mineral particles (Gu et al., 1995). It is also likely that a significant portion of biochar occurs in aggregate-occluded organic matter in soil (see Section 3.2.5.3).

Biochar is no longer considered inert, although mechanisms involved in biochar degradation in soil not being fully understood (Hammes and Schmidt, 2009). It has been demonstrated that exposure to strong chemical oxidants (e.g. Skjemstad et al., 1996), including ozone (Kawamoto et al., 2005), and to high temperatures (Morterra et al., 1984; Cheng et al., 2006) can cause oxidation in charcoal over short periods of time. In natural environments, photochemical and microbial breakdown appear to be the primary degradation mechanisms (Goldberg, 1985), which can result in alteration of the charcoal’s surface chemistry and functional properties (e.g. CEC, nutrient retention; Glaser et al., 2002). Such mechanisms have been assessed by a relatively small number of short-term experiments involving biochar-enriched soils in the presence and absence of added substrates (e.g. Hamer et al., 2004; Cheng et al., 2006). Incubation studies appear to indicate that biological decomposition is very slow (see Section 3.2.5.1) and might be of minor relevance compared to abiotic degradation (see Section 3.2.5.1), particularly when fresh biochars are concerned (Cheng et al., 2006).

Surfaces of fresh biochars are generally hydrophobic and have relatively low surface charges (Lehmann et al., 2005). However, over time, biochar oxidation in the soil environment due to aging, may reflect in accumulation of carboxylic functionalities at the surfaces of biochar particles (Brodowski et al., 2005), promoting, perhaps, further interactions between biochar and other soil components (Cheng et al., 2006), including organic and mineral matter (Brodowski et al., 2005), as well as contaminants (Smernik et al., 2006). It is reasonable to hypothesize that solubilisation, leaching and translocation of biochar within the soil profile and into water systems is also expected to be gradually enhanced for longer exposure periods in soil (Cheng et al., 2006). Whether the relative importance of microbial decomposition increases over time (as biochar particle size decreases) remains largely unknown and attempts to determine actual mineralisation rates are still scarce.

Although biochar characteristics (e.g. particle and pore size distribution, surface chemistry, relative proportion of readily available components), as well as physical and chemical stabilisation mechanisms may contribute to the

long mean residence times of biochar in soil, the relative contribution of each factor to short- and long-term biochar loss has been poorly assessed, particularly when influenced by environmental conditions. Biochar characteristics are largely determined by the feedstock and pyrolysis conditions, as previously discussed. For instance, particle size is likely to influence the rate of both abiotic and biotic degradation in soil, as demonstrated for biochar particles $>50\ \mu\text{m}$ in a Kenyan Oxisol (Nguyen et al., 2008 in Lehmann et al., 2009). Therefore, processes which favour biochar fragmentation into smaller particles (e.g. freeze-thaw cycles, rain and wind erosion, bioturbation) may not only enhance its degradation rate, but also render it more susceptible to transport (reviewed by Hammes and Schmidt, 2009).

Processes which may influence biochar fate in soil might be the same as those for other natural organic matter (NOM), although little experimental evidence on this is still available. If that is the case, a lower clay content and an increase in soil temperature and water availability will probably enhance biochar degradation and loss, as previously suggested by Sohi et al. (2009). For example, mean annual temperature of the site that biochar is applied to has shown to be a contributing factor in accelerating biochar oxidation in soil (Cheng et al., 2008). One could hypothesize that the same might apply to tillage (Sohi et al., 2009) through altering soil aggregate distribution. Interestingly, Brodowski et al. (2006) did not find evidence that different management practices have an effect on BC contents in Haplic Luvisol topsoil (0-30 cm; $13.4\pm 0.2\ \text{g kg}^{-1}$ organic C) from continuous wheat and maize plots. Adjacent grassland (0-10 cm; $10.3\ \text{g kg}^{-1}$ organic C; since 1961) and spruce forest (0-7 cm; $41.0\ \text{g kg}^{-1}$ OC; since ca. 1920) topsoil were also sampled (Brodowski et al., 2006).

Sohi et al. (2009) and Collison et al. (2009) proposed that feedstock material (including its degree of aromaticity) and cropping patterns (which influences nutrient composition in the rhizosphere) are contributing factors in determining biochar degradation rates in soil. These authors provided the following example: Pyrolysis of wood-based feedstocks generate coarser and more resistant biochars explained by the rigid xylemic structure of the parent material, whereas biochars produced from crop residues (e.g. rye, maize) and manures are generally finer and nutrient-rich, therefore more readily degradable by microbial communities (Collison et al., 2009).

Cheng et al. (2008) have recently assessed the effects of climatic factors (mainly temperature) on biochar oxidation in natural systems. The cation exchange capacity of biochar was correlated to the mean temperature and the extent of biochar oxidation was related to its external surface area, being seven times higher on the external surfaces than in its interior (Cheng et al., 2008). In addition, X-ray photoelectron spectroscopy (Cheng et al., 2006) and later, near-edge X-ray absorption fine structure spectroscopy (Lehmann et al., 2005) have shown that abiotic oxidation occurs mainly in the porous interior of biochar, while biotic oxidation is the predominant process on external surfaces. This probably means that biotic oxidation may become more relevant as particle size decrease as a consequence of biochar weathering, although there are doubts on the relative importance of such a process (Cheng et al., 2006). Nevertheless, the influence of increasingly warmer

climates on biochar degradation rates in natural systems has not been resolved yet.

Translocation of biochar within the soil profile and into water systems may also be a relevant process contributing to explain biochar loss in soil (Hockaday et al., 2006). Such a translocation via aeolian (e.g. Penner et al., 1993) and mostly fluvial (e.g. Mannino and Harvey, 2004) long-range transport has been previously proposed for other forms of BC, in order to explain its occurrence in deep-sea sediments (Masiello and Druffel, 1998), as well as in natural riverine (Kim et al., 2004) and estuarine (Mannino and Harvey, 2004) water.

Soil erosion (in a global context) might result in greater amounts of BC being redistributed onto neighbouring hill slopes and valley beds (Chaplot et al., 2005), or enriching marine and river sediments through long-range transport, as recently suggested by Rumpel et al. (2006a;b) for tropical sloping land under slash and burn agriculture. Partially, this can be explained by the light nature (low mass) of biochar (Rumpel et al., 2006a;b), and may be particularly relevant for finer biochars or those with higher dust contents. Similarly, this might apply predominantly to soils and sites which are more prone to erosion (Hammes and Schmidt, 2009).

Up to now, biochar loss and mobility through the soil profile and into the water resources, has been scarcely quantified and translocation mechanisms are poorly understood. This is further complicated by the limited amount of long-term studies and the lack of standardized methods for simulating biochar aging and for long-term environmental monitoring (Sohi et al., 2009). Sound knowledge at this level will not only enable for a more robust estimate of global BC budget to be put forward (through an improved understanding of the role of BC as a global environmental carbon sink) but also attenuate uncertainties in relation to current estimates of BC environmental fluxes.

The finest biochar dust fraction, comprising condensed aromatic carbon in the form of fullerene-like structures (Harris, 1997), is thought to be the most recalcitrant portion of the BC continuum in natural systems (Buzea et al., 2006). Interactions between this ultrafine fraction and soil organic and mineral surfaces has been suggested to contribute to biochar's inherent recalcitrance (Lehmann et al., 2009), although quantifying its relative importance by experimental evidence, may render difficult. Free sub-micron BC particles are primarily transported to the oceans, where the majority is deposited on coastal shelves, while smaller amounts continue on to deep-ocean sediments (Masiello and Druffel, 1998; Mannino and Harvey, 2004) with expected residence times of thousands of years (Masiello and Druffel, 1998). The remaining fraction remains suspended in the atmosphere in the form of aerosols (Preston and Schmidt, 2006) and can be transported over long distances, eventually reaching the water courses and sediments (Buzea et al., 2006).

3.2.2 Sorption of Hydrophobic Organic Compounds (HOCs)

The sorption of anthropogenic hydrophobic organic compounds (HOC) (e.g. PAHs, polychlorinated biphenyl - PCBs, pesticides and herbicides) in soils and sediments, is generally described based on two coexisting and

simultaneous processes: absorption into natural (amorphous) organic matter (NOM) and adsorption onto occurring charcoal materials (Cornelissen et al., 2005; Koelmans et al., 2006). Comparatively to that of NOM, charcoals (including soot) generally hold up to 10-1000 times higher sorption affinities towards such compounds (Chiou and Kile, 1998; Bucheli and Gustafsson, 2000, 2003). It has been estimated that BC can account for as much as 80-90% of total uptake of trace HOC in soils and sediments (Cornelissen et al., 2005), and that it applies to a much broader range of chemical species than previously thought (Bucheli and Gustafsson, 2003; Cornelissen et al., 2004).

Biochar application is, therefore, expected to improve the overall sorption capacity of soils (Chiou 1998), and consequently, influence toxicity, transport and fate of trace contaminants, which may be already present or are to be added to soils. Enhanced sorption capacity of a silt loam for diuron (Yang and Sheng, 2003) and other anionic (Hiller et al., 2007) and cationic (Sheng et al., 2005) herbicides has previously been reported following the incorporation of biochar ash from crop (wheat and rice) residues. The relative importance of these latter studies is justified by the fact that charring of crop residues is a widespread agricultural practice (Hiller et al., 2007). Nevertheless, while the feasibility for reducing mobility of trace contaminants in soil might be beneficial (see Section 4.3), it might also result in their localised accumulation, with potentially detrimental effects on local flora and fauna if at some point in time the sorbed compounds become available to organisms. Experimental evidence is required to verify this.

Despite that little is still known on the micro-scale processes controlling sorption to biochar (Sander and Pignatello, 2005) in soils and sediments, it has been suggested that it is mechanistically different from the traditional sorption models for NOM, and that it is also a less reversible process (Gustafsson et al., 1997; Chiou and Kile, 1998; Jonker et al., 2005). While absorption to NOM has little or no concentration dependence, adsorption to biochars has been shown to be strongly concentration dependent (e.g. Gustafsson et al., 1997; Sander and Pignatello, 2005; Pastor-Villegas et al., 2006; Wang et al., 2006; Chen et al., 2007), with affinity decreasing for increasing solute concentrations (Cornelissen et al., 2004; Wang et al., 2006). Several equations have been employed to describe such a behaviour, including that of Freundlich (e.g. Cornelissen et al., 2004) and Langmuir (e.g. van Noort et al., 2004), although more recent equations based on pore-filling models have shown better fits (e.g. Kleineidam et al., 2002).

Previous studies have convincingly demonstrated that adsorption to charcoals is mainly influenced by the structural and chemical properties of the contaminant (i.e. molecular weight, hydrophobicity, planarity) (Cornelissen et al., 2004, 2005; Zhu and Pignatello, 2005; Zhu et al., 2005; Wang et al., 2006), as well as pore size distribution, surface area and functionality of the charcoal (e.g. Wang et al., 2006; Chen et al., 2007). For example, sorption of tri- and tetra-substituted-benzenes (such as trichlorobenzene, trinitrotoluene and tetramethylbenzene) to maple wood charcoal (400°C) was sterically restricted, when comparing to that of the lower size benzene and toluene (Zhu and Pignatello, 2005). Among most classes of common organic compounds, biochar has been shown to adsorb PAHs particularly strongly, with desorption having been regarded as 'very slow' (rate constants for desorption in water of

10^{-7} - 10^{-1} h^{-1} , and even lower in sediments) (Jonker et al., 2005). This can be explained both by the planarity of the PAH molecule, allowing unrestricted access to small pores (Bucheli and Gustafsson, 2003; van Noort et al., 2004), and the strong π - π interactions between biochar's surface and the aromatic molecule (e.g. Sander and Pignatello, 2005).). In fact, experimental evidence has recently demonstrated that organic structures in the form of BC (including biochar) or NOM, which are equipped with strong aromatic π -donor and -acceptor components, are capable of strongly adsorbing to other aromatic moieties through specific sorptive forces other than hydrophobic interactions (Keiluweit and Kleber, 2009).

Although a large body of evidence is available on the way the characteristics of HOC influence sorption to biochars, the contribution of the char's properties to that process has been far less evaluated. It is generally accepted that mechanisms leading to an increase in surface area and/or hydrophobicity of the char, reflected in an enhanced sorption affinity and capacity towards trace contaminants, as demonstrated for other forms of BC (Jonker and Koelmans, 2002; Noort et al., 2004; Tsui and Roy, 2008). The influence of pyrolysis temperatures mostly in the 340-400°C range (James et al., 2005; Zhu et al., 2005; Tsui and Roy, 2008) and feedstock type (Pastor-Villegas et al., 2006) on such a phenomena has been recently evaluated for various wood chars by a number of authors. Interestingly, sorption to high-temperature chars appear to be exclusively by surface adsorption, while that to low-temperature chars derive from both surface adsorption and (at a smaller scale) absorption to residual organic matter (Chun et al., 2004).

The influence of micropore distribution on sorption to biochars has been clearly demonstrated by Wang et al. (2006). Diminished O functionality on the edges of biochar's graphene sheets due to heat treatment (e.g. further charring), resulted in enhanced hydrophobicity and affinity for both polar and apolar compounds, by reducing competitive adsorption by water molecules (Zhu et al., 2005; Wang et al., 2006). The treated char also revealed a consistent increase in micropore volume and pore surface area, resulting in better accessibility of solute molecules and an increase in sorption sites (Wang et al., 2006).

Once released in the environment, the original adsorption properties of biochar may be affected by 'aging' due to environmental factors, such as the impact of coexisting substances. The presence of organic compounds with higher hydrophobicity and/or molecular sizes have shown reduce adsorption of lower molecular weight compounds to biochars (e.g. Sander and Pignatello, 2005; Wang et al., 2006). In the same way, some metallic ions (e.g. Cu^{2+} , Ag^+) present at environmental relevant concentrations (50 mg L^{-1}) may significantly alter surface chemistry and/or pore network structure of the char through complexation (Chen et al., 2007).

Perhaps a more important mechanism to consider, is the influence of dissolved NOM, including the humic, fulvic (Pignatello et al., 2006) and lipid (Salloum et al., 2002) fractions, on the physical-chemical properties and adsorption affinity and capacity of biochars (Kwon and Pignatello, 2005). Similar evidence has long been reported for activated carbon (Kilduff and Wigton, 1999). "Aging" of maple wood charcoal (400°C) particles in a

suspension of Amherst peat soil (18.9% OC)-water has demonstrated that NOM reduced affinity of the char for benzene (Kwon and Pignatello, 2005), corroborating other research (Cornelissen and Gustafsson, 2005; Pignatello et al., 2006). Similar observation over a period of 100 years has been reported for pyrene in forest soil enriched with charcoal (Hockaday, 2006). In both cases, such a behaviour was explained by mechanisms of pore blockage (Kwon and Pignatello, 2005; Pignatello et al., 2006), and by the capacity of NOM to compete with (e.g. Cornelissen and Gustafsson, 2005) and displace the organic compound from the sorption sites (Hockaday, 2006). A wider range of soil characteristics remain to be tested.

Frequently, contaminated soils contain a mix of organic solvents, PAHs, heavy metals and pesticides, adding to the naturally occurring mineral and organic matter (Chen et al., 2007). Nevertheless, most studies on organic sorption to charred materials have relied on single-solute experiments, whereas those using multiple solutes hold more practical relevance (Sander and Pignatello, 2006). Competitive sorption can be a significant environmental process in enhancing the mobility as well as leaching potential of HOC in biochar-enriched soil.

Most of the evidence of increased sorption to HOC by biochar incorporation into soil is indirect (i.e., bulk and biochar or soot sorption is determined separately and biochar's contribution is then proved comparatively to a treatment without biochar) and earlier attempts for its direct assessment overestimated it (Cornelissen and Gustafsson, 2004). Yet, the potential of biochar amendment of soils for enhancing soil sorption capacity and, therefore mitigating the toxicity and transport of relevant environmental contaminants in soils and sediments appears undeniable. One can suggest that such an enhancement of soil sorption capacity may result in long mean residence times and accumulation of organic contaminants with potentially hazardous health and environmental consequences. At this stage, very little is known about the short- and long-term distribution, mobility and bioavailability of such contaminants in biochar-enriched soils.

It is worth underlining that although such a strong adsorptive behaviour appears to imply a reduced environmental risk of some chemical species (e.g. PAHs), very little data is, in fact, currently available which confirms this. The underlying sorption mechanism, including the way it is influenced by a wide range of factors inherent to the contaminant, to the char material and to the environment, remains far from being fully understood (Fernandes and Brooks, 2003), and thus it is identified in this report as a priority for research. In this context, it is vital to comprehensively assess the environmental risk associated to these species in biochar-enriched soils, while re-evaluating both the use of generic OC-water distribution coefficients (Jonker et al., 2005) and of remediation endpoints (Cornelissen et al., 2005). For instance, remediation endpoints (undetectable, non-toxic or environmentally acceptable concentrations, as set by regulatory agencies) for common environmental contaminants in biochar-enriched soils would need to be assessed based on dissolved (bioavailable) concentrations rather than on total concentrations (Pointing, 2001; Cornelissen et al., 2005). In order to achieve that, prior careful experimental evaluation of the contaminant distribution, mobility and availability in the presence of biochar is paramount.

3.2.3 Nutrient retention/availability/leaching

Reduction of nutrient leaching from agriculture is an objective in line with the Water Framework Directive (WFD). The WFD promotes an integrated management approach to improve the water quality of European water bodies. Application of fertilisers has led to increased concentrations of nitrates and phosphates in European surface and ground waters. Specific water quality targets have been set by the Water Framework Directive with respect to nitrates, which are very susceptible to leaching (European Parliament and the Council of the European Union, 2000). Improved agricultural management practices are increasingly stimulated by the Common Agricultural Policy (cf. CAP Health Check).

Evidence from several laboratory and field studies suggests that the application of biochar may lead to decreased nutrient leaching (studies particularly focussed on nitrates) and contaminant transport below the root zone. Several mechanisms contribute to the decrease in nutrient leaching which are related to increased nutrient use efficiency by increased water and nutrient retention (residence time in the root zone) and availability, related to an increased internal reactive surface area of the soil-biochar matrix, decreased water percolation below the root zone related to increased plant water use (increased evaporative surface), and increased plant nutrient use through enhanced crop growth. Higher retention times also permit a better decomposition of organic material and promote the breakdown of agrichemicals. Nevertheless, mechanisms such as colloid-facilitated transport of contaminants by biochar particles, or preferential flow induced by biochar applications, and long term stability of biochar in soil, are potential factors that may increase the leaching of nutrients and/or contaminants.

The magnitude and dynamics resulting from biochar application are time, space and process specific. The myriad of interactions within the soil-plant-atmosphere, and the range of potential feedstock specific effects of biochar on these interactions, makes it inherently difficult to formulate generic qualities of "biochar". It also has to be kept in mind that other factors, such as rainfall patterns and agricultural management practices, will be more strongly determining the loss of nutrients from the root zone.

The mobility of the water percolating beyond the root zone depends on the infiltration capacity, hydraulic conductivity and water retention of the root zone, the amount of crop transpiration dependent on the density and capability of the root network to extract water, and the prevalent meteorological conditions at the site. These factors are largely dependent on the proportion and connections between micro, meso and macro pores.

The partitioning of groundwater recharge, surface-water runoff and evapotranspiration is affected by changes in the soil's water retention capacity. In those situations where biochar application improves retention (of plant available water) and increases plant transpiration (Lehmann et al., 2003), percolation below the root zone can be reduced, leading to the retention of mobile nutrients susceptible to leaching such as nitrates, or base cations at low pH.

Biochar directly contributes to nutrient adsorption through charge or covalent interactions on a high surface area. Major et al. (2002) showed that biochar

must be produced at temperatures above 500°C or be activated to results in increased surface area of the biochar and thus increased direct sorption of nutrients. Glaser et al. (2002) conclude that 'charcoal may contribute to an increase in ion retention of soil and to a decrease in leaching of dissolved OM and organic nutrients' as they found higher nutrient retention and nutrient availability after charcoal additions to tropical soil. A possible contributing mechanism to increased N retention in soils amended with biochar is the stimulation of microbial immobilisation of N and increased nitrates recycling due to higher availability of carbon (see Section 3.2.3). Biological N fixation by common beans was reported to increase with biochar additions of 50 g kg⁻¹ soil (Rondon et al., 2007), although soil N uptake decreased by 50%, whereas the C:N ratios increased with a factor of two.

Lehmann et al. (2003) reported on lysimeter experiments which indicated that the ratio of uptake to leaching for all nutrients increases with charcoal application to the soil. However they also concluded that it could not clearly be demonstrated which role charcoal played in the increased retention, although, in these experiments, water percolation was not decreased. Therefore, nutrients must have been retained on electrostatic adsorption complexes created by the charcoal. Similarly, Steiner et al. (2004) attributed decreased leaching rates of applied mineral fertiliser N in soils amended with charcoal to increased nutrient use efficiency. Nevertheless, the interaction between mineral fertiliser and biochar seems critical. Lehmann et al. (2003) found that while cumulative leaching of mineral N, K, Ca and Mg in an Amazonian Dark Earth was lower compared to a Ferralsol in unfertilised experiments, leaching from the ADE exceed that from the Ferralsol in fertiliser experiments.

If biochar applications lead to improved soil aggregation, this may lead to an increase in the soil's water infiltration capacity. Using measured properties such as saturated hydraulic conductivity and total porosity in a modelling assessment of the impact of charcoal production, Ayodele et al. (2009) showed that infiltration was enhanced and runoff volume reduced. The increase in infiltration may be accompanied by improved water retention in the root zone in coarse soils. On the other hand, however, since a large percentage of the pores in biochar are very small (<2 x 10⁻³ µm, following Tseng and Tseng, 2006), it may also reduce the mobility of water through the soil. If the increased infiltration is not off-set by increased retention and transpiration, due to factors related to the native soil, and/or if crop nutrient uptake is not increased, the net results may be an increased percolation below the root zone, especially of soluble and mobile nutrients such as nitrates.

Fine biochar particles resulting from transportation, application, and further weathering in the field, may facilitate the colloidal transport of nutrients and contaminants (Major et al., 2002).

Hydrophobicity (see Section 3.2.2) induced by biochar is thought to be most significant in the first years after application since 'fresh' biochar contains a large fraction of hydrophobic groups. The implications of biochar hydrophobicity on runoff and unwanted export of nutrients from the field has not been investigated in detail. Another potential concern in certain soils is preferential flow induced by the incorporation of biochar in the soil matrix, it

has been suggested that biochar can alter percolation patterns, residence times of soil solution, and affect flow paths (Major et al., 2002).

3.2.4 Contamination

Given that the widespread interest in biochar applications to soils continues to rise, so does the concern regarding the potential for soil contamination associated to some of its components. It is crucial to ensure that soil functions and processes as well as water quality are not put at risk as a consequence of biochar application to soils, which would carry severe health, environmental and socio-economic implications (Collison et al., 2009). Mineral contaminants like salts that are often present in some biochars and may be detrimental to soil functioning rather than to human and animal health, and have been discussed previously. This section is dedicated to contaminants such as heavy metals, PAHs and dioxins, which remain major issues of concern with regard to potential for soil contamination and health hazards, and yet have surprisingly received very little attention.

The occurrence of these compounds in biochar may derive either from contaminated feedstocks or from pyrolysis conditions which favour their production. For example, slow pyrolysis at temperatures below 500°C is known to favour the accumulation of readily available micronutrients (e.g. Sulphur) in biochar (Hossain et al., 2007). However, heavy metals, PAHs and other species with disinfectant and antibiotic properties (e.g. formaldehydes, creosols, xylenols, acroleyn) may also accumulate under such operating conditions (Painter, 2001). Full and careful risk assessment for such contaminants is urgently required, in order to relate contaminant toxicity to biochar type, safe application rates and operating pyrolysis conditions.

Organic wastes (e.g. biosolids, sewage sludge, tannery wastes) are known to generally contain high levels of light and heavy metals, which remain in the final biochar product following pyrolysis (Hospido et al., 2005; Chan and Xu, 2009). Bridle and Pritchard (2004) reported high concentrations of Copper (Cu), zinc (Zn), chromium (Cr) and nickel (Ni) in biochar produced from sewage sludge. Muralidhar (1982) has long found that Cr, which accounts for up to 2% (total dry weight) of tannery wastes, is commonly found in biochar produced from this material. On the other hand, relatively low concentrations of aluminium (Al), Cr, Ni and molybdenum (Mo) have been recently detected in poultry litter, peanut hull and pine chip biochars produced between 400-500°C, while poultry litter biochar generally contained the highest levels of these metals (Gaskin et al., 2008). In contrast, Zn, Cu, Al and Fe were lower in the poultry litter biochar compared to that in pine chip and peanut hulls biochars, which pattern seem to be reverse to that observed in the feedstock materials. Although one could suggest pyrolysis as means of reducing metal availability in some feedstocks (such as poultry litter), and be encouraged to use biochar (instead of poultry litter) for mitigating some of the concerns relating to soil contamination, there is no clear evidence to confirm this (Gaskin et al., 2008).

Metal concentration in the biomass feedstock often determines biochar's safe application rate (McHenry, 2009). Preliminary data seems to suggest that, at current ordinary biochar application rates, there is little environmental risk by metal species within biochar, which McHenry (2009) describes as similar to

that associated to the use of conventional fertilisers. In fact, for contaminants such as Zn, mercury (Hg), arsenic (As), lead (Pb) and Ni, it is likely that significant risk can only be expected from exceedingly high biochar application rates ($>250 \text{ t ha}^{-1}$) (McHenry, 2009). A wider range of biochars and soil types remains to be tested, which would undoubtedly shed more light onto the potential for soil and water contamination by metals.

Secondary chemical reactions during thermal degradation of organic material at temperatures exceeding 700°C , is generally associated to the generation of heavily condensed and highly carcinogenic and mutagenic PAHs (Ledesma et al., 2002; Garcia-Perez, 2008). Nevertheless, little evidence exists that PAHs can also be formed within the temperature range of pyrolysis ($350\text{-}600^\circ\text{C}$), although these appear to carry lower toxicological and environmental implications (Garcia-Perez, 2008). Nevertheless, their potential occurrence in the soil and water environments via biochar may constitute a serious public health issue. Evidence seems to show that biomass feedstock and operation conditions are influencing factors determining the amount and type of PAHs generated (Pakdel and Roy, 1991), and therefore, there is great need to assess the mechanisms, as well as identify specific operational and feedstock conditions, which lead to their formation and retention in the final biochar product.

Very little data is available on the occurrence of PAHs in pyrolysis products, compared to that from combustion or incineration. Among such studies, Fernandes and Brooks (2003), Brown et al. (2006) and Jones (2008) do stand out. Pea straw and eucalyptus wood charcoal produced at 450°C for 1 h, exhibited low PAHs concentrations ($<0.2 \mu\text{g g}^{-1}$), although their levels in straw ($0.12 \mu\text{g g}^{-1}$) were slightly higher than that from the denser feedstock material ($0.07 \mu\text{g g}^{-1}$) (Fernandes et al., 2003). Similarly, Brown et al. (2006) reported that PAHs concentrations in several chars produced at temperatures exceeding 500°C , ranged between $3\text{-}16 \mu\text{g g}^{-1}$ (depending on peak treatment temperature), compared to that ($28 \mu\text{g g}^{-1}$) in char from prescribed burn in pine forest. The range of producing conditions and feedstock materials employed in the latter studies was narrow. In contrast, Jones (2008) studied twelve biochar products from a variety of biomass sources and producers, with evidence that PAHs levels in biochar were often comparable or even lower than those found in some rural urban and urban soils. This finding corroborates previous studies (reviewed by Wilcke, 2000), in which topsoil concentration ranges of several PAHs were found to increase in the order of arable < grassland < forest < urban. For example, at the lower end (arable soil), concentration ranges for naphthalene, fluorene, phenanthrene, anthracene and pyrene were up to 0.02, 0.05, 0.067, 0.134 $\mu\text{g g}^{-1}$ (respectively). At the top end of the concentration range (urban soil), levels of those compounds (respectively) were up to 0.269, 0.55, 2.809, 1.40 and 11.90 $\mu\text{g g}^{-1}$ (reviewed by Wilcke, 2000). It is important to note, however, that the latter data refers to initial concentrations in soil, not taking into account interactions with organic and mineral fractions, and most importantly, not providing information on the bio-available fraction.

Recently, however, the mild (supercritical fluid) extraction of pyrogenic PAHs from charcoal, coal and different types of soot, including coal soot, showed promising results (Jonker et al., 2005). To the best of our knowledge, this

study was pioneer in reporting desorption kinetics of pyrogenic PAHs from their 'natural' carrier under conditions which mimic those in natural environments. Such "soot and charcoal-associated PAHs" were found to be strongly sorbed to their carrier matrix (e.g. charcoal, soot) by means of physical entrapment within the matrix nanopores (so called "occlusion sites") in charcoal and sequestration within the particulate matter. Consequently, it is anticipated "very slow desorption" (rate constants of up to 10^{-7} to 10^{-6} h⁻¹) of these compounds from the carrier in natural environments, which can range from several decades to several millennia (Jonker et al., 2005). PAHs sorption to charcoals has been reviewed extensively in Section 3.2.2 of this report, including the mechanisms leading to increases in their accessibility, such as interactions with NOM and coexisting chemical species.

To the best of our knowledge, there are no toxicological reports involving PAHs incorporated in soil due to biochar application, nor have biochar application rates have been defined in terms of PAHs accumulation and bioavailability, both in soil and water systems. Further research is paramount on the behaviour of such contaminants in biochar-enriched natural systems. In this context, a re-evaluation of risk assessment procedures for these compounds needs to be put in place, which takes into account the influence of NOM on their desorption from biochar, transport and bioavailability.

Dioxins and furans are planar chlorinated aromatic compounds, which are predominantly formed at temperatures exceeding 1000°C (Garcia-Perez, 2008). Although data exists confirming their presence in products from combustion reactions, such as incineration of landfill and municipal solid wastes (as cited by Garcia-Perez, 2008), no reports were found on their content in biochar derived from traditional biomass feedstocks. In contrast, char from automobile shredder residues was shown to contain up to 0.542 mg kg⁻¹ of dioxins, while their generation and accumulation in the char was dependent on the operational conditions (Joung et al., 2007). Scarce experimental evidence on dioxin levels in pyrolysis products (biochar in particular) in the range of temperatures between 350-600°C, is largely limiting towards our knowledge on potential dioxin contamination of soil via biochar. More research on this matter is urgently needed. It appears that pyrolysis of strongly oxygenated feedstocks under low temperatures (400 and 600°C) do not favour the generation of dioxins and dioxin-related compounds. Based on the current knowledge, it is likely that such a risk is low for the aforementioned biochar production factors, particularly when using low-chlorine and low-metal containing feedstocks (Garcia-Perez, 2008).

At this stage, extrapolating a link between the presence of contaminants on biochar and a detrimental effect on human and animal health, particularly in regard to bioaccumulation and bioamplification in the food chain, can only be hypothesised. One can suggest that potential uptake and toxicity of such contaminants is perhaps more prominent in the case of microbial communities, sediment-dwelling organisms and filter feeders. In note of the application of biochar into soil being an irreversible process, Blackwell et al. (2009) emphasised the need for full case-by-case characterisation and risk assessment of each biochar product previous to its application to soil, accounting not only for heterogeneity among biochars, but also for soil type and environmental conditions. There are no current standards for biochar or

processing conditions which can provide sound basis for biochar quality regulations with regard to the presence of contaminants, thus ensuring soil and water protection. Also lacking is a clearly defined set of conditions under which biochar and related materials can be applied to soil without licensing (Sohi et al., 2009).

As Collison et al. (2009) noted, the natural occurrence of BC in soils is widespread and detrimental effects on environmental quality are generally not apparent. However, it is the perspective of an extensive and indiscriminate incorporation of biochars into soils, derived from some feedstock materials under specific operation conditions, without previous full risk assessment, which constitutes the main issue of concern. This is particularly the case for small-scale and on-farm pyrolysis units using local biomass resources (e.g. forestry and agricultural wastes), which may not hold the necessary technological and economic infrastructures to tackle this matter. Also, it is likely that these small landholders in rural areas might prefer using low-temperature pyrolysis, thereby reducing operation costs. Farmers should be made aware that sub-optimal pyrolysis operating conditions and certain feedstocks may not only reduce the benefits associated to biochar application, but also enhance the risk of land and water contamination.

3.2.5 Soil Organic Matter (SOM) Dynamics

SOM stabilisation mechanisms for temperate soils have been researched comprehensively and reviewed recently (Von Lützow et al, 2006; 2008 2008; Kögel-Knabner et al., 2008; Marschner et al., 2008).

Primary recalcitrance refers to the recalcitrance of the original plant matter, while secondary recalcitrance refers to that of its charred product, i.e. pyrogenic BC. For biochars from feedstocks that have already undergone selective preservation, i.e. any process leading to the relative accumulation of recalcitrant molecules, it may be appropriate to consider tertiary recalcitrance. Stability of SOM is the result of recalcitrance, organo-mineral interactions, and accessibility. Because biochar is OM but also has many properties functionally similar to mineral matter, it is necessary to consider the stability of biochar in soils as well as the stability of native SOM, or OM that is added with, or after, the biochar.

3.2.5.1 Recalcitrance of biochar in soils

Studies of charcoal produced by wildfires have shown that abiotic processes generally have more impact on the decomposition of charcoal than biotic processes, in the short term (Cheng et al 2006; Bruun and Luxhøi. 2008). However, abiotic oxidation can only occur on the surface and as such once the surface of biochar has been oxidised biotic process are thought to become more important. The fact that the soil microbiota is capable of oxidising graphitic carbon, which is thermodynamically stable and recalcitrant carbon, was first demonstrated by Shneour (1966). This author found that a 'substantially higher' oxidation rate, being at least a 3-fold increase, was found in non-sterile soils than in sterilised soils.

More work regarding recalcitrance has been conducted on BC, specifically pyrogenic BC, rather than on biochar *per se*. Nevertheless, owing to its relatively similar physical and chemical composition BC is an acceptable

analogue and it is likely that the recalcitrance of biochars will function according to similar mechanisms.

As graphite has been shown to be oxidised by microbial activity, albeit very slowly (Shneour 1966), a degree of decomposition of biochars can be expected. Contradictory experimental results exist, with both rapid (Bird et al. 1999) and slow (Shindo 1991) decomposition of biomass-derived BC being reported. This difference is likely to be an artefact of the different microbial communities to which the BC was exposed. Although precise details regarding the turnover of BC in soils remain unknown, and due to the complexity of its interaction within the soil system and its biota exact details are unlikely to be found, BC has been found to be the oldest fraction of C in soil, being older than the most protected C in soil aggregates and organo-mineral complexes (Pessenda et al., 2001), which are commonly the most stable forms of C in soil. This demonstrates that even without knowing the precise details of turnover of BC in soil, it at least has highly stable components with “decomposition leading to subtle, and possibly important, changes in the bio-chemical form of the material rather than to significant mass loss” (Lehmann et al 2006).

It has been noted that the recalcitrance of BC in soils cannot be characterised by a single number (Hedges et al., 2000; Von Lützow et al., 2006). This is because pyrogenic BC is an amalgamation of heterogeneous compounds and, as such, different fractions of it will decompose at different rates under different conditions (Hedges et al., 2000). According to Preston & Schmidt (2006) the more recalcitrant compounds in pyrogenic BC, created by wildfire and therefore of a woody feedstock, can be expected to have a half life in the region of thousands of years (possibly between 5 and 7 thousand years) in cold and wet environments. However, some fractions of pyrogenic BC which may have undergone less thermal alteration (being more analogous to biochars which have also undergone less thermal alteration due to low heat pyrolysis, a half life in the region of hundreds of years as opposed to thousands may be expected (Bird et al., 1999). This agrees with work reported by Brunn et al. (2008) who found that the rate of microbial mineralisation of charcoal decreases with increasing mineralisation temperature (see also Section 1.6).

Besides physical and chemical stabilization mechanisms, another important factor that may affect the residence time of biochar in soils is the phenomenon of co-metabolism. This is where biochar decomposition is increased due to microbial metabolism of other substrates, which is often increased when SOM is ‘unlocked’ from the soil structure due to disturbance (e.g. incorporating biochar into the soil via tillage).

3.2.5.2 Organomineral interactions

The interactions between SOM and soil minerals have received considerable attention in the literature. Von Lützow et al. (2006) concluded that some evidence exists for interactions between biochar and soil minerals, leading to accumulation in soil, but that the mechanisms responsible are still unknown. One potential mechanism is the oxidation of the functional groups at the surface of the charcoal, which favours interactions with soil organic and

mineral fractions (Lehmann et al., 2005; Glaser et al., 2002). Section 3.2.1 explores further the interaction between biochar and other soil components.

3.2.5.3 Accessibility

Biochar can both increase and decrease the accessibility of SOM to microorganisms and enzymes. Brodowski et al. (2006) provided evidence that a significant portion of BC occurs in the aggregate-occluded OM in soil. Interestingly, the largest BC concentrations occurred in microaggregates (<250 µm) and it has been suggested that it may be actively involved in the formation and stabilisation of microaggregates, comparatively to other forms of organic matter (Brodowski et al., 2006). At the present, one can only speculate on such a role of biochar in soil. Most importantly, organo-mineral interactions may be relevant in determining the environmental behaviour and fate of biochar (Hammes and Schmidt, 2009; Section 3.2.1) and can contribute to physically protecting it from degradation, while promoting its long mean-residence times in soil (Glaser et al., 2002; Lehmann et al., 2005; Brodowski et al., 2006).

3.2.5.4 Priming effect

The priming effect has been defined as being “the acceleration of soil C decomposition by fresh C input to soil” (Fontaine et al., 2004) and are generally considered to be short-term changes in the turnover of SOM (Kuzyakov et al., 2000). The priming effect is thought to be a function of changes in microbial community composition upon fresh C input into soil (e.g. cellulose, Fontaine et al., 2004). This means that addition of a ‘new’ source of carbon into the soil system can potentially lead to a priming effect whereby SOC is reduced. Several mechanisms may be involved: changes in pH, changes in water-filled pore space, changes in habitat structure, or changes in nutrient availability.

Following cellulose addition, Fontaine et al. (2004) found that decomposition rate of soil humus stock in savannah soil increased by 55%. Kuzyakov et al. (2009) demonstrated that BC in soil underwent increased decomposition upon the addition of glucose to soil. They concluded that while soil microorganisms were not dependant on BC as an energy source, the extracellular enzymes produced by the microbial community for the decomposition of the glucose (and its metabolites) also decomposed the BC, albeit at a vastly decreased rate when compared to the added glucose. They estimated the mean decomposition time of black carbon to be in the range of 0.5% per year and concluded that the mean residence time of black carbon in soil is likely to be in the range of about 2000 years. This provides some further evidence of priming effects occurring with regard to mineralisation of C in soils, in this case BC, upon addition of a substance, in this case glucose. As to whether the addition of biochar to soil can lead to a priming effect leading to accelerated mineralisation of SOM is still a matter of debate.

This then leads to the question as to whether biochar addition to soils can cause a priming effect. Kuzyakov et al. (2000) stated that the most important mechanisms concerning priming effects are due to increased activity or quantity of the microbial biomass. Biochar has been shown to increase both of these factors (Section 3.2.6.1), and as such there is the clear potential for

biochar to cause a priming effect on SOM. There is a paucity of data on the possible priming effect of biochar on SOM, but some initial data is available. Steinbeiss (2009) found that the addition of homogeneous biochars, made from glucose and yeast to produce N-free biochar and biochar with a N content of ~5%, respectively. When these biochars were mixed with arable soils and forest soils in controlled microcosm experiments a clear priming effect could be observed with between 8% and 12% of carbon from the SOC pool being lost in 4 months after addition of either type of biochar to either type of soil. The addition of nitrogen containing biochar to forest soil had the largest effect (13% loss) with addition of the nitrogen free biochar to arable soil having the smallest effect (8%). That said, it is important to note that the controls of both the arable soil and the forest soil which had no biochar addition but were subject to the same disturbance (sieved to 2 mm and mixed) also showed a loss of carbon from the SOC pool of 4% and 6% respectively. This demonstrates that disturbance to the soil which is sufficient to break up soil aggregates and expose previously protected soil organic matter to microbial decomposition and mineralisation itself has a strong priming effect on SOC.

Biochars made from these specific feedstocks are unlikely to be used in reality particularly as they were almost certainly lacking in micronutrients such as P and K which would be introduced into the soil with most biochar types. Also, they were produced by hydrothermal pyrolysis, which is not the most commonly used or posited method of pyrolysis. This, combined with large amount of variance seen within each treatment group means that the results must be extrapolated with caution. However, it appears to be preliminary evidence that biochars can instigate, or at least increase the priming effect and accelerate the decomposition of SOC. There is some evidence that the availability of N in a soil is the main factor affecting the priming effect, with more available N leading to a reduced priming effect (Neff et al., 2002; Fontaine, 2007). This suggests that the priming effect could perhaps be reduced or eliminated though the co-addition of N fertiliser along with biochar.

If biochar components are highly recalcitrant in soil, as evidence suggests, and its addition, in some scenarios at least, speeds up the decomposition, and thereby depletion of SOC, soil fertility and the ecosystem services which it provides may be negatively affected. It is conceivable that, through biochar addition to soil, it may be possible to increase the level of C in soils beyond what is found in most given soils on average at the moment. However, if this is C in the form of a highly recalcitrant substance that does not take part in the cycling of C in the soil (i.e. biochar) and not the highly chemically complex and dynamic substance (i.e. humus) and other SOM fractionations, then ecosystem functioning of soils may well be compromised. This is because it is well recognised that it is not the presence of C within the soil which is important for functioning, but rather it is the decomposition of SOC which drives the soil biota and leads to the provision of ecosystem services. This was recognised even before Russell (1926) who stated that SOM must be decomposed before it has 'served its proper purpose in the soil'. This is clearly an area that warrents further research.

3.2.5.5 Residue Removal

One of the often proposed methods of obtaining biomass for use as a feedstock to make biochar is the removal of crop residues for pyrolysis. The removal of residues, and the possible associated impacts has already been discussed extensively from the point of view of biofuels (Wilhelm et al., 2004; Lal, 2007; Blanco-Canqui and Lal, 2008; Lal, 2009). Removal of crop residues is associated with increased risk of soil loss by both water and wind erosion with associated off-site effects, depletion of SOM, degradation of soil quality leading to decrease in agronomic productivity and a reduction in crop yields per unit input of fertiliser and water, thereby compromising the sustainability of agriculture (Lal, 2007).

Removal of crop residues for biochar production, therefore, has the potential to have multiple negative effects on the soil, which may only be partially outweighed, if at all, by the positive effects of biochar addition. While it is possible that the inclusion of biochar into the soil system may aid the reduction of atmospheric CO₂, it is also feasible that more CO₂ will be required to be produced as a by-product of processes undertaken to remediate the damage done by crop residue removal, such as increased production of fertiliser which may need to be undertaken to keep yields stable.

Furthermore, as discussed above, the soil biota relies on the breakdown of SOM to provide energy for it to perform the multitude ecosystem services which it provides. It is the SOM *dynamics* that helps drive the system, not just the presence of SOM. If the potential new inputs of SOM, being crop residues in many agricultural situations, are removed, and converted into a substantially more recalcitrant form which does not function as an energy source for the edaphic microflora and fauna, then ecosystem services may well be compromised and reduced.

3.2.6 Soil Biology

The soil biota is vital to the functioning of soils and provides many essential ecosystem services. Understanding the interactions between biochar, when it is used as a soil amendment, and the soil biota is therefore vital. It is largely through interactions with the soil biota, such as promoting arbuscular mycorrhizal fungi (AMF) as well as influences on water holding capacity, which leads to the reported effects of biochar on yields (see Section 3.3).

Soil is a highly complex and dynamic habitat for organisms, containing many different niches due to its incredibly high levels of heterogeneity at all scales. On the microscale, soil is often an aquatic habitat, as micropores in soil are full of water at all times, apart from very extreme drought, due to the high water tension which exists there. This is vital for the survival of many microbial species which require the presence of water for mobility as well as to function. Indeed, many soil organisms, specifically nematodes and microorganisms such as protozoa enter a state of cryptobiosis, whereby they enter a protective cyst form and all metabolism stops in the absence of water. When biochar application leads to an increased water retention of soils (see Section 3.1.2), it seems likely, therefore, that this will have a positive effect on soil organism activity, which may well lead to concurrent increases in soil functioning and the ecosystem services which it provides.

Organisms in the soil form complex communities and food webs and engage in many different techniques for survival and to avoid becoming prey, ranging from hiding in safe refuges, through to conducting forms of chemical 'warfare'. Biochar, due to its highly porous nature, has been shown to provide increased levels of refugia where smaller organisms can live in small spaces which larger organisms cannot enter to prey on them. Microorganisms within these micropores are likely to be restricted in growth rate due to relying on diffusion to bring necessary nutrients and gases, but as this occurs in micropores within the soil, this demonstrates that microorganisms utilising these refugia almost certainly would not be reliant of decomposition of the biochar for an energy source. This is likely to be one of the mechanisms for the demonstrated increases in microbial biomass (Steiner et al., 2008; Kolb et al., 2009), and combined with the increased water holding potentials of soil is a possible mechanisms for the increased observed basal microbial activity (Steiner et al., 2008; Kolb et al., 2009). However, due to the complexities of the soil system and its biota, it is probable that many more mechanisms are at work. For example Kolb et al. (2009) demonstrated that while charcoal additions affected microbial biomass and microbial activity, as well as nutrient availability, differences in the magnitude of the microbial response was dependent on the differences in base nutrient availability in the soils studied. However, they noted that the influences of biochar on the soil microbiota acted in a relatively similar way in the soils they studied, albeit at different levels of magnitude, and so suggested that there is considerable predictability in the response of the soil biota to biochar application.

As with all interactions between the soil biota and biochar, there is a scarcity of data regarding the interaction of biochar with fungi. However, considering the diverse saprophytic abilities of fungi it is probable that the interaction between fungi and biochar is most likely to affect the stability and longevity of biochar within the soil. While there is evidence of long residence times of biochar in soils from Terra Pretas, biochar from different sources and exposed to different fungal communities may well have differing levels of recalcitrance and hence residence times in soils. This is therefore a highly pertinent area for further research.

There is some evidence that the positive effects of biochar on plant production may be attributable to increased mycorrhizal associations (Nisho and Okano, 1991). The majority of studies concerning biochar effects on mycorrhiza show that there is a strong positive effect on mycorrhizal abundance associated with biochar in soil (Harvey et al., 1976; Ishii and Kadoya, 1994; Vaario et al., 1999). The possible mechanisms were hypothesised by Warnock et al. (2007) to include (in decreasing order of currently available experimental evidence)

- a) alteration of soil physico-chemical properties
- b) indirect effects on mycorrhizae through effects on other soil microbes
- c) plant–fungus signalling interference and detoxification of allelochemicals on biochar
- d) provision of refugia from fungal grazers

Biochar, immediately after pyrolysis, can have a wide range of compounds on its surface. These can include ones that are easily metabolised by microbes, such as sugars and aldehydes which are turned over quickly, but may also include compounds which have bactericidal and fungicidal properties such as formaldehyde and cresols (Painter, 2001). However, residence times of these substrates has been shown to be in the range of one to two seasons and, therefore, long term effects of these chemicals on the soil biota are unlikely (Zackrisson et al., 1996).

The structure of biochar provides a refuge for small beneficial soil organisms, such as symbiotic mycorrhizal fungi which can penetrate deeply into the pore space of biochar and extraradical fungal hyphae (fungal hyphae which are found outside of roots) which sporulate in the micropores of biochar where there is lower competition from saprophytes (Saito and Marumoto, 2002). Nishio (1996) stated that "the idea that the application of charcoal stimulates indigenous arbuscular mycorrhiza fungi in soil and thus promotes plant growth is relatively well-known in Japan, although the actual application of charcoal is limited due to its high cost". The specifics of the cost-benefit relationship of biochar application to soil and its associated effects on yield have not yet been covered in depth by the scientific community and is subject of discussion in Section 5.4.

The relationship between mycorrhizal fungi and biochar may be important in realising the potential of charcoal to improve fertility. Nishio (1996) also reported that charcoal was found to be ineffective at stimulating alfalfa growth when added to sterilised soil, but that alfalfa growth was increased by a factor of approximately 1.8 when unsterilised soil containing native mycorrhizal fungi was also added. This demonstrates that it is the interaction between the biochar and the soil biota which leads to positive effects on yield, and not just the biochar itself (See Section 3.3).

3.2.6.1 Soil microbiota

It has long been assumed that soil biodiversity and SOM are positively correlated although experimental evidence for this is scarce. Even if this assumption is proven to be true, it is unclear as to what role biochar will play in this interaction. This is because, for the majority of the soil biota at least, biochar appears to function more as the mineral constituent of the soil, than the OM *per se*. Nevertheless, there is experimental evidence that microbial communities are directly affected by the addition of biochar to soils (Ogawa, 1994; Rondon et al., 2007; Warnock et al., 2007; Steiner et al., 2008).

Due to the fact that experiments involving the addition of biochar to soils are relatively new, with only relatively few experiments being more than a decade old, quantifying the long term effects of biochar addition to soil is problematic. While not perfect analogies to the addition of biochar to temperate soils, investigation of Terra Preta soils in the Amazon Basin does have the potential to lead to insights regarding the long term effects of biochar addition to soil.

O'Neill et al. (2009) performed 16s rRNA analysis on Terra Pretas and their surrounding soils. Although their experiment was limited by the fact that they isolated microorganisms through culturing techniques, they did find numerous differences between Terra Pretas and their surrounding soils. Firstly, higher

numbers of culturable bacteria, by over two orders of magnitude were found in the Terra Pretas consisting of five possible new bacterial families. They also reported greater diversity being isolated from the Terra Preta soils. This increase in culturable bacterial populations and a greater culturable diversity were found in all of the Anthrosols, to a depth of up to 1 m, when compared to adjacent soils located within 50-500 m of terra preta. Although using culturing of the microorganisms as a form of isolation is undoubtedly a weakness in this experiment design owing to the fact that the vast majority of soil microorganisms are not culturable in the laboratory (Torsvik et al., 1990; Ritz, 2007), soil extract media was used which when compared to standard culture media revealed an increased diversity in the soil microbial populations of the Terra Pretas

As well as affecting the inherent recalcitrance of biochar, the pyrolysis temperature range also affects how the biochar will interact with the soil community. This is particularly true of woody charcoal which, at lower pyrolysis temperatures retains an interior layer of bio-oil which is equal to glucose in its effect on microbial growth (Steiner, 2004). When pyrolysed at higher temperatures, this internal layer of bio-oil is lost and so it is likely that the biochar will have less impact with regard to promoting soil fertility when compared to biochar which does have the internal layer of bio-oil.

When added to soil, biochar has been shown to cause a significant increase in microbial efficiency as a measure of units of CO₂ released per microbial biomass carbon in the soil as well as a significant increase in basal respiration (Steiner et al., 2008). Steiner et al. (2008) also found that the addition of organic fertiliser amendments along with biochar lead to further increases in microbial biomass, efficiency in terms of CO₂ release per unit microbial carbon, as well as population growth and concluded that biochar can function as valuable component of the soil system, especially in fertilised agricultural systems.

As well as increasing basal respiration and microbial efficiency, there is experimental evidence that biochar addition to soil increases N₂ fixation by both free living and symbiotic diazotrophs (Ogawa, 1994; Rondon et al., 2007). Rondon et al. (2007) reported that the positive effects of biochar, including increased N₂ fixation, lead to a between 30 and 40% increase in bean (*Phaseolus vulgaris* L.) yield at biochar additions of upto 50 g kg⁻¹. However, they found that at an application rate of 90 g kg⁻¹ a negative effect with regard to yield occurred. It should be noted that this appears contrary to data shown in Figure 3.1 which shows a general trend for positive crop productivity effects upon biochar addition to soil. This may be due to the Rondon et al. (2007) study being excluded from the meta-analysis owing to the study not reporting the variance of within their treatments meaning that the data could not be included. This means that a possible negative weighting was not included in the meta-analysis which could have caused a slight sciew of the results. However, as n was low in the Rondon study when compared to the combined data used in the meta-analysis, the effects of this omission are likely to be minimal and this highlights the need of accurate reporting of variances in experimental data to both allow effective interpretation of the results, and to allow further analyses such as statistical meta-analyses to be undertaken. Furthermore, many more studies which are reported in the meta-

analysis showed a positive effect on crop productivity at similar or higher application rates. However, this highlights the fact that while biochar addition to soil is potentially positive with regard to crop yield, situations also exist where negative effects can occur regarding yield. There is currently no clear mechanism which may lead to positive effects on yield can become negative once a threshold has been crossed regarding the amount of biochar which is added to soil. While it is possible to hypothesise mechanisms responsible for this effect, there is, as yet, no experimental evidence to confirm or refute any hypothesis and this highlights the need for further research.

3.2.6.2 Soil meso and macrofauna

There is a current paucity of research with regard to the interaction of biochar with the soil meso and macrofauna, with the exception of earthworms.

Both the application rate of biochar and the original feedstock used have been shown to affect the soil biota. Weyers et al. (2009) reported that application rates higher than 67 t ha⁻¹ of biochar made from poultry litter had a negative impact on earthworm survival rates. They hypothesised that increased soil pH or salt levels may have been the reason for the observed reduced survival rates. They noted that earthworm activity was greater in soil amended with pine chip biochar than with poultry litter biochar and so concluded that different types of biochar can have different effects on the soil biota. This confirmed work reported by Chan et al. (2008) who found that earthworms had different preferences for different types of biochar, but noted that the underlying mechanisms driving these preferences required further work.

Recent work by Van Zwieten et al. (2009) has shown that earthworms preferred biochar-amended Ferrosols over control soils, although they found no significant difference for Calcarosols. This shows that it is not just the application rate or feedstock of the biochar which is important to consider when predicting possible effects, but the soil to which it is added must also be taken into account. This highlights the complex dynamic interactions which can vary greatly with soil type, application rate and feedstock used and shows that predicting the effects of biochar application on the soil biota of a given soil, whilst very important, is inherently very difficult.

Some work has been undertaken looking at the effects of charcoal ingestion on earthworms (Hayes, 1983). When charcoal is ingested by an earthworm, along with other soil particles, the two are mixed with mucus secreted in the oesophagus and finely ground in the muscular gizzard. When excreted, the charcoal/soil paste is stabilised by Van der Waals forces after drying and forms a dark-coloured humus (Hayes, 1983). Ponge et al. (2006) reported that in laboratory experiments the earthworm *Pontoscolex corethrurus* was found to prefer to ingest a mixture of charcoal and soil compared to either pure soil or pure charcoal. Because of this, Ponge et al (2006) concluded that *Pontoscolex corethrurus* was the organisms most responsible for the incorporation of charcoal into the topsoil in the form of silt size particles which aids the formation of stable humus in Terra Pretas.

In further laboratory experiments on the effects of charcoal on populations of earthworms, Topoliantz and Ponge (2003) found differences in the way in which different populations of the earthworm species *P. corethrurus*, taken

from either forest soil or fallow soil, were adapted to the presence of charcoal, implying that the addition of charcoal to soil is exerting a selective influence on the worms although what the specific effects of this selective pressure may eventually be is unclear. They also reported that the observed transport of charcoal within the soil demonstrated the importance of *P. corethrurus* in the incorporation of charcoal particles into the soil.

No research has yet been undertaken investigating the effects of biochar addition to soil on soil microarthropods such as collembola or acari, or on other soil dwelling organisms such as rotifers and tardigrades. Any negative effect on these organisms seems likely to only occur as a result of any contamination which exists in the biochar, if that contaminant is bioavailable (Section 3.2.4). Stimulation of the microbial community may or may not have concurrent effects on soil invertebrates depending on whether the increase in microbial biomass is exposed for predation. If the majority of the increase in microbial biomass occurs within biochar particles in the soil, then the microorganisms may not be available as a food source for soil invertebrates. However, if the stimulated growth in microbial biomass also occurs outside of biochar particles within the soil, then it is possible that an increase in the soil invertebrate community may also occur. This could have implications for nutrient cycling, crop yield and other ecosystem services which are hard to predict owing to a paucity of experimental data and the high intrinsic complexity and dynamic nature of the edaphic community.

3.2.6.3 Soil megafauna

There is no research reported in the literature on the effects of charcoal or biochar addition to soil on soil megafauna such as badgers, moles or other vertebrates. As these organisms are not generally found in the arable environment it is likely that any effects may be minimal if biochar addition is limited to agricultural land. However, should biochar addition be planned for other soils, including forest soils, then an impact assessment may well need to be carried out to investigate any possible impacts.

Off-site effects of biochar addition to arable soils are possible, and are likely to include any contaminants such as heavy metals moving up through the food chain. This is likely to be particularly true of moles that have a diet high in earthworms. As it has been shown that earthworms ingest charcoal which exists within the soil profile, it is probable that moles will in turn ingest charcoal particles when they ingest worms. It is still currently unclear what quantity of heavy metals, if any, will be able to pass from the biochar, if present, into the tissues of other organisms and this is an area which requires significant further work to ensure the safety of heavy metal containing biochars in soils (see also Section 3.2.4).

The main point of contact between biochar in the soil and other megafauna such as rabbits, badgers and foxes is likely to be through skin contact when the animals are building and resting in their burrows, sets and 'earths'. Heavy metal absorption is extremely limited through skin, with the exception of mercury which is likely to exist in biochars in extremely minute amounts, if at all. It is possible that some small amount of biochar may enter these organisms' digestive tracts and airways if it is in the form of very small particles, as well as through ingestion of earthworms in the case of some

organisms such as moles, as earthworms have been shown to ingest charcoal in soil (Topoliantz and Ponge, 2005).

Concerning possible ingestion of biochar fragments from the soil by soil megafauna there is no published data in the primary literature. However, Van et al. (2006) found that incorporation of bamboo charcoal (0.5 to 1.0 mg kg⁻¹ of body weight) into the feed of growing goats resulted in enhanced growth and no adverse effects were observed at the study concentrations. Clearly care must be taken when extrapolating data to other animals and to biochars made from alternative feedstocks and this area warrants further research.

Ingestion is not the only mode of possible uptake of biochar fragments by the soil megafauna. Biochar dust particles may possibly be inhaled by the soil megafauna. However, there is currently no research reported in the primary literature concerning the effect of charcoals on the respiratory systems of soil megafauna and as such robust predictions concerning the possible effects is currently not possible and requires further research.

3.3 Production Function

Increased yields are the most commonly reported benefits of adding biochar to soils. Nearly all experiments have been conducted in the tropics, while field trials in temperate regions have been set up only recently. Taking a step back, SOM is generally believed to be correlated positively with crop yields in modern arable agriculture, although there is still poor scientific understanding of the strength of this relationship, the influence of environmental conditions (sandy or clayey soil, wet, dry, etc.), crop types (combinable vs. root crops) and the underlying mechanisms. Loveland and Webb (2003) reviewed 1200 papers in the scientific literature on the relationship between SOC and crop yield in temperate regions and concluded that a consensus does not exist.

Diaz-Zorita et al. (1999) performed stepwise regression analysis between wheat yields and soil properties and found different relationships in different years. In a year without a water deficit, N and P influenced yield, in drought years however, yields were correlated to water availability and OM. Pan and Smith (2009) investigated the relationship between SOM and yield by using statistical data for China (1949-1998) and found a particularly strong relationship between yield stability and SOM.

Considering the poor understanding of the relationship between SOM and crop yield or plant production, it may be expected that similar challenges exist regarding the scientific understanding of the relationship between biochar and plant productivity. However, to investigate the relationship between biochar additions to soils and crop productivity in more detail, new tools can be used. Therefore, a meta-analysis on this relationship was performed (see next sections).

3.3.1 Meta-analysis methods

Objectivity of systematic reviews on biochar is paramount. In the medical sciences this has been resolved by the founding of an independent organisation (the Cochrane Collaboration) that provides regularly updated systematic reviews on specific healthcare issues using a global network of volunteers and a central database/library. The methodologies used in medical

science can be transferred to ensure objectivity when compiling literature reviews in other research areas such as those related to biochar, even though the amount of literature and information available on biochar is currently limited. One such methodology which was developed for objective analysis of a range of different medical studies testing the same (or similar) hypothesis was that of meta-analysis which is being increasingly used across a range of scientific disciplines.

Here, meta-analysis techniques (Rosenberg et al., 1997) were used to quantify the effect of biochar addition to soil on plant productivity. For each study the control mean and experimental means were recorded, or calculated where necessary. Standard deviation was used as a measure of variance and this was reported where given or calculated from the published measure of variance from each study. To maximise the number of studies used in the analysis, both pot and field experiments were recorded, providing the results were quantitative.

Standardisation of the results from the studies was undertaken through calculation of the “effect size” which allows quantitative statistical information to be pooled from and robust comparisons of effects from studies with different variables to be made. Data was square root transformed to normalise the distribution. Effect size was calculated using the transformed data taken as the natural logarithm of the response ratio by using the following equation:

$$\ln R = \ln \left(\frac{\bar{x}^E}{\bar{x}^C} \right)$$

Where \bar{x}^E = mean of experimental group; and \bar{x}^C = mean of control group

For the meta-analysis, the following nine studies concerning the effects of biochar addition to soil on crop production were used: Van Zwieten et al. (2008); Yamato (2006); Chan (2007); Chan (2008); Lehmann (2003); Ishii and Kadoya (1994); Nehls (2002); Kimetu et al. (2008) and Blackwell (2007). These studies combined produced 86 different ‘treatments’ for use in the meta-analysis.

In order to use change in pH as a grouping category, changes were grouped by ‘no change’ (0 – representing no change from soil starting pH upon addition of biochar) and in consecutive changes in pH of 0.5 for both increasing and decreasing pH values upon biochar addition. For calculation of grouped effect sizes a categorical random effects model was used. Groups with fewer than two variables were excluded from each analysis. Resampling tests were generated from 999 iterations. For each of the analyses, grouped by different categorical predictors, the data was analysed using a fixed effects model if the estimate of the pooled variance was less than or equal to zero. When plotting figures, the effect size was unlogged (exponentially transformed) and the result multiplied by 100 to obtain the percentage change in effect size upon biochar addition in each category. Analysis was undertaken using MetaWin Version 2 statistical software (Rosenberg et al., 2000). While more than the nine reported studies looking at the effect of

biochar addition to soil on crop productivity, studies were excluded from the analysis when no quantitative results or measures or variance were available, leaving the nine studies reported above.

3.3.2 Meta-analysis results

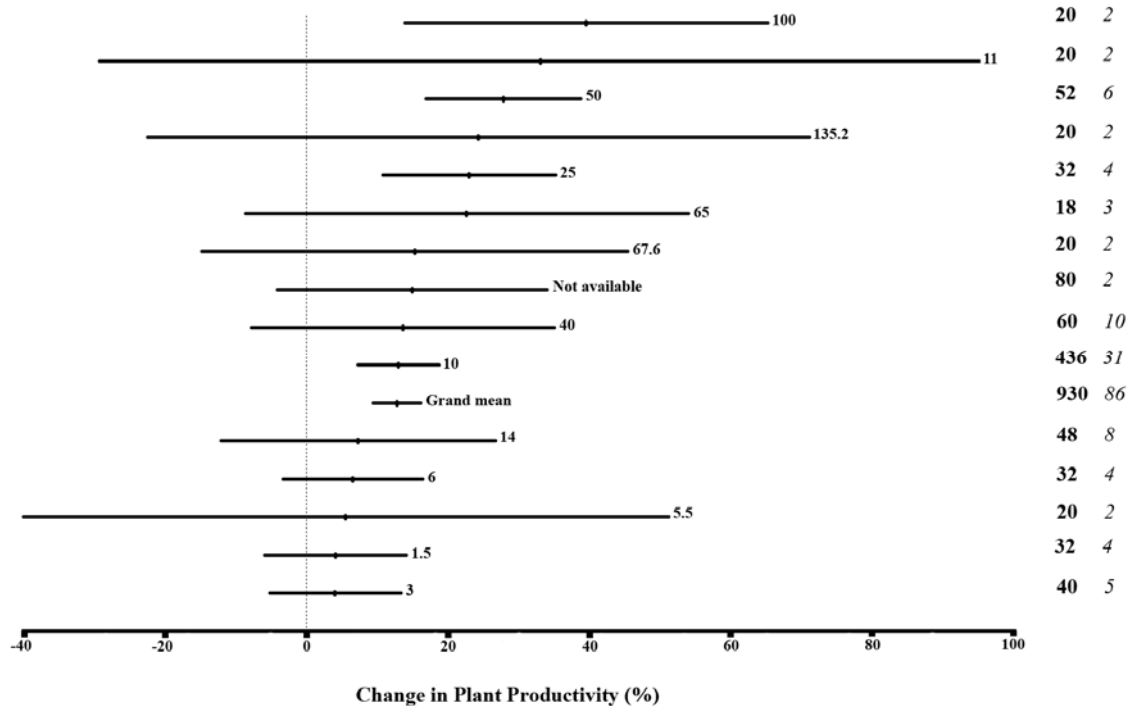


Figure 3.2 The percentage change in crop productivity upon application of biochar at different rates, from a range of feedstocks along with varying fertiliserco-amendments. Points represent mean and bars represent 95% confidence intervals. Numbers next to bars denote biochar application rates (t ha⁻¹). Numbers in the two columns on the right show number of total ‘replicates’ upon which the statistical analysis is based (**bold**) and the number of ‘experimental treatments’ which have been grouped for each analysis (*italics*)

Figure 3.2 shows the effect of biochar addition to soil on crop productivity, grouped by application rate and vertically partitioned by effect size. The sample means seem to indicate a small but positive effect on crop productivity with a grand mean (being the mean of all effect sizes combined) of about 10%. There appears to be a general trend, when looking at the sample means, for increased biochar application rate to be correlated with increased crop productivity (Figure 3.2). However, there was no statistically significant difference (at $P = 0.05$) between any of the application rates as is evident from the overlapping error bars which represent the 95% confidence intervals. Application rates of 10, 25, 50 and 100 t ha⁻¹ were all found to significantly increase crop productivity when compared to controls which received no biochar addition. However, other application rates which fall within the range of these statistically significant application rates, such as 40 and 65 t ha⁻¹ showed no statistically significant effect of biochar addition to soil on crop yield, demonstrating that while biochar addition to soil may increase crop productivity it is not linearly correlated.

It can be seen from Figure 3.2 that even with the same application rate of biochar, a large variation in effect size occurs. This is particularly true of the

lower application rates of 5.5 and 11 t ha⁻¹ and also for the large application rate of 135.2 t ha⁻¹. Other application rates also have a large variance in their effect size, but to a lesser extent. The reason for this large variation is likely to be due to the different biochar feedstocks used, the different crops assessed and differences in soil type to which the biochar was added. It is interesting to note that while there was often large variation in the data for a given application rate, the means for each application rate all fall on the positive productivity effect side, and no single biochar application rate was found to have a statistically significant negative effect on the crops from the range of soils, feedstocks and application rates studied. It should be noted that while no negative effects have been detected by this meta-analysis with regard to the effect of application rate on crop productivity, the studies used in the meta-analysis do not cover a wide range of latitudes and the data used was heavily skewed towards (sub)tropical conditions. This means that while this analysis provides good evidence of the generally positive effects of biochar addition to soil on crop productivity, care needs to be taken when extrapolating these results to European latitudes, crops and soil types.

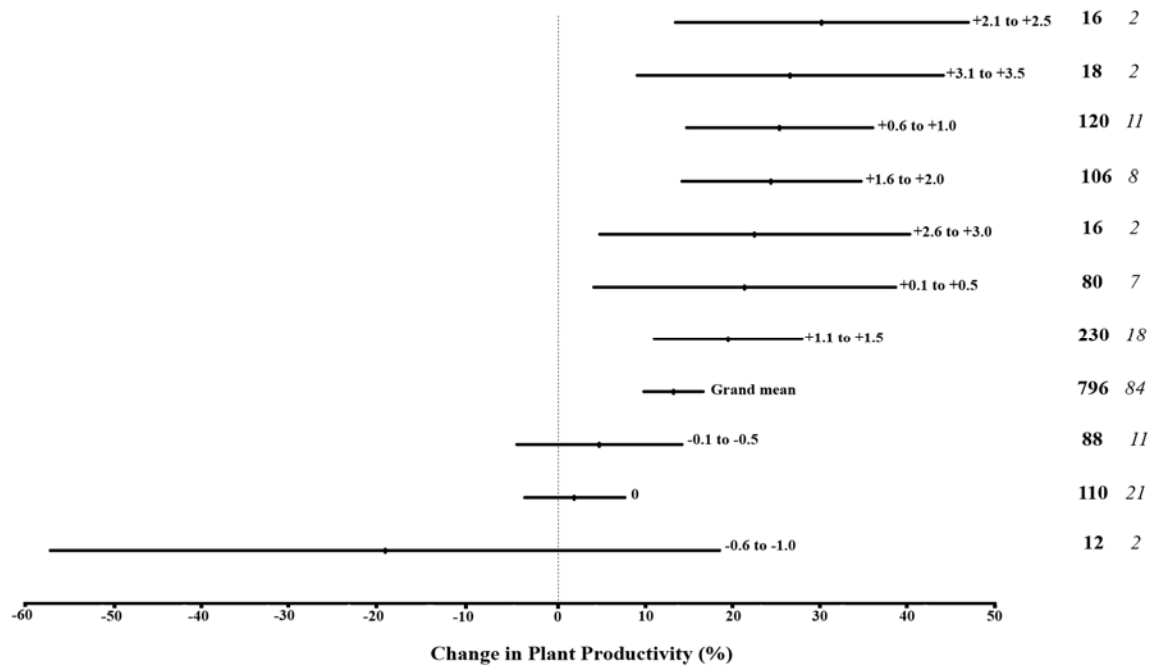


Figure 3.3 Percentage change in crop productivity upon application of biochar at different rates along with varying fertiliserco-amendments grouped by change in pH caused by biochar addition to soil. Points represent mean and bars represent 95% confidence intervals. Values next to bars denote change in pH value. Numbers in the two columns on the right show number of total ‘replicates’ upon which the statistical analysis is based (**bold**) and the number of ‘experimental treatments’ which have been grouped for each analysis (*italics*)

Figure 3.3 shows the effect of biochar addition to soil on crop productivity, grouped by liming effect. It should be noted that where the biochar addition to soil lead to a liming effect (i.e. the pH of the soil was increased), there was a significant increase in crop productivity compared to controls, although there were no significant differences between treatments which lead to a positive liming effect.

Regarding those treatments that showed no change, or a reduction in pH upon biochar addition to soil, biochar addition to soil showed no statistically significant effect. All other groupings where biochar addition to soil led to an increase in soil pH, a concurrent increase in crop productivity was seen. This effect was not strictly linear, with the mean increase in crop productivity where biochar caused a liming effect (with an increase in pH units ranging from 1.1-1.5), was lower when compared to those treatments where the liming effect resulted in an increase ranging from 0.6 to 1.0 pH units. This may be due to differences in initial pH, before biochar addition to soil, meaning that a lesser increase was still sufficient to pass a tipping point with regard to metal ion availability for example, meaning a slightly increased crop productivity effect even with a decreased liming effect.

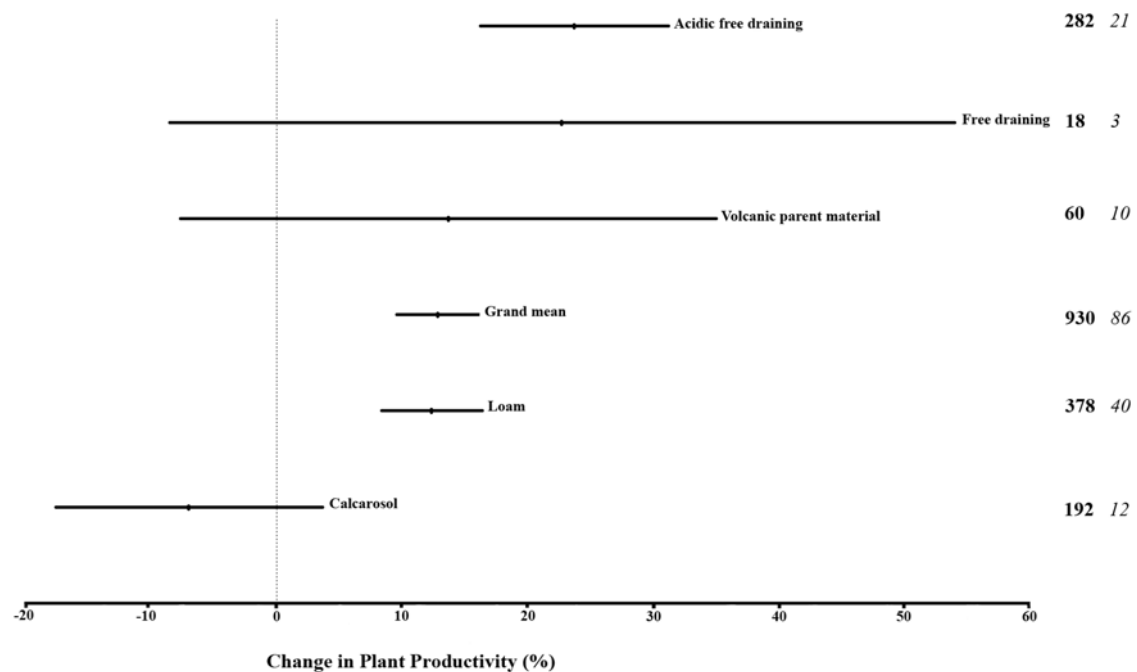


Figure 3.4 The percentage change in crop productivity upon application of biochar at different rates along with varying fertiliserco-amendments to a range of different soils. Points shows mean and bars so 95% confidence intervals. Numbers in the two columns on the right show number of total ‘replicates’ upon which the statistical analysis is based (**bold**) and the number of ‘experimental treatments’ which have been grouped for each analysis (*italics*)

Figure 3.4 shows the effect of biochar addition to soil on crop productivity, grouped by soil type. As with the previous meta-analysis figures, the error bars are again very large. Again, there were found to be no statistically significant negative effects of biochar to soil on crop productivity when grouped by soil type. The trend of the effect in Calcarosols was towards the negative, but this effect was not statistically significant when compared to control soils, although it was significantly less than the positive effects seen upon biochar addition to both loam soils and acidic free draining soils. The effect of biochar addition to these soils (‘loam’ and ‘acidic free draining’) was also found to show a statistically significant increase when compared to control soils with no biochar addition. For the other soil types investigated by this analysis (‘volcanic parent material’ and ‘free draining’), there was a general trend towards a positive effect as evidenced by the means being on

the positive effect side of 0. However, the effect for these soils was not found to be statistically significant owing to the large variation from the samples.

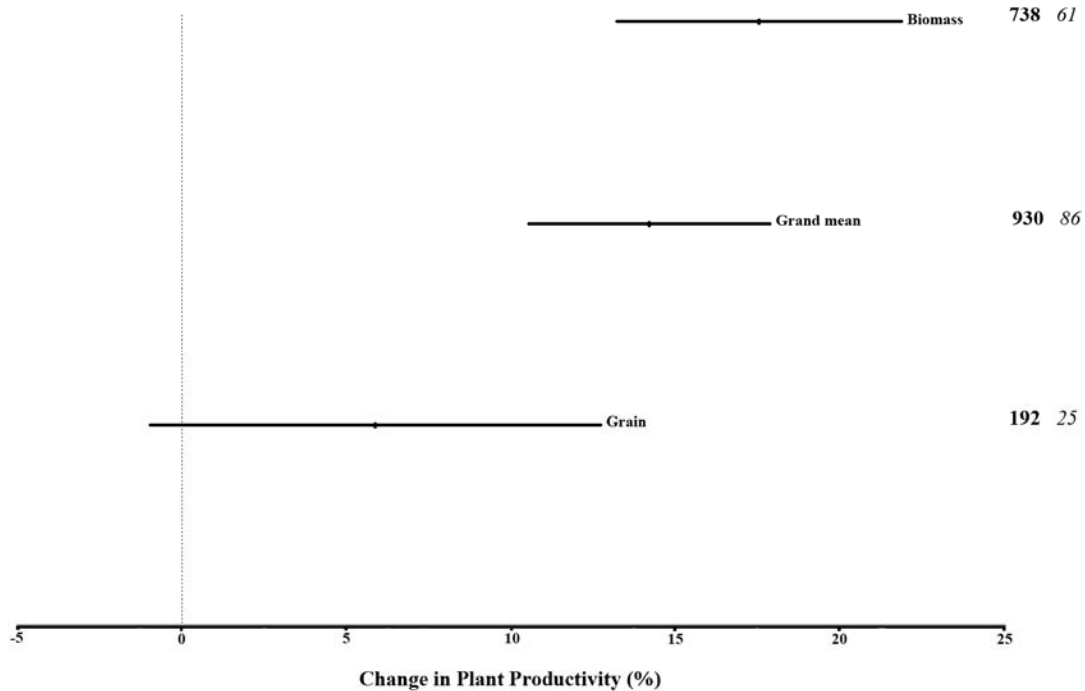


Figure 3.5 The percentage change in crop productivity of either the biomass or the grain upon application of biochar at different rates along with varying fertiliserco-amendments. Points shows mean and bars so 95% confidence intervals. Numbers in the two columns on the right show number of total ‘replicates’ upon which the statistical analysis is based (**bold**) and the number of ‘experimental treatments’ which have been grouped for each analysis (*italics*)

Figure 3.5 shows the effect of biochar addition to soil on crop productivity, grouped by overall biomass productivity vs. grain yield. There was no significant difference in grain yield for those crops grown in biochar amended soils compared to non-biochar amended soils. There was a significant increase in overall crop biomass production in biochar amended soils compared to non-biochar amended soils, although this difference was not significant when compared to the impact of growth on biochar amended soils on grain production.

The fact that biomass was positively affected by growth on biochar amended soils whereas grain was not is possibly due to grain being a relatively small part of the biomass and so any slight change would be more difficult to detect. Again, the error bars show that there was considerable variation within treatments, as would be expected due to the data being amalgamated from several different studies, and each treatment in the above figure includes data obtained from different crops, soils and biochar feedstocks.

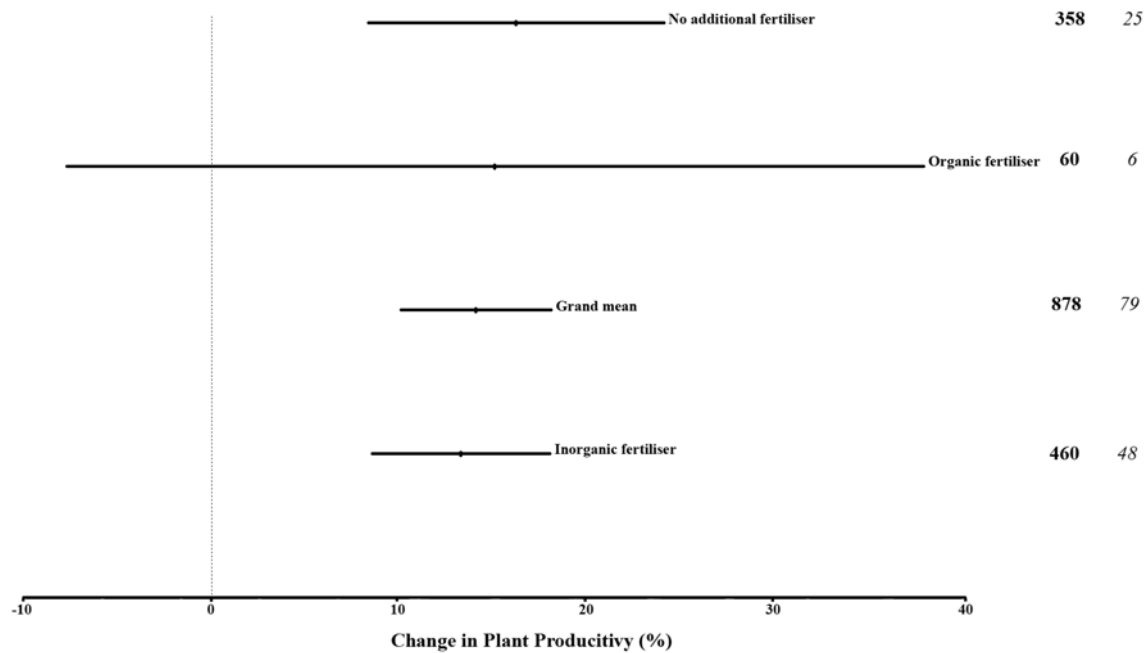


Figure 3.6 The percentage change in crop productivity upon application of biochar along with a co-amendment of organic fertiliser(o), inorganic fertiliser(I) or no fertiliser(none). Points shows mean and bars so 95% confidence intervals. Numbers in the two columns on the right show number of total ‘replicates’ upon which the statistical analysis is based (**bold**) and the number of ‘experimental treatments’ which have been grouped for each analysis (*italics*)

There was no statistically significant difference between biochar application to soil whether no concurrent fertiliser addition was used, or whether organic or inorganic fertiliser was used (Figure 3.6). This is contrary to what is often reported in the literature where specific recommendations often state that fertiliser addition is necessary to maximise crop yields.

Care must be taken when interpreting Figure 3.6, as it appears at first glance to show no difference in effect size between addition of biochar alone, or with fertiliser. It is important to remember that the effect sizes are between ‘controls without biochar’ vs ‘treatments with biochar’. This means that the no fertiliser application treatment shows the effect of biochar addition to soil alone. In the other treatments, the control includes the addition of fertiliser, but without the addition of biochar, compared to the experimental treatments which include both fertiliser and biochar. Figure 3.6 shows, therefore, that the impact of biochar addition to soil was not significantly different whether fertiliser, either organic or inorganic was used. This does not show, as appears at first glance, that there was no significant effect of co-addition of fertiliser with biochar, over addition of biochar to soil alone.

While there was found to be no significant difference between the effects of inorganic fertiliser with biochar compared to no fertiliser with biochar, both of these treatments showed increased crop productivity when compared to control non-biochar amended soils. Chan et al. (2007) reported a lack of response upon addition of biochar without the co-addition of N and as such it seems likely that in those studies available N in the soil was not a limiting factor, possibly due to previous cropping with legumes, or owing to the quantity and quality of SOM meaning that available N levels were not limiting.

The addition of organic fertiliser along with biochar to soils was found to have no statistically significant effect when compared to application of organic fertiliser to non-biochar amended soils. This is due to extreme levels of variance in results of the biochar plus organic fertiliser treatments, as shown by the large error bars.

3.3.3 *Meta-analysis recommendations*

As was shown in this report, soils are very heterogeneous systems, in both time and space and at a multitude of scales, and biochar is a very heterogeneous material. Meta-analysis is a valuable tool for amalgamating, summarising and reviewing studies on biochar. It can elucidate trends in a quantitative way that in conventional reviews might be perceived as being biased by personal judgement. A combination of meta-analysis with a qualitative review of the literature will provide the most comprehensive discussion of both the status of scientific knowledge on a specific 'effect' and the possible underlying mechanisms and exceptional or marginal conditions. As new studies are published, the meta-analyses on the effect of biochar application to soil on productivity can be updated (and refined) periodically. In addition, many other effects of biochar (see Chapter 3) can be analysed by meta-analyses once a large enough body of research has been established.

From this work it is strongly recommended that scientists publishing results on effects of biochar describe the data, and the variance of those data, consistently and completely. This means including the Z or F statistic for regression data and clear measures of variance for comparative analysis data, such as standard deviations or standard errors for each treatment, including the control, rather than an LSD (least significant difference) which has been pooled for several treatments. In all cases, it should be absolutely clear what the sample number is for every treatment (including control). Clearly this should be normal scientific conduct, but unfortunately does not seem to occur in all cases. To enable meta-analyses on effects of a factor that is not the dependent variable of a study, it is also recommended to include all sample numbers, standard deviations or standard errors of other parameters measured in the study, e.g. CEC, pH, bulk density, microbial activity, etc. Finally, it is recommended to report all the data in tabular format, possibly as an annex.

3.3.4 *Other components of crop production function*

Crop production is, however, only one possible agronomic effect of on-farm benefit from biochar. Many other effects still need to be investigated, for example i) direct impacts on yields (seed rate); ii) crop-related impacts (crop establishment, fertiliser, disease and weeds); and iii) non-crop-related impacts (workability, soil hydrology, soil degradation).

3.4 Summary

This section has highlighted the relative paucity of knowledge concerning the specific mechanisms behind the reported interactions of biochar within the soil environment. However, while there is still much that is unknown, large steps have been taken towards increasing our understanding of the effects of biochar on soil properties and processes. Biochar interacts with the soil

system on a number of levels. Sub-molecular interactions with clay and silt particles and SOM occur through Van der Waals forces and hydrophobic interactions. It is the interactions at this scale which will determine the influence of biochar on soil water repellency and also the interactions with cations and anions and other organic compounds in soil. These interactions are very char specific, with the exact properties being influenced by both the feedstock and the pyrolysis conditions used.

There has been some evidence to suggest that biochar addition to soil may lead to loss of SOM via a priming effect in the short term. However, there is only very little research reported in the literature on this subject, and as such it is a highly pertinent area for further research. The fact that Terra Pretas contain SOM as well as char fragments seems to demonstrate that the priming effect either does not exist in all situations or if it does, perhaps it only lasts a few seasons and it appear not to be sufficient to drive the loss of all native SOM from the soil. Biochar has the potential to be highly persistent in the soil environment, as evidenced both by its presence in Terra Pretas, even after millennia, and also as evidenced by studies discussed in this section. While biochars are highly heterogeneous across scales, it seems likely that properties such as recalcitrance and effects on water holding capacity are likely to persist across a range of biochar types. It also seems probable, that while difference may occur within biochars on a microscale, biochars produced from the same feedstocks, under the same pyrolysis conditions are likely to be broadly similar, with predictable effects upon application to soil. What remains to be done are controlled experiments with different biochars added to a range of soils under different environmental conditions and the precise properties and effects identified. This may lead towards biochars possibly being engineered for specific soils and climate where specific effects are required.

After its initial application to soil, biochar can function to stimulate the edaphic microflora and fauna due to various substrates, such as sugars, which can be present on the biochar's surface. Once these are metabolised, biochar functions more as a mineral component of the soil rather than an organic component, as evidenced by its high levels of recalcitrance meaning that it is not used as a carbon source for respiration. Rather, the biochar functions as a highly porous network the edaphic biota can colonise. Due to the large inherent porosity, biochar particles in soil can provide refugia for microorganisms whereby they may often be protected from grazing by other soil organisms which may be too large to enter the pores. This is likely to be one of the main mechanisms by which biochar-amended soils are able to harbour a larger microbial biomass when compared to non-biochar amended soils. Biochar incorporation into soil is also expected to enhance overall sorption capacity of soils towards trace anthropogenic organic contaminants (e.g. PAHs, pesticides, herbicides), in a stronger way, and mechanistically different, from that of native organic matter. Whereas this behaviour may greatly contribute to mitigating toxicity and transport of common pollutants in soil, biochar aging over time may result in leaching and increased bioavailability of such compounds. On the other hand, while the feasibility for reducing mobility of trace contaminants in soil might be beneficial, it might

also result in their localised accumulation, although the extent and implications of this have not been experimentally assessed.

Soil quality may not be necessarily improved by adding biochar to soil. Soil quality can be considered to be relatively high for supporting plant production and provision of ecosystem services if it contains carbon in the form of complex and dynamic substances such as humus and SOM. If crop residues are used for biochar, the proportion of carbon going into the dynamic SOM pool is likely to be reduced, with the carbon being returned to the soil in a relatively passive biochar form. The proportion of residues which are removed for pyrolysis versus the proportion which is allowed to remain in the soil will determine the balance between the dynamic SOM and the passive biochar and so is likely to affect soil quality for providing the desired roles, be it provision of good use as crop or timber, or functioning as a carbon pool. Biochar also has the potential to introduce a wide range of hazardous organic compounds (e.g. heavy metals, PAHs) into the soil system, which can be present as contaminants in biochar that has been produced either from contaminated feedstocks or under processing conditions which favour their production. While a tight control over the feedstock type and processing conditions used can reduce the potential risk for soil contamination, experimental evidence of the occurrence and bioavailability and toxicity of such contaminants in biochar and biochar-enriched soil (over time) remain scarce. A comprehensive risk assessment of each biochar product prior to its incorporation into soil, taking into account the soil type and environmental conditions, is therefore paramount.

Increased crop yields are the most commonly reported benefits of adding biochar to soils. A full search of the scientific literature led to a compilation of studies used for a meta-analysis of the effects of biochar application to soils and plant productivity. Meta-analysis techniques (Rosenberg et al., 1997) were used to quantify the effect of biochar addition to soil on plant productivity from a range of experiments. Our results showed a small overall, but statistically significant, positive effect of biochar application to soils on plant productivity in the majority of cases, covering a range of both soil and crop types. The greatest positive effects were seen on acidic free-draining soils with other soil types, specifically Calcarosols showing no significant effect. No statistically significant negative effects were found. There was also a general trend for concurrent increases in crop productivity with increases in pH up on biochar addition to soils. This suggests that one of the main mechanisms behind the reported positive effects of biochar application to soils on plant productivity may be a liming effect. These results underline the importance of testing each biochar material under representative conditions (i.e. soil-environment-climate-management factors).

The degree and possible consequences of the changes biochar undergo in soil over time remain largely unknown. Biochar loss and mobility through the soil profile and into water resources has so far been scarcely quantified and the underlying transport mechanisms are poorly understood. This is further complicated by the limited amount of long-term studies and the lack of standardized methods for simulating biochar aging and for long-term environmental monitoring.

4. BIOCHAR AND 'THREATS TO SOIL'

This chapter summarises the findings and gaps in the biochar literature relevant to the threats to soil, as identified by the Thematic Strategy for Soil Protection ([COM\(2006\) 231](#)). For a more in-depth discussion of patterns, effects, processes and mechanisms, please refer to the relevant Sections in this report. For the threats to soil of 'soil sealing' and 'landslides', biochar holds no relevance at present.

4.1 Soil loss by erosion

In the context of threats to soil, soil loss by erosion is specified by being “as a result of anthropogenic activity, in excess of natural soil formation rates causing a deterioration or loss of one or more soil functions” (Jones et al., 2008). Experimental studies on the effects of biochar application on soil erosion have not been found. Even erosion of charcoal particles from the soil surface after wildfires is a topic that has only started being researched relatively recently. However, an obvious potential effect is the wind erosion of biochar particles during application to soils. For application strategies where the biochar is incorporated into the soil, further erosion by either wind is likely to be reduced to the 'normal' erosion rates of the site. For application strategies where the biochar is applied to the soil surface only, the risk of erosion increases strongly because biochar generally has a relatively low density and, therefore, a greater erodibility by wind for smaller particles and by water for also the larger biochar particles. Surface application has been discussed for grassland and forest land uses mostly (and no-till systems). The greater risk may be expected for grasslands since these are open systems with generally greater wind velocities than forests.

Biochar application to soils can also be considered from a soil formation perspective. Verheijen et al. (2009) reviewed soil formation rates in Europe to be in the range of 0.3-1.4 t ha⁻¹ yr⁻¹. Considering the human life span, these very low formation rates (measurable only in geological terms) mean that soil is a non-renewable resource. Even low application rates of biochar are likely to outstrip natural soil formation rates by physicochemical weathering and dust deposition (i.e. mineral dust mainly from the Sahara). However, great care must be taken when considering biochar application to soils as constituting towards soil formation rates, and thereby tolerable soil erosion rates. Most notably, the residence time of biochar particles in soils needs to be considered, which depends on i) decomposition rates of biochar components (physicochemical and biological degradation), and ii) mobility and fate of biochar particles (movement through the soil matrix and into ground/surface waters). Both these factors are likely to be influenced strongly by variation in soil properties, climatic conditions, biochar properties, and land use and soil management. A substantial body of experimental scientific research into the mechanisms affecting the residence time of biochar particles in soils is required before biochar application to soils might be considered in the context of tolerable soil erosion rates. Conventionally, SOM build up is not considered for soil formation rates of mineral soils. Under what conditions those components of biochar that are very recalcitrant (e.g. residence time >1,000 yr) will reside in the soil matrix during their 'life span', is unknown at present. The interaction between biochar particles, mineral soil particles and

native organic matter (NOM), or OM that is applied with (or after) the biochar, is likely to play a major role (see Section 3.2.1 and 3.2.5).

Wind erosion is caused by the simultaneous occurrence of three conditions: high wind velocity; susceptible surface of loose particles; and insufficient surface protection. Theoretically, if biochar particles are produced with water retention properties greater than the water retention capacity of the soil surface at a site, and if the biochar particles become a structural component of that surface soil (e.g. not residing on top of the soil surface), and possibly interacting with OM and mineral particles, then wind erosion rates at that site may be reduced, all other factors remaining equal. The application of biochar dust to the soil surface (i.e. not incorporated) can pose risks via wind erosion of the dust particles and subsequent inhalation by people. Strict guidelines on biochar application strategies under specific environmental and land use conditions could prove sufficient to prevent this risk.

Water erosion takes place through rill and/or inter-rill (sheet) erosion, and gullies, as a result of excess surface runoff, notably when flow shear stresses exceed the shear strength of the soil (Kirkby et al., 2000, 2004; Jones et al., 2004). This form of erosion is generally estimated to be the most extensive form of erosion occurring in Europe. If biochar reduces surface runoff, then, logically, it will reduce soil loss by water erosion, all other factors remaining equal. Surface runoff can be reduced by increased water holding capacity (decreasing saturation overland flow) or increased infiltration capacity (decreasing infiltration excess – or Hortonian - overland flow) of the topsoil. Under specific environmental conditions, it seems that biochar with large water retention properties could diminish the occurrence of saturation overland flow. This effect could be enhanced when biochar addition leads to stabilisation of NOM, or OM that is added with, or after, the biochar. Infiltration excess overland flow depends more on soil structure and related drainage properties. In particular the soil surface properties are important for this mechanism. It is not inconceivable that specific biochar particles can play a role in increasing infiltration rates, however, other biochar particles could also lead to reduced infiltration rates when fine biochar particles fill in small pore spaces in topsoils, or increased hydrophobicity (Section 3.1). In addition, and this could be an overriding factors at least in the short term, the biochar application strategy and timing is a potential source of topsoil and/or subsoil compaction (Section 1.8) and, thereby, reduced infiltration rates.

It stands to reason that under those conditions where surface runoff is reduced by biochar application, possibly as part of a wider package of soil conservation measures, a concomitant reduction in flooding occurrence and severity may be expected, all other factors remaining equal. However, as stated at the beginning of this section, experimental evidence of biochar application on erosion was not encountered in the scientific literature, nor was it for flooding. On the other hand, under conditions where biochar application leads to soil compaction (see Section 1.8) runoff may be increased leading to more erosion. Research is needed into all aspects of effects from biochar addition to soil loss by erosion described here, and in particular into the mechanisms behind the effects. Even a small effect may be worthwhile considering estimates of the cost to society from erosion. For example annual costs have been estimated to be £205 million in England and Wales alone

and \$44 billion in the U.S.A. (Pimentel et al., 1995). In addition, active and targeted modification of the water retention function of specific soils could be considered in the context of scenarios of adapting to changing rainfall patterns (seasonal distribution, intensity) with climate change. In the future, climate change looks likely to increase rainfall intensity over large areas of Europe, if not annual totals, thereby increasing soil erosion by water, although there is much uncertainty about the spatio-temporal structure of this change as well as the socio-economic and agronomic changes that may accompany them (e.g. Boardman and Favismortlock, 1993; Phillips et al., 1993; Nearing et al., 2004).

4.2 Decline in soil organic matter

Decline in SOM is defined as a negative imbalance between the build-up of SOM and rates of decomposition leading to an overall decline in SOM contents and/or quality, causing a deterioration or loss of one or more soil functions (Jones et al., 2008).

The interaction between biochar and NOM, or OM that is added with the biochar, or afterwards, is complex. Many mechanisms have been identified and are discussed in this report, i.e. priming effect, residue removal, liming effect, organomineral interactions, aggregation and accessibility.

Biochar replacing peat extraction

If biochar is engineered to have good plant-available water properties as well as nutrient retention, it could come to replace peat as a growing medium in horticulture (also agriculture), and as a gardening amendment sold in garden centres. Peatlands currently used ('mined') for peat extraction could then be restored with substantial benefits to their functioning and the ecosystem services which they provide, e.g. maintenance of biodiversity, C sequestration, water storage, etc. Janssens et al. (2005) reported that undisturbed European peatlands sequester C at a rate of 6 g m⁻² total land area, while peat extraction caused a C loss of 0-36 g m⁻² total land area. Janssens et al. (2003) estimated a net loss of 50 (±10) Mt yr⁻¹ for the European continent, which is equivalent to around 1/6 of the total yearly C loss from European croplands. However, this value is likely to be greater when also considering C emissions associated with continued decomposition at abandoned peat mines (Turetsky et al., 2002), transport to processing plant, transport to market, and decomposition of the applied peat (e.g. in a life cycle assessment; Cleary et al., 2005).

4.3 Soil contamination

Recently, increasing knowledge on the sorption capacity of biochar has had two environmentally important outcomes. Firstly, the realisation that biochar addition to a soil can be expected to improve its overall sorption capacity, and consequently influence the toxicity, transport and fate of any organic compounds, which may be already present or are to be added to that soil (see Section 3.2.2). Secondly, enhanced awareness that biochar from widely available biomass resources can be applied to soils and sediments as a low-

cost and low-environmental-impact mitigation/remediation strategy for common environmental pollutants.

The latter outcome appears to be even more attractive when considering the time and cost benefits associated to biochar production, relatively to that of activated carbon in various applications. Activated carbon results from activating (involving partial oxidation) a charcoal precursor by means of exposing it to CO₂, steam or acid at high temperatures, in order to further increase its surface area (per gram; McHenry, 2009). Overall, evidence suggests that biochar and activated carbon have comparable sorption affinities, as demonstrated by Tsui and Roy (2008), using compost biochar (pyrolysis temperatures ranging between 120-420°C) and corn stillage activated carbon for removal of the herbicide atrazine in solution (1.7 mg L⁻¹). In fact, the effectiveness of activated carbon over that of wood biochar has been questioned in some instances (Pulido et al., 1998; Wingate et al., 2009), but this aspect remains far from fully evaluated.

Wingate et al. (2009) have very recently patented the development and application of charcoal from various plant and crop tissues (leaves, bark and stems) of ammonium (NH₄⁺) and heavy metal-contaminated environments (soil, brown-field site, mine tailings, slurry, and aqueous solution). Heavy metal ions are strongly adsorbed onto specific active sites containing acidic carboxyl groups at the surface of the charcoal (e.g. Machida et al., 2005). Surprisingly, the mechanism of metal uptake by charcoals appears to involve replacing pre-existing ions contained in the charcoal (e.g. K, Ca, Mg, Mn, excluding Si), with the metal ion, suggesting a relationship between the mineral content of the charcoal and its remediation potential for heavy metals (Wingate et al., 2009).

In the soil environment, biochar has already been shown to be effective in mitigating mobility and toxicity of heavy metals (Wingate et al., 2009) and endocrine disruptors (Smernik, 2007; Winsley, 2007). However, very little work of this kind has been accomplished and data is still scarce. It is likely that soil heterogeneity and the lack of monitoring techniques for biochar in this environment may partly explain such a gap. The previous discussion on contaminant leaching over time as a consequence of biochar aging in the environment (see Section 3.2.1) does not necessarily mean that its high remediating potential should be disregarded. For example, it could be employed as a 'first-instance' pollutant immobilisation from point sources. Also, biochar's highly porous matrix might be ideal as carrier for microorganisms as part of bioaugmentation programs for specific sites, where indigenous microbial populations are scarce or have been suppressed by the contaminant (Wingate et al., 2009). In this context, for instance, Wingate et al. (2009) have reported the successful application of charcoal carrying 10¹⁰ hydrocarbon degraders (per gram of charcoal) in diesel-polluted sites, resulting in 10 fold enhancement of hydrocarbon degradation in this environment. Clearly, it is likely that appropriate regulatory requirements for cleanup and closure would be needed before any remediation plan involving biochar could be implemented. Experimental evidence is required in order to verify this.

There is also evidence that it is possible to use biochar's sorptive capacity in water and wastewater treatments (Wingate et al., 2009), whereas the use of activated carbon for removal of chlorine and halogenated hydrocarbons, organic compounds (e.g. phenols, PCBs, pesticides) and heavy metals (Boateng, 2007) has long been established. Crop residue (mainly wheat) biochar produced at temperatures between 300°C and 700°C has already shown potential for removal of sulphate (Beaton, 1960), benzene and nitrobenzene from solution (Chun et al., 2004), while bamboo charcoal powder has been effective in uptake of nitrate from drinking water (Mizuta et al., 2004). Other studies in aqueous media have reported biochar's capacity to adsorb phosphate and ammonium (Lehmann et al., 2002; Lehmann et al., 2003, 2003b), with further applications having been reviewed by Radovic et al. (2001). In the context of water treatment, Sohi et al. (2009) have pointed out that a higher control over the remediation process would be achievable, comparatively to that in soil.

The possibility of using 'engineered' (or 'tailor-made') biochar (Pastor-Villegas et al., 2006) in order to meet the requirements for a specific remediation plan looks increasingly promising. As the mechanisms of biochar production, behaviour and fate, as well as its impact on ecosystem health and functioning become increasingly well understood, biochar can be optimised to deliver specific benefits (Sohi et al., 2009). Nevertheless, data on competitive sorption in soils and sediments emphasize the need for a full characterisation of the contaminated site and the coexisting chemical species before any remediation plan involving biochar is put in place.

4.4 Decline in soil biodiversity

Decline in soil biodiversity is defined as a 'reduction of forms of life living in the soil (both in terms of quantity and variety) and of related functions, causing a deterioration or loss of one or more soil functions' (Jones et al., 2008). There is evidence of decline in soil biodiversity in some specific cases. For example, the Swiss Federal Environment Office has published the first-ever "Red List" of mushrooms detailing 937 known species facing possible extinction in the country (Swissinfo 2007). In another instance, the New Zealand flatworm is increasing in numbers and extent and potentially poses a great threat to earthworm diversity in the UK with a 12% reduction in earthworm populations in some field sites in Scotland already reported (Boag et al. 1999). Changes in earthworm community structure have been also recorded (Jones et al., 2001).

The exact impacts of a decline in soil biodiversity are far from clear, due to complications by such phenomena as functional redundancy. However, it is clear that any decline in soil biodiversity has the potential to compromise ecosystem services, or at least reduce the resistance of the soil biota to further perturbations. Although evidence exists for declines in soil biodiversity in some specific cases, it is a highly depauperate area of research. However, no studies have been published to date looking at how biochar additions to soil can be used to restore soil biodiversity to previous levels in any given area.

Threats to soil biodiversity consist of those soil threats as described in the Thematic Strategy for Soil Protection (COM(2006) 231) and as such, in those

situations where biochar either helps the mitigation of, or increases the problem of, it is likely that knock on effects for the soil biota will occur.

4.6 Soil compaction

Soil compaction is defined as the densification and distortion of soil by which total and air-filled porosity are reduced, causing a deterioration or loss of one or more soil functions (Jones et al., 2008).

The effects of biochar on soil compaction have been studied very little. Both potential positive and negative effects may occur, for topsoil as well as subsoil compaction. Whereas topsoil compaction is 'instantaneous', subsoil compaction is a cumulative process leading to densification just below the topsoil over the years. A biochar application strategy, where application occurs every year, is, therefore, a greater risk of subsoil compaction than a 'single application' biochar strategy. An obvious risk of compaction is the actual application of biochar itself. When applied with heavy machinery and while the water-filled pore volume of soil is high, the risk of compaction increases. Biochar also has a low elasticity, measured by the relaxation ratio (R), which is defined as the ratio of the bulk density of the test material under specified stress to the bulk density after the stress has been removed. Straw has a very high elasticity ratio and, therefore, when straw is charred and applied as biochar instead of fresh straw, the resilience of the soil to compactive loads is reduced, all other factors remaining equal. The bulk density of biochar is low and, therefore, adding biochar to soil can lower the bulk density of the soil thereby reducing compaction. However, when biochar is applied as very fine particles, or when larger biochar particles disintegrate in arable soils under influence of tillage and cultivation operations, these can fill up small pores in the soil leading to compaction.

Compaction by machinery may be prevented relatively easily by promoting sound soil management. However, compaction by the behaviour of biochar particles in the soil has received very little attention in research so far and mechanisms are understood poorly.

4.7 Soil salinisation

Soil salinisation is defined as the accumulation of water soluble salts in the soil, causing a deterioration or loss of one or more soil functions. The accumulated salts include sodium-, potassium-, magnesium- and calcium-chlorides, sulphates, carbonates and bicarbonates (Jones et al., 2008). A distinction can be made between primary and secondary salinisation processes. Primary salinisation involves accumulation of salts through natural processes as physical or chemical weathering and transport processes from salty geological deposits or groundwater. Secondary salinisation is caused by human interventions such as inappropriate irrigation practices, use of salt-rich irrigation water and/or poor drainage conditions (Huber et al., 2009). Salts associated with biochar should be considered as a potential source for secondary salinisation.

Various salts can be found in the ash fraction of biochar, depending mostly on the mineral content of the feedstock. Indications are that the ash content of biochar varies from 0.5% - 55%. In classic charcoal manufacturing, 'good

quality' charcoal is referred to as having 0.5% – 5.0% ash (Antal and Gronli, 2003). However, biochar produced from feedstocks such as switchgrass and maize residue have been reported to have an ash content 26% - 54% much of which as silica, while hardwood ash contains mainly alkali metals (Brewer et al., 2009). A wide range of trace elements have been measured in biochar ash, e.g. boron, copper, zinc, etc., however, the most common elements are potassium, calcium, silicon and in smaller amounts aluminium, iron, magnesium, phosphorus, sodium and manganese. These elements are all in oxidised form, e.g. Na_2O , CaO , K_2O , but can be reactive or soluble in water to varying degrees. It is the ash fraction that provides the liming effects of biochar that is discussed as a potential mechanism of some reported increases in plant productivity (see Section 3.3). However, for soils that are salinised or are sensitive to become salinised, that same ash fraction might pose an increased threat. Surprisingly little work has been found on biochar ash and under what conditions it may become soluble and contribute to salinisation.

4.8 Summary

This chapter has described the interactions between biochar and 'threats to soil'. For most of these interactions, the body of scientific evidence is currently insufficient to arrive at a consensus. However, what is clear is that biochar application to soils will effect soil properties and processes and thereby interact with threats to soil. Awareness of these interactions, and the mechanisms behind them, is required to lead to the research necessary for arriving at understanding mechanisms and effects on threats to soil, as well as the wider ecosystem.

5. WIDER ISSUES

5.1 Emissions and atmospheric pollution

The high load of aerosol and pollutant emissions generated by wildfires and the combustion of fossil fuels explain much of the concern on biochar production being associated to high levels of particulate matter and atmospheric pollutants. Nevertheless, the type and composition of such emissions, including the way these are influenced by pyrolysis conditions and factors associated to biomass feedstock, are considerably less well understood (Fernandes and Brooks, 2003).

Particulate matter emitted during pyrolysis is a main focus of human and environmental health concern based on what is known regarding the inherent toxicity associated to some types of fine and ultrafine particles, due to their small size and large surface area (Fernandes and Sicre, 1999). Whereas until recently, some cases of disease (e.g. respiratory and cardiac) associated to atmospheric pollution were thought to be caused by some particle types with dimensions up to 10 μm , recent progress has demonstrated that those responsible are mainly within the nano-size range. The U.S.A. Environment Protection Agency (EPA) has responded by putting forward new ambient standards on Air Quality for particulate matter $<2.5 \mu\text{m}$ (PM_{2.5}). Current annual mean limits are 40 $\mu\text{g m}^{-3}$ and 20 $\mu\text{g m}^{-3}$ for PM₁₀ ($<10 \mu\text{m}$) and PM_{2.5} respectively (EPA, 2007), whereas ambient standards for sub-micron particles in the environment were not found. Besides the potential health risks associated to fine and ultrafine particle emissions, their direct and indirect role in climate change has also granted them wide attention. Further research involving characterisation of biochar-related particulate emissions during pyrolysis would be vital for assessing the true contribution of such emissions to ambient aerosols, as well as identifying processing conditions and technologies that may help reducing them.

Typically, large amounts of organic and inorganic volatile compounds are emitted during biomass pyrolysis, particularly at temperatures exceeding 500°C (Greenberg et al., 2005; Gaskin et al., 2008; Chan and Xu, 2009). Major volatile organic compounds emissions from pyrolysis (30 to 300°C) of leaf and woody plant tissue (pine, eucalyptus and oak wood, sugarcane and rice) included acetic acid, furfuraldehyde, methyl acetate, pyrazine, terpenes, 2,3 butadione, phenol and methanol, as well as smaller quantities of furan, acetone, acetaldehyde, acetonitrile and benzaldehyde (Greenberg et al., 2005). At treatment temperatures between 300 and 600°C, heat- and mass-transfer rates are high, resulting in a gas-forming pathway dominating the pyrolysis process, being linked to the production of heavy molecular weight (tarry) vapours of highly diverse composition (Amonette and Joseph, 2009). At temperatures around that lower limit, these tars remain trapped within micropores of the carbonaceous residue but become volatile for higher temperatures. While the majority of such vapours are commonly recovered from the gas stream as bio-oil using a condensation tower (Amonette and Joseph, 2009), a significant proportion is still emitted into the atmosphere, especially where simple charcoal kilns are used.

Emissions of PAHs resulting from both natural (e.g. forest fires, volcanic eruptions) and anthropogenic sources (e.g. burning of fossil fuels) are recognized as relevant environmental pollutants (Pakdel and Roy, 1991). Secondary chemical reactions during thermal degradation of organic material at high temperatures (>700°C), is generally associated to the generation and emission of heavily condensed and highly carcinogenic and mutagenic PAHs (Ledesma et al., 2002; Garcia-Perez, 2008). Nevertheless, some evidence also exists that PAHs can be formed within the temperature range of pyrolysis (350-600°C). These low-temperature generated PAHs are highly branched in nature and appear to carry lower toxicological and environmental implications (Garcia-Perez, 2008). Preliminary results from a recent study have shown that the amount of biochar-related PAH emissions from traditional feedstocks remain within environmental compliance (Jones, 2008).

Dioxins (PCDD) and furans (PCDF) are planar chlorinated aromatic compounds, which are predominantly formed by combustion of organic material in the presence of chlorine and metals, at temperatures exceeding 1000°C (Lavric et al., 2005; Garcia-Perez, 2008). Wood (accidental fires, wildfires and wood wastes) is an important air emission source for dioxins (Lavric et al., 2005). While combustion of firewood and pellets in residential stoves, as well as paper and plastic wastes, are well known for emitting high loads of dioxins (Hedman et al., 2006), actual emission factors and corresponding activity rates remain poorly assessed (Lavric et al., 2005). No experimental evidence was found confirming dioxin emissions from pyrolysis of traditional biomass feedstocks used in biochar production.

The emission of atmospheric pollutants during biochar production requires a full evaluation. This assessment is vital for establishing whether such emissions may cancel out benefits such as carbon sequestration potential. Such an evaluation should focus beyond a qualitative and quantitative characterisation of those pollutants, and should include the pyrolysis operational conditions and technologies required to reduce their emissions to acceptable levels. Evidence in the literature suggests that a certain degree of control in respect to biochar-related emissions can be achieved through the use of traditional feedstock materials and lower (<500°C) temperature pyrolysis. Whereas this aspect looks promising in relation to Air Quality, current biochar-producing technologies remain largely inefficient. According to Brown (2009), there is still wide room for improvement in the context of both energy consumption and atmospheric emissions, particularly when traditional gasifiers are concerned. At this level, the author identifies specific goals for optimal biochar production, among which are the use of continuous feed pyrolysis and an effective recovery of co-products (Brown, 2009). A detailed analysis on current and future biochar technologies aiming for a more 'environmentally friendly' biochar production is also provided.

Collison et al. (2009) in a report to EEDA, reminded that generation and emission of environmental pollutants as well as the incidence of health and safety issues associated to biochar production, transport and storage, is probably of greater concern for small-scale pyrolysis units, particularly in developing countries. It is often the case, that such smaller units lack the knowledge and/or financial support, to comply to the environmental standards (Brown, 2006). A joint effort is necessary to overcome this gap, which

includes the use of clean pyrolysis technologies (Lehmann et al., 2006) and the establishment of tight policy and regulations in respect to biochar production and handling. Furthermore, adequate educating and training, and perhaps the granting of governmental financial support would allow putting in place equipment and measures, aiming to minimise environmental and human exposure to emissions linked to biochar production.

5.2 Occupational health and safety

Biochar production facilities, as well as those associated to transportation and storage may pose an Occupational Health hazard for the workers involved, particularly when exposure to biochar dust is concerned (Blackwell et al., 2009). In addition, health and fire hazards are related directly to the key physical properties of biochar determining the suitability for a given application method (Blackwell et al., 2009). However, any discussions and recommendations in the context of health and safety can only be addressed generally, given the heterogeneity among biochars. Further research on acute and chronic exposure to biochar dust, in particular to its nano-sized fraction, remains scarce and is thus identified as a priority.

'Nanoparticle' has been used broadly to refer to those particles within biochar dust (e.g. fullerenes or fullerene-like structures, crystalline forms of silica, cristobalite and tridymite), with at least one dimension smaller than 100 nm. Two major aspects distinguish them from the remaining larger-sized microparticles: large surface area and high particle number per unit of mass, which may signify a 1000-fold enhanced reactive surface (Buzea et al., 2007). Such reactivity and their small size widely explain their hazardous potential. Several reports have focused on their ability to enter, transit within and damage living cells and organisms. This capacity is partly consequence of their small size, enabling easy penetration through physical barriers, translocation through the circulatory system of the host, and interaction with various cellular components (Buzea et al., 2007), including DNA (Zhao et al., 2005).

Most toxicological and epidemiological studies using fish, mice and mammalian cell lines (Andrade et al., 2006; Moore et al., 2006; Oberdorster et al., 2006; Nowack et al., 2007) demonstrate an inflammatory response in the cell or animal host (Donaldson et al., 2005). In biological systems, nanoparticles are known to generate disease mainly by mechanisms of oxidative stress, either by introducing oxidant species into the system or by acting as carriers for trace metals (Oberdorster, et al., 2004; Sayes et al., 2005). Those studies have also demonstrated that oxidative stress may result ultimately in irreversible disruption of basic cellular mechanisms such as proliferation, metabolism and death. However, extrapolating such effects to humans remains a challenge, and any outcomes are expected to be dependent on various factors relating to exposure conditions, residence time and inherent variability of the host (Buzea et al., 2007).

Exposure to nanoparticles within biochar dust (e.g. carbon-based NP, crystalline silica) appears to have associated health risks primarily for the respiratory system (e.g. Borm et al., 2004; Knaapen et al., 2004) and the gastrointestinal tract (e.g. Hussein et al., 2001). If inhalation of biochar dust should occur, measures which rapidly enhance airway clearance (e.g.

mucociliary rinsing with saline solution), and reduce inflammatory and allergic reactions (e.g. sodium cromoglycate) should be promptly carried out (Buzzea et al., 2007). On the other hand, dermal uptake of combustion-derived nanoparticles was also found to occur, although this issue remains a controversial one. It has been suggested that nanoparticle incursion through the skin may occur at hair follicles (Toll et al., 2004), as well as broken (Oberdörster et al., 2005) or flexed (Tinkle et al., 2003) skin, depending mainly on particle size.

Besides unusually high levels (up to 220 g kg^{-1}) of silica, highly toxic crystalline forms of cristobalite and tridymite have also been found in rice husk biochars produced at temperatures above 550°C . Blackwell et al. (2009) did not hesitate in recommending careful handling, transport and storage of rice husk biochar as well as strict quality control measures for its production. Regarding those mineral forms, Stowell and Tubb (2003) have recommended maximum exposure limits of 0.1, 0.05 and 0.05 mg m^{-3} for crystalline silica, cristobalite and tridymite respectively. In comparison, those authors have suggested that current maximum exposure limits for crystalline silica (given as an example) assigned by the UK (0.3 mg m^{-3}) and the US (10 mg m^{-3} divided by the percentage of SiO_2) may be too high.

In the context of Occupational Health, reducing biochar dust exposure requires tight health and safety measures to be put in place. For biochars containing a large proportion of dust, health risks associated to safe transport and storage, as well as application, may be reduced using dust control techniques (Blackwell et al., 2009). For example, covering or wrapping biochar heaps or spraying the surface with stabilising solutions can minimise the risk of exposure during transport and storage. In regard to reducing dust formation during application, especially with concern to uniform topsoil mixing and top-dressing, water can be used to support on-site spreading (when spreading is appropriate) (Blackwell et al., 2009).

It has been reported that generation of free-radicals during thermal ($120^\circ\text{C} < T < 300^\circ\text{C}$) degradation of lignocellulosic materials, may be responsible for the propensity of fresh biochars to spontaneously combust (Amonette and Joseph, 2009), particularly at temperatures $< 100^\circ\text{C}$ (Bourke et al., 2007). The free-radicals are primarily produced by thermal action on the O-functionalities and mineral impurities within the source material. Under certain conditions, an excessive accumulation of free-radicals at the biochar surface (Amonette and Joseph, 2009) and within its micropores (Bourke et al., 2007) might occur. The proportion of free-radicals in biochar is primarily dependent on the temperature of pyrolysis, and generally decrease with increasing operation temperatures (Bourke et al., 2007).

There is also evidence that an excessive accumulation of biochar dust in enclosed spaces may enhance its pyrophoric potential, as recently reported with coal dust in mines (Giby et al., 2007). To tackle this issue, increasing biochar density through pelleting may be advisable (Werther et al., 2000). In addition, the volatile (e.g. aldehydes, alcohols and carboxylic acids) content of biochar (as influenced by biomass feedstock and operation conditions; Brown 2009) may also constitute a fire hazard during transport, handling and storage (Werther et al., 2000), and should be taken into account.

Overall, increasing awareness of biochar flammability means that avoiding biochar storage with neighbouring residential buildings and goods is advisable. Nevertheless, successful attempts to reduce the risk of combustion of rice husk char by adding fire retardants (e.g. boric acid, ferrous sulphate; Maiti et al., 2006) and inert gases for removal of atmospheric O₂ (Naujokas, 1985) have been reported. There is also sound proof of the effective use of water in assisting cooling of a wide range of carbonaceous materials, including charcoals (Naujokas, 1985).

5.3 Monitoring biochar in soil

Research methodologies for comparing different biochars produced under laboratory conditions already have been put in place, based on work involving charcoal and other BCs. Currently, ¹³C nuclear magnetic resonance (NMR) and mid-infrared spectroscopy appear to be reliable methods for providing compositional characterisation (at the functional group level) of biochar, as well as differentiation between biochar products. Nevertheless, using such methods for routine purposes is expensive and time consuming, particularly when a large number of samples is involved. An efficient, rapid and economically feasible method for long-term routine assessment of biochar in soil has not yet been described. Furthermore, at the present, it is perhaps more important for research to focus on assessing and comparing between biochar produced under industrial and field conditions.

5.4 Economic Considerations

There is no established business model in the sense of industry-wide accepted set of standards of production, distribution and use of biochar. In fact, even the term “biochar industry” would be misplaced. What exists currently is a multitude of start-up companies and other entities experimenting with alternative pyrolysis technologies operating at various scales.

Two important considerations with respect to the operation of any biochar system are: the scale of the biochar operation, and how the feedstock is sourced (intentional or dedicated). Biochar can be produced in a centralised, industrial fashion, or can adopt a small-scale, local approach. Regarding feedstocks, one can distinguish between an open and a closed system. In a closed system, the pyrolysed material essentially consists of agricultural and forestry residues (byproduct), whereas the open system envisages the growing of biomass dedicated to pyrolysis as well as off-site waste products (e.g. sewage sludge). The distinction along these lines is important because of the different economic implications associated with the respective biochar systems and it also gives rise to another distinction between private and social costs and benefits.

5.4.1 Private costs and benefits

The private costs and benefits determine the commercial viability of any biochar operation and are a combination of biochar’s value as a soil additive, as a source of carbon credits and as an energy source. Crudely, the cost-revenue structure of a biochar system could be broken down as follows (McCarl et al., 2009; Collison et al., 2009). On the revenue side, the following sources of value should be considered:

- sale of pyrolysis-derived energy co-products;
- value of biochar as a soil amendment;
- value of biochar as a source of carbon credits.

Potential value to farmers, if any, could arise from increases in crop yield, although current evidence indicates a relatively small overall effect (see Section 3.3) and plant production is likely to vary considerably for combinations of environmental factors and crop types (see Sections 3.3).

Additional economic benefits, in the form of reduced production costs, may also come about from a reduction in fertilizer application or liming (both very dependent on biochar quality and quantity as well as frequency of application, see Section 1.8). Irrigation costs could also potentially be reduced if biochar application leads to enhanced water retention capacity, which evidence suggests may be possible at least for sandy soils (see Section 3.1.2). However, although the intention of biochar is to improve the soil it can also be envisaged that unforeseen effects on the soil, due to improper management, would actually lead to an increase in production costs.

For example, when (sub)soil compaction is caused during biochar application to the soil, subsequent subsoiling operations to alleviate the compaction would incur a cost. Due to the lack of a functioning biochar industry, it is not yet clear whether any payments for carbon credits will accrue to the land owners or the biochar producers. Either way, the economic viability of the carbon offsetting potential could be limited owing to the potentially high monitoring and verification costs (Gaunt and Cowie, 2009). Regardless whom the proceeds from carbon credits accrue to, their value should reflect not only the carbon sequestration potential of biochar but also the reduced emissions due to lower fertiliser applications, as well as emissions from the transportation needs of biomass and biochar. Accounting for these indirect emissions might add to the costliness of certifying any carbon credits and, thus, further undermine its profitability.

The cost elements of the equation are the following:

- cost of growing the feedstock (in case of an open system);
- cost of collecting, transporting and storing the feedstock;
- cost of pyrolysis operation (purchase of equipment, maintenance, depreciation, labour);
- cost of transporting and applying the biochar

Despite the large uncertainties on biochar costs and benefits, the following factors ought to be taken into account. First, it is clear that the private costs and benefits of a biochar operation will vary depending on the scale of the operation. Biochar production at an industrial scale implies significantly higher costs of transporting the feedstock and the biochar produced from it than when produced at a small scale. System analysis studies will be of great help in understanding these issues. Higher transportation needs also lead to higher GHG emissions, as more fuel is needed for hauling the biomass and the biochar. The increased emissions need to be accounted for and included in the carbon offsetting potential of biochar, which would reduce the biochar's

value as a source of carbon credits. On the other hand, industrial production of biochar means that bigger pyrolysis plants could generate economies of scale, which would bring the average cost of producing biochar down.

Another factor that may influence the commercial appeal and the reliability in the supply of biochar is the fact that biochar is only one co-product of pyrolysis, the other ones being syngas and bio-oil. Different types of pyrolysis (fast vs. slow) will yield different proportions of these products (see Section 1.6), and biochar with varying properties, for a given amount of feedstock. This means that decisions pertaining to the quantity and quality of produced biochar will depend on the economic attractiveness of the other two products and not just on the cost elements of biochar production and the demand for biochar. For instance, if demand for bio-oil and syngas increases, the opportunity cost of biochar production will increase, thus shifting production away from it and rendering it relatively more expensive. Such flexibility in production is, of course, a welcome trait for pyrolysis operators, but adds an extra layer of unpredictability that might dampen demand for biochar as a soil amendment and as a potential source of carbon credits.

As biochar development and adoption are still at an early stage, there is currently very little quantitative information on these costs and benefits. McCarl et al. (2009) undertook a cost benefit analysis (CBA) of a pyrolysis operation in Iowa that uses maize crop residues as feedstock. Assuming a 5 t ha⁻¹ biochar application and a 5% increase in yields, they conclude that both fast and slow operations are not profitable at current carbon and energy prices, with a net present value of about -\$44 and -\$70 (per tonne of feedstock) respectively.

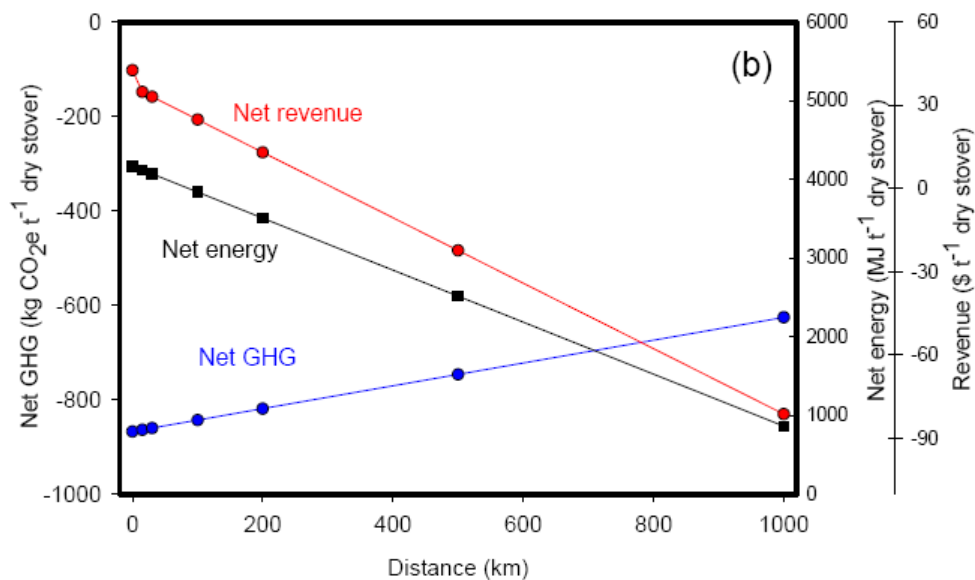


Figure 5.1 Effect of transportation distance in biochar systems with bioenergy production using the example of late stover feedstock on net GHG, net energy and net revenue (adopted from Roberts et al., 2009)

Roberts et al. (2009) calculate the economic flows associated with the pyrolysis of three different feedstocks (stover, switchgrass and yard waste). They find that the economic profitability depends very much on the assumed

value of sequestered carbon. At $\$20 \text{ t}^{-1} \text{ CO}_{2\text{e}}$, only yard waste makes pyrolysis operation profitable, whereas at a higher assumed price of $\$80 \text{ t}^{-1} \text{ CO}_{2\text{e}}$, stover is moderately profitable ($\$35 \text{ t}^{-1}$ of stover), yard waste significantly so ($\$69 \text{ t}^{-1}$ of waste), but switchgrass is still unprofitable. The point that is made is that despite the revenues from the biochar and energy products for all feedstocks, the overall profitability is reduced by the cost of feedstock collection and pyrolysis, even when CO_2 is valued at $\$80 \text{ t}^{-1}$, while the costs of feedstock and biochar transport and application play a smaller role. Figure 5.1 illustrates the effect that increased transportation distance has on net GHG, net energy and net revenue for a pyrolysis operation using stover as a feedstock.

In a somewhat less sophisticated attempt to estimate costs and benefits, Collison et al. use a hypothetical case study of biochar application in the East of England, without, however, taking into account the costs of biochar production, distribution and application. They estimate an increase in profitability of the order of $\text{£}545 \text{ ha}^{-1}$ for potatoes and $\text{£}143 \text{ ha}^{-1}$ for feed wheat.

Similarly, Blackwell et al. (2007) estimated the wheat income benefits for farmers in Western Australia by carrying out a series of trials of applying varying rates of mallee biochar and fertiliser. The trials produced benefits of up to $\$96 \text{ ha}^{-1}$ of additional gross income at wheat prices of $\$150 \text{ ha}^{-1}$. Again, no account was taken of the costs of biochar production.

The lesson to be taken from such studies is that at this early stage, any CBA is an assumption-laden exercise that is prone to significant errors and revisions as more information becomes available on pyrolysis technologies and the agronomic effects of biochar.

5.4.2 Social costs and benefits

The social costs and benefits closely follow from the private ones but can be quite hard to monetize, or even model. Like the private ones, they also depend on the type of biochar system that is adopted. If an open system is adopted, the biggest concern is that the drive for larger volumes of biochar may lead to unsustainable land practices, causing significant areas of land to be converted into biomass plantations. Such competition for land could encourage the destruction of tropical forests directly or indirectly, via the displacement of agricultural production. The latter possibility could also have negative consequences on the prices and the availability of food crops, much like in the case of the market for biofuels.

However, these social costs are not inevitable. Tropical deforestation could be avoided if, for instance, biomass is grown sustainably on land previously deforested. Moreover, any adverse effects of growing biochar feedstock on food security and availability could be mitigated by the biochar-induced gains in crop yields (see Section 3.3). Furthermore, wide, health-related social benefits can be ascribed to biochar's potential for land remediation and decontamination. Of course, the biggest source of social benefits would be biochar's climate change mitigation potential.

This section has briefly sketched the economic considerations that ought to be taken into account when planning for the development of a biochar system.

For biochar to be successful it must not only deliver on its environmental promise but it should also be commercially viable.

The profitability of any biochar operation will depend mainly on its potential to attract revenue as a soil additive and carbon sink and will be affected by the type of production (open vs. closed, local vs. centralised), which can in turn result in environmental and economic spillovers. Moreover, the demand for biochar will be influenced by, and will indeed influence the demand for biofuels, as a byproduct of pyrolysis, the demand for products such as manure and compost and the price of carbon in the carbon markets.

Which shape and direction the biochar industry is likely to take is very much unknown at this stage. However, any outcomes will be greatly influenced by policy measures on energy, agriculture and climate change. The interplay and interdependence of such policies call for a holistic, systemic assessment of the opportunities and pitfalls presented by biochar.

5.5 Is biochar soft geo-engineering?

Geo-engineering is the artificial modification of Earth systems to counteract the consequences of anthropogenic effects, such as climate change. Large-scale (industrial) deployment of biochar thus qualifies as a geo-engineering scheme. Geo-engineering is very controversial and the primitive nature of geo-engineering schemes has been likened to a planetary version of 19th century medicine (Lovelock, 2007). Furthermore, panaceas often fail (Ostrom et al., 2007). However, biochar may be considered a 'softer' form of geo-engineering compared to more intrusive schemes. Especially if used with certain feedstocks under certain conditions and compared to those geo-engineering proposals that focus on lowering temperature rather than reducing GHG emissions or sequestering carbon. Indeed, biochar has been promoted as a lower-risk strategy compared to other sequestration methods (Lehmann, 2007). Nevertheless, deploying biochar on a scale with a mitigative effect entails a large construction of necessary infrastructure and a very intrusive impact on the way agriculture is performed.

The scalability of biochar is both a potential strength and a potential weakness. As noted by Woods et al. (2006) 'one is sometimes left the impression that the biochar initiative is solely directed towards agribusiness applications'. However, several trials exist in collaboration with smallholder farmers, the closest approximation to the original Terra Preta formation. Small scale biochar systems that lead to a reduction of net GHG emissions have been suggested to be part of C offset mechanisms and so possibly contribute to soil C storage in Africa (Whitman and Lehmann, 2009). However, given the extensive use of biomass burning for energy in Africa, one of the potential problems will relate to the willingness of farmers to forego an energy source (biochar) once it has been created, which requires transparent certification and monitoring schemes if it is to be used in C credit trading schemes.

To what extent are the motives, practices and input materials that led to the creation of the Terra Preta soils similar or different compared to today's application of biochar to soil? A first obvious difference relates to the variety of inputs used in the formation of Terra Preta, compared to the limited number of

inputs (e.g. biochar, or mixtures of biochar and manure) currently proposed. This is an important consideration that determines how far the carbon storage properties (relative to 'average' agricultural soil with organic matter) and agronomic benefits of Terra Preta can reasonably be extrapolated.

The recalcitrance of biochar components is estimated to be potentially hundreds or thousands of years (dependent on biochar properties, environmental conditions, and land use/soil management), or roughly one to two magnitudes higher than the breakdown of OM in the soil (Sections 3.2.1 and 3.2.5.1). Biochar has been identified as the oldest fraction of SOM, confirming its recalcitrance to decomposition and mineralisation (Lehman and Sohi, 2007). The residence time and stability of biochar in Terra Preta soil are fairly robust, but are the result of extensive smallholder agriculture over tens to hundreds of years as opposed to intensive agriculture. The direct translation of these residence times to today's intensive agricultural systems with the use of heavy machinery, and the possible accelerated disintegration and decomposition of biochar particles, with possible effects on biochar recalcitrance, remains questionable.

Sequestering carbon with biochar seems to have potential in theory. Choices of feedstocks are critically related to the larger scale impacts and benefits of biochar. Use of specific organic waste (e.g. papermill waste) may be a reasonable first approach that circumvents the food vs. fuel debate (cf. biofuels, van der Velde et al., 2009). Hansen et al. (2008), using illustrative climate change mitigation scenarios, assumed waste-derived biochar to provide only a small fraction of the land use related CO₂ drawdown, with reforestation and curtailed deforestation providing a magnitude more (Kharecha and Hansen, 2009). In line with estimates by Lehman et al. (2006), Hansen et al. (2008) assumed waste-derived biochar to "be phased in linearly over the period 2010-2020, by which time it will reach a maximum uptake rate of 0.16 Gt C yr⁻¹". This illustrates that waste-derived biochar can be a part of the mitigation options, although fundamental uncertainties associated with biochar remain.

5.6 Summary

Biochar can be produced from a wide range of organic feedstocks under different pyrolysis conditions and at a range of scales. The original feedstock used, combined with the pyrolysis conditions will affect the exact physical and chemical properties of the final biochar, and ultimately, the way and the extent to which soil dependent ecosystem services are affected. Preliminary evidence appears to suggest that a tight control on the feedstock materials and pyrolysis conditions (mainly temperature) may be enough in attenuating much of the current concern relating to the high levels of atmospheric pollutants (e.g. PAHs, dioxins) and particulate matter that may be emitted during biochar production, while implications to human health remain mostly an occupational health issue. Health (e.g. dust exposure) and fire hazards associated to production, transport, application and storage need to be considered when determining the suitability of the biochar for a given application, while tight health and safety measures need to be put in place to mitigate such risks for the worker, as well as neighbouring residential areas.

The profitability of any biochar operation will depend mainly on its potential to attract revenue as a soil additive and C sink and will be affected by the type of biomass feedstock and that of production (open vs closed, local vs centralised), which can, in turn, result in environmental and economic spillovers. Moreover, the demand for biochar, as a byproduct of pyrolysis, will be influenced by, and will indeed influence, the demand for biofuels, the demand for products such as manure and compost and the price of carbon in the carbon markets. Furthermore, the costs and benefits of a range of biochar operations and scenarios need to be quantified. Cost-benefit analyses ought to cast the net wide by accounting not only for commercial factors but also for social costs and benefits.

6. KEY FINDINGS

This chapter summarises the main findings of the previous chapters, synthesises between these and identifies the key research gaps.

6.1 Summary of Key Findings

This report has highlighted that large gaps in knowledge still exist regarding the effects (including the mechanisms involved) of biochar incorporation into soils. Considerable further research is required in order to maximise the possible advantages of such an application, while minimizing any possible drawbacks. For some potential effects very few or no data are available. For other effects data exist but they do not cover sufficiently the variation in relevant soil-environment-climate-management factors. Table 6.1 provides an overview of the key findings. In view of this, the possibility of qualifying biochar for carbon offset credits within the UNFCCC as part of a post-Kyoto treaty seems premature at the present stage. Although an inclusion in the carbon credit systems would certainly boost the nascent biochar industry, current scientific knowledge of large-scale use of biochar in intensive agricultural systems has not reached a sufficient level for safe deployment. Best practices associated with production and application, quality standards, specifications that clarify land use conflicts and opportunities, monitoring of utilisation, and details on minimal qualification requirements for certification of biochar products, require further understanding of the C-sequestration potential and behaviour of biochar in the environment.

Table 6.1 Overview of key findings (numbers in parentheses refer to relevant sections)

	Description	Conditions
Positives	Empirical evidence of charcoal in soils exists (long term)	Biochar analogues (pyrogenic BC and charcoal) are found in substantial quantities in soils of most parts of the world (1.2-1.4)
	The principle of improving soils has been tried successfully in the past	Anthrosols can be found in many parts of the world, although normally of very small spatial extent. Contemplation of Anthrosol generation at a vast scale requires more comprehensive, detailed and careful analysis of effects on soils as well as interactions with other environmental components before implementation (1.2-1.3 and throughout)
	Plant production has been found to increase significantly after biochar addition to soils	Studies have been reported almost exclusively from tropical regions with specific environmental conditions, and generally for very limited time periods, i.e. 1-2 yr. Some cases of negative effects on crop production have also been reported (3.3).
	Liming effect	Most biochars have neutral to basic pH and many field experiments show an increase in soil pH after biochar application when the initial pH was low. On alkaline soils this may be an undesirable effect. Sustained liming effects may require regular applications (3.1.4)
	High sorption affinity for HOC may enhance the overall sorption capacity of soils towards these trace contaminants	Biochar application is likely to improve the overall sorption capacity of soils towards common anthropogenic organic compounds (e.g. PAHs, pesticides and herbicides), and therefore influence toxicity, transport and fate of such contaminants. Enhanced sorption capacity of a silt loam for diuron and other anionic and cationic herbicides has been observed following incorporation of biochar from crop residues (3.2.2)

	Microbial habitat and provision of refugia for microbes whereby they are protected from grazing	Biochar addition to soil has been shown to increase microbial biomass and microbial activity, as well as microbial efficiency as a measure of CO ₂ released per unit microbial biomass C. The degree of the response appears to be dependent on nutrient availability in soils
	Increases in mycorrhizal abundance which is linked to observed increases in plant productivity	Possibly due to: a) alteration of soil physico-chemical properties; b) indirect effects on mycorrhizae through effects on other soil microbes; c) plant–fungus signalling interference and detoxification of allelochemicals on biochar; or d) provision of refugia from fungal grazers (3.2.6)
	Increases in earthworm abundance and activity	Earthworms have been shown to prefer some soils amended with biochar than those soils alone. However, this is not true of all biochars, particularly at high application rates (3.2.6)
Negatives	The use of biochar analogues for assessing effects of modern biochars is very limited	Charcoal in Terra Preta soils is limited mainly to Amazonia and have received many diverse additions other than charcoal. Pyrogenic BC is found in soils in many parts of the world but are of limited feedstock types and pyrolysis conditions (Chapter 1)
	Soil loss by erosion	Top-dressing biochar to soil is likely to increase erosion of the biochar particles both by wind (dust) and water. Many other effects of biochar in soil on erosion can be theorised, but remain untested at present (4.1)
	Soil compaction during application	Any application carries a risk of soil compaction when performed under inappropriate conditions. Careful planning and management could prevent this effect (4.6)
	Risk of contamination	Contaminants (e.g. PAHs, heavy metals, dioxins) that may be present in biochar may have detrimental effects on soil properties and functions. The occurrence of such compounds in biochar is likely to derive from either contaminated feedstocks or the use of processing conditions that may favour their production. Evidence suggests that a tight control over the type of feedstock used and lower pyrolysis temperatures (<500°C) may be sufficient to reduce the potential risk for soil contamination (3.2.4)
	Residue removal	Removal of crop residues for use as a feedstock for biochar production can forego incorporation of the crop residue into the soil, potentially leading to multiple negative effects on soils (3.2.5.5)
	Occupational health and fire hazards	Health (e.g. dust exposure) and fire hazards associated to the production, transport, application and storage of biochar need to be considered when determining the suitability for biochar application. In the context of occupational health, tight health and safety measures need to be put in place in order to reduce such risks. Some of these measures have already proved adequate (5.2)
	Reduction in earthworm survival rates (limited number of cases)	High biochar application rates of >67 t ha ⁻¹ (produced from poultry litter) were shown to have a negative effect on earthworm survival rates, possibly due to increases in pH or salt levels (3.2.6)
Unknown	Empirical evidence is extremely scarce for many modern biochars in soils under modern arable management	Biochar analogues do not exist for many feedstocks, or for some modern pyrolysis conditions. Biochar can be produced with a wide variety of properties and applied to soils with a wide variety of properties. Some short term (1-2 yr) evidence exists, but only for a small set of biochar, environmental and soil management factors and almost no data is available on long term effect (1.2-1.4)
	C Negativity	The carbon storage capacity of biochar is widely hypothesised, although it is still largely unquantified and depends on many factors (environmental, economic, social) in all parts of the life cycle of biochar and at the several scales of operation (1.5.2 and Chapter 5)
	Effects on N cycle	N ₂ O emissions depend on effects of biochar addition on soil hydrology (water-filled pore volume) and associated microbial processes. Mechanisms are poorly understood and thresholds largely unknown (1.5.2)

Biochar Loading Capacity (BLC)	BLC is likely to be crop as well as soil dependent leading to potential incompatibilities between the irreversibility of biochar once applied to soil and changing crop demands (1.5.1)
Environmental behaviour mobility and fate	The extent and implications of the changes that biochar undergoes in soil remain largely unknown. Although biochar physical-chemical properties and stabilization mechanisms may explain biochar long mean residence times in soil, the relative contribution of each factor for its short- and long-term loss has been sparsely assessed, particularly when influenced by soil environmental conditions. Also, biochar loss and mobility through the soil profile and into the water resources has been scarcely quantified and transport mechanisms remain poorly understood (3.2.1)
Distribution and availability of contaminants (e.g. heavy metals, PAHs) within biochar	Very little experimental evidence is available on the short- and long-term occurrence and bioavailability of such contaminants in biochar and biochar-enriched soil. Full and careful risk assessment in this context is urgently required, in order to relate the bioavailability and toxicity of the contaminant to biochar type and 'safe' application rates, biomass feedstock and pyrolysis conditions, as well as soil type and environmental conditions (3.2.4)
Effect on soil organic matter dynamics	Various relevant processes are acknowledged but the way these are influenced by combinations of soil-climate-management factors remains largely unknown (Section 3.2.5)
Pore size and connectivity	Although pore size distribution in biochar may significantly alter key soil physical properties and processes (e.g. water retention, aeration, habitat), experimental evidence on this is scarce and the underlying mechanisms can only be hypothesised at this stage (2.3 and 3.1.3)
Soil water retention/availability	Adding biochar to soil can have direct and indirect effects on soil water retention, which can be short or long lived, and which can be negative or positive depending on soil type. Positive effects are dependent on high applications of biochar. No conclusive evidence was found to allow the establishment of an unequivocal relation between soil water retention and biochar application (3.1.2)
Soil compaction	Various processes associated with soil compaction are relevant to biochar application, some reducing others increasing soil compaction. Experimental research is lacking. The main risk to soil compaction could probably be reduced by establishing a guide of good practice regarding biochar application (3.1.1 and 4.6)
Priming effect	Some inconclusive evidence of a possible priming effect exists in the literature, but the evidence is relatively inconclusive and covers only the short term and a very restricted sample of biochar and soil types (3.2.5.4)
Effects on soil megafauna	Neither the effects of direct contact with biochar containing soils on the skin and respiratory systems of soil megafauna are known, nor the effects or ingestion due to eating other soil organisms, such as earthworms, which are likely to contain biochar in their guts (3.2.6.3)
Hydrophobicity	The mechanisms of soil water repellency are understood poorly in general. How biochar might influence hydrophobicity remains largely untested (3.1.2.1)
Enhanced decomposition of biochar due to agricultural management	It is unknown how much subsequent agricultural management practices (planting, ploughing, etc.) in an agricultural soil with biochar may influence (accelerate) the disintegration of biochar in the soil, thereby potentially reducing its carbon storage potential (3.2.3)
Soil CEC	There is good potential that biochar can improve the CEC of soil. However, the effectiveness and duration of this effect after addition to soils remain understood poorly (2.5 and 3.1.4)
Soil Albedo	That biochar will lower the albedo of the soil surface is fairly well established, but if and where this will lead to a substantial soil warming effect is untested (3.1.3)

6.1.1 Background and Introduction

As a concept biochar is defined as 'charcoal (biomass that has been pyrolysed in a zero or low oxygen environment) for which, owing to its inherent properties, scientific consensus exists that application to soil at a specific site is expected to sustainably sequester carbon and concurrently improve soil functions (under current and future management), while avoiding short- and long-term detrimental effects to the wider environment as well as human and animal health'. Inspiration is derived from the anthropogenically created Terra Preta soils (Hortic Anthrosols) in Amazonia where charred organic material plus other (organic and mineral) materials appear to have been added purposefully to soil to increase its agronomic quality. Ancient Anthrosols have been found in Europe as well, where organic matter (peat, manure, 'plaggen') was added to soil, but where charcoal additions appear to have been limited or non-existent. Furthermore, charcoal from wildfires (pyrogenic black carbon - BC) has been found in many soils around the world, including European soils where pyrogenic BC can make up a large proportion of total soil organic carbon.

Biochar can be produced from a wide range of organic feedstocks under different pyrolysis conditions and at a range of scales. Many different materials have been proposed as biomass feedstocks for biochar. The suitability of each biomass type for such an application is dependent on a number of chemical, physical, environmental, as well as economic and logistical factors. The original feedstock used, combined with the pyrolysis conditions will determine the properties, both physical and chemical, of the biochar product. It is these differences in physicochemical properties that govern the specific interactions which will occur with the endemic soil biota upon addition of biochar to soil, and hence how soil dependent ecosystem functions and services are affected. The application strategy used to apply biochar to soils is an important factor to consider when evaluating the effects of biochar on soil properties and processes. Furthermore, the biochar loading capacity of soils has not been fully quantified, or even developed conceptually.

6.1.2 Physicochemical properties of Biochar

Biochar is comprised of stable carbon compounds created when biomass is heated to temperatures between 300 to 1000°C under low (preferably zero) oxygen concentrations. The structural and chemical composition of biochar is highly heterogeneous, with the exception of pH, which is typically > 7. Some properties are pervasive throughout all biochars, including the high C content and degree of aromaticity, partially explaining the high levels of biochar's inherent recalcitrance. Nevertheless, the exact structural and chemical composition, including surface chemistry, is dependent on a combination of the feedstock type and the pyrolysis conditions (mainly temperature) used. These same parameters are key in determining particle size and pore size (macro, meso and micropore; distribution in biochar. Biochar's physical and chemical characteristics may significantly alter key soil physical properties and processes and are, therefore, important to consider prior to its application to soil. Furthermore, these will determine the suitability of each biochar for a given application, as well as define its behaviour, transport and fate in the

environment. Dissimilarities in properties between different biochar products emphasises the need for a case-by-case evaluation of each biochar product prior to its incorporation into soil at a specific site. Further research aiming to fully evaluate the extent and implications of biochar particle and pore size distribution on soil processes and functioning is essential, as well as its influence on biochar mobility and fate.

6.1.3 Effects on soil properties, processes and functions

This section has highlighted the relative paucity of knowledge concerning the specific mechanisms behind the reported interactions of biochar within the soil environment. However, while there is still much that is unknown, large steps have been taken towards increasing our understanding of the effects of biochar on soil properties and processes. Biochar interacts with the soil system on a number of levels. Sub-molecular interactions with clay and silt particles and SOM occur through Van der Waals forces and hydrophobic interactions. It is the interactions at this scale which will determine the influence of biochar on soil water repellency and also the interactions with cations and anions and other organic compounds in soil. These interactions are very char specific, with the exact properties being influenced by both the feedstock and the pyrolysis conditions used.

There has been some evidence to suggest that biochar addition to soil may lead to loss of SOM via a priming effect in the short term. However, there is only very little research reported in the literature on this subject, and as such it is a highly pertinent area for further research. The fact that Terra Pretas contain SOM as well as char fragments seems to demonstrate that the priming effect either does not exist in all situations or if it does, perhaps it only lasts a few seasons and it appears not to be sufficient to drive the loss of all native SOM from the soil. Biochar has the potential to be highly persistent in the soil environment, as evidenced both by its presence in Terra Pretas, even after millennia, and also as evidenced by studies discussed in this section. While biochars are highly heterogeneous across scales, it seems likely that properties such as recalcitrance and effects on water holding capacity are likely to persist across a range of biochar types. It also seems probable, that while difference may occur within biochars on a microscale, biochars produced from the same feedstocks, under the same pyrolysis conditions are likely to be broadly similar, with predictable effects upon application to soil. What remains to be done are controlled experiments with different biochars added to a range of soils under different environmental conditions and the precise properties and effects identified. This will lead towards biochars possibly being engineered for specific soils and climate where specific effects are required.

After its initial application to soil, biochar can function to stimulate the edaphic microflora and fauna due to various substrates, such as sugars, which can be present on the biochar's surface. Once these are metabolised, biochar functions more as a mineral component of the soil rather than an organic component, as evidenced by its high levels of recalcitrance meaning that it is not used as a carbon source for respiration. Rather, the biochar functions as a highly porous network the edaphic biota can colonise. Due to the large inherent porosity, biochar particles in soil can provide refugia for

microorganisms whereby they may often be protected from grazing by other soil organisms which may be too large to enter the pores. This is likely to be one of the main mechanisms by which biochar-amended soils are able to harbour a larger microbial biomass when compared to non-biochar amended soils. Biochar incorporation into soil is also expected to enhance overall sorption capacity of soils towards trace anthropogenic organic contaminants (e.g. PAHs, pesticides, herbicides), in a stronger way, and mechanistically different, from that of native organic matter. Whereas this behaviour may greatly contribute to mitigating toxicity and transport of common pollutants in soil, biochar aging over time may result in leaching and increased bioavailability of such compounds. On the other hand, while the feasibility for reducing mobility of trace contaminants in soil might be beneficial, it might also result in their localised accumulation, although the extent and implications of this have not been experimentally assessed.

Soil quality may not be necessarily improved by adding biochar to soil. Soil quality can be considered to be relatively high for supporting plant production and provision of ecosystem services if it contains carbon in the form of complex and dynamic substances such as humus and SOM. If crop residues are used for biochar, the proportion of carbon going into the dynamic SOM pool is likely to be reduced, with the carbon being returned to the soil in a relatively passive biochar form. The proportion of residues which are removed for pyrolysis versus the proportion which is allowed to remain in the soil will determine the balance between the dynamic SOM and the passive biochar and so is likely to affect soil quality for providing the desired roles, be it provision of good use as crop or timber, or functioning as a carbon pool. Biochar also has the potential to introduce a wide range of hazardous organic compounds (e.g. heavy metals, PAHs) into the soil system, which can be present as contaminants in biochar that has been produced either from contaminated feedstocks or under processing conditions which favour their production. While a tight control over the feedstock type and processing conditions used can reduce the potential risk for soil contamination, experimental evidence of the occurrence and bioavailability and toxicity of such contaminants in biochar and biochar-enriched soil (over time) remain scarce. A comprehensive risk assessment of each biochar product prior to its incorporation into soil, which takes into account the soil type and environmental conditions, is therefore, paramount.

Increased crop yields are the most commonly reported benefits of adding biochar to soils. A full search of the scientific literature led to a compilation of studies used for a meta-analysis of the effects of biochar application to soils and plant productivity. Meta-analysis techniques (Rosenberg et al., 1997) were used to quantify the effect of biochar addition to soil on plant productivity from a range of experiments. Our results showed a small overall, but statistically significant, positive effect of biochar application to soils on plant productivity in the majority of cases, covering a range of both soil and crop types. The greatest positive effects were seen on acidic free-draining soils with other soil types, specifically Calcarosols showing no significant effect. No statistically significant negative effects were found. There was also a general trend for concurrent increases in crop productivity with increases in pH up on biochar addition to soils. This suggests that one of the main mechanisms

behind the reported positive effects of biochar application to soils on plant productivity may be a liming effect. These results underline the importance of testing each biochar material under representative conditions (i.e. soil-environment-climate-management factors).

The degree and possible consequences of the changes biochar undergo in soil over time remain largely unknown. Biochar loss and mobility through the soil profile and into water resources has so far been scarcely quantified and the underlying transport mechanisms are poorly understood. This is further complicated by the limited amount of long-term studies and the lack of standardised methods for simulating biochar aging and for long-term environmental monitoring.

6.1.4 Biochar and soil threats

This chapter has described the interactions between biochar and 'threats to soil'. For most of these interactions, the body of scientific evidence is currently insufficient to arrive at a consensus. However, what is clear is that biochar application to soils will effect soil properties and processes and thereby interact with threats to soil. Awareness of these interactions, and the mechanisms behind them, is required to lead to the research necessary for arriving at understanding mechanisms and effects on threats to soil, as well as the wider ecosystem.

6.1.5 Wider issues

Biochar can be produced from a wide range of organic feedstocks under different pyrolysis conditions and at a range of scales. The original feedstock used, combined with the pyrolysis conditions will affect the exact physical and chemical properties of the final biochar, and ultimately, the way and the extent to which soil dependent ecosystem services are affected. Preliminary evidence appears to suggest that a tight control on the feedstock materials and pyrolysis conditions (mainly temperature) may be enough in attenuating much of the current concern relating to the high levels of atmospheric pollutants (e.g. PAHs, dioxins) and particulate matter that may be emitted during biochar production, while implications to human health remain mostly an occupational health issue. Health (e.g. dust exposure) and fire hazards associated to production, transport, application and storage need to be considered when determining the suitability of the biochar for a given application, while tight health and safety measures need to be put in place to mitigate such risks for the worker, as well as neighbouring residential areas. The profitability of any biochar operation will depend mainly on its potential to attract revenue as a soil additive and C sink and will be affected by the type of biomass feedstock and that of production (open vs closed, local vs centralised), which can, in turn, result in environmental and economic spillovers. Moreover, the demand for biochar, as a byproduct of pyrolysis, will be influenced by, and will indeed influence, the demand for biofuels, the demand for products such as manure and compost and the price of carbon in the carbon markets. Furthermore, the costs and benefits of a range of biochar operations and scenarios need to be quantified. Cost-benefit analyses ought to cast the net wide by accounting not only for commercial factors but also for social costs and benefits.

6.2 Synthesis

The aim of this report was to review the state-of-the-art regarding the interactions between biochar application to soils and effects on soil properties, processes and functions. Adding biochar to soil is not an alternative to reducing the emissions of greenhouse gasses. Minimising future climate change requires immediate action to lower greenhouse gas emissions and harness alternative forms of energy (IPCC, 2007).

6.2.1 Irreversibility

The irreversibility of biochar application to soils has implications for its development. Once biochar has been applied to soils, it is virtually impossible to remove. This irreversibility does not have to be a deterrent from considering biochar. Rather, the awareness of its irreversibility should lead to a careful case-by-case assessment of its impacts, underpinned by a comprehensive body of scientific evidence gathered under representative soil-environment-climate-management conditions. Meta-analyses, an example of which on the relationship between biochar and crop productivity is presented in this report, can provide a valuable method for both signalling gaps in knowledge as well as providing a quantitative review of published experimental results. The results of meta-analyses can then be used to feed back to directing funding for more research where needed, and/or to inform specific policy development. Objectivity of systematic reviews on biochar is of paramount importance. In the medical sciences this has been resolved by the founding of an independent organisation (the Cochrane Collaboration), which provides regularly updated systematic reviews on specific healthcare issues using a global network of volunteers and a central database/library. A similar approach, although at a different scale, could be envisaged to ensure that the most robust and up to date research informs policy concerning biochar. Alternatively, this task could be performed by recognised, independent scientific institutions that do not (even partially) depend on conflicting funding, and that have the necessary expertise.

6.2.2 Quality assessment

The evidence reviewed in this report has highlighted potential negative as well as positive effects on soils and, importantly, a very large degree of unknown effects (see Table 6.1; and Section 6.3). Some of the potential negative effects can be 'stopped at the gate', i.e. by not allowing specific feedstocks that have been proven to be inappropriate, and by regulating pyrolysis conditions to avoid undesirable biochar properties (a compulsory biochar quality assessment and monitoring approach could prove effective). Other potential negative effects on soils, or the wider ecosystem, need to be regulated on the application side, i.e. at the field scale, taking into account the soil properties and processes as well as threats to soil functions. Similarly, biochar properties can be 'engineered' (to an extent), through controlled use of feedstocks and pyrolysis conditions, to provide necessary benefits to soil functions and reduce threats when applied to fields that have specific soil-environmental-climatic-management conditions. However, the current state-of-the-art regarding the effects of biochar on soils has a substantial lack of

information on relevant factors (see Section 6.3). Results from research into the relative importance of these factors, and the associated environmental and soil management conditions, needs to drive further extension and development of a biochar quality assessment protocol.

6.2.3 Scale and life cycle

Relevant factors for producing biochar with specific properties are feedstock characteristics and pyrolysis conditions, thereby affecting the scale and method of operation. The optimal scale of operation, from a soil improvement and climate adaptation perspective, will differ for different locations, as the availability of feedstocks and the occurrence of soil-environment-climate-management conditions changes along with land use. The optimal scale of operation, from a climate mitigation perspective, is, intuitively, the smallest scale. However, full life cycle assessment studies to evidence this have not been found. It is possible that at a larger scale of operation, if not production then at least application, a more complementary situation exists with larger concomitant reductions in CO₂ equivalent emissions by the ability to forego or reduce certain operations. For example, a farm on a fertile floodplain, with good water availability, may produce biochar from feedstocks on the farm with good water and nutrient retention properties. If this is applied to soils on the same farm, it may allow a reduction of a single fertiliser pass. However, if the biochar is sold (or traded) to the farm next door, which may be on soils with low water and nutrient retention, then there may be a reduction of two fertiliser passes and a substantial reduction in irrigation, for example. It is possible, therefore, that the CO₂ equivalents saved on the farm next door are more than the CO₂ equivalent emissions produced during transport from one farm to the other. This is of course just one hypothetical example of how off-site biochar distribution does not necessarily decrease the carbon negativity of the technology. One critical factor affecting this is the way long-lived specific beneficial effects of specific biochars will be under specific conditions. Experimental studies of sustained effects, e.g. nutrient and water retention, of different biochars in different soil-environment-climate-management combinations are needed to feed into life cycle assessment studies. It is possible that the optimum scale of operation, in terms of global warming mitigation, will be different in different parts of Europe and the world.

6.2.4 Mitigation/adaptation

Besides global warming mitigation, biochar can also be viewed from the perspective of adaptation to climate change. In the future, climate change looks likely to increase rainfall intensity, if not annual totals, for example thereby increasing soil loss by water erosion, although there is much uncertainty about the spatio-temporal structure of this change as well as the socio-economic and agronomic changes that may accompany them. Independent from changes in climate, the production function of soil will become increasingly more important, in view of the projected increase in global human population and consequent demands for food. More than 99% of food supplies (calories) for human consumption come from the land, whereas less than 1% comes from oceans and other aquatic ecosystems (FAO, 2003).

A common way of thinking about adapting food production to climate change is by genetically engineering crops to survive and produce under adverse and variable environmental conditions. This may well work, if risks to the environment are minimised and public opinion favourable. However, other soil functions are likely to still be impaired and threats exacerbated, such as increased loss of soil by erosion. Improving the properties of soil will increase the adaptive capacity of our agri-environmental systems. The ClimSoil report (Schils et al., 2008) reviews in detail the interrelation between climate change and soils. One of their conclusions is that land use and soil management are important tools that affect, and can increase, SOC stocks. In this way, the soils will be able to function better, even under changing climatic conditions. In arable fields, SOM content is maintained in a dynamic equilibrium. Arable soil is disturbed too much for it to maintain greater contents of SOM than a specific upper limit, which is controlled by mainly clay contents and the soil wetness regime. Biochar, because of its recalcitrance, and possibly because of its organo-mineral interaction and accessibility, provides a means of potentially increasing the relevant functions of soils beyond that which can be achieved by OM alone in arable systems.

Biochar application to soils, therefore, may play both a global warming mitigation and a climate change adaptation role. For both, more research is needed before conclusive answers can be given with a high degree of scientific certainty, particularly when considering specific soil-environment-climate-management conditions and interactions. However, it may be the case that in certain situations the biochar system does not mitigate global warming, i.e. is C neutral or positive, but that the enhanced soil functions from biochar application may still warrant contemplation of its use.

As far as the current scientific evidence allows us to conclude, biochar is not a 'silver bullet' or panacea for the whole host of issues ranging from food production and soil fertility to mitigating (or more correctly 'abating') global warming and climate change for which it is often posited. The critical knowledge gaps are manifold, mainly because the charcoal-rich historic soils, as well as most experimental sites, have been studied mostly in tropical environments, added to the large range of biochar properties that can be produced from the feedstocks currently available subjected to different pyrolysis conditions. Biochar analogues, such as pyrogenic BC, are found in varying, and sometimes substantial amounts in soils all over the world. As well as causing some difficulty with predicting possible impacts of biochar addition to soil, the large variety in biochar properties that can be produced actually provides an opportunity to 'engineer' biochar for specific soil-environment-climate-management conditions, thereby potentially increasing soil functioning and decreasing threats to soil (and/or adapting to climate change). What is needed is a much better understanding of the mechanisms concerning biochar in soils and the wider environment. Although the research effort that would be required is substantial, the necessary methods are available.

6.3 Knowledge gaps

Table 6.1 lists ‘unknown’ effects of biochar on soil properties, processes and functions. For ‘known’ positive or negative effects, Table 6.1 also discusses (briefly but with reference to more elaborate discussions in the report) the soil-environment-climate-management conditions for which the effects are valid and where they are not (known). From the viewpoint of biochar effects on soil functions and soil threats, a number of key issues emerge that are discussed in the subsections below. Biochar research should aim to reach a sufficient level of scientific knowledge to underpin future biochar policy decisions. This review indicates that a large number of questions related to biochar application to soils remain unanswered. The multitude of gaps in current knowledge associated with biochar properties, the long-term effects of biochar application on soil functions and threats, and its behaviour and fate in different soil types (e.g. disintegration, mobility, recalcitrance, interaction with SOM), as well as sensitivity to management practices, require more scientific research.

6.3.1 Safety

While the widespread interest in biochar applications to soils continues to rise, issues remain to be addressed concerning the potential for soil contamination and atmospheric pollution associated to its production and handling, with potentially severe health, environmental and socio-economic implications. The irreversibility of biochar incorporation into soil emphasises the urgent need for a full and comprehensive characterisation of each biochar type in regard to potential contaminants (mainly heavy metals and PAHs), as influenced by biomass feedstock and pyrolysis conditions. Very little focus has been paid to the long-term distribution of such contaminants in biochar-enriched soils and bioavailability to the micro- and macro-biota. In this context, risk assessment procedures for these compounds need to be re-evaluated on a case-by-case basis, based on bioavailable concentrations (rather than initial concentrations in biochar) and accounting for the influence of NOM on their desorption from biochar over time. This would allow understanding the true implications of their presence in biochar on human, animal and ecosystem health over a wide range of soil conditions, while enabling relation of toxicity to biochar type and safe application rates, as well as feedstock characteristics and pyrolysis conditions. Similarly, the emission of atmospheric pollutants during biochar production requires careful qualitative and quantitative analysis. It will provide a sound basis for the development and/or optimisation of feedstock and pyrolysis operational conditions (as well as technologies) required to tackle these pollutants.

6.3.2 Soil organic matter dynamics

Biochar can function as a carbon sink in soils under certain conditions. However, the reported long residence times of biochar have not been confirmed for today’s intensive agricultural systems in temperate regions. Disintegration of biochar is likely to be stimulated by intensive agricultural practices (tilling, ploughing, harrowing) and use of heavy machinery, thereby potentially reducing residence times. Work is required to better elucidate the biochar loading capacity of different soils, for different climatic conditions in order to maximise the amount of biochar which can be stored in soils without impacting negatively on soil functions. In addition to crop yields, research

should also focus on threshold amounts of biochar that can be added to soils without adverse consequences to soil physical properties, such as priming by increasing the pH or decreasing water-filled pore space, hydrophobic effects, or soil chemical properties, e.g. adding a high ash content (with salts) biochar to a soil already at risk of salinisation, or other ecosystem components, e.g. particulate or dissolved organic C reaching ground/surface waters. Therefore, the biochar loading capacity should vary according to environmental conditions as well as biochar 'quality', specific to the environmental conditions of the site (soil, geomorphology, hydrology, vegetation).

6.3.3 Soil biology

Owing to the vital role that the soil biota plays in regulating numerous ecosystem services and soil functions, it is vital that a full understanding of the effects of biochar addition to soil is reached before policy is written. Due to the very high levels of heterogeneity found in soils, with regard to soil physical, chemical and biological properties, extensive testing is needed before scientifically sound predictions can be made regarding the effects of biochar addition to soils on the native edaphic communities under a range of climatic conditions. Much of the data currently reported in the literature shows a slight, but significant positive effect on the soil biota, with increased microbial biomass and respiration efficiency per unit carbon, with associated increases in above ground biomass production reported in the majority of cases. There is currently a major gap in our understanding of the influence of biochar addition to soils on carbon fluxes. This is vital to increase our understanding of interactions between the soil biota and biochar as it will help to unravel the mechanisms behind any possible priming effect, as well as nutrient transfer and interactions with contaminants introduced with biochar. A very suitable method for probing this interaction would be the use of Stable Isotope Probing (SIP), which can be used with other molecular techniques to trace the flow of carbon from particular sources through the soil system. Pyrolysing biomass labeled with a stable isotope and measuring its emission from the soil will allow accurate measures of its recalcitrance over time. Conducting controlled atmosphere experiments with stable isotope-labelled CO₂ will enable assessing the observed increased microbial respiration and investigation of whether this increase is due to a more efficient use of plant provided substrates (in case the label is detected in soil respiration), or if a priming effect has occurred leading to increased metabolisation of the SOM (in case the label is not detected).

6.3.4 Behaviour, mobility and fate

Physical and chemical weathering of biochar over time has implications for its solubilisation, leaching, translocation through the soil profile and into water systems, as well as interactions with other soil components (including contaminants). Up to now, biochar loss and environmental mobility have been quantified scarcely and such processes remain poorly understood. In addition, the contribution of soil management practices and the effects of increasingly warmer climates, together with potential greater erosivity as potential key mechanisms controlling biochar fate in soil, have also been assessed insufficiently up to now.

An effective evaluation of the long-term stability and mobility of biochar, including the way these are influenced by factors relating to biochar physicochemical characteristics, pyrolysis conditions and environmental factors, is paramount to understanding the contribution that biochar can make to improving soil processes and functioning, and as a tool for sequestering carbon. Such knowledge should derive from long-term studies involving a wide range of soil conditions and climatic factors, while using standardised methods for simulating biochar aging and for long-term environmental monitoring.

6.3.5 Agronomic effects

Biochar has shown merit in improving the agronomic and environmental value of agricultural soils in certain pilot studies under limited environmental conditions, but a scientific consensus on the agronomic and environmental benefits of biochar has not been reached yet. It remains difficult to generalise these studies due to the variable nature of feedstocks, their local availability, the variability in resulting biochar and the inherent biophysical characteristics of the sites it has been applied to, as well as the variability of agronomic practices it could be exposed to. Furthermore, there is a lack of (long-term) studies on the effects of biochar application in temperate regions. Direct and indirect effects of biochar on soil hydrology (e.g. water availability to plants) need to be studied experimentally for representative conditions in the field and in the laboratory (soil water retention – pF - curves) before modelling exercises can begin. Ultimately, in those conditions where biochar application is beneficial to agriculture and environment, it should be considered as part of a soil conservation package aimed at increasing the resilience of the agro-environmental system combined with the sequestration of carbon. The key is to identify the agri-soil management strategy that is best suited at a specific site. Other carbon sequestration and conservation methods, such as no-till, mulching, cover crops, complex crop rotations, mixed farming systems and agroforestry, or a combination of these, need to be considered. In this context the interaction of biochar application with other methods warrants further investigation.

References

- Almendros, G., Knicker, H., González-Vila, F. J., 2003. Rearrangement of carbon and nitrogen forms in peat after progressive thermal oxidation as determined by solid-state ^{13}C - and ^{15}N -NMR spectroscopy. *Organic Geochemistry* 34: 1559-1568.
- Amonette, J.E., Joseph, S., 2009. Characteristics of Biochar: Microchemical Properties. In: J. Lehmann, Joseph, S. (Editor), *Biochar for Environmental Management Science and Technology*. Earthscan, London.
- Anikwe, M.A.N. and Nwobodo, K.C.A., 2002. Long term effect of municipal waste disposal on soil properties and productivity of sites used for urban agriculture in Abakaliki, Nigeria. *Bioresource Technology* 83(3): 241-250.
- Antal Jr, M.J. and Grönli, M., 2003. The art, science, and technology of charcoal production. *Industrial and Engineering Chemistry Research* 42(8): 1619-1640.
- Ascough, P.L., Bird, M.I., Wormald, P., Snape, C.E. and Apperley, D., 2008. Influence of production variables and starting material on charcoal stable isotopic and molecular characteristics. *Geochimica et Cosmochimica Acta* 72(24): 6090-6102.
- Augusto, L., Bakker, M.R. and Meredieu, C., 2008. Wood ash applications to temperate forest ecosystems - Potential benefits and drawbacks. *Plant and Soil* 306(1-2): 181-198.
- Ayodele, A, Oguntunde, P, Joseph, A and de Souza Dias Junior, M, 2009. Numerical analysis of the impact of charcoal production on soil hydrological behavior, runoff response and erosion susceptibility. *Revista Brasileira de Ciência do Solo*, 33:137-145.
- Baldock, J. A., Smernik, R. J., 2002. Chemical composition and bioavailability of thermally altered *Pinus resinosa* (red pine) wood. *Organic Geochemistry* 33: 1093-1109.
- Bird, M. I., Moyo, C., Veenendaal, E. M., Lloyd, J., Frost, P., 1999. Stability of elemental carbon in a savanna soil. *Global Biogeochemical Cycles* 13: 923-932.
- Bird, M.I., Ascough, P.L., Young, I.M., Wood, C.V. and Scott, A.C., 2008. X-ray microtomographic imaging of charcoal. *Journal of Archaeological Science* 35(10): 2698-2706.
- Blackwell, P., Reithmuller, G. and Collins, M., 2009. Biochar application to soil. In: J. Lehmann and S. Joseph (Editors), *Biochar for Environmental Management: Science and Technology* Earthscan.
- Blanco-Canqui, H. and Lal, R., 2008. Corn stover removal impacts on micro-scale soil physical properties. *Geoderma* 145(3-4): 335-346.
- Blume, H.P. and Leinweber, P., 2004. Plaggen soils: Landscape history, properties, and classification. *Journal of Plant Nutrition and Soil Science* 167(3): 319-327.

- Boag B., J., H. D., Neilson, R., Santoro, G., 1999. Spatial distribution and relationship between the New Zealand flatworm *Arthurdendyus triangulatus* and earthworms in a grass field in Scotland. *Pedobiologia*,43: 340-344.
- Boardman, J., Favismortlock, D.T., 1993. Climate-change and soil-erosion in Britain. *Geographical Journal* 159: 179–183.
- Borm, P. J. A., Kreyling, W., 2004. Toxicological hazards of inhaled nanoparticles: implications for drug delivery. *Journal of Nanoscience and Nanotechnology* 4: 1-11.
- Borm, P.J.A., Robbins, D., Haubold, S., Kuhlbusch, T., Fissan, H., Donaldson K., Schins, R., Stone, V., Kreyling, W., Lademann, J., Krutmann, J., Warheit, D., Oberdorster, E., 2006. The potential risks of nanomaterials: a review carried out for ECETOC. *Particle and Fibre Toxicology* 3: 11.
- Borm, P.J.A., Cakmak, G., Jermann, E., Weishaupt, C., Kempers, P., Van Schooten, F. J., Oberdärster, G., and Schins, R. P. F., 2005. Formation of PAH-DNA adducts after in vivo and vitro exposure of rats and lung cells to different commercial carbon blacks. *Toxicology and Applied Pharmacology* 205(2): 157-167.
- Borm, P.J.A., Schins, R.P.F. and Albrecht, C., 2004. Inhaled particles and lung cancer, part B: Paradigms and risk assessment. *International Journal of Cancer* 110(1): 3-14.
- Bourke, J., Manley-Harris, M., Fushimi, C., Dowaki, K., Nunoura, T., Antal, M. J. Jr., 2007. Do all carbonised charcols have the same structure? A model of the chemical structure of carbonized charcoal. *Industrial and Engineering Chemistry Research* 46: 5954-5967.
- Boxall, A.B.A., Tiede, K., Chaudhry, Q., 2007. Engineered nanomaterials in soils and water: how do they behave and how could they pose a risk to human health? *Nanomedicine* 2 (6): 919-927.
- Brady, N. C., 1990. The nature and properties of soils. 10th Ed. Prentice-Hall.
- Brewer, C.E., Schmidt-Rohr, K., Satrio, J.A. and Brown, R.C., 2009. Characterization of biochar from fast pyrolysis and gasification systems. *Environmental Progress and Sustainable Energy* 28(3): 386-396.
- Bridle, T. R., Pritchard, D., 2004. Energy and nutrient recovery from sewage sludge via pyrolysis. *Water Science Technology* 50: 169-175.
- Briggs, C.M., Breiner, J., and Graham, R.C., 2005. Contributions of Pinus Ponderosa Charcoal to Soil Chemical and Physical Properties. The ASA-CSSA-SSSA International Annual Meetings (November 6-10, 2005), Salt Lake City, U.S.A.
- Briones, M.J.I., Ineson, P. and Heinemeyer, A., 2007. Predicting potential impacts of climate change on the geographical distribution of enchytraeids: A meta-analysis approach. *Global Change Biology* 13(11): 2252-2269.

- Brodowski, S., Amelung, W., Haumaier, L., Abetz, C., Zech, W., 2005. Morphological and chemical properties of black carbon in physical soil fractions as revealed by scanning electron microscopy and energy-dispersive X-ray spectroscopy. *Geoderma* 128: 116-129.
- Brodowski, S., John, B., Flessa, H. and Amelung, W., 2006. Aggregate-occluded black carbon in soil. *European Journal of Soil Science* 57(4): 539-546.
- Brown, M. A., Levine, M. D., Short, W., and Koomey, J. G., 2001. Scenarios for a clean energy future. *Energy Policy* 29: 1179-1196.
- Brown, R., 2009. Biochar Production Technology. In: *Biochar for Environmental Management: Science and Technology* (Eds. Lehmann, J. & Joseph, S.), Earthscan.
- Bruun, S. and Luxhøi, J., 2008. Is biochar production really carbon-negative? *Environmental Science and Technology* 42(5): 1388.
- Bucheli, T., Gustafsson, Ö., 2000. Quantification of the soot-water distribution coefficients of PAHs provides mechanistic basis for enhanced sorption observations. *Environmental Science and Technology* 34: 5144-5151.
- Bucheli, T., Gustafsson, Ö., 2001. Ubiquitous observations of enhanced solid affinities for aromatic organochlorines in field situations: are in situ dissolved exposures overestimated by existing partitioning models? *Environmental Toxicology and Chemistry* 20: 1450-1456.
- Bucheli, T., Gustafsson, Ö., 2003. Soot sorption of non-ortho and ortho substituted PCBs. *Chemosphere* 53: 515-522.
- Buzea, C., Pacheco, I.I. and Robbie, K., 2008. Nanomaterials and nanoparticles: Sources and toxicity. *Biointerphases* 2(4): 17-71.
- Cetin, E., Moghtaderi, B., Gupta, R., Wall, T. F., 2004. Influence of pyrolysis conditions on the structure and gasification reactivity of biomass chars. *Fuel* 83: 2139-2150.
- Chan, K. Y., van Zwieten, L., Meszaros, I., Downie, A. Joseph, S., 2007a. Assessing the agronomic values of contrasting char materials on Australian hardsetting soil. *Proceedings Conference of the International Agrichar Initiative, 30 May – 2 April, 2007, Terrigal, Australia.*
- Chan, K. Y., Xu, Z., 2009. Biochar: Nutrient Properties and Their Enhancement. In: *Biochar for Environmental Management: Science and Technology* (Eds. Lehmann, J. & Joseph, S.), Earthscan.
- Chan, K.Y., Van Zwieten, L., Meszaros, I., Downie, A. and Joseph, S., 2007. Agronomic values of greenwaste biochar as a soil amendment. *Australian Journal of Soil Research* 45(8): 629-634.
- Chan, K.Y., Van Zwieten, L., Meszaros, I., Downie, A. and Joseph, S., 2008. Using poultry litter biochars as soil amendments. *Australian Journal of Soil Research* 46(5): 437-444.
- Chaplot, V. A. M., Rumpel, C., Valentin, C., 2005. Water erosion impact on soil and carbon redistributions within uplands of Mekong River. *Global Biogeochemical Cycles* 19 (4): 20-32.

- Chen, J., Zhu, D., Sun, C., 2007. Effect of heavy metals on the sorption of hydrophobic organic compounds to wood charcoal. *Environmental Science and Technology* 41: 2536-2541.
- Cheng, C. H., Lehmann, J., Engelhard, M., 2008. Natural oxidation of black carbon in soils: changes in molecular form and surface charge along a climosequence. *Geochimica et Cosmochimica Acta* 72: 1598-1610.
- Cheng, C-H, Lehmann, J., Thies, J., Burton, S. D., Engelhard, M. H., 2006. Oxidation of black carbon by biotic and abiotic processes. *Organic Geochemistry* 37: 1477-1488.
- Chiou, C. T., Kile, D. E., 1998. Deviations from sorption linearity on soils of polar and nonpolar organic compounds at low relative concentrations. *Environmental Science and Technology* 32: 338-343.
- Chun, Y., Sheng, G., Chiou, C. T., Xing, B., 2004. Compositions and Sorptive Properties of Crop Residue-Derived Chars. *Environmental Science and Technology* 38: 4649-4655.
- Cleary, J., Roulet, N.T. and Moore, T.R., 2005. Greenhouse gas emissions from Canadian peat extraction, 1990-2000: A life-cycle analysis. *Ambio* 34(6): 456-461.
- Cohen-Ofri, I., Popovitz-Niro, R., Weiner, S., 2007. Structural characterization of modern and fossilized charcoal produced in natural fires as determined by using electron energy loss spectroscopy. *Chemistry – A European Journal* 13: 2306-2310.
- Cornelissen, G., Gustafsson, Ö., 2004. Sorption of phenanthrene to environmental black carbon in sediment with and without organic matter and native sorbates. *Environmental Science and Technology* 38: 148-155.
- Cornelissen, G., Gustafsson, Ö., 2005. Importance of unburned coal carbon, black carbon, and amorphous organic carbon to phenanthrene sorption in sediments. *Environmental Science and Technology* 39: 764-769.
- Cornelissen, G., Gustafsson, Ö., Bucheli, T. D., Jonker, M. T. O., Koelmans, A. A., van Noort, P. C. M., 2005. Extensive sorption of organic compounds to black carbon, coal and kerogen in sediments and soils: mechanisms and consequences for distribution, bioaccumulation and biodegradation. *Environmental Science and Technology* 39: 6881-6895.
- Curtis, P.S. and Wang, X., 1998. A meta-analysis of elevated CO₂ effects on woody plant mass, form, and physiology. *Oecologia* 113(3): 299-313.
- Davidson, D.A., Dercon, G., Stewart, M. and Watson, F., 2006. The legacy of past urban waste disposal on local soils. *Journal of Archaeological Science* 33(6): 778-783.
- Day, D., Evans, R.J., Lee, J.W. and Reicosky, D., 2005. Economical CO₂, SO_x, and NO_x capture from fossil-fuel utilization with combined renewable hydrogen production and large-scale carbon sequestration. *Energy* 30(14): 2558-2579.

- De Graaff, M.A., van Groenigen, K.J., Six, J., Hungate, B. and van Kessel, C., 2006. Interactions between plant growth and soil nutrient cycling under elevated CO₂: A meta-analysis. *Global Change Biology* 12(11): 2077-2091.
- De Jonge, L.W., Jacobsen, O.H., Moldrup, P., 1999. Soil water repellency: effects of water content, temperature, and particle size. *Soil Science Society of America Journal* 63: 437–442.
- DeBano, L. F., 2000. Water repellency in soils: a historical overview. *Journal of Hydrology* 231-232: 4-32.
- Demirbas, A., 2004. Effects of temperature and particle size on bio-char yield from pyrolysis of agricultural residues. *Journal of Analytical and Applied Pyrolysis* 72(2): 243-248.
- Demirbas, A., 2008. Biofuels sources, biofuel policy, biofuel economy and global biofuel projections. *Energy Conversion and Management* 49(8): 2106-2116.
- Derfus, A., Chan, W., Bhatia, S. N., 2004. Probing the cytotoxicity of semiconductor quantum dots. *Nanoletters* 4 (1): 11-18.
- Derfus, A.M., Chan, W.C.W. and Bhatia, S.N., 2004. Probing the Cytotoxicity of Semiconductor Quantum Dots. *Nano Letters*, 4(1): 11-18.
- Diaz-Zorita, M., Buschiazzo, D. E., and Peinemann, N. (1999). Soil organic matter and wheat productivity in the semiarid Argentine pampas. *Agronomy Journal* 91: 276-279.
- Dickens, A.F., Gudeman, J.A., Gélinas, Y., Baldock, J.A., Tinner, W., Hu, F.S., and Hedges, J.I., 2007. Sources and distribution of CuO-derived benzene carboxylic acids in soils and sediments. *Organic Geochemistry* 38(8): 1256-1276.
- Ding, Q., Liang, P., Song, F., Xiang, A., 2006. Separation and preconcentration of silver ion using multi-walled carbon nanotubes as solid phase extraction sorbent. *Separation Science and Technology* 41: 2723-2732.
- Doerr, S. H., Shakesby, R.A., Walsh, R.P.D., 2000. Soil water repellency: its causes, characteristics and hydro-geomorphological significance. *Earth Science Reviews* 51: 33-65.
- Downie, A., Crosky, A., Munroe, P., 2009. Physical properties of biochar. In: *Biochar for Environmental Management: Science and Technology* (Eds. Lehmann, J. & Joseph, S.), Earthscan.
- Downie, A., van Zwieten, L., Doughty, W., Joseph, F., 2007. Nutrient retention characteristics of chars and the agronomic implications. *Proceedings, International Agrichar Initiative Conference, 30th April - 2nd May 2007, Terrigal, Australia.*
- Earl, B., 1995. Tin smelting. *The Oriental Institute News and Notes*, 146.
- Edwards, J., 2009. Pyrolysis of Biomass to Produce Bio-oil, Biochar and Combustible Gas Energy Postgraduate Conference 2008. School of Engineering and Advanced Technology Massey University.

- EPA, 2007. Nanotechnology White Paper. U.S. Environmental Protection Agency Report EPA 100/B-07/001, Washington DC 20460, USA.
- Falloon, P. D., Smith, P., Smith, J. U., Szabo, J., Coleman, K., and Marshall, S., 1998. Regional estimates of carbon sequestration potential: linking the Rothamsted Carbon Model to GIS databases. *Biology and Fertility of Soils* 27: 236-241.
- FAO, 2003. Food Balance Sheet. Last modified 08/06/2008: <http://faostat.fao.org/site/502/default.aspx>.
- Fernandes, M. B. and Sicre, M.A., 1999. Polycyclic aromatic hydrocarbons in the Arctic: Ob and Yenisei estuaries and Kara Sea shelf. *Estuarine, Coastal and Shelf Science* 48: 725-737.
- Fernandes, M.B. and Brooks, P., 2003. Characterization of carbonaceous combustion residues: II. Nonpolar organic compounds. *Chemosphere* 53(5): 447-458.
- Fernandes, M.B., Skjemstad, J.O., Johnson, B.B., Wells, J.D. and Brooks, P., 2003. Characterization of carbonaceous combustion residues. I. Morphological, elemental and spectroscopic features. *Chemosphere*, 51(8): 785-795.
- Fontaine, S., Bardoux, G., Benest, D., Verdier, B., Mariotti, A., and Abbadie, L., 2004. Mechanisms of the Priming Effect in a Savannah Soil Amended with Cellulose. *Soil Science Society of America Journal* 68(1): 125-131.
- Fontaine, S., 2007. The priming effect and its implication for soil modeling, Disentangling Abiotic and Biotic Effects on Soil Respiration. Innsbruck, 12th - 13th March 2007.
- Forbes, M. S., Raison, R. J., Skjemstad, J. O., 2006. Formation, transformation and transport of black carbon (charcoal) in terrestrial and aquatic ecosystems. *Science of the Total Environment* 370: 190-206.
- Fortner, J.D., Lyon, D.Y., Sayes, C.M., Boyd, A.M., Falkner, J.C., Hotze, E.M., Alemany, L.B., Tao, Y.J., Guo, W., Ausman, K.D., Colvin, V.L., Hughes, J.B., 2005. C60 in water: nanocrystal formation and microbial response. *Environmental Science and Technology* 39: 4307-4316.
- Fowles, M., 2007. Black carbon sequestration as an alternative to bioenergy. *Biomass and Bioenergy* 31(6): 426-432.
- Freibauer, A., rounsevell, M.D.A., Smith, P. and Verhagen, J., 2002. "Background paper on carbon sequestration in agricultural soils, under article 3.4 of the Kyoto Protocol," Rep. No. Contract N°.2001.40.CO001.
- Garcia-Perez, M., 2008. The formation of polyaromatic hydrocarbons and dioxins during pyrolysis. In: Washington State University.
- Gaskin, J.W., Steiner, C., Harris, K., Das, K.C. and Bibens, B., 2008. Effect of low-temperature pyrolysis conditions on biochar for agricultural use. *Transactions of the ASABE* 51(6): 2061-2069.

- Gaunt J. and Cowie A., 2009. Biochar, Greenhouse Gass Accounting and Emissions Trading. In: Biochar for environmental management: Science and technology. (eds. Lehmann, J., and Joseph, S). Earthscan Ltd, London.
- Gaunt, J.L. and Lehmann, J., 2008. Energy balance and emissions associated with biochar sequestration and pyrolysis bioenergy production. *Environmental Science and Technology* 42(11): 4152-4158.
- Giani, L., Chertov, O., Gebhardt, C., Kalinina, O., Nadporozhskaya, M., and Tolkdorf-Lienemann, E., 2004. Plagganthrepts in northwest Russia? Genesis, properties and classification. *Geoderma* 121(1-2): 113-122.
- Giby, J., Blair, A., Barab, J., Kaszniack, M., MacKensie, C., 2007. Combustible dusts: a serious industrial hazard. *Journal of Hazardous Materials* 142: 589-591.
- Glaser B., Guggenberger G., Zech W, 2004. Identifying the Pre-Columbian anthropogenic input on present soil properties of Amazonian Dark Earth (Terra Preta). In: Glaser, B., Woods, W. (Eds.) Amazonian Dark Earths: Explorations in Space and Time. Springer, Heidelberg, 215 pp.
- Glaser, B., Balashov, E., Haumaier, L., Guggenberger, G. and Zech, W., 2000. Black carbon in density fractions of anthropogenic soils of the Brazilian Amazon region. *Organic Geochemistry* 31(7-8): 669-678.
- Glaser, B., Haumaier, L., Guggenberger, G. and Zech, W., 2001. The 'Terra Preta' phenomenon: A model for sustainable agriculture in the humid tropics. *Naturwissenschaften* 88(1): 37-41.
- Glaser, B., Lehmann, J., Zech, W., 2002. Ameliorating physical and chemical properties of highly weathered soils in the tropics with charcoal: a review. *Biology and Fertility of Soils* 35: 219-230.
- Glaser, B., Parr, M., Braun, C. and Kopoló, G., 2009. Biochar is carbon negative. *Nature Geoscience* 2(1): 2.
- Goldberg, E. D., 1985. Black carbon in the Environment: properties and distribution. Wiley, NY.
- González, J. F., Román, S., Encinar, J. M., Martínéz, G., 2009. pyrolysis of various biomass residues and char utilization for the production of activated carbons. *Journal of Analytical and Applied Pyrolysis* 85: 134-141.
- Goodman, C.M., McCusker, C.D., Yilmaz, T. and Rotello, V.M., 2004. Toxicity of gold nanoparticles functionalized with cationic and anionic side chains. *Bioconjugate Chemistry* 15(4): 897-900.
- Grierson, S., Strezov, V., Ellem, G., McGregor, R. and Herbertson, J., 2009. Thermal characterisation of microalgae under slow pyrolysis conditions. *Journal of Analytical and Applied Pyrolysis* 85(1-2): 118-123.
- Gu, B., Schmitt, J., Chen, Z., Liang, L., McCarthy, J. F., 1995. Adsorption and desorption of different organic matter fractions on iron oxide.

- Geochimica et Cosmochimica Acta* 59: 219-229.
- Gustafsson, Ö., Haghseta, F., Chan, C., Macfarlane, J., Gschwend, P., 1997. Quantification of the dilute sedimentary soot phase: implications for PAH speciation and bioavailability. *Environmental Science and Technology* 31: 203-209.
- Hamer, U., Marschner, B., Brodowski, S. and Amelung, W., 2004. Interactive priming of black carbon and glucose mineralisation. *Organic Geochemistry* 35(7): 823-830.
- Hansen, J., Mki. Sato, P. Kharecha, D. Beerling, R. Berner, V. Masson-Delmotte, M. Pagani, M. Raymo, D.L. Royer, and J.C. Zachos, 2008: Target atmospheric CO₂: Where should humanity aim? *Open Atmosphere Science. Journal*, 2: 217-231, doi:10.2174/1874282300802010217.
- Harris, P. J. F., 1997. Structure of non-graphitising carbons. *International Materials Reviews* 42 (5): 206-218.
- Harris, P. J. F., Tsang, S. C., 1997. High resolution of electron microscopy studies of non-graphitizing carbons. *Philosophical Magazine A* 76 (3): 667-677.
- Harris, P.J.F., 2005. New perspectives on the structure of graphitic carbons. *Critical Reviews in Solid State and Materials Sciences* 30(4): 235-253.
- Harvey, A.E., Jurgensen M. F., Larsen, M. J., 1976. Comparative distribution of ectomycorrhizae in a mature Douglas-fir/Larch forest soil in western Montana. *Forest Science*: 22: 350-358.
- Hata, T., Imamura, Y., Kobayashi, E., Yamane, K., Kikuchi, K., 2000. Onion-like graphitic particles observed in wood charcoal. *Journal of Wood Science* 46: 89-92.
- Haumaier, L. and Zech, W., 1995. Black carbon-possible source of highly aromatic components of soil humic acids. *Organic Geochemistry* 23(3): 191-196.
- Hays, M. D., van der Wal, R. L., 2007. Heterogenous soot nanostructure in atmospheric and combustion source aerosols. *Energy and Fuels* 21: 801-811.
- Hedges, J.I., Eglinton, G., Hatcher, P.G., Kirchman, D.L., Arnosti, C., Derenne, S., 2000. The molecularly-uncharacterized component of nonliving organic matter in natural environments. *Organic Geochemistry* 31: 945–958.
- Hedman, B., Naslund, M., Marklund, S. L., 2006. Emission of PCDD/F, PCB and HCB from combustion of firewood and pellets in residential stoves and boilers. *Environmental Science and Technology* 40: 4968-4975.
- Heymann, D., Jenneskens, L.W., Jehlička, J., Koper, C. and Vlietstra, E., 2003. Terrestrial and extraterrestrial fullerenes. *Fullerenes Nanotubes and Carbon Nanostructures* 11(4): 333-370.
- Hiller, E., Fargasova, A., Zemanova, L., Bartal, M., 2007. Influence of wheat ash on the MCPA immobilization in agricultural soils. *Bulletin of*

- Environmental Contamination and Toxicology 78: 345-348.
- Hockaday, W. C., 2006. The organic geochemistry of charcoal black carbon in the soils of the University of Michigan Biological Station. Doctoral Thesis, Ohio State University, US.
- Hockaday, W.C., Grannas, A.M., Kim, S. and Hatcher, P.G., 2006. Direct molecular evidence for the degradation and mobility of black carbon in soils from ultrahigh-resolution mass spectral analysis of dissolved organic matter from a fire-impacted forest soil. *Organic Geochemistry* 37(4): 501-510.
- Hockaday, W.C., Grannas, A.M., Kim, S. and Hatcher, P.G., 2007. The transformation and mobility of charcoal in a fire-impacted watershed. *Geochimica et Cosmochimica Acta* 71(14): 3432-3445.
- Holownicki, R., Doruchowski, G., Godyn, A. and Swiechowski, W., 2000. Variation of spray deposit and loss with air-jet directions applied in orchards. *Journal of Agricultural and Engineering Research* 77(2): 129-136.
- Hospido, A., Moreira, M. T., Martin, M., Rigola, M., Feijoo, G., 2005. Environmental evaluation of different treatment processes for sludge from urban wastewater treatments: anaerobic digestion versus thermal processes. *International Journal of Life Cycle Analysis* 5: 336-345.
- Hossain, M. K., Strezov, V., Nelson, P., 2007. Evaluation of agricultural char from sewage sludge. *Proceedings International Agrichar Initiative, 2007 Terrigal, Australia.*
- Hubbe, A., Chertov, O., Kalinina, O., Nadporozhskaya, M., and Tolkdorf-Lienemann, E., Giani, L., 2007. Evidence of plaggen soils in European North Russia (Arkhangelsk region). *Journal of Plant Nutrition and Soil Science* 170(3): 329-334.
- Huber, S., Prokop, G., Arrouays, D., Banko, G., Bispo, A., Jones, R.J.A., Kibblewhite, M.G., Lexer, W., Möller, A., Rickson, R.J., Shishkov, T., Stephens, M., Toth, G. Van den Akker, J.J.H., Varallyay, G., Verheijen, F.G.A., Jones, A.R. (eds) (2008). *Environmental Assessment of Soil for Monitoring: Volume I Indicators & Criteria.* EUR 23490 EN/1, Office for the Official Publications of the European Communities, Luxembourg, 339pp.
- Hungerbuhler, H., Guldi, D. M., Asmus, K. D., 1993. Incorporation of C60 into artificial lipid membranes. *Journal of American Chemistry Society* 115: 3386-3387.
- Husain, L., Khan, A. J., Shareef, A., Ahmed, T., 2008. Forest Fire Derived Black Carbon in the Adirondack Mountains, NY, ~1745 to 1850 A.D.
- Hussain, N., Jaitley, V. and Florence, A.T., 2001. Recent advances in the understanding of uptake of microparticulates across the gastrointestinal lymphatics. *Advanced Drug Delivery Reviews* 50(1-2): 107-142.
- Hyung, H., Fortner, J. D., Hughes, J. B., Kim, J. H., 2007. Natural organic matter stabilizes carbon nanotubes in the aqueous phase. *Environmental Science and Technology* 42: 179-184.

- Intergovernmental Panel on Climate Change (2001). "Atmospheric Chemistry and Greenhouse Gases". Climate Change 2001: The Scientific Basis. Cambridge, UK: Cambridge University Press.
- International Energy Agency, 2006. Annual Report - IEA Bioenergy. Task 34 Pyrolysis of Biomass.
<http://www.ieabioenergy.com/DocSet.aspx?id=5566&ret=lib> (last accessed: 11-12-2009).
- Ishii, T., Kadoya, K., 1994. Effects of charcoal as a soil conditioner on citrus growth and vesicular–arbuscular mycorrhizal development. *Journal of the Japanese Society for Horticultural Science* 63: 529-535.
- Iwai, K., Mizuno, S., Miyasaka, Y. and Mori, T., 2005. Correlation between suspended particles in the environmental air and causes of disease among inhabitants: Cross-sectional studies using the vital statistics and air pollution data in Japan. *Environmental Research* 99(1): 106-117.
- James, G., Sabatini, D. A., Chiou, C. T., Rutherford, D., Scott, A. C., Karapanagioti, H. K., 2002. Evaluating phenanthrene sorption on various wood chars. *Water Research* 39: 549-558.
- Janssens, I.A., Freibauer, A., Ciais, P., Smith, P., Nabuurs, G.J., Folberth, G., Schlamadinger, B., Hutjes, R.W.A., Ceulemans, R., Schulze, E.D., Valentini, R., and Dolman, A.J., 2003. Europe's terrestrial biosphere absorbs 7 to 12% of European anthropogenic CO₂ emissions. *Science*, 300(5625): 1538-1542.
- Janssens, I.A., Freibauer, A., Schlamadinger, B., Ceulemans, R., Ciais, P., Dolman, A.J., Heimann, M., Nabuurs, G.J., Smith, P., Valentini, R., and Schulze, E.D., 2005. The carbon budget of terrestrial ecosystems at country-scale - A European case study. *Biogeosciences* 2(1): 15-26.
- Janzen, H. H., 2004. Carbon cycling in earth systems - a soil science perspective. *Agriculture Ecosystems & Environment* 104: 399-417.
- Janzen, H.H., 2006. The soil carbon dilemma: Shall we hoard it or use it? *Soil Biology and Biochemistry* 38(3): 419-424.
- Johnson, E., and Heinen, R., 2004. Carbon trading: time for industry involvement. *Environment International* 30 : 279-288.
- Jones H.D., G.S., B. Boag, R. Neilson., 2001. The diversity of earthworms in 200 Scottish fields and the possible effect of New Zealand land flatworms (*Arthurdendyus triangulatus*) on earthworm populations. *Annals of Applied Biology* 139: 75-92.
- Jones, D. M., 2008. Polycyclic aromatic hydrocarbons (PAHs) in biochars and related materials. *Biochar: sustainability and security in a changing climate. Proceedings 2nd International Biochar Initiative Conference 2008, Newcastle, UK.*
- Jones, R.J.A., Verheijen, F.G.A., Reuter, H.I., Jones, A.R. (eds), 2008. *Environmental Assessment of Soil for Monitoring Volume V: Procedures & Protocols. EUR 23490 EN/5, Office for the Official Publications of the European Communities, Luxembourg, 165pp.*

- Jonker, M. T. O., Hawthorne, S. B., Koelmans, A. A., 2005. Extremely Slowly Desorbing Polycyclic Aromatic Hydrocarbons from Soot and Soot-like Materials: Evidence by Supercritical Fluid Extraction. *Environmental Science and Technology* 39: 7889-7895.
- Jonker, M. T. O., Koelmans, A. A., 2002. Sorption of polycyclic aromatic hydrocarbons and polychlorinated biphenyls to soot and soot-like materials in the aqueous environment: mechanistic considerations. *Environmental Science and Technology* 36: 3725-3734.
- Joseph, S., Peacock, C., Lehmann, J., Munroe, P., 2009. Developing a Biochar Classification and Test Methods. In: *Biochar for Environmental Management: Science and Technology* (Eds. Lehmann, J. & Joseph, S.), Earthscan.
- Joung, H-T., Seo, Y-C., Kim, K-H., 2007. Distribution of dioxins, furans, and dioxin-like PCBs in solid products generated by pyrolysis and melting of automobile shredder residues. *Chemosphere* 68: 1636-1641.
- Karajanagi, S. S., Yang, H. C., Asuri, P., Sellitto, E., Dordick, J. S., Kane, R. S., 2006. Protein-assisted solubilization of singled-walled nanotubes. *Langmuir* 22: 1392-1395.
- Kawamoto, K., Ishimaru, K., Imamura, Y., 2005. Reactivity of wood charcoal with ozone. *Journal of Wood Science* 51: 66-72.
- Kearney, P. and Roberts, T. (Eds), 1998. *Pesticide Remediation in Soils and Water*. Wiley Series in Agrochemicals and Plant Protection. John Wiley & Sons Ltd, UK.
- Keiluweit, M., Kleber, M., 2009. Molecular level interactions in soil and sediments: the role of aromatic π -systems. *Environmental Science and Technology* 43: 3421-3429.
- Kharecha and Hansen, 2009. 'We never said biochar is a miracle cure', *The Guardian*, Wednesday 25 March 2009, <http://www.guardian.co.uk/environment/2009/mar/25/hansen-biochar-monbiot-response>.
- Kilduff, J. E., Wigton, A., 1999. Sorption of TCE by humic-preloaded activated carbon: Incorporating size-exclusion and pore blockage phenomena in a competitive adsorption model. *Environmental Science and Technology* 33: 250-256.
- Kim, S., Kaplan, L. A., Brenner, R., Hatcher, P. G., 2004. Hydrogen-deficient molecules in natural riverine water samples - Evidence for the existence of black carbon in DOM. *Mar. Chemistry* 92: 225-234.
- Kimetu, J.M., Lehmann, J., Ngoze, S. O., Mugendi, D. N., Kinyangi, J. M., Riha, S., Verchot, L., Recha, J. W., and Pell, A. N., 2008. Reversibility of soil productivity decline with organic matter of differing quality along a degradation gradient. *Ecosystems* 11(5): 726-739.
- King, J. A., Bradley, R. I., Harrison, R., and Carter, A. D., 2004. Carbon sequestration and saving potential associated with changes to the management of agricultural soils in England. *Soil Use and Management* 20: 394-402.

- King, P.M., 1981. Comparison of methods for measuring severity of water repellence of sandy soils and assessment of some factors that affect its measurement. *Australian Journal of Soil Science* 19: 275–285.
- Kirkby, M.J., Jones, R.J.A., Irvine, B., Gobin, A., Govers, G., Cerdan, O., Van Rompaey, A.J.J., Le Bissonais, Y., Daroussin, J., King, D., Montanarella, L., Grimm, M., Vieillefont, V., Puigdefabregas, J., Boer, M., Kosmas, C., Yassoglou, N., Tsara, M., Mantel, S., Van Lynden, G.J., and Huting, J., 2004. Pan-European Soil Erosion Risk Assessment: the PESERA map. Version 1 October 2003. Explanation of Special Publication Ispra 2004 No.73 (S.P.I.04.73), European Soil Bureau Research Report No.16, EUR 21176. Office for Official Publications of the European Communities, Luxembourg. 18 pp.
- Kirkby, M.J., Le Bissonais, Y., Coulthard, T.J., Daroussin, J., and McMahon, M.D., 2000. The development of land quality indicators for soil degradation by water erosion. *Agriculture Ecosystems and Environment* 81: 125–136.
- Kishimoto S, and Sugiura, G., 1985. Charcoal as a soil conditioner, in: *Symposium on Forest Products Research, International Achievements for the Future* 5:12–23.
- Kittelson, D. B., 2001. Proceedings of the conference on Current Research on Diesel Exhaust Particles of the Japan Association of Aerosol Science and Technology, Tokyo, 9 January 2001 (unpublished data).
- Kleineidam, S. Schuth, C., and Grathwol, P., 2002. Solubility-normalized combined adsorption-partitioning sorption isotherms for organic pollutants. *Environmental Science and Technology* 36: 4689-4697.
- Knaapen, A.M., Borm, P.J.A., Albrecht, C. and Schins, R.P.F., 2004. Inhaled particles and lung cancer. Part A: Mechanisms. *International Journal of Cancer* 109(6): 799-809.
- Knicker, H., Totsche, K. U., Almendros, G., and Gonzalez-Vila, F. J., 2005. Condensation degree of burnt peat and plant residues and the reliability of solid state VACP MAS 13C NMR spectra obtained from pyrogenic humic material. *Organic Geochemistry* 36: 1359-1377.
- Knox, E.G., 2005. Oil combustion and childhood cancers. *Journal of Epidemiology and Community Health*, 59(9): 755-760.
- Koelmans, A. A., Jonker, M. T. O., Cornelissen, G., Bucheli, T. D., van Noort, P. C. M., and Gustafsson, Ö., 2006. Black carbon: the reverse of its black side. *Chemosphere* 63: 365-377.
- Kögel-Knabner, I., Ekschmitt, K., Flessa, H., Guggenberger, G., Matzner, E., Marschner, B., and Von Lützw, M., 2008. An integrative approach of organic matter stabilization in temperate soils: Linking chemistry, physics, and biology. *Journal of Plant Nutrition and Soil Science*, 171(1): 5-13.
- Kolb, S.E., Fermanich, K.J. and Dornbush, M.E., 2009. Effect of Charcoal Quantity on Microbial Biomass and Activity in Temperate Soils. *Soil Science Society of America Journal* 73(4): 1173-1181.

- Kuzyakov, Y., Friedel, J.K., and Stahr, K., 2000. Review of mechanisms and quantification of priming effects. *Soil Biology and Biochemistry* 32: 11-12: 1485-1498
- Kuzyakov, Y., Subbotina, I., Chen, H., Bogomolova, I. and Xu, X., 2009. Black carbon decomposition and incorporation into soil microbial biomass estimated by ¹⁴C labeling. *Soil Biology and Biochemistry* 41(2): 210-219.
- Kwon, S. and Pignatello, J. J., 2005. Effect of Natural Organic Substances on the Surface and Adsorptive Properties of Environmental Black Carbon (Char): Pseudo Pore Blockage by Model Lipid Components and Its Implications for N₂-Probed Surface Properties of Natural Sorbents. *Environmental Science and Technology* 39: 7932-7939.
- Laird, D.A., 2008. The charcoal vision: A win-win-win scenario for simultaneously producing bioenergy, permanently sequestering carbon, while improving soil and water quality. *Agronomy Journal* 100(1): 178-181.
- Laird, D.A., Chappell, M.A., Martens, D.A., Wershaw, R.L. and Thompson, M., 2008. Distinguishing black carbon from biogenic humic substances in soil clay fractions. *Geoderma* 143(1-2): 115-122.
- Lal, R. and Pimentel, D., 2007. Biofuels from crop residues. *Soil and Tillage Research* 93(2): 237-238.
- Lal, R., 2004. Soil carbon sequestration impacts on global climate change and food security. *Science* 304: 1623-1627.
- Lal, R., 2008. Crop residues as soil amendments and feedstock for bioethanol production. *Waste Management* 28(4): 747-758.
- Lal, R., 2009. Soil quality impacts of residue removal for bioethanol production. *Soil and Tillage Research* 102(2): 233-241.
- Lang, T. Jensen, A. D., Jensen, P. A., 2005. Retention of organic elements during solid fuel pyrolysis with emphasis on the peculiar behaviour of nitrogen. *Energy and Fuels* 19: 1631-1643.
- Ledesma, E. B., Marsh, N. D., Sandrowitz, A. K., Wornat, M. J., 2002. Global kinetics rate parameters for the formation of polycyclic aromatic hydrocarbons from the pyrolysis of catechol, a model compound representative of solid fuels moieties. *Energy and Fuels* 16: 1331-1336.
- Lehmann, J. and Sohi, S., 2008. Comment on "fire-derived charcoal causes loss of forest humus". *Science* 321: 5894.
- Lehmann, J., 2007. A handful of Carbon. *Nature* 447: 143-144
- Lehmann, J., 2007. Bio-energy in the black. *Frontiers in Ecology and the Environment* 5: 381-387.
- Lehmann, J., Czimczik, C., Laird, D., and Sohi, S., 2009. Stability of biochar in the soil. In: *Biochar for Environmental Management: Science and Technology* (Eds. Lehmann, J. & Joseph, S.), Earthscan.
- Lehmann, J., da Silva Jr., J. P., Rondon, M. C. M., Greenwood, J., Nehls, T. Steiner, C., and Glaser, B., 2002. Slash-and-char – a feasible

- alternative for soil fertility management in the Central Amazon? In: 17th World Congress of Soil Science, Bangkok.
- Lehmann, J., da Silva Jr., J. P., Steiner, C., Nehls, T., Zech, W., and Glaser, B., 2003b. Nutrient availability and leaching in an archaeological Anthrosol and a Ferralsol in the Central Amazon basin: Fertiliser, manure and charcoal amendments. *Plant and Soil* 249: 343-357.
- Lehmann, J., Gaunt, J. and Rondon, M., 2006. Bio-char sequestration in terrestrial ecosystems - A review. *Mitigation and Adaptation Strategies for Global Change* 11(2): 403-427.
- Lehmann, J., Kern, D. C., Glaser, B., and Woods, W. I., 2003. *Amazonian Dark Earths: Origin, Properties and Management*. Kluwer Academic Publishers, The Netherlands.
- Lehmann, J., Lan, Z., Hyland, C., Sato, S., Solomon, D., and Ketterings, Q. M., 2005. Long term dynamics of phosphorus and retention in manure amended soils. *Environmental Science and Technology* 39 (17): 6672-6680.
- Levis, S., Bonan, G.B. and Bonfils, C., 2004. Soil feedback drives the mid-Holocene North African monsoon northward in fully coupled CCSM2 simulations with a dynamic vegetation model. *Climate Dynamics* 23(7-8): 791-802.
- Liang, B., Lehmann, J., Solomon, D., Kinyangi, J., Grossman, J., O'Neill, B., Skjemstad, J.O., Thies, J., Luizão, F.J., Petersen, J., and Neves, E.G., 2006. Black carbon increases cation exchange capacity in soils. *Soil Science Society of America Journal* 70(5): 1719-1730.
- Liang, B., Lehmann, J., Solomon, D., Sohi, S., Thies, J., Skjemstad, J.O., Luizão, F.J., Engelhard, M.H., Neves, E.G., and Wirrick, S., 2008. Stability of biomass-derived black carbon in soils. *Geochimica et Cosmochimica Acta* 72(24): 6069-6078.
- Liang, P., Ding, Q., and Song, F., 2005a. Application of multi-walled carbon nanotubes as solid phase adsorbent for the preconcentration of trace copper in water samples. *Journal of Separation Science* 28: 2339-2343.
- Liang, P., Liu, Y, Guo, L., Zeng, J., and Lu, H. B., 2004. Multi-walled carbon nanotubes as solid phase adsorbent for the preconcentration of trace metal ions and their determination by inductively coupled plasma atomic emission spectrometry. *Journal of Analytical Atomic Spectrometry* 19: 1489-1492.
- Lima, I. M. and Marshall, W. E., 2005. Granular activated carbons from broiler manure: physical, chemical and adsorptive properties. *Bioresource Technology* 96: 699-706.
- Linak, W.P., Miller, C.A. and Wendt, J.O.L., 2000. Comparison of particle size distributions and elemental partitioning from the combustion of pulverized coal and residual fuel oil. *Journal of the Air and Waste Management Association* 50(8): 1532-1544.
- Long, R. Q., Yang, R. T., 2001. Carbon nanotubes as superior sorbent for

- dioxin removal. *Journal of American Chemistry Society* 123: 2058-2059.
- Loveland, P., and Webb, J., 2003. Is there a critical level of organic matter in the agricultural soils of temperate regions: a review. *Soil & Tillage Research* 70: 1-18.
- Lovelock, J. A geophysicist's thoughts on geoengineering. *Philosophical Transactions of the Royal Society A* 366, 3883-3890, doi:10.1098/rsta/2008.0135.
- Lua, A. C., Yang, T., and Guo, J., 2004. Effects of pyrolysis conditions on the properties of activated carbons prepared from pistachio-nut shells. *Journal of Analytical and Applied Pyrolysis* 72: 279-287.
- Lützow, M.V., Kögel-Knabner, I., Ekschmitt, K., Matzner, G., Guggenberger, G., Marschner, B., and Flessa, H., 2006. Stabilization of organic matter in temperate soils: Mechanisms and their relevance under different soil conditions - A review. *European Journal of Soil Science* 57(4): 426-445.
- Machida, M., Yamzaki, R., Aikawa, M., and Tatsumoto, H., 2005. Role of minerals in carbonaceous adsorbents for removal of Pb (II) ions from aqueous solution. *Separation Purification Technology* 46: 88-94.
- Maiti, S., Dey, S., Purakayastha, S., and Ghosh, B., 2006. Physical and thermochemical characterisation of rice husk char as a potential biomass source. *Bioresource Technology* 97: 2065-2070.
- Mannino, A. and Harvey, H. R., 2004. Black carbon in estuarine and coastal ocean dissolved organic matter. *Limnology and Oceanography* 49: 735-740.
- Marris, E., 2006. Putting the carbon back: Black is the new green. *Nature* 442(7103): 624-626.
- Marschner, B., Brodowski, S., Dreves, A., Gleixner, G., Gude, A., Grootes, P. M., Hamer, U., Heim, A., Jandl, G., Ji, R., Kaiser, K., Kalbitz, K., Kramer, C., Leinweber, P., Rethemeyer, J., Schäffer, A., Schmidt, M. W. I., Schwark, L., and Wiesenberger, G. L. B., 2008. How relevant is recalcitrance for the stabilization of organic matter in soils? *Journal of Plant Nutrition and Soil Science*, 171(1): 91-110.
- Marsh, H., Heintz, E. A., Rodriguez-Reinoso, F., 1997. *Introduction to Carbon Technologies*. University of Alicante, Alicante, Spain.
- Martínez, M. L., Torres, M. M., Guzmán, C. A., Maestri, D. M., 2006. Preparation and characteristics of activated carbon from olive stones and walnut shells. *Industrial crops and products* 23: 23-28.
- Masiello, C. A. and Druffel, E. R. M., 1998. Black carbon in deep-sea sediments. *Science* 280: 1911-1913.
- Mathews, J.A., 2008. Carbon-negative biofuels. *Energy Policy* 36(3): 940-945.
- Maynard, R., 2004. Key airborne pollutants - The impact on health. *Science of the Total Environment* 334-335: 9-13.
- Mbagwu, JSC and Piccolo, A., 1997. Effects of humic substances from

- oxidized coal on soil chemical properties and maize yield. In: Drozd J, Gonet SS, Senesi N, Weber J (eds) *The role of humic substances in the ecosystems and in environmental protection*. IHSS, Polish Society of Humic Substances, Wroclaw, Poland: pp 921–925.
- McCarl B., Peacocke G.V.C., Chrisman R., Kung C., and Sands R. D., 2009. Economics of biochar production, utilisation and emissions. In: *Biochar for environmental management: Science and technology*. (eds. Lehmann, J., and Joseph, S). Earthscan Ltd, London.
- McHenry, M.P., 2009. Agricultural bio-char production, renewable energy generation and farm carbon sequestration in Western Australia: Certainty, uncertainty and risk. *Agriculture, Ecosystems and Environment* 129(1-3): 1-7.
- Meharg, A.A., Deacon, C., Edwards, K.J., Donaldson, M., Davidson, D., Spring, C., Scrimgeour, C.M., Feldmann, J., and Rabb, A., 2006. Ancient manuring practices pollute arable soils at the St Kilda World Heritage Site, Scottish North Atlantic. *Chemosphere* 64(11): 1818-1828.
- Mercado, L.M., Bellouin, N., Sitch, S., Boucher, O., Huntingford, C., Wild, M., and Cox, P.M., 2009. Impact of changes in diffuse radiation on the global land carbon sink. *Nature* 458(7241): 1014-1017.
- Mizuta, K., Matsumoto, T., Hatate, Y., Nishihara, K. and Nakanishi, T., 2004. Removal of nitrate-nitrogen from drinking water using bamboo powder charcoal. *Bioresource Technology* 95(3): 255-257.
- Moore, M.N., 2006. Do nanoparticles present ecotoxicological risks for the health of the aquatic environment? *Environment International* 32(8): 967-976.
- Morterra, C., Low, M J. D., and Severdia, A. G., 1984. IR studies of carbon. 3. The oxidation of cellulose chars. *Carbon* 22: 5-12.
- Muralidhara, H. S., 1982. Conversion of tannery waste to useful products. *Resources and Conservation* 8: 43-59.
- NASA, 2008. Carbon Cycle.
http://www.nasa.gov/centers/langley/images/content/174212main_rn_berrien2.jpg Accessed June 2009.
- Naujokas, A. A., 1985. Spontaneous combustion of carbon beds. *Plant Operations Progress* 4: 120-2070.
- Nearing, M.A., Pruski, F.F., and O'Neal, M.R., 2004. Expected climate change impacts on soil erosion rates: a review. *Journal of Soil and Water Conservation* 59(1): 43–50.
- Neff, J.C., Townsend, A.R., Gleixner, G., Lehman, S.J., Turnbull, J. and Bowman, W.D., 2002. Variable effects of nitrogen additions on the stability and turnover of soil carbon. *Nature* 419(6910): 915-917.
- Nehls, T., 2002. Fertility improvement of a terra firme oxisol in central Amazonia by charcoal application. Final thesis in Geoecology, University of Bayreuth, Institute of Soil Science and Soil Geography: 81

pp.

- Nelson, P.F., 2007. Trace metal emissions in fine particles from coal combustion. *Energy and Fuels* 21(2): 477-484.
- Nguyen, B.T. and Lehmann, J., Black carbon decomposition under varying water regimes. *Organic Geochemistry* 40: 846-853.
- Nguyen, B.T., Lehmann, J., Kinyangi, J., Smernik, R., Riha, S. J., and Engelhard, M. H., 2008. Long-term black carbon dynamics in cultivated soil. *Biogeochemistry*, 89(3): 295-308.
- Nguyen, B.T., Lehmann, J., Kinyangi, J., Smernik, R., Riha, S. J., and Engelhard, M. H., 2009. Long-term black carbon dynamics in cultivated soil. *Biogeochemistry* 92(1-2): 163-176.
- Nisho, M.a.O., S. , 1991. Stimulation of the growth of alfalfa and infection of mycorrhizal fungi by the application of charcoal. *Bulletin of the National Grassland Research Institute*, 45: 61-71.
- Niyogi, S., Abraham, T. E. and Ramakrishna, S. V., 1998. Removal of chromium (VI) from industrial effluents by immobilized biomass of *Rhizopus arrhizus*. *Journal of Scientific and Industrial Research* 57: 809-816.
- Nowack, B. and Bucheli, T.D., 2007. Occurrence, behavior and effects of nanoparticles in the environment. *Environmental Pollution* 150(1): 5-22.
- Oberdörster, G., 2002. Toxicokinetics and effects of fibrous and non-fibrous particles. *Inhalation Toxicology* 14 (1): 29-56.
- Oberdörster, G., Stone, V. and Donaldson, K., 2007. Toxicology of nanoparticles: A historical perspective. *Nanotoxicology* 1(1): 2-25.
- Ogawa, M., 1994. Symbiosis of people and nature in the tropics. *Farming Japan*, 28: 10-34.
- Ogawa, M., Okimori, Y. and Takahashi, F., 2006. Carbon sequestration by carbonization of biomass and forestation: Three case studies. *Mitigation and Adaptation Strategies for Global Change* 11(2): 429-444.
- Oguntunde, P.G., Abiodun, B.J., Ajayi, A.E. and Van De Giesen, N., 2008. Effects of charcoal production on soil physical properties in Ghana. *Journal of Plant Nutrition and Soil Science* 171(4): 591-596.
- Oguntunde, P.G., Fosu, M., Ajayi, A.E. and Van De Giesen, N.D., 2004. Effects of charcoal production on maize yield, chemical properties and texture of soil. *Biology and Fertility of Soils* 39(4): 295-299.
- Okimori, Y., Ogawa, M. and Takahashi, F., 2003. Potential of CO₂ emission reductions by carbonizing biomass waste from industrial tree plantation in South Sumatra, Indonesia. *Mitigation and Adaptation Strategies for Global Change* 8(3): 261-280.
- O'Neill, B., Grossman, J., Tsai, M. T., Gomes, J. E., Lehmann, J., Peterson, J., Neves, E., and Thies, J. E., 2009. Bacterial Community Composition in Brazilian Anthrosols and Adjacent Soils Characterized Using Culturing and Molecular Identification. *Microbial Ecology*: 1-13.

- Ostrom, E., Janssen, M.A., and Anderies, J.M., 2007. Going beyond panaceas. *Proceedings of the National Academy of Sciences of the U.S.A.* 104 (39): 15176-15178.
- Painter, T.J., 2001. Carbohydrate polymers in food preservation: An integrated view of the Maillard reaction with special reference to the discoveries of preserved foods in *Sphagnum* dominated peat bogs. *Carbohydrate Polymers* 36: 335-347.
- Pakdel, H., and Roy, C., 1991. Hydrocarbon Content of Liquid Products of Tar from Pyrolysis and Gasification. *Energy & Fuels*: 427-436.
- Pastor-Villegas, J., Pastor-Valle, J. P., Meneses Rodriguez, J. M., and García García, M., 2006. Study of commercial wood charcoals for the preparation of carbon adsorbents. *Journal of Analytical and Applied Pyrolysis* 76: 103-108.
- Pendall, E., Bridgham, S., Hanson, P. J., Hungate, B., Kicklighter, D. W., Johnson, D. W., Law, B. E., Luo, Y. Q., Megonigal, J. P., Olsrud, M., Ryan, M. G., and Wan, S. Q., 2004. Below-ground process responses to elevated CO₂ and temperature: a discussion of observations, measurement methods, and models. *New Phytologist* 162: 311-322.
- Penner, J. E., Eddleman, H., and Novakav, T., 1993. Towards the development of a global inventory for black carbon. *Atmospheric Environment* 27 A (8): 1277-1295.
- Pessenda, L.C.R., Gouveia, S.E.M., and Aravena, R., 2001. Radiocarbon dating of total soil organic matter and humin fraction and its comparison with ¹⁴C ages of fossil charcoal. *Radiocarbon* 43 (2001): 595-601.
- Petrus, L. and Noordermeer, M.A., 2006. Biomass to biofuels, a chemical perspective. *Green Chemistry* 8, The Royal Society of Chemistry: 861-867.
- Phillips, D.L., White, D., and Johnson, B., 1993. Implications of climate-change scenarios for soil-erosion potential in the USA. *Land Degradation and Rehabilitation* 4 (2): 61-72.
- Piccolo, A. and Mbagwu, J.S.C., 1997. Exogenous humic substances as conditioners for the rehabilitation of degraded soils. *Agro-Foods Industry Hi-Tech*: 8(2): 2-4.
- Piccolo, A., Pietramellara, G. and Mbagwu, J.S.C., 1996. Effects of coal derived humic substances on water retention and structural stability of mediterranean soils. *Soil Use and Management*, 12(4): 209-213.
- Piccolo, A., Pietramellara, G. and Mbagwu, J.S.C., 1997. Use of humic substances as soil conditioners to increase aggregate stability. *Geoderma*, 75(3-4): 267-277.
- Pignatello, J. J., Kwon, S., and Lu, Y., 2006. Effect of Natural Organic Substances on the Surface and Adsorptive properties of Environmental Black Carbon (Char): Attenuation of Surface Activity by Humic and Fulvic Acids. *Environmental Science and Technology* 40: 7757-7763.

- Pointing, S., 2001. Feasibility of bioremediation by white rot fungi: *Applied Microbiology and Biotechnology* 57, 20-33.
- Ponge, J.-F., Topoliantz, S., Ballof, S., Rossi, J.P., Lavelle, P., Betsch, J.M., and Gaucher, P., 2006. Ingestion of charcoal by the Amazonian earthworm *Pontoscolex corethrurus*: A potential for tropical soil fertility. *Soil Biology and Biochemistry* 38(7): 2008-2009.
- Post, D.F., Fimbres, A., Matthias, A.D., Sano, E.E., Accioly, L., Batchily, A.K., and Ferreira, L.G., 2000. Predicting soil albedo from soil color and spectral reflectance data. *Soil Science Society of America Journal*, 64(3): 1027-1034.
- Post, W. M., Peng, T. H., Emanuel, W. R., King, A. W., Dale, V. H., and Deangelis, D. L., 1990. The Global Carbon-Cycle. *American Scientist* 78: 310-326.
- Preston, C. M., and Schmidt, M. W. I., 2006. Black (pyrogenic) carbon in boreal forests: a synthesis of current knowledge and uncertainties. *Biogeosciences Discussions* 3:211-271.
- Pulido, L. L., Hata, T., Imamura, Y., Ishihara, S., and Kajimoto, T., 1998. Removal of mercury and other metals by carbonized wood powder from aqueous solution of their salts. *Journal of Wood Science* 44(3): 237-243.
- Quénéa, K., Derenne, S., Rumpel, C., Rouzaud, J.N., Gustafsson, O., Carcaillet, C., Mariotti, A., and Largeau, C., 2006. Black carbon yields and types in forest and cultivated sandy soils (Landes de Gascogne, France) as determined with different methods: Influence of change in land use. *Organic Geochemistry*, 37(9): 1185-1189.
- Radovic, L. R., Moreno-Castilla, C., and Rivera-Utrilla, J., 2001. Carbon materials as adsorbents in aqueous solutions. In: *Chemistry and Physics of Carbon* (ed. L. R. Radovic): 227-405.
- Renner, R., 2007. Rethinking biochar. *Environmental Science and Technology* 41(17): 5932-5933.
- Ritsema, C. J., and Dekker, L. W., 1996. Water repellency and its role in forming preferred flow paths in soils. *Australian Journal of Soil Research* 34: 475-487.
- Ritz, K., 2007. The plate debate: cultivable communities have no utility in contemporary environmental microbial ecology. *FEMS Microbiology Ecology* 60: 358-362.
- Roberts, K., Gloy, B., Joseph, S., Scott, N. and Lehmann, J., (2009), Life cycle assessment of biochar systems: Estimating the energetic, economic and climate change potential. *Environment Science and Technology* 44: 827-833.
- Rogers, F., Arnott, P., Zielinska, B., Sagebiel, J., Kelly, K.E., Wagner, D., Lighty, J., and Sarofim, A.F., 2005. Real-time measurements of jet aircraft engine exhaust. *Journal of the Air and Waste Management Association* 55(5): 583-593.

- Rondon, M.A., Lehmann, J., Ramírez, J. and Hurtado, M., 2007. Biological nitrogen fixation by common beans (*Phaseolus vulgaris* L.) increases with bio-char additions. *Biology and Fertility of Soils* 43(6): 699-708.
- Rosenberg, M.S., Adams, D.C., and Gurevitch, J., 2000. *MetaWin Statistical Software for Meta-Analysis, Version 2*. Department of Ecology and Evolution, State University of New York at Stony Brook. Sinauer Associates, Inc., Sunderland, Massachusetts, U.S.A.
- Rumpel, C., Chaplot, V., Planchon, O., Bernadoux, J., Valentin, C., and Mariotti, A., 2006b. Preferential erosion of black carbon on steep slopes with slash and burn agriculture. *Catena* 65 (1): 30-40.
- Rumpel, C., Alexis, M., Chabbi, A., Chaplot, V., Rasse, D. P., Valentin, C., and Mariotti, A., 2006a. Black carbon contribution to soil organic matter composition in tropical sloping land under slash and burn agriculture. *Geoderma* 130: 35-46.
- Russell, E.J., 1926. *Plant nutrition and crop production*. University of California Press, Berkeley, California: 115 pp.
- Rustad, L.E., Campbell, J.L., Marion, G.M., Norby, R.J., Mitchell, M.J., Hartley, A.E., Cornelissen, J.H.C., and Gurevitch, J., 2001. A meta-analysis of the response of soil respiration, net nitrogen mineralisation, and aboveground plant growth to experimental ecosystem warming. *Oecologia*, 126(4): 543-562.
- Saito, M., and Marumoto, T., 2002. Inoculation with arbuscular mycorrhizal fungi: the status quo in Japan and the future prospects. *Plant and Soil* 244: 273–279.
- Salloum, M. J., Chefetz, B., Hatcher, P. G., 2002. Phenanthrene sorption by alliphatic-rich natural organic matter. *Environmental Science and Technology* 36: 1953-1958.
- Sánchez, M.E., Lindao, E., Margaleff, D., Martínez, O. and Morán, A., 2009. Pyrolysis of agricultural residues from rape and sunflowers: Production and characterization of bio-fuels and biochar soil management. *Journal of Analytical and Applied Pyrolysis* 85(1-2): 142-144.
- Sander, M., and Pignatello, J. J., 2005. Characterisation of charcoal adsorption sites for aromatic compounds: Insights drawn from single and bi-solute competitive experiments. *Environmental Science and Technology* 39: 1606-1615.
- Schils, R., Kuikman, P., Liski, J., van Oijen, M., Smith, P., Webb, J. Alm, J., Somogyi, Z., van den Akker, J., Billett, M., Emmett, B., Evans, C., Lindner, M., Palosuo, T., Bellamy, P., Jandl, R., and Hiederer, R., 2008. Review of existing information on the interrelations between soil and climate change. Final Report. Contract number 070307/2007/486157/SER/B1, 208 pp.
- Schmidt, M.W.I., Skjemstad, J.O. and Jäger, C., 2002. Carbon isotope geochemistry and nanomorphology of soil black carbon: Black chernozemic soils in central Europe originate from ancient biomass burning. *Global Biogeochemical Cycles* 16(4): 70-1.

- Schmidt, M.W.I., Skjemstad, J.O., Gehrt, E. and Kögel-Knabner, I., 1999. Charred organic carbon in German chernozemic soils. *European Journal of Soil Science* 50(2): 351-365.
- Schnitzer, M.I., Monreal, C.M., Facey, G.A., and Fransham, P.B., 2007. The conversion of chicken manure to biooil by fast pyrolysis I. Analyses of chicken manure, biooils and char by ¹³C and ¹H NMR and FTIR spectrophotometry. *Journal of Environmental Science and Health, Part B: Pesticides, Food Contaminants and Agricultural Wastes* 42 (1): 71-77.
- Schwartz, J. and Morris, R., 1995. Air pollution and hospital admissions for cardiovascular disease in Detroit, Michigan. *American Journal of Epidemiology* 142(1): 23-35.
- Seifritz, W., 1993. Should we store carbon in charcoal? *International Journal of Hydrogen Energy* 18(5): 405-407.
- Weyers, S.L., Liesch, A.M., Gaskin, J.W., Das, K.C. 2009. Earthworms Contribute to Increased Turnover in Biochar Amended Soils [abstract][CD-ROM]. ASA-CSSA-SSSA Annual Meeting Abstracts. ASA-CSSA-SSSA Annual Meeting. Nov. 1-5, 2009, Pittsburgh, PA.
- Sheng, G., Yang, Y., Huang, M., and Yang, K., 2005. Influence of pH on pesticide sorption by soil containing wheat residue-derived char. *Environmental Pollution* 134: 457-463.
- Shindo, H., 1991. Elementary composition, humus composition, and decomposition in soil of charred grassland plants. *Soil Science and Plant Nutrition* 37: pp. 651-657.
- Shneour, E.A., 1966. Oxidation of graphitic carbon in certain soils. *Science* 151(3713): 991-992.
- Sjöström, E., 1993. *Wood Chemistry: Fundamentals and Applications*, second edition, Academic Press, San Diego, U.S.A.
- Skjemstad, J. O., Taylor, J. A., Oades, J. M., and McClure, S. G., 1996. The chemistry and nature of protected carbon in soil. *Australian Journal of Soil Resources* 34: 251-271.
- Sleutel, S., De Neve, S., Hofman, G., Boeckx, P., Beheydt, D., Van Cleemput, O., Mestdagh, I., Lootens, P., Carlier, L., Van Camp, N., Verbeeck, H., Vande Walle, I., Samson, R., Lust, N., and Lemeur, R., 2003. Carbon stock changes and carbon sequestration potential of Flemish cropland soils. *Global Change Biology* 9: 1193-1203.
- Smernik, R.J., Kookana, R.S. and Skjemstad, J.O., 2006. NMR characterization of ¹³C-benzene sorbed to natural and prepared charcoals. *Environmental Science and Technology* 40(6): 1764-1769.
- Smith, P., Powlson, D. S., Smith, J. U., Falloon, P., and Coleman, K., 2000a. Meeting Europe's climate change commitments: quantitative estimates of the potential for carbon mitigation by agriculture. *Global Change Biology* 6: 525-539.
- Smith, P., Powlson, D. S., Smith, J. U., Falloon, P., and Coleman, K., 2000b. Meeting the UK's climate change commitments: options for carbon

- mitigation on agricultural land. *Soil Use and Management* 16: 1-11.
- Soane, B. D., 1990. The Role of Organic-Matter in Soil Compactibility - a Review of Some Practical Aspects. *Soil & Tillage Research* 16: 179-201.
- Sohi, S., Lopez-Capel, E., Krull, E., and Bol, R., 2009. Biochar, climate change and soil: a review to guide future research. CSIRO Land and Water Science Report.
- Solomon, D., Lehmann, J., Thies, J., Schäfer, T., Liang, B., Kinyangi, J., Neves, E., Petersen, J., Luizão, F., and Skjemstad, J., 2007. Molecular signature and sources of biochemical recalcitrance of organic C in Amazonian Dark Earths. *Geochimica et Cosmochimica Acta* 71(9): 2285-2298.
- Star, A., Steuerman, D. W., Heath, J. R., and Stoddart, J. F., 2002. Starched carbon nanotubes. *Angewandte Chemie -International Edition* 41: 2508-2512.
- Steinbeiss, S., Gleixner, G. and Antonietti, M., 2009. Effect of biochar amendment on soil carbon balance and soil microbial activity. *Soil Biology and Biochemistry* 41(6): 1301-1310.
- Steiner, C., 2004. Plant nitrogen uptake doubled in charcoal amended soils, Energy with Agricultural Carbon Utilization Symposium, Athens, Georgia, U.S.A.
- Steiner, C., 2007. Slash and Char as Alternative to Slash and Burn: soil charcoal amendments maintain soil fertility and establish a carbon sink. Cuvillier Verlag, Gottingen.
- Steiner, C., De Arruda, M.R., Teixeira, W.G. and Zech, W., 2007. Soil respiration curves as soil fertility indicators in perennial central Amazonian plantations treated with charcoal, and mineral or organic fertilisers. *Tropical Science* 47(4): 218-230.
- Steiner, C., Glaser, B., Teixeira, W. G., Lehmann, J., Blum, W. E. H., and Zech, W., 2008. Nitrogen retention and plant uptake on a highly weathered central Amazonian Ferralsol amended with compost and charcoal. *Journal of Plant Nutrition and Soil Science* 171(6): 893-899.
- Steiner, C., Teixeira, W., Lehmann, J., Nehls, T., de Macêdo, J., Blum, W., and Zech, W., 2007. Long term effects of manure, charcoal and mineral fertilization on crop production and fertility on a highly weathered Central Amazonian upland soil. *Plant and Soil* 291(1): 275-290.
- Stowell, G., Tubs, V., 2003. Rice husk and market study. EXP 129. ETSU U/00/0061/REP.DTI/Pub URN 03/665.
- Strezov, V., Morrison, A. and Nelson, P.F., 2007. Pyrolytic mercury removal from coal and its adverse effect on coal swelling. *Energy and Fuels* 21(2): 496-500.
- Subke, J.A., Inglima, I. and Cotrufo, M.F., 2006. Trends and methodological impacts in soil CO₂ efflux partitioning: A metaanalytical review. *Global*

- Change Biology 12(6): 921-943.
- Sundquist, E. T., 1993. The Global Carbon-Dioxide Budget. *Science* 259: 1812-1812.
- Swissinfo, 2007. Hundreds of mushroom species face extinction, Swissinfo.
- Tinkle, S. S., Antonini, J. M., Rich, B. A., Roberts, J. R., Salmen, R., DePree, K., and Adkins, A. J., 2003. Skin as a route of exposure and sensitization in chronic beryllium disease. *Environmental Health Perspectives* 111: 1202-1208.
- Toll, R., Jacobi, U., Richter, H., Lademann, J., Schaefer, H., and Blume-Peytavi, U., 2004. Penetration profile of microspheres in follicular targeting of terminal hair follicles. *Journal of Investigative Dermatology* 123: 168-176.
- Topoliantz, S. and Ponge, J.F., 2003. Burrowing activity of the geophagous earthworm *Pontoscolex corethrurus* (Oligochaeta: Glossoscolecidae) in the presence of charcoal. *Applied Soil Ecology* 23(3): 267-271.
- Topoliantz, S. and Ponge, J.F., 2005. Charcoal consumption and casting activity by *Pontoscolex corethrurus* (Glossoscolecidae). *Applied Soil Ecology* 28(3): 217-224.
- Torsvik, V., Goksoyr, J. and Daae, F., 1990. High diversity in DNA of soil bacteria. *Applied Environmental Microbiology* 56: 782-787.
- Tóth, G., Montanarella, L., Stolbovoy, V., Máté, F., Bódis, K., Jones, A., Panagos, P. and van Liedekerke, M., 2008. Soils of the European Union. Luxembourg: Office for Official Publications of the European Communities. EUR – Scientific and Technical Research series – ISSN 1018-5593; ISBN 978-92-79-09530-6; DOI 10.2788/87029: 85 pp.
- Tryon, E.H., 1948. Effect of charcoal on certain physical, chemical, and biological properties of forest soils. *Ecological Monographs* 18(1): 83-113.
- Tsui, L. and Roy, W.R., 2008. The potential applications of using compost chars for removing the hydrophobic herbicide atrazine from solution. *Bioresource Technology* 99(13): 5673-5678.
- Turetsky, M., Wieder, K., Halsey, L. and Vitt, D., 2002. Current disturbance and the diminishing peatland carbon sink. *Geophysical Research Letters* 29(11):21-1 – 21-4.
- U.S. Environmental Protection Agency, 2002. Atmospheric Concentrations of Greenhouse Gases
<http://cfpub.epa.gov/eroe/index.cfm?fuseaction=detail.viewPDF&ch=46&IShowInd=0&subtop=342&lv=list.listByChapter&r=209837>. Accessed July 2009
- Vaario, L.M., Tanaka, M., Ide, Y., Gill, W. M., Suzuki, K., 1999. *In vitro* ectomycorrhiza formation between *Abies firma* and *Pisolithus tinctorius*. *Mycorrhiza* 9: 177-183.
- Van der Velde, M, Bouraoui, F and Aloe, A, 2009. Pan-European regional-scale modelling of water and N efficiencies of rapeseed cultivation for

- biodiesel production. *Global Change Biology* 15: 24-37. doi: 10.1111/j.1365-2486.2008.01706.x.
- Van Groenigen, K.J., Six, J., Hungate, B.A., de Graaff, M.A., van Breemen, N., and van Kessel, C., 2006. Element interactions limit soil carbon storage. *Proceedings of the National Academy of Sciences of the United States of America*, 103(17): 6571-6574.
- Van Genuchten, M.T. 1980. A Closed-form Equation for Predicting the Hydraulic Conductivity of Unsaturated Soils. *Soil Science Society of America Journal* 44: 892-898.
- Van Kooten, G.C., Eagle, A.J., Manley, J. and Smolak, T., 2004. How costly are carbon offsets? A meta-analysis of carbon forest sinks. *Environmental Science and Policy* 7(4): 239-251.
- Van Zwieten, L., Kimber, S., Morris, S., Chan, K.Y., Downie, A., Rust, J., Joseph, S., and Cowie, A., 2009. Effects of biochar from slow pyrolysis of papermill waste on agronomic performance and soil fertility. *Plant and Soil*: 1-12.
- Van Zwieten, L., Kimber, S., Downie, A., Joseph, F., Chan, K. Y., Cowie, A., Wainberg, R., and Morris, S., 2007. Paper mill char: benefits for soil health and plant production. *Proceedings, International Agrichar Initiative Conference, 30th April - 2nd May 2007, Terrigal, Australia.*
- Van Zwieten, L., Singh, B., Joseph, S., Kimber, S., Cowie, A., and Chan, K. Y., 2009. Biochar and Emissions of Non-CO₂ Greenhouse Gases from Soil. In: *Biochar for Environmental Management: Science and Technology* (Eds. Lehmann, J. & Joseph, S.), Earthscan.
- Van, D. T. T., Mui, N. T., and Ledin, I., 2006. Effect of processing foliage of *Acacia mangium* and inclusion of bamboo charcoal in the diet on performance of growing goats. *Animal Feed Science and Technology* 130: 242-256.
- Velasco-Santos, C., Martinez-Hernandez, A. L., Consultchi, A., Rodriguez, R., and Castaño, V. M., 2003. Naturally produced carbon nanotubes. *Chemical Physics Letters* 373: 272-276.
- Verheijen, F.G.A. and Cammeraat, L.H., 2007. The association between three dominant shrub species and water repellent soils along a range of soil moisture contents in semi-arid Spain. *Hydrological Processes* 21(17): 2310-2316.
- Verheijen, F.G.A., Jones, R.J.A., Rickson, R.J. and Smith, C.J., 2009. Tolerable versus actual soil erosion rates in Europe. *Earth-Science Reviews* 94(1-4): 23-38.
- Von Lützow, M., Kögel-Knabner, I., Ludwig, B., Matzner, E., Flessa, H., Ekschmitt, K., Guggenberger, G., Marschner, B., and Kalbitz, K., 2008. Stabilization mechanisms of organic matter in four temperate soils: Development and application of a conceptual model. *Journal of Plant Nutrition and Soil Science* 171(1): 111-124.
- Wang, K., Wang, P., Jingmiao, L., Sparrow, M., Haginoya, S., and Zhou, X., 2005. Variation of surface albedo and soil thermal parameters with soil

- moisture content at a semi-desert site on the western Tibetan Plateau. *Boundary-Layer Meteorology* 116(1): 117-129.
- Wang, X., Sato, T., and Xing, B., 2006. Competitive sorption of pyrene on wood chars. *Environmental Science and Technology* 40: 3267-3272.
- Wardle, D.A., Nilsson, M.C. and Zackrisson, O., 2008. Fire-derived charcoal causes loss of forest humus. *Science* 320(5876): 629.
- Wardle, D.A., Nilsson, M.C. and Zackrisson, O., 2008. Response to comment on "fire-derived charcoal causes loss of forest humus". *Science* 321(5894): 1295d.
- Warnock, D.D., Lehmann, J., Kuyper, T.W. and Rillig, M.C., 2007. Mycorrhizal responses to biochar in soil - Concepts and mechanisms. *Plant and Soil* 300(1-2): 9-20.
- Warren, G.P., Robinson, J.S. and Someus, E., 2009. Dissolution of phosphorus from animal bone char in 12 soils. *Nutrient Cycling in Agroecosystems* 84(2): 167-178.
- West, T. O., and Post, W. M., 2002. Soil organic carbon sequestration rates by tillage and crop rotation: A global data analysis. *Soil Science Society of America Journal* 66: 1930-1946.
- Wilcke, W., 2000. Polycyclic aromatic hydrocarbons (PAHs) in soil - A review. *Journal of Plant Nutrition and Soil Science* 163(3): 229-248.
- Wilhelm, W.W., Johnson, J.M.F., Hatfield, J.L., Voorhees, W.B. and Linden, D.R., 2004. Crop and Soil Productivity Response to Corn Residue Removal: A Literature Review. *Agronomy Journal* 96(1): 1-17.
- Winsley P., 2007. Biochar and Bionenergy Production for Climate Change. *New Zealand Science Review* 64 (1): 1-10.
- Woods, WI, Falcao, NPS and Teixeira, WG, 2006. Biochar trials aim to enrich soil for smallholders, *Nature* 443: 144.
- Wu, Y., Hudson, J. S., Lu, Q., Moore, J. M., Mount, A. S., Rao, A. M., Alexov, E., and Ke, P. C., 2006. Coating single-walled carbon nanotubes with phospholipids. *Journal of Physical Chemistry B* 110: 2475-2478.
- Yamato, M., Okimori, Y., Wibowo, I.F., Anshori, S. and Ogawa, M., 2006. Effects of the application of charred bark of *Acacia mangium* on the yield of maize, cowpea and peanut, and soil chemical properties in South Sumatra, Indonesia. *Soil Science and Plant Nutrition*, 52(4): 489-495.
- Yanai, Y., Toyota, K. and Okazaki, M., 2007. Effects of charcoal addition on N₂O emissions from soil resulting from rewetting air-dried soil in short-term laboratory experiments: Original article. *Soil Science and Plant Nutrition* 53(2): 181-188.
- Yang, K., Wang, X. L., Zhu, L. Z., and Xing, B. S., 2006b. Competitive sorption of pyrene, phenanthrene and naphthalene on multi-walled carbon nanotubes. *Environmental Science and Technology* 40: 5804-5810.
- Yang, Y., and Sheng, G., 2003. Enhanced pesticide sorption by soils

- containing particulate matter from crop residue burns. *Environmental Science and Technology* 37: 3635-3639.
- Yu, C., Tang, Y., Fang, M., Luo, Z., and Ceng, K., 2005. Experimental study on alkali emission during rice straw Pyrolysis. *Journal of Zhejiang University (Engineering Science)* 39: 1435-1444.
- Zackrisson, O., Nilsson, M. C. and Wardle, D. A., 1996. Key ecological function of charcoal from wildfires in the Boreal forest. *Oikos*: 77: 10-19.
- Zhu, D., Kwon, S., and Pignatello, J. J., 2005. Adsorption of Single-Ring Organic Compounds to Wood Charcoals Prepared to under Different Thermochemical Conditions. *Environmental Science and Technology* 39: 3990-3998.
- Zhu, D., and Pignatello, J. J., 2005. Characterization of Aromatic Compound Sorptive Interactions with Black Carbon (Charcoal) Assisted by Graphite as a Model. *Environmental Science and Technology* 39: 2033-2041.
- Zhu, Y., Zhao, Q., Li, Y., Cai, X., and Li, W., 2006c. The interaction and toxicity of multi-walled carbon nanotubes with *Stylonychia mytilus*. *Journal of Nanoscience and Nanotechnology* 6: 1357-1364.

European Commission

EUR 24099 - EN – Joint Research Centre – Institute for Environment and Sustainability

Title: Biochar Application to Soils - A Critical Scientific Review of Effects on Soil Properties, Processes and Functions

Author(s): F. Verheijen, S. Jeffery, A.C. Bastos, M. van der Velde, I. Diafas

Luxembourg: Office for Official Publications of the European Communities

2009 – 151 pp. – 21.0 x 29.7 cm

EUR – Scientific and Technical Research series – ISSN 1018-5593

ISBN 978-92-79-14293

DOI 10.2788/472

Abstract

Biochar application to soils is being considered as a means to sequester carbon (C) while concurrently improving soil functions. The main focus of this report is providing a critical scientific review of the current state of knowledge regarding the effects of biochar application to soils on soil properties and functions. Wider issues, including atmospheric emissions and occupational health and safety associated to biochar production and handling, are put into context. The aim of this review is to provide a sound scientific basis for policy development, to identify gaps in current knowledge, and to recommend further research relating to biochar application to soils. See Table 1 for an overview of the key findings from this report. Biochar research is in its relative infancy and as such substantially more data are required before robust predictions can be made regarding the effects of biochar application to soils, across a range of soil, climatic and land management factors.

Definition

In this report, biochar is defined as: "charcoal (biomass that has been pyrolysed in a zero or low oxygen environment) for which, owing to its inherent properties, scientific consensus exists that application to soil at a specific site is expected to sustainably sequester carbon and concurrently improve soil functions (under current and future management), while avoiding short- and long-term detrimental effects to the wider environment as well as human and animal health." Biochar as a material is defined as: "charcoal for application to soils". It should be noted that the term 'biochar' is generally associated with other co-produced end products of pyrolysis such as 'syngas'. However, these are not usually applied to soil and as such are only discussed in brief in the report.

Biochar properties

Biochar is an organic material produced via the pyrolysis of C-based feedstocks (biomass) and is best described as a 'soil conditioner'. Despite many different materials having been proposed as biomass feedstock for biochar (including wood, crop residues and manures), the suitability of each feedstock for such an application is dependent on a number of chemical, physical, environmental, as well as economic and logistical factors. Evidence suggests that components of the carbon in biochar are highly recalcitrant in soils, with reported residence times for wood biochar being in the range of 100s to 1,000s of years, i.e. approximately 10-1,000 times longer than residence times of most soil organic matter. Therefore, biochar addition to soil can provide a potential sink for C. It is important to note, however, that there is a paucity of data concerning biochar produced from feedstocks other than wood, but the information that is available is discussed in the report. Owing to the current interest in climate change mitigation, and the irreversibility of biochar application to soil, an effective evaluation of biochar stability in the environment and its effects on soil processes and functioning is paramount. The current state of knowledge concerning these factors is discussed throughout this report.

Pyrolysis conditions and feedstock characteristics largely control the physico-chemical properties (e.g. composition, particle and pore size distribution) of the resulting biochar, which in turn, determine the suitability for a given application, as well as define its behaviour, transport and fate in the environment. Reported biochar properties are highly heterogeneous, both within individual biochar particles but mainly between biochar originating from different feedstocks and/or produced under different pyrolysis conditions. For example, biochar properties have been reported with cation exchange capacities (CECs) from negligible to approximately 40 cmolc g⁻¹, and C:N ratios from 7 to 500, while the pH is normally neutral to basic. While this heterogeneity leads to difficulties in identifying the underlying mechanisms behind reported effects in the scientific literature, it also provides a possible opportunity to engineer biochar with properties that are best suited to a particular site (depending on soil type, hydrology, climate, land use, soil contaminants, etc.).

Effects on soils

Biochar characteristics (e.g. particle and pore size distribution, surface chemistry, relative proportion of readily available components), as well as physical and chemical stabilisation mechanisms of biochar in soils, determine the effects of biochar on soil functions. However, the relative contribution of each of these factors has been assessed poorly, particularly under the influence of different climatic and soil conditions, as well as soil management and land use. Reported biochar loss from soils may be explained to a certain degree by abiotic and biological degradation and translocation within the soil profile and into water systems. Nevertheless, such mechanisms have been quantified scarcely and remain poorly understood, partly due to the limited amount of long-term studies, and partly due to the lack of standardised methods for simulating biochar aging and long-term environmental monitoring. A sound understanding of the contribution that biochar can make as a tool to improve soil properties, processes and functioning, or at least avoiding negative effects, largely relies on knowing the extent and full implications of the biochar interactions and changes over time within the soil system.

Extrapolation of reported results must be done with caution, especially when considering the relatively small number of studies reported in the primary literature, combined with the small range of climatic, crop and soil types investigated when compared to possible instigation of biochar application to soils on a national or European scale. To try and bridge the gap between small scale, controlled experiments and large scale implementation of biochar application to a range of soil types across a range of different climates (although chiefly tropical), a statistical meta-analysis was undertaken. A full search of the scientific literature led to a compilation of studies used for a meta-analysis of the effects of biochar application to soils and plant productivity. Results showed a small overall, but statistically significant, positive effect of biochar application to soils on plant productivity in the majority of cases. The greatest positive effects were seen on acidic free-draining soils with other soil types, specifically calcarosols showing no significant effect (either positive or negative). There was also a general trend for concurrent increases in crop productivity with increases in pH up on biochar addition to soils. This suggests that one of the main mechanisms behind the reported positive effects of biochar application to soils on plant productivity may be a liming effect. However, further research is needed to confirm this hypothesis. There is currently a lack of data concerning the effects of biochar application to soils on other soil functions. This means that although these are qualitatively and comprehensively discussed in this report, a robust meta-analysis on such effects is as of yet not possible. Table 1 provides an overview of the key findings - positive, negative, and unknown - regarding the (potential) effects on soil, including relevant conditions.

Preliminary, but inconclusive, evidence has also been reported concerning a possible priming effect whereby accelerated decomposition of soil organic matter occurs upon biochar addition to soil. This has the potential to both harm crop productivity in the long term due to loss of soil organic matter, as well as releasing more CO₂ into the atmosphere as increased quantities of soil organic matter is respired from the soil. This is an area which requires urgent further research.

Biochar incorporation into soil is expected to enhance overall sorption capacity of soils towards anthropogenic organic contaminants (e.g. PAHs, PCBs, pesticides and herbicides), in a mechanistically different (and stronger) way than amorphous organic matter. Whereas this behaviour may greatly mitigate toxicity and transport of common pollutants in soils through reducing their bioavailability, it might also result in their localised accumulation, although the extent and implications of this have not been assessed experimentally. The potential of biochar to be a source of soil contamination needs to be evaluated on a case-by-case basis, not only with concern to the biochar product itself, but also to soil type and environmental conditions.

Implications

As highlighted above, before policy can be developed in detail, there is an urgent need for further experimental research in with regard to long-term effects of biochar application on soil functions, as well as on the behaviour and fate in different soil types (e.g. disintegration, mobility, recalcitrance), and under different management practices. The use of representative pilot areas, in different soil ecoregions, involving biochars produced from a representative range of feedstocks is vital. Potential research methodologies are discussed in the report. Future research should also include biochars from non-lignin-based feedstocks (such as crop residues, manures, sewage and green waste) and focus on their properties and environmental behaviour and fate as influenced by soil conditions. It must be stressed that published research is almost exclusively focused on (sub)tropical regions, and that the available data often only relate to the first or second year following biochar application.

Preliminary evidence suggests that a tight control on the feedstock materials and pyrolysis conditions might substantially reduce the emission levels of atmospheric pollutants (e.g. PAHs, dioxins) and particulate matter associated to biochar production. While implications to human health remain mostly an occupational hazard, robust qualitative and quantitative assessment of such emissions from pyrolysis of traditional biomass feedstock is lacking.

Biochar potentially affects many different soil functions and ecosystem services, and interacts with most of the 'threats to soil' outlined by the Soil Thematic Strategy (COM (2006) 231). It is because of the wide range of implications from biochar application to soils, combined with the irreversibility of its application that more interdisciplinary research needs to be undertaken before policy is implemented. Policy should first be designed with the aim to invest in fundamental scientific research in biochar application to soil. Once positive effects on soil have been established robustly for certain biochars at a specific site (set of environmental conditions), a tiered approach can be imagined where these combinations of biochar and specific site conditions are considered for implementation first. A second tier would then consist of other biochars (from different feedstock and/or pyrolysis conditions) for which more research is required before site-specific application is considered.

From a climate change mitigation perspective, biochar needs to be considered in parallel with other mitigation strategies and cannot be seen as an alternative to reducing emissions of greenhouse gases. From a soil conservation perspective, biochar may be part of a wider practical package of established strategies and, if so, needs to be considered in combination

with other techniques.

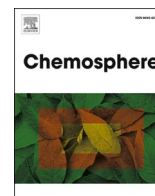
How to obtain EU publications

Our priced publications are available from EU Bookshop (<http://bookshop.europa.eu>), where you can place an order with the sales agent of your choice.

The Publications Office has a worldwide network of sales agents. You can obtain their contact details by sending a fax to (352) 29 29-42758.

The mission of the JRC is to provide customer-driven scientific and technical support for the conception, development, implementation and monitoring of EU policies. As a service of the European Commission, the JRC functions as a reference centre of science and technology for the Union. Close to the policy-making process, it serves the common interest of the Member States, while being independent of special interests, whether private or national.





Competitive adsorption of multicomponent volatile organic compounds on biochar

Hamid Rajabi^a, Mojgan Hadi Mosleh^{a,*}, Tirto Prakoso^b, Negin Ghaemi^{a,c}, Parthasarathi Mandal^a, Amanda Lea-Langton^a, Majid Sedighi^a

^a Department of Mechanical, Aerospace and Civil Engineering, School of Engineering, The University of Manchester, Manchester, M13 9PL, UK

^b Department of Bioenergy Engineering and Chemurgy, Faculty of Industrial Technology, Bandung Institute of Technology (ITB), Indonesia

^c Campus Technology Hub, Sci-Tech Daresbury, Keckwick Lane, Daresbury, Warrington, WA4 4AD, UK

ARTICLE INFO

Handling Editor: Y Yeomin Yoon

Keywords:

VOCs
Biochar
Crude oil-contaminated soil
Multi-component sorption
Desorption

ABSTRACT

Crude oil contaminated lands are recognised to have significant contributions to airborne volatile organic compounds (VOCs) with adverse effects on human health and tropospheric ozone. Soil capping systems for controlling harmful emissions are critical engineering solutions where advanced soil remediation techniques are neither available nor feasible. Studies on the adsorption of single VOC species in biochar have shown promising results as a potential capping material; however, current understanding of mixed gas system and multi-component adsorption of VOCs on biochar which would represent more realistic in situ conditions is very limited. We present, for the first time, the results of a study on competitive adsorption of mixed VOCs, including aromatic and non-aromatic VOCs commonly emitted from crude oil contaminated sites on two types of biochar pyrolysed at 500°C from wheat straw and bagasse as feedstock. The kinetics of sorption of multicomponent VOCs including acetone, hexane, toluene and p-xylene in biochar are studied based on the results of an extensive experimental investigation using a bespoke laboratory setup. Both biochar types used in this study presented a high sorption capacity for VOC compounds when tested individually (51–110 mg/g). For the multicomponent mixture, the competition for occupying sorption sites on biochar surface resulted in a lower absolute sorption capacity for each species, however, the overall sorption capacity of biochar remained more or less similar to that observed in the single gas experiments (50–109 mg/g). The chemical interactions via hydrogen bonds, electrostatic attraction, and pore-filling were found to be the main mechanisms of adsorption of VOC in the biochar studied. The efficiency of biochar regeneration was assessed through five cycles of adsorption-desorption tests and was found to be between 88% and 96%. The incomplete desorption observed confirm the formation of likely permanent bonds and heel build-ups during the sorption process.

1. Introduction

Crude oil contaminated lands are recognised to be one of the major sources of volatile organic compounds (VOCs). VOCs are categorised as hazardous chemicals and can cause a wide range of adverse effects on human health and contribute to the tropospheric ozone (Wang et al., 2015b). The crude oil-associated VOC emissions (CVEs) from contaminated lands can not only affect the neighbouring communities but also be capable of travelling extensive distances (tens of miles) to exacerbate atmospheric pollution in metropolitan areas. High infant mortality rates and severe health problems have been frequently reported near major

petroleum spillage sites with alarming cancerous/non-cancerous symptoms of human liver and kidney malfunction, respiratory and neurological system disorders, skin and eye irritations (Rajabi et al., 2020). The technologies for the remediation of oil-contaminated soil are usually time-consuming (e.g., bioremediation), costly (e.g., thermal desorption), environmentally unfriendly for certain approaches (e.g., oxidation) and sensitive to the operating conditions (physicochemical techniques) (Lim et al., 2016; Rajabi and Sharifipour, 2017, 2018, 2019). Such constraints make the conventional remediation techniques unfeasible for applications in large polluted lands or deprived regions. Therefore, an easy-to-localise solution to contain the VOC emissions

* Corresponding author. Department of Mechanical, Aerospace and Civil Engineering, The University of Manchester, Pariser Building, Sackville Street, Manchester, M13 9PL, United Kingdom.

E-mail address: mojgan.hadimosleh@manchester.ac.uk (M. Hadi Mosleh).

<https://doi.org/10.1016/j.chemosphere.2021.131288>

Received 6 April 2021; Received in revised form 15 June 2021; Accepted 17 June 2021

Available online 22 June 2021

0045-6535/© 2021 Elsevier Ltd. All rights reserved.

would protect the health of large communities living near oil-contaminated regions. Examples of such communities affected by VOC contaminated lands have been reported in Latin America (Coronel Vargas et al., 2020) and central Africa (Onyena and Sam, 2020), where affordability to benefit from effective remedial technologies is limited.

Adsorption through carbonaceous materials is a reliable technique and practised in landfill capping systems to remove gas emissions from buried wastes (Xie et al., 2016, 2017, 2018; Wang et al., 2019). Such sorption-based capping systems have the potential to be adopted and redesigned to manage hazardous emissions from contaminated soil. However, containment through engineered organic/inorganic sorbents (e.g., activated carbon or silica gel) are unfeasible for extensive polluted areas due to the cost and advanced technology required for mass production. Biochar, on the other hand, is a low-cost carbonaceous by-product of biomass pyrolysis which has been particularly utilised in a wide variety of applications including separation, carbon sequestration, energy storage/conversion and water filtration (Ahmad et al., 2014; Wang et al., 2020; Yaashikaa et al., 2020). The partial pyrolysis process can convert biomass (e.g., biowaste, agriculture waste) into porous structures which consist of a carbonised mass with reactive superficial chemistry. Such highly reactive and porous material can act as a sink to capture various types of organic and inorganic chemicals (Zhang et al., 2017a). Biochar can be utilised as an affordable sorbent for managing CVEs from contaminated soil since it can be supplied in large quantities from widespread feedstock through the low-tech low-cost combustion process. Interests in applications of biochar in environmental control systems and treatment processes have recently emerged (e.g., soil remediation, carbon sequestration, decontaminations, catalysts, organic solid waste composting, etc.) (Wang and Wang, 2019).

Char-based removals of volatile chemicals have been studied by other researchers too, e.g. benzene (Kumar et al., 2020), cyclohexane (Zhang et al., 2017b, 2019, 2020b; Xiang et al., 2020), ethylbenzene (Kim et al., 2019), toluene (Zhang et al., 2017b; Xiang et al., 2020; Yang et al., 2020), and xylenes (Zhang et al., 2020a). Biochar from a range of feedstock has also been tested for the removal of xylene isomers which are among high-detected high-concentrated CVEs (Rajabi et al., 2020). The existing limited studies which have only looked at the adsorption of individual VOC species on biochar provide an incomplete understanding of the biochar potential for containment of VOCs in a multispecies/multi-component system. The competitive adsorption under realistic multispecies systems has received very little attention. This paper, for the first time, provides an insight into the sorption of multicomponent VOC systems on biochar as an exploratory research to provide a scientific base (concept development and validation) of a low-cost system to contain the hazardous emissions from crude oil-contaminated lands with certain level of similarity to the capping systems conventionally used in landfills. Two types of biochar from prevalent agricultural wastes were used as sorbents in this study. The VOC species of toluene, p-xylene, and hexane were used as aromatic/non-aromatic examples of CVEs which are abundantly detected near petroleum polluted sites. Acetone was also considered as it has been frequently used in studies of VOC adsorption in carbon-based adsorbents due to its high volatility and very small molecule size. The rationale was to compare our results with other studies on biochar-based removal of VOCs (Zhang et al., 2017). The competitive sorption of acetone with a lower molar mass (58 g/mol), kinetic diameter (3.8 Å) and boiling point (56 °C) and without a benzene ring in its molecular shape could further reveal the governing mechanisms of VOC adsorption on biochar under competitive inhibition. Physicochemical properties of biochar samples were studied through elemental analysis, Fourier-transform infrared spectroscopy (FTIR), scanning electron microscopy (SEM), and Brunauer–Emmett–Teller (BET) surface area analysis. A bespoke experimental setup with an in-line GC-FID was developed to investigate the kinetics of both single- and multi-component sorption of VOCs on the samples and to assess their reliability and reusability through five cyclic single-component

adsorption-desorption tests on acetone and toluene as representative non-aromatic and aromatic VOCs.

2. Materials and methods

2.1. Biochar and chemicals

Two types of biochar, both formed by pyrolysis at 500 °C sourcing from wheat straw (WS) and bagasse sugarcane (BG), were chosen as commonly available agricultural waste (Yuan and Sun, 2010). These were obtained from Nanjing Zhironglian Technology (China) and Bandung Institute of Technology (Indonesia), respectively. High purity (+99%) analytical grades of acetone, hexane, toluene, and p-xylene were purchased from Acros Organics as adsorbates (Table S1). Biochar samples were manually grounded using a mortar and pestle, then sieved to obtain a size range between 0.5 and 1 mm. The sieved samples were then washed thoroughly using deionised water to remove any impurities, and then oven-dried at 85°C for 24 h until the weight stabilised. The dried samples were stored in sealed containers and used for characterisation and sorption tests.

2.2. Biochar characterisation

CHNS elemental analyser (Thermo Scientific™) and scanning electron microscopy (SEM, FEI Quanta™ 650 FEG) were utilised to analyse the elemental composition and structural features of the used biochar, respectively. SEM images were taken under a low accelerating voltage (2.00 kV) via Everhart-Thornley Detector (ETD) mode at various magnifications up to 1000×. Detailed information of the porous system of the samples (e.g., BET surface area and pore volume) was determined by the N₂ adsorption-desorption isotherms (Micromeritics® Surface Area Analyser). The samples (typically 0.1–0.2 g) were initially degassed using a Micromeritics FlowPrep 060 under a flow of CP grade N₂ at 80°C for 18 h before BET surface area measurements. Infrared spectra of the samples were taken by Spotlight 200i FTIR Spectroscopy (PerkinElmer®) in the range of 400–4000 cm⁻¹ as an identification tool to describe the biochar surface functional groups.

2.3. Adsorption and desorption tests

The experimental setup designed and used for investigating the single gas sorption process (details can be found in (Rajabi et al., 2021)) was further extended to create the capability for studying the kinetics of multicomponent sorption processes as well as gas desorption (Fig. S1). The stripping method (pure nitrogen as carrier gas regulated at 0.2 ml/min) was used to convert liquid VOCs (injected into carrier gas at specific rates via a set of syringe pumps). A concentration of 200–220 ppmv was considered for all chemicals in single- and multi-component tests. This range was selected to represent the maximum concentrations reported in the literature for VOC emissions from petroleum contaminated sites (Pandya et al., 2006; Bocos-Bintintan et al., 2019; Rajabi et al., 2020). In order to ensure intended VOC concentrations are achieved in the mixed gas system, four gas-tight microsyringes (Hamilton-1725 TLL; 250 µl) driven by two dual-syringe infusion pumps (Cole-Parmer and Chemyx) at different injection rates of 0.008–0.02 ml/h were employed to gradually inject the liquid chemicals into the flow of carrier gas (0.02 ml/min). On average, 3–4 h were required to produce a steady gas stream of desired VOC concentrations. Further details about experimental methodology, calibrations and adjustment of VOC concentrations can be found in (Rajabi et al., 2021). The mixed gas was then passed through a mixing bottle packed with glass beads to ensure its homogeneity before injection into the adsorption column. Based on a careful review of the literature, it appears that both terms (i. e., gas and vapour) are commonly used to refer to VOCs. For example VOCs have been considered as vapours by (Feng et al., 2020) and (Mızrak et al., 2017), whereas (Cheng et al., 2020) and (Minella and

Minero, 2021) referred to them as gases. The United States Environmental Protection Agency (EPA) also states that “Volatile organic compounds (VOCs) are emitted gases from certain solids or liquids” (EPA, 2019). Moreover, in this study N₂ was used as a stripping gas, and therefore the mixture is also referred to as gas for consistency and clarity. The temperature of the adsorption column was maintained at 25°C during all adsorption tests using a digital water bath. An in-line GC-FID (Chromatotec®) was utilised for continuous analysis of the outflow gas composition at 15-min intervals. The injection of mixed gas with desired VOC concentration into the sorption column (gas-tight solvent-resistant Plexiglass cell) was continued until the biochar samples (0.5 ± 0.01 g) reached saturation. The saturation state was considered when the stabilised composition of the outflow gas was observed for at least 1 h. Once the sorption was completed, desorption was initiated by stopping the gas injection and increasing the temperature of the sorption column by submerging that in a water bath to accelerate the process. The temperature was increased at a rate of approximately 4.8 °C/min to a maximum temperature of 95°C to initiate/accelerate the desorption process as a technical procedure frequently used in the literature (Xiang et al., 2020; Zhang et al., 2020b). Five single adsorption/desorption cycles were carried out on selected sorbents/sorbates to evaluate the reusability of the biochar. Data collected by the GC-FID were analysed based on the mass conservation equations (Eqs. (S1-2) in supplementary materials). Each test was repeated three times, and the mean value with an absolute uncertainty (absolute error) was reported. To obtain further insight into the governing sorption mechanism, the experimental results were compared against well-established kinetic models including pseudo-first and second-order models (PFOM & PSOM), the Elovich model (ELM) and the intra-particle diffusion model (IPDM) (Eqs. (S3-7)).

3. Results and discussion

3.1. Biochar characterisation

Physicochemical properties of carbonaceous materials govern their sorption mechanisms for the removal of organic/inorganic pollutants (Zhu et al., 2020). Such properties are mainly characterised through elemental composition, porous structure and surface chemistry. CHNS/O elemental composition and porous characteristics of the biochar are presented in Table 1. The oxygen content was measured using the mass balance technique (Chen et al., 2008). Both types of biochar are rich in carbon with 67% and 76% carbonised mass for WS and BG, respectively. The atomic ratios of aromaticity (H/C), hydrophilicity (O/C) and polarity (O + N)/C for WS char are nearly doubled in comparison to BG. The lower polarity of BG can be attributed to its higher carbon content compared to the high-organic structure of WS with more polar compounds (e.g., cellulose, fatty acids, and lignin) and more aromatic cores, which elevate its polarity too (Cao et al., 2019). FTIR spectra of biochar samples (Fig. 1) indicate a wide variety of oxygen- and hydrogen-containing functional groups on biochar surface which can interact with organic compounds. Similar peaks were found on both samples at 748–874 cm⁻¹ (C-H bending), 1512–1692 cm⁻¹ (C=O stretching), 1980–1982 cm⁻¹ (C-H aromatic bending), 2162–2166 cm⁻¹ (C=C=O stretching) and 2958–3044 cm⁻¹ (C-H stretching). BG lacks few peaks at 1314–1378 cm⁻¹ which can be associated with the absence of polar compounds in BG (e.g., lignin, cellulose, and hemicelluloses) which also shows the lower polarity of BG in comparison to WS deduced from the elemental analysis. A lower

hydrophilic surface of BG with fewer polar groups can be also confirmed by its lower ratio of O/C (hydrophilicity) and (O + N)/C (polarity). BG has a higher SSA/PV from BET analysis compared with WS (Table 1). Similar observations have been also reported for biochar produced from wheat straw and sugarcane bagasse (Chatterjee et al., 2020). Differences in pore size and shape of both samples can be evaluated using SEM images (Fig. S2). Both samples have a wide range of pore sizes (magnification of 100 & 50 μm); however, BG has a more homogeneous pattern of smaller pores (5 μm) in comparison to WS having fewer but bigger pores/canals at the same scale.

3.2. Single-component sorption

The single-component sorption kinetics of selected VOCs on BG and WS biochar are presented in Fig. 2. The highest sorbed mass was observed for acetone on BG, followed by p-xylene, toluene, and hexane. The overall differences in adsorption quantities can be attributed to (i) molecular characteristics of the VOCs with different kinetic diameters and non-identical conformation and configuration (steric hindrance), and (ii) biochar surface chemistry and porosity. Acetone can combine with carbonised mass of both samples mostly through carboxylic groups (Yu et al., 2018), and a low kinetic diameter (3.8 Å) enables acetone molecules to interact with more active sites and enter smaller pores/canals (Zhang et al., 2017b). The maximum adsorption (Q_{eq}) of acetone on BG (110.1 ± 5.4 mg/g) is more than doubled the adsorbed mass on WS (44.5 ± 2.1 mg/g). This is due to the higher SSA/PV of BG which elevates the pore-filling and access to active sites. On the other hand, the lowest sorption capacity on both samples is related to hexane mainly because of its specific molecular arrangements which affect its success rate for adsorbing onto the carbon surface of the biochar. Hexane molecules (C₆H₁₄) are normally aligned parallel (an elongated cylinder (Wang et al., 2015a)) to carbon surface and can interact with carbon molecules by seven hydrogen atoms only through CH-π bonding, while other aromatic chemicals (e.g., toluene and p-xylene) utilise not only CH-π interactions but also π-π stacking and other functional groups in combination with carbon surfaces (Thongsai et al., 2019). Hexane was also found to be more adsorbed on BG (36.8 ± 1.5 mg/g) in comparison to WS (19.7 ± 0.9 mg/g) which can be related to its higher inclination towards hydrophobic carbon surfaces with fewer oxygenated groups and greater porosity (e.g., BG) (Hernández-Monje et al., 2018).

Aromatic structures of toluene and p-xylene can be adsorbed onto carbon surface through π-π stacking (Navarro Amador et al., 2018), electrostatic attraction (Solanki and Boyer, 2019) and functional groups (Kim et al., 2019) as well as partitioning into non-carbonised mass (Chen et al., 2017). It should be added that adsorption of VOCs on carbon-based materials mainly is a physicochemical process mostly controlled by physical attraction through pore-filling and van der Waals forces in addition to chemical attractions via functional groups and stacking (reversible) rather than chemical reactions (irreversible). The ultimate sorption of toluene on BG (45.2 ± 1.7 mg/g) is slightly higher than WS (32.5 ± 1.6 mg/g) which can be related to the increased pore-filling within BG mass and higher SSA; however, different behaviour was observed for the case of p-xylene. P-xylene molecules with para-substituted benzene cores are more accumulated onto the low-SSA structure of wheat straw due to higher polarity (more polar groups) of wheat straw biochar compared with bagasse (more details in Fig. 1). In addition, the kinetic behaviour of p-xylene sorption on both types of biochar is more or less similar (Fig. 2) since its big molecules and higher steric hindrance might have prevented p-xylene to enter more available

Table 1
Physicochemical properties and pore characteristics of biochar samples.

Biochar	C (%)	H (%)	N (%)	S (%)	O (%)	O/C	H/C	(O + N)/C	S _{BET} (m ² .g ⁻¹)	V _{Total-BET} (cm ³ .g ⁻¹)
BG	75.94	1.77	0.40	NF	21.89	0.289	0.024	0.293	78.15	0.1448
WS	66.57	2.66	0.98	<0.3	29.49	0.443	0.040	0.458	58.38	0.0786

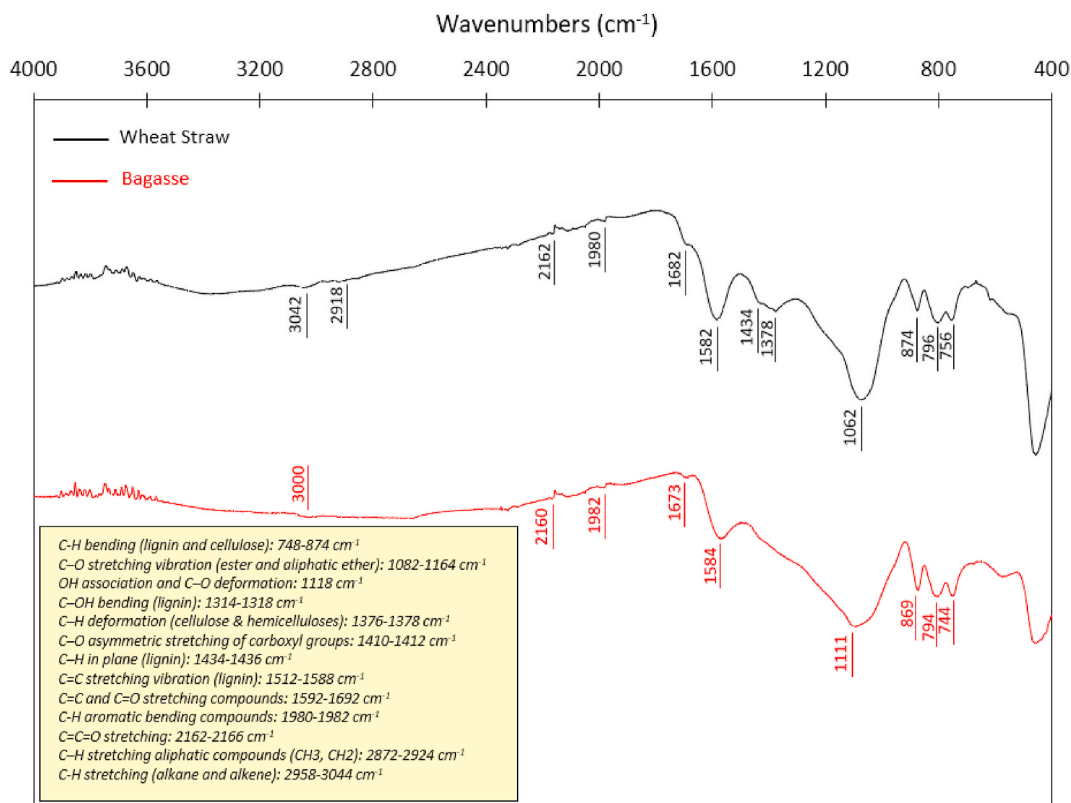


Fig. 1. FTIR spectra of WS and BG biochar.

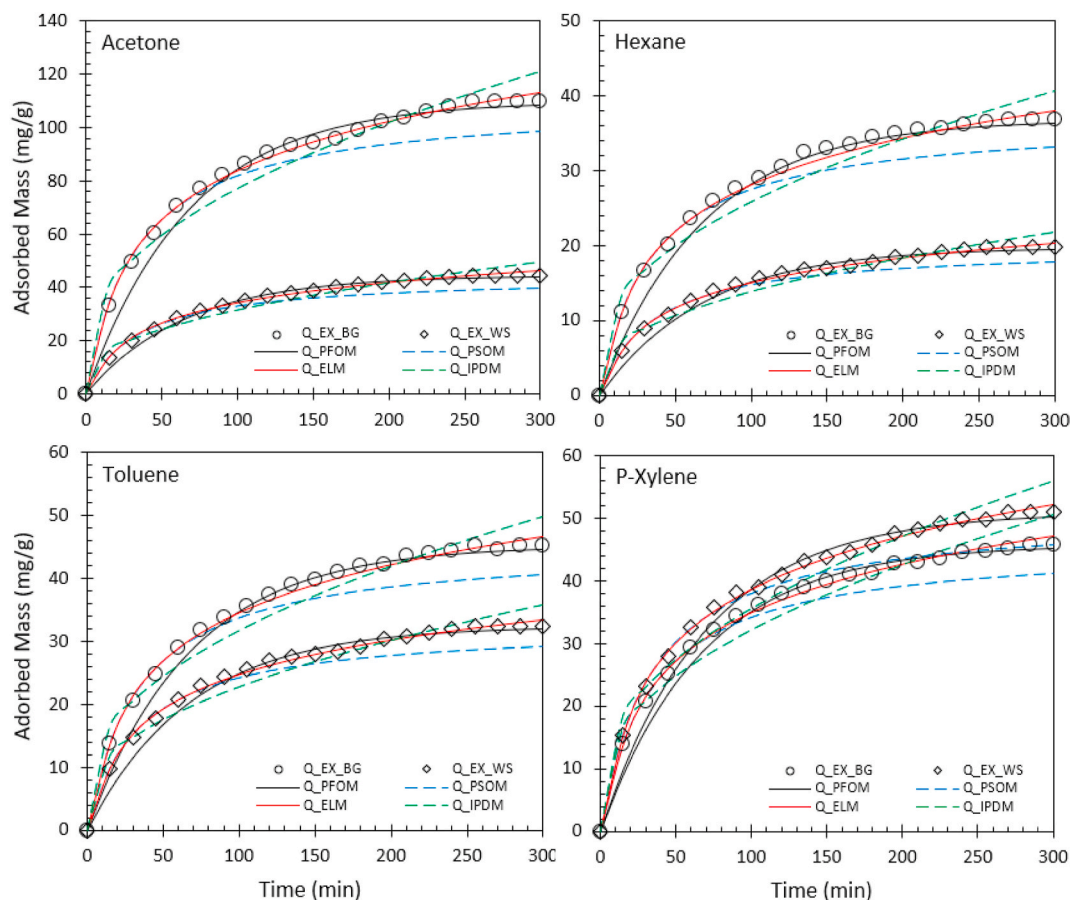


Fig. 2. Kinetics of single-component sorption of VOCs on WS and BG biochar.

pores within the BG structure. Overall, adsorption kinetics of both types of biochar showed reasonable removal capacities up to 110.1 ± 5.4 mg/g compared to the rate of VOC emissions reported for oil-contaminated lands (Ausma et al., 2002; Wang et al., 2015b; Rajabi et al., 2020). It should be noted that the used biochar showed reliable potentials for removal of acetone (44.5 and 110.9 mg/g), hexane (36.8 and 19.7 mg/g), toluene (32.4 and 45.2 mg/g) and p-xylene (24.8 and 51.1 mg/g) in comparison to other reported figures for adsorption on non-activated/non-modified biochar such as acetone: 7.6–50.2 mg/g (Xiang et al., 2020); 7.1–91.2 mg/g (Zhang et al., 2017b); 17.9–25.2 mg/g (Zhang et al., 2020b), toluene: 13.8–65.5 mg/g (Kumar et al., 2020); 12.7–55.1 mg/g (Xiang et al., 2020); 31.2 mg/g (Yang et al., 2020); 12.7–62.9 mg/g (Zhang et al., 2017b); and xylenes: 1.5–60.2 mg/g (Kumar et al., 2020). A statistical analysis also showed a non-linear relationship between each adsorbates' property (molar mass, boiling point, and kinetic diameter) and adsorption capacity of the used biochar. It revealed that the sorption mechanism of VOCs on biochar may not be only controlled by the molecular properties of VOCs, and other mechanisms such as adsorbent's surface chemistry and porous structure are also involved. The FTIR spectra taken from clean and saturated samples (WS biochar as an example) by all chemicals are provided in Fig. S3. The characteristic peaks corresponding to acetone (at 529, 1220, 1358, and 1710 cm^{-1}), hexane (at 723, 1379, and 1459 cm^{-1}), toluene (at 464, 693, 726, and 1495 cm^{-1}) and p-xylene (at 482, 793, and 1516 cm^{-1}) on saturated samples in addition to sorption tests can confirm that biochar from agricultural waste can effectively adsorb both aromatic and non-aromatic VOCs.

3.3. Multi-component sorption

Figs. 3 and 4 present the results from multi-component adsorption

experiments for mixed VOCs on both biochar types. The presence of chemicals on the biochar surface was confirmed by the corresponding peaks on FTIR spectra of the saturated samples, as shown in Fig. S4. Higher SSA/PV of BG provides more accessible active sites to the mixed gas molecules resulting in higher sorption capacity (109.1 ± 4.3 mg/g) in comparison to that of WS (50.1 ± 2.1 mg/g). The total adsorbed mass of multi-component tests is very slightly lower than that of single gas for both samples which might be due to few active sites left vacant in the competitive process of adsorption. The total adsorbed mass of each VOC in multi-compound tests is noticeably lower (27–75%) than that of the single gas in both samples. This shows that the adsorption capacity of all adsorbates was limited due to the competitive inhibition.

The reduction in total adsorption capacity of multicomponent gas compared to the single component can be explained by increased competitive inhibition of the sorption process (Fig. 5), which leads to a lower sorbed mass and slightly rapid saturation (Vikrant et al., 2020). The reductions in the saturation time were in the range of 7.1–16.7% and 5.3–13.2% for all the chemicals on WS and BG, respectively. This is attributed to a higher molecular diffusion under competitive inhibition (Jahandar Lashaki et al., 2016). A higher reduction in the overall sorption capacity of each compound in multi-component tests was observed in WS (51–75%) in comparison to BG (27–70%). This is expected to be associated with the lower SSA/PV which gives fewer active sites within the WS structure to adsorbates. The reductions in maximum sorption between individuals and mixtures are more significant for lighter VOCs (acetone) than heavier VOCs considered in this study (hexane, toluene, and p-xylene). This is particularly highlighted on bagasse which can be related to greater van der Waals' interactions between carbon surface and heavier compounds having more carbon atoms (Samaddar et al., 2019). The sorption order also remained unchanged for BG in both single and multi-component tests (acetone >

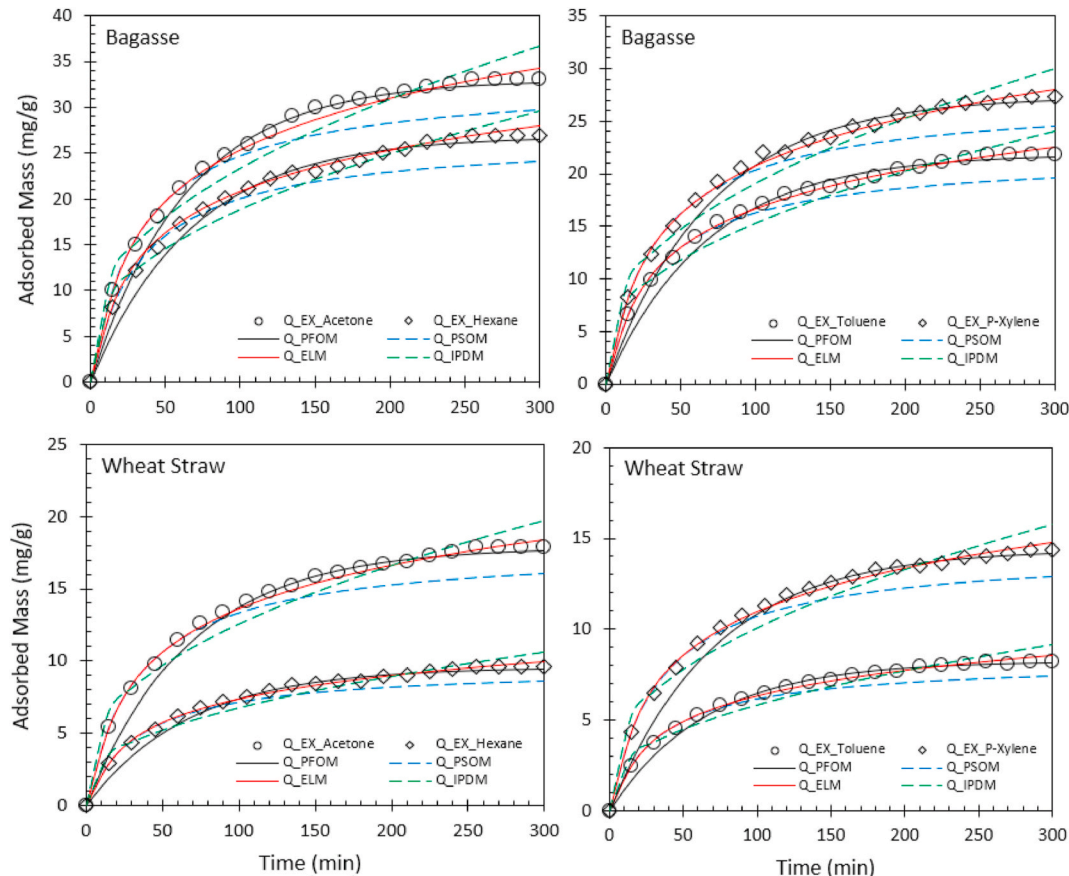


Fig. 3. Kinetics of multi-component sorption of acetone, hexane, toluene, and p-xylene on WS and BG biochar.

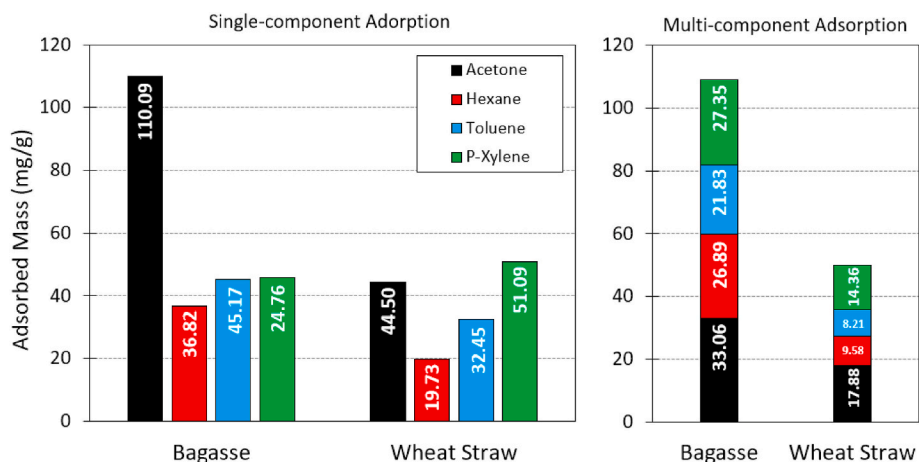


Fig. 4. Comparison of adsorption capacity of BG and WS biochar in single and multi-component experiments.

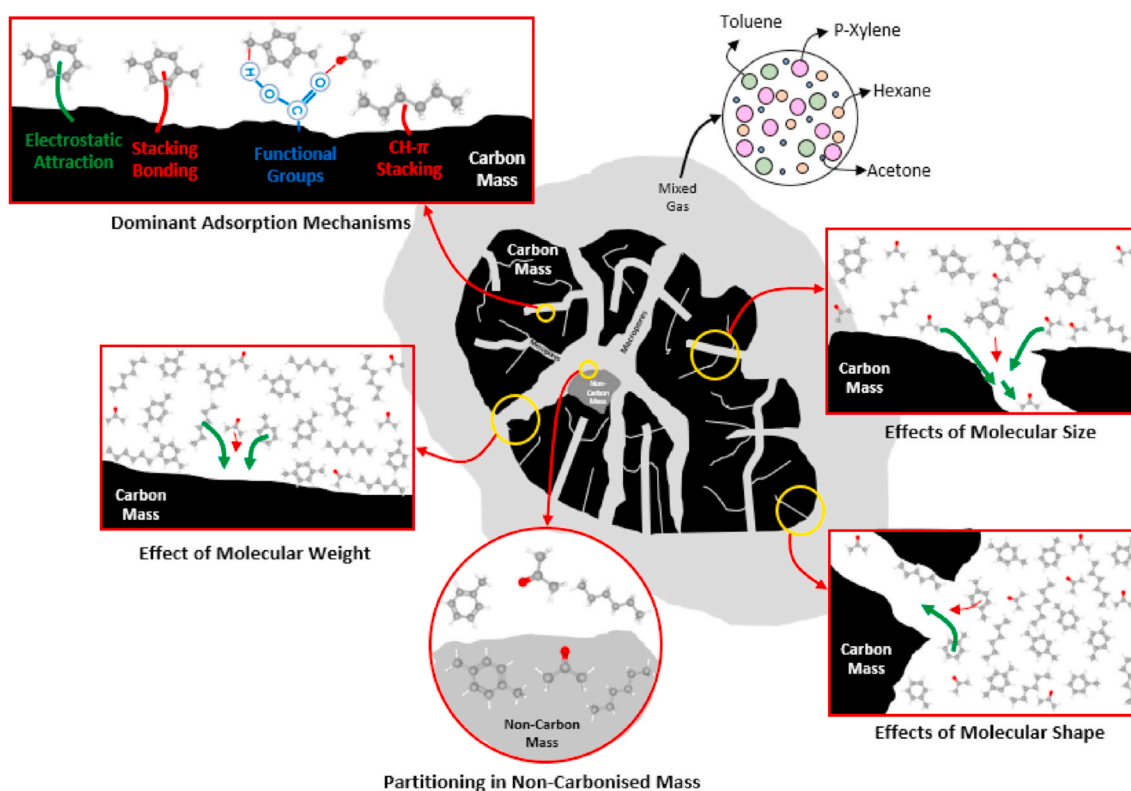


Fig. 5. Graphical description of dominant mechanisms in competitive adsorption.

p-xylene > toluene > hexane), for WS however, there was a slight discrepancy in this order for hexane and toluene. A higher uptake of hexane by WS in comparison to toluene may be attributed to the greater molecular diffusivity within the pores. In addition, the larger kinetic diameter of toluene molecules can also act as a barrier to their competitive sorption with hexane to secure access to the active sites.

This behaviour is not valid for acetone with smaller molecules (3.8 Å) than hexane since its multi-component uptake by BG is seen to reduce by 65.12%. Larger individual uptake of acetone may be related to the greater contributions of smaller pores in capturing acetone of which a large quantity is now blocked by larger molecules of hexane, toluene, and p-xylene in the competitive process. Similar behaviour observed in uptakes of toluene and p-xylene from mixed gas on both biochar types can be related to their similar kinetic diameter (5.9 Å) and molecular shape (aromaticity); however, their sorbed amounts were more reduced

by competitive sorption on WS (29–36%) mainly due to its lower SSA/PV compared with BG (10–27%). The results of multi-component experiments provide confidence in the reliability of biochar as an efficient adsorbent with adequate sorption capacity to control VOC emissions from crude oil contaminated lands for a range of aromatic/non-aromatic chemicals with different molecular characteristics.

3.4. Desorption

Desorption is an important index for adsorbents commercialisation since regeneration potential is a critical property of an adsorbent demonstrating its reusability for adsorption system as well as safety/reliability for ex-situ regeneration process (Jang et al., 2020; Feizbakhshan et al., 2021). With regards to the effects of elevated temperature on the desorption process of VOCs on biochar, studies reported

indicate that the saturated biochar (from a range of feedstocks) can retain between 50 and 95% of the adsorbed volatile chemicals at 50–60°C (Xiang et al., 2020; Zhang et al., 2020). It shows the reliability of biochar materials for containment purposes to retain adsorbed volatile chemicals even under extreme operating conditions. The desorption process should also be investigated to better comprehend the dominant mechanisms of adsorption (Zhang et al., 2020a). The regeneration potential of the used biochar was investigated through five successive adsorption-desorption tests with acetone and toluene as (Feizbakhshan et al., 2021) non-aromatic and aromatic CVEs, respectively. The experimental procedure for the assessment of VOC desorption from biochar is described in Section 2.3, and the results are presented in Fig. 6. Both samples (BG and WS) indicated regeneration efficiency (RE) (Eq. S2) of approximately 86.9–96.4% overall cyclic tests as a reliable range for biochar. From the results, it can be observed that the majority of gas desorption occurs in the first cycle. Depending on the biochar type and gas specie, on average, 4–13% of adsorbed gas was released during the first cycle, whereas in subsequent cycles, there were slight fluctuations in the detected regeneration efficiency. The results of desorption tests show that the majority of adsorbed gas remains within the structure

of biochar which can be related to the creation of some permanent bonds between VOC molecules and functional groups on biochar surface (Zhang et al., 2017b) and/or heel build-ups during cyclic adsorption-desorption of VOCs (Jahandar Lashaki et al., 2020). Acetone presented the highest and lowest RE for WS (95.4%) and BG (90.1%), respectively, because of its different desorption mechanisms in these samples. Desorption of acetone from wheat straw is simpler than from bagasse since BG has a high-SSA structure in which pore filling is dominant, and more pore blockage and oligomerization are probable during desorption (heel formation) (Lashaki et al., 2012).

Compared to acetone, toluene showed relatively similar desorption behaviour and RE, although its desorption mechanisms may have been different. More molecules of toluene retained within WS after desorption due to its higher boiling point in comparison to acetone and better surface chemistry of WS with more active sites (than BG). However, a higher desorption rate from BG was observed for toluene. Toluene has relatively large molecules and therefore its access to the adsorption sites in smaller pores and canals of BG are limited which leads to an easier release of gas molecules of toluene in larger channels and pores (Yang et al., 2020).

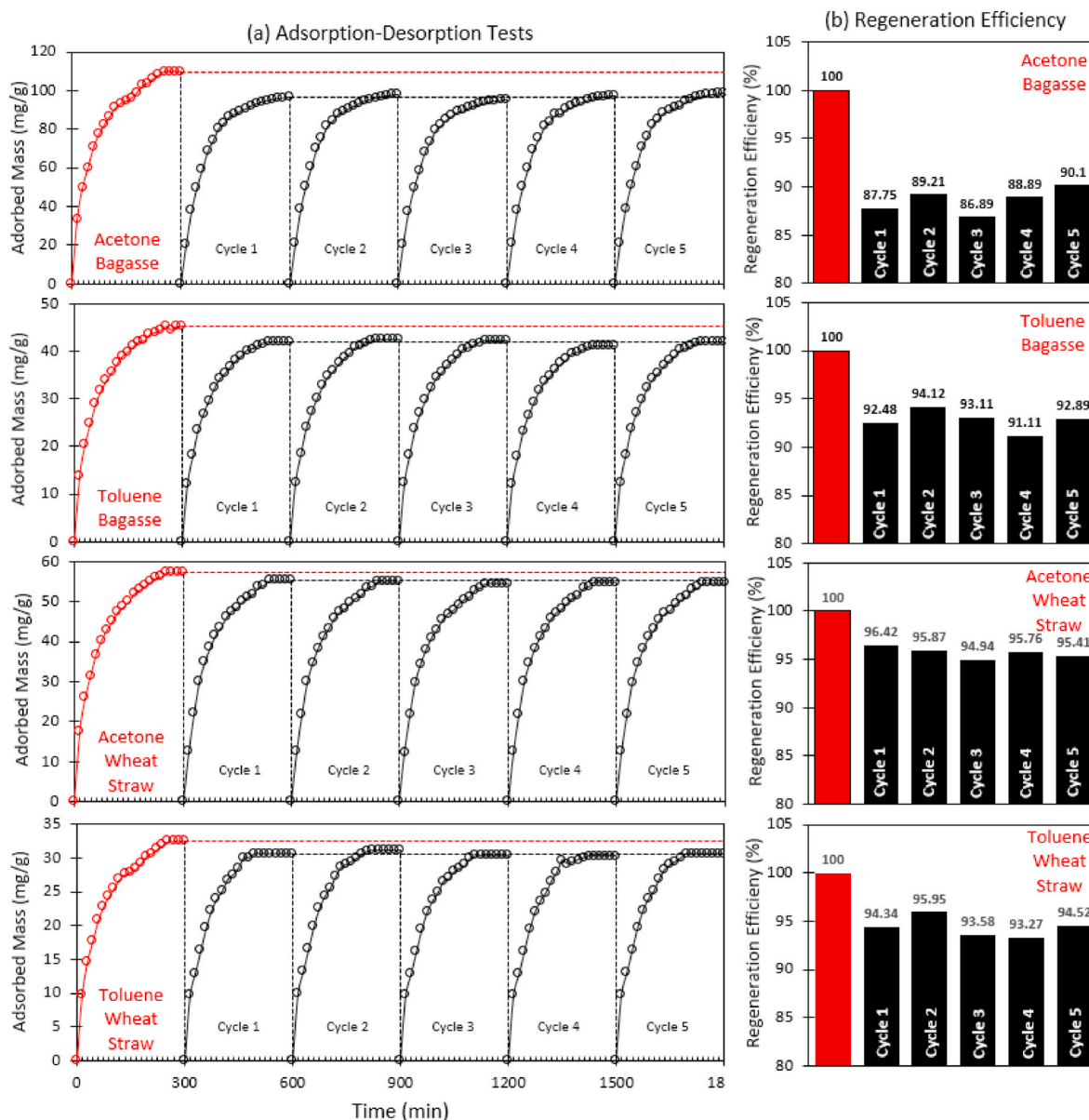


Fig. 6. Adsorption-desorption cycles of acetone and toluene on BG and WS biochar.

3.5. Sorption modelling

Figs. 2 and 3 also present a comparison of the experimental results with the sorption dynamics anticipated by the conventional kinetic models including PFOM, PSOM, ELM and IPDM. The coefficients of determination (R^2) and the sum of the squared errors (SSE) are provided in Table S2–3. Overall, there are strong correlations between the kinetic models and the experimental data. However, the data from the ELM model showed the best fits to the test results in both single gas (e.g., $R^2 = 0.998$ and $SSE = 1.33$ for hexane on WS) and multi-component sorption experiments (e.g., $R^2 = 0.998$ and $SSE = 1.63$ for toluene on BG). Based on the results, PFOM and PSOM underestimated the amount of sorption at equilibrium up to 1.23% and 11.53% in single gas and 0.98% and 10.42% in the mixed gas, respectively, while ultimate sorption was overestimated by IPDM up to 9.34% and 9.98% in single and multi-component tests. The robust agreement between the ELM data and experimental results may be attributed to the Elovich equation assumption. The Elovich kinetic model is the best fit for the experimental data when chemical adsorption on heterogeneous adsorbing surfaces is the dominant mechanism (Wu et al., 2009). This agreement indirectly confirms that the chemical interactions of hydrogen bonding (CH- π & π - π stacking) and electrostatic attraction through functional groups served as chemisorption sites are the main mechanisms of adsorption in the system, as previously discussed in sections 3.2 and 3.3 along with pore-filling. The curve-fitting plots of IPDM (Q_t^{IPDM} versus $t^{0.5}$) for both single- and multi-component sorption were found not to pass through the starting point, showing that the intraparticle diffusion is not the only rate-limiting process in adsorption mechanisms of these VOCs on the samples (Yang et al., 2014).

4. Conclusions

In this paper, we presented an experimental investigation on single and multicomponent sorption kinetics of aromatic and non-aromatic volatile organic compounds on two types of biochar sourcing from commonly available agricultural wastes (wheat straw and bagasse). Investigations of the single and competitive experiments revealed sufficiently high adsorption capacities for both types of biochar, indicating the efficiency of biochar for the removal of VOC emissions from in-land oil spills under more realistic in situ conditions. The tested types of biochar showed relatively similar total adsorption capacity for single (51–110 mg/g) and mixed gases (50–109 mg/g). Bagasse showed the highest sorption capacity in both single and multi-component tests, mainly due to its higher SSA and PV. The highest adsorption on the used biochar was recorded for acetone with the smallest molecular diameter; however, its uptake was reduced up to 65% by competitive inhibition of the multi-component adsorption process. Hydrogen bonding, electrostatic interaction, and π -stacking, as well as partitioning, were found to be the main sorption mechanisms in both single and competitive VOC uptake by biochar. The Elovich model presented the best fit for the experimental data providing further confirmation for chemical interactions to be the dominant mechanism. The sorption capacity of the biochar samples was adequately sustained after five cycles of sorption-desorption tests (88–96%). The regeneration efficiency is a crucial parameter where adsorbent reproduction is required. The comprehensive experimental work carried out in this study has demonstrated for the first time the promising potentials of biochar as a sustainable, low-cost and effective capping system to uptake and contain the mission of harmful VOCs from crude oil-contaminated lands.

Credit author statement

Hamid Rajabi: Conceptualization, Methodology, Formal analysis, Investigation, Validation, Writing - Original Draft. Mojgan Hadi Mosleh: Conceptualization, Methodology, Formal analysis, Writing-Review &

Editing, Supervision, Project administration, Funding acquisition. Tirtu Prakoso: Methodology, Writing-Review & Editing, Funding acquisition. Negin Ghaemi: Methodology, Formal analysis, Writing-Review & Editing. Parthasarathi Mandal: Conceptualization, Writing-Review & Editing, Supervision. Amanda Lea-Langton: Conceptualization, Writing-Review & Editing. Supervision. Majid Sedighi: Conceptualization, Methodology, Writing-Review & Editing, Funding acquisition.

Declaration of competing interest

The authors declare that they have no known competing financial interests or personal relationships that could have appeared to influence the work reported in this paper.

Acknowledgements

H Rajabi acknowledges the financial support through Dean's Awards of the Faculty of Science and Engineering at the University of Manchester. M Hadi Mosleh and M Sedighi gratefully acknowledge the financial support provided for the project VOCaL by the University of Manchester Research England GCRF QR Allocation and the Department for Business, Energy and Industrial Strategy via British Council by grant 527663638 (GeoGrab). The authors would like to thank Prof. Yazid Bindar and Mr Pandit Hernowo from Bandung Institute of Technology (ITB) for their support in this project and the production of biochar.

Appendix A. Supplementary data

Supplementary data to this article can be found online at <https://doi.org/10.1016/j.chemosphere.2021.131288>.

References

- Ahmad, M., Rajapaksha, A.U., Lim, J.E., Zhang, M., Bolan, N., Mohan, D., Vithanage, M., Lee, S.S., Ok, Y.S., 2014. Biochar as a sorbent for contaminant management in soil and water: a review. *Chemosphere* 99, 19–33.
- Ausma, S., Edwards, G.C., Fitzgerald-Hubble, C.R., Halfpenny-Mitchell, L., Gillespie, T.J., Mortimer, W.P., 2002. Volatile hydrocarbon emissions from a diesel fuel-contaminated soil bioremediation facility. *J. Air Waste Manag. Assoc.* 52, 769–780.
- Bocos-Bintintan, V., Ratiu, I.A., Al-Suod, H., 2019. Real time monitoring of soil contamination with diesel fuel using photoionization detectors. *Arab J. Basic Appl. Sci.* 26, 446–452.
- Cao, Y., Xiao, W., Shen, G., Ji, G., Zhang, Y., Gao, C., Han, L., 2019. Carbonization and ball milling on the enhancement of Pb(II) adsorption by wheat straw: competitive effects of ion exchange and precipitation. *Bioresour. Technol.* 273, 70–76.
- Chatterjee, R., Sajjadi, B., Chen, W.-Y., Mattern, D.L., Hammer, N., Raman, V., Dorris, A., 2020. Impact of biomass sources on acoustic-based chemical functionalization of biochars for improved CO₂ adsorption. *Energy Fuels* 34, 8608–8627.
- Chen, B., Zhou, D., Zhu, L., 2008. Transitional adsorption and partition of nonpolar and polar aromatic contaminants by biochars of pine needles with different pyrolytic temperatures. *Environ. Sci. Technol.* 42, 5137–5143.
- Chen, Y., Zhang, X., Chen, W., Yang, H., Chen, H., 2017. The structure evolution of biochar from biomass pyrolysis and its correlation with gas pollutant adsorption performance. *Bioresour. Technol.* 246, 101–109.
- Cheng, J., Li, H., Zhou, J., Lin, Z., Wu, D., Liu, C., Cao, Z., 2020. Laser induced porous electropun fibers for enhanced filtration of xylene gas. *J. Hazard. Mater.* 399, 122976.
- Coronel Vargas, G., Au, W.W., Izzotti, A., 2020. Public health issues from crude-oil production in the Ecuadorian Amazon territories. *Sci. Total Environ.* 719, 134647.
- EPA, U., 2019. Volatile Organic Compounds' Impact on Indoor Air Quality. <https://www.epa.gov/indoor-air-quality-iaq/volatile-organiccompounds-impact-indoor-air-quality#intro>.
- Feizbakhshan, M., Amdebrhan, B., Hashisho, Z., Phillips, J.H., Crompton, D., Anderson, J.E., Nichols, M., 2021. Effects of oxygen impurity and desorption temperature on heel build-up in activated carbon. *Chem. Eng. J.* 409, 128232.
- Feng, S.-J., Zhu, Z.-W., Chen, H.-X., Chen, Z.-L., 2020. Two-dimensional analytical solution for VOC vapor migration through layered soil laterally away from the edge of contaminant source. *J. Contam. Hydrol.* 233, 103664.
- Hernández-Monje, D., Giraldo, L., Moreno-Piraján, J.C., 2018. Study of Hexane Adsorption on Activated Carbons with Differences in Their Surface Chemistry, 23. *Molecules*, Basel, Switzerland.
- Jahandar Lashaki, M., Atkinson, J.D., Hashisho, Z., Phillips, J.H., Anderson, J.E., Nichols, M., 2016. The role of beaded activated carbon's surface oxygen groups on irreversible adsorption of organic vapors. *J. Hazard. Mater.* 317, 284–294.

- Jahandar Lashaki, M., Hashisho, Z., Phillips, J.H., Crompton, D., Anderson, J.E., Nichols, M., 2020. Mechanisms of heel buildup during cyclic adsorption-desorption of volatile organic compounds in a full-scale adsorber-desorber. *Chem. Eng. J.* 400, 124937.
- Jang, Y., Bang, J., Seon, Y.-S., You, D.-W., Oh, J.-S., Jung, K.-W., 2020. Carbon nanotube sponges as an enrichment material for aromatic volatile organic compounds. *J. Chromatogr. A* 1617, 460840.
- Kim, J., Lee, S.S., Khim, J., 2019. Peat moss-derived biochars as effective sorbents for VOCs' removal in groundwater. *Environ. Geochem. Health* 41, 1637–1646.
- Kumar, A., Singh, E., Khapre, A., Bordoloi, N., Kumar, S., 2020. Sorption of volatile organic compounds on non-activated biochar. *Bioresour. Technol.* 297, 122469.
- Lashaki, M.J., Fayaz, M., Wang, H., Hashisho, Z., Phillips, J.H., Anderson, J.E., Nichols, M., 2012. Effect of adsorption and regeneration temperature on irreversible adsorption of organic vapors on beaded activated carbon. *Environ. Sci. Technol.* 46, 4083–4090.
- Lim, M.W., Lau, E.V., Poh, P.E., 2016. A comprehensive guide of remediation technologies for oil contaminated soil — present works and future directions. *Mar. Pollut. Bull.* 109, 14–45.
- Minella, M., Minero, C., 2021. Evaluation of gas/solid photocatalytic performance for the removal of VOCs at ppb and sub-ppb levels. *Chemosphere* 272, 129636.
- Mızrak, B., Altındal, A., Abdurrahmanoğlu, Ş., 2017. Synthesis, characterization and partition coefficients for VOC vapor adsorption onto novel pyridine derivatives Co (II) phthalocyanines. *Prog. Org. Coating* 109, 92–96.
- Navarro Amador, R., Cirre, L., Carboni, M., Meyer, D., 2018. BTEX removal from aqueous solution with hydrophobic Zr metal organic frameworks. *J. Environ. Manag.* 214, 17–22.
- Onyena, A.P., Sam, K., 2020. A review of the threat of oil exploitation to mangrove ecosystem: insights from Niger Delta, Nigeria. *Global Ecol. Conserv.* 22, e00961.
- Pandya, G., Gavane, A., Bhanarkar, A., Kondawar, V., 2006. Concentrations of volatile organic compounds (VOCs) at an oil refinery. *Int. J. Environ. Stud.* 63, 337–351.
- Rajabi, H., Hadi Moseleh, M., Mandal, P., Lea-Langton, A., Sedighi, M., 2020. Emissions of volatile organic compounds from crude oil processing – global emission inventory and environmental release. *Sci. Total Environ.* 727, 138654.
- Rajabi, H., Moseleh, M.H., Mandal, P., Lea-Langton, A., Sedighi, M., 2021. Sorption behaviour of xylene isomers on biochar from a range of feedstock. *Chemosphere* 268, 129310.
- Rajabi, H., Sharifipour, M., 2017. An experimental characterization of shear wave velocity (vs) in clean and hydrocarbon-contaminated sand. *Geotech. Geol. Eng.* 35, 2727–2745.
- Rajabi, H., Sharifipour, M., 2018. Influence of weathering process on small-strain shear modulus (Gmax) of hydrocarbon-contaminated sand. *Soil Dynam. Earthq. Eng.* 107, 129–140.
- Rajabi, H., Sharifipour, M., 2019. Geotechnical properties of hydrocarbon-contaminated soils: a comprehensive review. *Bull. Eng. Geol. Environ.* 78, 3685–3717.
- Samaddar, P., Kim, K.-H., Yip, A.C.K., Zhang, M., Szulejko, J.E., Khan, A., 2019. The unique features of non-competitive vs. competitive sorption: tests against single volatile aromatic hydrocarbons and their quaternary mixtures. *Environ. Res.* 173, 508–516.
- Solanki, A., Boyer, T.H., 2019. Physical-chemical interactions between pharmaceuticals and biochar in synthetic and real urine. *Chemosphere* 218, 818–826.
- Thongsai, N., Jaiyong, P., Kladsomboon, S., In, I., Paoprasert, P., 2019. Utilization of carbon dots from jackfruit for real-time sensing of acetone vapor and understanding the electronic and interfacial interactions using density functional theory. *Appl. Surf. Sci.* 487, 1233–1244.
- Vikrant, K., Kim, K.-H., Kumar, V., Giannakoudakis, D.A., Boukhvalov, D.W., 2020. Adsorptive removal of an eight-component volatile organic compound mixture by Cu-, Co-, and Zr-metal-organic frameworks: experimental and theoretical studies. *Chem. Eng. J.* 397, 125391.
- Wang, G., Dou, B., Zhang, Z., Wang, J., Liu, H., Hao, Z., 2015a. Adsorption of benzene, cyclohexane and hexane on ordered mesoporous carbon. *J. Environ. Sci.* 30, 65–73.
- Wang, H., Fischer, T., Wieprecht, W., Möller, D., 2015b. A predictive method for volatile organic compounds emission from soil: evaporation and diffusion behavior investigation of a representative component of crude oil. *Sci. Total Environ.* 530, 38–44.
- Wang, J., Wang, S., 2019. Preparation, modification and environmental application of biochar: a review. *J. Clean. Prod.* 227, 1002–1022.
- Wang, Q., Zuo, X., Xia, M., Xie, H., He, F., Shen, S., Bouazza, A., Zhu, L., 2019. Field investigation of temporal variation of volatile organic compounds at a landfill in Hangzhou, China. *Environ. Sci. Pollut. Control Ser.* 26, 18162–18180.
- Wang, Z., Sedighi, M., Lea-Langton, A., 2020. Filtration of microplastic spheres by biochar: removal efficiency and immobilisation mechanisms. *Water Res.* 184, 116165.
- Wu, F.-C., Tseng, R.-L., Juang, R.-S., 2009. Characteristics of Elovich equation used for the analysis of adsorption kinetics in dye-chitosan systems. *Chem. Eng. J.* 150, 366–373.
- Xiang, W., Zhang, X., Chen, K., Fang, J., He, F., Hu, X., Tsang, D.C.W., Ok, Y.S., Gao, B., 2020. Enhanced adsorption performance and governing mechanisms of ball-milled biochar for the removal of volatile organic compounds (VOCs). *Chem. Eng. J.* 385, 123842.
- Xie, H., Wang, Q., Bouazza, A., Feng, S., 2018. Analytical model for vapour-phase VOCs transport in four-layered landfill composite cover systems. *Comput. Geotech.* 101, 80–94.
- Xie, H., Wang, Q., Yan, H., Chen, Y., 2017. Steady-state analytical model for vapour-phase volatile organic compound (VOC) diffusion in layered landfill composite cover systems. *Can. Geotech. J.* 54, 1567–1579.
- Xie, H., Yan, H., Thomas, H.R., Feng, S., Ran, Q., Chen, P., 2016. An analytical model for vapor-phase volatile organic compound diffusion through landfill composite covers. *Int. J. Numer. Anal. Methods GeoMech.* 40, 1827–1843.
- Yaashikaa, P.R., Kumar, P.S., Varjani, S., Saravanan, A., 2020. A critical review on the biochar production techniques, characterization, stability and applications for circular bioeconomy. *Biotechnol. Rep.* 28, e00570.
- Yang, G., Chen, H., Qin, H., Feng, Y., 2014. Amination of activated carbon for enhancing phenol adsorption: effect of nitrogen-containing functional groups. *Appl. Surf. Sci.* 293, 299–305.
- Yang, Y., Sun, C., Lin, B., Huang, Q., 2020. Surface modified and activated waste bone char for rapid and efficient VOCs adsorption. *Chemosphere*, 127054.
- Yu, X., Liu, S., Lin, G., Zhu, X., Zhang, S., Qu, R., Zheng, C., Gao, X., 2018. Insight into the significant roles of microstructures and functional groups on carbonaceous surfaces for acetone adsorption. *RSC Adv.* 8, 21541–21550.
- Yuan, T.Q., Sun, R.C., 2010. Introduction. *Cereal Straw as a Resource for Sustainable Biomaterials and Biofuels*, pp. 1–7.
- Zhang, X., Gao, B., Creamer, A.E., Cao, C., Li, Y., 2017a. Adsorption of VOCs onto engineered carbon materials: a review. *J. Hazard. Mater.* 338, 102–123.
- Zhang, X., Gao, B., Fang, J., Zou, W., Dong, L., Cao, C., Zhang, J., Li, Y., Wang, H., 2019. Chemically activated hydrochar as an effective adsorbent for volatile organic compounds (VOCs). *Chemosphere* 218, 680–686.
- Zhang, X., Gao, B., Zheng, Y., Hu, X., Creamer, A.E., Annable, M.D., Li, Y., 2017b. Biochar for volatile organic compound (VOC) removal: sorption performance and governing mechanisms. *Bioresour. Technol.* 245, 606–614.
- Zhang, X., Miao, X., Xiang, W., Zhang, J., Cao, C., Wang, H., Hu, X., Gao, B., 2020a. Ball milling biochar with ammonia hydroxide or hydrogen peroxide enhances its adsorption of phenyl volatile organic compounds (VOCs). *J. Hazard. Mater.*, 123540.
- Zhang, X., Xiang, W., Wang, B., Fang, J., Zou, W., He, F., Li, Y., Tsang, D.C.W., Ok, Y.S., Gao, B., 2020b. Adsorption of acetone and cyclohexane onto CO₂ activated hydrochars. *Chemosphere* 245, 125664.
- Zhu, L., Shen, D., Luo, K.H., 2020. A critical review on VOCs adsorption by different porous materials: species, mechanisms and modification methods. *J. Hazard. Mater.* 389, 122102.

ATTACHMENT C
Professional Engineer Certifications

**REMEDIAL ACTION OPTIONS REPORT – NR 712.09 CERTIFICATIONS
COMMUNITY WITHIN THE CORRIDOR – EAST BLOCK
2748 N 32ND STREET, MILWAUKEE, WI 53210
BRRTS #: 02-41-263675, FID #: 241025400
JULY 20, 2023**

This report was prepared by: Robert T. Reineke, P.E. P.E. # 32737 – 006
Senior Engineer Date: July 20, 2023

"I, Robert T. Reineke, hereby certify that I am a registered professional engineer in the State of Wisconsin, registered in accordance with the requirements of ch. A-E 4, Wis. Adm. Code; that this document has been prepared in accordance with the Rules of Professional Conduct in ch. A-E 8, Wis. Adm. Code; and that, to the best of my knowledge, all information contained in this document is correct and the document was prepared in compliance with all applicable requirements in chs. NR 700 to 726, Wis. Adm. Code."

Robert T. Reineke

This report was prepared by: Pratap N. Singh, Ph.D., PE P.E. # 22177-6
Principal Engineer Date: July 20, 2023

"I, Pratap N. Singh, hereby certify that I am a registered professional engineer in the State of Wisconsin, registered in accordance with the requirements of ch. A-E 4, Wis. Adm. Code; that this document has been prepared in accordance with the Rules of Professional Conduct in ch. A-E 8, Wis. Adm. Code; and that, to the best of my knowledge, all information contained in this document is correct and the document was prepared in compliance with all applicable requirements in chs. NR 700 to 726, Wis. Adm. Code."

Pratap N. Singh
